National Aeronautics and
Space Administration

Document Number CxP 72103
Revision A

Crew Exploration Vehicle Project Office
National Aeronautics and Space Administration
Johnson Space Center, TX 77058

CEV Reference Configuration Study

CRC-3 Design Definition Document

October 2006

Document Number	Document Title	Office of Primary Responsibility
CxP 72103	CEV Reference Configuration DDD	CEV VIO

Document Errata Sheet

The issues listed below are KNOWN errors/issues/gaps acknowledged and in work by the document owners.

Included on the first page are those major concerns. The second page provides space for lesser issues.

Please do not write RIDS for TBD/TBR data as we are including TBD/TBR tables at the end of each document. For your convenience, the issues are listed by section number.

Please do not write RIDS for these known errors/issues/gaps.

Known Major Issues/Gaps

Known Major Issues / Gaps with Product:

#1 Note: this document contains an old configuration.

#2

Forward Plan for Issues / Gaps:

#1 Will be replaced by Lockheed Martin's Architecture Design Document when enough detail is available.

#2

Document History Log

Status (Baseline/ Revision/ Canceled)	**Document Revision**	**Effective Date**	**Description**
Baseline	-	August 2006	Covers the CRC-2 reference configuration
Revision	A	October 2006	Updated for CRC-3

CEV Reference Configuration
Design Definition Document

Signature Page

SUBMITTED BY:

_______________________________ _______________

Name: Jim Geffre — Date
Title: Lead, CEV Reference Configuration Study
Vehicle Integration Office

APPROVED BY:

_______________________________ _______________

Name: Ed Robertson — Date
Title: Manager, Integrated Vehicle Performance Analysis
Vehicle Integration Office

_______________________________ _______________

Name: Scott Gahring — Date
Title: Manager, Vehicle Integration Office

TABLE OF CONTENTS

****

LIST OF FIGURES

****

LIST OF TABLES

****

Acronyms and Symbols

Al-Li	Aluminum-Lithium
APAS	Androgynous Peripheral Assembly System
AR	Area Ratio
ARC	Ames Research Center
ARU	Array Regulator Unit
ATCS	Active Thermal Control System
BFS	Backup Flight System
BMI	Bismaleimide
BPC	Boost Protective Cover
C&DH	Command and Data Handling
C&T	Communications and Tracking
CARD	Constellation Architecture Requirements Document
CBE	Current Best Estimate
CBM	Common Berthing Mechanism
CEV	Crew Exploration Vehicle
CFD	Computational Fluid Dynamics
CG	Center of Gravity
CLV	Crew Launch Vehicle
CM	Crew Module
CONUS	Continental United States
COPV	Composite Overwrapped Pressure Vessel
COTS	Commercial Off the Shelf
CRC	CEV Reference Configuration
CSFDR	Crash-Survivable Flight Data Recorder
CxP	Constellation Program
D&C	Displays and Controls
DAC	Design Analysis Cycle
DAU	Data Acquisition Unit
DDD	Design Definition Document
DFMR	Design for Minimum Risk
DOF	Degrees Of Freedom
DSNE	Design Specification for Natural Environments
ECLSS	Environmental Control and Life Support System
EDS	Earth Departure Stage
EPS	Electrical Power System
ESAS	Exploration Systems Architecture Study
EVA	Extravehicular Activity
FCC	Flight Critical Computer
FCE	Flight Crew Equipment
FDIR	Fault Detection, Isolation, and Recovery
g	Acceleration of Gravity
GN&C	Guidance, Navigation, and Control
GOX	Gaseous Oxygen
GPS	Global Positioning System
GRAM	Global Reference Atmospheric Model
GRC	Glenn Research Center

GSE	Ground Support Equipment
HSIR	Human System Integration Requirements
IMU	Inertial Measurement Unit
IRD	Interface Requirements Document
Isp	Specific Impulse
ISS	International Space Station
JSC	Johnson Space Center
KSC	Kennedy Space Center
L/D	Lift to Drag Ratio
LaRC	Langley Research Center
LAS	Launch Abort System
LAV	Launch Abort Vehicle
lbf	pounds force
lbm	pounds mass
LCG	Liquid Cooling Garment
LEO	Low Earth Orbit
LIDAR	Light Detection and Ranging
LIDS	Low Impact Docking System
LLO	Low Lunar Orbit
LOI	Lunar Orbit Insertion
LS	Landing System
LSAM	Lunar Surface Access Module
LVLH	Local Vertical Local Horizontal
MEL	Master Equipment List
MIMU	Miniature Inertial Measurement Unit
MLI	Multi-Layer Insulation
MMH	Monomethyl Hydrazine
MMOD	Micrometeoroid and Orbital Debris
MR	Mixture Ratio
MSL	Mean Sea Level
NASA	National Aeronautics and Space Administration
nmi	Nautical Miles
NTO	Nitrogen Tetroxide
OML	Outer Mold Line
OMS	Orbital Maneuvering System
Pc	Chamber Pressure
PDU	Power Distribution Unit
PMA	Pressurized Mating Adapter
PMD	Propellant Management Device
psf	Pounds per Square Foot
psi	Pounds per Square Inch
PTCS	Passive Thermal Control System
RAC	Requirements Analysis Cycle
RCS	Reaction Control System
RPOD	Rendezvous Proximity Operations and Docking
SA	Spacecraft Adapter
SM	Service Module
SPDU	Secondary Power Distribution Unit
SPS	Service Propulsion System
SRB	Solid Rocket Booster

SRD	System Requirements Document
SSME	Space Shuttle Main Engine
STS	Space Transportation System
TBD	To Be Determined
TBR	To Be Resolved
TEI	Trans-Earth Injection
TLI	Trans-Lunar Injection
TPS	Thermal Protection System
TRL	Technology Readiness Level
WCS	Waste Collection System

****

This Page Intentionally Left Blank

1.0 Introduction and Study Overview

The CEV Reference Configuration (CRC) study was initiated by the CEV Project Office in November 2005 to develop a NASA-internal CEV design concept. This reference concept has been used to support the CEV Project and Constellation Program Offices, including CEV and architecture requirements validation, Crew Module cockpit layout requirements development, aerothermodynamic assessments, integrated CLV-CEV stack analyses, and numerous other activities. While the CEV procurement is in a competitive phase, the CRC study is also used to merge the most favorable design aspects of the two Phase 1 contractor concepts (teams from Lockheed Martin and Northrop Grumman/Boeing) and the NASA team concept into a single CEV design. This Design Definition Document (DDD) describes the results of those efforts – a CEV reference configuration as baselined at the conclusion of a design analysis cycle (DAC). This particular version of the DDD captures the reference configuration from design analysis cycle-3 (DAC-3), and the final CEV reference configuration (CRC) resulting from DAC-3 will hereafter be referred to in this document as CRC-3. The DDD also serves as the initialization point for the subsequent design cycle.

The CRC study has focused on developing a reference concept for the lunar CEV mission as that configuration results in the maximum total CEV mass and therefore is most constrained in terms of meeting CLV payload mass limits. However, the overarching design philosophy throughout the study has been that the reference concept must be designed to satisfy all CEV requirements and not only those applicable to the lunar mission – requirements for ISS crew rotation, ISS pressurized cargo delivery, and lunar missions must be met with a single CEV design. An example of this single-CEV design philosophy is that the CEV crew cabin structure is designed for an ISS-compatible 14.7 psia internal pressure even though the nominal operating pressure for lunar missions will be 10.2 psia.

Since its inception, the CRC study has completed three design analysis cycles. The first, DAC-1, was a brief cycle with a primary goal of updating the Exploration System Architecture Study CEV design to comply with CEV requirements described in the November 2005 release of its System Requirements Document (SRD). The final configuration from DAC-1, CRC-1, was reviewed and baselined on 20 January 2006. DAC-1A then commenced in early February and its primary goal was to revise CRC-1 as quickly as possible to incorporate several major architecture changes made by the Constellation Program in early January. These changes included the following:

- Eliminate the requirement to use oxygen and methane as the Service Module propulsion system's propellant type. The result of this change in CRC-1A was a hypergolic propulsion system using nitrogen tetroxide and monomethyl hydrazine as propellants, similar to the Apollo Service Propulsion System and Shuttle Orbital Maneuvering System. The hypergolic system is expected to have lower cost, schedule, and risk than the oxygen/methane system, albeit with lower performance (higher mass).
- Reduce the CEV outer moldline diameter from 5.5 m to 16.5 ft (~5.0 m). This mass-saving reduction was necessary following a loss in CLV payload capability when the baseline CLV configuration was changed from a four-segment SRB First Stage and single SSME Upper Stage to a five-segment SRB and single J-2X.

- Eliminate the requirement for a common docking mechanism for ISS and lunar CEV missions. This resulted in a Crew Module design that could accommodate either an APAS (ISS) or LIDS (lunar) mechanism.
- Transfer responsibility for the CEV-CLV Spacecraft Adapter from CLV to the CEV Project Office.

CRC-1A was reviewed and baselined on 24 February 2006.

The third design cycle (DAC-2) proceeded from March until 30 April with an interim briefing to the Constellation Systems Engineering Control Board on 07 April. This design cycle finally afforded the team sufficient time to analyze and optimize the CEV design using a stable CEV requirements set, the results of which are described in subsequent sections of this DDD.

DAC-2 began with a maximum CEV effective payload mass limit of 50,785 lbm as levied by the CEV System Requirements Document. The effective payload mass is the theoretical net payload mass the CLV could deliver from Earth to the ascent target if no payload mass were jettisoned during ascent, and in the case of CEV, its effective payload mass can be calculated by summing the mass of the Crew Module, Service Module, Spacecraft Adapter, and $1/6^{th}$ of the Launch Abort System mass. The Launch Abort System only contributes $1/6^{th}$ of its mass to this calculation as it is jettisoned shortly after CLV Upper Stage ignition (currently 30 seconds after) and is not carried to orbit. The final concept resulting from DAC-2, the configuration referred to as CRC-2, has an effective payload mass including mass growth of 50,679 lbm.

The fourth and final reference configuration, CRC-3, was developed between June and August of 2006. Design changes, refinements, and requirements changes during the development of CRC-3 increased the predicted effective payload mass to 51,607 lbm. After completion of this design cycle, Lockheed Martin was selected as the CEV prime contractor and work on the NASA reference configuration ceased. The CEV prime contractor is responsible for overall design and integration of the CEV.

The Call for Improvements requirements set released to the CEV Phase 1 contractors in February 2006 served as initialization documents for the CRC-2 and CRC-3 configurations.

2.0 CEV Overview

The Crew Exploration Vehicle (CEV) is the spacecraft used to transfer flight crews, cargo, and support equipment from Earth to Low Earth Orbit (LEO) or lunar orbit and subsequently return the crew to Earth's surface. For an International Space Station crew rotation or pressurized cargo delivery mission, the CEV is delivered by the Crew Launch Vehicle (CLV) to a suborbital -30 x 100 nmi orbit where the CEV then separates from CLV and transfers to the ISS. After completion of its mission, the CEV undocks from the ISS and returns the crew to Earth. For a lunar mission, the CEV is again delivered to a -30 x 100 nmi where it instead transfers to a waiting Lunar Surface Access Module (LSAM) and Earth Departure Stage (EDS). In conjunction with the LSAM and EDS, the CEV delivers the flight crew to low lunar orbit and subsequently loiters there without crew on board while the lunar surface expedition is performed. After returning to orbit with the LSAM, the crew transfers back to the CEV and the CEV returns the crew to Earth.

The CEV is comprised of four distinct modules: a Launch Abort System (LAS), a Crew Module (CM), a Service Module (SM), and a Spacecraft Adapter (SA). These modules are seen from right to left in Figure 2.0-1 and are described below and in subsequent sections (3.0-6.0).

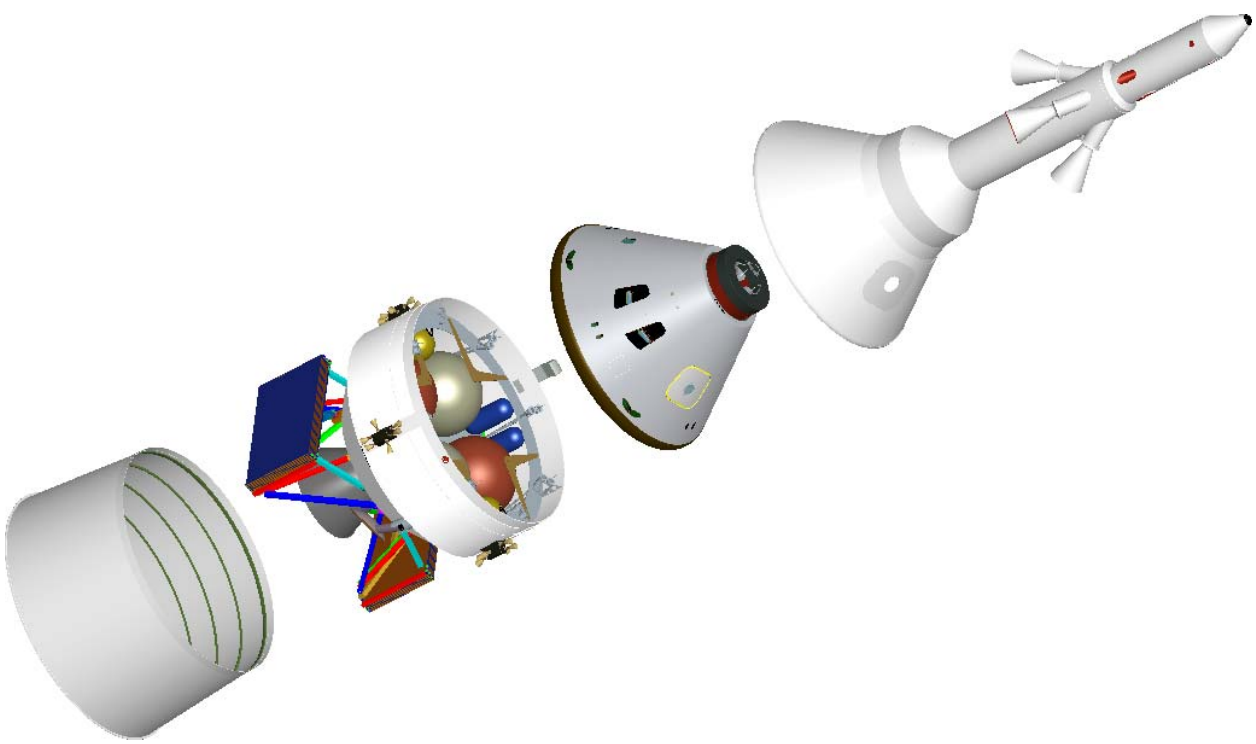

Figure 2.0-1 CEV Exploded View – LAS, CM, SM, and SA

The function of the CEV's Launch Abort System is to separate the Crew Module and its crew quickly from the CLV in case an abort is necessary during pre-launch, launch, or ascent mission phases. It also protects the CM thermal protection system and windows against ascent heating, debris, and motor exhaust with a Boost Protective Cover (BPC). The LAS nominally becomes active after shortly prior to launch and is jettisoned from the CEV shortly after CLV Upper Stage ignition (approximately 30 seconds after ignition, or at an altitude of 300,000 ft). Three solid rocket motors are included on the LAS to perform its function: a jettison motor to jettison the LAS from the CEV, an active control motor to control the orientation of the LAS and CM, and an abort motor. The abort motor supplies the large impulse and thrust needed to separate the CM from the launch vehicle under high-drag abort conditions or to reach a suitable parachute deployment altitude following a pad abort.

The CEV CM is the center for CEV command, control, and habitation functions, and is the only portion of the CEV recovered at the end of its mission. It provides all pressurized volume for the crew and after the LAS is jettisoned, can be used for docking and pressurized transfer to other architecture elements such as the ISS or LSAM. It also includes a thermal protection system and landing and recovery system for safe landing on Earth. The CM is closely derived from the shape of the Apollo Command Module, with a conical side wall and blunt end for atmospheric entry.

All power generation and translational ΔV capabilities for the CEV reside in the SM. It also provides all attitude control function during on-orbit mission phases, and may be used for ascent aborts after LAS jettison. The SM separates from the SA following orbit insertion and separates from the CM prior to atmospheric entry at the end of the mission. The SM is a short cylinder with a single main engine attached to the aft end.

The final CEV module, the SA, provides for physical mating and data transfer with the CLV. It is a truncated hollow cone to provide a smooth transition from the CLV Upper Stage's 18.05 ft (5.50 m) diameter to the 16.5 ft diameter of the CEV SM and CM. The SA also provides protection for the SM's main engine, solar arrays, and high gain antenna during ascent. After reaching orbit, the SA remains attached to the CLV while the SM separates from the SA and the CEV continues on with its mission.

2.1 Subsystem Mass Estimates

Tables 2.1-1 through 2.1-4 provide CRC-3 final mass estimates for lunar variants of the four CEV modules – the Crew Module, Service Module, Launch Abort System, and Spacecraft Adapter. The first column of masses represents the current best estimates (CBE) as supplied by the system and subsystem engineers. The next two columns are the average dry mass growth applied to each system. Dry mass growth was applied according to the mass growth allowance schedule seen in Table 2.1-5. The predicted mass is the sum of the CBE and mass growth allowance. The right column provides the sizing target masses supplied to each system at the start of the design cycle.

Module and system mass targets for CRC-3 were allocated using the 50,785 lbm effective payload mass limit in the SRD and system mass estimates from CRC-2. The CEV effective payload mass is calculated from the sum of the CM, SM, SA, and 1/6th of the LAS mass. This is the theoretical payload mass that the CLV could deliver to orbit if no payload was jettisoned between launch and insertion. The LAS mass only counts 1/6th of its mass against the effective payload mass limit because the LAS is jettisoned shortly after CLV Upper Stage ignition and therefore is not carried to orbit. The CRC-3 final configuration has an effective payload mass of 51,607 lbm, or 822 lbm more than the CLV limit.

Crew Module	**CBE Mass (lbm)**	**Growth (%)**	**Growth (lbm)**	**Predicted Mass (lbm)**	**Target Mass (lbm)**
Active Thermal Control	506	13%	65	570	605
Avionics	553	12%	65	618	618
GN&C	163	9%	14	177	158
ECLSS	516	12%	61	577	1,336
Instrumentation & Wiring	-	-	-	-	720
Landing System	264	14%	36	300	444
Mechanisms	1,488	19%	282	1,770	1,724
Passive Thermal Control	234	17%	41	275	200
Power & Wiring	1,529	14%	209	1,738	1,034
Propulsion	572	11%	65	637	869
Pyros	245	16%	38	283	301
Parachute System	764	17%	131	895	895
Seats	100	25%	25	125	125
Structure	3,199	25%	796	3,995	4,097
TPS	1,888	25%	472	2,360	2,210
Crew & Flight Crew Equipment	1,982	6%	116	2,098	1,915
ECLSS & ATCS Fluids	767	0%	0	767	-
Propellant	434	0%	0	434	-
			TOTAL MASS	**17,621**	**17,252**
			DRY MASS	**14,322**	
			AVG DRY MASS GROWTH	**19.1%**	
			FLUIDS	**1,201**	
			CREW & FCE	**2,098**	

Table 2.1-1 Crew Module Mass Summary

The CRC-3 final CM predicted mass is 17,621 lbm, or 369 lbm over its target mass (the final mass from CRC-2). The predicted mass includes 19.1% average growth for dry mass components, with fluids and crew receiving no mass growth allowance. Fluids included on the CM are a propylene glycol/water blend, water, and Freon for active thermal control; potable water for life support; oxygen and methane for reaction control propulsion; and solid rocket propellant for retrorockets in the landing system.

The Crew Module system masses changed in several areas going from CRC-2 to CRC-3. A brief summary of the major changes are listed by system below.

- The active control system predicted mass decreased by 35 lbm largely due to a bookkeeping change. In CRC-2, the water tank and water used for the fluid evaporator were included in ECLSS, and in CRC-3, responsibility for those components shifted to ATCS. However, all ATCS fluids are now listed separately from ATCS dry mass components.
- Flight crew equipment increased by 184 lbm in CRC-3 due to a 10% growth allocation mandated by the Program and the addition of WCS supplies previously carried under ECLSS.

- GN&C hardware mass increased by 20 lbm with the addition of an altimeter/velocimeter system for the retrorocket landing system.
- The CRC-3 estimate for ECLSS decreased by 759 lbm. Most of this is due to transfer of ECLSS items to other systems, while some mass savings were realized in the swing bed design and mass increased for the suit/ECLSS interfaces. Potable water is now listed separate from ECLSS dry mass components.
- Landing system mass was essentially unchanged from CRC-2 to CRC-3 though the landing system design changed from airbags to retrorockets. The switch to retrorockets did increase the GN&C system mass. The retrorocket propellant is bookkept with the CM RCS propellant.
- Mechanisms increased by 46 lbm, mostly due to mass increases in the tension ties and LIDS/APAS jettison system.
- The passive thermal control system added an extra MLI blanket and pressure vessel heaters which increased its system mass by 75 lbm.
- All wiring mass for CRC-3 (720 lbm) was consolidated under the power system, therefore its mass experienced the most growth. The power management and distribution hardware mass decreased by 16 lbm.
- The CM RCS mass in CRC-3 decreased by 232 lbm when the design changed from GOX/ethanol to GOX/GCH4 and propellant was bookkept as a separate line item.
- Pyros decreased by 18 lbm when the landing system changed from airbags to retrorockets. Pyro hardware for airbag initiation was eliminated.
- The CRC-3 predicted mass estimate for structures decreased by 102 lbm, largely due to a lower mass allocation for secondary structure.
- TPS increased by 150 lbm over CRC-2. In CRC-2, the TPS mass was based on a PICA heat shield and LI-900/LI-2200 tiles for the back shell. The TPS in CRC-3 switched to BRI-8/BRI-18 tiles for the back shell and the heat shield mass was based on the average mass of all five candidate ablator materials.

Service Module	**CBE Mass (lbm)**	**Growth (%)**	**Growth (lbm)**	**Predicted Mass (lbm)**	**Target Mass (lbm)**
Active Thermal Control	666	19%	129	795	834
Avionics	99	12%	12	111	111
ECLSS	236	19%	46	283	524
Instrumentation & Wiring	-	-	-	-	468
Mechanisms	275	25%	69	344	171
Passive Thermal Control	91	20%	18	109	109
Power & Wiring	1,749	17%	306	2,055	1,355
Propulsion	2,483	18%	446	2,929	23,928
Pyros	125	20%	25	149	149
Structure	1,819	25%	455	2,274	2,274
ECLSS & ATCS Fluids	261	0%	0	261	-
Unusable Propellant	687	0%	0	687	-
Propellant	20,500	0%	0	20,500	-
			TOTAL MASS	**30,496**	**29,924**
			DRY MASS	**9,048**	
			AVG DRY MASS GROWTH	**19.9%**	
			FLUIDS	**21,448**	

Table 2.1-2 Service Module Mass Summary

The Service Module predicted mass for CRC-3 is 30,496 lbm with 19.9% average dry mass growth. Fluids included on the SM are a propylene glycol/water blend for active thermal control, oxygen and nitrogen for life support, and nitrogen tetroxide (NTO), monomethyl hydrazine (MMH), and helium for translation and attitude control propulsion. The CRC-3 SM mass is 572 lbm over its target mass.

The major system changes in CRC-3 are as follows:

- Active thermal control dry mass decreased by 28 lbm with refined plumbing mass estimates. ATCS fluids are now bookkept separately.
- An extra 7 lbm of ECLSS oxygen and nitrogen was needed to support one full cabin repressurization and one "feed the leak" event. Like ATCS, ECLSS fluids are bookkept individually.
- The mechanisms mass increased by 172 lbm when solar array mechanisms were resized for launch and TLI burn loads and responsibility for those mechanisms was transferred from the power system to the mechanisms system.
- The power system mass increased by 700 lbm in CRC-3. This was due to the consolidation of wiring mass under the power system, the addition of two thruster control units, and refined estimates for the solar arrays and array launch support structure. All solar array mechanisms were transferred to the mechanisms system in CRC-3.
- SM propulsion increased by 188 lbm largely due to the addition of a main engine gimbal system and four aft-firing RCS thrusters. Usable and unusable propellant is tracked in CRC-3 as individual categories.

Launch Abort System	**CBE Mass (lbm)**	**Growth (%)**	**Growth (lbm)**	**Predicted Mass (lbm)**	**Target Mass (lbm)**
Active Control Motor	335	30%	100	435	327
Abort Motor	2,780	14%	387	3,167	2,747
Jettison Motor	548	21%	115	663	150
Structures & Mechanisms	1,236	15%	184	1,420	1,532
Avionics & Power	170	20%	34	204	77
Guidance, Navigation, & Control	-	-	-	-	125
Passive Thermal Control	989	25%	247	1,236	1,575
Ordnance	-	-	-	-	52
Propellant	6,271	10%	652	6,923	5,453
			TOTAL MASS	**14,049**	**12,038**
			DRY MASS	**7,126**	
			AVG DRY MASS GROWTH	**17.6%**	
			FLUIDS	**6,923**	
			MASS WITH MANAGEMENT RESERVE	**14,049**	**13,200**

Table 2.1-3 Launch Abort System Mass Summary

The CRC-3 Launch Abort System predicted mass is 14,049 lbm, an increase of 849 lbm over the CRC-2 estimate. Much of the mass increase is due to refined component designs and a larger CM/LAS adapter needed to accommodate a raised APAS or LIDS docking mechanism. In CRC-2, the docking mechanism was partially embedded in the CM forward compartment.

Spacecraft Adapter	**CBE Mass (lbm)**	**Growth (%)**	**Growth (lbm)**	**Predicted Mass (lbm)**	**Target Mass (lbm)**
Structure	741	25%	185	926	1,080
Wiring	20	25%	5	25	25
Pyrotechnics	68	25%	17	85	85
Mechanisms	90	25%	23	113	113
			TOTAL MASS	**1,149**	**1,302**
			DRY MASS	**1,149**	
			AVG DRY MASS GROWTH	**25.0%**	
			FLUIDS	**0**	

Table 2.1-4 Spacecraft Adapter Mass Summary

The Spacecraft Adapter predicted mass for CRC-3 is 1,149 lbm with 25% average dry mass growth. This is 154 lbm less than its target mass at the start of the design cycle, and is due to a switch from aluminum to composite as the construction material for the Spacecraft Adapter skin panels.

2.1.1 Mass Growth Allowance

Mass is included in the CRC-3 concept in addition to the current best estimates supplied by the system engineers to account for expected future mass growth in the CEV. Mass growth allowance was allocated to CRC-3 component mass estimates according to the nature of the individual component and its design maturity for this design cycle. The growth allocation schedule, seen in Table 2.1-5, was developed specifically for the CEV Reference Configuration study though is closely derived from recommended standards of the American Institute of Aeronautics and Astronautics and Society of Allied Weight Engineers. According to the schedule, component mass growth ranges from 0-30%, with study goal of having 20-25% dry mass growth for each CEV module (such as the Crew Module). Components receiving no mass growth include fluids, crew, cargo, flight crew equipment, or components that exist today and will be included in the CEV without modification. Components receiving the most mass growth are those with the least design fidelity, typically structures, wiring, plumbing, and small electrical components. Mass growth for a component is summed with its current best estimate to produce a predicted mass, and all predicted masses are summed for the overall module and CEV masses.

Design Maturity	Structure Mech Pyros TPS	Propulsion	Environmental Control	Batteries	Wiring & Plumbing	Electrical/Electronic Components		
						0-10 lb	10-30 lb	>30 lb
Parametric & New Design	25%	20%	20%	17%	30%	30%	20%	15%
Existing Similar Hardware Requiring Major Mods	17%	15%	15%	10%	20%	20%	12%	10%
Prototype Hardware	10%	8%	8%	8%	10%	10%	8%	8%
Minor Mods to Existing Hardware	5%	5%	5%	5%	5%	5%	5%	5%
Actual Mass	0%	0%	0%	0%	0%	0%	0%	0%
Flight Crew Equipment	0%	0%	0%	0%	0%	0%	0%	0%

Table 2.1-5 Mass Growth Allowance Schedule

2.1.2 SM Propellant Budget

The CRC-3 SM propulsion system is designed to store 20,500 lbm of usable propellant for orbital maneuvering (OMS) and reaction control (RCS) maneuvers. This allocation was based on a total SM ΔV of 6,087 ft/s and the initial subsystem mass targets for CRC-3. The required ΔV is derived from the CEV SRD, and the CRC-3 mass targets were assumed to be the following:

- CM: 17,300 lbm
- SM: 29,870 lbm

- SA: 1,400 lbm
- LAS: 13,290 lbm

Table 2.1-6 details the propellant consumption calculations that resulted in the total usable propellant mass of 20,500 lbm. Service Module propellant tank sizing and CRC-3 mass properties are based on this propellant mass. However, as the final system mass estimates exceeded their mass targets, the vehicle design is not closed. Additional propellant would be required to accommodate the higher predicted inert masses of the final CRC-3 configuration while meeting the delta-V requirement. This sizing iteration was not performed in CRC-3 because the CLV effective payload mass limit was exceeded even with the 20,500 lbm propellant mass allocation.

Updated 26 Feb 2006

	Isp	Thrust (lbf)
OMS	323.0	10,000
RCS*	287.0	100

Propulsive Maneuver	OMS ΔV (ft/s)	RCS ΔV (ft/s)	Initial CEV Mass (lbm)	OMS Prop Used (lbm)	RCS Prop Used (lbm)	Final CEV Mass (lbm)	Usable Prop Remaining (lbm)	Initial OMS T/W	Final OMS T/W
Insertion			48,570				20,492		
Rendezvous w/ LSAM	504.9	106.1	47,170	2,237	539	44,394	17,716	0.21	0.23
Lunar Orbit Maneuvering	590.6	49.2	43,134	2,383	229	40,522	15,104	0.23	0.25
Trans-Earth Injection	4,753.9		40,767	14,966		25,801	138	0.25	0.39
Mid-Course Correction(s)		32.8	25,801		91	25,710	46		
SM Disposal		49.2	8,725		46	8,678	0		
Totals	5,849	237		19,586	906				
* RCS Isp is an average of thruster Isp for short and long impulses (assumed to be 275 and 300 s)									
CEV Mass Gained or Lost During the Mission	Crew 820	Suits 440	Lunar Samples 280	Food Trash 163	Water 371		Water Tanks 89	LIDS Mech 672	
Pre-LO Maneuvering Mass Gains/Losses	Crew, Suits (Losses)								
Pre-Trans-Earth Injection Mass Gains/Losses	Crew, Suits, Lunar Samples (Gains); Food Trash, Water, Water Tanks, LIDS Mechanism (Losses)								
Pre-SM Disposal Mass Gains/Losses	Crew Module (Losses)								

CEV Effective P/L Mass	50,785	lbm
LAS	-13,290	lbm
SA	-1,400	lbm
CSM Insertion Mass	47,170	lbm

Note: Insertion mass penalty for LAS is 1/6 of total LAS mass

Table 2.1-6 SM Usable Propellant Budget

The CEV begins with an inserted mass of 48,570 lbm, which results from subtracting the LAS mass penalty from the CEV effective payload mass limit of 50,785 lbm listed in the SRD. The assumed LAS penalty for carrying the LAS to Upper Stage ignition + 30 seconds and then jettisoning it was 1/6th of its total mass. After separating from the SA, the total CEV mass then decreases to 47,170 lbm and it begins consuming SM propellant. The ΔV allocated for CLV separation, circularization, and rendezvous, proximity operations, and docking with the LSAM is 504.9 ft/s for OMS and 106.1 ft/s for RCS. Assuming an OMS specific impulse (Isp) of 323 seconds for OMS and an average Isp of 287 seconds for RCS results in a total propellant consumption of 2,776 lbm by the time of docking.

The next period of CEV propellant use comes during the uncrewed flight portion of lunar orbit operations. The CEV performs periodic attitude control maneuvers and a major plane change to align its orbit with the ascending LSAM Ascent Stage. However, prior to this event, the CEV mass has substantially changed – the flight crew and their EVA equipment have transferred to the LSAM. This results in a 1,260 lbm CEV mass decrease. Assuming ΔVs of 590.6 ft/s for OMS and 49.2 ft/s for RCS, the CEV consumes 2,612 lbm of propellant during this mission phase.

Following ascent from the lunar surface and docking with the CEV, the crew then transfers themselves, their suits, and 280 lbm of lunar samples from the LSAM to the CEV. The crew also transfers any unnecessary trash from the CEV to the LSAM and during undocking, the CEV leaves the LIDS docking mechanism with the LSAM. Overall, the CEV mass increases 245 lbm from its pre-docked condition. The next burn for the CEV is trans-Earth injection (TEI), which has an OMS ΔV of 4,753.9 ft/s. TEI is the main contributor to propellant consumption with it accounting for 15,104 lbm or 74% of the overall budget. The last two CEV maneuvers are relatively minor RCS burns: trajectory correction maneuvers and an SM disposal burn. The SM disposal burn comes after the CM has separated from the SM.

2.1.3 CM Propellant Budget

The CM usable propellant budget is based on an entry ΔV requirement of 164 ft/s listed in the CEV SRD. RCS propellant on the CM may be used to reorient the vehicle to a proper attitude for entry, and during atmospheric flight to provide roll torque to control the direction of the CM lift vector and to counteract induced spin torques; to provide dampening of induced pitch and yaw instabilities; and to correct range dispersions during skip-out portions of a lunar skip return trajectory. Using a target CM mass of 16,354 lbm at entry interface and average Isp of 315 seconds for a GOX/GCH4 system results in a total CM RCS propellant mass of 288 lbm. This mass includes a 26 lbm allocation for unusable propellant.

2.2 CEV Mass Properties

CEV mass properties for several critical mission phases of the four-crew lunar sortie mission are provided in Table 2.2-1. These mission phases are:

- Launch
- Pad Abort (Ignition and Burnout)
- Post-LAS Jettison
- Separation from CLV (Solar Arrays and High Gain Antenna Stowed and Deployed)
- Docked to the LSAM and EDS for TLI
- Lunar Orbit Loiter
- SM Burnout
- Entry
- Landed

LUNAR SORTIE: CRC-3 CONFIGURATION	Predicted Mass (lbm)	Center of Gravity X (in)	Center of Gravity Y (in)	Center of Gravity Z (in)	Moments of Inertia Ixx (slug-ft^2)	Moments of Inertia Iyy (slug-ft^2)	Moments of Inertia Izz (slug-ft^2)	Products of Inertia Ixy (slug-ft^2)	Products of Inertia Ixz (slug-ft^2)	Products of Inertia Iyz (slug-ft^2)
CREW MODULE	17,621	131.1	1.0	-7.3	12,482	11,724	11,086	-139	-346	180
SERVICE MODULE	30,496	222.5	0.8	2.3	26,668	18,102	16,947	-79	-186	-1,650
LAUNCH ABORT SYSTEM	14,049	-49.2	0.1	0.1	2,909	25,173	25,196	70	32	11
SPACECRAFT ADAPTER	1,149	280.1	0.0	2.2	2,560	1,636	1,583	0	6	0
LAUNCH	63,314	137.8	0.7	-0.9	44,846	215,212	213,163	186	1,009	-1,466
CREW MODULE	17,621	131.1	1.0	-7.3	12,482	11,724	11,086	-139	-346	180
LAUNCH ABORT SYSTEM	14,049	-49.2	0.1	0.1	2,909	25,173	25,196	70	32	11
PAD ABORT (IGNITION)	31,670	51.1	0.6	-4.0	15,482	91,816	91,111	202	-2,541	181
CREW MODULE	17,621	131.1	1.0	-7.3	12,482	11,724	11,086	-139	-346	180
LAUNCH ABORT SYSTEM	7,304	-45.7	0.3	0.1	2,509	20,604	20,626	68	31	11
PAD ABORT (BURNOUT)	24,925	79.3	0.8	-5.1	15,052	67,230	66,554	79	-1,770	185
CREW MODULE	17,621	131.1	1.0	-7.3	12,482	11,724	11,086	-139	-346	180
SERVICE MODULE	30,496	222.5	0.8	2.3	26,668	18,102	16,947	-79	-186	-1,650
SPACECRAFT ADAPTER	1,149	280.1	0.0	2.2	2,560	1,636	1,583	0	6	0
LAS JETTISON (NOMINAL ASCENT)	49,265	191.1	0.9	-1.1	41,932	53,806	51,738	-291	1,651	-1,476
CREW MODULE	17,606	131.1	1.0	-7.3	12,474	11,718	11,080	-139	-346	180
SERVICE MODULE	30,496	222.5	0.8	2.3	26,668	18,102	16,947	-79	-186	-1,650
SEPARATION FROM CLV	48,102	189.0	0.9	-1.2	39,362	50,142	48,128	-272	1,571	-1,475
CREW MODULE	17,606	131.1	1.0	-7.3	12,474	11,718	11,080	-139	-346	180
SERVICE MODULE	30,496	221.4	0.8	2.3	45,880	26,769	25,614	-77	-177	-11,235
SOLAR ARRAYS DEPLOYED	48,102	188.4	0.9	-1.2	58,574	58,367	56,353	-266	1,561	-11,060
CREW MODULE	17,606	131.1	1.0	-7.3	12,474	11,718	11,080	-139	-346	180
SERVICE MODULE	27,720	221.6	0.9	2.5	43,960	25,678	24,526	-78	-179	-11,033
TLI - DOCKED TO LSAM	45,326	186.5	0.9	-1.3	56,657	56,662	54,648	-248	1,538	-10,856
CREW MODULE	16,391	131.5	0.9	-8.3	12,112	11,441	10,945	-132	-341	173
SERVICE MODULE	27,720	221.6	0.9	2.5	43,960	25,678	24,526	-78	-179	-11,033
LUNAR ORBIT LOITER (UNCREWED)	44,110	188.1	0.9	-1.5	56,334	55,458	53,549	-207	1,655	-10,859
CREW MODULE	16,451	134.6	1.0	-8.6	12,367	10,142	9,371	-165	-263	192
SERVICE MODULE	9,996	225.3	2.5	7.1	31,651	18,635	17,544	-97	-235	-9,756
SERVICE MODULE BURNOUT	26,447	168.9	1.5	-2.7	44,351	40,144	37,953	-81	1,411	-9,532
CREW MODULE	16,451	134.6	1.0	-8.6	12,367	10,142	9,371	-165	-263	192
ENTRY (NOMINAL)	16,451	134.6	1.0	-8.6	12,367	10,142	9,371	-165	-263	192
CREW MODULE	12,107	130.3	0.9	-10.7	7,964	6,350	5,499	-126	-418	210
TOUCHDOWN (NOMINAL)	12,107	130.3	0.9	-10.7	7,964	6,350	5,499	-126	-418	210

Notes

1) Module mass properties are calculated at the module's center of gravity
2) CEV mass properties are calculated at the CEV's center of gravity
3) Products of Inertia are calculated using a "positive integral" formulation
4) All mass properties are calculated using the CEV Structural Frame centered at theoretical apex of the Crew Module conical section
5) All mass properties are calculated including mass growth allocations

Table 2.2-1 CRC-3 Mass Properties for the Lunar Sortie Mission

Moments and products of inertia for the CEV are given about each configuration's center of gravity, and center of gravity locations are measured relative to the CEV structural coordinate system that has its origin at the theoretical apex of the Crew Module cone. It should also be noted that the products of inertia listed in Table 2.2-1 correspond to a positive integral formulation. Simulations assuming negative integral calculations for I_{XY}, I_{XZ}, and I_{YZ} must first reverse the signs of the listed values.

The X_{CG} and Z_{CG} locations for a nominal lunar entry are shown in Figure 2.2-1. The Crew Module mass at entry interface is 1,170 lbm less than at launch, and the center of gravity has shifted 3.5 inches in +X and 1.3 inches in –Z. These changes are due to mass that has been added or removed from the CM over the course of the nominal mission. Specifically, the LIDS mechanism is jettisoned with the LSAM Ascent Stage (-807 lbm), waste water is vented and trash is transferred to the empty Ascent Stage (-628 lbm), the CM cabin pressure is lowered to 10.2 psia (-15 lbm), and lunar sample containers are shifted from the LSAM to the CEV (+280 lbm). The resulting CM at Mach 25 has a lift-to-drag (L/D) ratio of 0.35. The L/D goal was 0.4 at the start of CRC-3 but was not achieved in the final configuration.

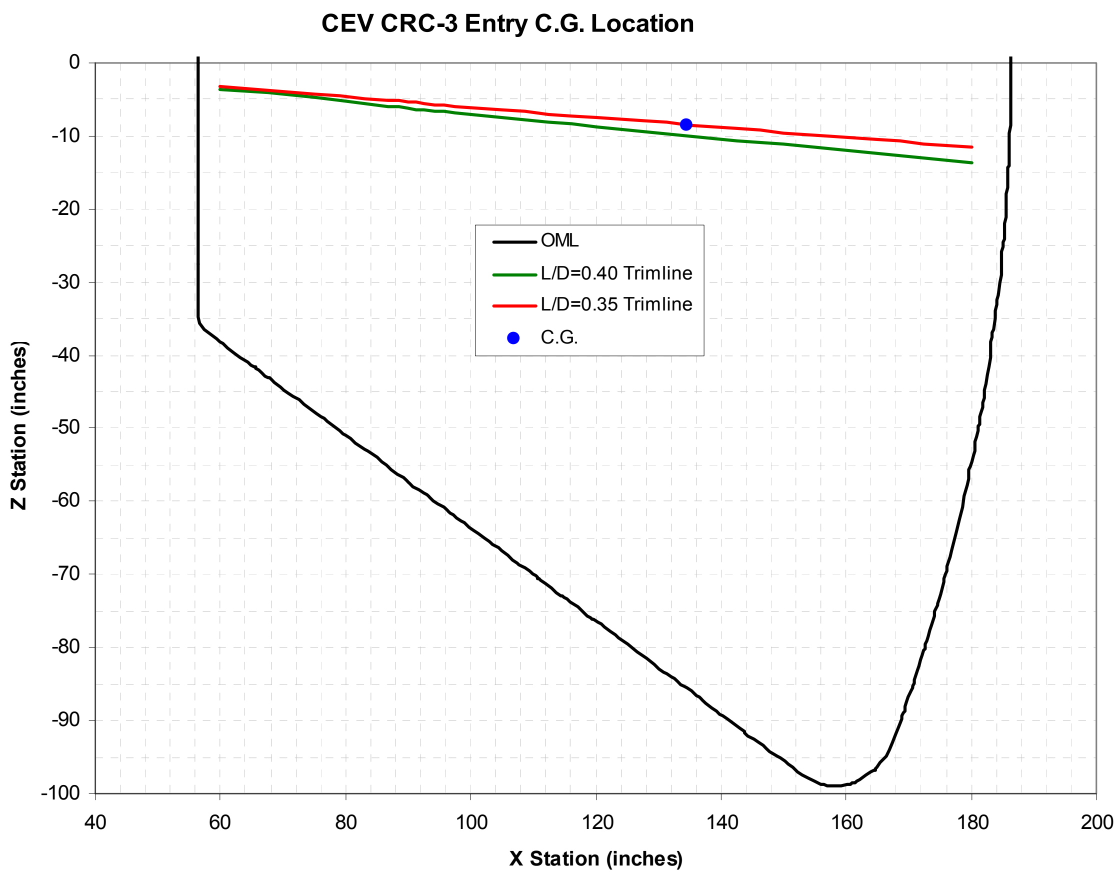

Figure 2.2-1 Entry CG Location and L/D Trim Lines (M=25)

2.3 Mission Timeline

The CEV nominal lunar mission timeline used for CRC-3 included five major mission phases: (1) pre-launch, launch, ascent, and low Earth orbit operations; (2) trans-lunar coast; (3) lunar orbit operations; (4) trans-Earth coast; and (5) entry, descent, landing, and recovery. The mission timeline is described below and in Table 2.3-1.

Pre-Launch, Launch, Ascent, and Low Earth Orbit Operations

This mission phase includes all activities beginning with crew ingress into the CEV on the launch pad through completion of the trans-lunar injection (TLI) burn. Six hours of CEV- or Ground Systems-provided life support is included for pre-launch activities such as crew ingress and systems checkout. The expected duration for this mission phase will be closer to 3 hours with the remainder being included for launch delays and margin. The next activity, launch and ascent, lasts approximately 10 minutes from liftoff to Upper Stage engine cutoff at the desired ascent target conditions (-30x100 nmi orbit). After engine cutoff, the CEV Service Module separates from the Spacecraft Adapter and begins a 12-hour rendezvous, proximity operations, and docking sequence for a flight day one docking with the LSAM and EDS. After docking with the LSAM, 18 hours has been bookkept for crew sleep and vehicle checkout prior to the TLI burn. However, as the Constellation Program desires a capability for four successive CEV launch opportunities before the TLI window closes, an on-time CEV launch means the crew must wait for several days until the TLI window opens. This is because the LSAM and EDS are launched to orbit prior to the CEV, and in doing so, the TLI opportunities become fixed in time. The TLI window must be set up such that the CEV can launch on its fourth opportunity, dock with the LSAM, and have enough time for TLI preparation before the window opens. The timeline assumes the CEV launches on its first opportunity and therefore must wait 70.5 hours for the window opening.

The TLI window of the Constellation Architecture is assumed to be such that there are five discrete TLI burn opportunities (one per orbit). With the first opportunity at the start of the first orbit and the fifth opportunity near the end of the fourth orbit, the overall TLI window extends 6 hours. The nominal TLI burn will occur at the middle of the window for maximum performance. This means the CEV waits for 3 hours until the nominal TLI and then the EDS performs a 6-minute TLI burn.

Trans-Lunar Coast

After a nominal TLI burn, the CEV coasts for 72 hours to the Moon. The transfer time may vary, though, depending on which TLI opportunity is used. The lunar arrival time is held approximately constant, which means that if TLI occurs on the last opportunity or 3 hours past the middle of the window, the transfer time will be approximately 69 hours. The overall effect is that the total time between the opening of the TLI window and lunar arrival is 75 hours. During the trans-lunar coast, the crew will check out the LSAM in preparation for lunar orbit insertion and will periodically perform trajectory correction maneuvers to correct TLI burn errors. According to the current baseline, the LSAM is required to perform the correction maneuvers, though there is an on-going trade to determine if that function should more appropriately belong to the CEV.

Lunar Orbit Operations

The next major CEV mission phase begins with the lunar orbit insertion (LOI) burn and ends with completion of the trans-Earth injection (TEI) burn. The architecture utilizes a three-burn sequence to transfer from a hyperbolic lunar fly-by trajectory to a low lunar orbit set up for a 7-day sortie mission. This sequence nominally lasts 24 hours from the LOI burn to the lunar orbit circularization burn. After this, the crew begins preparation for descent by checking out the LSAM, transferring themselves and equipment to the LSAM, and undocking. Six complete orbit revolutions or 12 hours has been allocated to these tasks. The CEV then transforms to uncrewed free-flight operation which lasts until the LSAM Ascent Stage docks with the CEV approximately 7 days later. CEV activities during free-flight include attitude maintenance, possibly serving as a LSAM-to-Earth communications relay, and performing an ascent plane change burn near liftoff to align its orbit with the Ascent Stage's target orbit plane. Once the vehicles have re-docked, 10 hours have been included for crew and equipment transfer, Ascent Stage undocking, and TEI preparation. Like lunar orbit capture, lunar departure is a three-burn, 24-hour sequence from the orbit apolune raise burn to TEI burn completion. A large plane change burn is performed in the middle of this sequence.

Trans-Earth Coast

Trans-Earth Coast encompasses all operations between TEI burn completion and arrival at Earth entry interface. This entire mission phase nominally lasts as little as 3.5 days or 84 hours, though the total flight time may vary by as much as 24 hours in order to move the Earth longitude of the lunar antipode for a skip entry trajectory to a single Continental United States (CONUS) landing site. In this time, the CEV performs trajectory correction maneuvers to correct TEI errors, separates the Crew Module from the Service Module, and prepares for Earth entry. The timeline puts the time between separation and entry interface at 25 minutes, which leaves 83.6 hours for coast time. Any coast time increases come out of the CEV contingency time allocation.

Entry, Descent, Landing, and Recovery

The fifth and final major mission phase lasts from entry interface through connection of ground support equipment following touchdown. If the CEV performs a maximum-range skip entry to a CONUS landing site, the time to drogue parachute deployment may be 31 minutes. Another six minutes is required on the drogue and main parachutes to touchdown. Finally, 45 minutes of CEV support has been allocated for ground crews to reach the Crew Module and connect support equipment.

Phase Name	Duration (hr)	Start MET (hr:min)	Environment	OMS DV (ft/s)	RCS DV (ft/s)	Crew On-Board?
Pre-Launch	6	-6:00	On-Pad			Yes w/ Pad Umbilical
Ascent	0.2	0:00	Ascent			Yes
Rendezvous Sequence	10	0:10	Low Earth Orbit	505	106	Yes
Terminal Phase Initiation to Docking	2	10:10				Yes
Checkout	18	12:10				Yes
Loiter to TLI Window Opening	70.5	30:10				Yes
TLI Opening to Ignition	3	100:40				Yes
TLI Burn	0.1	103:40				Yes
Trans-Lunar Coast	72	103:43	Earth-Moon Space			Yes
Lunar Orbit Capture Burn	0.1	175:40	Low Lunar Orbit			Yes
Coast	8.3	175:43				Yes
LOI Plane Change Burn	0.1	184:02				Yes
Coast	15.5	184:05				Yes
Lunar Orbit Circularization Burn	0.1	199:32				Yes
Checkout and Prepare for Undocking	12	199:35				Yes
Lunar Surface Activities	168	211:35		591	49	No
Prepare for TEI	10	379:35				Yes
TEI Apolune Raise Burn	0.1	389:35		1,872		Yes
Coast	16.7	389:38				Yes
TEI Plane Change Burn	0.1	406:17		1,199		Yes
Coast	6.8	406:20				Yes
TEI Completion Burn	0.1	413:09		1,683		Yes
Trans-Earth Coast	83.6	413:12	Earth-Moon Space		33	Yes
SM Separation to Entry Interface	0.42	496:45	Low Earth Orbit		49	Yes
Entry Interface to Drogue Deploy	0.53	497:10	Entry		164	Yes
On-Chute to Landing	0.1	497:42				Yes
Recovery	0.75	497:47	Landing Site			Yes w/ Hatches Open

Total Stand-Alone Mission Duration	**497.8 hr**	**20.7 days**
Total Duration w/ Crew	**329.8 hr**	**13.7 days**
Contingency Time	**102.2 hr**	**4.3 days**

Table 2.3-1 CEV Mission Timeline

The nominal active duration for this lunar mission is 13.7 days. Active mission time is time in which the crew is on-board the CEV and utilizing on-board CEV life support and power resources. Since the CEV is required to provide an 18-day active mission duration, this leaves 4.3 days of contingency time. The trans-Earth coast may vary by up to 24 hours, so the remaining 3.3 days can be used for other mission phases or for an extended post-LOI loiter in the case of particular hard-to-reach lunar landing sites.

2.4 Integrated Flight Attitude Performance Analysis

An inter-system team was formed to examine the effects of flight attitudes on the performance of the vehicle. The study goal was to develop a reference set of vehicle flight attitudes that will yield acceptable performance of the CEV throughout all mission phases. Several systems are affected by flight attitude and those include:

- Power: Power generation from the solar arrays
- Propulsion: Propellant consumption to maintain vehicle attitude/altitude
- Active Thermal: Heat rejection capability from radiators
- Passive Thermal: Hot/cold conditions for sensitive hardware and the amount of heater power required
- Communication: Antenna pointing and data rate
- GN&C: Attitude knowledge, instrument pointing & pointing targets for arrays & antennas

Since it is likely that no one attitude (or set of attitudes) will be optimal for all effected systems, the team sought to find a reference set of attitudes which will be acceptable for overall vehicle performance, that will meet the CEV SRD, IRD(s), and CARD requirements. Therefore, the team set out to develop a set of candidate flight modes for each mission phase, and examine the performance of each system in those flight attitudes. The results from each system would be compared against requirements, and, looking across all systems, a determination would be made as to whether the flight mode is acceptable or not. The team focused on the low lunar orbit (LLO) and low Earth orbit (LEO) phases of the mission.

2.4.1 Attitudes Assessed and Coordinate System Used

The team considered several attitudes of the LVLH and solar inertial varieties. LVLH, or local vertical, local horizontal, attitudes are orientations in which the CEV's attitude is constant with respect to the Moon (for LLO cases), or Earth (for LEO cases). These attitudes are usually defined by specifying which vehicle axis is aligned with the orbit velocity vector, and which vehicle axis is aligned with the orbit nadir vector (otherwise known as the local vertical vector, which is the vector that points from the CEV to the center of the Earth or Moon). For example:

- +Xvv+Znadir would mean that the vehicle positive X axis is aligned with the velocity vector and the vehicle positive Z axis is pointed nadir.

For this assessment, the team used a GN&C-based system which is different from the vehicle, or structural coordinate system. This system has +X forward along the nose of the vehicle, so that roll, pitch, and yaw maneuvers are in the expected directions. The origin of this coordinate system is at the vehicle CG. This is illustrated in Figure 2.4-1.

The attitudes considered for this study require having the solar arrays aligned either in the plane of the orbit, or perpendicular to the plane. Since the CEV design concept has the solar arrays clocked 45° to the vehicle axes, this means flying in attitudes with roll angles of ±45° such that the vehicle principle axes are not necessarily aligned with the velocity or nadir vectors. To make it easier to refer to these attitudes without using a yaw-pitch-roll angle sequence, some mnemonics were developed to help easily identify different attitude variants. These are:

- AOP, which stands for *Arrays Out of Plane* and is used to signify an attitude which has the solar arrays oriented perpendicular to the plane of the orbit, and

- AIP, which stands for *Arrays In Plane* and is used to signify an attitude which has the solar arrays oriented in the plane of the orbit.

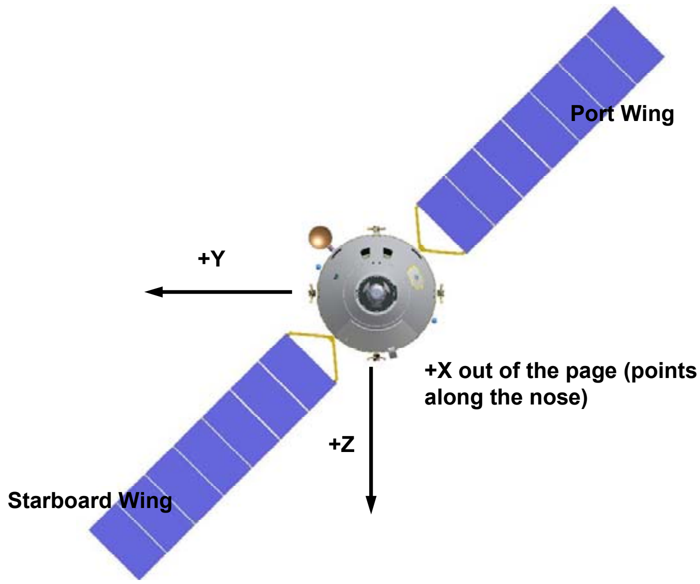

Figure 2.4-1 GN&C-based Coordinate System

Given the short time available for the assessment, only a small subset of potential attitudes could be looked at in detail. The team concentrated on the LVLH attitudes which have the vehicle ±X-axis aligned with the velocity vector, and those with the vehicle +X axis aligned with the orbit nadir vector. Each of those attitudes has a variant with the solar arrays either in-plane or out of plane, which yields for main attitude variants that were considered. These four variants are shown in Figure 2.4-2.

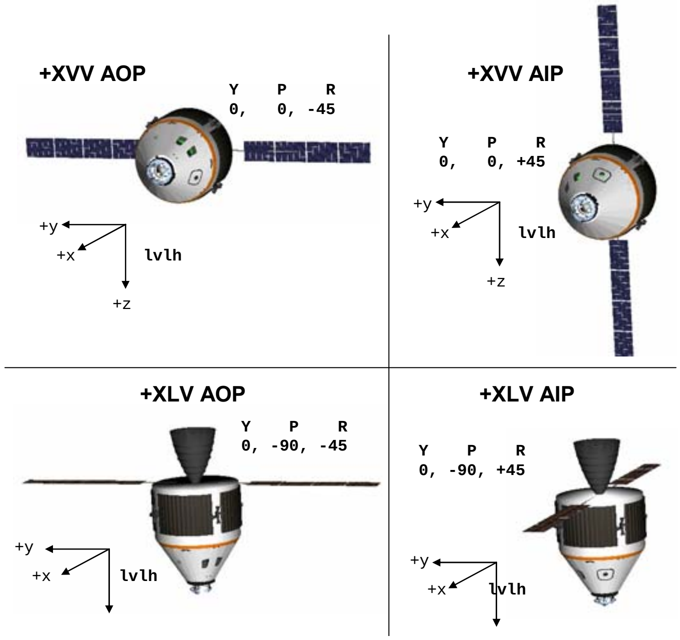

Figure 2.4-2 Attitudes Considered

2.4.2 Low Lunar Orbit Results

The LLO phase of the mission was determined to be the most challenging for many of the systems. No single attitude or set of attitudes was demonstrated to be good for all systems across all solar β angles. Nose-Down (+Xnadir) attitudes seem to be the best identified thus far:

a) These were demonstrated to be good for both active and passive thermal, and to be good for power, although power requires that two different variations be flown, depending on the solar β:

- Solar arrays out of plane (AOP) for low solar βs (|β| < ~35°) (See Figure 2.4-2)
- Solar arrays in plane (AIP) for high solar βs (|β| > ~35°)

b) Comm determined that nose-down attitudes are marginal-to-good for communications coverage.

c) Initial ΔV and fuel consumption assessments by GN&C indicate potentially insufficient fuel for the 210 day outpost mission (which includes fuel for attitude maintenance). This fuel consumption assessment continues to be refined. Nevertheless, GN&C and Propulsion have concluded that there are not significant discriminators in fuel consumption between the various attitudes that were assessed. However, a potential issue was identified with the need for star tracker alignment maneuvers. If the star trackers (which are located on the CM) are aligned perpendicular to the surface of the CM, they cannot see the sky in a nose-down attitude. Therefore, they would require brief, periodic vehicle maneuvers so the trackers can see the target stars. The frequency that these maneuvers would be required has not been completely determined, but is currently estimated to be approximately once per day. During the outpost missions (up to 210 days in LLO) these regular attitude maneuvers would increase fuel consumption and could be fuel-prohibitive. This issue is alleviated if at least one star-tracker is oriented so that it points perpendicular to the X-axis of the vehicle. In this orientation, the star-trackers can see the sky even in the nose-down attitude, which makes this attitude acceptable for both GN&C and propulsion.

Color-coded, summary results for each subsystem assessed for the LLO CEV-alone flight attitude cases are shown below in Figure 2.4-3.

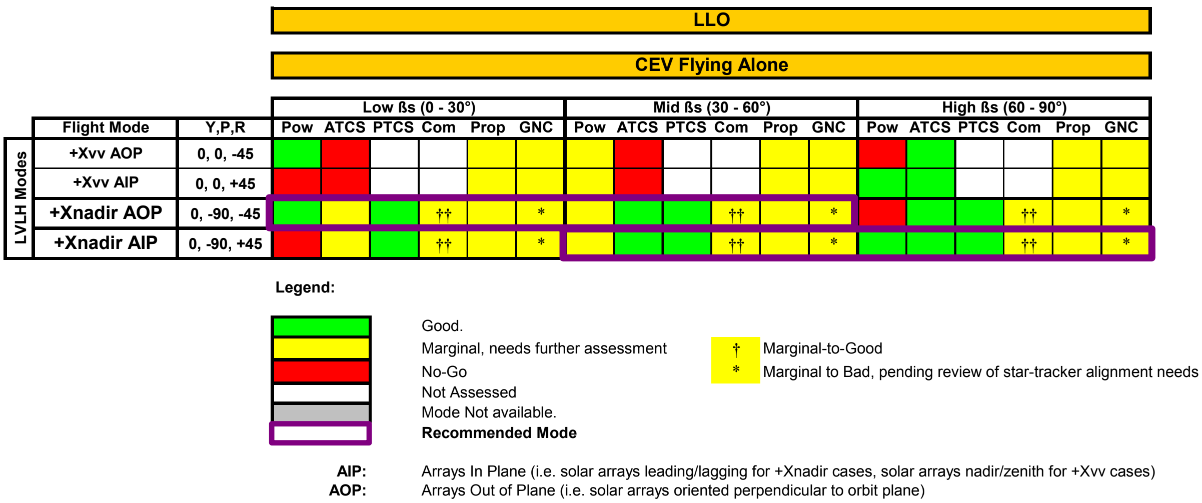

Figure 2.4-3 Flight Mode Assessment for LLO CEV - Alone Case

An example result for CEV power generation capability while mated to the LSAM in LLO is shown in Figure 2.4-4. These results indicate that the CEV can produce ~6.0 kWe in all cases assuming there are no EPS hardware failures. This capability increases to ~6.8 kWe if appropriate roll angles can be used at mid-βs (20° to 50°). The nose-down (+Xnadir) flight attitudes are better for power generation at low β values while the nose-forward flight attitudes (±Xvv) are better for power at high β values.

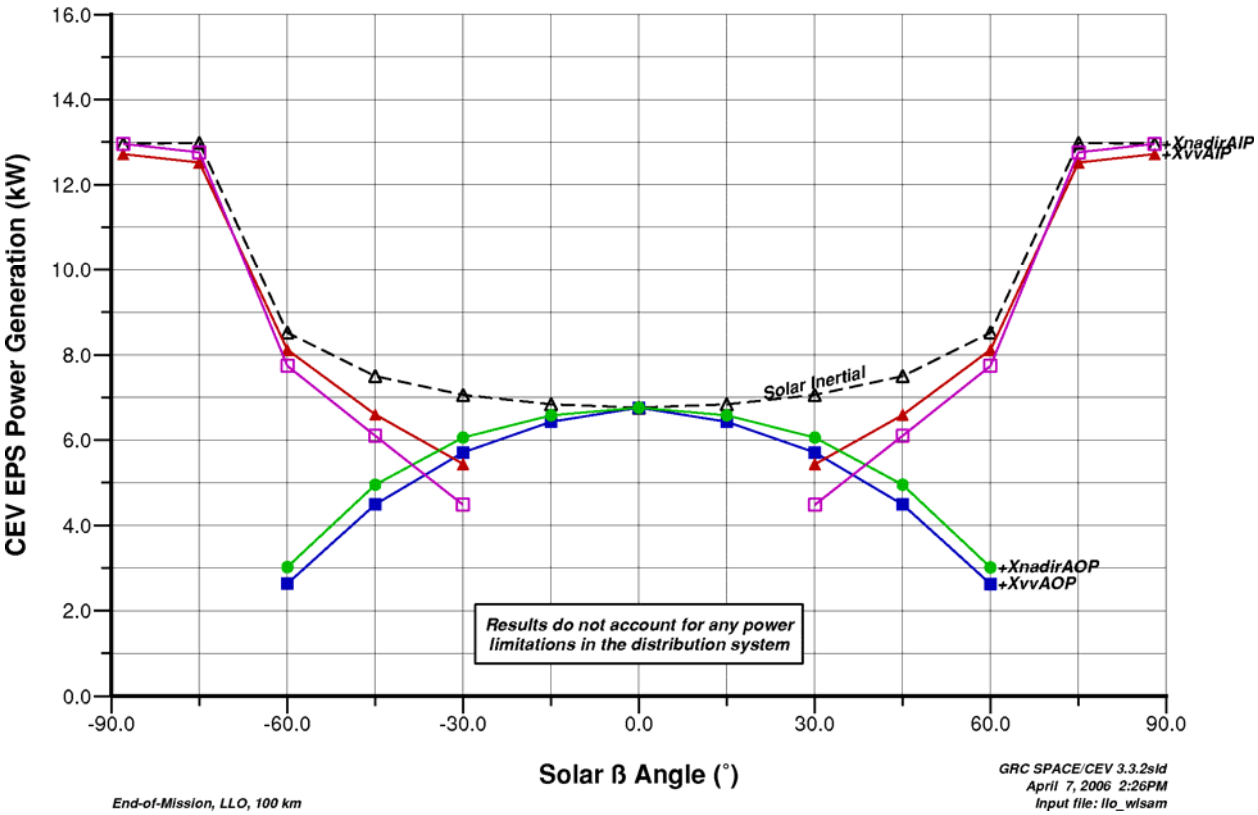

Figure 2.4-4 Power Generation Capability: CEV Mated to LSAM in LLO

2.4.3 Low Earth Orbit Results

As with LLO, no single attitude examined thus far has been demonstrated to be good for all systems across all solar β angles, but LEO is a much more benign environment for many of the CEV systems. Unlike LLO, Xvv attitudes (either nose or tail forward) seem to be the best attitudes found thus far:

a) Initial ΔV and fuel consumption assessments by GN&C indicate potentially insufficient fuel They are show to be good for both active and passive thermal, GN&C and propulsion

b) They are better for communications than the nose-down cases

c) They have been shown to be good for power in most cases, and like LLO, require two variants depending on the solar β angle:

- Solar Arrays Out of Plane (AOP) for low solar βs (|β| < ~45°)
- Solar Arrays In Plane (AIP) for high solar βs (|β| > ~45°)

d) There is still a shortfall of power at mid-βs (30° - 56°) when mated to LSAM/EDS. This is due to the need to supply an additional 1.5 kWe of power for transfer to LSAM. The CEV cannot supply that much power at those mid βs, unless an additional small vehicle roll is used. This additional roll, which places the solar arrays 45° out of plane, allows the power system to produce the necessary power for LSAM transfer.

Color-coded, summary results for each subsystem assessed for the LEO CEV-alone and CEV-mated to LSAM, flight attitude cases are shown below in Figure 2.4-5. Note that there are significantly more "green" cases, than for the LLO assessment.

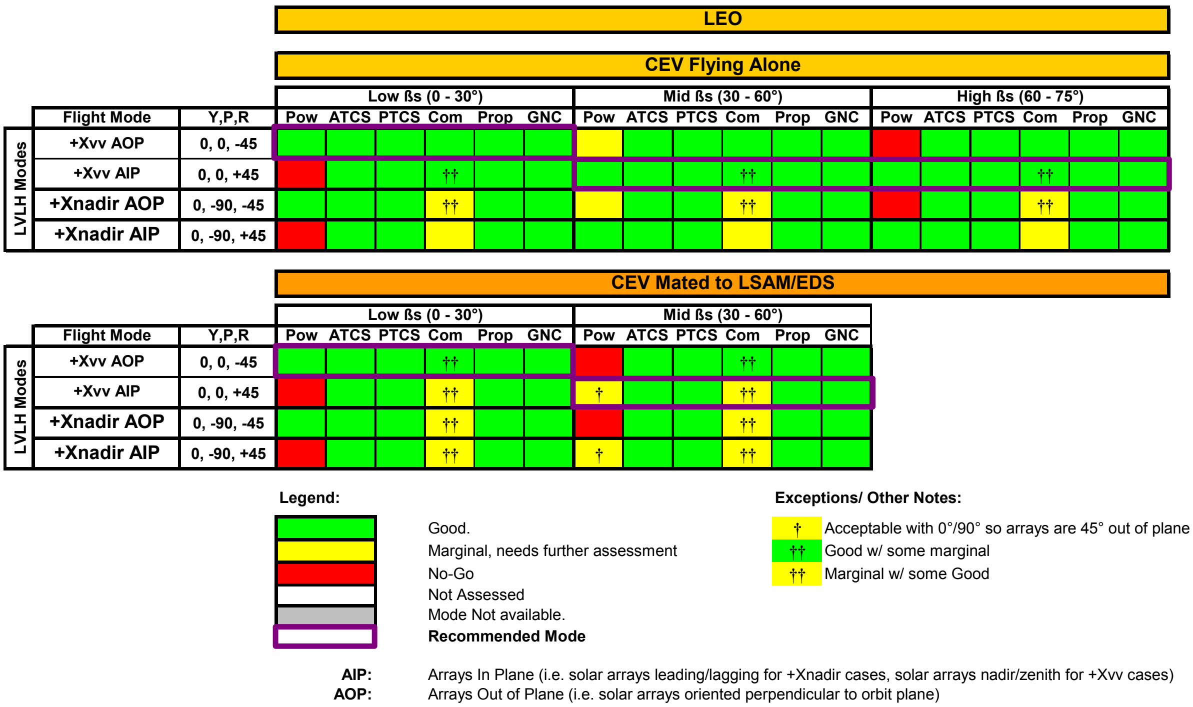

Figure 2.4-5 Flight Mode Assessment for LEO CEV - Alone Case & CEV Mated to LSAM

2.4.4 Proximity Operations

Although time was not available to do a thorough assessment of proximity operations across all subsystems, a quick assessment of the power generation during proximity operations with the ISS was performed. Power is expected to be one of the most sensitive systems to proximity operations, since constraints may limit solar array pointing for one or more hours during maneuvers.

The assessment used the ISS docking as a proxy for the various docking maneuvers that the CEV will need to perform (e.g. LSAM docking in LLO or LEO) and since preliminary prox ops timelines have been developed for the ISS docking. The current prox ops definition has a fairly detailed event timeline from Terminal Phase Initiation (TPI) to docking, for both Node 2 and Node 3 docking. However, it has not yet been determined whether there will be any need to feather (or lock) the CEV solar arrays at any point during the procedure.

So, in order to get a preliminary feel for robust the CEV power system would be to this scenario, the team assessed how long the CEV could sustain itself with no power generation at all from the solar arrays. This turns out to be approximately 2.1 hours at a 5 kW load demand. The current timeline shows the time from TPI to docking to be less than one orbital period (i.e., less than 90 minutes), and so the CEV should be able to complete that maneuver even with no power generation, which is an extremely conservative assumption. Therefore, it appears that there should not be any major issues with power generation during proximity operations.

2.4.5 ISS Mated Operations

One additional important CEV power generation capability result is shown below in Figure 2.4-6 and covers the cases of CEV mated with the ISS. When mated with ISS, the CEV will either be docked to the Node 2 forward (into the velocity vector) docking adaptor or the Node 3 nadir (Earth facing) docking adaptor. The ISS flight attitude will be Xvv+Znadir (in ISS coordinates). Results below indicate that in general, the Node 2 forward cases generate more power than Node 3 nadir cases, for all βs. This is due to less shadowing of CEV solar arrays at the Node 2 location. The CEV solar array 45° clocking case results in improved power generation at high βs but reduced power at some mid-βs. Power generation is estimated to be > 2 kWe for all solar βs while the 0° clocking approach results in < 2 kWe generation at the highest β cases (|β| > ~62°). For reference, the ISS spends approximately 30 days per year in that β range. Given the CEV docked power draw estimate of ~1.9 kWe and the ability to transfer ~1 kWe from ISS to the CEV, the CEV-ISS mated power system performance is acceptable based on the assumed CEV docked configuration and assuming CEV solar arrays are clocked 45°.

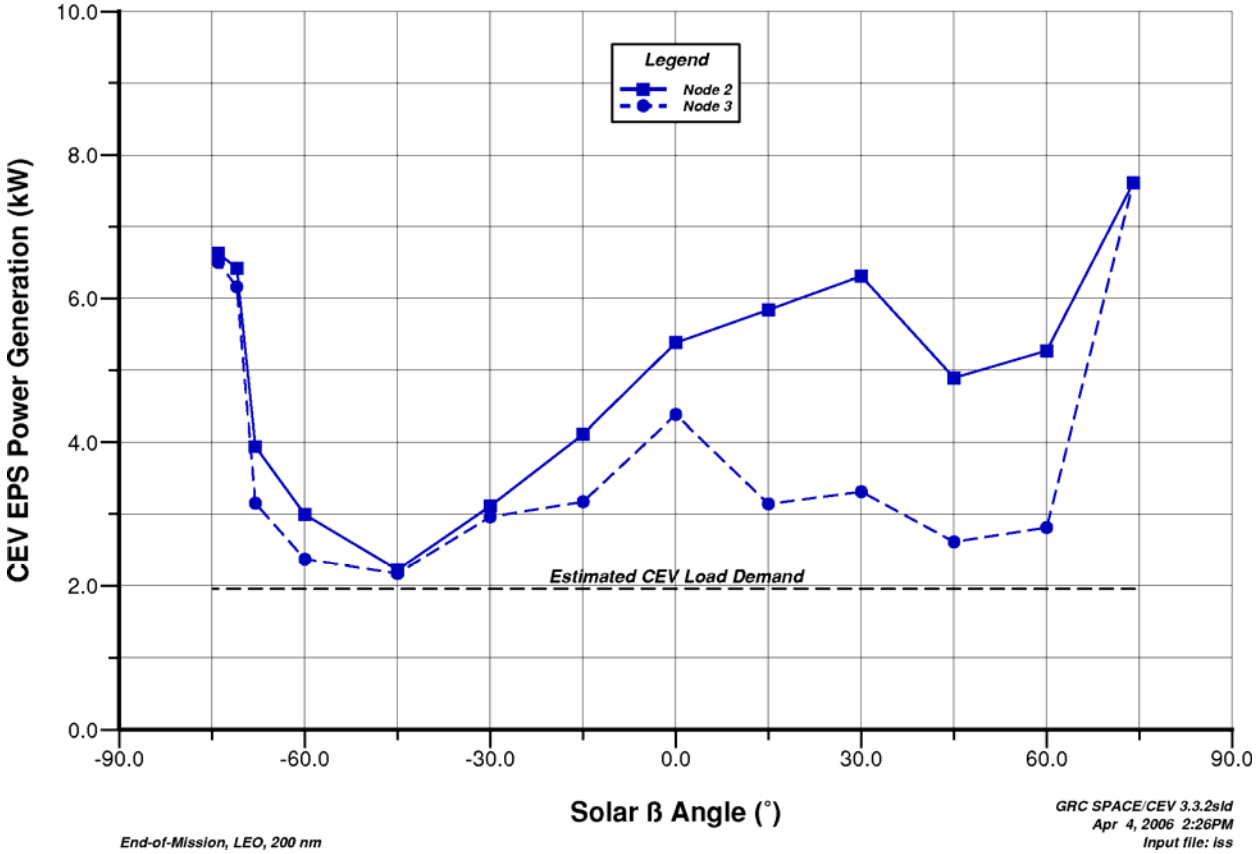

Figure 2.4-6 Power Generation Capability: CEV Mated to ISS

Forward Work for Integrated Flight Attitude Performance Analysis

The integrated flight attitude performance analysis team has identified forward work in many various areas including: 1) confirm that the star tracker placement is such that attitude maneuvers will not be required during LLO, 2) further examine rendezvous & proximity operations cases to include realistic array power scenarios, assessments of the performance of the other subsystems, and assessment of docking in LLO, 3) define time period of steady attitudes (orbital revolution, days, weeks) and determine number of attitude maneuvers required throughout mission. In addition to these team forward work items, each subsystem has specific forward work elements that should be addressed to enhance the fidelity of integrated flight attitude performance analysis results.

2.5 OML and Coordinate Systems

Figure 2.5-1 presents an outer mold line (OML) drawing of the mated CEV stack.

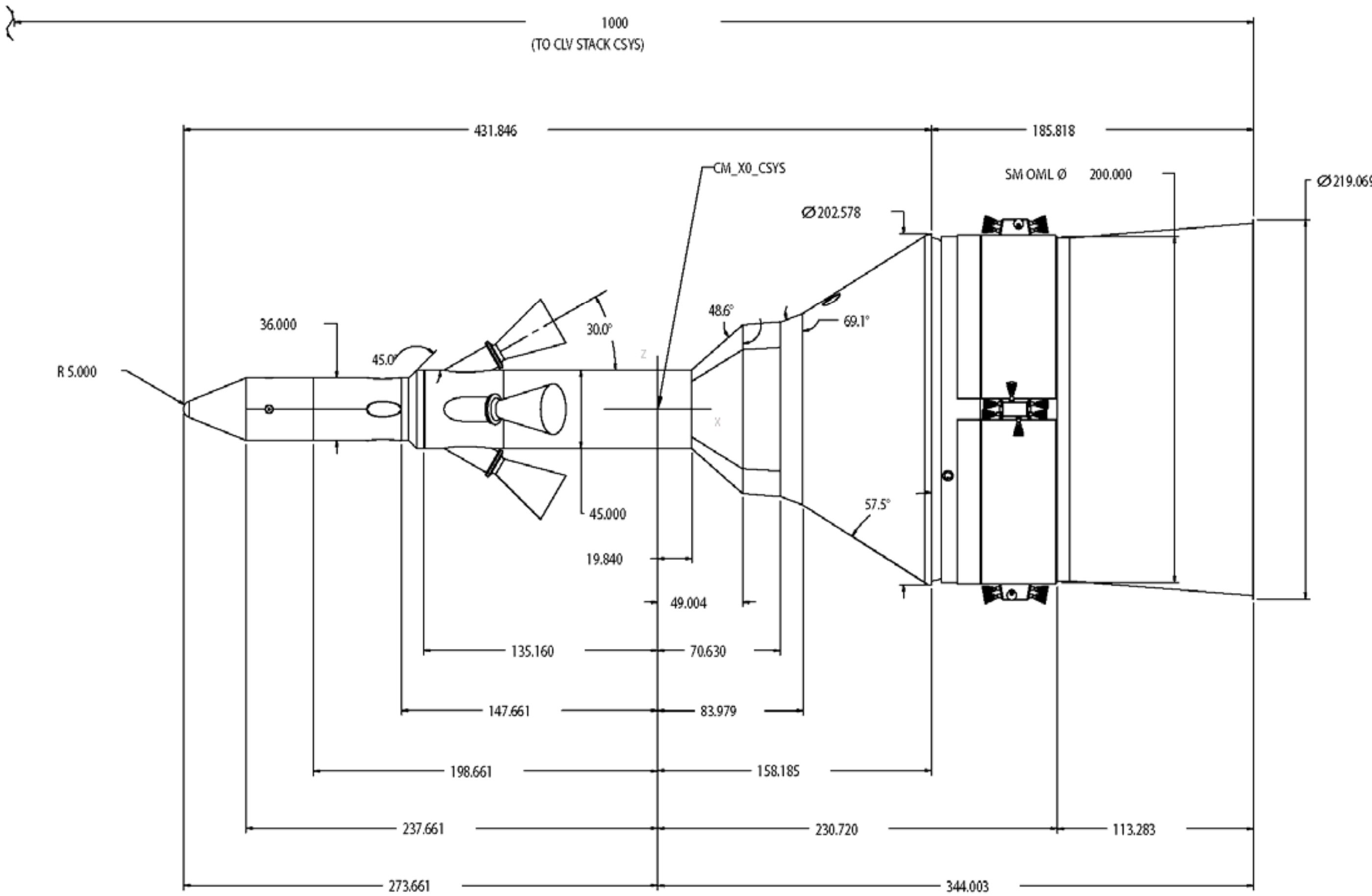

Figure 2.5-1 CEV Outer Mold Line

The CEV includes two structural coordinate systems – one for the CEV and one for the mated CEV-CLV stack. The CEV structural coordinate system has its origin at the theoretical apex of the Crew Module conical section. Its directionality is as follows:

- X-axis: The CEV structural X coordinate axis runs along the centerline of the cone, and is positive from the cone apex toward the heat shield. This orientation is dictated due to the use of heritage shuttle hardware as components of the CLV stack.
- Z-axis: The structural Z axis is defined positive running from the centerline in the feet to head direction for a seated crew member.
- Y-axis: Completes the right-handed system, resulting in the positive direction toward the crew's right as they are seated facing the cone apex.

The stack coordinate system has an origin 1000.0 inches (25.4 m) forward of the CEV/CLV interface plane with the same directionality as the CEV coordinate system.

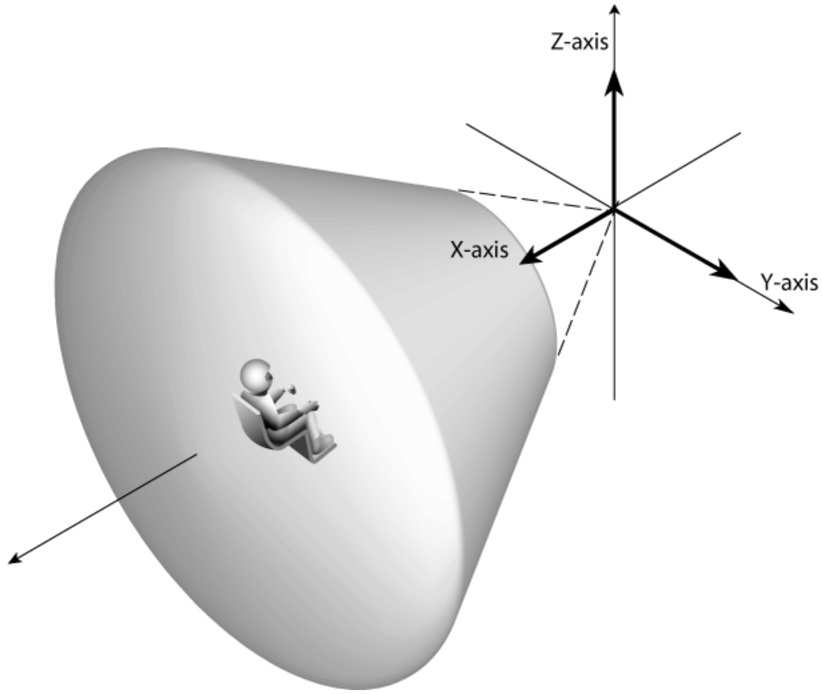

Figure 2.5-2 CEV Structural Coordinate System

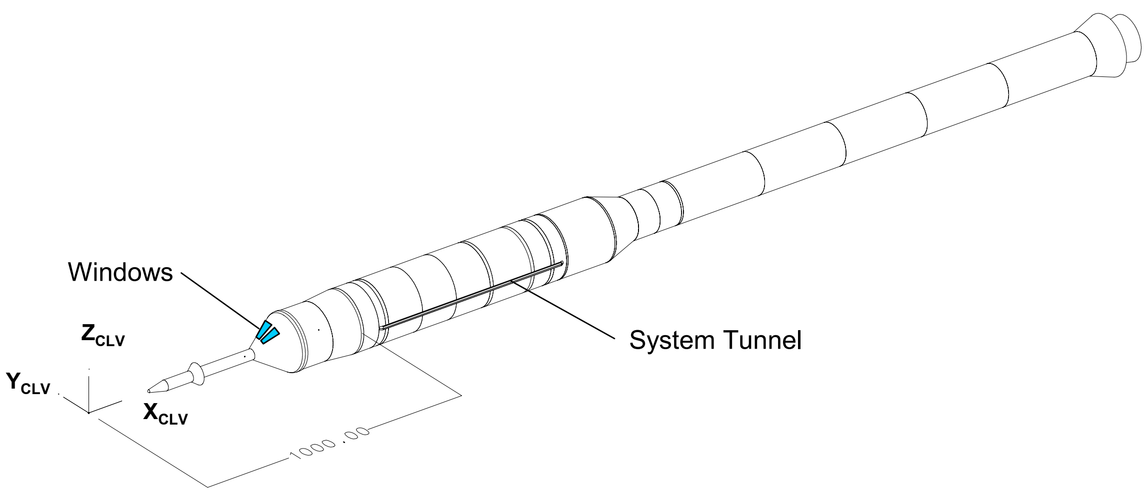

Figure 2.5-3 CLV/CEV Stack Structural Coordinate System

3.0 Launch Abort System Overview

The LAS provides safe mission abort from the launch pad prior to vehicle liftoff to after successful Upper Stage ignition. The LAS consists of the Launch Abort Tower (LAT) and the Boost Protective Cover (BPC). During a nominal mission, the LAS is jettisoned (jettison motor fires) approximately 30 seconds after Upper Stage ignition. For an abort case, the LAS pulls the Crew Module (CM) from the Crew Launch Vehicle (CLV) at the Service Module (SM) interface (abort motor fires and attitude control is activated providing guidance). The free-flying vehicle consisting of the LAS and the CM is the Launch Abort Vehicle (LAV). An Apollo-style diagram illustrating the functionality of the LAS is shown in Figure 3.0-1.

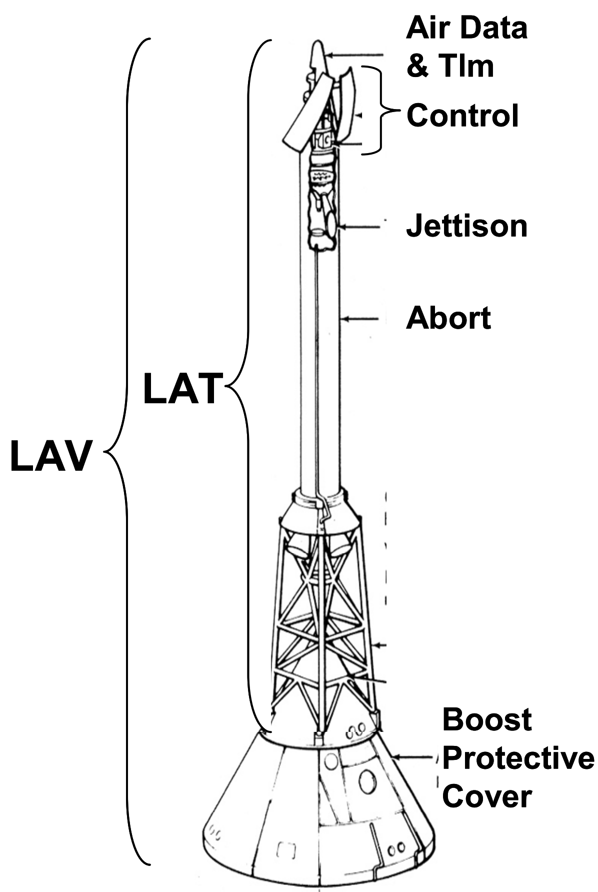

Figure 3.0-1 LAS Functionality Diagram

The sequence of events for an abort is shown in Figure 3.0-2.

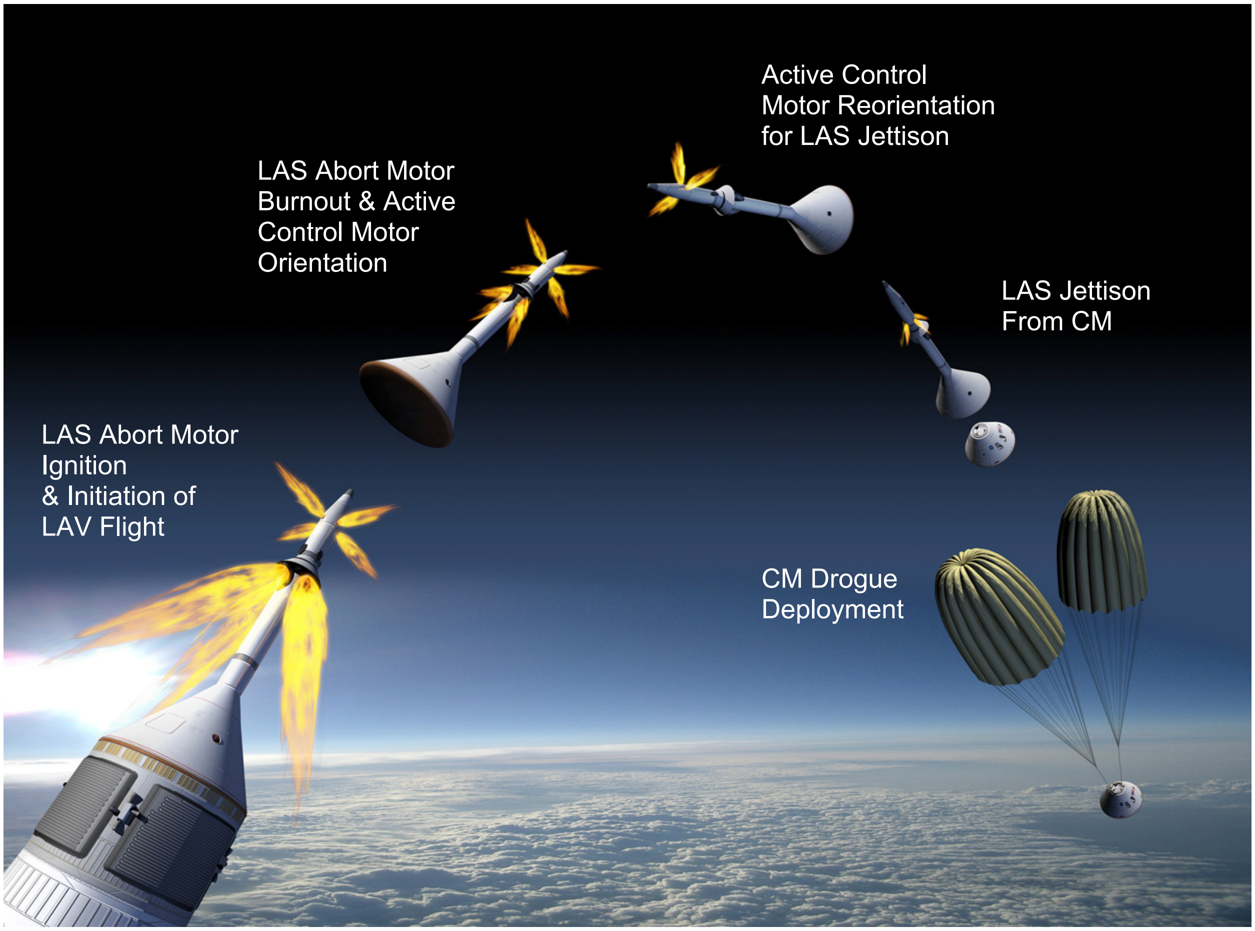

Figure 3.0-2 Abort Sequence of Events

For the CRC-3 design, the LAV control function is accomplished by an attitude control motor (see section 3.2) instead of canards as shown in the Figure 3.0-1. In addition, the abort motor employs a reverse flow nozzle configuration. This configuration provides sufficient stand-off distance between the abort motor nozzles and the CM surface and takes the place of the truss structure utilized in the Apollo-style system to reduce plume impingement effects on the CM (see section 3.1). The CRC-3 design is shown (and compared to Apollo LES) in Figure 3.0-3.

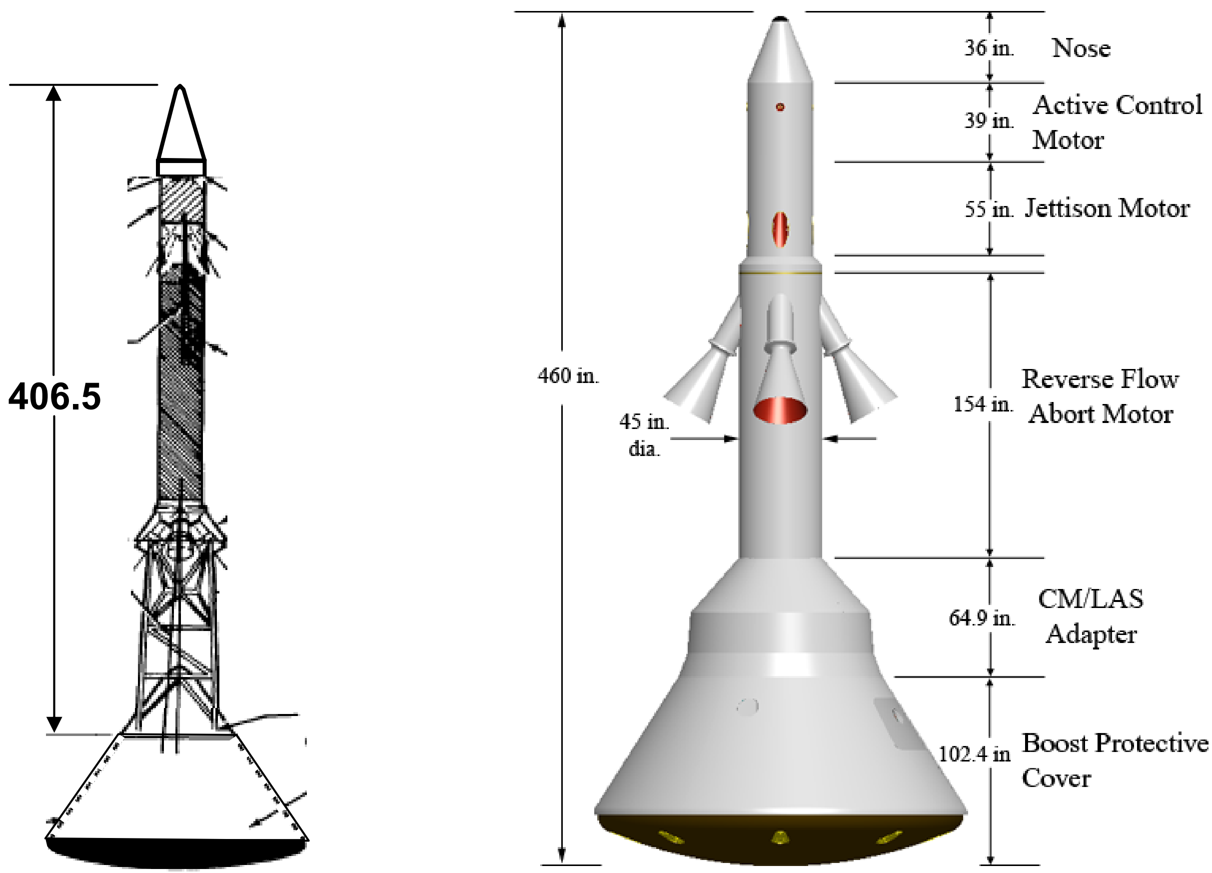

Figure 3.0-3 CRC-3 LAS Design Overview

3.1 Driving Requirements, Groundrules, and Assumptions

The following is a compendium of the System Requirements Document (SRD) requirements and the derived requirements that drive the design of the LAS.

3.1.1 Interface Requirements

[CEV/CLV IRD 3.3.4] Stiffness for Controllability - The CEV shall provide minimum cantilevered natural frequencies of 5 Hz (TBR) laterally and 25 Hz (TBR) axially.

[CEV/CLV IRD 3.5.3.5.2] CEV Lightning Protection - The CEV shall be designed and fabricated so that, when mated with the CLV, the mated configuration does not reduce nor compromise protection against damage from the direct and indirect effects of lightning in accordance with CXP-00102, Constellation Program Design Specification for Natural Environments (DSNE).

[ISS-CEV IRD 3.2.3.1.1 /CV0602] Docking Interfaces - The CEV shall dock with the ISS at PMA-2 (Node 2 Forward port) and PMA-3 (Node 3 Nadir port) via an ISS Androgynous Peripheral Assembly System (APAS).

3.1.2 SRD Requirements

[CV0042] Launch Abort System Sizing – The CEV Launch Abort System shall provide a thrust of not less than 15 (TBR-002-12) times the combined weight of the CM + LAS for a duration of 2 (TBR-002-149) seconds. (Affects LAS abort motor sizing)

[CV0043] Blast Overpressure – The CEV shall withstand a maximum blast overpressure of 20 psid (TBR-002-150) over ambient conditions for crew survival. (Affects LAS structural design and structural interface to CM)

[CV0058] Abort Initiation Latency - The CEV shall provide a latency of less than 300 milliseconds (TBR-002-013) from abort command initiation receipt until abort engine start. (Affects LAS abort motor sizing)

[CV0052] CEV Ascent Abort Maneuvers – The CEV shall provide automated maneuvers to depart from the launch vehicle and to target abort landing locations. (Affects LAS abort design aspects for the ascent abort phase, including LAS avionics)

[CV0188] CEV Mass Limit for Lunar Mission - The CEV shall have an effective payload mass no greater than 50,785 lb (23,036 kg) (TBR-002-029) where the effective payload mass includes the mass of the Crew Module, Service Module, Spacecraft Adapter, and 1/6 of the Launch Abort System.

[CV0194] CEV Ascent and Pad Abort Reliability Allocation – The CEV shall provide a risk of loss of crew during a pad or ascent abort no greater than 1 in 10 (TBR-002-145). (Affects LAS ascent and pad abort phases)

[CV0207] General Natural Environments Data Specification - Be able to withstand collision with an avian species with a maximum mass of 4.9 lb (2.2 kg) up to a maximum altitude of 3.5km. CLV trajectory conditions: Relative velocity @ ~3.5km is ~800 fps

[CV0219] Launch Environments – Flora and Fauna – The CEV shall meet its functional and performance requirements during and after exposure to launch phase flora and fauna hazards as defined in the CXP-00102, Constellation Program Design Specification for Natural Environments (DSNE), section 3.2.11.

[CV0315] LIDS Interface - The CEV shall interface with the LIDS mating mechanism in accordance with the CXP-01008 Low Impact Docking System (LIDS) to Element Interface Definition Document (IDD).

3.1.3 Derived Requirements

Separation Distance Achieved – LAS shall achieve at least 350 feet separation distance from CLV during an ascent abort within 3 seconds of LAS ignition (TBR). (Affects LAS abort motor sizing. This defines the level of thrust necessary to ensure a safe and adequate ascent abort. (Originated with the Apollo Program)) SRD Par. 3.2.2.3.3.2

Separation Distance Maintained – LAS shall maintain at least 350 feet separation distance from CLV during an ascent abort after 3 seconds of LAS ignition (TBR). (Affects LAS motor sizing. This defines the level of thrust necessary to ensure a safe and adequate ascent abort. (Originated with the Apollo Program)) SRD Par. 3.2.2.3.3.2

Abort Thrust Level – LAS shall be at 90% of full thrust within 0.3 seconds of receiving an abort command. (Affects LAS abort motor sizing and amount of latency allowed once an abort command has been received.) SRD Par. 3.2.2.3.1.8

Downrange Distance – LAS shall provide pad abort capability to reach a downrange distance of (3,500 to 6,000) feet (TBR) to ensure water depth of at least 10 feet at low tide. (Affects LAS abort motor sizing and trajectory specifications) SRD Par. 3.2.2.3.3.2.1

Parachute Deployable Attitude/Altitude – LAS shall provide pad abort capability to reach an altitude of at least (4,000 to 5,200) feet (TBR) to place the CM into a parachute deployable altitude and configuration. (Affects LAS abort motor sizing and trajectory specifications) SRD Par. 3.2.2.3.3.2.1

LAS Jettison Motor Thrust – LAS shall be jettisoned under normal launch conditions at 300,000 feet or no greater than 1.5 g CLV acceleration during 2nd Stage CLV burn. (This drives the jettison motor sizing, which could impact weight allocations.) The LAS shall maintain positive clearances between the LAS and CM after LAS jettison, except for those features that are designed for contact, such as bumpers and abrasion pads. SRD Par. TBD

LAS Attitude Control Motor Thrust – LAS shall position the LAV to the CM command orientation prior to LAS abort jettison. (Drives LAV attitude control and control motor sizing) SRD Par. 3.2.2.3.3.2.1

LAS Jettison Motor Failure – The LAS shall be able to use the abort engine for jettison for normal profile jettison failures. SRD Par. TBD

LAS Structural Loads – In addition to the normal launch and ascent loads (SRD Par. 3.3.1.6), other loads must be assessed to ensure worst case loads have been included in the structural analysis such as pad abort loads, blast overpressure loads and ascent abort loads. SRD Par. TBD

System Safety Review Process of LAS Design to Demonstrate Compliance with all Applicable NASA Safety Requirements for Spacecraft – The NASA Phased Safety Review process is performed in parallel with the design, development, testing, and verification of the LAS, and can result in design changes to critical hardware late in the development flow. The implication here is for close coordination with the panel early in the design phase. SRD Par. TBD

3.2 LAS Subsystem Design

The Launch Abort System (LAS) contains three solid rocket motors: the abort motor, the active control motor, and the jettison motor. None of the LAS motors has thrust vector control, nor does the LAS provide roll control. Roll control for all phases of LAV flight is provided by the Crew Module.

The abort motor is the largest of the three motors. It provides thrust to pull the Launch Abort Vehicle away from the Ares-I stack whenever an abort is necessary. This may be any time during the launch trajectory – from a pad abort at sea level, through a mid-flight max Q abort, to a high-altitude abort in the case of a failed second stage ignition.

The active control motor provides control authority for pitch and yaw during all phases of LAV flight. Its four nozzles point outward from the centerline of the LAV to provide directional control to the LAV. Each nozzle contains its own actuated pintle assembly to independently set its thrust level. The summed area of the four nozzles sets the total thrust output of the active control motor.

The jettison motor separates the LAS from the Crew Module and is used in both nominal and aborted flight. On a nominal flight, the LAS is jettisoned approximately 30 seconds after ignition of the second stage of the CLV after which the Service Module provides thrust for aborts.

Both the abort motor and the jettison motor produce net axial thrust using sets of canted nozzles. This can produce confusion when discussing motor performance since it is not always clear from context whether the parameter has or has not had cosine losses subtracted. For this reason, two prefixes are applied to propulsion properties to indicate whether or not the cosine losses have been applied. Axial properties are those that have had cosine losses applied and absolute properties have not. Typically, specific impulse is reported as absolute, but both axial and absolute thrust levels are discussed. It is highly recommended that subsequent documentation adopt this or some other clear distinction between effective and absolute values.

3.2.1 Abort Motor

The abort motor is shown in Figure 3.2-1. By requirement, abort motor impulse is set to provide an axial thrust to weight ratio of fifteen to the LAV for 2 seconds. The abort motor consists of a composite motor case capped by a titanium upper manifold and a titanium bottom dome and a steel skirt to interface with the structural adapter below it. The manifold feeds four titanium nozzles canted 30 degrees from the vehicle centerline to direct the abort motor plume around the Crew Module. The motor has a “reverse flow nozzle” configuration in that the flow is turned 150 degrees before exiting the motor. Reverse flow nozzle losses are estimated to be about 2% of the overall Isp based on subscale flow testing. This design has the igniter at the bottom and the nozzles on the top of the abort motor to provide additional standoff distance between the nozzles and the Crew Module. In comparison, the Apollo Launch Escape System (LES) used a lower truss to distance its abort motor nozzles from the Command Module. The reverse flow configuration stiffens the overall LAS and reduces mass by eliminating the tower structure below the abort motor.

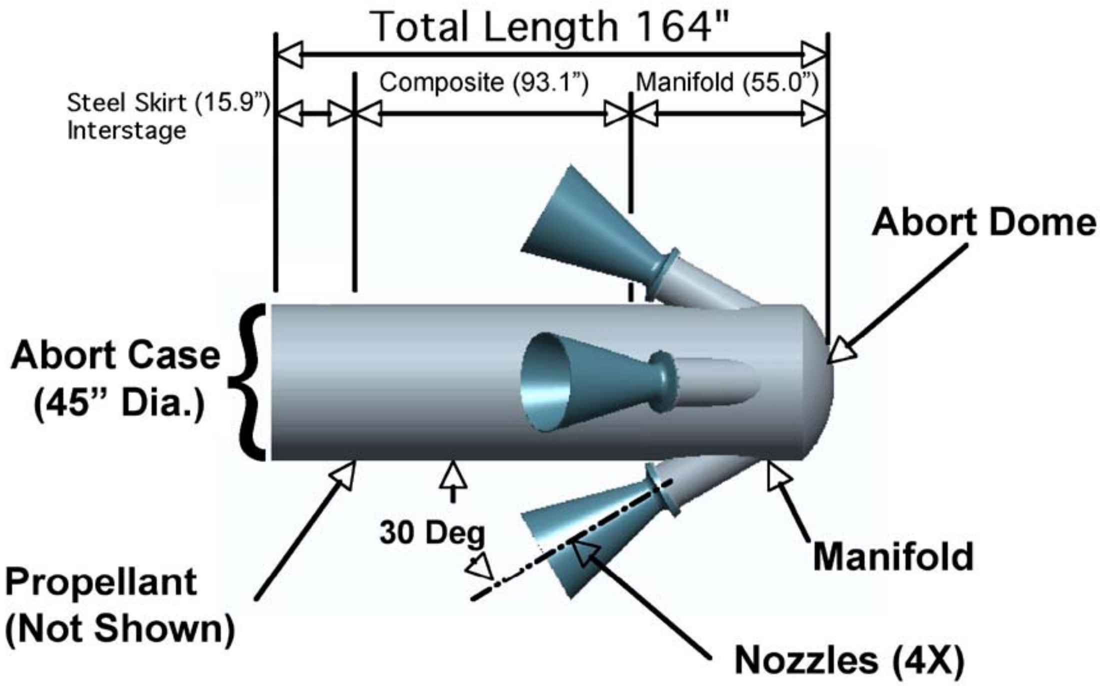

Figure 3.2-1 Abort Motor

The abort motor uses a low aluminum content (~2 %) propellant similar to that used in the Shuttle Booster Separation Motor (BSM) with a burn rate of 0.95 inches per second at 1000 psi. By design, minimum thrust is produced by a cold motor (30 °F) at sea level. An average absolute specific impulse of 237 seconds over its web time (2.12 seconds) is assumed. Web time is the time it takes for the motor to consume the web section of its propellant grain. Each of the four nozzles has an expansion ratio of about 9.3:1 and the average chamber pressure is 1460 psia. The motor provides approximately 80% of its impulse in the first 2 seconds with the remaining 20% produced during tail off. The current estimate for the abort motor propellant mass is 5609 lbm, and the total abort motor mass is 8389 lbm, resulting in a propellant mass fraction of about 0.67. Abort motor performance data are summarized in Table 3.2-1 below. Material properties are summarized in Table 3.2-2 below.

Nozzle Cant Angle	30 degrees
Web Time	2.12 seconds
Average Chamber Pressure, Pc	1460 psia
Average Thrust @ Web Time (axial)	443,000 lbf
Propellant Burn Rate	0.950 in./sec. @ 1000 psi
Isp, absolute	237.0 seconds
Propellant Mass	5,609 lbm
Motor Inert Mass	2780 lbm

Table 3.2-1 Abort Motor Performance Summary

Component	**Material**	**Density (lbm/in^3)**	**Weight (lb) EA.**	**QTY:**
Manifold	Ti	.164	738	1
Abort Dome	Ti	.164	238	1
Abort Case	Composite	.057	1408	1
Nozzles	Ti	.164	99	4
Propellant	TP-H1262 (2% Al content, HTPB / AP)	.065	5609	1

Table 3.2-2 Abort Motor Material Summary

The center of mass of the CM is about one foot off from its centerline in order to produce aerodynamic lift on re-entry. This also means that the center of mass of the LAV is off from its centerline and that it moves outward as the Abort motor burns off. The net thrust vector of the Abort motor is aligned slightly off the centerline through the loaded LAV's center of mass. This reduces the pitch produced by the interaction of the static thrust vector and the moving center of mass.

Figures 3.2-2 and 3.2-3 show abort motor thrust and LAV acceleration as a function of time. The three curves on each graph represent cold, nominal, and hot motor performance. The thrust is tailored to compensate for decreased LAV mass as propellant burns resulting in a flat acceleration profile over the first two seconds or the web time of the motor.

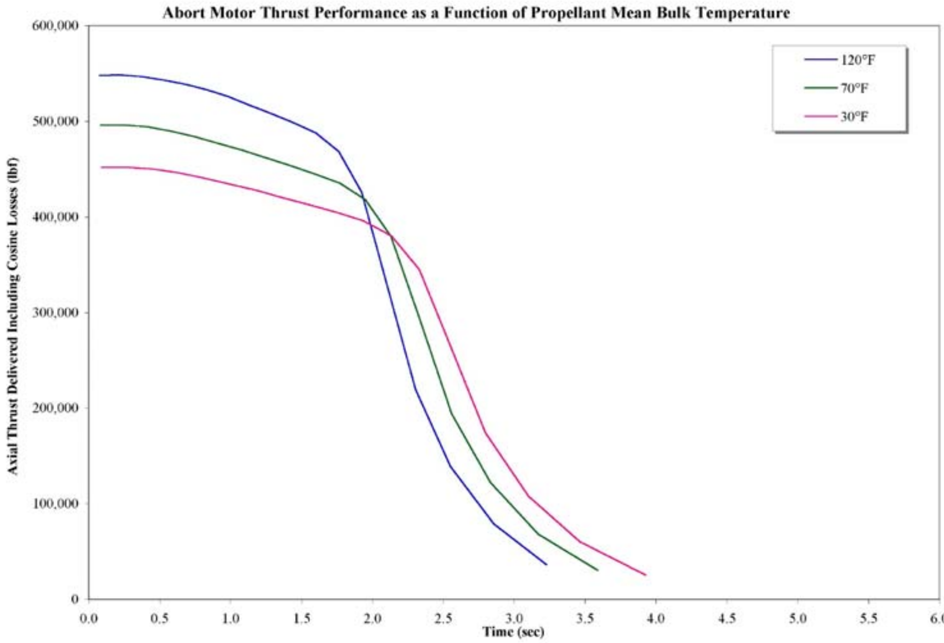

Figure 3.2-2 Launch Abort Motor Axial Thrust as a Function of Temperature

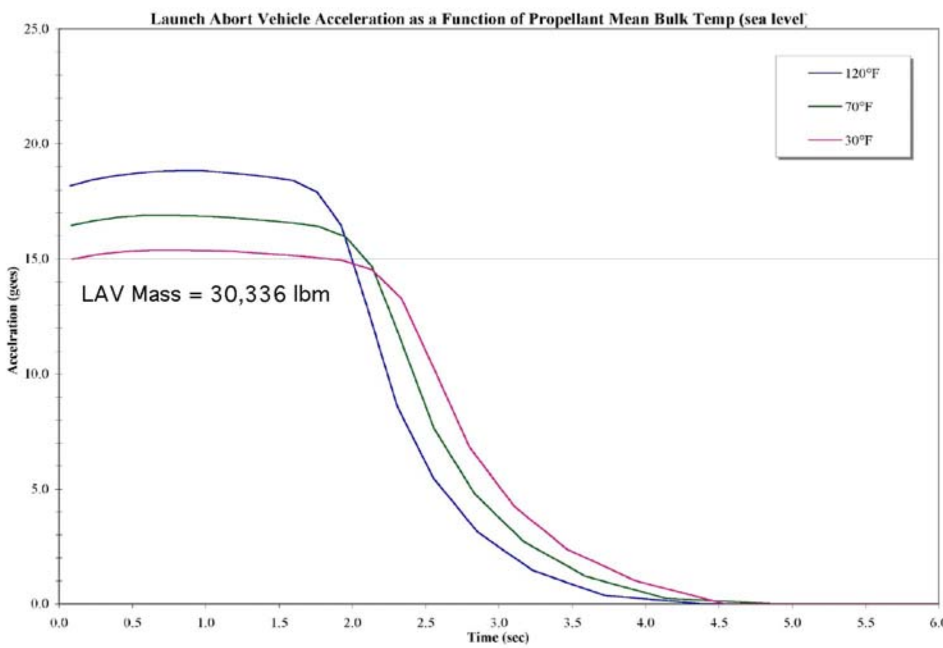

Figure 3.2-3 Launch Abort Vehicle Acceleration as a Function of Temperature

3.2.2 Active Control Motor

The active control motor provides three functions during a launch abort sequence. First, the active control motor provides pitch thrust during abort motor firing (2 seconds) to rotate the LAV's direction of travel away from the path of the CLV. This is particularly important during a pad abort where downrange and altitude requirements are to be met. Second, the ACM provides attitude adjustments during the coast phase of the abort (about 20 seconds) to maintain angle of attack and overall stability of the vehicle. Lastly, the active control motor provides pitching moment for about 10 seconds to "flip" the LAV such that the heat shield of the CM is down and the parachutes can deploy out of the top of the CM. The LAS is then jettisoned from the CM. Estimates of the thrust required during these phases are 4800 lbf for initial pitch, 500 lbf for coast, and 1500 lbf for reorientation. The active control motor is shown in Figure 3.2-4.

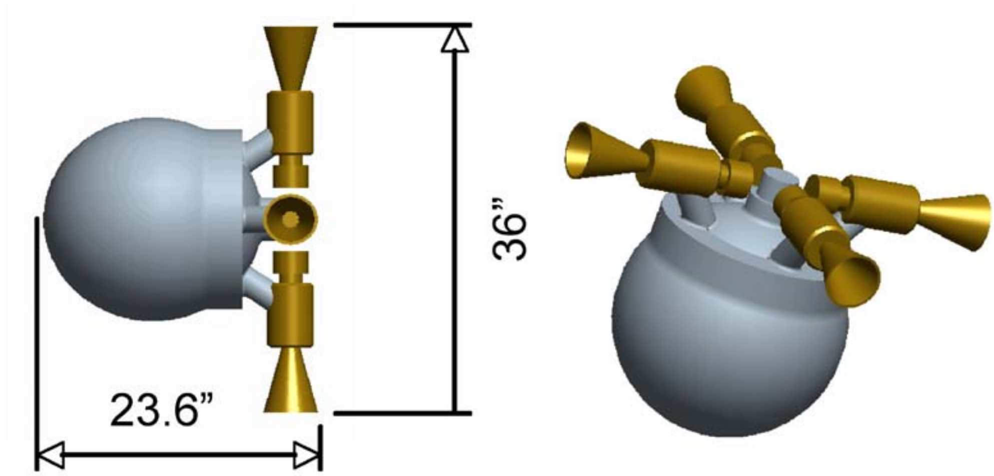

Figure 3.2-4 Active Control Motor

Nominal Burn Time	30 seconds
Average Chamber Pressure, Pc	Variable
Avg. Thrust @ Burn Time	Minimum 6000 lbf in a given lateral direction
Propellant Burn Rate	0.50 in./sec. @ 1000 psi
Isp	247.0 seconds
Propellant Mass	500 lbm
Motor Inert Mass including Structural Skin	335 lbm

Table 3.2-3 Active Control Motor Performance Summary

Component	**Material**	**Density (lbm/in³)**	**Mass ea. (lbm)**	**QTY:**
Case	Ti	.164	31.3	1
Cap	Ti	.164	24.94	1
Propellant	Current production propellant containing no aluminum	.1854	500	1
Liner Case	Insulation densities based industry standard materials	.05	.88	1
Insulation Case	Insulation densities based on industry standard materials	.05	3.45	1
Liner Cap	Insulation densities based on industry standard materials	.05	.2	1
Insulation Cap	Insulation densities based on industry standard materials	.05	1.53	1
Pintle Valve	A-286 STEEL ALY	.283	28.34	4
Igniter	A-286 STEEL ALY	.283	7.48	1
Structural Skin	AL 2195	.098	151.5	1

Table 3.2-4 Active Control Motor Material Summary

3.2.3 Jettison Motor

The jettison motor is shown in Figure 3.2-5. It is designed to separate the LAS from the CM during either a nominal ascent or a launch abort. For both scenarios, the boost protective cover (BPC) is part of the LAS. This thrust is generated by a solid rocket motor consisting of a titanium motor case and four steel scarfed nozzles that have been canted 30 degrees from the vehicle centerline. Scarfing the nozzles provides less drag and reduces the potential for negative interactions between jettison and abort motor nozzles.

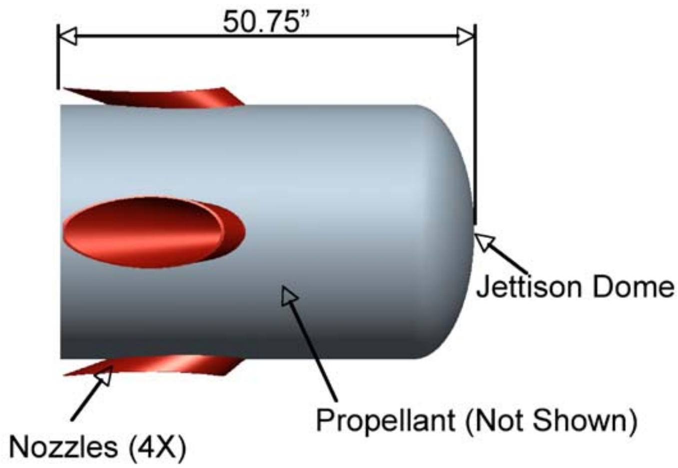

Figure 3.2-5 Jettison Motor

The jettison motor produces 30,000 lbf axial thrust after cosine losses are applied. It provides the loaded LAS a thrust to weight of 2.4 for 1 second on a nominal launch jettison. Some thrust tail off is also present as shown in Figure 3.2-6. This axial thrust is offset eight degrees from the LAS centerline to pitch the jettisoned LAS away from the flight path of the CLV. This thrust off-set leaves the LAS with a 120 degree/second pitch rate after jettison.

The time between second stage ignition and LAS jettison is long enough to verify proper ignition and operation of the second stage engine. From a mission perspective, one would want to jettison the LAS as soon as possible in order to reduce accelerated vehicle weight. Clearly, there is a trade between earlier LAS jettison to improve payload to orbit, and later LAS jettison to provide longer LAS abort coverage. This trade is handled elsewhere in the Constellation Program and was not determined by the LAS team.

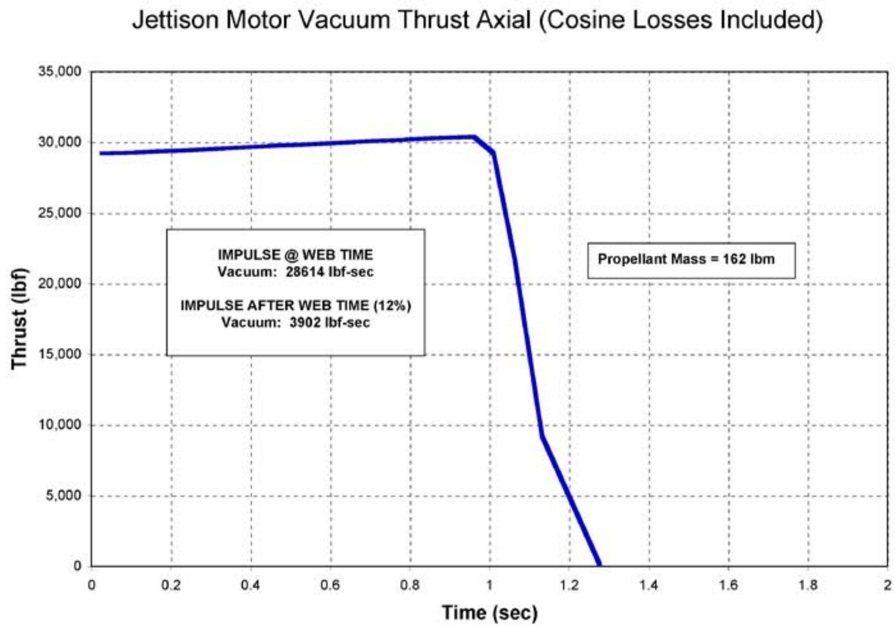

Figure 3.2-6 Jettison Motor Thrust at Vacuum

The jettison motor uses a low aluminum content (~2 %) solid propellant similar to that of the Shuttle Booster Separation Motor (BSM). The motor has an average specific impulse of 231.6 seconds over its entire burn time as calculated by dividing total impulse (37526 lbf-sec) by propellant weight (162 lbf). Since the nozzles are canted at 30 degrees, cosine losses reduce the effective impulse to 32516 lbf-sec, for an axial specific impulse of 200.6 seconds. The jettison motor provides approximately 88% of its total impulse during main stage and another 12% during tail off. This assumes operation of the jettison motor at vacuum with a 30 °F propellant mean bulk temperature (PMBT). A summary of the jettison motor propulsion characteristics is presented in Table 3.2-5.

Nozzle Cant Angle	30 degrees
Web Time	1.01 seconds
Average Chamber Pressure, Pc	1214 psia
Average Thrust @ Web Time w/ cosine losses	29,766 lbf
Thrust offset angle	8 degrees
Propellant Burn Rate	0.950 in./sec. @ 1000 psi
Isp, Absolute	231.0 seconds
Propellant Mass	162 lbm
Motor Inert Mass including Structural Skin	710 lbm

Table 3.2-5 Jettison Motor Performance Summary

Based on the current design parameters, the estimated jettison motor propellant mass is 162 lbm, and the total jettison motor mass is 710 lbm, including its aeroshell.

Component	**Material**	**Density (lbm/in^3)**	**Mass EA. (lbm)**	**QTY:**
Jettison Dome	Ti	.164	170	1
Nozzles	A-286 STEEL ALY	.283	40.20	4
Propellant	TP-H1262 (2% Al content, HTPB)	.065	162	1
Structural Skin	AL 2195	.098	217	1

Table 3.2-6 Jettison Motor Material Summary

Vehicle dynamics analyses were performed to validate the design of the jettison motor. An Excel based time marching flyout model was used to run trade studies on motor thrust, burn time, and thrust offset angle. The model tracked CLV and LAS position as well as LAS pitch angle and thrust. The CLV accelerated in the X direction and the jettisoned LAS traveled in both X and Y directions. The model updated the positions of the two vehicles, the angle of the LAS, and the X and Y thrust vectors of the LAS. Aerodynamics is not included since the normal LAS jettison takes place in vacuum conditions. The mass of the LAS is assumed constant as is the JM thrust level. JM burn time is extended slightly to account for thrust tail off, but total motor impulse is matched. Table 3.2-7 shows some of the jettison model parameters for easy reference.

CLV acceleration	0.85 g
LAS Mass	12329 lbm
LAS CG	18.69 ft
LAS MMI	653454 lbm-ft^2
Jettison Motor Location	9.17 ft
Jettison Motor Thrust	29445 lbf
Jettison Motor Offset Angle	8 degrees
Jettison Motor Axial Thrust Component	29158 lbf
Jettison Motor Lateral Thrust Component	4098 lbf
Angular Acceleration During Thrust	112 degrees / $second^2$
Angular Velocity at JM burn out	121 degrees / second
Time Step	0.02 seconds

Table 3.2-7 LAS Jettison Model Parameter Summary

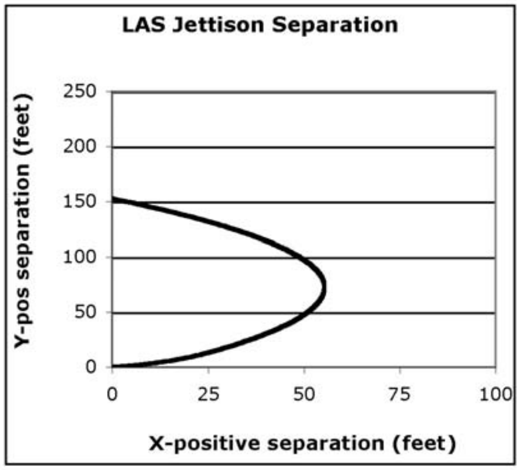

Figure 3.2-7 LAS Jettison Separation Dynamics

Figure 3.2-7 shows the lateral separation distance during a nominal LAS jettison. Separation distance can be read as the intersection of the curve with the Y-axis (150 feet). At time zero, the two vehicles are at the origin of graph. As the LAS lifts from the CLV, the X-distance between the two vehicles increases to the right, as does the Y-distance as the LAS is translated out of the CLV's flight path. The jettison motor rotates the LAS and as time progresses, the thrust is more lateral.

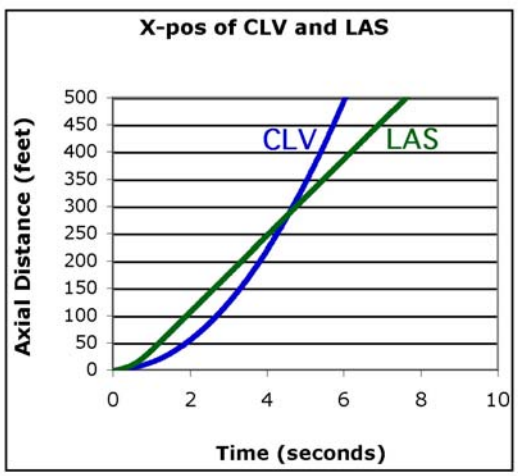

Figure 3.2-8 Axial Distance Traveled by CLV and LAS Post Jettison

Figure 3.2-8 shows the distance both vehicles have traveled post LAS jettison. When the lines cross (at about 4.6 seconds), both vehicles are at the same "altitude" so to speak, but the LAS is 150 feet to the side of the CLV. Optimizing separation distance involves jettison motor thrust, burn time, and offset angle. For a given jettison motor, varying offset angle produces very different separation dynamics. The following figure (3.2-9) shows LAS jettison dynamics for offset angles 4, 6, 8, 10, 12, and 14 degrees respectively.

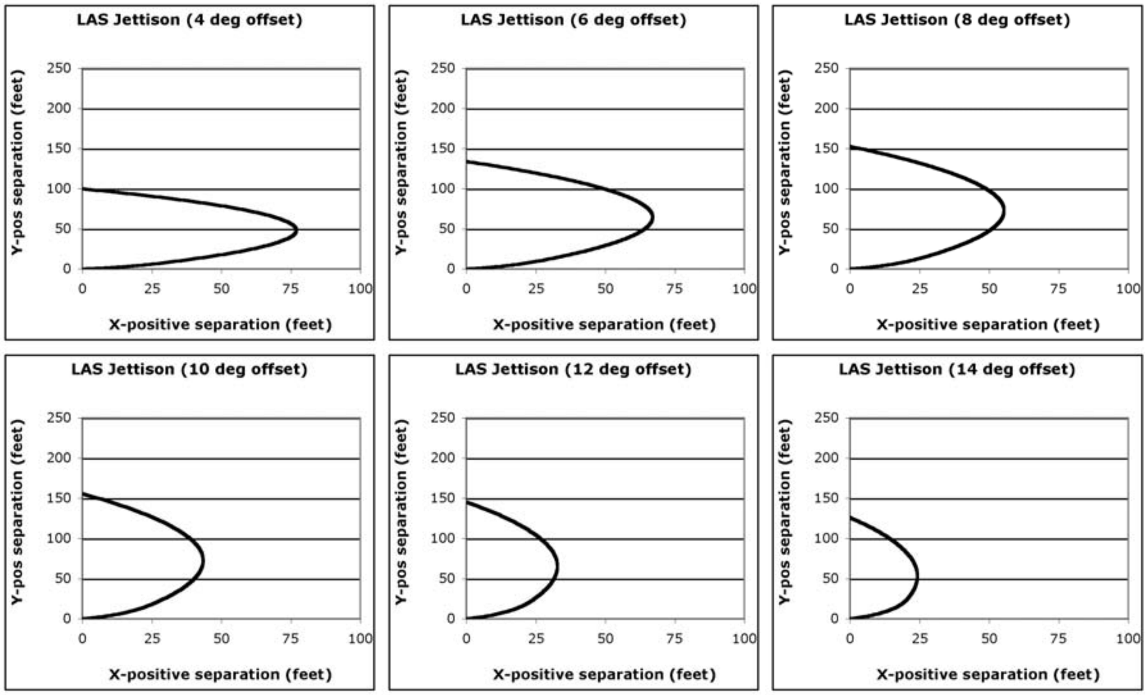

Figure 3.2-9 Effect of Offset Angle on LAS Jettison Separation

Looking at the series of separation graphs shows some expected trends. At low offset angles, the jettison motor thrust propels the LAS to high X-distances ("altitudes"), but does not translate the LAS adequately. More thrust can be placed in the Y-direction by increasing offset angle. Separation clearances were not investigated in this study, but are certainly affected by the offset angle – higher thrust offset angles being of more concern. For this reason, the lowest offset angle that produced a high LAS separation was selected (8 degrees). Propellant mean bulk temperature (PMBT) might also affect jettison separation. To investigate effects of jettison motor temperature, burn time was varied by +/- 20% while holding motor impulse and offset angle constant. Separation distance was found to be surprisingly insensitive to this variation (See Figure 3.2-10).

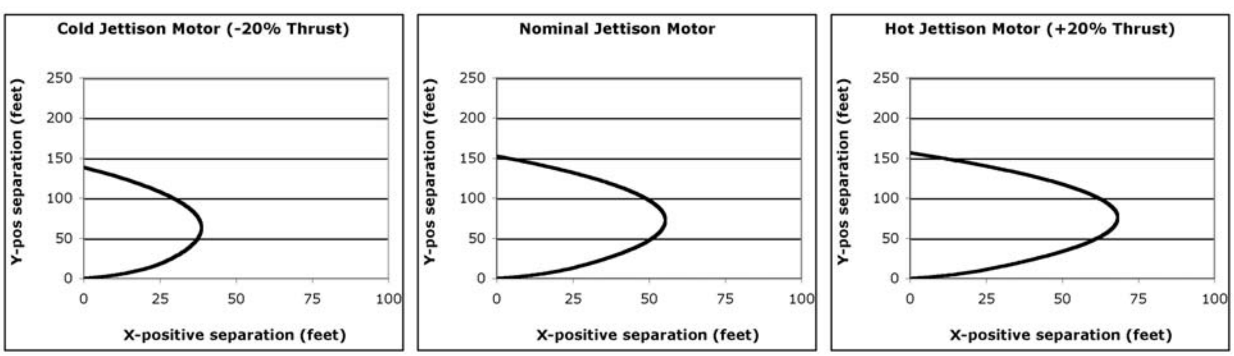

Figure 3.2-10 Effect of Temperature on LAS Jettison Separation (8 deg offset)

3.2.4 Boost Protective Cover

The boost protective cover (BPC) is part of the Launch Abort System (LAS) and is designed to protect the Crew Module (CM) from the aerodynamic environment during CEV nominal ascent and abort flight modes. Designed to survive re-entry, the CM thermal protection system (TPS) can easily tolerate the anticipated ascent and abort aerodynamic heating rates. The primary function of the BPC is to protect certain CM surfaces that are sensitive to abrasive forces unique to the ascent and abort flight environment. These abrasive forces include the following:

1) High velocity impacts from particles ejected by the LAS abort and jettison motors;
2) High velocity impacts from environment related debris (hail, bird-strike, etc.); and
3) Friction due to aerodynamic shear and LAS motor plume impingement.

The CM surfaces that require protection from abrasion include the following:

4) CM crew and hatch windows;
5) Catalytic and optical coatings applied to the surface of the CM TPS; and
6) CM outer mold line (OML) protrusions (e.g., RF antennas).

The BPC will need to tolerate temperatures up to about 900 °F. The BPC will be designed to minimize overall weight while still providing an acceptable level of abrasion protection. Potential material concepts for the BPC include:

1) Composite substrate (e.g., IM6) bonded to a low temperature ablative coating (e.g., cork);
2) Aluminum honeycomb core bonded to thin Titanium alloy faceplates.

The BPC separates from the CM during LAS jettison. This is allowable as the post LAS flight environment will not subject the aforementioned CM surfaces to abrasion. Prior to LAS jettison, the BPC must be designed to withstand all flight related stresses (aerodynamic, acceleration, blast pressure, etc.). Following LAS jettison, the BPC must maintain its structural integrity long enough to preclude any risk of debris impact with the CM.

It is important that the BPC design not visually obstruct the CM windows, or at least be designed to leave a minimum set of windows unobstructed. This can be accomplished by integrating appropriately located windows or cut-outs within the BPC structure or by keeping the BPC aft OML forward of the CM windows. It is important that the BPC design not impede CM hatch access or operation. This can be accomplished by integrating an appropriately located hatch or cut-out within the BPC structure or by keeping the BPC aft OML forward of the CM hatch. The BPC is shown in Figure 3.0-3.

3.3 Optional Design Consideration - Dual Thrust Launch Abort Motor

The Launch Abort System must be ready to operate at any altitude from sea level to 300,000 feet, at any range of temperature from 30 °F to 120 °F, and at any range of dynamic pressure from 0 psf to 750 psf. Each of these three ranges has an effect on the LAV's performance. Ambient pressure affects the thrust output of the abort motor. Propellant mean bulk temperature (PMBT) affects burn rate and hence, thrust. The aerodynamic drag on a vehicle is directly proportional to dynamic pressure. The result is that a motor designed to produce 15 g acceleration on a vehicle when cold and at sea level will produce much more when hot and at altitude.

The single thrust abort motor is a one size fits all approach to the launch abort mission. The high thrust produced is only necessary at transonic aborts where most of the thrust is consumed overcoming aerodynamic drag. Ironically, perhaps, the "softest" abort happens at this transonic condition where the LAV only accelerates at between 2.5 g to 5 g. The LAV is overpowered for about 80% of the launch trajectory when it produces greater than 5 g acceleration to the LAV. Indeed, it is estimated that the LAV will experience better than 20 g with a hot abort motor at vacuum conditions.

So, why not just be grateful that the thrust is there and accept the single thrust motor?

First, the high acceleration loading requires the CM internals to be designed to handle 20 g structurally. Additionally, the propellant and all inert components of all the motors in the LAS must also be able the bear that load. This complicates grain design for high burn rate propellants, as they are the least able to withstand high structural loading.

Second, the fast-burning abort motor drives the thrust of the active control motor up and its technology readiness level (TRL) down, thus introducing unnecessary risk to the program. The LAV must be quickly pitched in order to meet the downrange requirements for pad abort. This pitch-over must be completed early in the abort motor burn for it to be effective. Having the option of a lower thrust, longer burning abort motor reduces the active control motor maximum thrust required and the resultant TRL is increased when compared to that of an active control motor with a higher thrust.

Lastly, failure mode and blast analysis studies have shown that it is primarily warning time, and not high acceleration, that has the greater effect on saving the crew. Aborting from a catastrophic launch failure is like avoiding being hit by a train. It's a lot more important to see it coming than it is to be able to jump out of the way twice as quickly. The LAS needs to perform its abort safely and reliably.

Allowing for dual thrust opens the design space to improve LAV and CLV performance, as well as to allow additional methods of providing launch abort. An abort motor with two thrust levels could use the high thrust level when necessary for transonic aborts, but otherwise could use the lower thrust setting. Peak acceleration loads on the CM could be reduced from 20 g to perhaps 8 or 9 g. The active control motor maximum thrust level could also be reduced, raising its TRL, reducing its mass, and giving it more time to pitch the LAV over at pad abort. A reduced thrust setting might also make ascent assist feasible by reducing tension stress on the CM. Ascent assist involves firing the abort motor on nominal launch to gain payload benefit. In any case, the impulse of the motor remains nearly constant – it just produces less thrust for a longer time.

There are essentially three ways to alter the thrust of a solid rocket motor system: increase the number of motors or grains in the motor, increase the burn area of the grain, or increase the burn rate of the grain. Combining multiple motors in a single case is a very simple solution. Containing multiple grains separated by bulkheads that can be breached is lighter, but more complex. Employing grain inhibitor with multiple igniters is the lightest solution.

Varying the burn rate of the propellant can be achieved by varying the chamber pressure. For a given burn area, increasing throat area decreases burn rate by reducing chamber pressure. Reduced burn rate decreases mass flow through the nozzle and therefore reduces thrust. Variance in nozzle area can occur by opening up more nozzles, increasing the throat area of existing nozzles by expelling inserts, or by incorporating a pintle such as that used on the active control motor.

A single pintle could be used in the existing abort motor. It would be placed in a more open position at the pad and would provide low thrust for pad aborts. As the launch vehicle neared transonic speed and high thrust was required for abort, the pintle would be moved to a narrower setting the reduce throat area. After the transonic portion of the trajectory had been successfully completed, the pintle would move back into the low thrust position.

The MSFC Power and Propulsion Team plans to investigate the dual thrust abort motor design in more detail in the coming months.

3.4 Optional Design Consideration - Ascent Assist using Launch Abort Motor

The payload performance benefit obtained by using the abort motor for additional ΔV prior to LAS jettison was investigated. This analysis compared the performance of two abort motor thrust levels and the impact both might have on the structure of the CLV.

Two cases were analyzed. Case 1 used the CRC-3 abort motor with a thrust-to-weight (T/W) equal to 15 applied for about 2 seconds. Case 2 used a lower thrust design with a T/W of about 7 applied for about 3 seconds. The Case 2 abort motor would have two thrust levels, one approximately twice the other.

Nozzle inserts are one method that would provide two available throat areas. A dual thrust abort motor would be fitted with inserts in each of the four nozzles that would be expelled to increase the throat area when lower thrust was desired. For a solid rocket motor, increasing the total throat area decreases chamber pressure, burn rate, and thrust, and increases motor burn time.

The total impulse in both the high T/W CRC-3 abort motor and lower T/W abort motor would be similar, with the CRC-3 motor having a slightly higher total impulse due its larger nozzle expansion ratio (exit area/throat area).

Nozzle insert technology has been used for such tactical missile concepts as the Integral-Rocket Ramjet and Ducted Rocket. As shown in Figure 3.4-1, the inserts are held in the nozzles with clamps. The nozzle inserts are expelled after the clamps are released either mechanically or pyrotechnically. Other methods exist for varying the thrust of a solid rocket motor, some of which do not expel debris. They are discussed in Section 3.3 above.

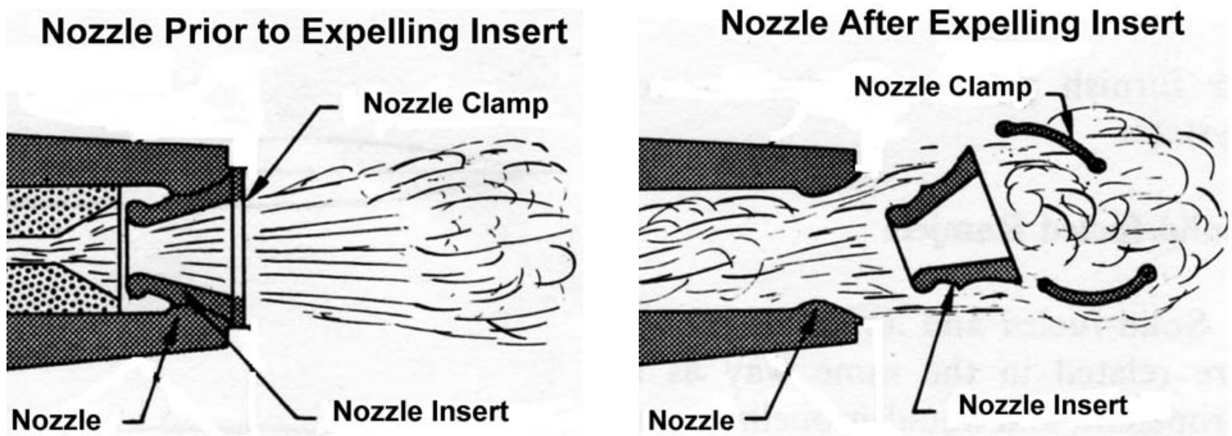

Figure 3.4-1 Nozzle Inserts in the Integral Rocket Ramjet

The thrust and acceleration for abort motor ascent assist is produced in addition to that nominally produced by the CLV second stage. The CLV second stage J-2X engine produces 273,750 lbf nominal vacuum thrust. The LAS abort motor was assumed to have a propellant mean bulk temperature of 70 °F for both the high T/W CRC-3 and lower T/W options. The abort motor ignited 30 seconds after the J-2X achieved nominal thrust during CLV second stage burn. The axial vacuum thrust profiles (including abort motor nozzle cant angle losses) for both the 15 g and the 7 g motors are shown in Figure 3.4-2.

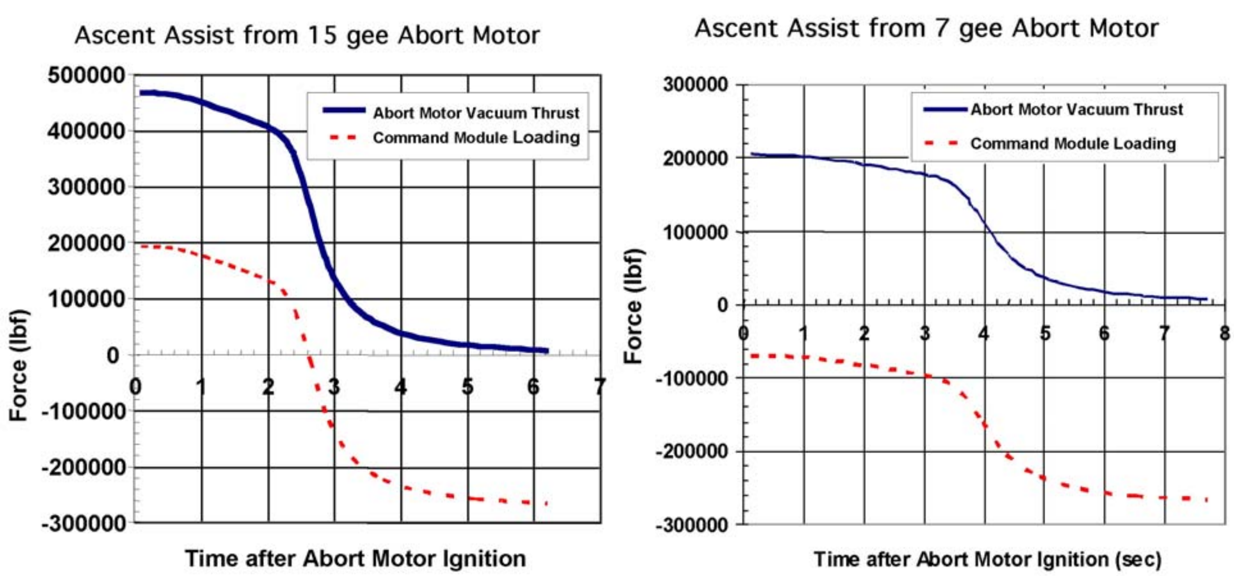

Figure 3.4-2 CRC-3 Ascent Assist

In addition to thrust profiles, the figure also shows the Crew Module loading values. Positive values indicate the CM is in tension and negative values indicate the CM is in compression. The effect on the CM is different in the two cases analyzed.

The high T/W case in Figure 3.4-3 shows that the CM experiences a change from compression to tension loading when the abort motor is fired. Essentially, the thrust from the 15 g abort motor is pulling the entire stack. Additional structural mass to account for this loading has not been assessed in this analysis, but some change in CM and SM structure might be expected. After abort motor burn out, the CM loading returns to compression. The lower T/W case in Figure 3.4-2 shows that the CM is always in compression during ascent assist. Ascent assist serves to "lighten the load" on the J-2X as opposed to "pull it along".

The acceleration on the CLV produced by the J-2X and the abort motor is shown in Figure 3.4-3 for both the high T/W CRC-3 and lower T/W cases. The entire CLV acceleration profile is shown in Figure 3.4-4.

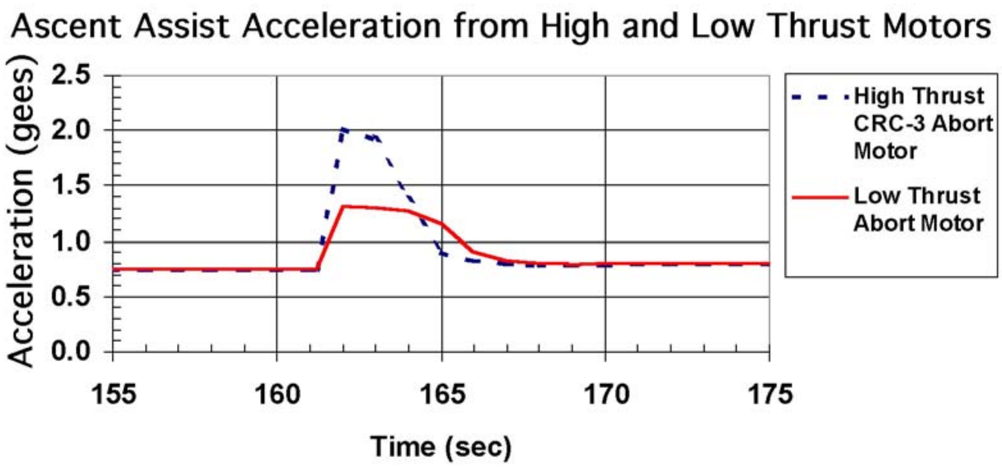

Figure 3.4-3 CLV Acceleration from High and Low Thrust Ascent Assist

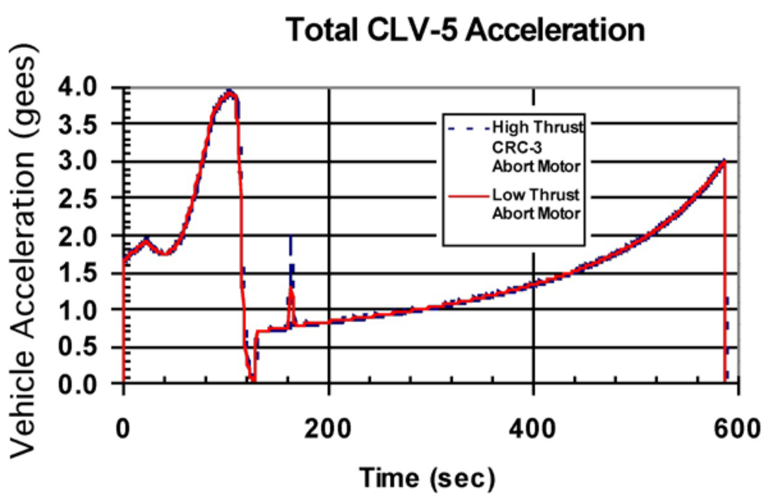

Figure 3.4-4 Total CLV Acceleration Profile with Ascent Assist

CLV trajectory analyses were performed to determine the additional payload to orbit capability realized from ascent assist. The revised 3M reference trajectory International Space Station mission was used, and the LAS abort motor burn time was optimized for maximum payload. Table 3.4-1 shows the LAS CRC-3 mass properties used in the trajectory analyses.

Abort Motor Useable Propellant Mass	5609 lbm
LAS Inert Mass	7619 lbm
LASTotal Mass	13228 lbm

Table 3.4-1 LAS Mass Properties Used in Ascent Assist Analysis

The payload increases due to the abort motor burn assist are shown in Table 3.4-2.

Vehicle	**Net Payload (lbm) (including Adapter)**	**Delta Payload (lbm)**
CLV (Unassisted)	43,025	0
High T/W CRC-3 Ascent Assist	44,042	1,017
Lower T/W Ascent Assist	43,672	646

Table 3.4-2 Payload Performance Comparison

The high thrust CRC-3 abort motor, if used for ascent assist, can provide a payload to orbit increase of 1017 lbm over the reference mission. However, structural mass will likely be required in the CM and the SM to bear the additional tension loading. The dual thrust abort motor reduces or eliminates the need for additional structural mass by negating the tension loading on the Crew Module, but this approach only increases the payload to orbit by 646 lbf over the reference mission. Additional optimization studies might trade the lower thrust level against structural weight to maximize payload benefit.

3.5 Mass Estimates and Design Maturity

The LAS mass estimates and bases of estimate are shown in Table 3.5-1.

Hardware Items	Quantity	Unit Mass (lbm)	Growth (%)	Total Mass (lbm)	LAS Mass (lbm)	CM Mass (lbm)	SM Mass (lbm)	Basis of Estimate
Launch Abort System				**14,049**	**14,049**	**0**	**0**	
Active Control Motor	1		30%	435.0	435.0			Performance Model
Structural Skin	1	152	30%					
Case	1	31	30%					
Cap	1	25	30%					
Liner Case	1	1	30%					
Insulation Case	1	3	30%					
Liner Cap	1	0	30%					
Insulation Cap	1	2	30%					
Pintle Valve	4	28	30%					
Igniter	1	7	30%					
Jettison Motor	1		21%	662.8	662.8			Performance Model
Structural Skin	1	217	21%					
Jettison Dome	1	170	21%					
Nozzles	4	40	21%					
Abort Motor	1		14%	3167.4	3167.4			Performance Model
Manifold	1	738	14%					
Abort Dome	1	238	14%					
Abort Case	1	1408	14%					
Nozzles	4	99	14%					
Nose Cone	1	106	25%	132.5	132.5			Performance Model
Interstage	1	222	25%	277.9	277.9			Performance Model
CM/LAS Adapter	1	792	10%	871.2	871.2			Performance Model
Avionics & Power	1	170	20%	204.0	204.0			Engineering Judgement
Avionics Mount	1	116	20%	139.2	139.2			Performance Model
BPC	1	989	25%	1236.3	1236.3			Performance Model
Active Control Motor Propellant	1	500	15%	575.0	575.0			Performance Model
Jettison Motor Propellant	1	162	10%	178.2	178.2			Performance Model
Abort Motor Propellant	1	5609	10%	6169.9	6169.9			Performance Model

Table 3.5-1 LAS Mass Estimates and Heritage

3.6 Plan Forward

The plan forward is to continue to refine the LAS design, interface with the CLV vehicle aero team to begin optimizing overall vehicle aerodynamics with the appropriate LAS trades (e.g., LAS control requirements/cost/complexity vs. LAS geometry), and complete the next design cycle. In addition, for the upcoming DAC, full structural models representing the most current LAS configuration will be built and analyzed. The analysis will encompass both static load and dynamic modal behavior. Structural interfaces can then be assessed, with attention to stiffness, strength and load-transfer.

4.0 Crew Module Overview

The Crew Module (CM) serves as the command, control, and habitation center of the CEV while transporting crews from Earth to lunar orbit or ISS and returning them to Earth. The Crew Module provides habitable volume for the crew, life support, docking and pressurized crew transfer to the ISS or LSAM, and atmospheric entry and landing capabilities. A scaled Apollo Command Module shape with a base diameter of 198 inches (16.5 feet) and side wall angle of 32.5° is the outer moldline for the CEV Crew Module. This configuration provides 685 cubic feet of pressurized volume for the crew during transits between Earth and the Moon. The CM can operate at a nominal internal pressure of 10.2 psia with 30% oxygen concentration for lunar missions, or at an ISS-compatible 14.7 psia for ISS missions. For the lunar mission, the Crew Module launches with a KSC sea level atmospheric pressure and the cabin is depressurized to 10.2 psia prior to docking with the LSAM.

The Crew Module propulsion system provides vehicle attitude control for atmospheric entry following separation from the Service Module and range error correction capability during the exoatmospheric portion of a lunar skip-entry return trajectory. The propulsion system is a combination of high pressure gaseous oxygen and liquid ethanol with a total ΔV of 164 ft/s. Upon return from ISS or lunar orbit, a combination of parachutes, retrorockets, and crushable structure provide for a nominal land touchdown at a Western Continental United States (CONUS) landing site, with water up-righting systems included for water landings following an aborted ascent or entry. Three main parachutes slow the CM to a steady-state sink rate of 24 ft/s, and prior to touchdown, the Crew Module's ablative base heat shield is jettisoned and eight retrorockets (four horizontal and four vertical) are deployed for soft landing. After recovery, the CM may be refurbished and reflown. The CM is the only portion of the CEV recovered after its mission.

The Crew Module includes the following fourteen subsystems:

1) Active Thermal Control
2) Avionics
3) Electrical Power
4) Environmental Control and Life Support
5) Flight Crew Equipment
6) Guidance, Navigation, and Control
7) Landing Attenuation
8) Mechanisms
9) Passive Thermal Control
10) Pyrotechnics
11) Reaction Control
12) Parachutes
13) Structure
14) Thermal Protection

<u>Physical Attributes</u>

- Height: 13 ft 4.5 in. (160.5 in.)
- Diameter: 16 ft 6 in. (198 in.)
- Sidewall Angle: 32.5°

- Launch Mass (4-crew Lunar): 17,621 lbm

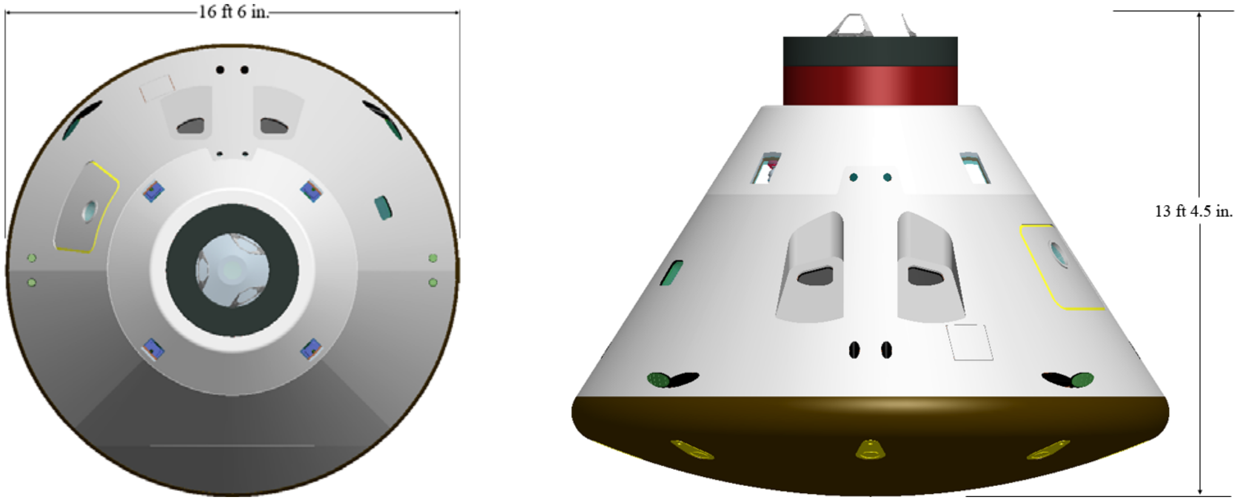

Figure 4.0-1 Crew Module External Arrangement

4.1 Crew Module Layout

The CM internal equipment is arranged within three different volumes or compartments: the forward compartment, the crew cabin, and the base compartment. In general, the forward compartment is the unpressurized internal volume at the forward (top) end of the vehicle. The forward compartment contains the CM recovery and landing equipment, navigation equipment, and docking mechanism. These components are covered for most of the CEV's mission by the forward bay cover and are exposed when the cover is jettisoned during the drogue parachute deployment sequence. Jettisoning the forward bay cover allows the parachutes to be deployed prior to touchdown.

The base compartment is the annular unpressurized volume formed at the base or aft end of the CM. This compartment houses the reaction control system equipment and some components of the active thermal control and communications and tracking system. It also contains eight retrorockets that are used to attenuate any residual energy and prevent roll-over during CM touchdown on land. Similar to the forward compartment, equipment in the base compartment (specifically the retrorockets) are exposed when the base heat shield is jettisoned following main parachute deployment.

Pressurized volume for crew habitation in the CM is provided by the crew cabin. The crew cabin is designed to hold an internal pressure of 14.7 psia for ISS missions (10.2 psia for lunar missions) and contains the bulk of the CM systems. The crew cabin is an irregular shape for traditional pressure vessels owing to the CM's unique aerodynamic shape. At the base is a bulkhead that follows the curved shape of the base heat shield and at the forward end is a flat circular bulkhead. The forward bulkhead is intersected along its centerline by a cylindrical tunnel that allows pressurized crew transfer between the CM and other elements such as the LSAM. Truncated cones make up the crew cabin side wall, with the upper cone following the 32.5° external back shell angle and the lower cone being inverted to provide equipment mounting volume in the base compartment.

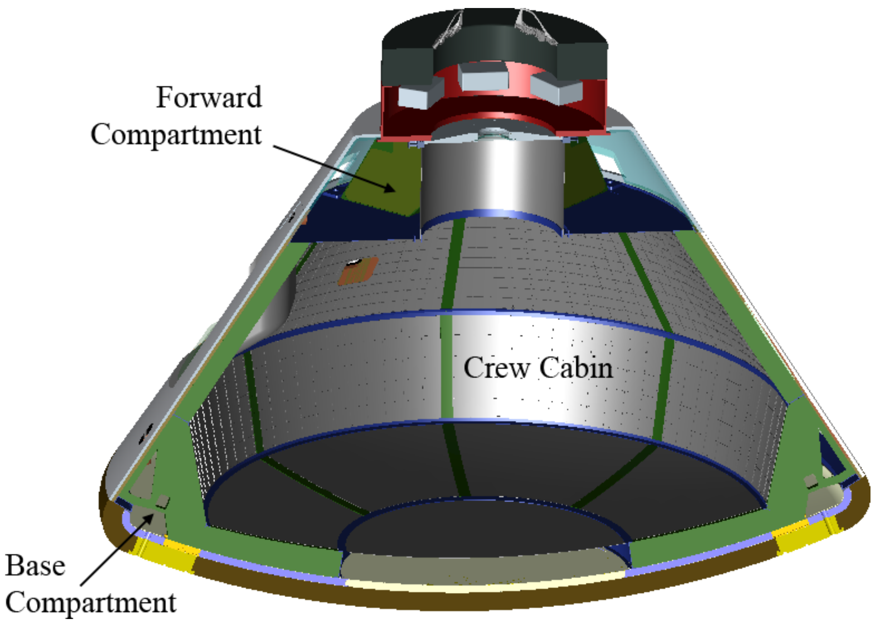

Figure 4.1-1 Crew Module Compartments

Figure 4.1-1 provides a labeled view of the Crew Module compartments.

4.1.1 Forward Compartment

The Crew Module forward compartment is defined as the unpressurized volume at the top of the vehicle enclosed by the docking tunnel, forward bulkhead, and forward bay cover. Upper gussets from the CM pressure vessel structure divide this volume into four bays, with each bay identified by its corresponding Y or Z axis. CM systems included in the forward compartment are the parachutes, up-righting airbags, RCS thrusters, and navigation sensors. The Launch Abort System also connects to attachment fittings located in this volume.

Two RCS thrusters are mounted in the forward compartment +Z bay. These thrusters provide negative pitch control for the CM during atmospheric flight. The complementary positive pitch thrusters are located in the base compartment. Also located in the +Z bay are the drogue parachutes and drogue mortars mounted symmetrically about the +Z axis. The drogue parachutes are deployed during entry to stabilize the vehicle and slow it sufficiently to allow the main parachutes to be deployed. Moving clockwise from the RCS thrusters is the first of three star trackers, part of the CM's navigation sensor suite. The CM star trackers are used to provide periodic attitude state vector updates to the inertial measurement units by measuring the orientation of the CEV relative to known stars. During rendezvous operations, the star trackers can also provide angular data between the CEV and ISS or LSAM. Star trackers are mounted in the forward compartment at approximately 120° intervals to enable a view of the sky regardless of the CEV attitude. On the opposite side of the RCS thrusters, roughly symmetric with the star tracker, are two light detection and ranging (LIDAR) optical sensors to provide range, bearing, and relative attitude information during rendezvous, proximity operations, and docking. The LIDAR sensors are positioned to enable viewing of the trajectory control sensor (TCS) target mounted on the ISS pressurized mating adapter through CEV hard capture.

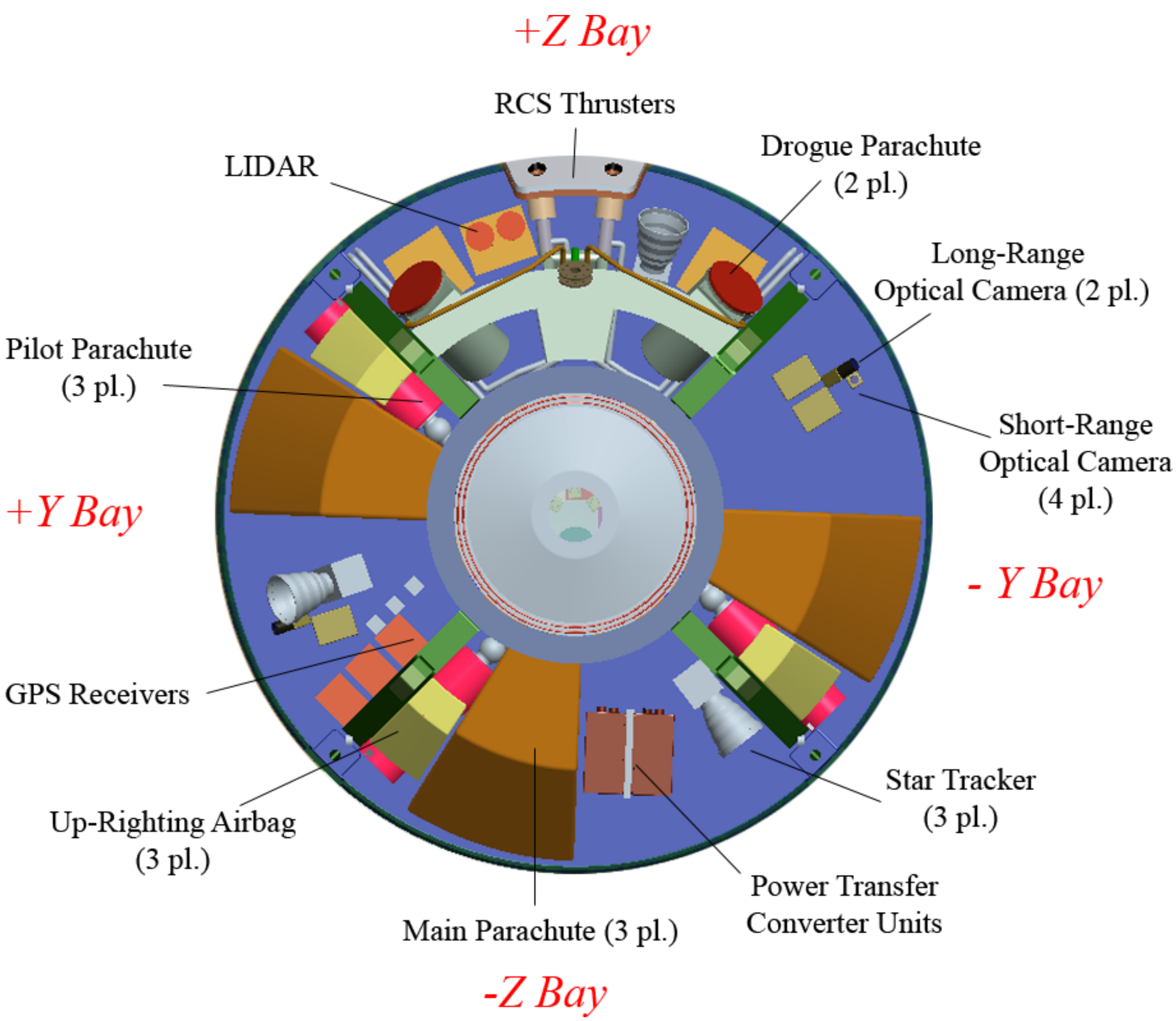

Figure 4.1-2 Forward Compartment Layout

The next forward compartment bay, the –Y bay, includes additional parachute and navigation equipment. A pilot parachute and mortar, used to deploy a main parachute, is mounted to an upper gusset to absorb shock loads from the pyrotechnic firing. Next to the pilot mortar is a packed main parachute. Above the mortar is the first of three up-righting airbags, which may be used to up-right the CM following a water landing. The –Y bay also includes the first of two long-range optical cameras, a short-range optical camera, and camera avionics boxes. These cameras are used to provide range, bearing, and relative attitude during rendezvous and proximity operations.

The long-range camera can also be used for celestial navigation. The second long-range camera is positioned approximately 180° from this one while three additional short-range cameras are located near the CM centerline on the docking hatch window.

The –Z bay consists of the second main parachute, pilot parachute and mortar, up-righting airbag, and star tracker. It also contains two power transfer converter units used to facilitate power transfer, conversion, and isolation between the CEV and LSAM or ISS.

The third set of main parachutes, pilot parachutes and mortars, up-righting airbags, and star trackers are found in the +Y bay. Also included here is the second long-range optical camera. The last components included in the forward compartment are three GPS receivers. These receivers collect GPS data from six GPS antennas mounted on the Crew Module while the CEV is in Earth vicinity, and transmit that data to the flight computers for processing.

4.1.2 Crew Cabin

Most CM systems, the flight crew, and their support equipment are housed in the pressurized volume of the Crew Module crew cabin. The crew cabin is the volume enclosed by two stacked truncated cones (the lower cone is inverted) and forward and aft bulkheads. This results in a total pressurized volume for the CM of 680 cubic feet. The crew cabin is nominally pressurized to 14.7 psia for ISS missions and 10.2 psia for lunar missions.

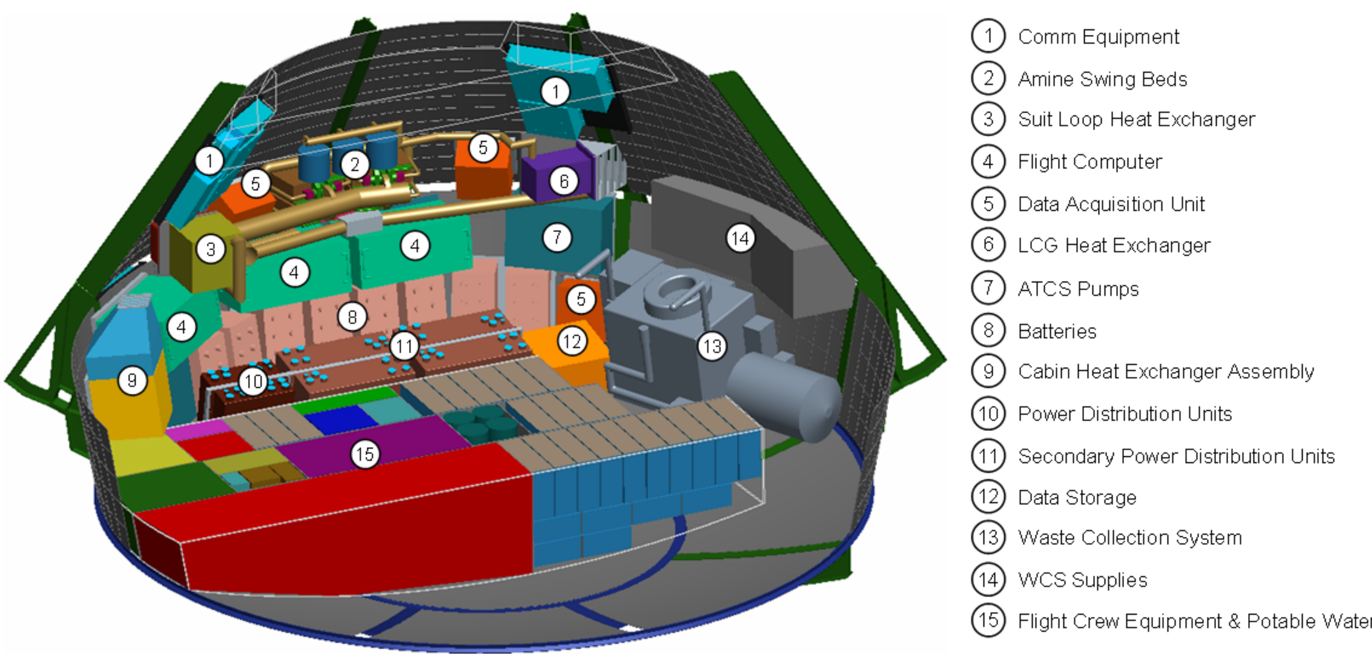

Figure 4.1-3 Crew Cabin - Right-Hand and Lower Bay Equipment

Internal equipment in the CM is arranged within five crew cabin bays: right-hand, left-hand, upper, lower, and aft. Right-hand (+Y), lower (-Z), and aft bay equipment is illustrated in Figure 4.1-3. The most massive CM hardware, the avionics and electrical power system equipment, is packaged as close to the base and as far in the –Z direction as possible for CG offset needs. Large +Xcg and –Zcg locations are desired for CM stability and a high trim angle of attack during atmospheric flight. Included in the avionics area are the flight computers, primary and secondary power distribution, batteries, data acquisition units, and pump packages. These boxes are rack-mounted with some equipment requiring structural cold plates, others simple structural shelving.

Above the avionics equipment are components of the environmental control and life support system and active thermal control system. An environmental control pallet near the avionics rack includes carbon dioxide and humidity control equipment, the suit heat exchanger, the trace contaminant control, and other miscellaneous fans and ducting.

The waste collection system is located in right-hand bay near the avionics rack. Layout considerations included crew accessibility, privacy, and proximity to the CM exterior for waste water disposal.

Mounted on the crew cabin aft bulkhead is the flight crew equipment within integral stowage cabinets. Flight crew equipment is stowed according to accessibility needs and availability of volume within the unique crew cabin geometry. Items include health and hygiene equipment, waste collection system supplies, photography, food stowage, clothing, and crew preference items. The required volume for flight crew equipment is driven by the lunar mission, which is support for four crew members for 18 days. The mission's potable water supply is also stored in 37 drink bag boxes, and these boxes cover the bulk of the aft bulkhead.

The crew cabin's left-hand (-Y) and upper (+Z) bay equipment is more sparsely populated than other areas of the crew cabin. This is due to the location of the crew, their seats, and the display and control panel, and the desire for a large CM –Zcg offset. The remainder of the vehicle's flight crew equipment – fire extinguishers and emergency oxygen masks - is wall-mounted here for rapid access. A cabin heat exchanger and fan assembly is located near the avionics rack.

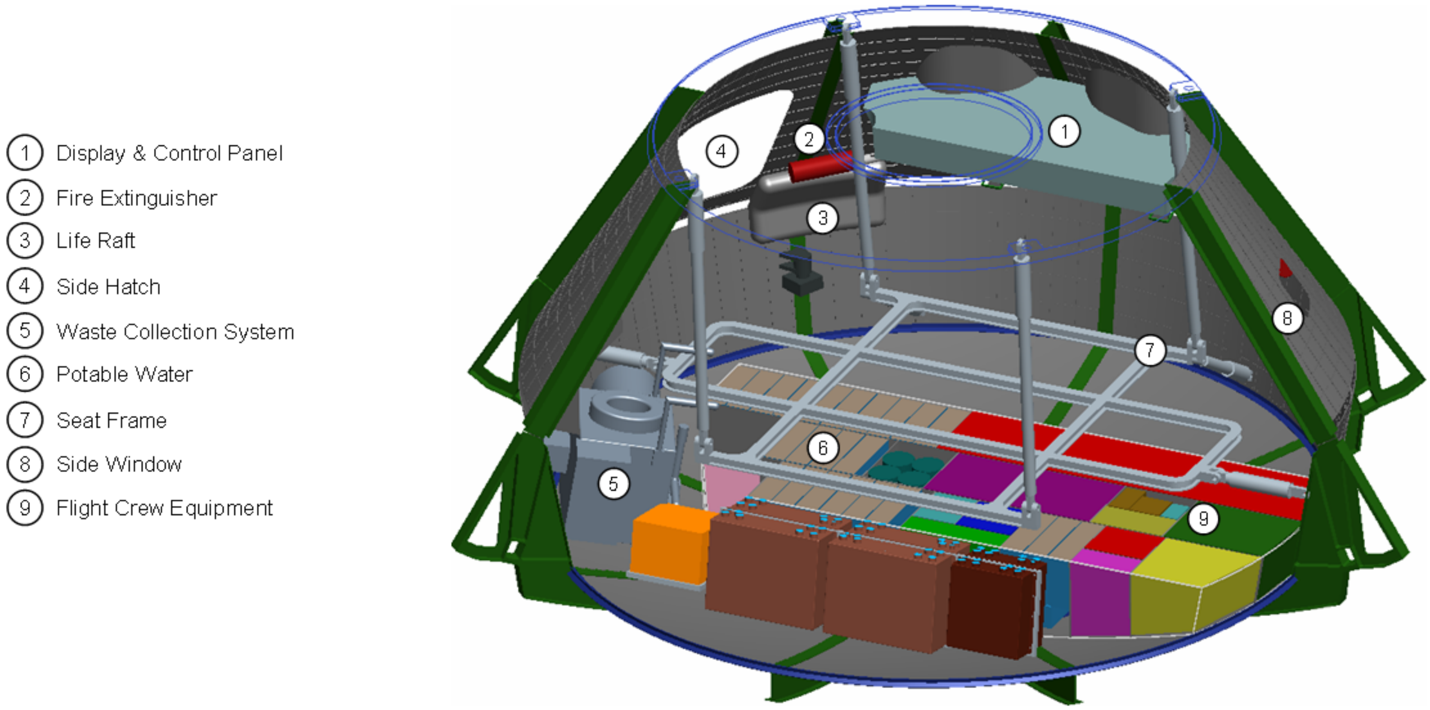

Figure 4.1-4 Crew Cabin Layout - Left-Hand and Upper Bay Equipment

Figure 4.1-5 illustrates how the crew is arranged within the crew cabin for lunar and ISS missions. These arrangements along with the size and location of the display and control panel was provided as an input to the CRC team from the CEV Cockpit Working Group, and this input was implemented in the CRC-3 configuration without modification. The Cockpit Working Group had explored numerous seating permutations before arriving at these arrangements. In this layout, the two operators are situated in the upper-most portion of the crew cabin under the display and control panel. Two more crew members are seated at their feet for ISS and lunar missions, and for maximum-crew ISS missions, a fifth and sixth crew member can be seated on the right- and left-hand sides. These seats are not used for lunar missions as the other two provide greater -Zcg offset (and thus greater L/D). The current layout can accommodate six maximum size male crew members as specified in the HSIR.

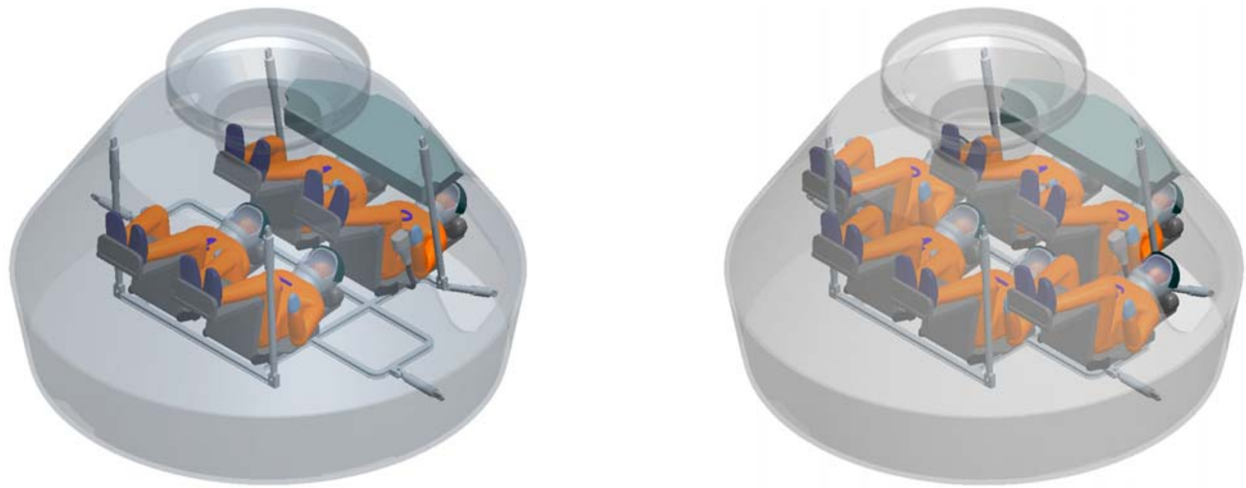

Figure 4.1-5 Crew Seating Arrangement for 4-Crew (Lunar) and 6-Crew (ISS)

4.1.3 Base Compartment

The CM's base compartment is the toroidal volume formed by the base heat shield, back shell, and crew cabin at the base of the CM. This volume includes components of the CM reaction control, communications and tracking, active thermal control, and landing system.

Figure 4.1-6 illustrates the upper (+Z) half of the CRC-3 base compartment. Eight of the twelve CM RCS thrusters are mounted in this space, including two thrusters for positive or negative yaw control, four for positive and negative roll control, and two positive pitch thrusters. The negative pitch thrusters are mounted in the forward compartment while the other two yaw thrusters are in the base compartment lower (-Z) half. Also included here from the RCS are two of the four gaseous oxygen tanks, the two methane tanks, and valve panels. Where possible, components are mounted symmetrically in the base compartment to maintain a CM Ycg location near the centerline, and as close to the lower half to maximize the -Zcg offset (for maximum L/D).

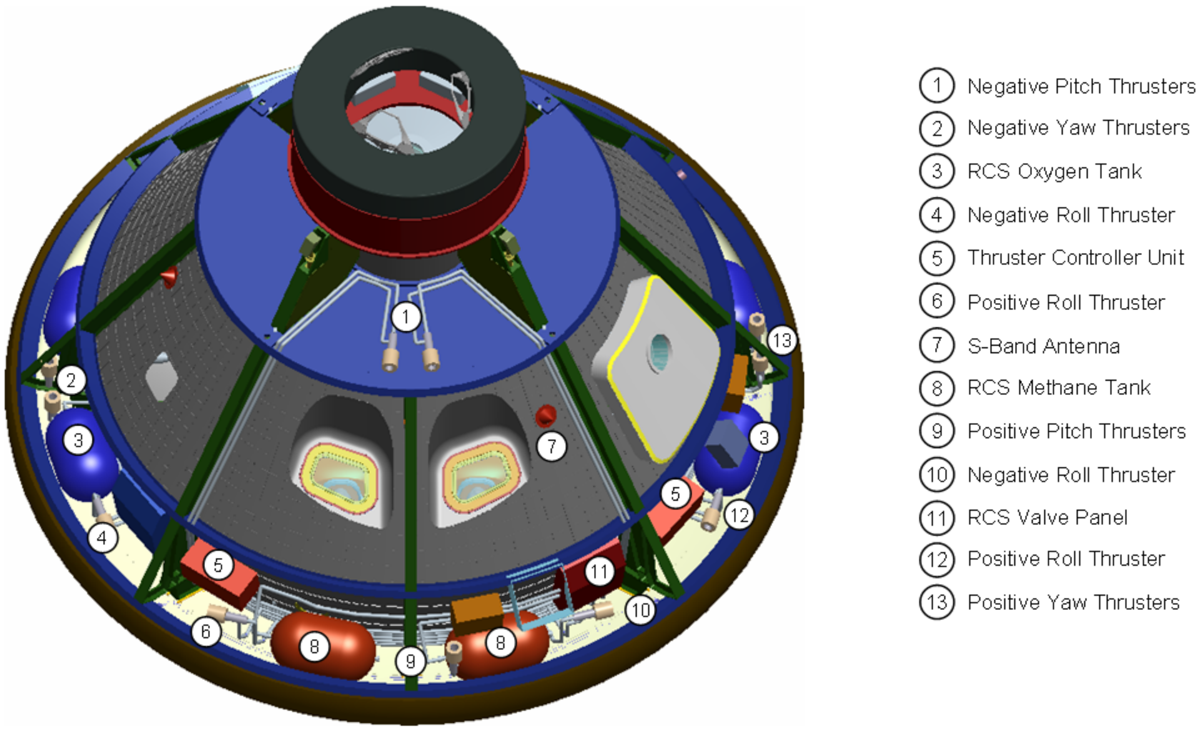

Figure 4.1-6 Base Compartment - Upper Bay Equipment

The lower (-Z) half of the base compartment is seen in Figure 4.1-7. Two yaw thrusters and two gaseous oxygen tanks are mounted on this half to complete the RCS as well as the second set of airbag inflation tanks. Not seen is a small gaseous oxygen surge tank to support the environmental control and life support system, mounted on a lower gusset near the inflation tanks. This surge tank maintains an on-demand breathable oxygen supply for the CM and is constantly replenished by the bulk oxygen storage on the SM. After CM-SM separation, the surge tank is the sole source for CM oxygen until landing. Lastly, mounted near the –Z extreme of the base compartment is a fluid evaporator, evaporator Freon and water tanks, and communications and tracking equipment mounted on cold plates. These components are mounted in their present locations primarily due to the active thermal control system (ATCS) architecture and location of the CM-SM umbilical. As currently envisioned, the ATCS pumps thermal control fluid after leaving the crew cabin through the external cold plates to acquire any excess heat. This occurs just prior to entering the umbilical and the SM radiators. After leaving the radiators and returning through the umbilical, the ATCS pumps the fluid through the fluid evaporator in case the radiators did not provide sufficient heat rejection. The CM-SM umbilical is located near the Freon and water tanks, therefore mounting this equipment in its present location minimizes fluid line length for multiple systems.

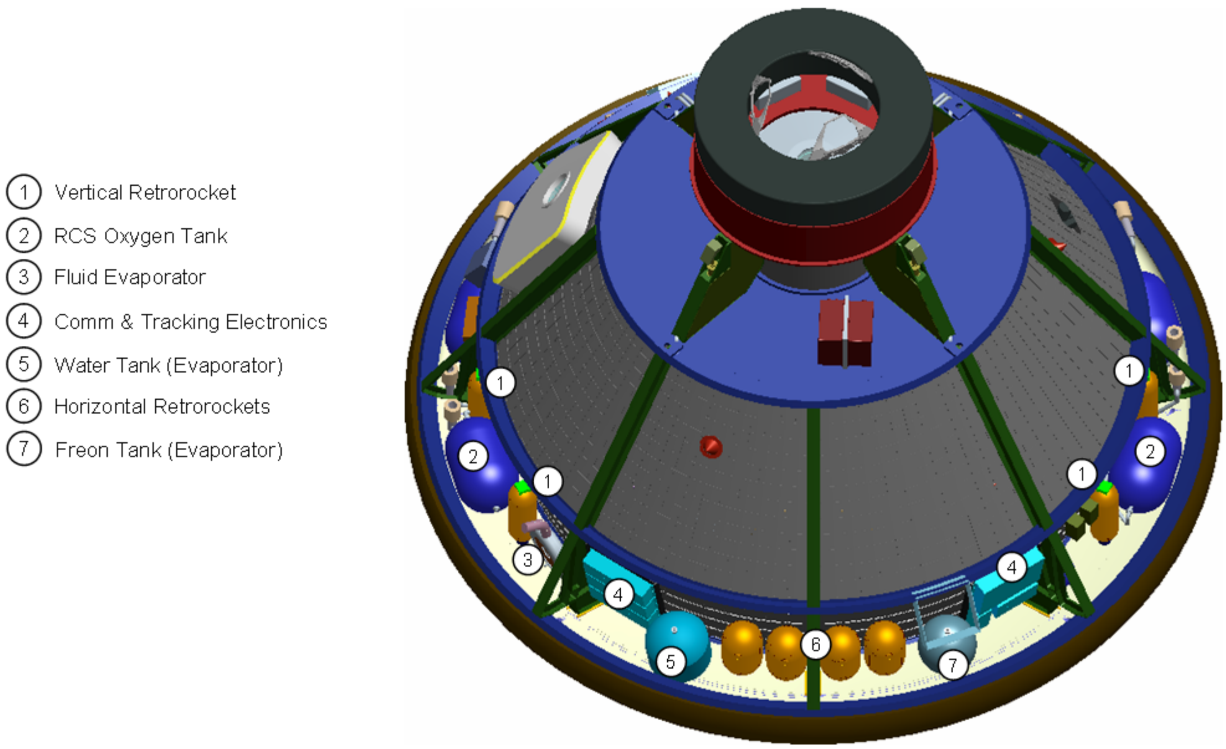

Figure 4.1-7 Base Compartment - Lower Bay Equipment

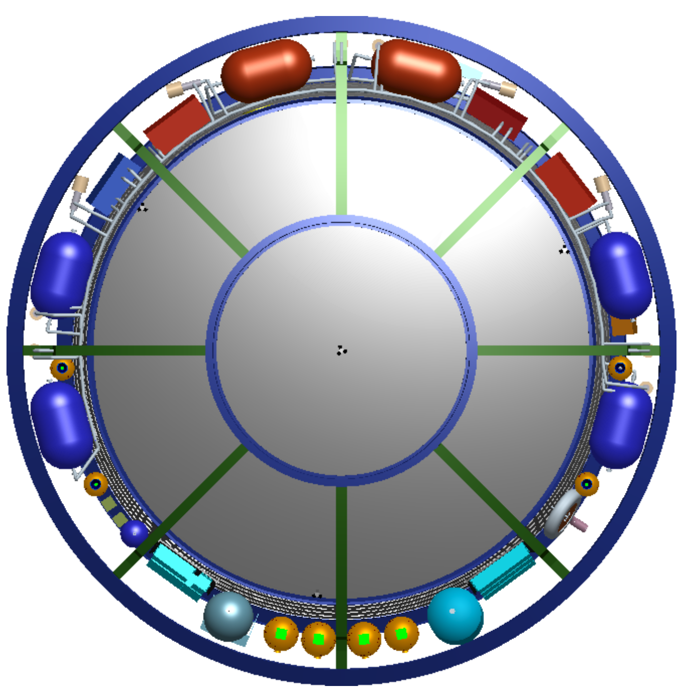

Figure 4.1-8 Base Compartment - Bulkhead

4.2 Crew Module External Features

The subsequent sections describe several key CM external features, including its structural construction, thermal protection system arrangement, provisions for docking and external viewing, approach for Earth recovery and landing, and inter-module connections.

4.2.1 Structure

The Crew Module is constructed from two primary structural elements: an internal pressure vessel to provide habitable space for the crew, and an external heat shield to give the CM an aerodynamic shape and to support the thermal protection system.

The pressure vessel structure provides volume for the crew and enclosure for necessary systems of the CM. The construction consists of aluminum orthogrid skin panels attached to eight aluminum longerons, ring frames, and a forward bulkhead. Skin panels serve to hold internal cabin pressure while the longerons, ring frames, and bulkhead react loads from the Crew Launch Vehicle, Service Module, parachutes, landing system, and Launch Abort System. The pressure vessel structure is constructed from the aluminum alloy Al-Li 2195-T8, selected for its relatively high strength-to-density ratio. This alloy is currently used on the Shuttle External Tank. Figure 4.2-1 provides a view of the CM pressure vessel structure.

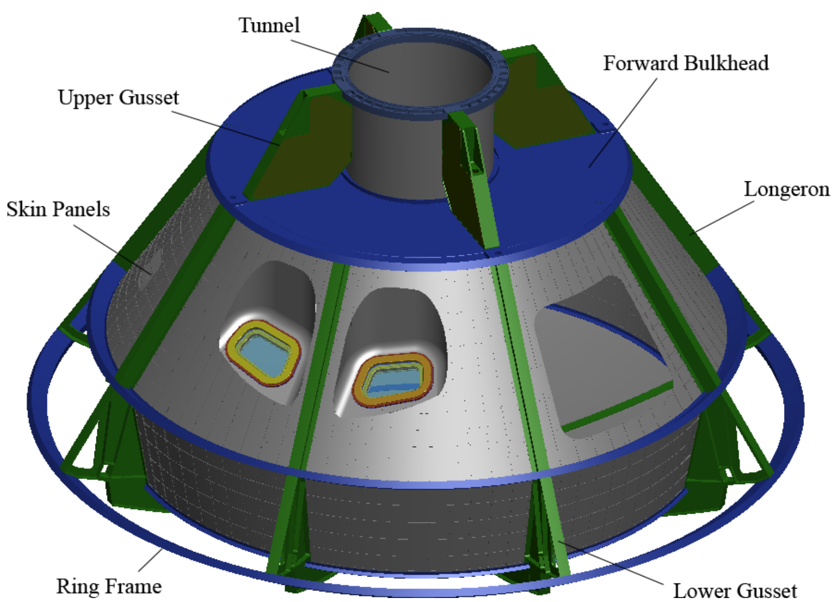

Figure 4.2-1 CM Pressure Vessel Structure

The external heat shield for the CEV Crew Module is sub-divided into three structural elements: the base heat shield, the back shell, and the forward bay cover. The base heat shield carrier structure gives the CM its distinct blunt body shape and is used to attach the vehicle's ablative thermal protection material. It is constructed from a titanium sandwich panel with 0.032 inch face sheets and a 2.0 inch titanium honeycomb core. For a nominal land landing, the base heat shield including structure and TPS is jettisoned following deployment of the main parachutes, though it may be retained for water landings. The other two elements, the back shell and forward bay cover, are truncated cone structures used to support the back shell TPS and to cover the crew cabin and forward compartments, respectively. Both structures are constructed from honeycomb sandwich panels with 0.04 inch graphite/BMI composite face sheets (eight plies of unidirectional tape in a quasi-isotropic layup) and a 0.75 inch aluminum honeycomb core. The forward bay cover is jettisoned during entry to allow deployment of the drogue, pilot, and main parachutes.

4.2.2 Thermal Protection

Thermal protection material on the Crew Module has the primary function of protecting the crew and vehicle systems from the extreme heating environments it sees during a mission. These environments include heating during Earth ascent, solar and planetary heating in Earth orbit, lunar orbit, and Earth-Moon transit, and the heat of Earth entry. For ascent, the Crew Module is protected with a Boost Protective Cover as described in the Launch Abort System section. The Crew Module thermal protection scheme consists of base heat shield TPS, back shell and forward bay cover TPS, and insulation blankets of Pyrogel and MLI between the pressure vessel and external heat shield structure. See Figure 4.2-2 for an illustration of the Crew Module TPS.

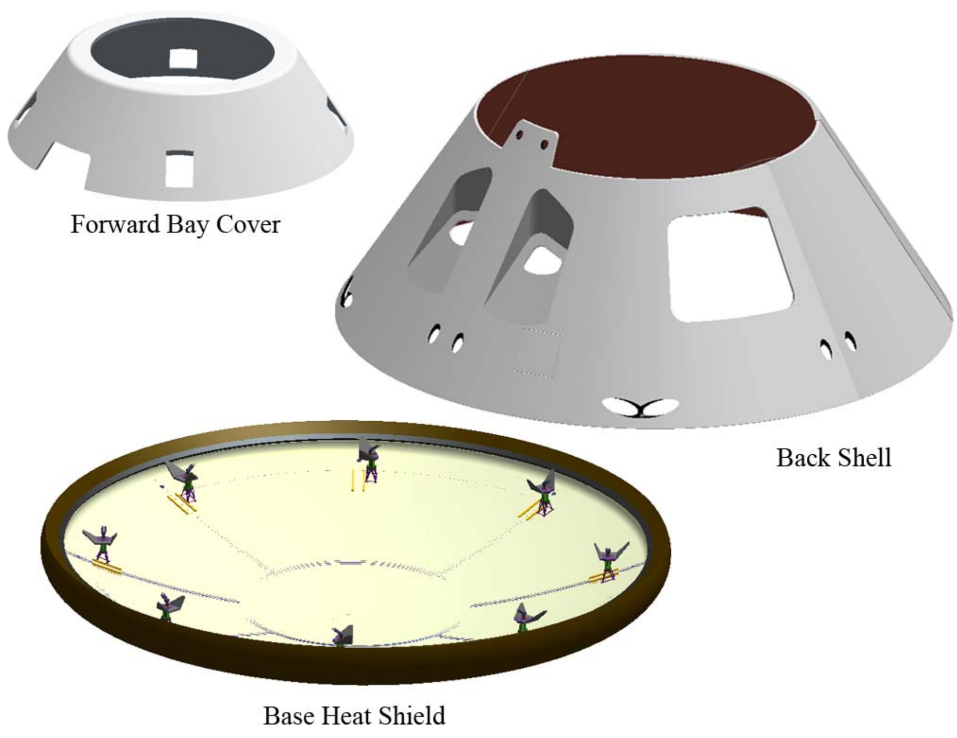

Figure 4.2-2 CM Thermal Protection

The base heat shield TPS includes material that chars (ablates) and pyrolizes to dissipate the bulk of the heat generated by the CM entering the atmosphere at 36,000 ft/s. Several candidate materials for the base heat shield TPS are being evaluated and considered at this time. The thickness of the base heat shield TPS is tailored according to the heat load distribution across its surface.

Back shell TPS on the CM is distributed between the crew cabin and forward compartment. The current reference material is the high-temperature reusable surface insulation (HRSI) tiles used on the Shuttle Orbiter. The back shell consists of both BRI-8 tiles and higher-density BRI-18 tiles for its higher temperature regions (Figure 4.2-3), while the forward bay cover uses only BRI-8 tiles.

Panel #	Area (ft^2)	Weight* (lbs)
1	34.531	44.0
2	34.531	44.0
3	34.531	53.0
4: BRI-18	13.080	47.5
BRI-8	21.451	44.0
SubTotal	34.531	90.0
5: BRI-18	13.080	47.5
BRI-8	21.451	44.0
SubTotal	34.531	90.0
6	34.531	53.0
7	34.531	44.0
8	34.531	44.0
Forward Bay Cover	63.42	95.0
Total	339.67	560.0

* *Includes 25% weight growth factor*

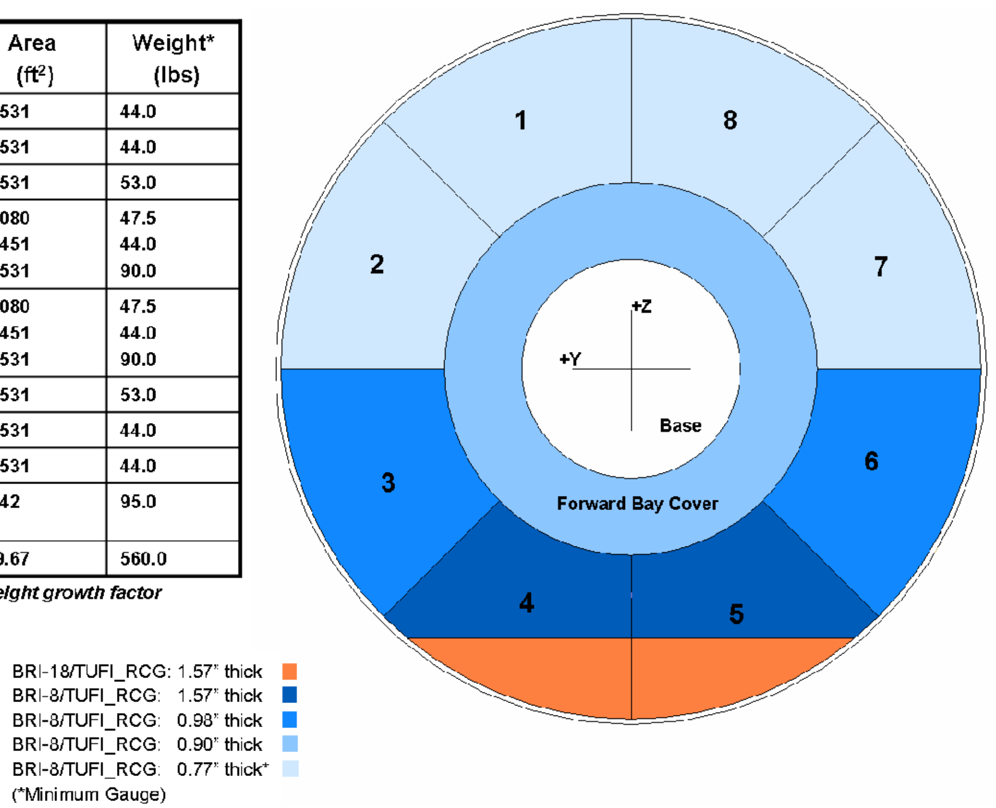

Figure 4.2-3 CM Back Shell and Forward Bay Cover TPS

4.2.3 Windows and Hatches

The Crew Module includes five windows for rendezvous and docking operations, observation, and photography. Two forward-facing windows on the vehicle sidewall provide crew operator views toward the apex of the Crew Module for rendezvous and docking with the International Space Station or Lunar Surface Access Module. A rectangular side window and a fourth circular window located within the side hatch provide additional external views. Finally, a fifth circular window is built into the forward docking hatch to provide a centerline view of the CEV's docking target. The rendezvous windows are quadruple-paned fused silica panels similar to the optical windows on the Shuttle Orbiter, including an outer thermal pane, outer and inner pressure panes, and a scratch pane. During launch and ascent, all Crew Module windows except the –Y operator's rendezvous window and the side hatch window are covered by the Boost Protective

Cover. The Boost Protective Cover is jettisoned with the LAS at an altitude between 250,000 and 300,000 feet (approximately 161 seconds after liftoff).

The CEV Crew Module has two hatches for crew ingress and egress. A side hatch located on the vehicle sidewall provides the primary means for crew entry and exit while the vehicle is on the launch pad or following landing, and may also serve as the primary translation path in the event of a contingency EVA. The side hatch is similar to the Apollo Command Module unified hatch in size (a trapezoid 33 inches wide at the top and 36 inches at the base) and operation (outward-opening). It can be opened rapidly by crew or ground personnel for emergency egress from inside the vehicle, or from the outside without requiring the use of a tool. The hatch also includes a valve to vent the internal cabin pressure prior to performing a contingency EVA. The contingency EVA scenario involving the Crew Module side hatch is a contingency external crew transfer from the LSAM to CEV following lunar ascent.

The side hatch was moved from the –Y to the +Y side of the Crew Module in CRC-3. This change was initiated when the Constellation Program baselined the Launch Complex-39 concept for launch of the CEV and CLV. In this concept, the crew is seated in the CEV with their heads pointed to the east to eliminate a CLV roll maneuver otherwise needed on lunar missions to put the crew in a heads-down orientation during ascent. The heads-down orientation is required for the crew to see the horizon when looking out the side windows. With the crew seated with their heads to the east and the Launch Complex-39 having its service structure to the north of the CEV and CLV, moving the side hatch to the +Y side of the Crew Module minimizes the length of the access arm that provides access to the CEV on the launch pad. Figure 4.2-4 provides the CEV and CLV orientation relative to the baselined launch pad concept.

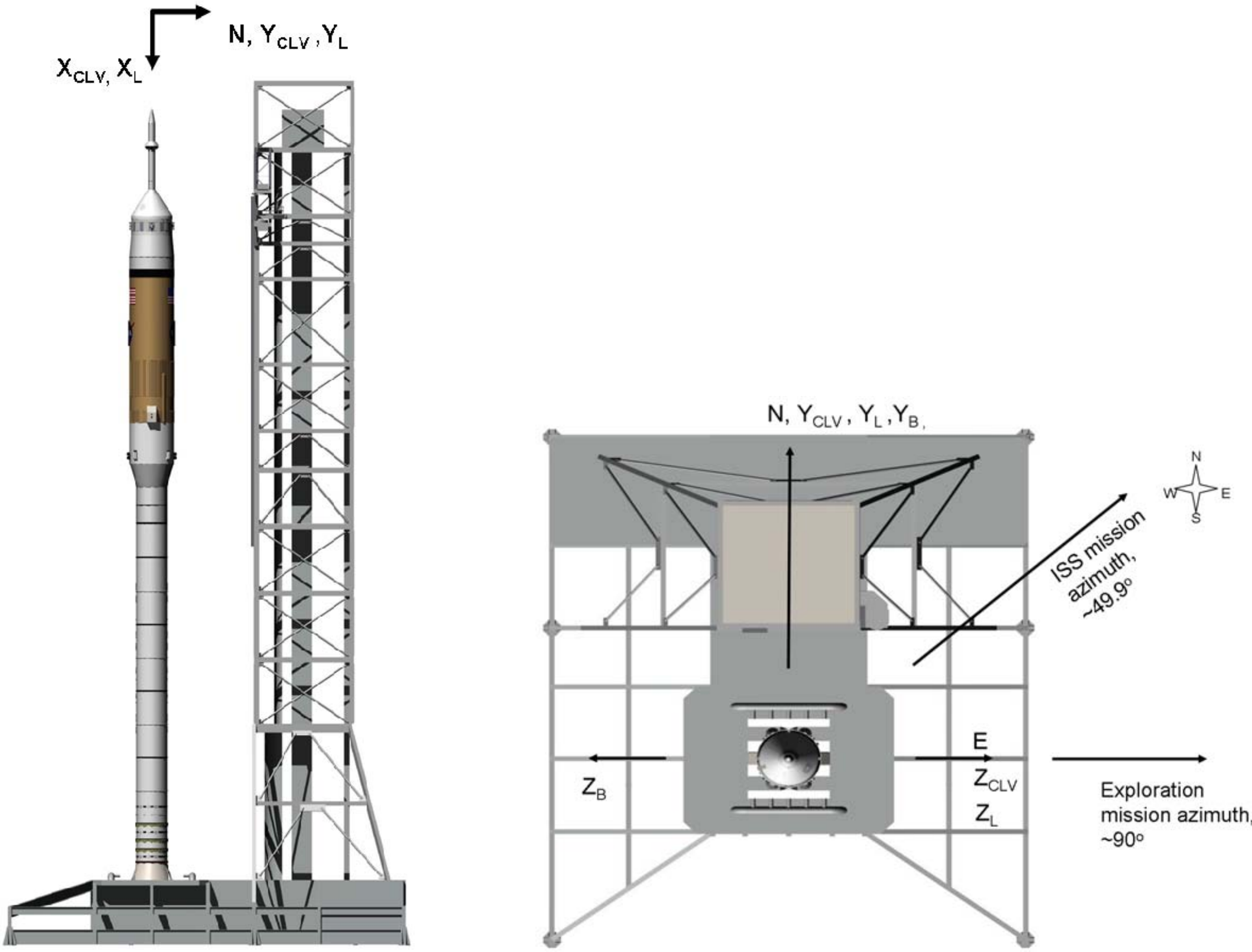

Figure 4.2-4 CEV Orientation for Launch

The forward hatch located near the vehicle apex is used nominally for pressurized transfer between the LSAM or ISS and CEV rather than the side hatch. The forward hatch is circular, approximately 32 inches in diameter, and is fully removable in-flight. Like the side hatch, the forward hatch can be opened from either side of the hatch. It also provides a secondary egress path from the vehicle.

Figure 4.2-5 illustrates the Crew Module windows and hatches.

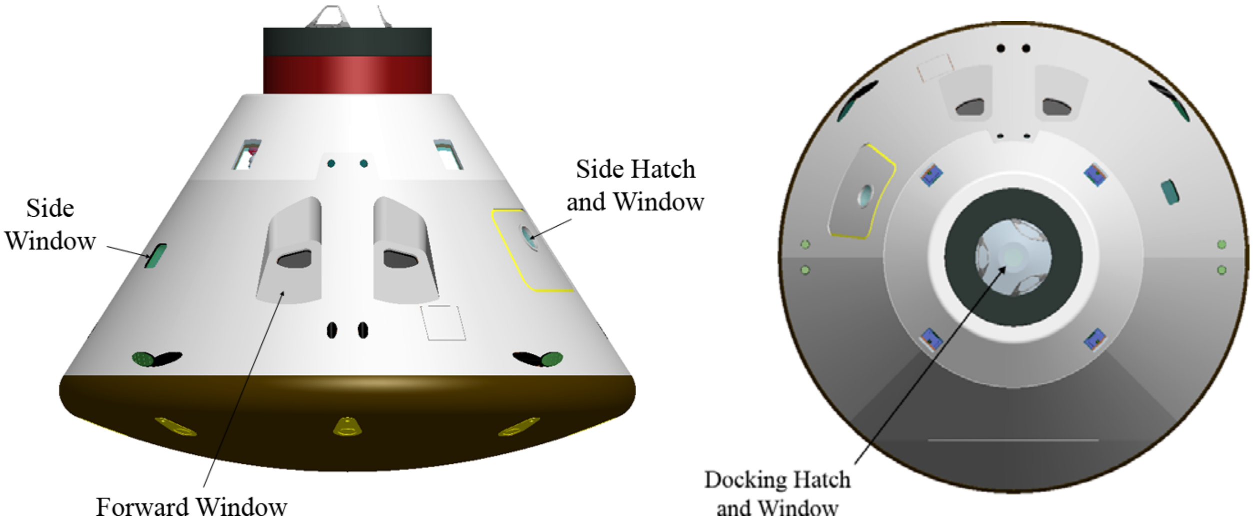

Figure 4.2-5 CM Window and Hatch Locations

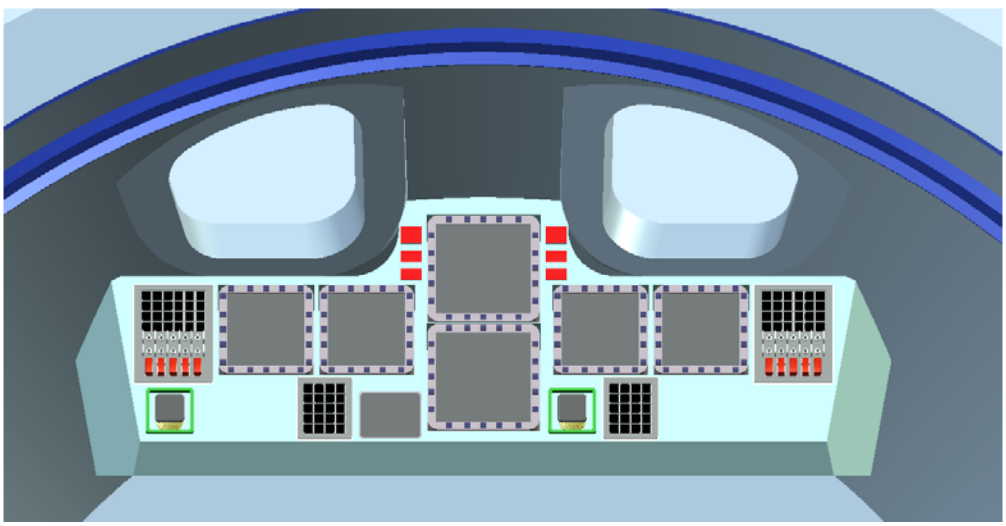

Figure 4.2-6 View Through the Rendezvous Windows

4.2.4 Earth Landing

The Crew Module utilizes three separate systems for attenuating energy associated with Earth landing: a parachute system, a retrorocket system, and seat struts. Landing may occur at one of several Western CONUS sites currently under consideration or in the water following an aborted ascent or entry.

The parachute system slows the CM from a nominal velocity of 600 ft/s at 44,000 feet mean sea level (MSL) altitude to 24 ft/s at touchdown. The CM parachute system is a scaled-up version of the Apollo parachutes in that two mortar-deployed drogue parachutes initially slow the vehicle to an appropriate deployment condition for the main parachutes. After the drogues are released, three mortar-deployed pilot parachutes extract the main parachutes. Main parachutes deploy at a dynamic pressure of 30 psf and 10,000 ft MSL (185 ft/s) and decelerate the vehicle to its nominal terminal velocity of 24 ft/s at 4,000 ft MSL. In the event of a chute failure, the terminal velocity under two working chutes increases to 29 ft/s.

The chosen landing system for the Crew Module includes four horizontal and four vertical retro-rockets for attenuating the energy remaining for a safe landing after the parachutes have slowed the vehicle to its 24 ft/s terminal velocity condition. Prior to touchdown, the CM base heat shield is jettisoned and the CM RCS reorients the vehicle for the –Z axis to point in the direction of wind drift. The Crew Module hangs from the parachutes at an angle of -20° so the –Z half of the vehicle impacts the ground first. This configuration (toe-in) allows for greater stability against roll-over with high horizontal wind speeds. Four horizontal retrorockets at the –Z shoulder are used to attenuate horizontal velocity, and four vertical retrorockets, two each on the +Y and –Y sides, are used to remove residual vertical velocity left from the parachutes. The vertical retro-rockets nominally slow the vehicle to from 24 ft/s to 5 ft/s and crushable structure at the base of the Crew Module pressure vessel attenuates the remaining energy upon touchdown.

A water up-righting system is also included in the CEV Crew Module to assure proper vehicle orientation in the event of a water landing. The CM has two possible stable orientations while floating in water: one with the CM X-axis perpendicular to the water surface and the docking hatch out of the water (preferred), and the other with the docking hatch submerged and the X-axis oriented approximately 45° to the surface. The up-righting system allows the vehicle to rotate to the preferred orientation for safe vehicle and crew extraction by recovery forces.

4.2.5 CM-SM Umbilical

Power, data, and fluids are shared between the CM and SM through an umbilical that connects the modules from launch until separation just prior to the CM entering the atmosphere. The CM-SM umbilical includes wiring to exchange power and data, fluid lines to pass propylene glycol-water thermal control fluid from the CM to the SM and return to the CM, and fluid lines to transfer high pressure oxygen and nitrogen from their storage tanks on the SM to the CM. The umbilical is located opposite from the rendezvous windows. During the CM-SM separation procedure, a guillotine mechanism of the SM portion of the umbilical severs the umbilical wiring and tubing near the CM outer mold line, and the umbilical hardware remains with the SM to be disposed.

4.2.6 Docking

The CM includes provisions for accommodating two different docking mechanisms depending on the mission being performed. A docking mechanism is used for physical attachment to other architecture elements, commodity transfer (e.g., power) between elements, and pressurized crew transfer between elements. Following conclusion of the ESAS study, the CEV was envisioned to use a single docking mechanism, the Low Impact Docking System (LIDS), for all missions. However the agency decided that given the limited number of Shuttle flights remaining prior to its retirement, it could not devote one or more Shuttle flights to delivering LIDS-compatible docking adapter to ISS. When CEV is operational, the ISS will have two ports available for CEV docking – Node 2 Forward and Node 3 Nadir. These locations will have Pressurized Mating

Adapters (PMAs) outfitted with the Androgynous Peripheral Assembly System (APAS) currently used for Shuttle Orbiter docking. A LIDS-compatible ISS would require either new PMAs with LIDS mechanisms or new APAS-to-LIDS adapters attached to the on-orbit APAS mechanisms. The design team received guidance from the CEV Project Office to develop a CM concept capable of utilizing either mechanism. While APAS and LIDS are similar in scale (LIDS is smaller) and appearance, there are several key differences between the two including capture technique and fault tolerance that require careful consideration. The two mechanisms are illustrated in Figure 4.2-7.

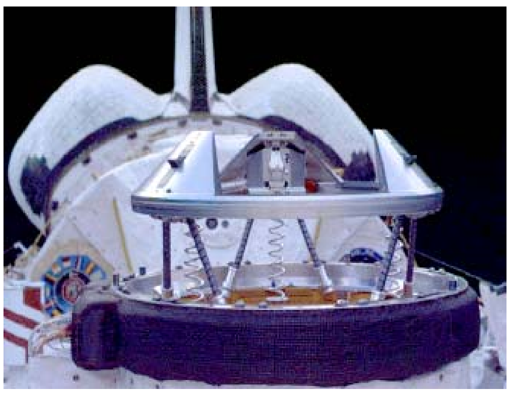

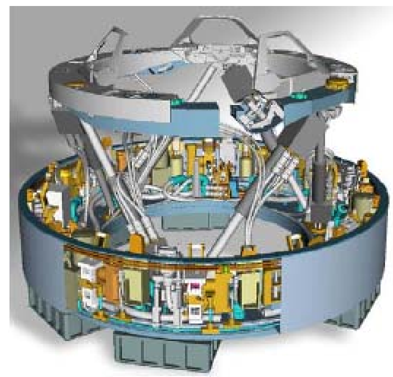

Figure 4.2-7 CM Docking Mechanisms: APAS (left) and LIDS (right)

The docking mechanism is jettisoned from the CM prior to entry for a nominal ISS mission, during LSAM Ascent Stage undocking for a lunar mission, or during LAS-CM separation following a LAS abort. Doing so has many advantages. It reduces the entry and landed mass of the CM, which reduces the necessary mass of the thermal protection, reaction control, recovery, and landing systems. Removing the LIDS mechanism during a lunar mission reduces TEI propellant and SM propulsion system mass. It also increases the CM's Xcg offset for entry, which increases pitch stability, and allows for a greater -Zcg offset by eliminating mass off the vehicle centerline. Jettisoning the docking mechanism means that it must be replaced for every flight, though.

In parallel with regular CRC design activities, the CEV Project Office is examining alternatives for delivering an APAS-to-LIDS or CBM-to-LIDS adapter to ISS using the capabilities of the CEV-CLV system. This would alleviate the need for the CM to accommodate multiple docking mechanisms and would allow for reliability growth on the LIDS system prior to engaging in lunar missions. The results of those trades will be reviewed prior to the CEV System Requirements Review in mid- to late-2006.

5.0 Service Module Overview

The function of the Service Module (SM) is to provide major translational maneuvering and attitude control capability, power generation, and heat rejection for the CEV. The Service Module has an integrated pressure-fed nitrogen tetroxide (NTO) / monomethyl hydrazine (MMH) orbital maneuvering and reaction control system to perform CEV-required propulsive maneuvers during its mission. For ISS missions, this includes rendezvous and docking with the ISS, the subsequent deorbit maneuver at the end of the mission, and self-disposal following separation from the Crew Module. For lunar missions, the required propulsive maneuvers are rendezvous and docking with the LSAM in Earth orbit, a plane change maneuver needed prior to lunar ascent, trans-Earth injection, post-TEI trajectory correction maneuvers, and disposal. A single 10,000 lbf main engine and twenty-four 25 lbf RCS thrusters are included to provide the thrust needed for these maneuvers. The Service Module propellant tanks are sized to perform up to 6,037 ft/s of ΔV with the Crew Module attached and 49 ft/s of ΔV after separation. In the event of a late ascent abort off the Crew Launch Vehicle, the Service Module propulsion system may also be used for separating from the launch vehicle and either aborting to near-coastline water landings or aborting to orbit.

Two deployable, single axis gimbaling solar arrays with 372 square feet of deployed area per wing are included with the SM to generate the necessary CEV power from Earth orbit insertion to CM-SM separation prior to entry. The Service Module distributes electrical power generated by the solar arrays to the CM and to its own internal loads. The SM also includes high pressure oxygen and nitrogen storage needed to provide a habitable environment for the crew. Oxygen and nitrogen are drawn from these tanks over the course of the mission and are delivered to the CM life support systems. Finally, the Service Module primary structure provides load transfer between the CM and SA and a mounting location for radiator panels. These panels enable radiative heat rejection capability for the CEV fluid loop heat acquisition and transport system. The total radiator acreage on the SM exterior is 395 square feet.

The Service Module includes the following nine subsystems:

1) Active Thermal Control
2) Avionics
3) Electrical Power
4) Environmental Control and Life Support
5) Mechanisms
6) Passive Thermal Control
7) Propulsion
8) Pyrotechnics
9) Structure

<u>Physical Attributes</u>

- Height: 14 ft 9.7 in. (177.7 in.)
- Diameter: 16 ft 10 in. (202 in.)
- Launch Mass (4-crew Lunar): 30,496 lbm

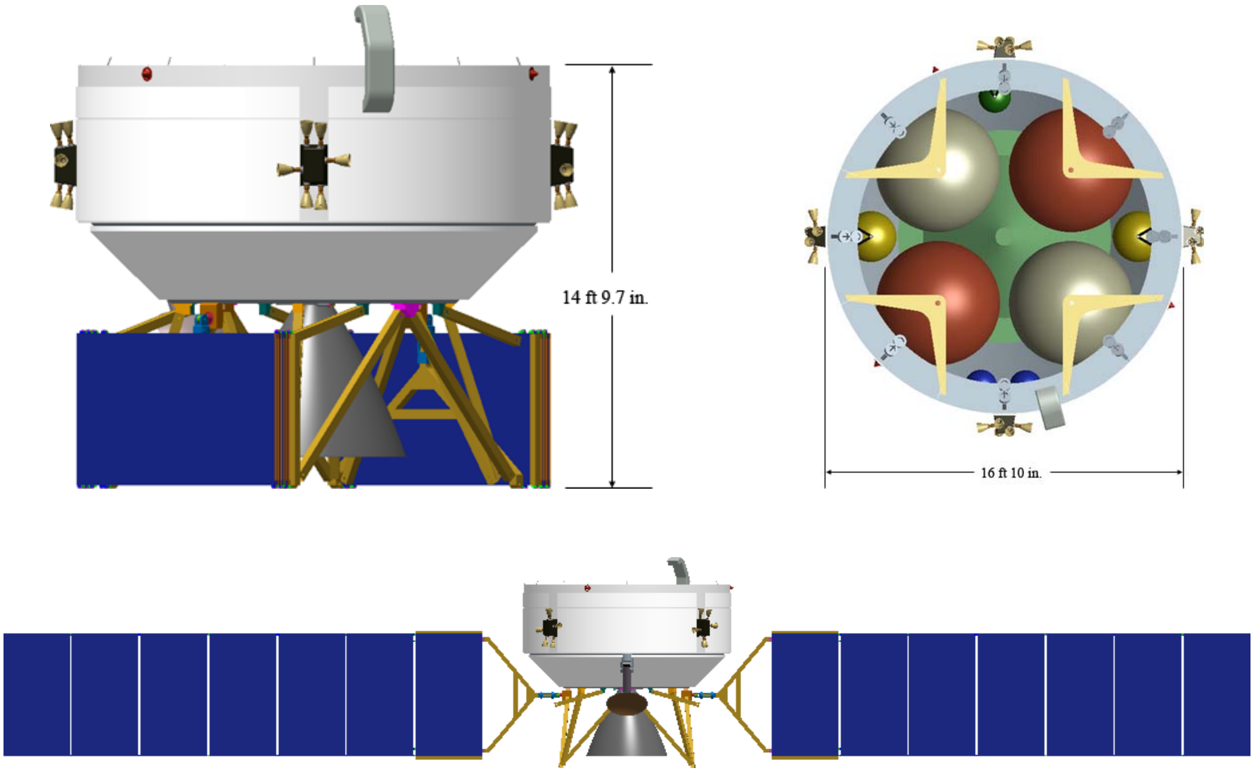

Figure 5.0-1 Service Module External Arrangement

5.1 Service Module Interior

The CRC-3 SM is a skin and stringer structural construction that provides for an unobstructed unpressurized internal volume (see Figure 5.1-1). This contrasts with the Apollo SM which had an alternate construction for load transfer and stiffness – its interior was intersected by six shear webs that transferred the primary loads between the CM and SLA. With the CRC-3 SM that function is served by the external SM skin and longerons.

The SM interior as currently envisioned provides mounting locations for electrical power system (EPS) and avionics controllers, and fluid storage tanks for the propulsion and environmental control and life support (ECLSS) systems. Two NTO and two MMH spherical tanks for bulk storage of translational and attitude control propellant occupy the majority of the SM's interior volume. The titanium-constructed tanks store 20,500 lbm of total usable propellant and sit on a tank support ring on the aft end of the SM. The tanks are attached to the SM sidewall by L-shaped supports at the forward tank domes. A series of five cylindrical, high-pressure, composite-overwrapped tanks mounted to the SM sidewall then occupy the space between the propellant tanks. Two gaseous oxygen tanks and one gaseous nitrogen tank supply life support gases to the CM pressure control system. These tanks are identical in size and construction. The remaining two tanks provide gaseous warm helium storage for pressurizing the propellant tanks – one tank supports NTO and the other MMH.

Other components attached in the SM interior volume are avionics and EPS equipment, including:

- Array Regulator Units (EPS)
- S-band and Ka-band Electronics (Avionics)
- Batteries (EPS)
- Ground Support Equipment Heat Exchanger (ATCS)
- Pyro Controllers (EPS)
- Primary and Secondary Power Distribution Units (EPS)
- Thruster Control Units (EPS)
- Data Acquisition Units (Avionics)

All boxes are mounted to the SM external skin with the exception of the Secondary Power Distribution Units (SPDUs), Thruster Control Units (TCUs), and Data Acquisition Units (DAUs). These boxes require active cooling and are mounted to structural cold plates, which are in turn mounted to the external skin.

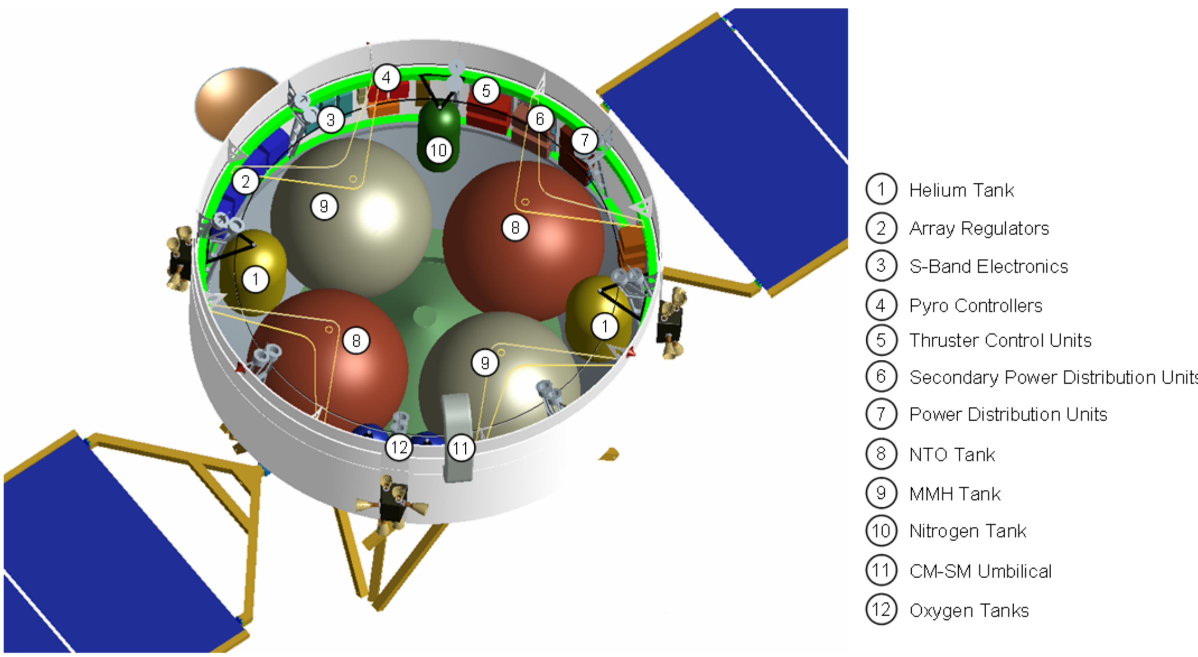

Figure 5.1-1 SM Interior Equipment

Power and data wiring and oxygen, nitrogen, and propylene glycol/water fluid lines from the SM interior are routed to the CM-SM umbilical for commodity exchange between modules.

5.2 Service Module Exterior

The SM exterior can be divided into two sections: a forward, cylindrical section, and an aft, conical section. The Spacecraft Adapter mates with the SM at the intersection of the cylindrical and conical sections.

The forward cylindrical section is the primary load-bearing and load-transfer portion of the SM structure. It is constructed from composite skin panels spanning between eight short longerons, and two ring frames to tie together the overall structure. The load path between the CM and the SA is the CM-SM tension ties near the SM perimeter, through the longerons and skin of the cylindrical section, and to the SA at the SM-SA attachment ring. As the tension ties are located slightly inboard of the perimeter and thus a short conical structure is needed, a cylindrical fairing is included at the top of the SM to provide a smooth aerodynamic transition between modules.

The structure of the forward section is primarily covered with radiator panels to reject heat from the CEV ATCS. Four pods of six 25 lbf RCS thrusters each are mounted to the structure between radiator panels on 90° intervals, and are mounted on the Y and Z axes. Each pod includes four ±X thrusters and two ±Y (or ±Z, depending on the pod) thrusters. The four pods provide two fault tolerant 6-DOF control.

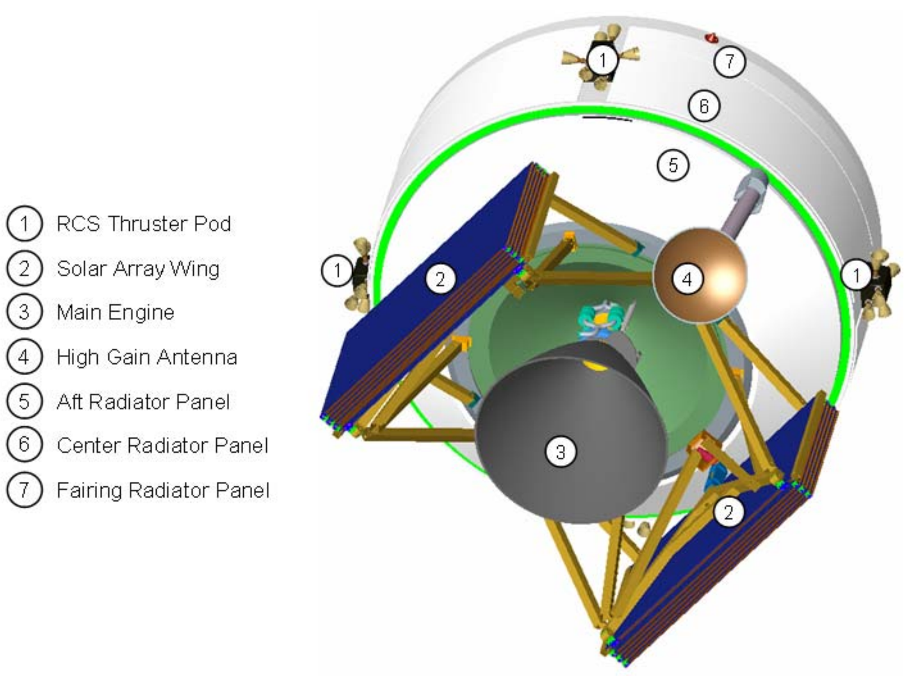

Figure 5.1-2 SM Exterior Equipment

Below the SM-SA attachment ring, two conical structures in the SM aft section provide load paths and attachment points for the propellant tanks and main engine. The inverted outer tension cone extends from the attachment ring downward to a tank support ring, upon which sits the weight of the SM propellant tanks. A high-gain S-/Ka-band antenna is also attached to the outer cone along with two solar array wings and a conical ATCS radiator panel. The antenna and array wings are stowed within the volume enclosed by the SA for ascent load protection, and are deployed shortly after the CEV separates from the SA. Both remain deployed for the remainder of the mission.

At the tank ring, the inner tension cone extends upward toward the vehicle centerline and provides attachment and load transfer for the CEV's single main engine. The main engine is an ablative, pressure-fed NTO/MMH engine capable of producing 10,000 lbf of thrust, and is closely derived from the AJ10-118K Delta II Upper Stage engine.

6.0 Spacecraft Adapter Overview

The Spacecraft Adapter (SA) is a simple conical structure used to structurally mate the CEV Service Module to the CLV Upper Stage and to protect equipment – a main engine, solar arrays, and deployable high-gain antenna – on the Service Module aft end during launch. The SA is a skin and stringer construction with intermediate ring frames for stiffness and forward and aft rings for attachment to the SM and Upper Stage, respectively. It also provides a smooth aerodynamic transition from the 16.5 ft (5.03 m) SM cylinder diameter to the 18.04 (5.50 m) diameter of the Upper Stage. Figure 6.0-1 illustrates the CRC-3 Spacecraft Adapter concept.

The Spacecraft Adapter includes the following four subsystems:

1) Mechanisms
2) Pyrotechnics
3) Structure
4) Wiring

Physical Attributes

- Height: 9 ft 5.3 in. (113.3 in.)
- Base Diameter: 18 ft 10 in. (220.4 in.)
- Launch Mass (4-crew Lunar): 1,149 lbm

Figure 6.0-1 Spacecraft Adapter External Arrangement

After ascent and Upper Stage engine shutdown, the CM sends a command to fire two redundant pyrotechnic linear shaped charges that run the circumference of the SA forward ring. This event severs the mechanical attachment between the SM and the SA as well as any wires passing between the CEV and CLV. The charges are redundant in that either charge can separate the modules and ignition of one charge will detonate the other. The CEV then maneuvers away from the SA and Upper Stage and performs the rest of its mission. The SA, meanwhile, remains intact and attached to the Upper Stage and is eventually disposed with it.

7.0 Avionics and Power

This section describes the CRC-3 trades, reference concepts, and mass estimates for the Avionics and Electrical Power Systems.

7.1 Avionics

The Avionics System provides the infrastructure through which most of the vehicle subsystems interact with one another, and external entities, via commanding, data transmission, and automatic processing. Avionics comprise these subsystems: command and data handling hardware, instrumentation, communication and tracking, display and control, and flight software. The reference architecture for these subsystems is presented here. Safety, fault tolerance, and redundancy management concerns, issues, and implementation design details are also provided in the following sections. The proposed avionics architecture design incorporates a 2-fault tolerant scheme for the Flight Critical Computers (FCCs) as well as providing redundancy capability up and downstream of flight critical components. Fault Tolerance (FT) and Redundancy Management (RM) coverage include Guidance, Navigation and Control (GN&C) computers, System Management/Display & Control/Communication & Tracking (SDC) computers, Data Acquisition Units (DAU), buses, sensors, and display and control human interfaces.

Command and Data Handling (C&DH)

The core avionics hardware consists of three highly-integrated FCCs that serve multiple functions, a Data Storage Unit (DSU), and FCC interconnecting data buses. Each FCC is partitioned into two distinct processing regions based on flight criticality and functionality. Each partition is electrically isolated from the other to provide containment of faults originating in one partition from propagating into the other. The most critical partition (GN&C) handles the guidance, navigation, and control processing. It processes only the information necessary to safely fly the spacecraft and keep the crew alive. The SDC partition handles all other processing required for systems management, crew display and control processing, communications & tracking functions, as well as other subsystem application processing. Also included within each FCC is an arbiter card that provides the means to communicate, share data, and vote amongst the FCCs. The interconnection between the arbiters is electrically isolated to help ensure Byzantine resilience and fault containment.

Instrumentation

Instrumentation is defined as the collection and processing of vehicle sensor information specified by CEV subsystems for use on the vehicle and ground.

Instrumentation consists of devices and sensors that measure specific parameters of physical phenomena such as pressure, temperature, vibration, acoustics, radiation, fuel flow rates, chemical content of gases, and structural flexing and bending. For vehicle health monitoring purposes, Instrumentation also includes the sensors that detect the state of each valve, actuator, switch, motor, rotator, mechanism, effector and anything else that can have more than one state.

Communications and Tracking (C&T)

The CEV Communications and Tracking system is comprised of the equipment and processes that enable the CEV to communicate with external elements and EVA. This includes transceivers/transponders, antennas and antenna electronics, audio and video equipment, communication outage recorder, etc. The C&T architecture also includes the crash survivable flight data recorder as of this writing. The Avionics C&T reference architecture is based on the February 3, 2006 version of the CEV SRD. Since then the C&T requirements for EVA communications and Ka-band are being reconsidered. Updates to the architecture will be made during the next analysis cycle based on the updated requirements.

Displays and Controls (D&C)

This displays and controls section encompasses devices intended for human interface with the avionic systems. It does not address mechanical human interfaces, such as hatch releases or seat adjustments. This section would address mechanical flight or system display devices used to supplement avionic systems, such as a mechanical attitude direction indicator, if such devices are required. This section addresses avionic devices such as primary and backup flight displays, hand controllers, caution and warning devices, keypads, and cursor control devices. Communication system components related to display and control, such as speakers for caution and warning or controls for the audio system, are covered in the communications and tracking section.

Flight Software

The flight software, running in the FCCs, and within embedded firmware controllers, provides the capability to command, control, and interface to the vehicle. The CEV Reference Avionic flight software that runs on each partition in the FCCs (the GN&C and SDC partitions) incorporates an embedded ARINC-653 compliant real-time operating system (RTOS), Board Support Package (BSP), and Arbiter interface software.

The GN&C partition also houses the GN&C application, Launch Abort System (LAS) application, and I/O interface software that drives the discrete, analog, and 1553 command and data interfaces.

The SDC partition also houses the System Management application, subsystems applications [D&C, C&T, Electrical Power System (EPS), Environmental Control and Life Support System (ECLSS), Propulsion, Active Thermal Control System (ATCS), Structures, Mechanisms, Pyros, Recovery, and Landing System)], and serial, discrete, analog, 1553 and 1394b I/O software.

7.1.1 Driving Requirements, Groundrules, and Assumptions

7.1.1.1 CEV Avionics Concept of Operations from MCC

General - The principle goals of CEV operation--performing a safe and successful mission--should be achievable with operational simplicity and a realistic degree of automation. Candidates for automation are those areas that require repetitive actions or that can be managed with fairly simplistic algorithms. Thus, it is hoped that most of the systems that have traditionally required heavy support from the Mission Control Center (MCC) can now be managed more efficiently using onboard applications. In order for this to work, there must be efficient monitoring and control interfaces between the onboard and ground applications. Of course, this does not negate the need to provide for direct crew action to respond to contingencies by whatever means necessary.

<u>Monitoring</u> - All critical parameters must be monitored onboard and on the ground simultaneously. In addition, routine management of onboard systems should be done by onboard and/or ground applications. In order for this to happen, the onboard and ground applications must be able to acquire the data needed to do their jobs. The infrastructure for acquiring data has been suggested by the C3I architecture team. This architecture provides a great deal of flexibility in customizing what data is being selected for onboard computation or for downlink. A certain degree of flexibility is important, whether the data formats end up rigidly defined or completely subscriber-based as some would propose.

<u>Commanding</u> - Ground control of onboard systems should be accomplished by way of the onboard applications. That is, the onboard applications will provide basic, routine management, such as closed-loop control, mode switching, limit monitoring, and reaction to expected exceedances. The ground would provide operational updates in the form of specified inputs to the onboard application, such as adjustments to operational limits, mode overrides, and computation corrections. There could also be a need for direct end-item commanding, where onboard applications may not be the most efficient means of control.

<u>Routine Operations</u> - It is anticipated that most routine system operations could be controlled by onboard applications. However, some types of systems may not have a “one size fits all” operation that is amenable to algorithmic control. There should be methods of ground control utilizing tools such as configuration files, schedule-related tools, time tagged files, and control tweaks (or software table maintenance). These products can be pre-planned and uplinked as required to achieve operational efficiency without crew interaction. However, the use of these tools should be carefully considered so as not to drive heavy ground support requirements.

<u>MCC Tools</u> - Flight Controllers will be using tools such as data monitoring displays, uplink file/command building displays, modeling displays, and interactive displays that will combine two or more of the above features. MCC displays will provide any required conversion between the user interface and the onboard application software interface.

7.1.1.2 Avionic System Drivers

The key CEV SRD and HSIR driving requirements for the CEV Avionic System can be described as fault tolerance and reliability, automated and autonomous operation, manual control capabilities, emergency entry mode, communications and interoperability. A summary of the key Avionics requirements are given below.

- Requirements for Fault Tolerance and Reliability
  - Two-fault tolerant for catastrophic hazards except for areas approved to use Design for Minimum Risk (DFMR) criteria
  - No single event or failure cause can eliminate more than one means of fault tolerance (i.e., the methods will have no common failure mode)
  - Provide a probability of 0.99999 (TBR-002-066), with the 90% confidence of no latch up, burn up, or other permanent failures due to single event effects …

  - Provide a probability of no functional ("soft") interrupts for avionic systems of 0.99 (TBR-002-037), per maximum duration mission within the single event effects …
  - The CEV shall provide protection from the effects of software common cause failures during the dynamic phases of the mission, when failure of a system function results in loss of life or loss of vehicle
  - The CEV shall fail safe in the event of software loss of output
- Requirements for Automated/Autonomous Operations
  - Automated ascent aborts, separation, and targeting of landing locations
  - Automatic execution of rendezvous, proximity operations, and docking for both nominal and abort conditions
  - Automated separation, proximity and departure operations
  - Return the crew to Earth with no communication with MPTFO during all mission phases
- Requirements for Manual Control
  - Crew override/inhibit of autonomous/automatic functions
  - Initiation of critical functions
  - Interfaces for manual vehicle control
- Requirement for Emergency Entry Mode
  - Provide emergency entry mode, terminal descent and landing without the use of primary systems for either power or attitude control
- Communications and Interoperability
  - Communicate using the data link and data protocols specified in CXP-00101 Constellation Command, Control, Communication, and Information (C3I) Interoperability Specification
  - Transmit real-time broadcast quality motion imagery and audio to the MPTFO element
  - Support of nominal data rates of 72 kbps/192 kbps during launch, ascent, and entry

7.1.1.3 Communications and Tracking Additional Drivers

There are several additional key CEV C&T driving requirements in the CARD and the CEV SRD. The requirements specify an S-band System, a Ka-band System, a Prox Ops System using IEEE 802.16e, and a Rendezvous Communications and Tracking System. There are requirements for the transfer of broadcast quality motion imagery, private crew audio, and Space Network signal formats. The driving requirement to comply with the Constellation Communications, Command, Control and Information (C3I) Interoperability Specification results in the need to support

Internet Protocol, Quality of Service, and other formats and protocols. The encryption algorithm baselined in the CEV SRD is the Advanced Encryption Standard (AES). The requirements in the CARD and the CEV SRD call for the CEV communication system to support radiometric tracking for obtaining range and range rate measurements.

The communication requirements by mission phase are given by the CEV SRD requirement CV0362, Table 4. This requires the CEV to transmit 192 kbps and receive 72 kbps to/from Mission Systems during launch, ascent, entry and post-landing. There are also requirements for the CEV to transmit 24 kbps and receive 18 kbps in any attitude for contingency/off-nominal communications.

There were several discussions on the criticality of the C&T system. There are requirements in the CARD and CEV SRD for autonomy and autonomous operations, crew return to earth with communication with Mission Control, so the question came up as to whether C&T was a mission-critical or safety-critical function. This discussion was taken to the Constellation Operations Panel on February 7, 2006. The communication functions by mission phase were discussed and it was determined that for all mission phases except the lunar orbit, lunar surface operations, and lunar rendezvous and docking cases, C&T was mission-critical, i.e., requiring single fault tolerance. For the lunar case, when the LSAM is relying on the CEV/Mission Control for CEV range, range rate, and bearing information, the integrated C&T system is safety-critical, requiring two-fault tolerance. Therefore the CEV reference architecture has three strings of C&T equipment to support the integrated two-fault tolerant requirement. The fault tolerance is met by two strings of S-band equipment and a single string of Ka-band equipment.

7.1.1.4 Displays and Controls Additional Drivers

At this writing, the project is in the very early stages of developing display and control requirements. Extensive work remains to be done, to define some critical requirements of the display and control subsystems, including:

- The number and size of displays required.
- The type of navigation devices desired (edge keys, cursor controls, etc.).
- A display and control-specific concept of operations and a task analysis.
- An evaluation of tasks as they relate to hardware redundancy (for example, if all critical tasks can be done on one display, the requirement for two-fault tolerance may drive a requirement for three displays).

Since the Cockpit Working Group is still developing detailed requirements, some preliminary requirements were developed by the Cockpit Working Group during this effort:

- Two workstations (a result of SRD requirements).
- Six aviation-style displays, arranged in two rows of three spanning across the two operator workstations. (Note: this requirement, in particular, is likely to change; that may have a significant impact on power, mass, volume, and avionic design.) Since the conclusion of CRC-3, the CWG recommendation for quantity, layout, and size of displays has

changed. Future work will involve assessment of Lockheed Martin's baseline three-display concept and a four-display concept.

- Edge keys for display navigation.
- Two 3-degree-of-freedom hand controllers per workstation.
- One aviation-style keypad (i.e., not a QWERTY keyboard) per workstation. (Note: this requirement is also under review to determine if a keyboard is required.)

Specific driving requirements from the SRD for the D&C subsystem include:

- The capability to operate in flight in an unpressurized state for not less than 120 hours.
- Allow control by a single crewmember, with ability to perform all CEV system functions.
- Redundant crew workstations to perform all CEV system functions.

7.1.2 Conceptual Design Overview

Figure 7.1-1 depicts the reference avionic architecture schematic.

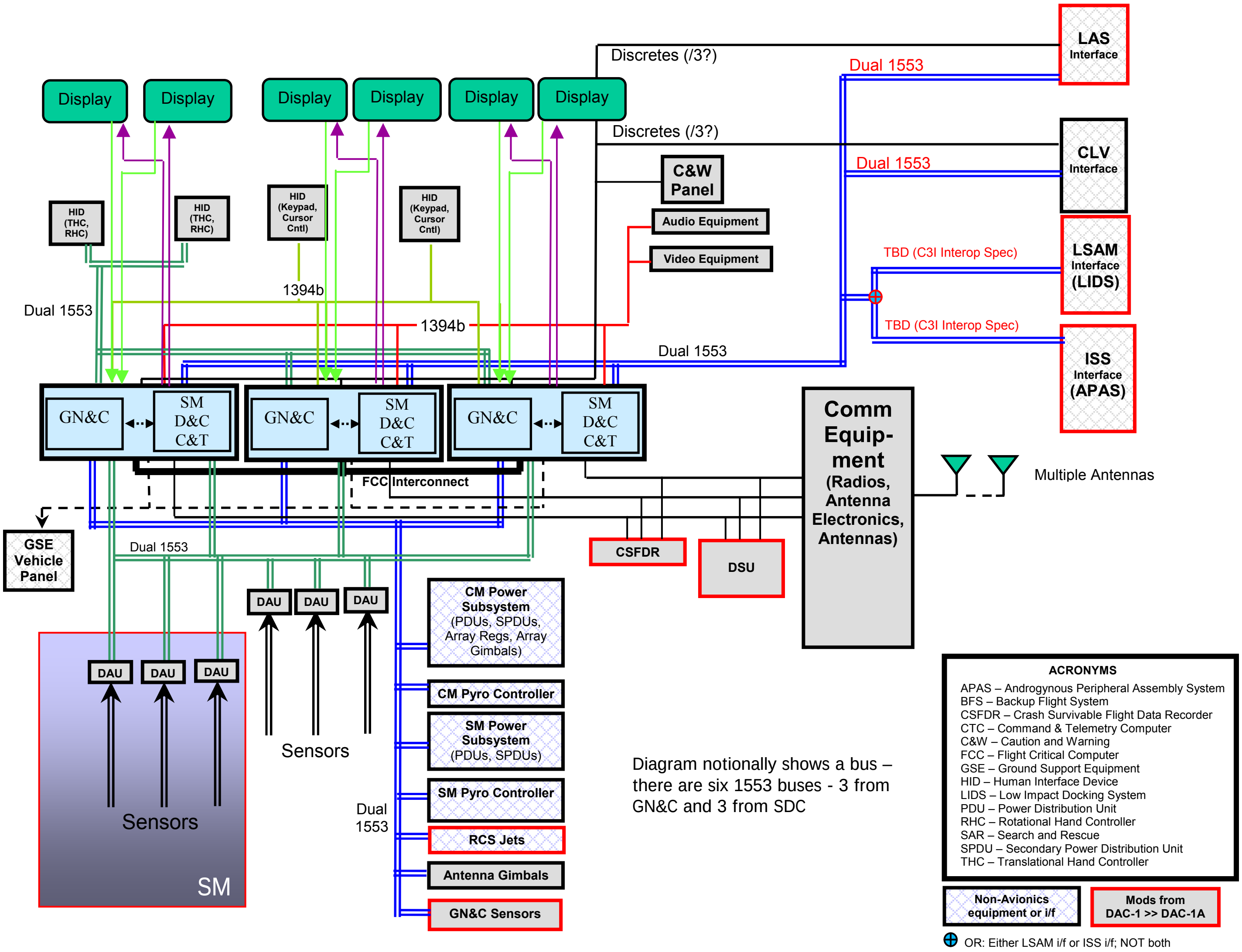

Figure 7.1-1 CEV Reference Avionics Architecture – DAC-2

The Avionics team considered several architectural options, but when evaluated as to how well they satisfied the driving requirements, the following option was selected for the baseline: **Byzantine Resilient using arbiters with integrated BFS and manual pass-through**. This option is a Byzantine resilient computer topology that partitions safety critical functions from other functionality. It also provides the capability for a Backup Flight System. Data acquisition will be accomplished via six Data Acquisition Units (DAUs), three located in the Crew Module and three located in the Service Module. One of the drivers for three DAUs per module was the need to provide dual fault tolerance.

7.1.2.1 Command and Data Handling

Flight Critical Computers (FCCs)

The FCCs are conduction-cooled chassis utilizing ruggedized 6U-size computer boards connected to a common Compact PCI backplane. Most of the hardware components are ruggedized COTS, based on commercial industry standards, but have specific design features to make them more reliable and fault-tolerant (e.g., watchdog timers, error detection & correction, etc.). In bounding our solution, this avionic architecture could be implemented using a completely radiation-hardened solution, or a COTS-based solution with appropriate software fault-detection, isolation & recovery (FDIR) provisions.

Each FCC is partitioned into two distinct processing regions based on flight criticality and importance. Each partition is electrically isolated from the other to provide containment of faults, i.e., faults originating in one partition are prevented from propagating into the other. Both partitions are housed in the same chassis (a.k.a. FCC), but share the common backplane. This thirteen-slot backplane actually contains separate backplane buses for each GN&C and SDC partition and thus the signals are physically and electrically isolated from each other, but they are fabricated on the same board. A common connector staging area is provided on the backplane for the internal I/O wiring harness. The three FCCs are mounted on cold plates inside the Crew Module. Figure 7.1-2 provides a functional depiction of the FCC.

The FCC chassis contains redundant 28-volt input power supplies that power all computer cards in a load-sharing arrangement. The input power feeds come from different power buses, and the supplies must be sized such that one power supply alone can provide adequate power to the entire FCC. A hard short-circuit in one processing partition also will not short the other partition.

GN&C Partition

This most critical partition handles the guidance, navigation, and control processing. It processes only that information necessary to fly the spacecraft safely and keep the crew alive. The intent is to keep this partition relatively simple and isolated from the rest of the vehicle's functions. This partition consists of a dedicated processor board (based on the PowerPC 750FX capability) with a two-channel MIL-STD-1553 daughter card, as well as a digital discrete and analog input/output card, and a custom-designed arbiter card.

SDC Partition

The SDC partition handles all other processing required for systems management, crew display and controls processing, and communications and tracking functions, in addition to other subsystem application processing. A similar PowerPC 750FX-based processor board is used, possibly the same one as in the GN&C partition. A digital discrete and analog input/output card and the custom-designed arbiter card are also included in this partition.

Arbiter and Interconnection Scheme

This arbiter card provides the means for the FCCs to communicate, share data, and vote amongst each other. The interconnects between the arbiters are electrically isolated to help ensure Byzantine resilience and fault-containment.

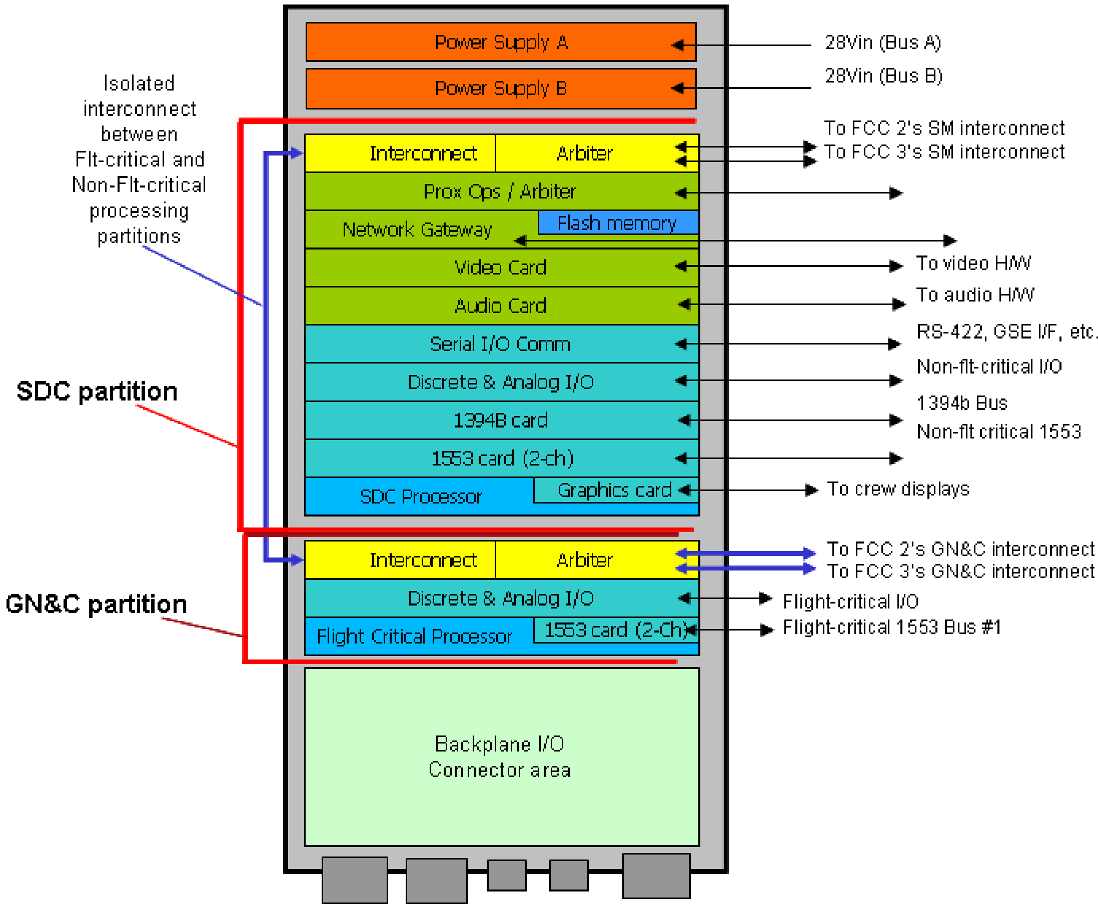

Figure 7.1-2 Functional Description of Each Flight Critical Computer

Data Storage Unit

A common Data Storage Unit (DSU) is included in the avionics architecture for recording long-term data to permanent memory. This may include motion imagery data, auxiliary data, etc. This also serves as the communication outage recorder. The DSU is considered non-flight critical hardware, so only one unit is provided on CEV. The current design approach utilizes a five-slot backplane, hosting 6U-size cards, with a single power supply. A processor card with a redundant MIL-STD-1553 daughter card is provided, along with a 1394B card, two Flash memory cards, and a motion imagery processing card. The data storage capacity has not been sized yet, but it is assumed to be in the tens- to hundreds- of Gigabytes range. All three FCCs have a direct connection to the DSU via the 1553 or 1394b bus. Figure 7.1-3 depicts the DSU.

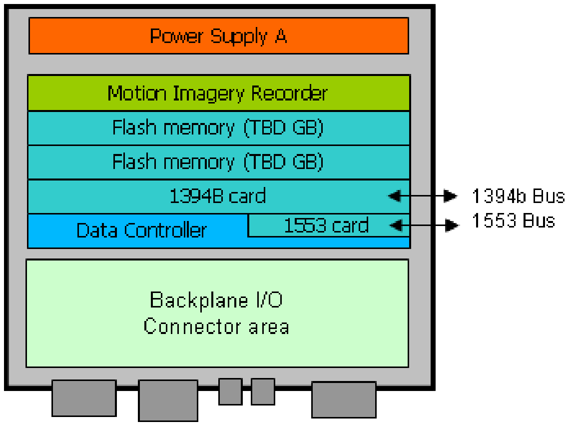

Figure 7.1-3 Functional Description of the Data Storage Unit

External Environmental Considerations

The hardware implemented must be able to survive in the space radiation environment. Three factors that must be evaluated are total ionizing dose, permanent latch-up failures, and single-event-upsets. The total ionizing dosage is not an issue for COTS in LEO and LLO environment. Permanent failures due to ionizing radiation must be a low probability, and this is possible with COTS components. The existing requirement for high probability of no functional upset during the entire mission duration is unlikely to be achieved with COTS hardware. This was demonstrated with the Space Shuttle Cockpit Avionics Upgrade project where the mean time to functional interrupt (MTTFI) was 41 days.

For Requirements Analysis Cycle-1 (RAC-1) an analysis task was initiated to realistically define the requirement for no functional upset. The analysis studies the critical mission phase durations and establishes high probability of no functional interrupt for those critical flight phases. The new requirement would lower the overall mean time between failures (MTBF) of the components, but would maintain a high POS. The analysis completes in June and the SRD will be updated.

C&DH Design Considerations

The FCC architecture fits into three chassis and remains two-fault tolerance. Partitioning the flight-critical from the non-critical processing yields a good fault-containment and design approach. This architecture utilizes COTS hardware standards for most boards. On the other hand, this FCC concept requires a large volume, generates a lot of heat, and uses bigger power feeds. The weight of the large FCC chassis is underestimated. It is becoming obvious that 49 pounds is too light for a chassis this size. The next analysis cycle will refine the size & mass estimates. The number of I/O signals, internal and external wire harnesses, and chassis connectors may be too great to fit them all on the FCC chassis and we may need to separate each FCC into two chassis. Custom design and development of the FCC Arbiter board is required since currently no existing board can provide this function.

7.1.2.2 Instrumentation

The major components of the CEV Instrumentation system are the sensors (typically provided by the using subsystems) and the Data Acquisition Units (DAUs). The DAUs are connected to the FCCs via dual redundant MIL-STD-1553 busses and have different I/O boards added for different sensor requirements (voltage range, single-ended vs. differential, analog vs. digital, etc.). The DAU I/O processor can also run algorithms on data if desired (e.g., digital filtering) prior to sending data to FCCs.

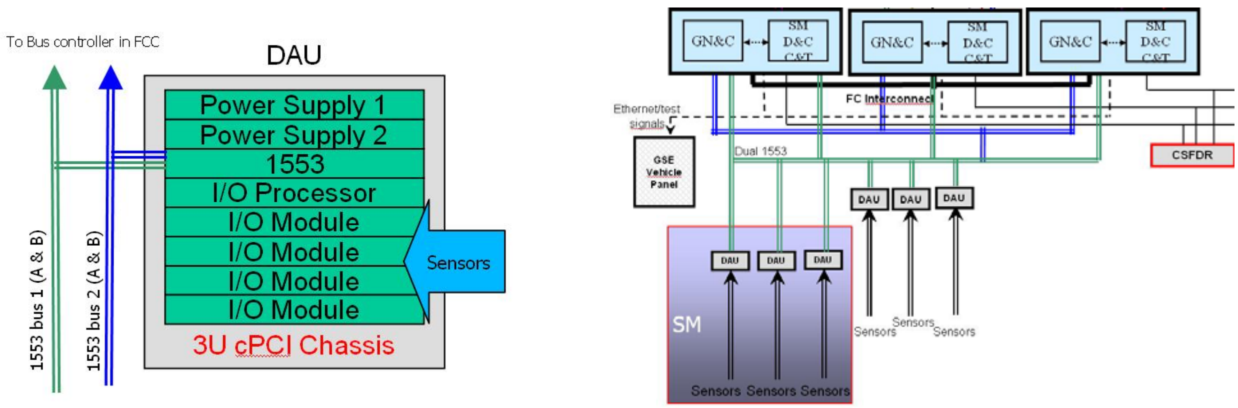

Figure 7.1-4 CEV Instrumentation Architecture

Instrumentation data is provided from the CEV subsystems in various formats, including analog voltages, discrete signal levels (on/off, high/low), serial digital data (e.g., RS-422), hard-wired bus-compliant data (e.g., MIL-STD-1553, IEEE 1394), or wireless data (e.g., IEEE 802.11).

The CEV Instrumentation system must collect all types of data and provide appropriate excitation, signal conditioning and processing to provide valid time-tagged data to the vehicle flight computers for further data processing and recording.

7.1.2.3 Communications and Tracking

The CEV C&T System is given in Figure 7.1-5 and is made of four main communication links:

- Space-to-Ground (Mission Control) link
- Prox Ops Link
- Rendezvous Link
- Search and Rescue Links

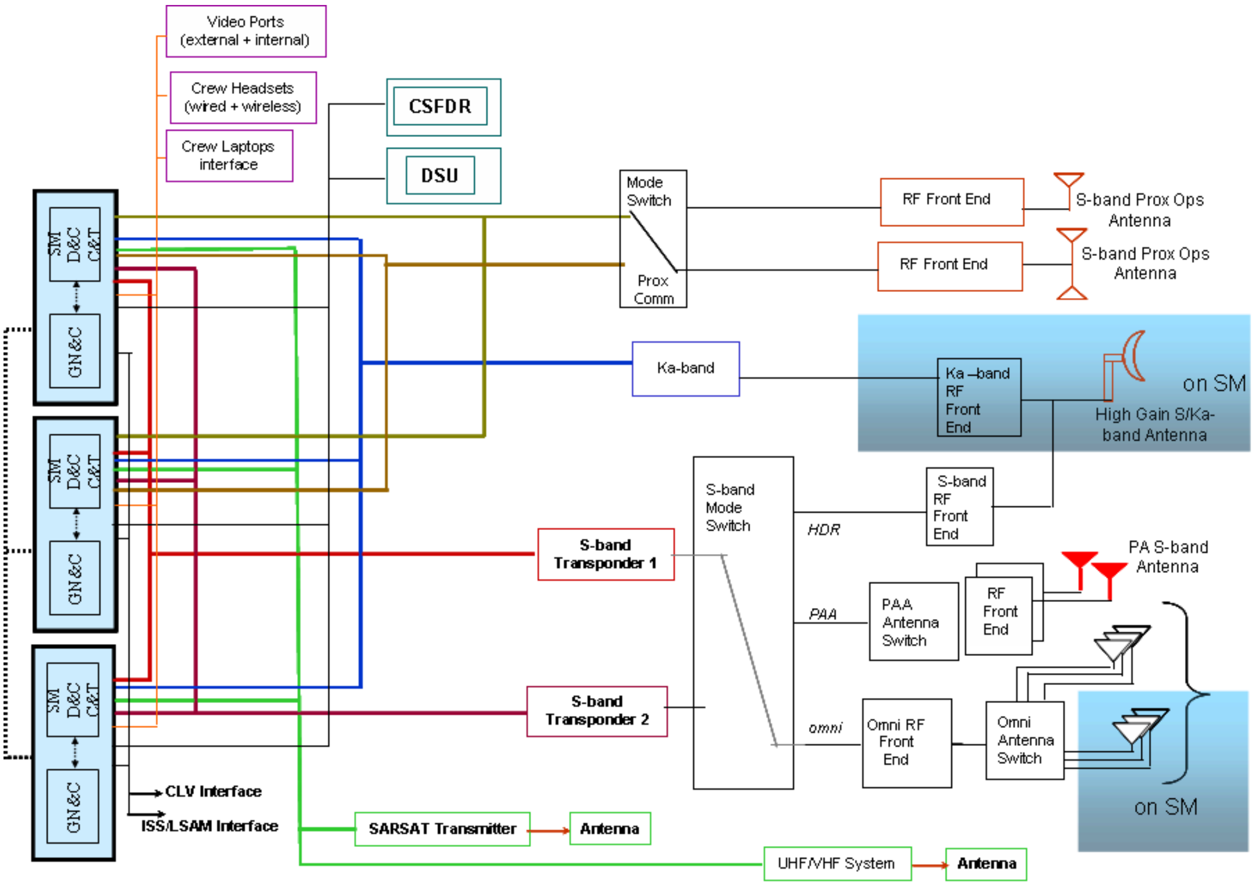

Figure 7.1-5 CEV C&T Reference Architecture – DAC-2

Communications Links

Space-to-Ground links

These (S-band and Ka-band) links provide data between the CEV and Mission Control. Based on the mission phase, it is either a direct link between CEV to ground or data is relayed through TDRS (Tracking and Data Relay Satellite) to ground. This link is used for commands, file transfer, motion imagery, telemetry, audio, etc. The S-band link also supports radiometric tracking to support tracking.

There are three data rates specified for the S-band link (in the CARD and the CEV/MS IRD; data rates were taken out of the CEV SRD). The nominal data rates are 192 kbps receive and 72 kbps transmit. The high data rate is 1 Mbps transmit and receive. The contingency, any attitude communication data rates are 24 kbps transmit and 18 kbps receive.

Prox Ops Link

Requirements for the Prox Ops link are:

- Provide point-to-point link out to a short distance (currently 5.4 nmi/10 km)
- Provide a mesh, multi-user communications (EVA-EVA-LSAM-CEV)

- Data rates suitable for commands, telemetry, audio and motion imagery

In the mesh mode, multiple proximity link users can be linked simultaneously - EVAs, CEV, LSAM. This then also becomes the "work area" wireless carried by the LSAM on the surface for EVA/rover communication within its line of sight. In that way, LSAM does not have to duplicate radios.

There are no requirements on this link to support radiometrics; the prox ops navigation sensors will provide the necessary information for prox ops and docking. There are several different communication protocols/systems that are in the trade space for the Prox Ops Link:

- Existing Space-to-Space Communication System (currently used on ISS / Shuttle for prox ops and EVAs)
  - Constrained by the data rates, encryption algorithm, and number of users on the network
- IEEE 802.11
  - Constrained by the range limitations of the protocol standard
- IEEE 802.16
  - Newly ratified standard (Dec. 7, 2005), can meet the range and mesh, point-to-point requirements
- Customized 802.11
  - Modify standard to extend the range capabilities
- Full Custom
  - Develop a custom TDMA standard
- Meet the range requirements and pick an optimum frequency band

The trade is on-going, but based on preliminary analysis, the IEEE 802.16e is currently specified in the C3I Interoperability Specification and the CEV SRD. The data rates on this link are not yet specified.

Rendezvous Link

This link was recently added to the CEV SRD based on navigation and ops requirements for when the LSAM is on the surface of the moon and CEV is in lunar orbit, and during LSAM liftoff and rendezvous operations with CEV. The primary capabilities and requirements on this link are:

- Provide radiometrics (range & range rate measurements) between CEV and LSAM from when the LSAM is on the lunar surface all the way in to a few kilometers.
- Provide CEV health and status to LSAM during the liftoff and rendezvous operations.
- Provide a contingency relay capability between CEV-LSAM-Mission Control of health, status, audio, etc.

This link is intended for the rendezvous, point-to-point operations and not for a mesh network to support EVA-EVA communications.

Search and Rescue Link

This link is to support communications between the CEV and pre- and post-landing forces to aid in the search and rescue of the crew. This system also provides an emergency locator beacon. This system is compatible with international standards as defined in the Constellation C3I Specification.

C&T Components

The main components of the reference C&T system are two S-band transponders that can support both the CEV-MPTFO link and the CEV-LSAM rendezvous link; a Ka-band transceiver; and two prox ops transceiver cards. The S-band transponders are cross strapped to: an omni antenna system to meet the any attitude communications requirement; a phased array system to support the launch, ascent, entry, and post-landing data rate requirements; a deployable high gain antenna (dual feed to support S-band and Ka-band) in the Service Module to support the high data rate requirements. The Ka-band transceiver is connected to the dual feed HGA. The prox ops transceiver cards are cross strapped to the S-band prox ops antenna system.

There are two Search and Rescue communication systems – a SARSAT and a VHF/UHF to provide compatibility with the international standards and some fault tolerance. It is also understood that the S-band link between CEV and Mission Control through TDRS will also be operational.

The audio and video processing, the baseband processing, and the communication outage recorder are located with the SDR side of the flight computer. Whether these functions reside inside the flight computer or are housed separately in a communications gateway is still being studied and will be addressed in the next design cycle.

7.1.2.4 Display and Control

As the avionic system design progressed, the team developed a goal to eliminate unique display and control (D&C) computers. This saved mass, volume, and power, while increasing the processing burden and decreasing the channel capacity of the resulting computing architecture. A thorough processing capacity analysis can't be done until the display and control tasks are better understood. Such an analysis will be an important trade study (see future work). The re-introduction of separate display and control processors will have significant ramifications.

Another goal was to design the display architecture with "dumb heads", that is, display devices that receive a screen of pixels over a video display line (as opposed to "clever heads", or "smart heads" which contain hardware that assembles data and creates a display at the head). Dumb heads are the simplest and cheapest devices (possibly with lower mass, volume, and power consumption). They provide greater flexibility for upgrades and they simplify test, verification, and maintenance. Using dumb heads can also minimize the amount of application-specific, and possibly proprietary, software development and maintenance. Both clever heads and smart heads also have significant advantages, and the trade between these three approaches should be the subject of future work.

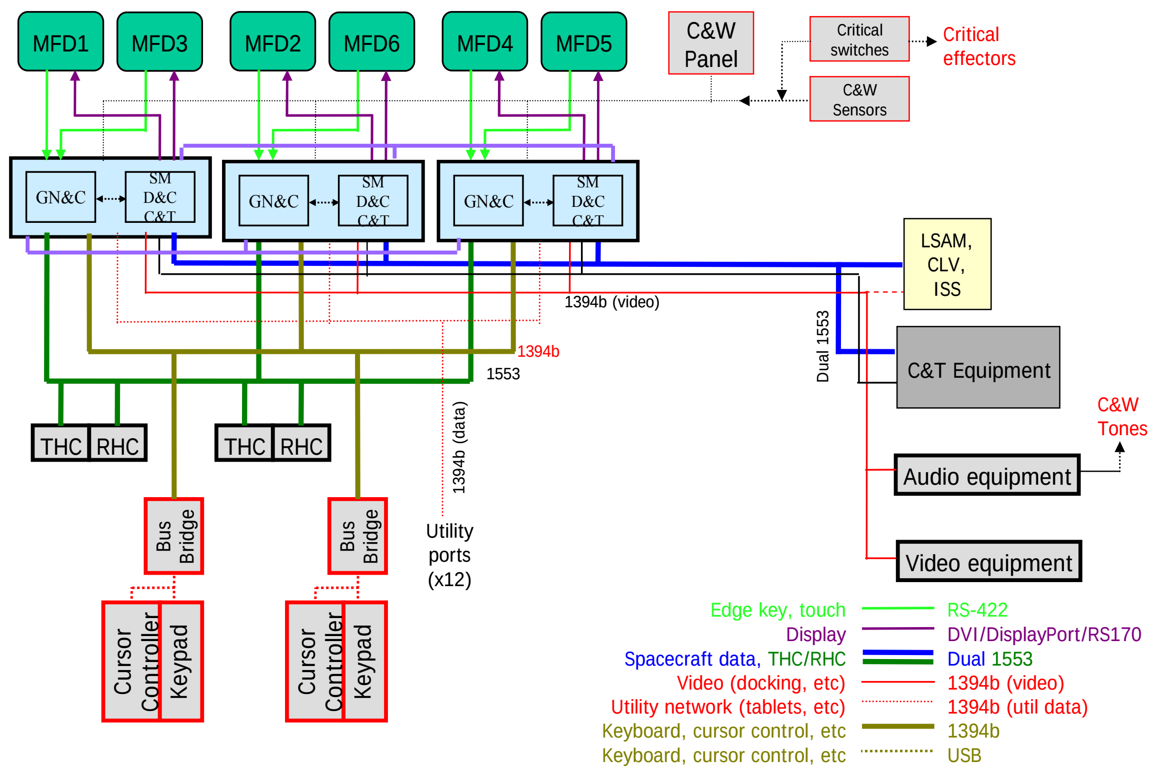

Figure 7.1-6 CEV Reference Avionics – Display & Control Details

See Figure 7.1-6 for a depiction of the CRC-3 proposed D&C architecture. The design consists of two 8 inch square and four 6.5 inch square multi-function displays (MFDs). The display sizes were chosen by the automation and robotics team members supporting the Cockpit Working Group, which used 3D CAD models to fit various components into the cockpit volume. The display sizes and layout chosen by the Cockpit Working Group were deemed acceptable for this design cycle, knowing that it would likely change as the cockpit requirements matures and additional evaluations are performed.

The MFDs are driven by a video graphics card in the SDC partition of the flight computer chassis. Each graphics card is capable of driving two displays, via a video display cable (ideally using a digital display technology, such as DVI, or the soon-to-be-released DisplayPort).

This design assumes that all *critical* functions can be performed on one display. This assumption means that no redundant cabling is required to meet requirements for two-fault tolerance (because any two faults will leave one display for each redundant workstation). As the cockpit requirements mature, this assumption is likely to be inaccurate. If redundant inputs to each head and redundant cabling are added, this architecture could still be used. But it appears likely that the required number of displays will drop as the cockpit requirements are refined; so this design will undergo significant modifications.

Significant early analysis was done on the use of projected, rather than direct-view displays. Projected displays use a light source, optics, and a tiny display generator (usually LCD or DLP technology), instead of a flat-panel LCD. Recent refinements in projected displays have made them a viable alternative for use in avionics. Projected displays can provide a large display surface, and might provide superior performance in vacuum. But after a number of discussions with vendors, we have tentatively accepted their assertion that projected display technology may not be practical for CEV, and conventional direct-view LCDs can be made to work within the CEV's environmental constraints. We believe LCD performance in the CEV environment is an area that requires further study (see forward work).

Although the heads are "dumb", RS-422 serial data lines provide Built-In-Test data, as well as data from edge keys and other hardware controls on the displays.

Motion video will be merged by the SDC into the video signal sent to the display head. This allows the SDC to insert camera video, such as video from a rendezvous and docking system. The SDC will get this data over a 1394b video bus.

The design includes a 1553 bus for the translational and rotational hand controllers (THC, RHC), and a 1394 bus for more modern crew interface devices, such as keypads and cursor controllers. Although this approach is more robust and flexible, it may be fodder for future simplification, since all the devices could be re-engineered to be compatible with a single bus interface. Bus channel capacity analysis will be an important part of these decisions.

Two hard switch panels (one for each workstation) are included in the design, because certain functions are likely to remain hard-wired to switches. Such functions might include power, fire suppression, and pyrotechnic system management switches.

The design also includes a single redundantly-wired caution and warning panel. A single panel visible to both workstations was chosen to simplify the design and ensure that both operators are using the same information in a shared area of the workspace. Some caution and warning sensors may be directly wired to this panel (for functions such as fire and cabin pressure detection), and/or wired to the flight computers.

7.1.2.5 Fault Tolerance/Redundancy Management Architecture

The proposed Fault Tolerant /RM Architecture is based on the following assumptions and ground rules:

- The Fault-Tolerant/RM Architecture is two-fault tolerant and specifically accommodates two non-simultaneous failures.
- The Arbiter votes, employing cryptography (authentication), as part of 1st round of exchange.
- A combination of a Triple Modular Redundant (TMR) processing board within a fault containment region of each Arbiter will provide a reasonable capability of detecting the malfunctioning computer / containment region in the case of the duplex dilemma (see Figure 7.1-7).
- A combination of a Triple Modular Redundant (TMR) processing board within a fault containment region of each Arbiter will provide the capability to adhere to a Byzantine-resilient architecture (see Figure 7.1-8).

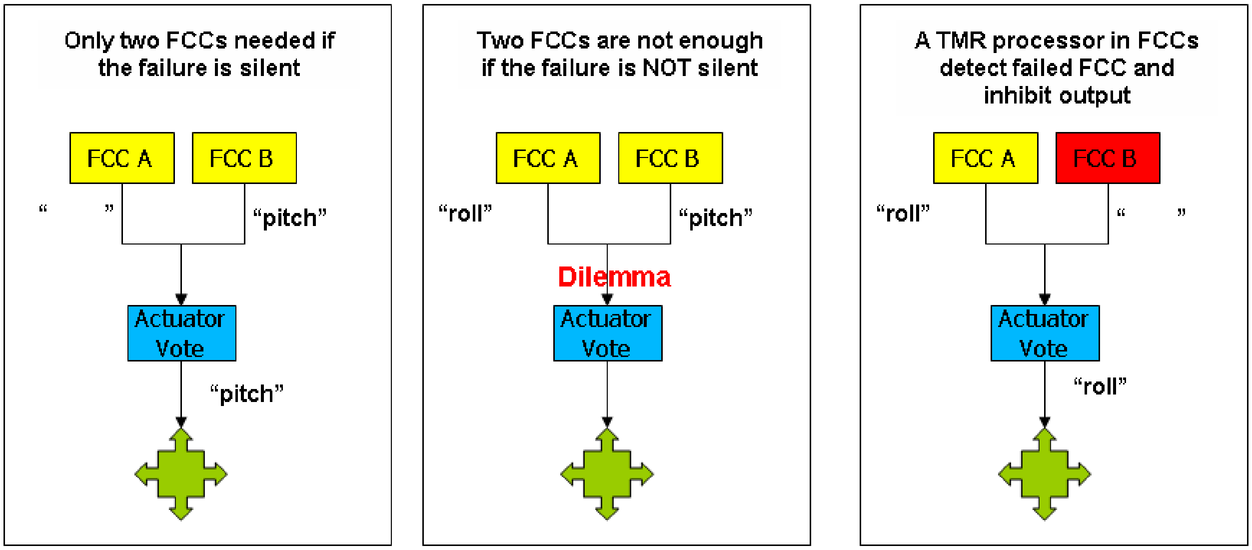

Figure 7.1-7 Using TMR processors to Solve the Dilemma Case

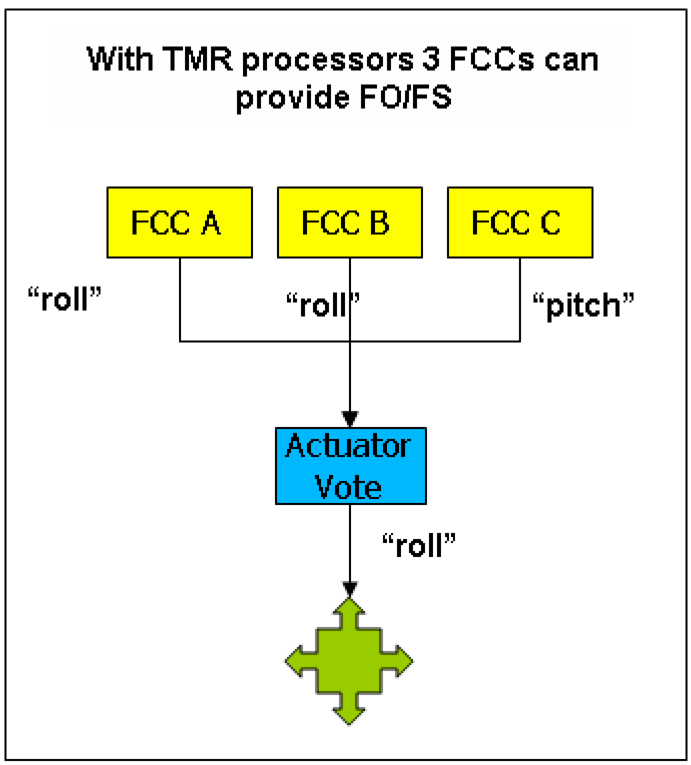

Figure 7.1-8 FO/FS with 3 FCCs using TMR Processors

The Fault Tolerant design adheres to project-levied requirements and assumptions. In order to achieve such a design an architecture that combines TMR processors for primary flight critical computers is used in combination with a Byzantine-resilient philosophy. The architecture provides Fail Op/Fail Safe (FO/FS) robustness, allowing a functioning avionics system after 2 non-simultaneous faults.

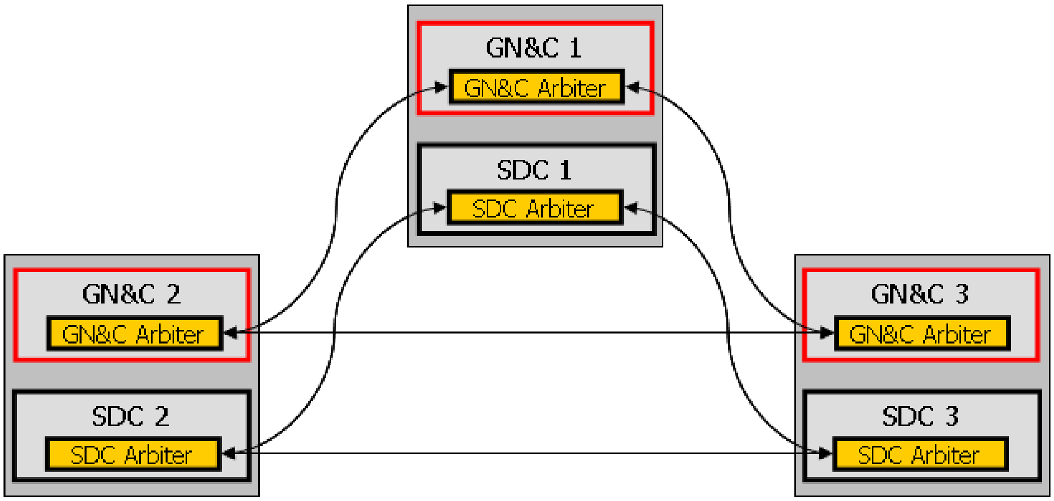

Figure 7.1-9 Proposed Fault Tolerant Architecture

Fault Containment Region (FCR)

A Fault Containment Region (FCR) contains a set of all the flight critical components required to control the CEV. A Fault Containment Region (FCR) isolates itself from the other FCRs. This prevents fault migration across channels. There are three FCRs within the proposed avionics architecture. In general terms, each chassis may represent an FCR, however an FCR also includes the entire string of capability (e.g., buses, effectors, sensors) and cannot be polluted by another FCR failure. Note: The proposed architecture allows the non-flight critical SDC FCR regions of the chassis to become a flight critical FCR if required.

GN&C and SDC

The GN&C and SDC partitions/computers are isolated from the normal input and output method. To maintain congruency, each of the computers receive and deliver inputs and outputs via the Arbiter. This provides a clean mechanism to isolate possible pollution activities that would otherwise occur in an open system. The computers run in lockstep with each other, synchronized by the Arbiter. The Arbiter also provides the computers congruent input and assures congruent output by voting the computer input and output. In the event of a common mode failure across the GN&C partitions, the proposed architecture allows the non-flight critical SDCs to be engaged as the primary system.

Arbiter

The Arbiter governs the avionics' FCRs. It provides the synchronizing mechanism for the FCCs, Byzantine resilience, fault isolation, fault detection, and fault recovery. In the proposed architecture, there are two sets of Arbiters: one flight-critical and the other non-flight critical. In the event the flight-critical fails, the architecture allows the non-flight critical Arbiter to be used as the flight critical path.

Parallel Processing

Each of the three GN&C computers run in parallel. Identical source code runs on the Flight Critical processors within each GN&C computer, each synchronizing at a frame boundary via the GN&C's local Arbiter. This provides the ability to withstand non-congruent faults within the channels and/or single event upsets (radiation).

On The Fly Redundancy

This architecture provides on the fly FO/FS redundancy. On the fly redundancy refers to the capability of "riding" one's redundancy as faults occur. If a fault is detected in one of the FCRs, that FCR is masked out of the group. This disallows the FCR and its components to affect the rest of the avionics system unless it is requested to rejoin the group.

Voting

Voting is provided by use of the Arbiter. By using a two-round voting exchange (adhering to Byzantine-resilient principles), a malicious computer/bus can be overcome (see Figure 7.1-10). The second round exchange also allows the system to identify which Fault Containment Channel provided the erroneous vote, thus isolating the source of error.

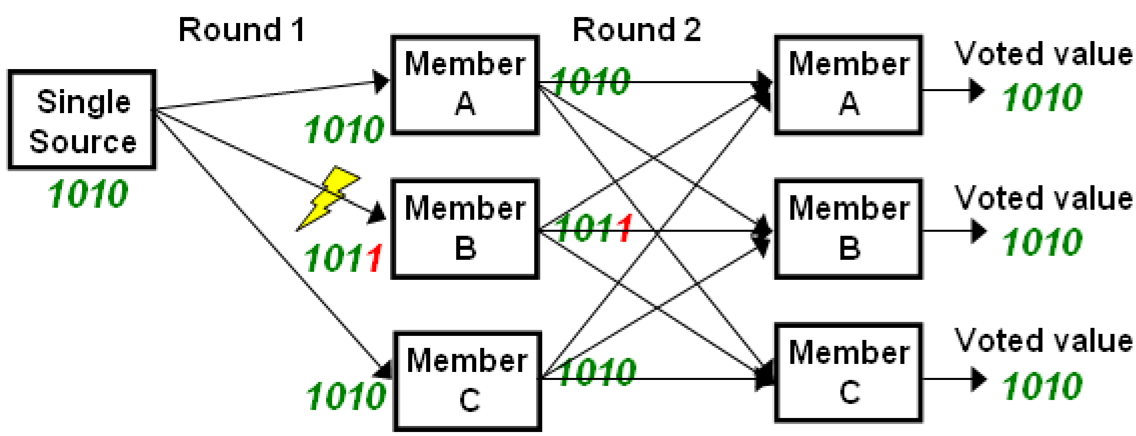

Figure 7.1-10 Voting Using Two Round Exchange

Voting Both Inputs and Outputs of Primary Avionics System

This proposed architecture provides voting on the input and output side of the primary avionics system. This provides the capability of detecting input or output errors at the primary avionics level.

Lower Level Actuator Voting

To complete the fault tolerant architecture, Actuator voting is necessary. Though the system votes outputs at the primary avionics level and enables identification of a faulty FCR, further corruption could occur downstream of the system. Therefore, voting at the actuator level ensures the full redundancy and reliability of the system.

Byzantine Resilience

The architecture provides Byzantine resilience, which is necessary in keeping erroneous software inputs and outputs from polluting the primary flight-critical avionics system. When distributing single-source data from one computer to the rest, it is necessary for all computers to end up with the same value. Otherwise they can take conflicting actions and system will fail. A "Byzantine" failure occurs when a computer fails in such a way that it tells its peers different things and thus puts at risk the principle that non-failed computers come to the same conclusion. The problem was identified by L. Lamport and colleagues at SRI (1980), originally called "interactive consistency" and then renamed to "Byzantine General's Problem".

A Byzantine Resilient system requires:

- For any simplex communication, each non-failed channel will receive the same value
- If the simplex originator is not failed, each non-failed recipient will receive the correct value

This architecture handles **f** simultaneous faults (where **f** = 1):

- **2f+1** "fault-containment" regions employing cryptography (authentication) as part of 1st round of exchange
- **2f+1** independent communication paths
- **f+1** rounds of exchange
- Bounded skew between channels
- Electrical isolation of channels
- Physical separation and channelized power and cooling

Reaction Concerns

Reaction time for several critical phases of flight were investigated based on analysis of requirements and assumptions levied upon the architecture (see Table 7.1-1). Therefore, the architecture lends itself to the capability of employing a "hot backup" or BFS.

Mission Phase	**Critical Phase**	**Failure**		**Reaction Time**	**Needed Capability**
Ascent	abort	CMF/RSE		~300 ms	Punch off
Ascent	abort	CMF/RSE		ms	Launch/Abort Active Control
Ascent	abort - chute	CMF/RSE		seconds	Deploy Chutes
Ascent	insertion burn	CMF/RSE		seconds(fail safe)/ms (hard over)	
Proximity Ops	approach	CMF/RSE		seconds/ms	Control authority - Backoff
Proximity Ops	docking	CMF/RSE		seconds/ms	Control authority - Backoff

Mission Phase	**Critical Phase**	**Failure**		**Reaction Time**	**Needed Capability**
Transit	Drift	CMF/RSE		Hours/days	Perform minimal functions for entire flight profile
Transit	Lunar TEI burn	CMF/RSE		Minutes(fail safe)/ms (har-dover)	Complete/Stop/Re-perform burn
Orbital Ma-neuvers	Stuck Thruster	CMF/RSE		second	Complete/Stop
Orbital Ma-neuvers	Rendezvous burns	CMF/RSE		Minutes(fail safe)/ms (har-dover)	Complete/Stop/Re-perform burn
Entry	De-orbit Burn	CMF/RSE		seconds	Complete/Stop/Re-perform burn
Landing	Parachute re-lease			seconds	Release Chutes
*Failures: CMF: Common Mode Failure RSE: Redundancy Set Exhausted					

Table 7.1-1 Failure Mitigation

Surveyed Architectures

Several architectures were investigated in order to meet the demand of the driving requirements for this vehicle. The goal of the architecture was to meet requirements and allow for the flexibility and modularity for future concerns. Weighing between what is needed now and what will be needed in the future is a difficult dilemma. However, the design proposed allows the scalability needed for successful development of this vehicle. During the architecture development, various kinds of alternative architectures were investigated and thus led to the proposed design (see Table 7.1-2).

	Byzantine-resilient using arbiters with integrated BFS and manual by-pass	**Byzantine-resilient with separate BFS and SM**	**Byzantine-resilient with inline SM and separate BFS**	**Prime/hot spare/cold spare inline CTC**	**Micro Wireless**
FT	2	2	2	2	2+
Byzantine Resi-lient	Yes	Yes	Yes	No	Yes
# Chassis	3 + Data Storage	8	5	4	N/A

	Byzantine-resilient using arbiters with integrated BFS and manual by-pass	**Byzantine-resilient with separate BFS and SM**	**Byzantine-resilient with inline SM and separate BFS**	**Prime/hot spare/cold spare inline CTC**	**Micro Wireless**
RM Scheme	▪ Voting Inputs & Outputs ▪ Using separate arbiters for critical and non-critical functions ▪ Uses TMR processor	▪ Voting Inputs & Outputs ▪ Using separate arbiters for critical and non-critical functions ▪ Uses TMR processor	▪ Voting Inputs and Outputs ▪ Uses TMR processor	▪ Uses TMR processor ▪ Health and fail silent checks	▪ Voting Inputs and Outputs ▪ Using separate arbiters for critical and non-critical functions
Flight critical electrically isolated from non-critical	Yes	Yes	Yes	Yes	Yes
Seamless fault Masking during critical phases	Yes	Yes	Yes	No	Yes
Other Considerations	▪ SDC may be used as a BFS	▪ Stand Alone FCC ▪ Stand Alone SDC ▪ Stand Alone BFS ▪ Robust	▪ Stand Alone BFS	▪ Difficult to determine switchover ▪ One computer controls vehicle ▪ TMR processor for self checking	▪ State machine electrically Isolated ▪ Low TRL Level ▪ EMI problems ▪ Synchronization Issues

Table 7.1-2 Surveyed Architectures

7.1.3 Mass Estimates and Design Maturity

The summary mass estimate for Avionics is given in Table 7.1-3. The estimates are grouped into C&DH and Wiring, Communications and Tracking, and Display and Control.

Hardware Items	Quantity	Unit Mass (lbm)	Growth (%)	Total Mass (lbm)	CM Mass (lbm)	SM Mass (lbm)	Basis of Estimate
Avionics - C&DH and Wiring				**785**	**635**	**150**	
Flight Computer	3	49	10%	161.7	161.7		Scaled SBS RCOM10 w ith 2 pow er supplies+13 cards)
Data Storage Unit	1	22	10%	24.2	24.2		Scaled SBS RCOM10 w ith 1 pow er supply+5 cards)
DAU (Data Acquisition Unit)	6	15	10%	99.0	49.5	49.5	Scaled SBS RCOM05+Aitech S950+2 pow er supplies+6 cards)
CM Wiring (Avionics specific)	1	400	0%	400.0	400.0		ESMD-RQ-0005
SM Wiring (Avionics specific)	1	100	0%	100.0		100.0	ESMD-RQ-0005

Hardware Items	Quantity	Unit Mass (lbm)	Growth (%)	Total Mass (lbm)	CM Mass (lbm)	SM Mass (lbm)	Basis of Estimate
Avionics - C&T				**316**	**255**	**61**	
Video Panel	1	6	20%	7.2	7.2		V. Studer
Headsets	10	0	20%	3.0	3.0		Phase 1 data
Headset control unit	2	3	20%	7.2	7.2		
Speakers	2	4	20%	9.6	9.6		Contractor data
CSFDR	1	10	10%	11.0	11.0		L3Com L-3/EDI spec sheet
S-band Transponder	2	12	5%	25.2	25.2		Alcatel Space product sheet
Ka-band Transceiver	1	12	5%	12.6	12.6		Best estimate P1 and LRO
S/Ka-band Antenna Dual Feed HGA	1	10	8%	10.8		10.8	Best estimate P1 and LRO
S/Ka-band Antenna Electronics	1	20	8%	21.6		21.6	Best estimate P1 and LRO
S-band Low Gain Antenna + Mount	6	2	20%	14.4	7.2	7.2	EDO Corporation AS48915
S-band Antenna Electronics	6	6	20%	43.2	21.6	21.6	Best estimate Phase 1
S-band Medium Gain Antenna	2	25	12%	56.0	56.0		ECOMM Phased array assembly
S-band MGA Electronics	2	18	12%	40.3	40.3		Best estimate from ECOMM
S-band Prox Ops Antenna + Mount	2	2	20%	4.8	4.8		EDO Corporation AS48915
S-band Prox Ops Antenna Electronics	2	10	12%	22.4	22.4		Best estimate
Sarsat Xmit Beacon	1	4	20%	4.3	4.3		
Sarsat Xmit Beacon Antenna	1	1	20%	0.6	0.6		
UHF/VHF ATC Antenna	2	3	20%	7.2	7.2		
UHF/VHF Antenna Electronics	2	1	5%	2.6	2.6		
UHF/VHF ATC Comm	1	10	20%	12.0	12.0		

Hardware Items	Quantity	Unit Mass (lbm)	Growth (%)	Total Mass (lbm)	CM Mass (lbm)	SM Mass (lbm)	Basis of Estimate
Avionics - D&C				**127**	**57**	**70**	
Display w/ Edge Keys	2	7	20%	16.8	16.8		Quantity & size per ER/Hnguyen
Display w/ Edge Keys	4	6	20%	28.8	28.8		Quantity & size per ER/Hnguyen
Translational Hand Controller	2	6	5%	11.8	11.8		Per Diana Schuler 2006/01/10
Rotational Hand Controller	2	10	5%	21.6		21.6	Per Diana Schuler 2006/01/10
Keypad	2	5	5%	10.5		10.5	From STS MCDS Rafael Munoz
Switch Panel	2	10	5%	21.0		21.0	Phase 1 info
Peripheral Bus Bridge	2	2	20%	4.8		4.8	Per Randy Wade 2006/01/10
C&W Panel	1	10	20%	12.0		12.0	Same as sw itch panel

Table 7.1-3 Avionics Mass Estimates

7.1.3.1 C&DH and Instrumentation Wiring

Each FCC measures 14 inches high, 10 inches wide, and 24 inches long, and weighs 49 lbm, for a total of 147 lbm for three FCCs. This is expected to increase in the next design cycle.

The current estimate for Instrumentation sensor and wiring mass is 500 lbm. Each DAU is estimated at 15 lbm, for a total of 90 lbm for six DAUs. The sensor and wiring mass is based on X-38 program actuals for an instrumentation system of approximately 1000 sensors. X-38 sensors primarily consisted of individually wired sensors, therefore additional usage of bussed data on CEV could reduce the weight per sensor ratio.

As sensor requirements mature, better estimates for system mass will be provided.

7.1.3.2 Communications and Tracking

The total C&T mass is 316 lbm with 255 lbm in the CM and 61 lbm in the SM. The C&T audio processing, video processing, C3I functions (baseband processing, forward error correction, encryption/decryption, frame formatting and synchronization, etc.) are currently performed in the SDC in the Flight Critical Computer.

The mass estimates for the C&T equipment (transponders, transceivers, antenna, audio/video equipment) are preliminary and based on available data sheets from vendors, information from Lunar Reconnaissance Orbiter (LRO), other available data, and engineering judgment. The mass estimates for the antenna electronics are very preliminary and will be further refined during the next analysis cycle.

7.1.3.3 Display and Control

The principal contributor of mass, power, and volume for the display and control system is the displays themselves, (assuming that channel capacity estimates do not indicate the need for a separate display and control computer). Because the number and size of the display heads has not yet been well defined, the display design maturity must necessarily be considered very low.

The relative dearth of potential display subcontractors further complicates the display estimates. Two suppliers stand out as being most capable of fielding hardware for CEV. Unfortunately, both of these suppliers are already teamed with Phase 1 contractors. This has greatly complicated our ability to independently discuss and evaluate the suppliers' product line.

As a result, most of the design information in this study comes from supplier data released to NASA by the Phase 1 contractors. The resulting lack of independence has been documented, and we continue to seek information from other suppliers with less sophisticated or less compatible hardware. We anticipate a more open dialogue with the primary suppliers in the next phase of the program.

Estimates for the hand controllers and keypad come from the Space Shuttle program. While the numbers are mature, the Shuttle-era devices are no longer available. It's likely that modern versions will be smaller, lighter, and consume less power.

Estimates for the switch panels and caution and warning panel come from a combination of Shuttle data, Phase 1 contractor data, and a rough estimate. Until the task analysis and operations are better defined, this estimate should be considered only slightly more mature than the display estimate.

7.1.4 Plan Forward

- As the other subsystems (including LAS) address their redundancy and fault tolerance schemes in the upcoming analysis cycle, those hazards or failures which utilize the Avionics architecture (hardware and/or software) as part of their control need to be identified to and addressed by the Avionics team. Integration with the Avionics architecture team is essential to providing an overarching CEV systems fault tolerance. For example, the Avionics team needs to ensure safety critical inputs have redundant paths.
- Several trades which potentially affect the Avionics architecture are also being conducted in parallel, such as the Backup Flight System Trade. The results of these trades will need to be factored into the Avionics architecture in the upcoming analysis cycle.
- It is anticipated that a Preliminary Hazard Analysis (PHA) will be performed on CEV Reference Configuration. The results of the PHA need to be provided to the Avionics architecture team to ensure that fault tolerance issues are addressed.
- Current research of 3U cPCI I/O cards indicates a capacity of up to 64 channels per card which in the current configuration would provide a capability 756 channels in the CM DAUs and 756 channels in the SM DAUs for a total of 1536 channel inputs.
    - Discussions are on-going with CEV subsystems to obtain more refined estimates for sensor requirements to determine if current architecture capability is adequate. Ensure the signal types, protocol, bandwidth, throughput, and data rate can be met with the proposed architecture.
    - In addition, as sensor needs are refined, the signal conditioning capabilities (excitation, filtering, amplification, compensation, bridge completion, etc) of the DAUs will be re-evaluated.
- Refine avionics wiring estimate based on sensor inputs.
- Perform vacuum testing on AMLCD direct-view devices. Evaluate displays that are similar to those being proposed by Phase 1 suppliers, perhaps in conjunction with Phase 1 suppliers. Evaluate an advanced fringe-field switching (AFFS) LCD device, if possible (AFFS is a promising type of LCD, currently in use in tablet computers). Tentative approval has been given to proceed with this testing.
- Perform a trade study to evaluate the benefits and drawbacks of using smart, clever, and dumb display heads.
- Participate in and track the development of the cockpit requirements document. Refine the number and size of the displays, as well as the types of interface devices.
- Participate in and track Cockpit Working Group trade studies of human interface technologies.

- Perform an analysis of channel capacity, and processor and bus loading, based on cockpit requirements, task analysis, etc.
- Develop a more robust analysis of redundancy requirements and redundancy management for the displays and controls, once the operations concepts are better understood.
- Clarify the operations concept for SRD requirement 2.8.2, “Emergency Entry Mode without Primary Systems”, and determine if it should trigger the design of an independent backup system for control and display.
- Determine if display heads can use passive conduction to eliminate heat. This would obviate the need to run plumbing to cold plates in the instrument panel.
- Obtain a human-factors position on the pros and cons of a single caution and warning panel vs two of them.
- Continue to work with other subsystems to determine interfaces and integration.
  - Processing
  - Bus loading analysis
- Refine power profiles.
- Refine software architecture.
- Evaluate use of small COTS electronics (ala PDA) to perform avionics, flight control functions.
  - Radiation
  - Reliability
  - EMI/EMC susceptibility
- Evaluate antenna type, placement, coverage, masking.
- Evaluate packaging options, and communication controller.
- Add more fidelity to the bus architecture and the audio video system.
- Provide a representative COTS solution for each circuit board, or detailing the design effort required if a COTS solution does not exist (e.g., the arbiter boards).
- Provide a refined FCC size, mass & power estimate, considering the number and placement of chassis I/O connectors, and the power requirements of each board.
- Evaluate TMR processor in solving dilemma case.

7.2 Power

The CEV electrical power system (EPS) encompasses both the SM and CM power. It is a 28 Vdc system with dual solar arrays on the SM for power generation, Li-Ion batteries for energy storage on both the SM and CM and numerous power distribution boxes. The power distribution boxes include solar array regulator units on the SM, primary and secondary power distribution units on both the SM and CM and pyrotechnic controller units on both the SM and CM, thruster control units on both the CM and SM, and power transfer converter units on the CM.

7.2.1 Driving Requirements, Groundrules, and Assumptions

The driving requirements for the EPS are listed below:

- The CEV shall provide 1.5 kW [TBR-007] continuous power transfer at 28 Vdc to LSAM. (CXP-01010: CEV to LSAM IRD, Draft – 3/29/06, Section 3.4.2.1)
- The CEV shall provide TBD-008 kW peak power transfer at 28 Vdc for periods up to TBD-009 minutes to LSAM. (CXP-01010: CEV to LSAM IRD, Draft – 3/29/06, Section 3.4.3.1)
- The CEV shall provide for crew survival for at least 36 hours (TBR-002-009) with the hatch closed following landing. (CXP-10001: CEV SRD, 2/3/06, CV0093)
- The CEV shall provide a minimum of 12 (TBR-002-152) common internal power utility outlets for general use by portable loads. (CXP-01006: CEV to Portable Equipment IRD, 1/9/06, CV0309)
- The CEV shall provide a minimum of 280 Watts (TBR-002-153) of power for each utility outlet intended for general portable load use. (CXP-01006: CEV to Portable Equipment IRD, 1/9/06, CV0310)
- The CEV shall dock with the ISS at PMA-2 (Node 2 Forward port) and PMA-3 (Node 3 Nadir port) via an ISS Androgynous Peripheral Assembly System (APAS). (CXP-01007: ISS to CEV IRD, 2/10/06, CV0602)
- The CEV shall be two-fault tolerant for catastrophic hazards, except for areas approved to use Design for Minimum Risk Criteria. (CXP-10001: CEV SRD, 2/3/06, CV0271)
- The CEV shall limit continuous power consumption from the ISS to less than or equal to 1 kW (TBR-002-018). (CXP-01007: ISS to CEV IRD, 2/10/06, CV0407)
- The CEV shall limit peak power draws from the ISS to less than 2 kW (TBR-002-078) for periods no more than 90 minutes (TBR-002-078) once per week. (CXP-01007: ISS to CEV IRD, 2/10/06, CV0408)
- The ISS shall provide 28 Vdc electrical power to CEV with 1.2 kW maximum capacity per channel, two channels per docking location. (CXP-01007: ISS to CEV IRD, 2/10/06, CV0686)

The groundrules and assumptions for the EPS are listed below:

- The EPS utilizes 28 Vdc power distribution
- The EPS is controlled via a 1553 data bus from the avionics computers
- Pyrotechnics are initiated by EPS pyrotechnic controllers via a 1553 data bus
- Thruster commands are initiated by EPS thruster controllers via a 1394 data bus

- The EPS is designed for the Block 2 lunar long-duration mission
- The EPS is designed to be two-fault tolerant (fail-op/fail-safe)
- The EPS utilizes two single axis solar array wings
- The EPS uses the same power interface for the LSAM and the ISS
- The EPS provides power management of subsystem loads
- The EPS power switching units provide internal software processing of all power instrumentation and control with all commands/feedback data coordinated with the avionics system
- The EPS system provides avionics with hardwired power inputs from multiple sources for automatic reboot during unmanned conditions
- The EPS system provides power and control to the SM for 15 minutes (TBR) after CM/SM separation for safe de-orbit of the SM
- The EPS provides control signals to the Launch Abort System during launch and ascent and battery charge power (TBD W) prior to launch
- The EPS provides power (1.5 kW) to the Lunar Surface Access Module while docked to the LSAM
- The EPS receives power (1.0 kW) from the ISS, while docked to the ISS
- The EPS receives power (TBD kW) from the LSAM, while docked to the LSAM
- The EPS receives power (TBD kW) from ground support equipment during testing and checkout, and on the launch pad

7.2.2 Conceptual Design Overview

7.2.2.1 Two-String Power Architecture Concept Features

- Provides two internally redundant strings of power system hardware to reduce weight/volume associated with baseplates & mechanical housings while isolating the two sub buses internally.
- Internal electrical channels provide required fault tolerance utilizing a total of four isolated sub-buses. Sub-buses can be cross-tied within each string after component failure isolation to recover functionality.
- Utilizes modular avionics approach to split out remote power control switching functions. Commonality of modules supported for CEV Crew and Service Modules and LSAM Ascent and Descent Modules.

A schematic of the CEV EPS conceptual design is shown in Figure 7.2-1 below.

Figure 7.2-1 Electrical Power System Architecture

7.2.2.2 Electrical Power Generation & Storage

Power Generation - Solar Arrays

The CEV EPS utilizes two single-axis solar array wings on the SM for power generation (see Figure 7.2-2). Each array wing consists of seven panels of approximately 5.38 ft by 9.88 ft, which results in a total array wing panel area of 372.2 square feet. For the four channel architecture, the arrays are oversized by 25%, which supports a fail-op/fail-safe EPS architecture. The array wings are designed to withstand all defined loading cases for the stowed and deployed configurations. The arrays were sized based upon utilization of Emcore Advanced Triple Junction with Monolithic by-pass diode (AJTM) solar cells for better performance during the low lunar orbit hot case. Array wing deployment is accomplished in a single step that moves the yoke to the saddle capture mechanism with also extending the solar array wing panel stack. The solar array wings panels are latched in the fully deployed position and are non-retractable. While in the stowed configuration, array panel stacks are covered by a metallic multi-layer insulation blanket to protect against over temperatures from the SM main engine nozzle and plume radiation heat transfer during the nominal low Earth orbit circularization burn and the abort-to-orbit SM main engine burn case.

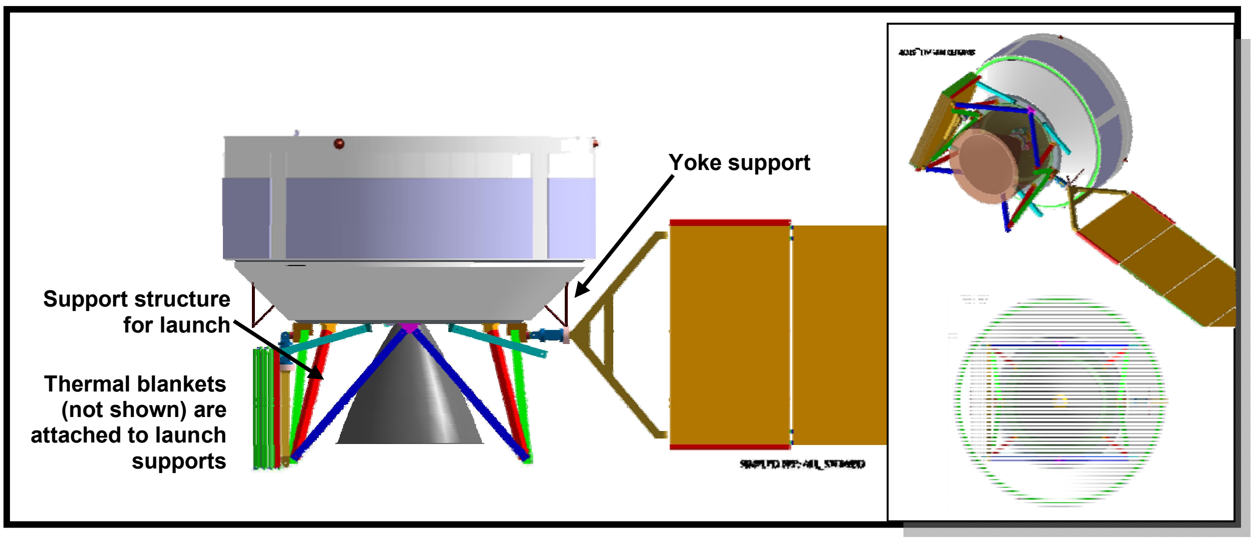

Figure 7.2-2 Solar Array Architecture (Stowed & Deployed Configuration)

Energy Storage - Lithium-Ion Batteries

The CEV EPS has ten Lithium-ion battery modules. Two of the battery modules are on the SM, and eight of the battery modules are on the CM. The CM point design selected a Li-ion cell design that achieved 180 Wh/kg and 400 Wh/L at C/2 charge and discharge rates in a 10 to 32 ºC pressurized cabin environment. This placement requirement is assumed to ease possible in flight replacement of battery modules. Several commercial off the shelf Li-ion cylindrical and pouch cell designs achieved these metrics. A greater challenge will be the later selection of a cell design that will have the >5 year calendar life necessary for Mars missions.

The redundancy factor simply multiplies the number of battery modules necessary to populate the four CM buses with two battery modules each. Estimating the battery mass and volume from the cell performance metrics requires applying parasitic mass and volume factors. The depth of discharge factor of 1.2 builds in a 20% capacity margin at the end of the discharge. The mass and volume packaging factors are based on those achieved while packaging the Electric Auxiliary Power Unit battery design with many 18650 cells and include the battery charging and gauging electronics in lieu of the high voltage dead-facing provisions. Although mass and volume savings could be achieved by implementing a unique design solution for the SM battery system, this study assumed commonality between the CM and SM battery modules. Therefore, the SM battery system simply utilizes 1/4th as many battery modules as in the CM.

A simple thermal analysis of each battery system indicates how much temperature rise would occur if the battery system could be adiabatically isolated. A full discharge of the CM battery system will result in a worst case 30 ºC temperature rise. Depending on the operational life requirements this may be acceptable for the battery to occasionally reach 62 ºC if it started at 32 ºC. No safety concerns exist with this rise. Therefore, the batteries are assumed to be passively cooled.

The battery module design will have to include electronics to take 28 Vdc power buses, when commanded by the CEV computers, and charge the battery module in less than 2 hours. The communication of charge enable, battery voltage, currents, and temperature, battery and charger faults, and capacity state of charge can be done via a USB interface to CEV computers. The charge control electronics will also manage cell balancing during charge. More importantly, this circuitry will have to be two-failure tolerant to a false positive indication that the battery is fully charged and thus, ready to proceed with an irreversible mission sequence. This is accomplished by having three independent microprocessors measure cell and battery voltage and assess whether charge is complete. This design complexity has been demonstrated in the spacesuit lithium ion battery charger. A false positive charge complete indication prior to an EVA is only given if three independent ICs are unanimously agreeing that charge is complete. These charge and gauging electronics are included in the mass and volume packaging factors.

The sizing case for the batteries derives from the requirement to perform safe reentry if there is an inability to deploy both solar arrays following ascent. Energy estimated for reentry including a 45 minute nominal recovery period is approximately 5.5 kWh and shown in Figure 7.2-8. Ascent energy is estimated by assuming a 5.6 kW power requirement for 1.5 hours for a total of ~8.4 kWh. The CEV 20 kWh battery sizing (8 x 2.5 kWh) allows for the nominal reentry power profile if emergency reentry is needed before being able to deploy both solar arrays. This assumes some battery capability needs to be reserved to meet the 36-hour post-landing requirement (36 x 170 W = 6.1 kWh). The other scenario for protecting batteries is post SM-CM separation where we have a two-failure case where we lose two main buses (10 kWh). With 10 kWh, a 4.5 kWh margin remains for 36-hour post landing support assuming a nominal reentry power profile (5.5 kWh). Here the post landing power would have to be managed at below approximately 125 Watts to meet sustain equipment operation over the 36-hour contingency recovery period. Power downs could help offset these failures but the desire is to maintain power levels in the first cut.

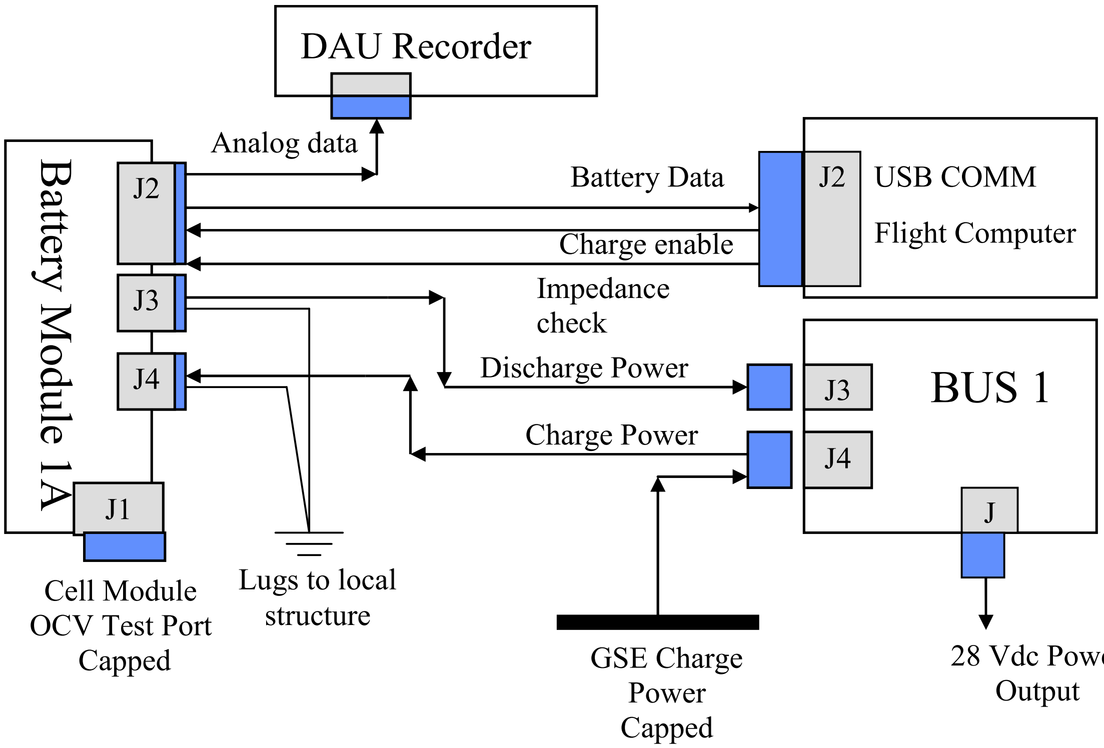

Figure 7.2-3 Lithium-Ion Battery Architecture

The next diagram shows the interfaces of the battery concept. Each battery module is tied to its electrical bus with separate discharge and charge relayed power feeds. The relays are not part of the battery system. To charge, the flight computer would close the charge relay and through a USB command, tell the battery electronics to start charging the battery.

7.2.2.3 Power Distribution and Control

Power Distribution Architecture

The CEV power system architecture utilizes a two main bus architecture with each main bus capable of being cross tied internally or isolated into four sub buses. The fourth bus has the capability to be isolated in the CM to provide power to the Emergency Ballistic Entry system which provided manual control of a minimal set of functions (e.g., attitude control, pyro events, life support, communications) need for entry in the event of loss of primary avionics.

Solar Array Regulator Units

The CEV EPS has four solar array regulator units (ARUs) on the SM. The ARUs are mounted by pairs in two common-chassis units that feed four independent power channels. The ARU design and scaled mass estimates are based on the Sequential Shunt Unit (SSU) technology being used on the International Space Station (ISS) photovoltaic power module. Each ARU has forty-two input power channels (representing half of the power channels of a single solar array wing) and two power output channels. The ARU voltage output set-point is maintained within a regulation band by coarse switching of input power channels (active or shunted) and rapid (e.g., at 20 kHz) pulse-width-modulated switching of one or two selected power channels. Channel shunting is accomplished using power field-effect-transistor (FET) switch technology. ARU output channel voltage ripple is managed via channel input and/out output RC filtering.

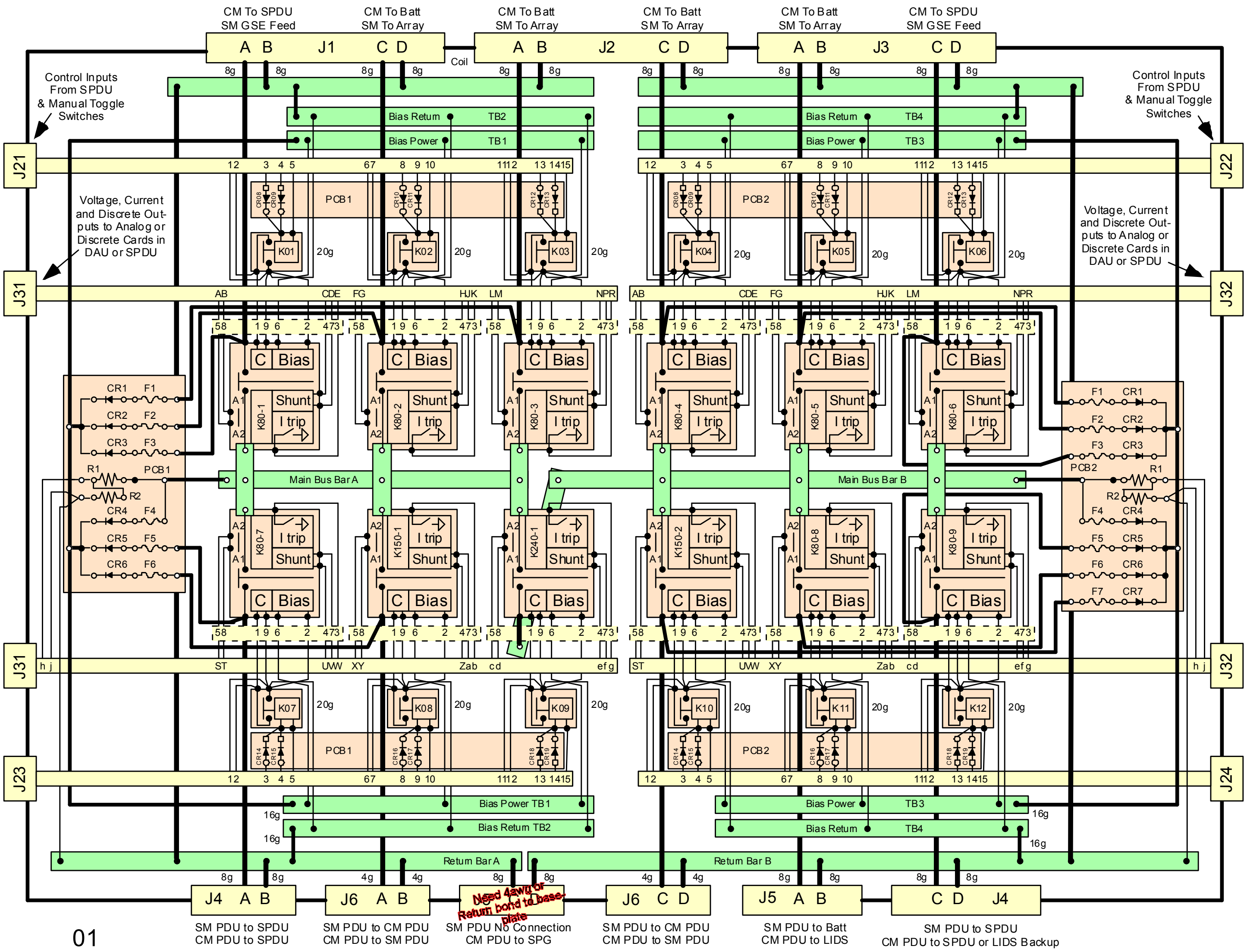

Figure 7.2-4 Power Distribution Unit

Power Distribution Units

The CEV EPS has four common power distribution units (PDUs). Two PDUs are on the SM, and two PDUs are on the CM. The primary purpose for these units is isolation of the primary distribution array and battery sources and distribution outputs. Each PDU has twelve relays. Each electro-mechanical relay provides latching input/output control and isolation, over-current protection of output wiring, analog current measurements and trip indication functions. They also provide voltage isolation during umbilical separation. Nine of the relays are 80 A for combinations of inputs and output channels. Two of the relays are 150 A for module to module power transfer, and one relay is 240 A for bus cross tie. The PDUs are passively cooled utilizing latching type contactor controls so that the units can function outside the pressurized volume and without cold plates. The PDU inputs/outputs can be controlled either by software or by manual toggle switch controls. The PDUs contain an essential sub bus for control to critical loads for initial power-up and reboots where multiple inputs sources feed the sub bus.

Secondary Power Distribution Units

The CEV EPS has six secondary power distribution units (SPDUs). The CM unpressurized volume, CM internal volume, and SM each contain two SPDUs, which are actively cooled by cold plates. SPDUs are controlled via redundant 1553 databus commands and have two inputs that are isolated from each other by DC/DC converters. SPDUs have two halves containing redundant mechanically isolated power supplies, control buses and power control modules. CM SPDUs are supplied by two different isolated sub buses. SPDUs are populated with three or five Power Control Modules (PCMs). PCMs have twelve channels consisting of two 20A-16awg outputs, four 10A-20awg outputs and six 5A-22awg outputs. Splitting the SPDUs to external and internal CM locations eliminates pressurized module feed-through connectors and frees up internal volume.

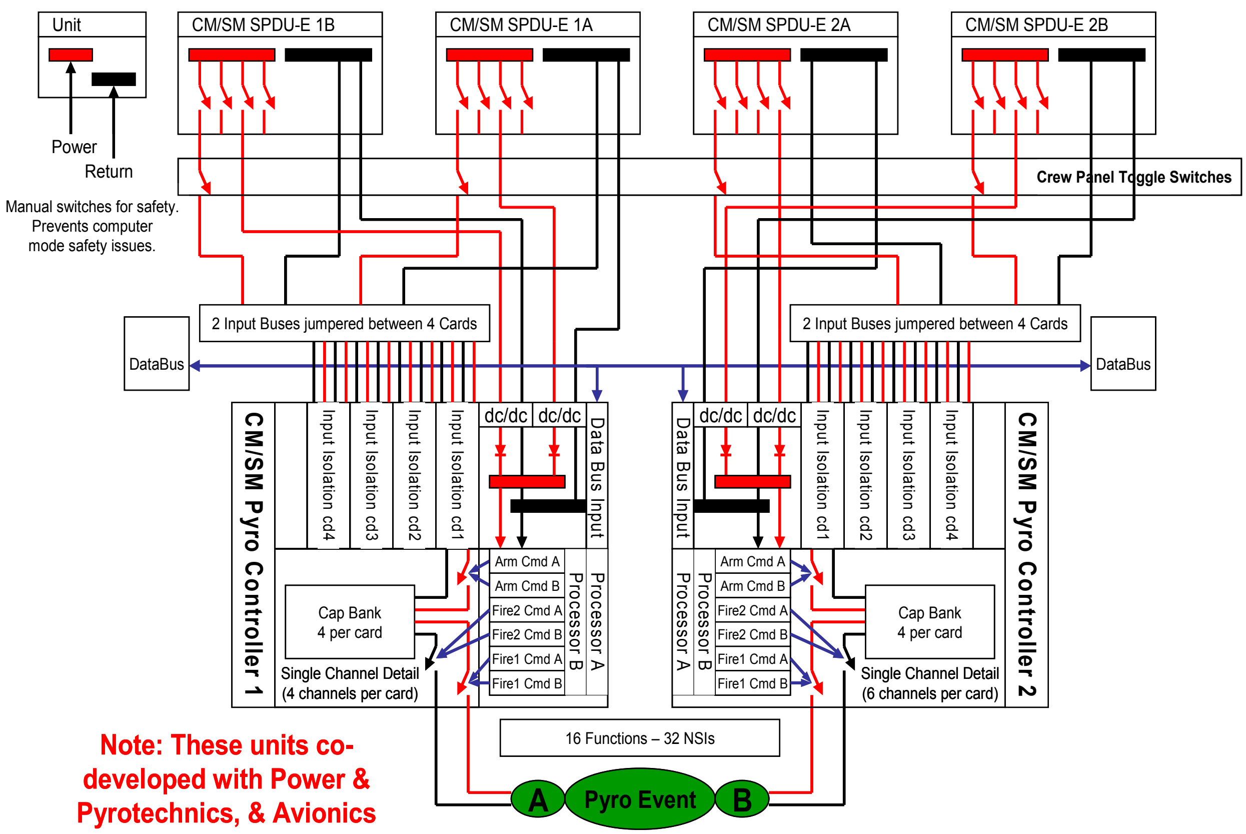

Figure 7.2-5 Crew Module Pyrotechnic Control Units A and B

Pyrotechnic Control Units

Pyrotechnic control units (PCUs) have small 1553-controlled processors with multiple Pyrotechnic Firing Cards (PFCs). The CEV EPS has two 6-card PCUs in the CM and two 2-card PCUs in the SM. The PCUs provide specialized cards that can be manually inhibited by crew controlled panels. Each card has an input capacitor bank and eight outputs and can be controlled via Arm, Fire1, and Fire2 commands for redundant firing of standard NSIs/Pyro functions. PCUs can provide circuit health to check out diagnostics such as firing line resistance on the pad or during flight. Ground checkout with GSE breakout box can facilitate energy measurements through dummy loads.

Thruster Control Units

Thruster Control Units (TCUs) provide specialized cards for both thruster power and return side switching. Two TCUs are located externally in both the CM and SM. TCUs provided specialized avionics for propulsion system power control featuring return side switching to thrusters. TCUs also include capabilities for igniter and thruster heater switching and solenoid driver power outputs for latching isolation valve operation. TCUs will be jointly developed hardware with avionics and propulsion subsystems. TCUs are actively cooled by cold plates and are controlled via 1394 data buses.

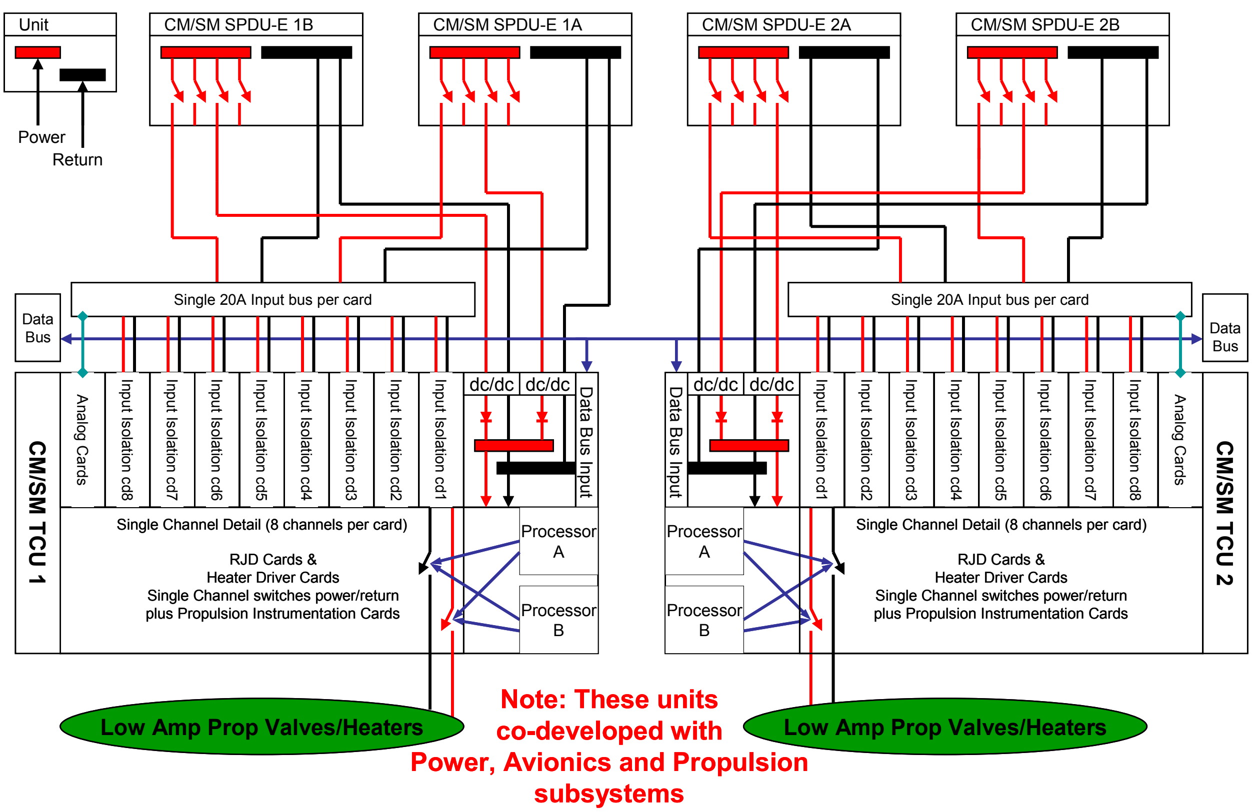

Figure 7.2-6 Crew and Service Module TCU A and B

Power Transfer Converter Units

Power Transfer Converter Units (PTCUs) provide ground/chassis isolation between the CEV and LSAM vehicles during mated operations. PTCUs provide two 1.5 kW feeds of regulated 28 Vdc power to simplify verification and system integration. The PTCU provides settable output voltage that each vehicles power system can utilize in their multi-source regulation scheme. The PTCU input/output can be swapped through relays to meet bi-directional power transfer requirement. There are two cold plated PTCUs in CM unpressurized volume.

7.2.2.4 Integrated Electrical-Thermal Power Profiles

Mission phase average power analysis was performed to understand the power and thermal resource utilization during the CEV Lunar and ISS missions. The electrical power load power profiles were updated to DAC2 (CRC-2) design reference data (with no added growth applied). The results showed no significant delta from previous total subsystem power demand assessed during DAC-1A. Therefore, CRC-3 battery energy capacity and mass properties (CM 8x2.5 kWh, 55 lbm each) were not changed the same as in CRC-2. Likewise, CRC-3 solar array wing panel area and power output remained the same as in CRC-2 (SM ~53 ft^2/panel, 7 panel/wing, ~10 kW max/wing). The Lunar mission phase integrated power utilization summary is provided in Table 7.2-1. Figures 7.2-7 through 7.2-10 provide graphical illustration of the mission electrical power and thermal heat load resource utilization profiles. Quiescent power during ISS docked phase was assessed to be slightly above 2 kW. CEV electrically powered functions during the quiescent ISS mated configuration are listed with their assumed average power levels and are shown as part of Figure 7.2-9.

Mission Phase	start MET hours	stop MET hours	Max SS Power (W)	Electric Energy (Wh)	Avg Power Load (W)
Launch to LSAM Docking	-0.2	16.0	7878	87567	5428
LEO & Lunar Transit	16.0	215.9	8212	1332891	6668
Untended CEV LLO	215.9	394.2	6096	610696	3425
Earth Transit	394.2	514.8	7145	606579	5028

Mission Phase	start MET hours	stop MET hours	Heat Energy (Wh)	Avg Heat Load (Wh/h) elec
Launch to LSAM Docking	-0.2	16.0	72707	4507
LEO & Lunar Transit	16.0	215.9	832475	4165
Untended CEV LLO	215.9	394.2	463431	2599
Earth Transit	394.2	514.8	501430	4157

Table 7.2-1 Total Electrical Power (left) and Thermal Heat (right) Load Summary

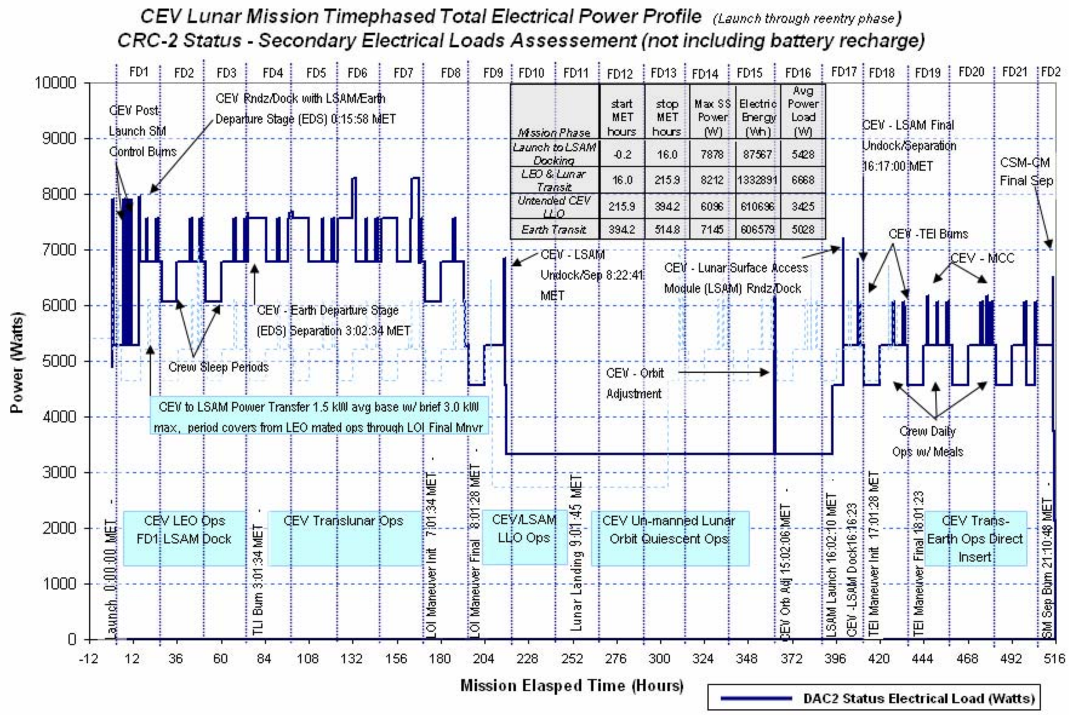

Figure 7.2-7 Total Integrated CEV Lunar Power Profile

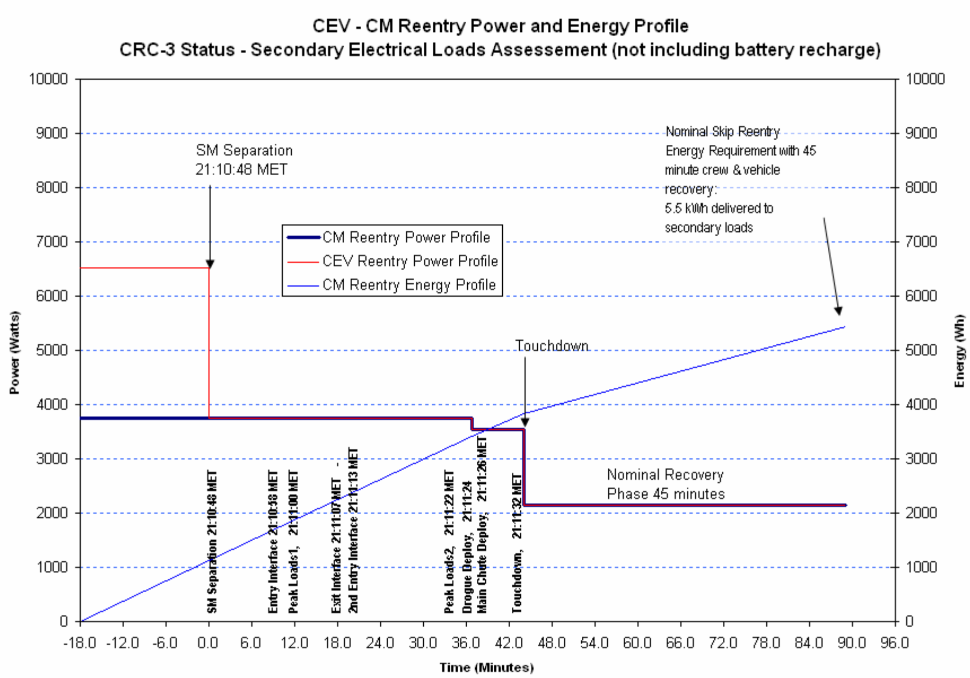

Figure 7.2-8 CM Nominal Reentry Power and Energy Profile

CEV ISS Mission Timephased Power Profile (Launch to prior to CM reentry phase)
CRC-2 CEV Reference Design - Secondary Loads Assessment (not including Power System battery recharge)

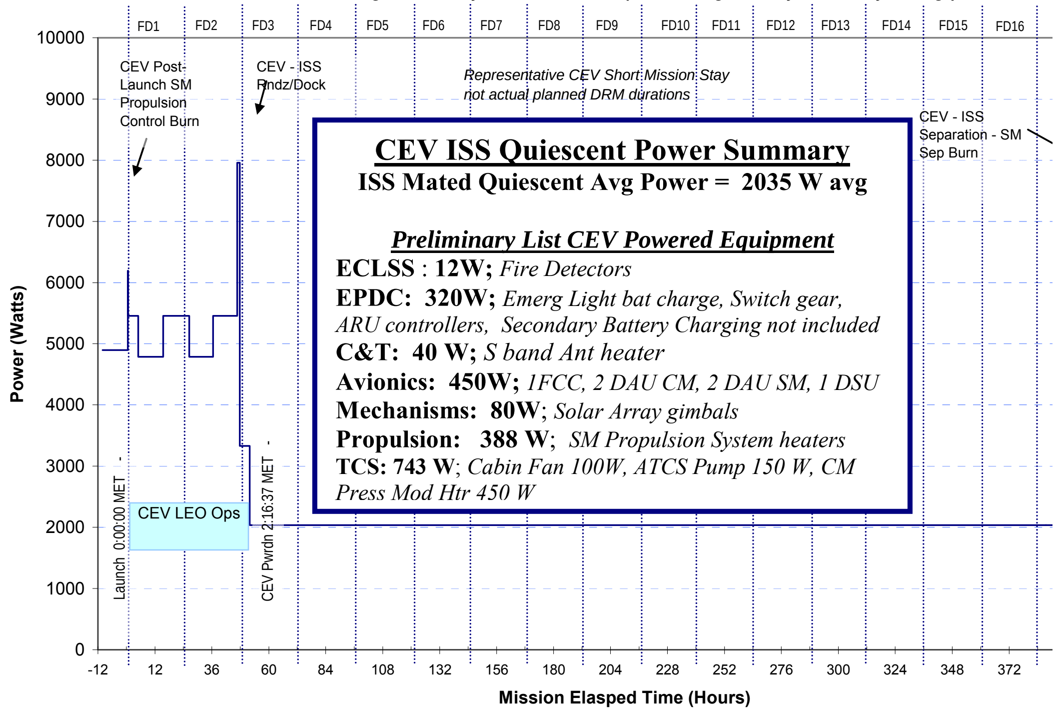

Figure 7.2-9 CEV ISS Mission Total Electrical Load Profile

CEV Lunar Mission Timephased Total Thermal Heat Load Profile *(Launch through reentry phase)*
CRC-2 Status - Thermal Heat Loads Assessement (not including crew metabolic)

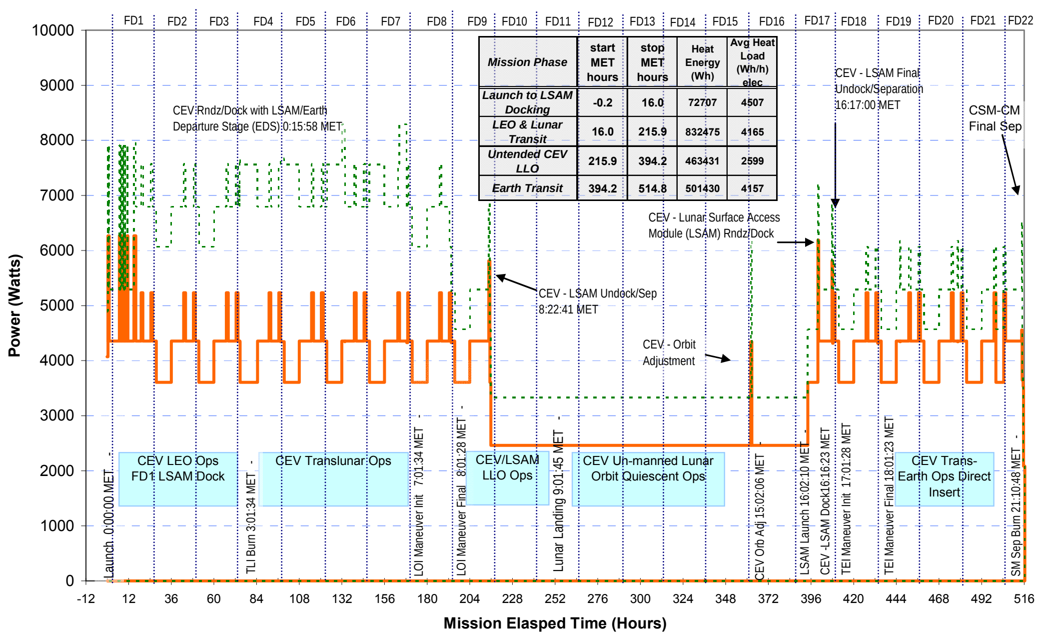

Mission Phase	start MET hours	stop MET hours	Heat Energy (Wh)	Avg Heat Load (Wh/h) elec
Launch to LSAM Docking	-0.2	16.0	72707	4507
LEO & Lunar Transit	16.0	215.9	832475	4165
Untended CEV LLO	215.9	394.2	463431	2599
Earth Transit	394.2	514.8	501430	4157

Figure 7.2-10 CEV Lunar Mission Total Thermal Heat Load Profile

7.2.3 Mass Estimates and Design Maturity

The mass estimates for the Electrical Power System and corresponding bases of estimate are provided in Table 7.2-2.

Hardware Items	Quantity	Unit Mass (lbm)	Growth (%)	Total Mass (lbm)	CM Mass (lbm)	SM Mass (lbm)	SA Mass (lbm)	Basis of Estimate
Electrical Power System				**3,319**	**1,338**	**1,955**	**25**	
Power Distribution Units	2	45	12%	100.8	100.8			Bottom's Up Component Summation
Secondary Power Distribution Units (Int.)	2	74	10%	162.8	162.8			Modified ISS FCF EPCU
Secondary Power Distribution Units (Ext.)	2	44	10%	96.8	96.8			Modified ISS FCF EPCU
Primary Power Wiring Harness	1	106	30%	137.8	137.8			Lengths: Guess; Gage: Calc based on Current
Secondary Power Wiring Harness	1	140	30%	182.2	182.2			Lengths: Guess; Bottom's Up Quantity Count
Power Transfer Converter Units	2	13	30%	33.8	33.8			Vicor VI-200 series conv. in SCBU topology
Pyro Controller	2	16	20%	38.4	38.4			
Thruster Control Units	2	16	20%	38.4	38.4			
Utility Outlet Panels (UOPs)	12	0.4	30%	6.2	6.2			
LithiumIon Rechargeable Batteries	8	55	17%	514.8	514.8			SOA Li-Ion Energy Density
General Internal Lighting	3	4	20%	15.8	15.8			
Tunnel Adapter Light Assy	1	4	20%	5.3	5.3			
External Floodlight	1	4	20%	5.3	5.3			
LithiumIon Rechargable Batteries	2	4	17%	9.6		9.6		SOA Li-Ion Energy Density
Off-line Charge Regulators	2	2	30%	5.2		5.2		Vicor VI series isolating converter
Solar Array Wings	2	311	13%	702.7		702.7		
SADA Power Harness	2	9	25%	22.0		22.0		
Solar Array Launch Support Structure	2	114	25%	286.0		286.0		
Array Regulator Units	4	43	15%	197.8		197.8		ISS SSU (scaled dow n to 5kW)
Power Distribution Units	2	45	12%	100.8		100.8		Bottom's Up Component Summation
Secondary Power Distribution Units	2	44	10%	96.8		96.8		Modified ISS FCF EPCU
Primary Power Wiring Harness	1	203	30%	263.5		263.5		Lengths: Guess; Gage: Calc based on Current
Secondary Power Wiring Harness	1	81	30%	104.7		104.7		Lengths: Guess; Bottom's Up Quantity Count
Pyro Controller	2	12	20%	28.8		28.8		
Thruster Control Units	2	42	20%	100.8		100.8		
SM-to-CM Umbilical	4	7	30%	36.4		36.4		
Wiring	1	20	25%	25.0			25.0	

Table 7.2-2 EPS Mass Estimates

7.2.4 Plan Forward

- Consider further size and mass reductions for solar array and battery systems
- Scrub subsystem loads and integrate low power switching into Avionics
    - Reduces SPDU switch count
    - Reduces SPDU mass and volume
    - Reduces ATCS
    - Reduces wire mass and routing

- Reduces bulkhead penetrations
- Solar Array Wing
  - Integrate stowed configuration with ascent loading
  - Enhance design of yoke capture mechanism
  - Expand deployed stress analysis cases for nominal and failure mode scenarios
  - Enhance design of hinges
  - Assess stowed wing power generation capability
  - Assess impacts of incorporating higher performance Emcore BTJM solar cells
- Further consideration of ISS and LSAM power transfer

7.2.5 Solar Array Wing Analysis Appendices

7.2.5.1 Solar Array Wing Stowed & Deployed Structural Dynamic Design/Performance

The following "Solar Array Structural Analysis and Sizing" report was written to document TDS CEV-08-005 by GRC/DES/T. Cressman on September 10, 2006.

Background

The purpose of this study was to address the impact of the structural loads on the solar array mass for all driving mission events. For CRC-2, very preliminary sizing was done due to the quick turnaround required. For the support structure that holds the stowed arrays during launch no actual sizing was done. Rather, a generic mass estimating relationship was used even though supporting the arrays during launch was considered challenging. For the deployed arrays the trans-lunar injection (TLI) burn was addressed but dynamic amplification due to engine transients was not included and generalized instability (buckling) was not included as a failure mode. ISS plume impingement loads and reboost loads were not considered.

Finally, the off-nominal case of a failed SADA (solar array tracking mechanism) post-TLI was not considered. In such an event the arrays could be stuck in their weakest orientation but may still need to survive a firing of the Service Module Main Engine (SMME) or even the engines on the lunar descent stage in order to assure safe return of the crew. This case could prove critical to array sizing or could require EVA or other contingencies to assure safe return.

An analysis was performed to determine the impact of static and dynamic loading on the CEV solar arrays during the CEV mission, including launch, reboost, the TLI burn, the LOI burn, and the TEI burn. Panels, hinges and booms and support structures were sized to meet this requirement. Fundamental natural frequencies were determined and deflections were predicted for assessing any clearance issues with ISS or the LSAM.

The requirements being addressed by this analysis are:

1) CEV-CLV IRD "The interface structure shall accommodate the loads defined in the CEV/CLV Loads Requirements Databooks (TBR)." [CXP-01001 – Section 3.3.1.1]

2) CEV-ISS IRD [CXP-01007] Effective Date 2/10/06
   - The CEV must withstand .2 g loads in any direction while mated. [CV0403]
   - The CEV shall withstand ISS plume loads of 7.2 psf for normal and 0.8 psf for shear (TBR-002-076) induced by attitude control and reboost. [CV0397]

In addition, there were no loads defined in the CEV-LSAM IRD and the CEV-EDS IRD.

Assumptions and Groundrules

Description of Arrays

The analysis and sizing use the CRC-2 design as a starting point. Figure 7.2-11 shows the overall array wing geometry. Each wing is about 44 ft long and 10 ft wide. The wings span 104 ft from tip to tip. The bottom half of Figure 7.2-11 shows the array design that resulted from this TDS, with launch sized launch support structure and the addition of large edge closeout on the in-board-most panel.

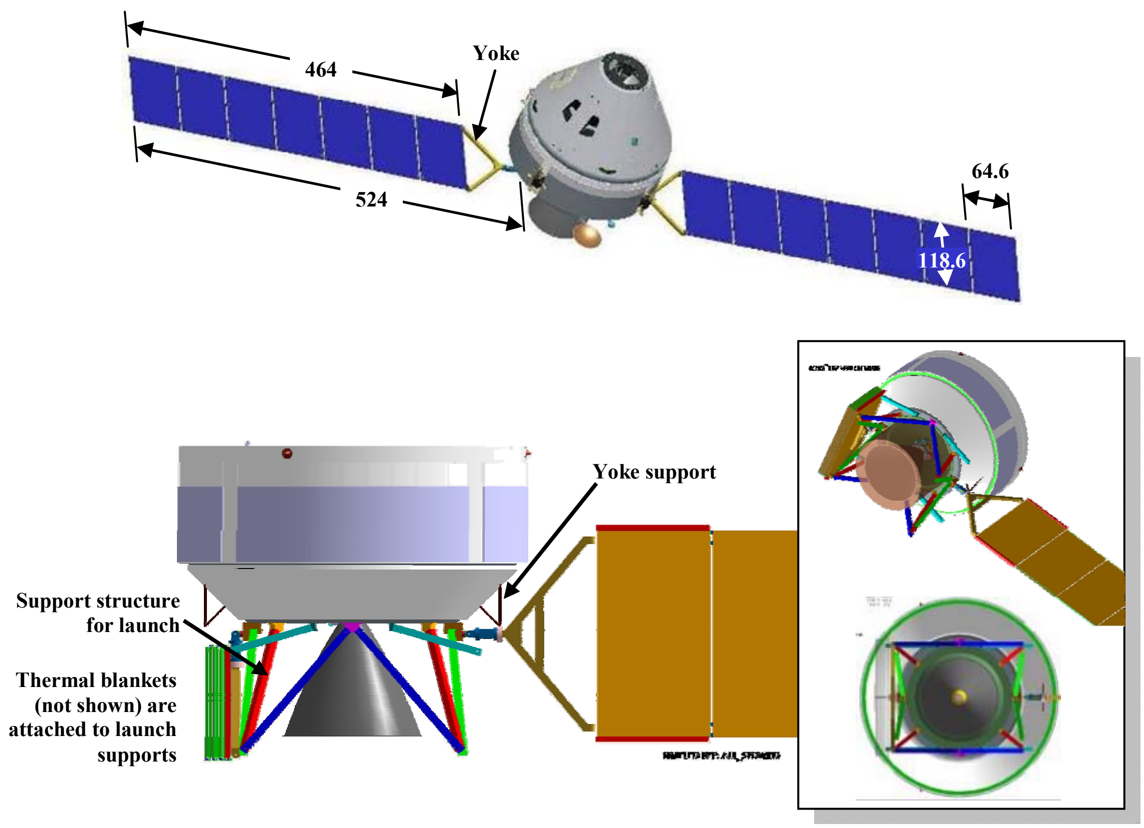

Figure 7.2-11 CRC-2 Arrays

Figure 7.2-12 shows the typical panel construction. The panel is of composite honeycomb sand-wich construction. Each face sheet consists of three 0.0075 inch carbon/cyanate ester face sheets with a 1 inch thick aluminum honeycomb core with 3/8 inch cells and 0.001 inch foil thickness. The face sheets are bonded to the core using reticulated adhesive for minimum weight. The construction is considered state of the art and flight proven. However the loads for the SM missions are considered out of family. For this reason it was expected that modifications would be required to survive the SM mission.

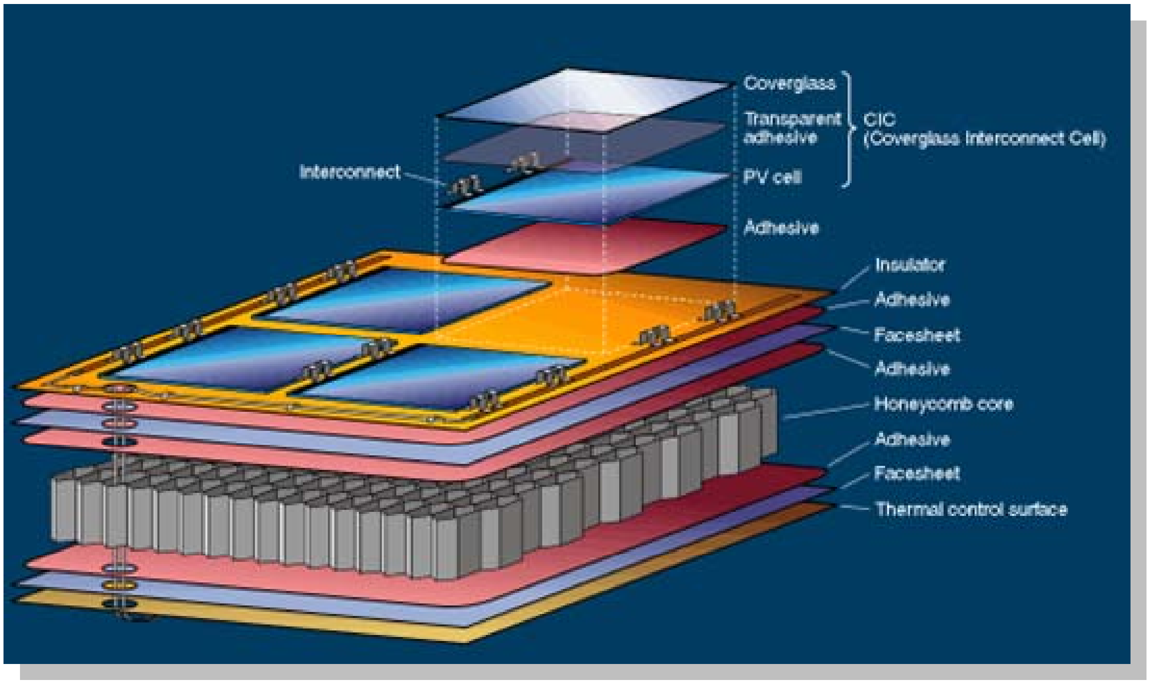

Notes:

- **Adhesive layer bonding face sheet to honeycomb core will actually be reticulated.**
- **Thermal control surface will actually be an environmental coating.**

Figure 7.2-12 CRC-2 Array Panel Construction

The hinges were also considered out of family due to the high loads. Previous designs for hinges on arrays and booms indicated low g load capability (~0.1-0.2 g). Therefore five hinge concepts were developed to obtain realistic mass and stiffness values for the hinges. The concept shown in Figure 7.2-13 was selected for further evaluation. Materials were chosen for high stiffness. The C channel at the back is bonded directly to the face sheets of the panel and protrudes 2 inches into the panel. Total mass of each hinge assembly is 1.73 lb not including deployment springs. Two hinges per panel edge were utilized in the stress analysis.

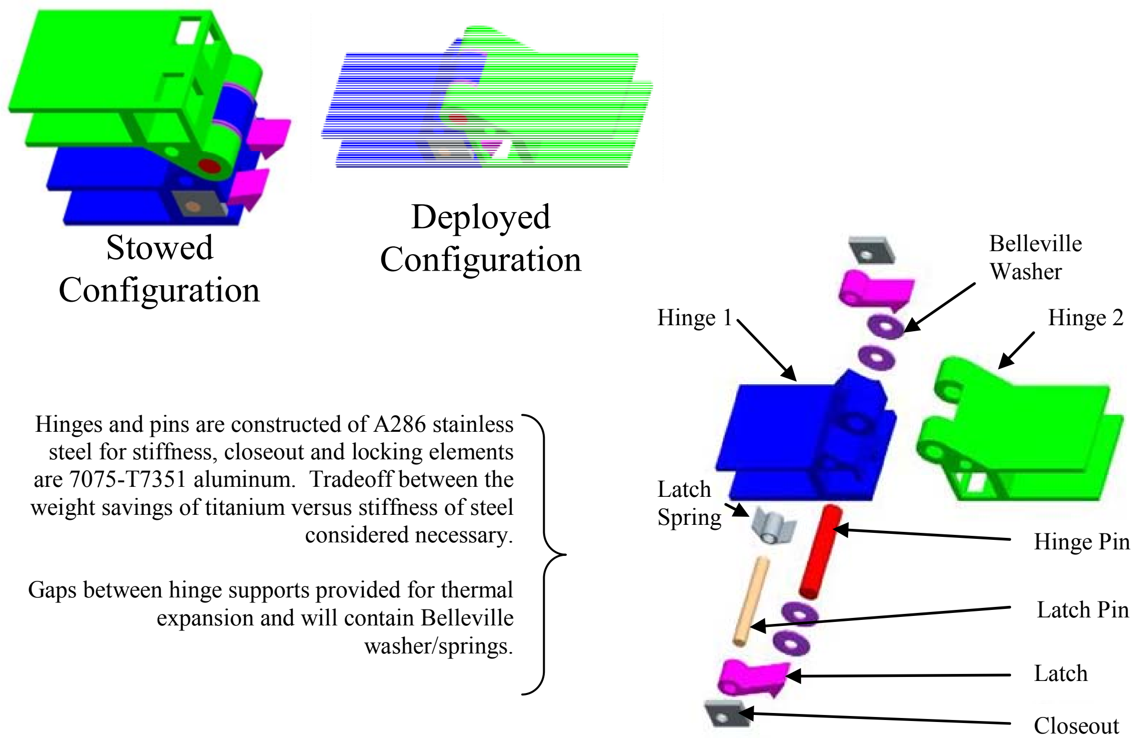

Figure 7.2-13 Array Hinge Concept for CRC-3

Loads

Figure 7.2-14 shows the load cases that were addressed. Launch and ascent loads were obtained from the CEV Loads Databook for CRC-2. The thrust/weight values for the TLI, LOI, and TEI burns were obtained from Jim Geffre on 6/29/06 for the latest mission analysis results.

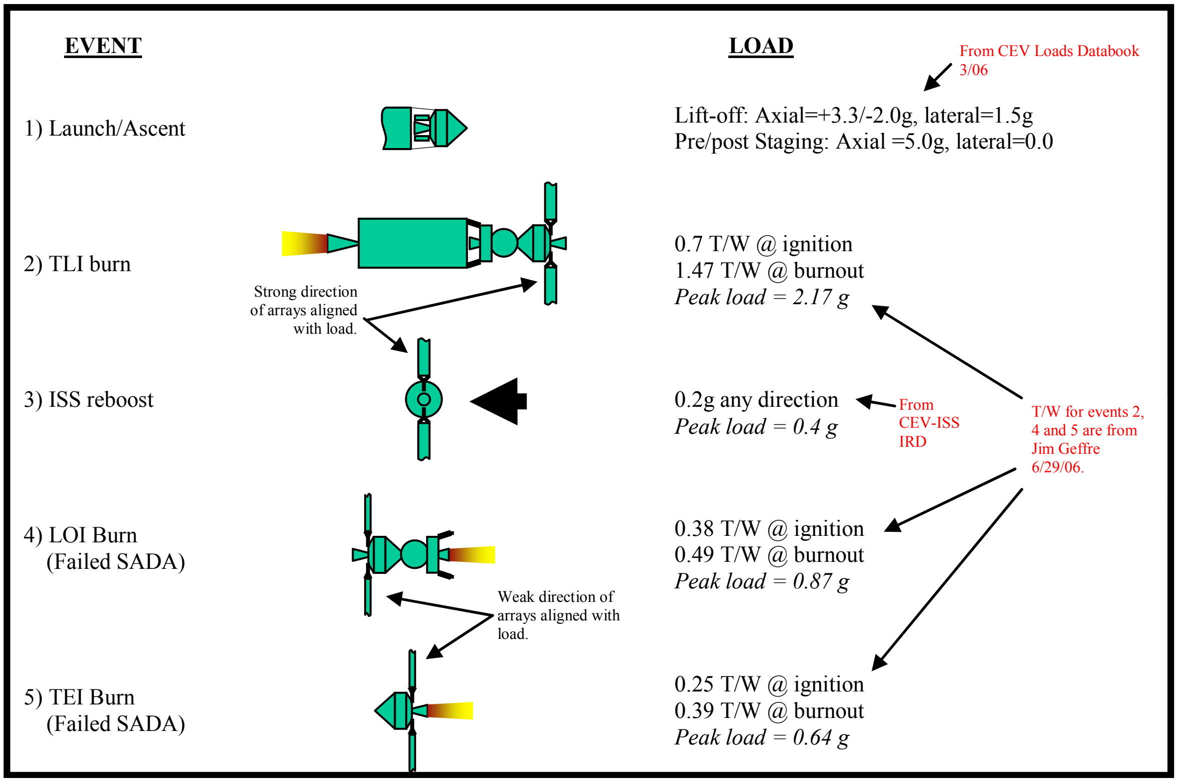

Figure 7.2-14 Array Load Cases Analyzed

Load Case 3 (ISS Reboost) was obtained from the CEV-ISS IRD. The acceleration value is considered ultra-conservative. At the time CEV is expected to dock to ISS, the ISS mass is expected to be > 800,000 lbm. A 0.2 g load would require a force of 160,000 lbf on the vehicle. In fact, the ISS arrays are only designed for a 0.1 g lateral load. Nevertheless, a dynamic amplification factor of 2 was applied. Even at 0.4 g's the reboost loads did not size anything.

Load Cases 4 and 5 are considered because the array rotation mechanism could fail with the arrays in the worst possible orientation. In this case the mission is expected to be aborted. However, if the SM is not on a free return trajectory, the SMME engine or the Lunar Descent Stage engines could be required for safe return of the crew. The term "LOI Burn" is a misnomer in this analysis. No lunar orbit insertion will be performed after an array mechanism failure. It simply refers to the case where the lunar descent engine is used for safe return, since the T/W will be the same. It can be argued that Case 4 would never occur since the SMME would be available to do the job and an Apollo 13-type return postulates a second failure in addition to the array mechanism. However, for this analysis, since Case 4 bounds Case 5, only Case 4 was analyzed.

Loads not considered were the ISS RCS impingement loads and the docking loads. The CEV-ISS IRD specified a 7.2 psf plume impingement load. Applied to the entire area this is equivalent to a 13 g inertial load on the arrays or a 2,700 lbf distributed force. This is well in excess of the thrust capability of any RCS on board. The impingement load will most likely be impulsive, applied to a limited area and cannot exceed the rated thrust of the RCS jets. The docking load is an impulsive load and will be attenuated by the intervening CEV structure. Therefore it was not considered for this analysis.

Dynamic amplification due to engine start and stop transients was considered an important factor to include. Figure 7.2-15 illustrates the assumed response to these transients. Undamped response to a unit step function was assumed. This gives a peak acceleration that is the sum of the initial and final thrust/weight for the vehicle 'stack' for a given burn. This acceleration is applied as a static load to the arrays. This is conservative since in reality there is damping and the engines ramp-up in thrust. Typical ramp-up time for a pump-fed engine is 3 seconds. For a pressure-fed engine it is 0.8 seconds. The deployed array fundamental modes are above 0.1 Hz.

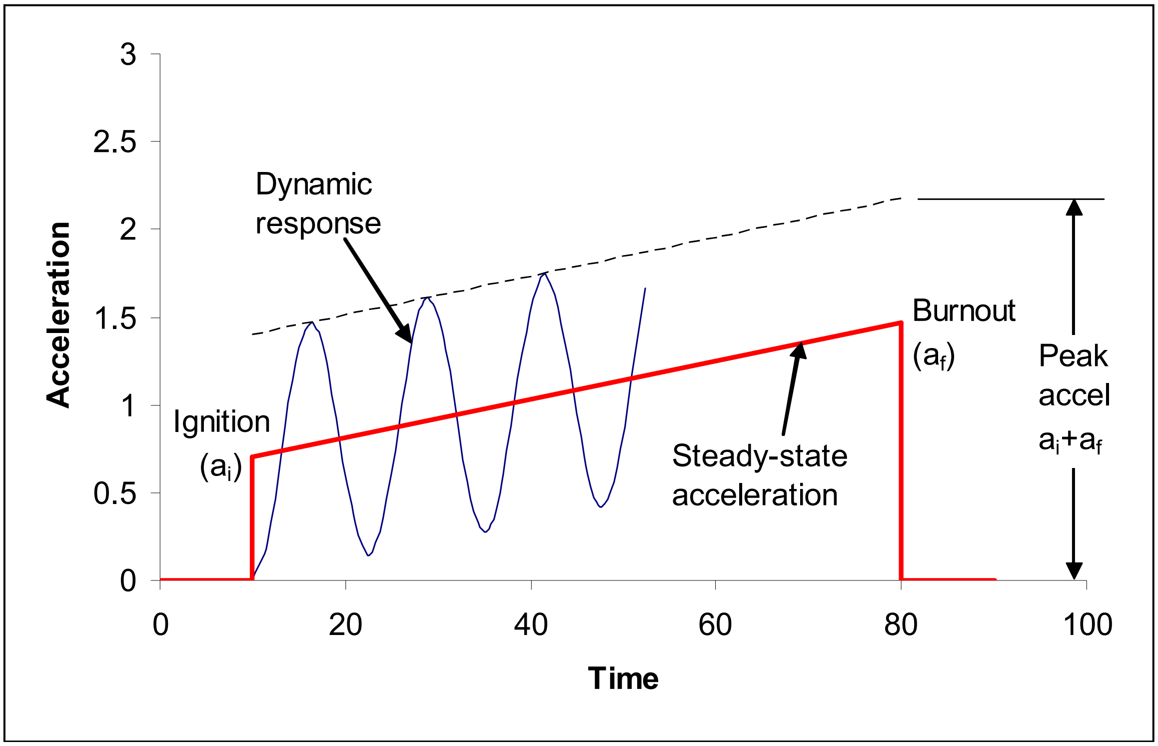

Figure 7.2-15 Array Dynamic Loads

Failure Modes

The failure modes considered for this analysis are listed below.

1) Array generalized instability (buckling): Coupled flexural/torsional and panel buckling.
2) Panel local modes: Face sheet wrinkling/core crush, inter-cell buckling, face sheet shear crimping, face sheet material failure
3) Hinges: Material failure
4) Arm/Yoke: Material failure
5) Yoke support: Material failure, buckling.
6) SM structure support: Material failure, buckling.
7) Material failure of composites: Tsai-Wu Failure Criteria.

A factor of safety of 1.4 was used for metallic material failure, for buckling and for composites away from fittings and discontinuities. A factor of safety of 2.0 was used for composite material failure at fittings and discontinuities. There were no known requirements for fundamental nodes. However, it was considered desirable to have axial natural frequencies above 25 Hz during launch and ascent to avoid coupling with vehicle modes and this was set as a goal. Fundamental modes for the deployed arrays was determined for comparison to engine transients

Analytical Models and Tools

ProEngineer was used for CAD modeling. MSC/NASTRAN version 2005 Solution Sequences 101, 103, 105 and 106 were used for linear static, model, bucking and non-linear finite element analyses respectively. Hypersizer Vxx was used for determining material properties for composite honeycomb sandwich panels.

Summary of Results

Load Case 1 – Launch and Ascent

A study was performed to design array supports for launch. Both mechanical design and finite element analysis were performed to determine mass, stresses, deformations and natural frequencies. It was assumed that the SM tension cone was perfectly rigid. Figure 7.2-16 shows the arrays without launch support structure, with the arrays cantilevered from the aft SM tension cone. The predicted displacements are 0.8 inches and the fundamental mode is 3.7 Hz, which is in the range predicted for the CEV 1st axial mode. Inclusion of SM structural compliance will result in considerably higher displacements and lower natural frequencies.

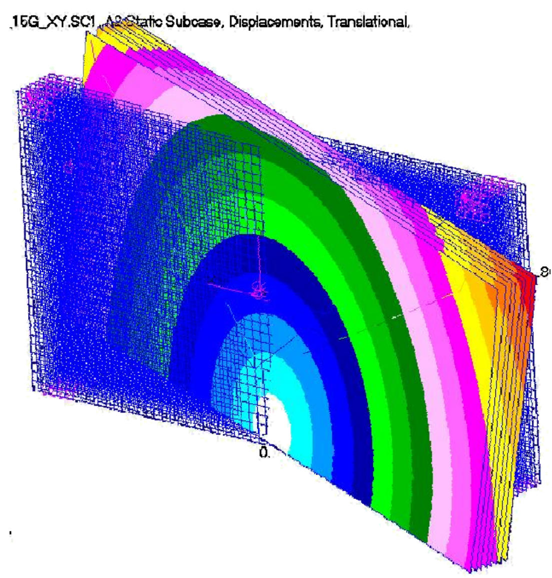

1st Mode: 3.7 Hz
2nd Mode: 5.0 Hz.
Max static deflection: 0.8”

1st mode is essentially a rigid body mode.

Figure 7.2-16 Launch/Ascent – Cantilevered Arrays

The added launch support structure shown in Figure 7.2-17 consisted of composite tube truss members and metallic fittings. The truss members are graphite-epoxy with a pseudo-isotropic lay up. Wall thickness of the tubes is 0.064 inches. Total mass of the structure is 60 lb plus about 35 lb of fittings. Thermal blankets would be attached to the launch supports but were not modeled for this analysis. Sizing of launch supports was driven by minimum gage and strength requirements. Margin of safety for material failure is 0.25 for F.S. = 2.0. The margin of safety for buckling is large. It was difficult to obtain a 1st mode above 25 Hz. Additional ties between the panels are required to raise the frequencies further. It is possible that the stowed arrays will couple with the CEV 1st axial mode, which is expected to be in the 15-20 Hz range, though structural damping of the array stack will be high.

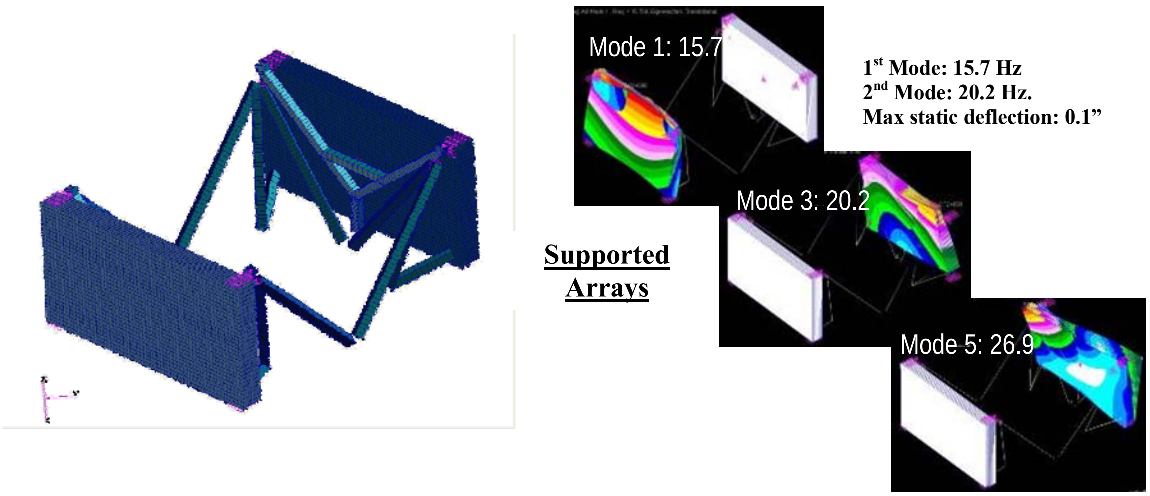

Figure 7.2-17 Launch/Ascent – Supported Arrays

Stability Analysis of Deployed Arrays

Stability (bucking) analysis was performed for the deployed arrays for load cases 2 (TLI burn) and 4 (LOI burn). Table 7.2-3 gives a summary of the results. For the old design (CRC-2) margins were negative for both the TLI and LOI burns. Panel edge closeouts were added to obtain positive margins for the TLI burn. Notice that the “General Bucking” is highly negative without these closeouts. This flexural/torsional mode is shown in Figure 7.2-18. An additional ply was added to each face sheet on the two inboard-most panels to get positive margins for the LOI burn. Figure 7.2-18 also shows the changes that were mode for the new design.

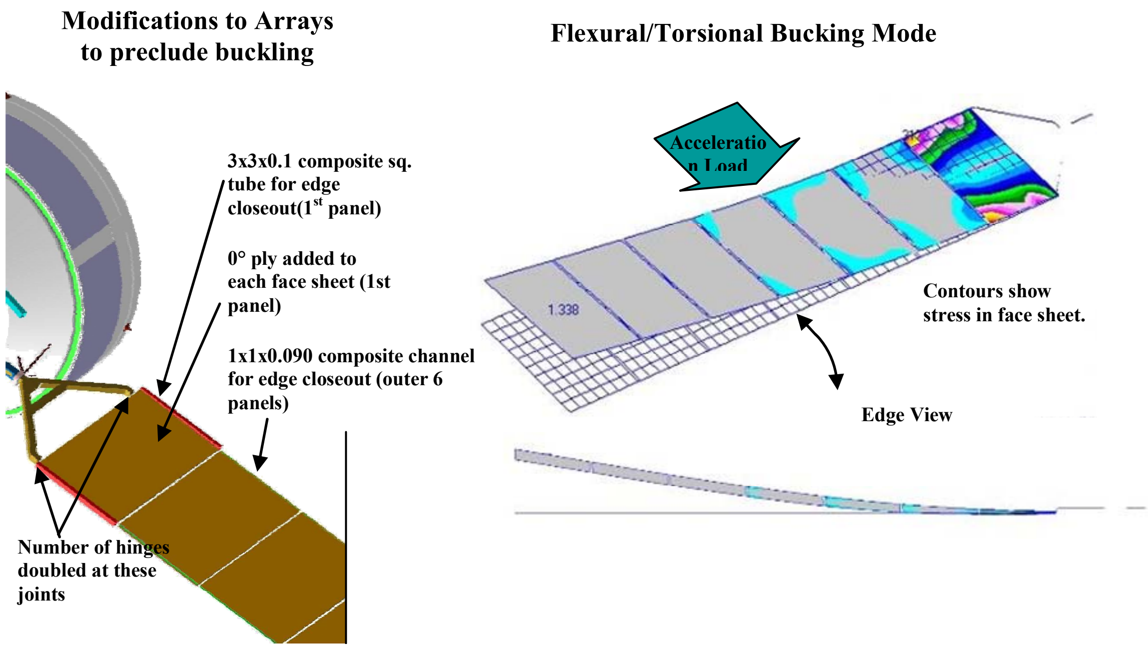

Figure 7.2-18 Stability Analysis of Arrays

	Margin of Safety		
Description	**Original Design**	**New Design**	**Remarks**
General Buckling InPlane Loading	-0.34	0.02	2.17 g's
General Buckling Normal Loading	-0.19	4.24	0.87g's
Local Facesheet Intracell Buckling	-0.93	0.71	Facesheet added (0/60/-60/0) to First 2 panels
Facesheet Wrinkling/Core Crush	0.07	0.07	3/8" Honeycomb cell size
Facesheet Shear Crimping	10.00	8.30	

Table 7.2-3 Stability Analysis of Arrays – TLI and LOI Burns

Deployed Array Displacements

A geometric non-linear elastic analysis was performed to determine the static deflections for the TLI burn. The deflections are shown in Figure 7.2-19 true to scale for both the old and new designs. The old design exhibits large and unacceptable post-buckled deflections. The new design shows reasonable deflections but some out-of-plane displacements, on the order of 7 ft, due primarily to offset hinges.

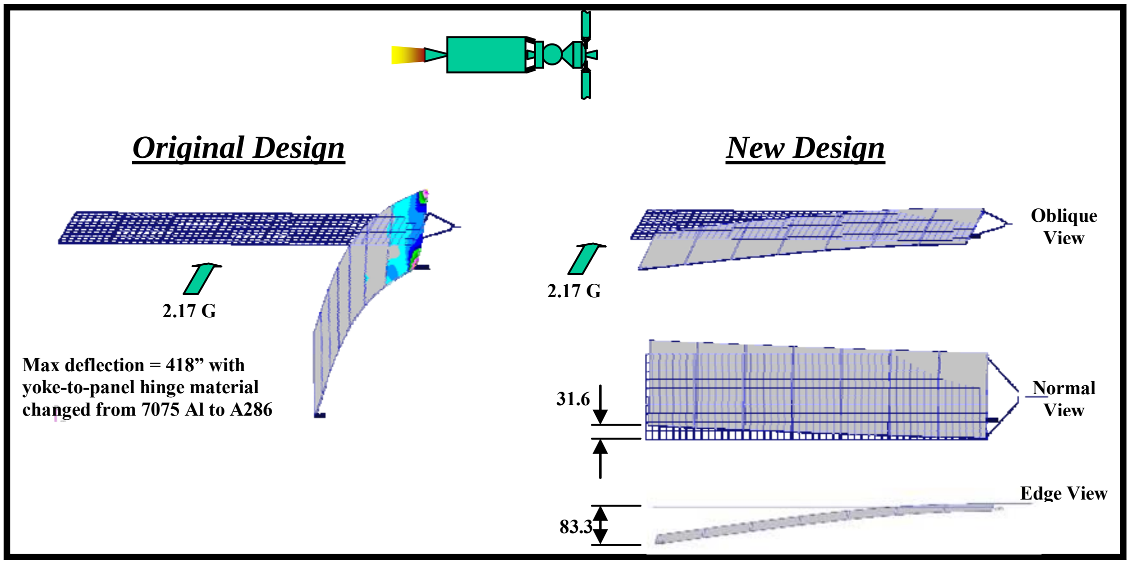

Figure 7.2-19 Deflection – TLI Burn

The analysis was repeated for the LOI burn case and the results are shown in Figure 7.2-20. Note that this is an 'off-nominal' case, i.e., the SADA is assumed to have failed with the arrays in the worst possible orientation. This case was not analyzed for CRC-2. The deformed shape is shown to true scale. The old design bows 24 feet and exhibits local bucking and material failure in the face sheets. The new design reduces tip deflection to 15 feet and eliminates buckling. The deflection for the new design needs to be evaluated to determine if there will be issues with plume impingement.

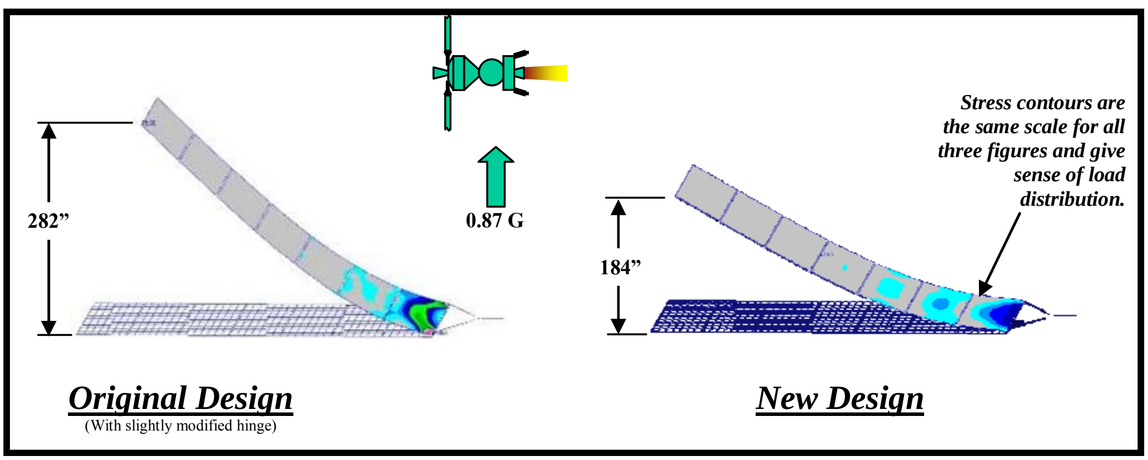

Figure 7.2-20 Deflection – LOI Burn

Hinges

The hinges were analyzed using hand calculations. Table 7.2-4 summarizes the results. Margin of safety for the bond joint between the hinge and panel is 0.69 assuming 4,000 psi for the strength of the adhesive. The minimum margin of safety of 0.02 is in the latching area of the hinge.

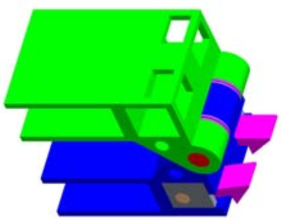

Stowed Configuration

Deployed Configuration

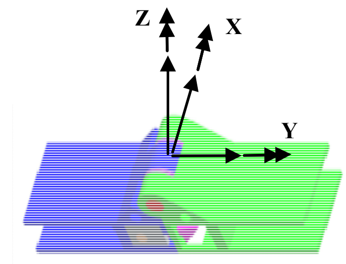

Margins of Safety on Hinge Components								
	M.S. Yoke to Panel 1 - *			M.S. Panel 1 to Panel 2			M.S. Panel 2 to Panel 3	
	Load Case1 Z direction (.87g) (1.4 F.S.)	Load Case2 X direction (2.17g) (1.4 F.S.)		Load Case1 Z direction (.87g) (1.4 F.S.)	Load Case2 X direction (2.17g) (1.4 F.S.)		Load Case1 Z direction (.87g) (1.4 F.S.)	Load Case2 X direction (2.17g) (1.4 F.S.)
Pin	6.11	0.45		9.12	19.02		16.57	32.07
Latches	0.19	0.06		0.16	14.89		1.05	22.55
Latch Pin	0.14	0.02		0.23	15.87		1.18	23.99
Attachment on Hinge	0.17	0.05		0.13	14.46		1.00	21.91
Material Strength								
Pin	65500.00	A286 Steel						
Latches	65500.00	A286 Steel						
Latch Pin	65500.00	A286 Steel						
Attachment on Hinge	65500.00	A286 Steel						

* - These Margins of Safety result from modifications to the standard hinge design due to the higher loads and differing interface at the yoke to panel interface. These modifications are an extra lug on one hinge side, an increase in the latch pin to .375" in diameter, and sectioning of the latch to provide for more shear area on the hinge

Table 7.2-4 Hinge Margins of Safety

Face Sheet Material Failure

Face sheet material failure was evaluated for the new design using the Tsai-Wu failure theory. Material failure is assumed for a Tsai-Wu failure index above 1.0. Thus a Tsai-Wu index below 0.72 gives positive margin of safety (MS) generally (factor of safety for 1.4), while a Tsai-Wu index below 0.5 gives a positive margin of safety for joints and discontinuities (F.S. 2.0).

Figure 7.2-21 shows the Tsai-Wu index for the new design for both the TLI and LOI burns. For the TLI case the stresses are generally low, though some hot spots occur on several of the panels near the hinges. It is thought that these margins can be made positive with proper tailoring of the interface between the metallic hinges and the carbon/cyanate ester plies. For the LOI Burn case the margins are lower but with local tailoring and with additional plies near the yoke attachment the margins should become positive.

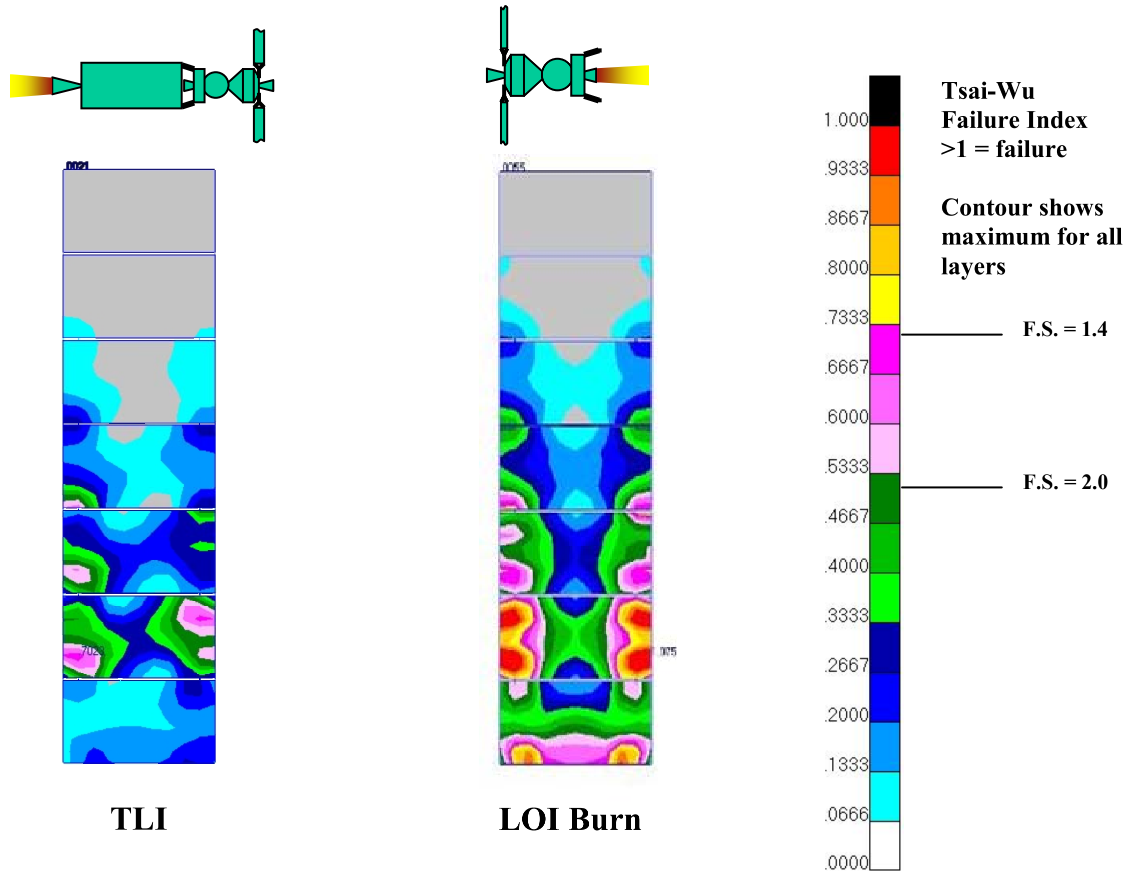

Figure 7.2-21 Face Sheet Material Failure

Yoke

The yoke was also examined for material failure and the results are summarized in Table 7.2-5. The critical sizing case for the yoke is the TLI burn. The margin of safety is negative for the new design (factor of safety = 2.0). The yoke wall thickness must be increased locally by 0.15 inches to obtain positive margin of safety. Resulting additional mass is no more than 5 lb.

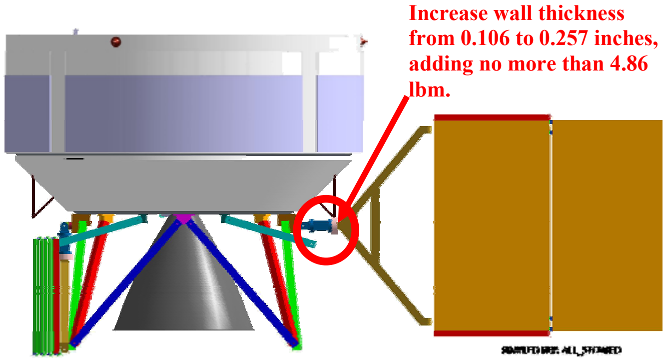

Load Case	Material	Thickness	*Max Stress (ksi)*	*Ult Strength (ksi)*	*Margin of Safety*
5.0 g	Gr/E	0.106	**25.**	**50.3**	**0.01**
2.17g	Gr/E	0.106	**41.9**	**50.3**	**-0.40**
0.87g	Gr/E	0.106	**16.8**	**50.3**	**0.50**

Table 7.2-5 Yoke Material Failure

Yoke Support

The yoke support was examined for the TLI and ISS Reboost cases combined. Figure 7.2-22 summarizes the results. Note that even with the combined load set, the margins of safety are positive. The yoke support mass is driven more by minimum gage.

Material: Ti-6Al-4V
X-Section: ¾” dia. x 1/8” thk wall
Length: 2 bars are 41.46”
1 bar is 21.2” long
Mass: 4.26 lbm for 3 bars combined
Loads: 200 lbf (0.4g) in X
1000 lbf (2.17g) in Y

Maximum Defl: 0.01 inches
Max Von Mises stress: 3292 psi
Minimum Buckling Factor: 6.45
Min. Mat. Safety Factor: 40

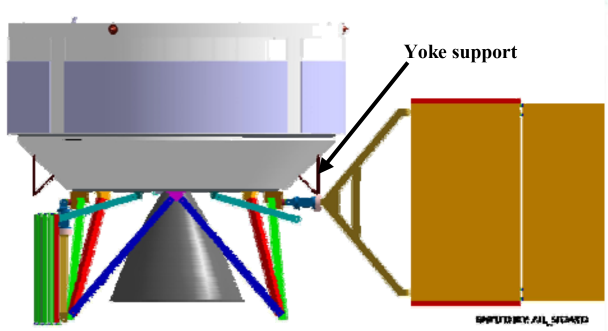

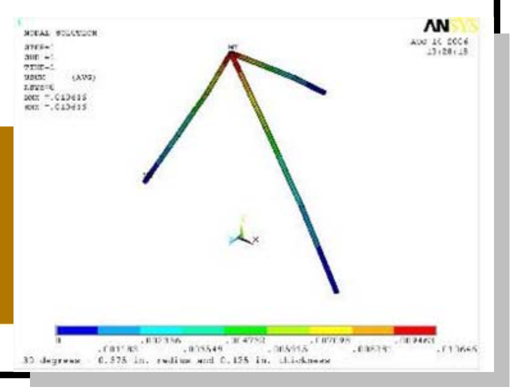

Figure 7.2-22 Yoke Support Margins of Safety

Deployed Array Modal Analysis

A modal analysis was also performed on the deployed arrays. Figure 7.2-23 shows the four lowest modes for both the old and new designs. The frequencies are typical of large solar array wings. The periods are on order of the engine ramp-up times, indicating that the assumed dynamic amplification factor of two could be reduced significantly with a coupled loads analysis.

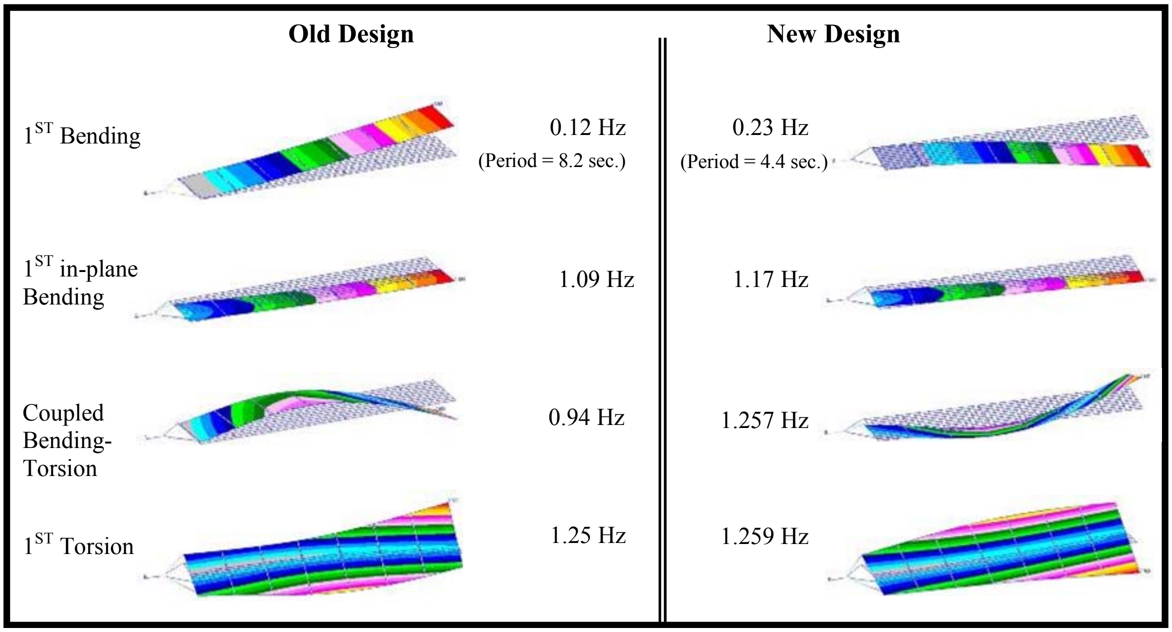

Figure 7.2-23 Deployed Arrays – Normal Modes

Mass Summary

Table 7.2-6 summarizes the structural mass difference between the old (CRC-2) and new (CRC-3) designs. 151 lb may be considered the mass impact of using deployed arrays during the in-space thrusting events compared to using them on a conventional low-thrust spacecraft. 96 lb, or 16% of the wing mass, is required to support the arrays during launch in the CRC-2 configuration.

Description	Old Design (CRC2) Qauntity	Old Design (CRC2) Unit Mass (lb)	Old Design (CRC2) Total CBE Mass (lb)	New Design Qauntity	New Design Unit Mass (lb)	New Design Total CBE Mass (lb)	Difference (lb)
Base Panels	14	28.4	397.6	2	43.1	86.2	
Outer Panels	-	-	-	12	34.1	409.2	
Panel Hinge	28	1.1	30.8	36	1.8	64.8	
Yoke	2	11.8	23.6	2	21.7	43.4	
Total for Wings			***452***			***603.6***	***151.6***
Yoke Support	0	-	-	2	10	20	
Launch Support Structure	2	24	48	2	48	96	
Total for Array Supports			***48***			***116***	***68***

Notes:
CBE = Current Best Estimate
Quantities are for both wings conbined.
Structural elements included only.

Table 7.2-6 Mass of Solar Arrays

Potential Ways to Reduce Array Mass

- Scrub CEV power loads, LSAM power transfer (reduced panel area).
- Refine solar cell string design for driving lunar hot case (reduced panel area).
- Utilize soon to be released SOA solar cell with higher efficiency (reduced panel area).
- Mass optimized launch support structure. (Fitting mass could be reduced).
- Mount the arrays flat against the aft end of the SM.
- Use picture frame panels in stead of sandwich panels.
- Perform coupled loads analysis to determine realistic dynamic loads (refinement over conservative amplification factor).

Conclusion and Issues

The following conclusions may be drawn from the work performed for this TDS.

1) Structure can be designed to adequately support the arrays during launch/ascent. But coupling with the CEV fundamental axial mode is possible.
2) Dynamic amplification has a significant impact on array mass and needs to be quantified for preliminary design.
3) Generalized instability (buckling) of the deployed array is a key failure mode for array structural sizing.
4) The arrays can be designed to structurally survive in-space acceleration events even in the event of a joint failure post-TLI, but resulting deflections will be large.
5) ISS acceleration loads do not affect array mass significantly even though they appear to be unrealistically conservative.

6) Plume impingement loads as specified in the ISS to CEV IRD will have a significant impact on array sizing and must be defined realistically.

Recommendations Follow-on Analysis

1) Need more realistic accelerations and plume impingement loads while mated to ISS. Perform coupled loads analysis to determine realistic loads on the arrays.
2) Need more realistic amplification factors for the arrays during engine start transients. Perform coupled loads analysis for TLI and TEI burns.

The analysis needs to be updated for the array concept chosen by the contactor.

7.2.5.2 Solar Array Wing Packaging Study

The following "Solar Array Wing Packaging Study," was performed by and documented by NASA GRC/DEC/Daniel A. Catalano.

CRC-2 (DAC-2)

The solar arrays were packaged in CRC-2 (DAC-2) as shown in Figure 7.2-24. Each array was positioned with the panels parallel to the vehicle centerline. The yoke structure was facing outboard and a notional structure with MLI, estimated at 38 lb per wing, was assumed to be in place provide support during launch and thermal protection during main engine firing.

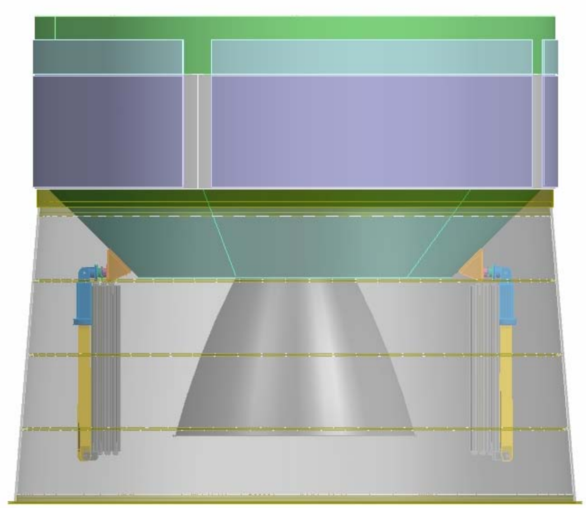

Figure 7.2-24 CRC-2 (DAC-2) Solar Array Configuration

The deployment kinematics of this array panel stack was evaluated using ADAMS analysis software, as shown in Figure 7.2-25. The deployment consisted of a two step process. First launch restraints holding the yoke are released and the yoke is rotated 90° and locked into position. Next, the array panel stack is released, deploying the array to its final position. A total deployment time of 120 seconds was assumed. The array panels deploy in an arching motion, which the ADAMS analysis showed to produce a maximum torque at the yoke hinge of 58.7 in-lb. This type of motion would be difficult to demonstrate on the ground due to the multi-axis motion and the challenges of off-loading the mass.

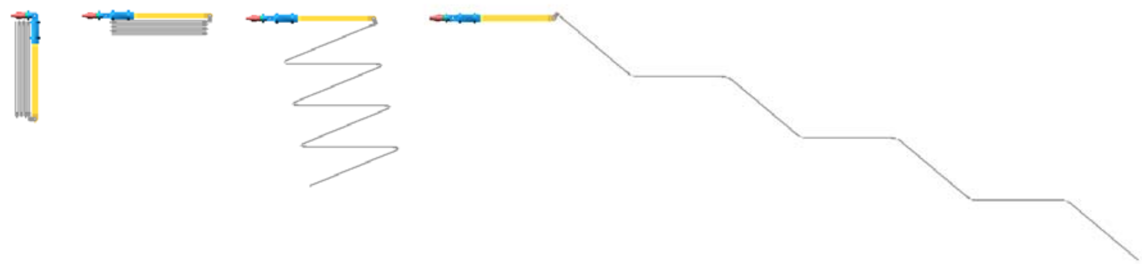

Figure 7.2-25 CRC-2 (DAC-2) ADAMS Analysis of Solar Array Deployment

CRC-3

CRC-3V (Vertically Stowed Array Configuration)

Additional focus on packaging the arrays was included in this design cycle. The first configuration investigated kept the arrays vertical, but flipped the stack such that the yokes were now inboard as shown in Figure 7.2-26. This configuration improved the deployment kinematics and launch support structure attachment, as shown in Figure 7.2-27.

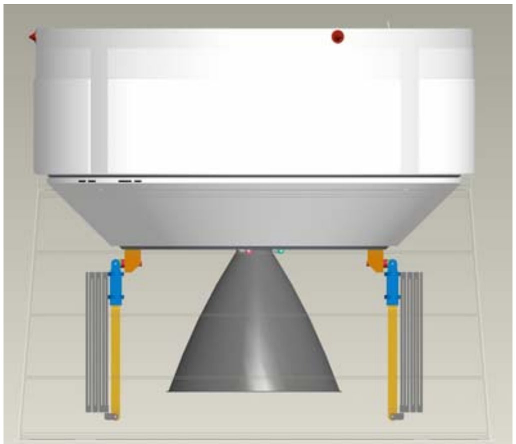

Figure 7.2-26 CRC-3V Solar Array Configuration

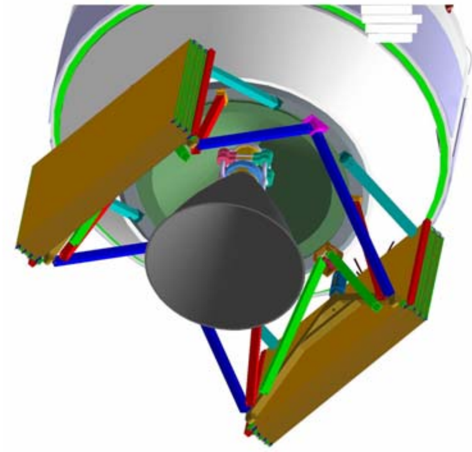

Figure 7.2-27 CRC-3V Solar Array Launch Support Structure

Some MMOD shielding will be required to protect the main engine. The design of the shield was not considered in much detail. Therefore, an approximate mass will be used for both array packaging concepts.

The thermal protection of the array stack will have MLI blankets that can be attached to the launch support structure. The shielding can be mounted such that it will not impede the deployment of the array stack and will remain on the vehicle.

In addition, the deployment now was a single step process. The array stack was secured to the yoke, which was also secure for launch. Once the restraints were released, the yoke and array panels were deployed in a more "traditional" linear motion. This motion can be demonstrated on the ground and off-loading the mass becomes easier. The configuration was also evaluated using ADAMS, as shown in Figure 7.2-28. As before, a total deployment time of 120 seconds was used. However, due to the simpler deployment kinematics, the maximum torque at the Yoke hinge was only 3.6 in-lb.

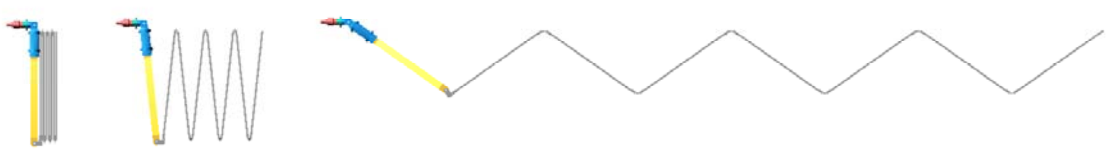

Figure 7.2-28 CRC-3V ADAMS Analysis of Solar Array Deployment

Based on the analysis and cleaner launch support structure attachment, it was decided that this array configuration would be considered the baseline for CRC-3.

CRC-3H (Horizontally Stowed Array Configuration)

An attempt was made to package the stowed arrays horizontally, thereby eliminating the need for additional launch support structure and to move them away from the engine exit. The individual panel size was reduced from 64 in. x 118 in. to 55 in. x 108 in. and the number of panels increased from 7 to 9 in order to maintain equivalent power generation. The reduction in panel size allowed the stack to be mounted flat against the bottom of the cone structure, as shown in Figure 7.2-29, and still fit within the Spacecraft Adapter. In addition, for this design cycle the main engine was allowed to gimbal 7°.

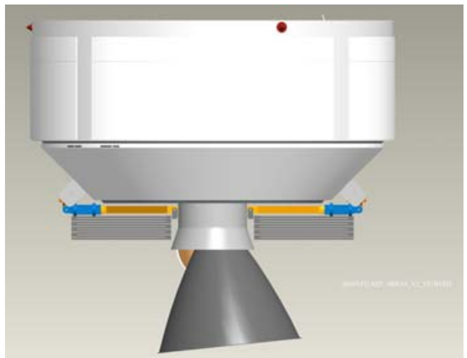

Figure 7.2-29 CRC-3H Solar Array Configuration

The position of the yoke eliminates any additional launch support structure since restraint points can be incorporated into the base of the cone as shown in Figure 7.2-30.

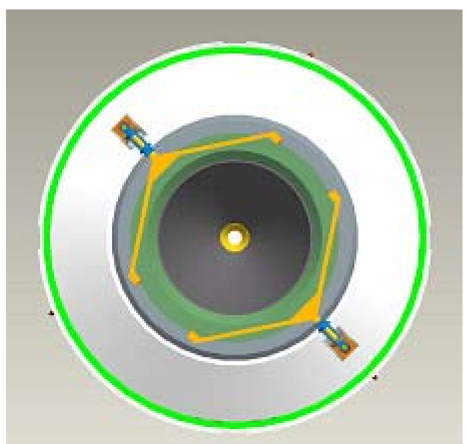

Figure 7.2-30 CRC-3H Yoke Launch Restraint

The main engine had to be moved down approximately 31 inches to accommodate the array position. Some additional structure would be required to lower the engine to this position, but detailed mass assessment of this structure was not done at this time. As shown in Figure 7.2-29, additional MMOD shielding will be required to protect the main engine power head, which is now exposed due to the lowering of the engine. The design of the shield was not optimized but an approximate mass was included in the overall mass roll-up. One concern with the notional shield shown above is the potential overheating of the main engine power head due to the close proximity. A preliminary thermal study was conducted and the results indicate that additional clearance between the power head and the shield is required. The intent of the proposed shield would be to also serve as thermal protection for the solar arrays. Additional MLI will be required to protect the stack and will need to be removed prior to panel stack deployment. The thermal protection scheme using MLI needs further work to optimize and position on the vehicle.

The deployment would be a two step process, with the yoke rotating 45° before the array panel stack release is initiated. However, the deployment kinematics would still be somewhat linear. As before, an ADAMS analysis was run with a total deployment time of 120 seconds as shown in Figure 7.2-31. The resulting maximum torque at the yoke hinge was found to be 20.2 in-lb, which is higher than CRC-3V, but still less than half of the CRC-2 (DAC-2) configuration.

Figure 7.2-31 CRC-3H ADAMS Analysis of Solar Array Deployment

Summary

This packaging investigation was also part of the solar array structural analysis that evaluated the array during boost conditions. Some of the array panels had to have additional stiffening in order to meet the mission defined acceleration loads. For the two cases described above, the CRC-3H needed additional support after deployment due to that longer length of the array. This added mass to the overall wing configuration. However, considering the wings, drive mechanisms, MMOD shielding, thermal protection and yoke support, the total mass for both arrays CRC-3H was about 120 lb lighter compared to CRC-3V.

The findings were discussed as part of a Service Module Engineering Panel held at GRC and the recommendation was to proceed with the CRC-3V configuration as the baseline. An analysis evaluating tip-off was conducted for both configurations after the Panel recommendation. It was discovered that if a 3.2°/s relative rotation occurs during the CEV separation from the CLV, then for CRC-3V, an extremely fast separation velocity of 20 ft/s would be required to clear the Spacecraft Adapter opening with no margin. The separation velocity for CRC-3H was found to only be 4.5 ft/s. It is likely that the Spacecraft Adapter would have to be of a clam-shell design to support the separation of the CRC-3V configuration. Additional work is required to optimize both the MMOD and thermal protection methods. The successful deployment of the array stack will depend on protecting the arrays from the induced environments.

7.2.5.3 Solar Array Wing Thermal Protection Study

The following "Radiation Thermal Analysis on CEV Service Module Main Engine," assessment was performed by Xiao-Yen Wang and James Yuko of the Thermal/Fluids System Branch at NASA Glenn Research Center.

Summary

The Service Module (SM) will experience heating from the rocket engine during phases of the mission circularization burn, contingency abort-to-orbit burn and the trans-Earth injection burn(s). The engine temperatures approach steady state conditions within seconds after firing. A simplified thermal model of the stowed solar array panels and engine was run to determine the transient response of the solar arrays to the engine thermal environment and it was determined that the solar array layer closest to the MLI shielding would reach steady state in about 100 seconds, so a steady state condition was analyzed. The calculation of the engine environment involved using the Chemical Equilibrium Analysis code, CFD software, CFX for the combustion flow analysis, and Thermal Desktop for the radiation and thermal analysis. The majority of the heating comes from gas radiation from the expanding exhaust gases and radiation from the outside of the rocket nozzle. The gas radiation is a function of the combustion products, their density, and pressure. As a result, over 95% of the heat produced in the exhaust plume is in the axial direction of the exhaust plume. The gas that expands toward the Prandtl-Meyer expansion limit near the SM components has a very low pressure and density and not much total heat to affect the components. However, the radiation from the hot engine nozzle will require that the adjacent components have radiation shielding. The stowed solar arrays will need a high temperature multi-foil insulation to insulate them from the hot radiating engine nozzle. The solar array drive assembly is protected from the environment with the MLI insulation and heaters that were baselined in the DAC-2 analysis cycle.

Introduction

The main engine and its plume radiate heat to deployed/stowed solar panel and radiator panels when it burns (see Figure 7.2-32). Thermal analysis is performed to compute the heat flux from both the main engine and its plume. A preliminary design on the thermal blanket for the solar panel is also performed.

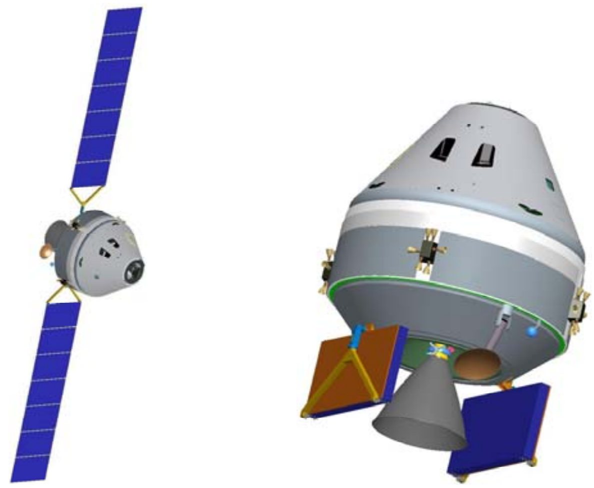

(a) Deployed solar panel (b) Stowed solar panel (old design)

Figure 7.2-32 Configuration of CEV (from DAC2 Database)

<u>Thermal Analysis on the Main Engine</u>

The main engine designation is listed in Table 7.2-7. The engine produces 10,000 lb thrust using monomethylhydrazine (MMH) and nitrogen tetroxide (NTO) as propellants with an oxidizer/fuel ratio of 1.9. The geometry of the thrust chamber of the main engine obtained from the DAC-2 CAD model is shown in Figure 7.2-33. The engine performance is computed using the chemical equilibrium compositions and applications (CEA) code. The flow properties at different locations inside the thrust chamber are listed in Table 7.2-7. At the nozzle exit, the mole fractions of the exhaust species based on chemical equilibrium are 33.56% of H_2O, 13.6% of CO_2, 3.22% of CO, 32.8% of N_2, and 16.9% of H_2, which will be used in the plume radiation calculation.

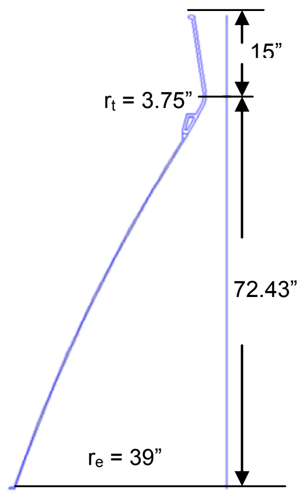

Figure 7.2-33 Sketch of the Main Engine Thrust Chamber

fuel	MMH(CH6N2)
oxidizer	NTO(N2O4)
chamber o/f ratio	1.9
chamber pressure (psia)	125
Propellant mass flow rate (lb/s)	30.63
nozzle throat diameter (in)	7.5
nozzle exit area ratio	108
chamber subtraction area ratio	2.54
chamber specific impulse (Isp, s)	323
thrust (lb)	10,000

	Injector	Combustion End	Throat	Exit
Pinjector/p	1	1.0679	1.7902	1886.54
p, BAR	8.6	8.07	4.81	0.00457
T, K	3137	3124	2967.8	915.6
ρ, kg/m^3	0.7092	0.6673	0.4237	0.001347
sonic velocity, m/s	1175.6	1172.7	1137.3	651.8
Mach number	0	0.244	1	5.082

Table 7.2-7 Main Engine Designation and Performance

Heat Transfer inside the Engine Thrust Chamber

A steady-state 1D model for isentropic flows of an ideal gas through a convergent-divergent nozzle is used to compute the flow variables of the hot gas inside the thrust chamber. The convective heat transfer coefficient that is function of Reynolds number and Prandtl number based on empirical equations [1] can be computed. Figure 7.2-34 shows the heat transfer coefficient and temperature of hot gas along the flow direction which will be used later in the thermal blanket design for the solar panel.

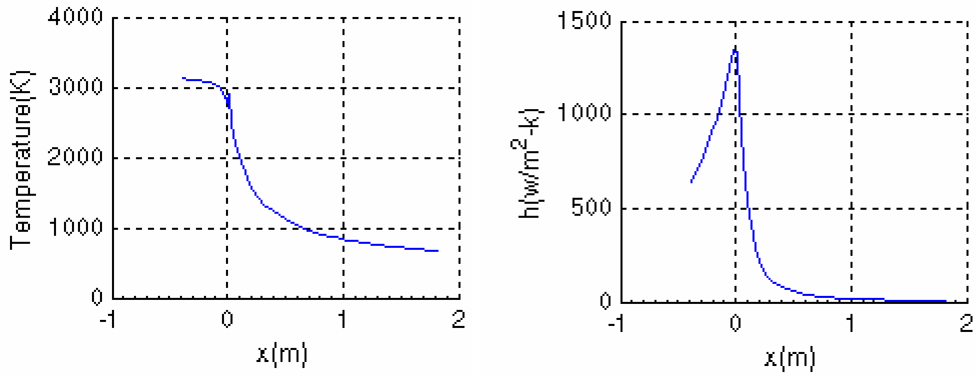

Figure 7.2-34 Gas Temperature (left) & Heat Transfer Coefficient (right) Inside the Chamber

Considering the MMH/NTO gas radiation, strong emission by carbon dioxide (CO_2) and water vapor (H_2O) (polar molecules) is in the infrared (IR) region and weaker emission is in the ultra-violet (UV) and visible ranges. Non-polar gases, such as O_2, N_2, and H_2, do not emit radiation and are transparent to incident thermal radiation. The approach for computing the gas radiation presented in [2] is used here and will be described briefly in the following.

The radiation heat flux $q = A_s \varepsilon_g \sigma T_g^{\,4}$, where A_s is the surface area, σ is Stephan-Boltzmann constant, ε_g is the gas emissivity, correlated in terms of gas temperature T_g, total pressure p of the gas, partial pressure p_g of the radiating species, and mean beam length $Le = 4V_s/A_s$ with V_s being the volume. Furthermore,

$$\varepsilon_g = \varepsilon_c + \varepsilon_w - \Delta\varepsilon$$

where ε_w is the emissivity of H_2O, ε_c is the emissivity of CO_2, $\Delta\varepsilon$ is the correction term for H_2O and CO_2 mixing. The partial pressure of CO_2 and H_2O are computed as

$$p_{CO2} = p\ m_{CO2},\ p_{H2O} = p\ m_{H2O}$$

where m_{CO2} and m_{H2O} are the mole fractions of CO_2 and H_2O, respectively. The data of ε_w , ε_c and $\Delta\varepsilon$ can be found in [2].

Since the flow properties change drastically along the flow direction, the hot gas is split into three parts to calculate the radiation heat flux and the results are listed in Table 7.2-8. Note that the regenerative cooling is not included here for hot gas.

$[x_s, x_e]$ (m)	height (m)	Volume (m^3)	Surface Area (m^2)	Le (m)	p_{CO2}Le (atm-ft)	p_{H2O}Le (atm-ft)	ε_g	T_g (K)	q (kw)
[0, 0.5]	0.5	0.1	0.864	0.466	0.454	1.122	0.207	2050	179
[0.5,1.0]	0.5	0.417	1.8059	0.92456	0.011	0.0275	0.0074	1050	0.92
[1.0,1.8]	0.8	1.7171	4.52	1.52	0.00427	0.0105	0.0024	950	0.5

Table 7.2-8 Radiation Heat Flux inside the Nozzle

Thermal analysis on the main engine exhaust plume

The exhaust plume is simulated using a finite-volume type 2D/axisymmetric CFD code. An ideal gas is assumed and the exhaust gas properties at the nozzle exit obtained from CEA is used. Three altitudes (75 km, 100 km, and 400 km) and two angles of attack α (0° and 180°) that is the angle between the vehicle velocity and thrust vectors are considered. At the inlet of the computational domain (nozzle exit), we define

$$p = 0.0045 \text{ atm}, T = 915.6 \text{ K}, \rho = 1{,}347 \text{ kg/m}^3, u = 3.312 \text{ km/s}, v = 0.0 \text{ km/s}$$

It should be pointed out that the nozzle cone half angle 20° at the exit of the chamber is not included here. The ambient conditions are

$$p = p_a, \rho = \rho_a, u = V\cos\alpha, \text{v} = \text{V}\sin\alpha$$

Where p_a and ρ_a are the pressure and density of the ambient air, respectively, $V = 7.8$ km/s is the vehicle velocity. For the 400 km altitude, the CFD code becomes unstable due to numerical issues related to very small density and pressure at that altitude. The code can produce converged plume results up to 100 km altitude. To approximate the ambient air condition at 400 km altitude above, the pressure and density of the ambient air at the altitude of 100 km with zero air velocity are used. It results in zero dynamic pressure ($\rho_a V^2$) of the ambient air and gives a reasonable approximation to the ambient condition at 400 km altitude and above since $\rho_a V^2$ (= 0.00017 N/m^2) at the altitude of 400 km is very small. The ambient air conditions at different altitudes are listed in Table 7.2-9.

Altitude (m)	Temperature (K)	Pressure (atm)	Density(kg/m^3)
75,000	206.65	2.04E-05	3.49E-05
100,000	195.08	3.16E-07	5.60E-07
130,000	469.27	1.23E-08	8.15E-09
160,000	696.3	3.00E-09	1.23E-09
200,000	845.56	8.36E-10	2.54E-10
400,000	995.83	1.43E-11	2.80E-12

Table 7.2-9 The Ambient Air Conditions at Different Altitudes

The computed numerical results are plotted in Figures 7.2-35 to 7.2-38. In Figure 7.2-35, $\log_{10}\rho$ contour is plotted for 75 km and 100 km altitudes at $\alpha = 0°$. It can be seen that the cone-shaped plume expands more when the altitude increases from 75 km to 100 km. The air shock, exhaust shock, and air/exhaust mixing are seen in the plume at both altitudes which agrees with some plume patterns shown in [3]. The $\log_{10} p$ and temperature contours are plotted in Figure 7.2-36 for the radiation heat flux calculation. Figure 7.2-37 shows the plume at the retro mode (α = 180°) at 100 km altitude. The major mass is within the plume intrinsic core near the nozzle exit. The altitude has negligible effect on the intrinsic core. The plume pattern is plotted in Figure 7.2-38 for altitudes 400 km and above. No shock waves are observed in the plume and the plume expands more. The Prandtl-Meyer expansion limit (for vacuum) is 103° [4] that include the half cone angle of 20°. For the vacuum case, the exhaust gas expands to reach the Prandtl-Meyer limit. However, the major mass is still within the intrinsic core.

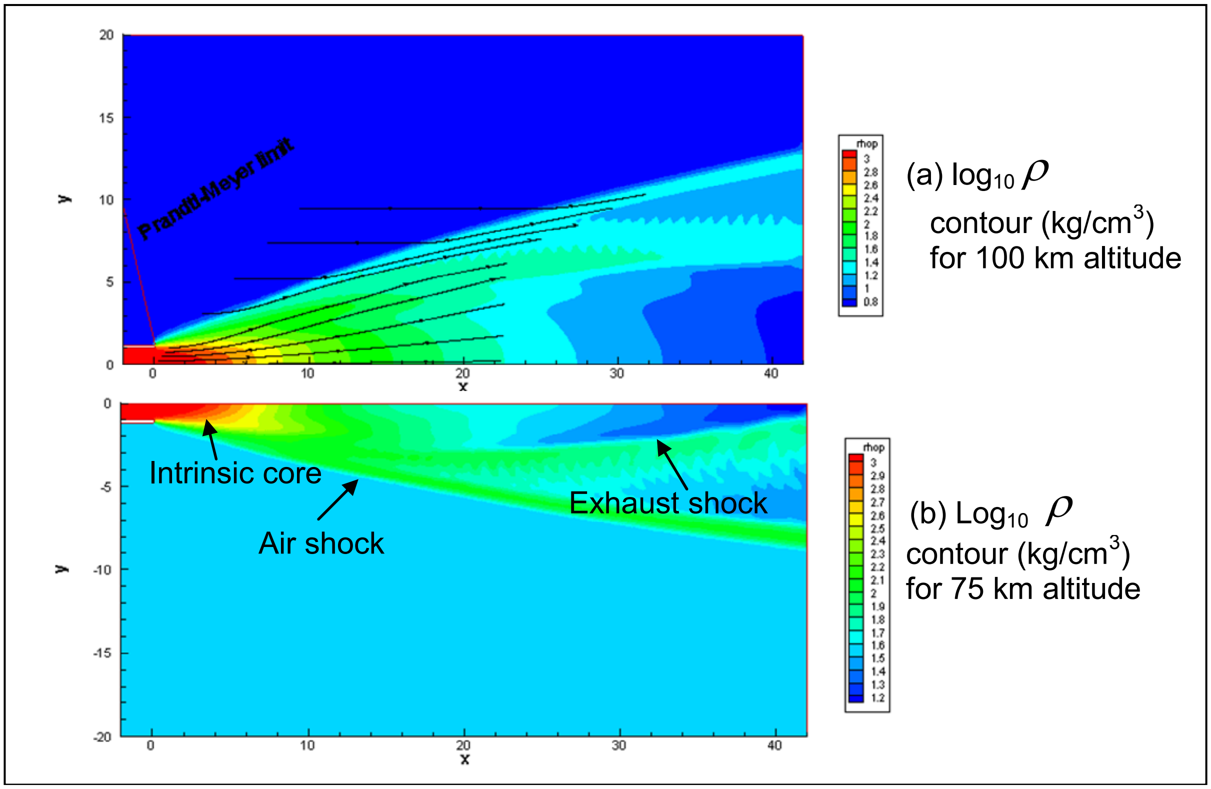

Figure 7.2-35 Comparison of Plume Shapes for Altitudes of 75 km and 100 km at α = 0°

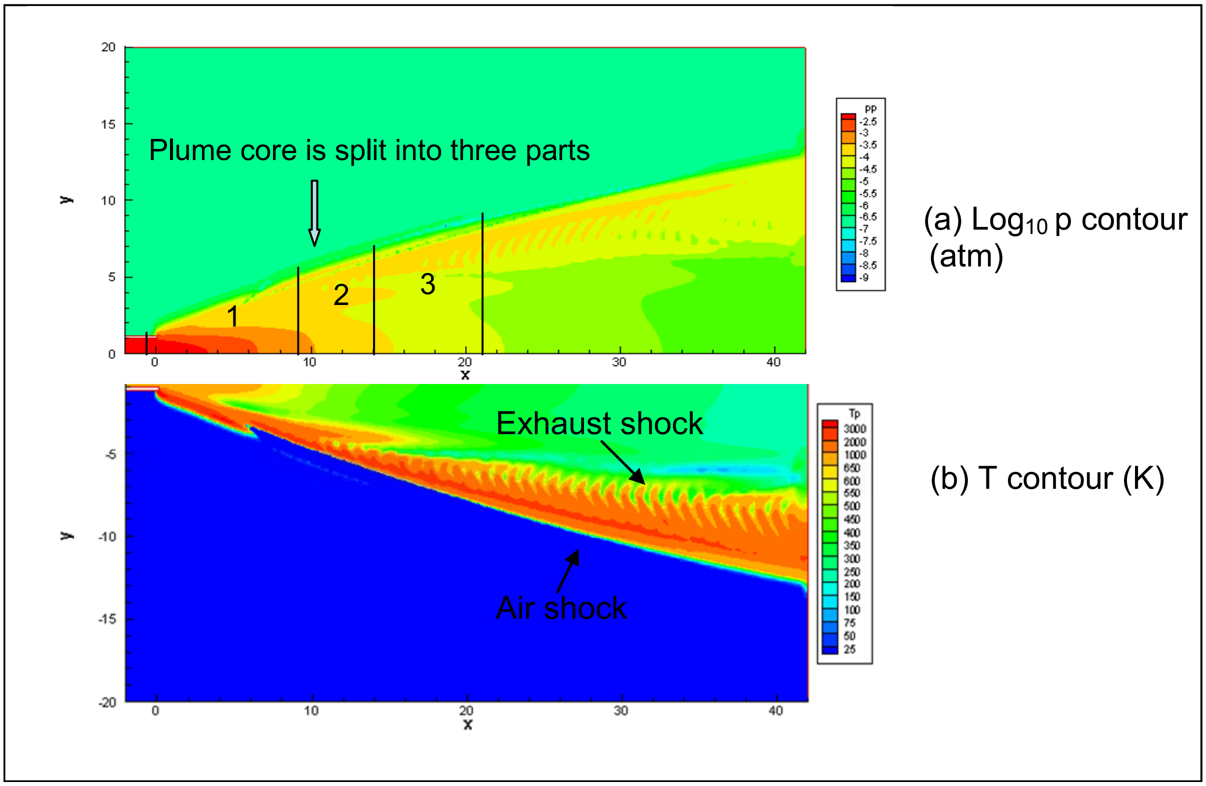

Figure 7.2-36 Plume at the Altitude of 100 km with α = 0°

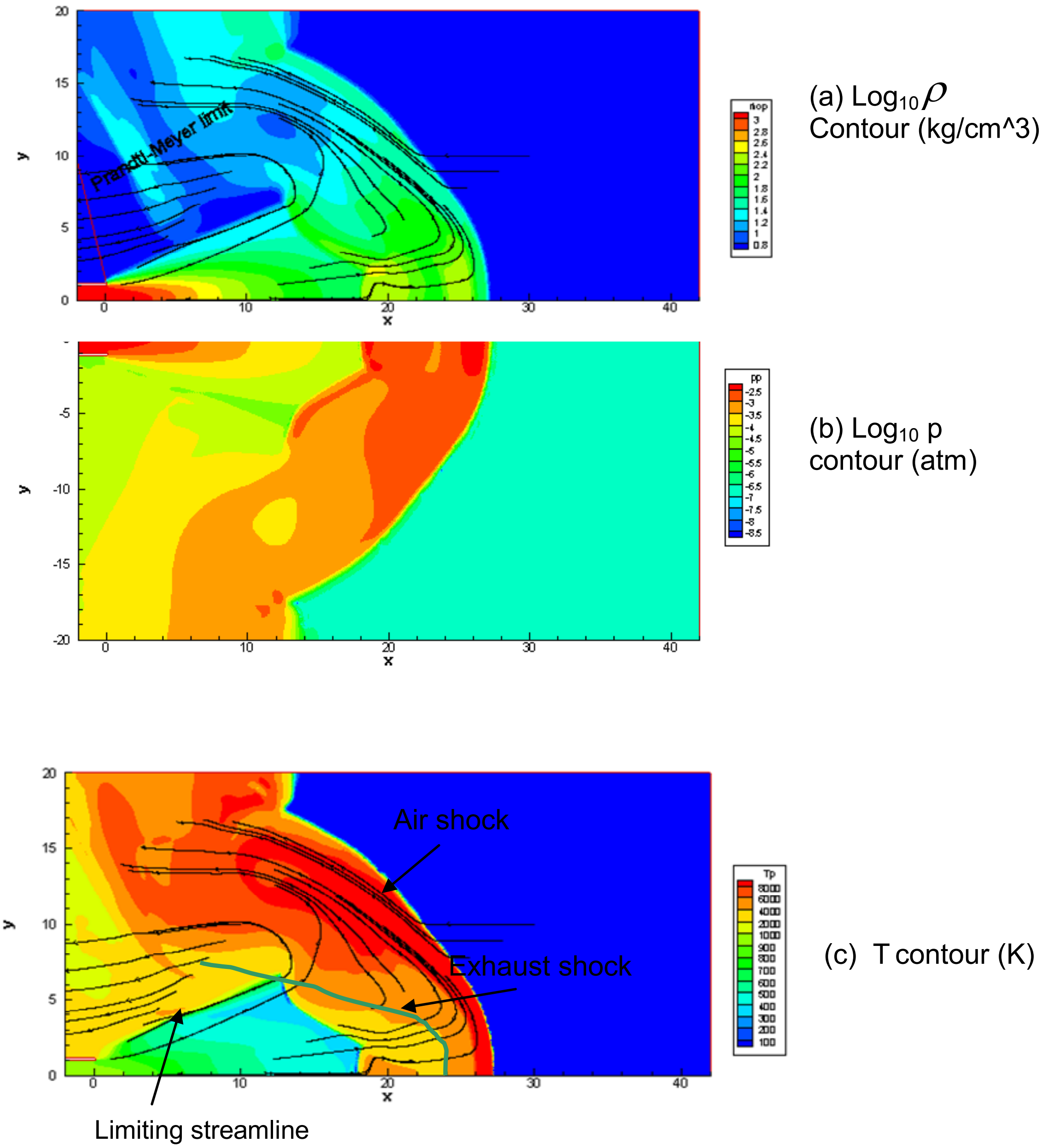

Figure 7.2-37 Plume at the Altitude of 100 km with α = 180°

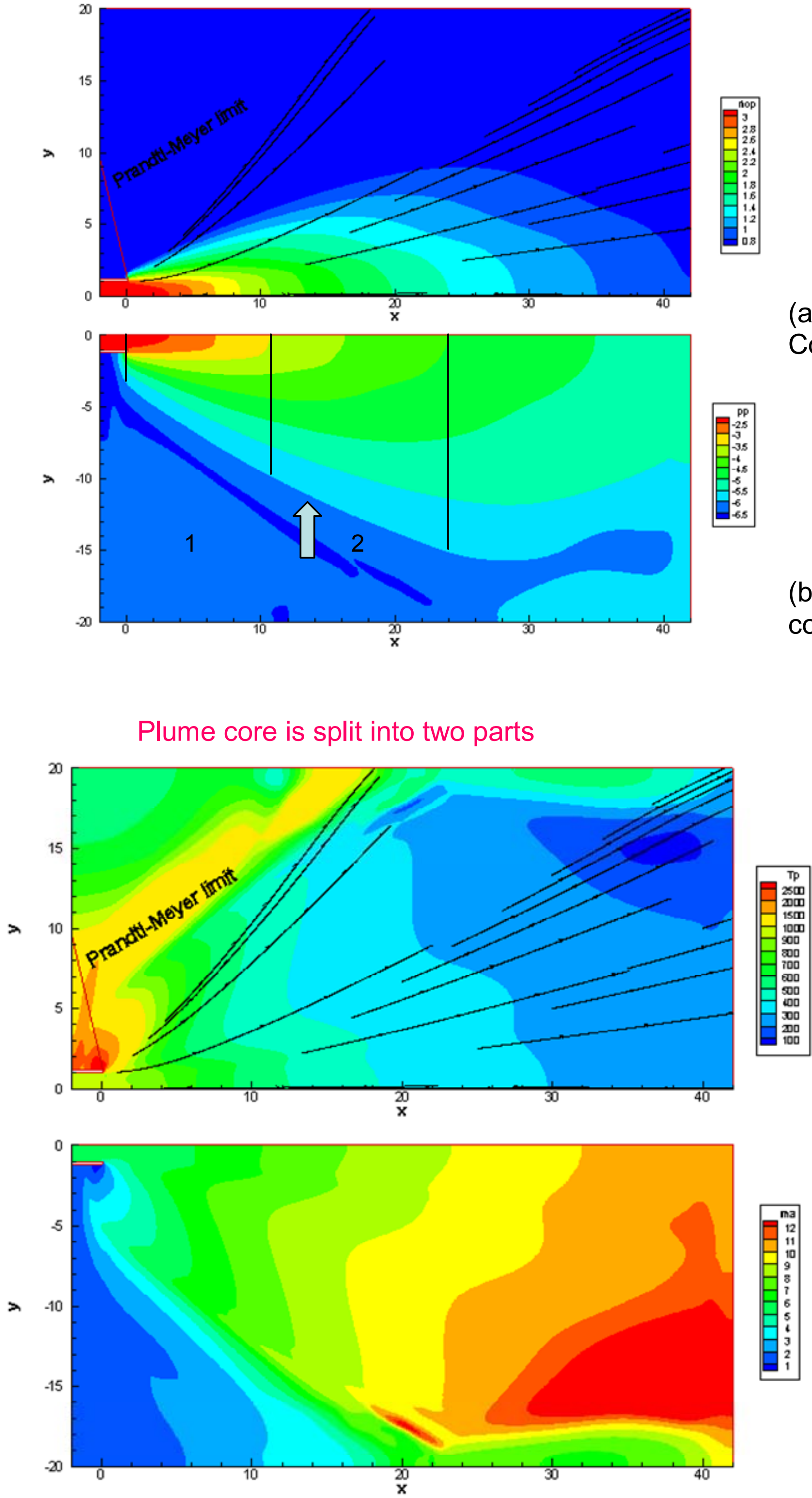

ρ

(a) Log_{10} Contour (kg/cm^3)

(b) Log_{10} p contour (atm)

(c) T contour (K)

(d) Mach contour

Figure 7.2-38 Plume at the Altitude of 400 km and Above

The radiation heat flux from the plume core is calculated using the same approach described previously for the hot gas inside the nozzle and is listed in Tables 7.2-10 and 7.2-11 for 100 km and 400 km altitudes, respectively. The volume-averaged gas pressure and temperature are used in the calculation. Since the regenerative cooling in the engine nozzle is not considered, the actual exhaust gas temperature will be lower. For the 100 km altitude, the plume core is split into three right circular cones (shown in Figure 7.2-35(a)) based on the pressure contour. The radiation due to the interaction between the exhaust and ambient air is not calculated here. For 400 km above altitudes, the plume core is split into two right circular cylinders (shown in Figure 7.2-38(b)). The radiation due to the interaction between ambient air and exhaust gas is negligible.

[r1,r2] (m)	Height (m)	Volume (m^3)	surface area (m^2)	Le (m)	p_{CO2}Le (atm-ft)	p_{H2O}Le (atm-ft)	ε_g	T_g (K)	q (kw)
[1.1,5.6]	10.1	410	233	4.89	0.0011	0.00275	0.0008	850	5.5
[5.6,7.0]	5.4	676	221	5.7	0.000688	0.0017	0.0005	600	0.8
[7.0,8.5]	7	1325	348.6	7.265	0.00029	0.0007	0.00025	500	0.3

Table 7.2-10 Main Engine Exhaust Plume Radiation Heat Flux (100 km, α = 0°)

[r1,r2] (m)	Height (m)	Volum (m^3)	surface area (m^2)	Le (m)	p_{CO2}Le (atm-ft)	p_{H2O}Le (atm-ft)	ε_g	T_g (K)	q (kw)
[4,10]	10.8	1764.3	543.4	7.774	0.00066	0.001635	0.0004	850	6.43
[10,15]	13.2	6566	1108.6	12.333	0.000456	0.001128	0.00018	550	1.03

Table 7.2-11 Main Engine Exhaust Plume Radiation Heat Flux (400 km Altitude Above)

Thermal Analysis on the Service Module Components

The CRC-3 thermal model of the SM was updated to add fidelity to the solar arrays, the solar array drive assemblies and the addition of a thermal insulation blanket between the stowed solar arrays and the engine nozzle. The thermal blankets are needed to protect the stowed solar arrays while the SM engine is firing during. This occurs during a circularization burn and the trans-earth injection burn. The SM engine was modeled after the Aerojet AJ10 118K engine which has a pressure-fed engine cycle, optimized for high-altitude operation. The oxidizer is nitrogen tetroxide flowing at 9.1 kg/s and the fuel is Aerozine-50 flowing at 4.76 kg/s. The mixture ratio is 1.9:1. The vacuum thrust and Isp are 43.38 kN and 320.5 seconds, respectively. The combustion chamber pressure is 8.84 atm. The engine is not regeneratively cooled, but instead utilizes an ablative chamber and radiative skirt cooling approach. The chamber wall ablator is comprised of rubber modified silica phenolic at the combustion flame front.

The high temperature insulation sized to protect the stowed solar arrays is a five layer blanket comprised of two layers of a nickel alloy 0.005 inches thick and three layers of Double Aluminized Mylar. The density of the nickel alloy is 0.3 lbm/in^3 and the areal density of a three layer DAM blanket is 0.023 lbm/ft^2. For a panel area of 7661.56 in^2 the mass of the total blanket, no structure, per array is 24.2 lbm. To hold the blanket in place a 0.5 inch nickel alloy “L” frame channel was sized for mounting around the perimeter. The mass was calculated to be 36 lbm per frame with a 20% margin on the size. The total blanket and frame mass is 120.4 lbm for the Service Module. The blanket mounting solution is not an optimized design and the potential for weight savings exists. An effective emissivity for the five layer blanket was calculated to be 0.031. The sizing condition for the blankets was to keep the layer of the solar arrays closest to the engine nozzle below their 302 °F non-operating high temperature limit.

The thermal analysis used the total heat produced by the plume and the calculated exterior wall temperature of the engine nozzle to provide the heat sources to the vehicle. The exhaust plume was modeled as a series of connected parabolas with the total heat produced from that section of the exhaust plume applied to that section of geometry. The total heat radiated from the exhaust plume was 7.46 kW (at a 400 km altitude Earth orbit). The engine conditions were calculated at 100 km altitude for the abort to orbit case. There is no difference in the calculated environment inside the engine, and the plume heating is less severe than that at the 400 km altitude. Therefore only the 400 km altitude orbit was analyzed. Thermal Desktop was used to calculate the view factors from the geometry and calculate the resulting temperatures. The heating from the exhaust plume did not apply any significant heating to the SM in the solar arrays deployed configuration. Up to 70 Watts of heat from the exhaust plume was calculated to provide additional heating to the arrays.

However, in the stowed configuration, see Figure 7.2-39, the stowed solar arrays extend beyond the exit plane of the engine nozzle.

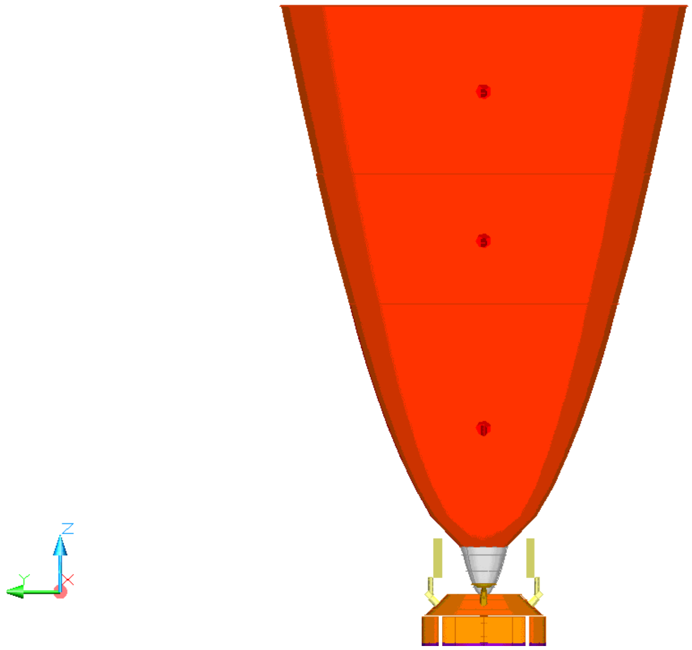

Figure 7.2-39 Engine Exhaust Plume (red), Nozzle (gray), and Stowed Solar Arrays (yellow)

The resulting temperature of the stowed solar array segment closest to the engine nozzle was 290 °F. The solar array insulation shield has a temperature of 528 °F. The surrounding structure will require MLI on it to shield it from the radiating engine nozzle. Temperatures up to 984 °F were calculated for the surfaces under the engine. See Figure 7.2-40 for a temperature contour plot of the analysis case.

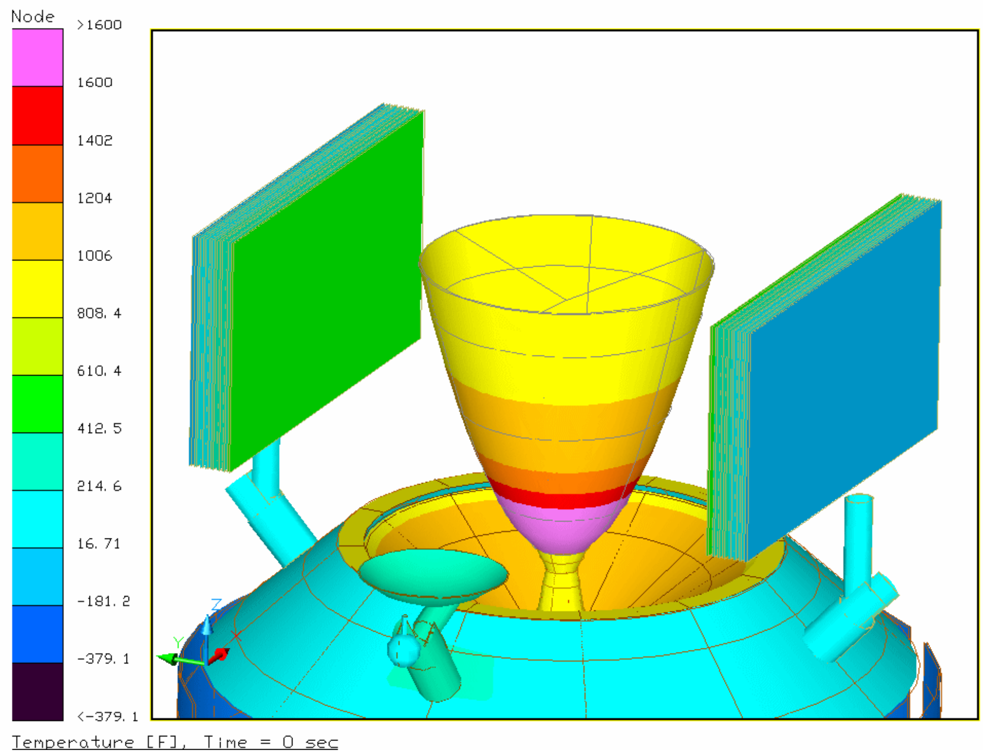

Figure 7.2-40 Stowed Solar Array Temperatures (°F) During an Engine Burn

Due to the MMOD requirements, a shield is being considered to be placed around the rocket injector head and combustion section. A parabolic shield was input in the model and the resulting calculated shield temperature was almost 800 °F. As long as the fuel injector and combustion chamber are regeneratively cooled, that should not be an issue.

Acknowledgement

The first author would like to thank Dr. Philip Jorgenson for his valuable help in the CFD simulation.

References

1) F.P. Incropera and D.P. DeWitt, "Fundamentals of heat and mass transfer", 5th Edition, John Wiley & Sons Inc., 2002.
2) R. Siegel and J.R. Howell, "Thermal radiation heat transfer", 3rd Ed, Hemisphere Publishing Corporation, Washington, 1992.
3) F.S. Simmons, "Rocket exhaust plume phenomenology", pp. 25, Aerospace Corporation, El Segundo, 2000,
4) M.A. Saad, "Compressible fluid flow", Prentice-Hall Inc., 1995.

8.0 Flight Dynamics

This section describes the trades, reference concepts, mass estimates, and analyses performed during CRC-3 as part of the Flight Dynamics functional area. Flight Dynamics for the purposes of this study includes Guidance, Navigation, and Control, Trajectories, and Aerodynamics and Aerothermal.

8.1 Guidance, Navigation, and Control (GN&C)

This document describes a preliminary navigation sensor suite design for systems integration of CEV mass, power, and volume within the government reference design. The sensor suite will include sensors for ascent, entry, LEO, cis-lunar transit, and LLO operations. In particular, this design is intended to address the needs of nominal flight operations; the demands of off-nominal and abort navigation may very well modify the composition and utilization of this sensor suite design. The implementation outlined in this document should not be taken as a requirement for navigation system design and is to be strictly limited to use in government analysis and validation efforts.

The reference CEV navigation sensor suite consists of four Honeywell Miniature Inertial Measurement Units (MIMU), three Viceroy GPS receivers, three Goodrich star trackers with target bearing tracking, two CSN010 LIDAR sensors, two Altasens short range optical cameras, two Altasens long range optical cameras, a communication system based on two way radiometric support with MPTFO, ISS, and LSAM, two radar altimeters/velocimeters, and three heat shield mounted pressure transducers. Details on the selection rationale, TRL, and utility of these sensors are provided in the following sections.

8.1.1 Driving Requirements, Groundrules, and Assumptions

The CEV GN&C mode teams selected the sensor suite for minimum mass, power, and volume with mature technologies that collectively provides the accuracies and redundancy needed to meet SRD requirements. The total GN&C sensor mass is approximately 177 lb including growth margins. Power consumption varies from 55 W during orbit coast to as high as 265 W during final approach and docking when powering relative navigation sensors. The following assumptions were made in implementing the GN&C design:

Assumptions

- The overall GN&C system functionality will utilize avionics system provided computers, data bus, and power.
- Ground tracking solutions provide the primary navigation update method beyond one-half the radius of GPS satellite orbits.
- No Lunar Communications and Navigation System (LCNS) assets will be in place for the early sortie missions.

- Targets and/or reflectors will be mounted in the vicinity of the target vehicle docking mechanism to enhance 6DOF (relative position and attitude) measurements and navigation during final approach and docking.

General satisfaction of the ISS crew rotation, ISS resupply, lunar sortie, and lunar outpost DRMs requires navigation during ascent, LEO, rendezvous proximity operations and docking (RPOD), direct entry from LEO, skip entry from lunar Earth return, cis-lunar transit, and LLO. The following requirements drive the navigation design:

CARD Requirements

- The Constellation Architecture shall provide the capability to return the crew to Earth without the ability to communicate with the ground during all mission phases. [CA0028-HQ]
- The Constellation Architecture shall provide the capability to perform an expedited return of the crew from the surface of the moon to the surface of the Earth in 120 hours (TBR-001-005) or less after the decision to return has been made. [CA0352-HQ]
- The Constellation Architecture shall provide the capability to perform Lunar Sortie missions without the aid of pre-deployed lunar surface infrastructure. [CA0208-HQ]
- The Constellation Architecture shall provide abort capability from the launch pad, after hatch closure, until reaching the mission destination. [CA0027-PO]
- The Spacecraft Segment shall be capable of returning the crew to Earth at any time after lunar landing during Lunar Sortie and Lunar Outpost Crew Missions in less than 120 hours with ΔV allocations in accordance with… [CA0055-PO]
- The CEV shall provide for return to Earth from any point in the mission while being operated by a single crewmember. [CA0448-PO]
- The CEV shall perform contingency rendezvous and approach proximity operations with the LSAM in Low Lunar Orbit with the un-crewed CEV functioning as the chaser vehicle. [CA0369-PO]
- The Constellation Architecture System shall be two-fault tolerant to catastrophic hazards, except for areas approved to use Design for Minimum Risk criteria. [CA0214-PO]

CEV SRD Requirements

- The CEV shall independently determine the ascent trajectory, attitude, and attitude rates to assess CLV ascent performance. [CV0110]
- The CEV shall provide automated ascent abort determination and initiation. [CV0053]
- The CEV shall utilize a common suite of relative navigation sensors. [CV0113]
- The CEV shall use at least two (TBR-002-089) dissimilar physical principles within its suite of relative navigation sensors during proximity and docking operations. [CV0114]
- The CEV shall determine the target vehicle relative attitude and relative attitude rate for docking operations. [CV0117]

- The CEV shall perform automatic execution of rendezvous, proximity operations, and docking for both nominal and abort conditions. [CV0121]
- The CEV shall dock with the target vehicle when the target vehicle is in an unplanned attitude with rate less than 1.0 deg/second (TBR-002-056). [CV0126]
- The CEV shall execute proximity operations and docking independent of orbital lighting conditions and ground overflight constraints. [CV0128]
- The CEV shall provide motion imagery of the proximity operations and docking. [CV0138]
- The CEV shall perform contingency rendezvous and approach proximity operations with the LSAM in Low Lunar Orbit with the un-crewed CEV functioning as the chaser vehicle. [CV0132]
- The CEV shall calculate the maneuver targets for return to Earth from Earth orbit, lunar transit, Earth Transit and lunar orbit. [CV0107]
- The CEV shall calculate Low Lunar Orbit (LLO) navigation solutions for TEI execution in less than 12 hours. (TBR-002-147) [CV0108]
- The CEV shall perform navigation for abort initiation and execution without MPTFO element communication. [CV0103]
- The CEV shall meet fault tolerance requirements such that no single event or failure cause can eliminate more than one means of fault tolerance (i.e., the methods will have no common failure mode). [CV0274]

8.1.2 Conceptual Design Overview

The CEV is responsible for monitoring inertial and/or relative navigation during Earth ascent as a passive vehicle on the CLV, LEO RPOD operations as the chase vehicle with the target EDS/LSAM and/or ISS, transit, lunar orbit, and at all times for aborts. The concept of operations for the CEV is under development at the time of this publication; however, the outline of CEV onboard and ground segment navigation functions as provided in Table 8.1-1, was used as an informed starting point around which to develop a reference sensor suite design.

Flight Phase	CEV Navigation	Ground Segment Navigation
Ascent to MECO	IMU based deduced reckoning navigation for the purpose of monitoring ascent stack mission progress, assessing abort options, and providing a CEV initial state in the event of abort initiation.	Skin tracking of ascent stack.
MECO to CEV injection into Earth Rendezvous Orbit (ERO)	IMU base deduced reckoning navigation with available GPS and MPTFO state updates.	Skin tracking and TDRSS tracking data based inertial navigation solutions as available.
ERO operations other than RPOD (coast, deorbit maneuver preparation, etc.)	GPS based state updates with IMU deduced reckoning propagation. Available MPTFO updates.	Skin tracking and TDRSS tracking data based navigation solutions as available.

Flight Phase	CEV Navigation	Ground Segment Navigation
ERO RPOD operations	Onboard processing of IMU and relative sensor data with available target state updates.	Skin tracking and TDRSS tracking data based inertial navigation solutions as available.
EDS execution of TLI	GPS based update provided to EDS flight computer. IMU deduced reckoning to monitor EDS execution of maneuver.	Skin tracking and TDRSS tracking data based inertial navigation solutions as available.
Transit operations post TLI and prior to LOI as well as post TEI and prior to Earth EI	IMU deduced reckoning propagation of MPTFO provided state updates as a backup to LSAM navigation. Celestial navigation optical sightings for calibration during nominal flight and support of autonomous return.	Two-way tracking of CEV/LSAM stack and calculation of Earth-Moon system inertial states.
LLO operations other than RPOD	IMU deduced reckoning propagation of MPTFO provided state updates, surface feature tracking, and celestial navigation processing.	Two-way tracking of CEV stack and calculation of Lunar system inertial states.
LLO RPOD operations	Onboard processing of IMU and relative sensor data with available target state updates.	Two-way tracking data based inertial navigation solutions as available to initialize LSAM ascent and RPOD operations.
Earth EI to Parachute Deploy	Onboard processing of IMU and atmospheric sensors with GPS updates.	Limited tracking capability with no state update.
Parachute Deploy to Touchdown	Onboard processing of IMU and terminal landing sensors with GPS updates.	Limited tracking capability with no state update.

Table 8.1-1 CEV Navigation Concept for Nominal Operations by Flight Phase

Sensor	Quantity	TRL	Comment
Honeywell MIMU	4	9	Used for navigation during highly dynamic events such as ascent/entry, during orbital maneuvers, and for attitude maintenance.
General Dynamics Viceroy GPS Receiver	3	9	Space heritage GPS receiver used for autonomous inertial navigation within HEO.
Goodrich Star Tracker	3	9	Used for attitude update and IMU bias calibration. Also has a non-inertial tracking capability to provide angles-only measurements to target vehicle at extreme ranges when target is illuminated.
LIDAR CSN010	2	7	Range and bearing at long and medium range, pose estimates at close range. May use targets as necessary/required. Also may be used as a common sensor for EDL. Flight heritage from XSS-11 mission.
Altasens Short Range Optical Camera (SROC)	2	6-8	Camera based system providing bearing and pose estimates at close range. Also serves for celestial and surface feature navigation.
Altasens Long Range Optical Camera (LROC)	2	6-8	Camera based system providing bearing at long and medium ranges. Also serves for celestial and surface feature navigation.

Sensor	Quantity	TRL	Comment
AST CSN006 Infrared Optical Camera (IROC)	2	6-8	Camera based system providing lighting independent bearing and pose estimates at close range. Also serves for celestial and surface feature navigation.
RF Transponder	2	6	Potentially integrated with communication system, this device provides tracking data to the MPTFO and generates LCNS and LSAM range, range, rate and bearing.
Radar Altimeter/Velocimeter	2	6-9	The Mars Surveyor Program Honeywell Altimeter is installed under the heat shield to be operated at heat shield deploy. Serves to support retro rockets with altitude and velocity data for precision landing.
Pressure Transducer	3	6-9	The Viking mission utilized heat shield mounted pressure sensors to estimate the Martian atmosphere. These pressure transducers can do the same when coupled with IMU sensed drag acceleration.

Table 8.1-2 CEV Sensor Suite Quantity and TRL

In addition to the actual sensors being carried under the first revision of the CEV master equipment list, there are four supporting hardware items being carried under the navigation sensor suite ledger: a proximity operations illuminator based upon the Boeing design for Orbital Express and an auxiliary video processing unit computer for dedicated processing of optical camera image data in backup mode to the avionics packaged in the optical cameras themselves. Two sets of antennas are also carried - four altimeter antennas mounted on the inside of the heat shield and six GPS antennas along the sides of the vehicle.

The specific roles of each sensor type are captured in Table 8.1-3 and Table 8.1-4 which respectively illustrate the utilization of each sensor by phase and the navigation application of each sensor. A quick summary of these roles follows. The IMUs will be mainly used for inertial position, velocity, and attitude propagation in all flight phases. The GPS receivers will be used for absolute position and velocity updates within the GPS shell as defined by "Technical Characteristics of the Navstar GPS", June 1991. Star trackers (ST) are used for fine attitude updates (platform alignment) and IMU gyroscope calibration in all orbital regimes and will also be used for long-range bearing-only observations to target vehicles when solar illumination permits observation during far-field and near-field rendezvous. The LIDAR device will provide 3DOF (bearing and range to centroid) observations during proximity operations and final approach and docking. The LIDAR will also provide 6DOF (target relative attitude and structure frame position) target observations during portions of proximity operations and all of final approach and docking. The long range optical cameras (LROC) will be used for 3DOF target observations during rendezvous and proximity operations and will provide limited 6DOF target measurements during proximity operations. The LROCs will also provide surface feature tracking during lunar orbit (i.e., tracking craters and similar planetary scale features) and could serve as the contingency sensor for celestial navigation in the event of loss of communications with the MPTFO element. The short-range optical cameras (SROC) provide 3DOF lighting-independent target observations during near-field rendezvous and proximity operations and will provide 6DOF target observations during parts of proximity operations and all of final approach and docking. The RF transponder will provide range and range rate between the target and chase vehicles during rendezvous. At this time it is unclear whether or not the RF system will also provide bearing angles for a complete 3DOF measurement set. The RF system also augments lunar surface operations by providing measurements between the landed LSAM and orbiting CEV. The radar altimeter velocimeters (RAV) are used during entry and landing to provide altitude and velocity measurements for retro rocket firing for precision landing. The pressure transducers (PT) are used during Earth entry along with IMU accelerometer measurements to update onboard atmospheric density models.

Phase	IMU	GPS	ST	LIDAR	LROC	SROC	RF	RAV	PT
Ascent	P								
Orbital Maneuvers	P								
Earth Orbit Coast	P	P	P						
Earth Far Field Rendezvous	P	P	P		P		P		
Earth Near Field Rendezvous	P	P	P		P	P	P		
Earth Prox Ops	P		P	P	P	P			
Earth Final Approach &Dock	P		P	P		P			
Lunar Transit	P		P		C				
Lunar Orbit	P		P		P		P		
Lunar Far Field Rendezvous	P		P		C		P		
Lunar Near Field Rendezvous	P		P		C	C	P		
Lunar Prox Ops	P		P	C	C	C			
Lunar Final Approach & Dock	P		P	C		C			
Earth Transit	P		P		C				
Entry	P	P						P	P
Landing	P	P						P	

Table 8.1-3 Sensor Utility by Flight Phase: (P)rimary or (C)ontingency

Navigation Application	IMU	GPS	ST	LIDAR	LROC	SROC	RF	RAV	PT
Absolute translation propagation	X								
Inertial attitude propagation	X								
LEO position and velocity update		X							
Ground tracking measurement support							X		
Inertial attitude update (all locations)			X						
Solar relative attitude update (all locations)									
Relative range (RPOD)				X	X	X	X		
Relative range rate (RPOD)							X		
Bearing to target			X	X	X	X			
Target relative attitude				X		X			
Target structure relative position				X		X			
Surface feature tracking (at moon)					X				
Celestial navigation (during transit)					X				
Atmospheric property estimation	X							X	X

Table 8.1-4 Sensor Navigation Application

The relative navigation sensor usage for rendezvous, proximity operations, and docking is shown in Figure 8.1-1. Not all sensors are required to be powered ON for every mission phase. The LROC and SROC cameras cannot be pointed at the target and used at the same time because of a field of view conflict.

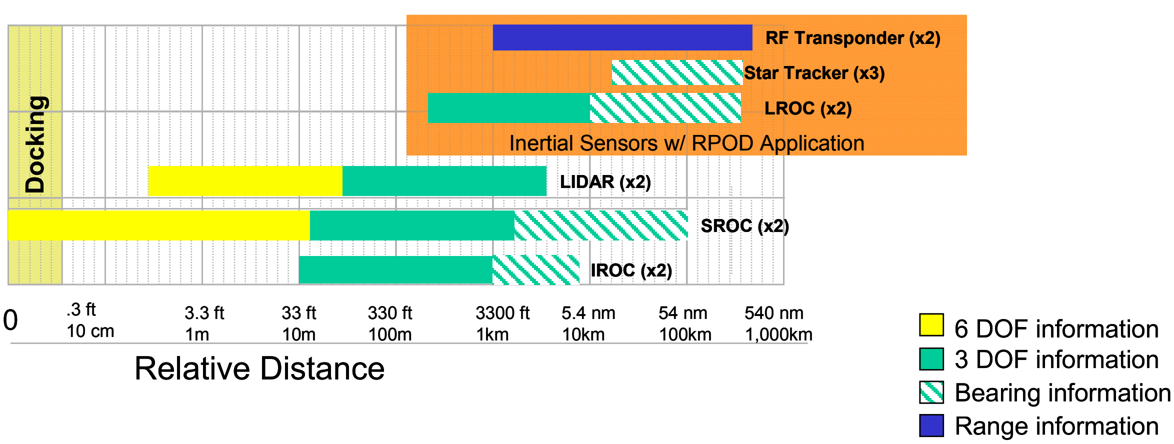

Figure 8.1-1 Relative Sensor Usage by Distance

A preliminary sensor power profile for lunar sortie missions (DRM2) has been compiled and is shown in Table 8.1-5. This profile gives a snapshot of a possible power usage by flight phase.

			Sensors																					
Event	Time	Duration	IMU1	IMU2	IMU3	IMU4	GPS1	GPS2	GPS3	ST1	ST2	ST3	Lidar O1	Lidar A1	Lidar O2	Lidar A2	LROC1	LROC2	SROC1	SROC2	RAV 1	RAV 2	Spotlight	SS Power	Peak Power
Liftoff	0:00:00		1	1	1	1	1	1	1															103	143
CLV MECO			1	1	1	1	1	1	1	1	1	1												121	161
ERO Orbit Insertion			1	1	1	1	1	1	1	1	1	1												121	161
Orbit Coast 1			1				1	1	1	1	1	1												55	65
Rendezvous		<1 day	1				1	1	1	1	1	1												55	65
Prox Ops 1		12 hours	1				1	1	1	1	1	1					1	1	1	1				67	97
Prox Ops 2		1 Hour	1				1	1	1	1	1	1	1	1	1	1	1	1	1	1				107	215
Prox Ops 3		1 Hour	1				1	1	1	1	1	1	1	1	1	1			1	1				101	199
Final Approach and Docking		30 Minutes	1				1	1	1	1	1	1	1	1	1	1			1	1			1	111	249
Docked to EDS/LSAM			1				1	1	1	1	1	1												55	65
TLI			1	1	1	1	1	1	1	1	1	1												121	161
Trans Lunar Cruise		2 days	1				1			1														33	43
Lunar Approach		2 days	1							1							1	1						34	54
LOI		30 minutes	1	1	1	1				1														100	150
Lunar Orbit 1		6 Days	1							1							1	1						34	54
Rendezvous		< 6 hours	1							1	1	1					1	1						46	66
Prox Ops 1		< 6 hours	1							1	1	1					1	1	1	1				52	82
Prox Ops 2		1 Hour	1							1	1	1	1	1	1	1	1	1	1	1				92	200
Prox Ops 3		1 Hour	1							1	1	1	1	1	1	1			1	1				86	184
Final Approach and Docking		30 Minutes	1							1	1	1	1	1	1	1			1	1			1	96	234
Docked to LSAM AS			1							1							1	1						34	54
LSAM Disposal			1							1			1	1			1	1	1	1			1	70	179
Lunar Orbit 2			1							1							1	1						34	54
TEI		30 minutes	1	1	1	1				1	1	1												106	146
Trans Earth Cruise		2 days	1							1							1	1						34	54
Earth Approach		2 days	1				1	1	1	1														43	53
Entry		30 minutes	1	1	1	1	1	1	1												1	1		119	159
Descent and Landing		30 minutes	1	1	1	1	1	1	1												1	1		119	159

Table 8.1-5 Preliminary Power Profile

IMU Specifics

The Honeywell Miniature Inertial Measurement Unit (MIMU) was selected as the IMU of choice over the HG1900 and SIRU products. It was selected based upon familiarity from the JPL-led Mars Science Lab and GSFC-led Hubble Recovery Vehicle (HRV) projects as well as comparisons of mass, power, accuracy, and redundancy with the MEMS HG1900, the SIRU, LN100G, SIGI, and LN200 units. Shuttle and Station experience determined four IMU units to be the optimum way to meet redundancy requirements for dynamic flight regimes such as ascent, entry, and critical powered trajectory maneuvers and the size of the MIMU lends itself to this philosophy. A trade study between the MIMU and GPS vs. a combined SIGI (Space Integrated GPS/INS) solution was also completed to examine the relative strengths of a consolidated GPS/INS implementation as opposed to a distributed GPS and INS system. Note that the SIGI and MIMU inertial sensor components are built upon the same accelerometer and gyroscope packages. The MIMU/GPS advantages were weight (total 52 lbm) and power (105 W typical to 155 W max) compared with 80 lbm and 136 W typical up to 180 W max for the SIGI. The SIGI's main advantage is the capability to blend INS and GPS data internally at higher rates (updating 200 Hz IMU data and 1 Hz GPS data to output 50 Hz data). However, it has been determined that blending at such high rates is not required for the CEV program based on the requirements and Shuttle/ISS experience. Ten Hz is the likely maximum the vehicle will require and keeping the filter within the flight computer instead of unavailable inside the SIGI has many more advantages as the Station and Shuttle programs have shown. Optimization of the flight string filter based on mission requirements can be achieved when the filter is decoupled from the

INS. Separation of the filtering and IMU responsibilities makes the IMUs less expensive and easier to replace and makes maintenance of the flight software more straight-forward. The MI-MU specifications are shown in Tables 8.1-6, 8.1-7, and 8.1-8.

IMU Accelerometer Uncertainty	Value (3σ)	Units
Accelerometer bias	.1	μg
Accelerometer scale factor	175	ppm
Accelerometer misalignment	5	arcsec
Accelerometer bias noise	10	μg/rt-s

Table 8.1-6 MIMU Accelerometer Specifications

IMU Gyro Uncertainty	Value (3σ)	Units
Bias Stability	0.005	deg/hr
Scale factor error	1	PPM
Misalignment	5	arcsec
Average random walk	0.005	deg/rt-hr

Table 8.1-7 MIMU Rate Gyro Specifications

Parameter	Value
Temperature	-30 to 65 °C
Pyrotechnic Shock	40,000 g
Acceleration	25 g
Rate Range	375 deg/s
Ang Accel Range	1500 deg/s^2
Power	32 W at 28 Vdc
Size	23.3 cm dia. x 16.9 cm
Weight	4.7 kg

Table 8.1-8 MIMU Operational Parameters

Star Tracker Specifics

The Goodrich HD-1005 Star Tracker has been selected to provide inertial attitude updates and target angles observations during rendezvous. This star tracker has flight time and extensive test time and provides a known quantity for navigation information. Model performance and parameters are shown in Tables 8.1-9 and 8.1-10. In order to accommodate viewing of the stars an opening or cutout of the vehicle in the Star Tracker vicinity will be required. The Star Tracker will then need thermal protection and Mylar blankets have been found to provide the appropriate amount of protection required.

Star Tracker Model Performance	Value (3σ)	Units
Inertial Attitude Max Meas Rate	2	Hz
Target Bearing Min Range (based upon HRV target properties)	2	km
Target Bearing Max Meas Rate	1	Hz

Table 8.1-9 Star Tracker Model Performance Parameters

Star Tracker Model Parameter	Value (3σ)	Units
Inertial Attitude Error (Gaussian)	180	Arcsec
Target Bearing Noise (floor of 10 m error at 2 km)	180	Arcsec
Target Bearing Bias	6	Arcsec
Target Bearing Bias Time Constant	3	orbit

Table 8.1-10 Star Tracker Model Error Parameters

RF Transponder Specifics

A dual-string RF transponder on C&T carried by the avionics system will be used to support ground tracking of the CEV beyond Low Earth Orbit and will be used as a lunar ascent and rendezvous link with the LSAM to generate range and range-rate observations. Model performance and parameters are shown in Tables 8.1-11 and 8.1-12.

RF Transponder Model Performance	Value	Units
Max Operating Range	200	km
Min Operating Range	10	m
Range Meas Rate	1	Hz
Range Rate Meas Rate	2	Hz
Bearing Meas Rate	TBD	TBD
Bearing Rate Meas Rate	TBD	TBD

Table 8.1-11 RF Transponder Model Performance Parameters

RF Transponder Model Parameter	Value (3σ)	Units
Range Noise Floor	1.0	m
Range Noise Scale Factor	.001	-
Range Bias	1.0	m
Range Bias Time Constant	1	Orbit
Range Rate Noise Floor	0.01	cm/s
Range Rate Noise Scale Factor	0.01	-
Range Rate Bias	0.01	cm/s
Range Rate Bias Time Constant	1	Orbit
Bearing Noise Floor	TBD	TBD
Additional Bearing Errors as Needed	TBD	TBD

Table 8.1-12 RF Transponder Model Error Parameters

Radar Altimeter Velocimeter Specifics

Two radar altimeter/velocimeters , the Mars Surveyor Program Modified Honeywell Altimeter will be used in support of retro rocket firing for precision landing. Four antennas underneath the heat shield are used to collect data. All antennas are on one plate with three antennas canted 40 degrees and spaced at 120 degree intervals surrounding one vertical antenna. Model performance and parameters are shown in Tables 8.1-13.

Radar Altimeter Velocimeter Model Parameter	Value (3σ)	Units
Altimeter Range	1.0 > 3,700	m
Altimeter Accuracy	<5%	-
Velocimeter Range	-32 to +128, vertical -80 to +80 horizontal 0 to 130 total velocity	m/s
Velocimeter Accuracy	H<1000m <4% H>1000m < (Hx.004%) X Velocity or 1.2 m/s	-
Velocimeter Quantization	V> 30; < 1.2 m/s V < 30; <.4m/s	m/s
Operation Range (Angle from Vertical)	+/- 30	deg
Update Rate (4 beams)	V>30: 400 ms V<30: 800 ms	m/s
Terrain	Constant slope, up to 20 deg from horizontal	Orbit

Table 8.1-13 Radar Altimeter Velocimeter Model Error Parameters

Pressure Transducer Specifics

Three pressure transducers, the LG-1237 Smart PT, will be used in support of atmospheric density estimation during Earth entry. This information along with the IMU and GPS will be used to meet the strict navigation requirements during entry and landing for the CEV.

GPS Specifics

The CEV program has many requirements for precision landing, anytime abort capability, autonomous crew return, and Earth orbit operations that were not placed upon the Apollo program. The reference navigation sensor suite accommodates these additional requirements by the inclusion of GPS as the primary means for inertial navigation updates within the GPS vicinity (approximately half the GPS orbital radius). A comparison to Shuttle ground tracking to on-orbit GPS navigation also demonstrates that GPS navigation is more accurate and flexible for orbital operations. Including GPS in the reference design takes advantage of these characteristics to meet the requirements of the CEV program. This additional accuracy translates into advantages such as fuel efficiency, operational flexibility, maneuver precision, and precision entry.

The reference GPS implementation is to utilize three General Dynamics Viceroy GPS receivers interfacing with six GPS antennas for attitude-independent operation. Therefore, each GPS receiver needs two antenna ports as provided in the Viceroy design. The Viceroy GPS receiver infrastructure will require modifications to support 1553 capability, the chosen communication standard for the CEV navigation sensors, adding some weight and power to the specifications on the standard housing. With these communication system modifications and additional flight requirements for ascent, entry, and human flight certification the following section describes pertinent lessons learned with regard to procurement and implementation of "smart" sensor systems with significant internal firmware processing such as GPS. Parameters for the Viceroy are shown in Table 8.1-14.

Parameter	Accuracy (3σ)
In Track Position	98 ft (30 m)
Cross Track Position	33 ft (10 m)
Radial Position	33 ft (10 m)
Semi-major Axis	98 ft (30 m)
Velocity	2.0 ft/s (0.6 m/s)
Startup	< 3 minutes
Time Offset 1 PPS	< 1500 nsecond

Table 8.1-14 Viceroy GPS Navigation Accuracy

GPS Lessons Learned

Lessons learned from the Shuttle, Station, and CRV programs indicate that sensor systems with significant internal firmware processing require end-user insight into coding implementation and standards to minimize life-cycle costs and avoid anomalous operational performance. Failure to achieve this insight has resulted in unexpected cost overruns from additional testing and verification required. Experience demonstrates that the most effective way to ensure this insight is through provisions in the original contract with the sensor vendor. Table 8.1-15 provides an overview of key requirements that should be placed on the sensor vendor for sensors with significant internal firmware processing requirements:

NASA/CEV Prime needs full insight into sensor firmware code to ensure a successful test program and flight maintenance/upgrade approach.
NASA/CEV Prime should have a contract mechanism for efficiently implementing code modifications as design problems emerge or mission objectives change during the CEV operational period. This capability would give us the most flexibility to modify code for mission objectives that will likely change as time goes on. The CEV end users in engineering and operations will have a better understanding of the changes needed than a sensor manufacturer.
NASA/CEV Prime should require flight qualified code with code inspections to insure that the quality of code will not contain legacy terrestrial code for aviation or automobile applications. In the past, the re-use of such code has led to unforeseen problems in space applications that have been costly to identify.

Table 8.1-15 Smart Sensor Lessons Learned

GPS Antenna Specifics

All three GPS receivers need to be operated simultaneously with unique antenna inputs in all two-fault tolerant mission phases. Combining GPS antenna signals is not recommended based on lessons learned from the Shuttle program. Two antennas will be placed on the Service Module in a 1-on-top and 1-on-bottom configuration and four will be placed on the cone of the Crew Module (CM) equidistant to each other to provide optimum coverage during ascent, entry, and Low Earth Orbit (LEO). Each antenna will provide a single RF input to a single input on a single receiver. In the event one SM antenna fails during orbital operations, the vehicle could be rotated if needed to use the opposite SM antenna. In the event of a second failure, a rotation to the cone antennas could be made if necessary as some of them will receive GPS visibility in most CEV orientations. The CM antenna placement was chosen to provide maximum coverage and fault tolerance during ascent and entry. Two antennas pointing slightly off of upward space-pointing during LEO would go to two separate receivers' ports. Two antennas approximately pointing slightly off of downward Earth-pointing during LEO would go to two separate receivers' ports. In this configuration, each receiver will have one antenna pointing approximately toward space during LEO and each will have an antenna pointing approximately toward Earth during LEO. During ascent and entry, the four cone antennas will all be facing approximately up.

There are many commercial GPS antennas that are unaffected by temperature that would be well-suited for the CEV. In order to reuse the antennas, a flat-styled antenna similar to the Shuttle's needs to be selected to fit under the CEV's thermal protection system (TPS). The effectors of TPS on GPS signal quality must be analyzed upon antenna selection. For this study the KSA-SP1575MS25-Y22 was chosen for its weight (approximately 0.3 lb) and size (1.4 by 1.4 inches, 0.16 inch height).

GPS Low Noise Amplifier

The GPS signal will have to travel a distance to the installed location of the GPS receivers and will need to be amplified to the receiver's requirements. A typical GPS receiver requires between 35 and 45 dB of gain at the RF input connector. The MITEQ AFD series low-noise amplifier has been selected to fulfill this requirement in the reference design. It provides 38 dB of gain, and has significant space flight experience. Additionally, MITEQ builds custom amplifiers for military and space applications with gains which are tailorable to meet the needs of the receiver. The amplifier is very small at 0.226 by 0.76 by 1.54 inches and would be mounted on the inside of CEV. It also uses little power, each drawing 125 mA each at 15 V, giving a total of 11.25 W for all six units.

Camera Specifics

For proximity operations and docking, cameras are required for relative navigation and situational awareness. Two long range optical cameras (LROC) made by Altasens (which will require some modifications for CEV use) have been selected to provide range, bearing (azimuth and elevation) and relative attitude during various phases of rendezvous and prox ops. They will also be used for celestial navigation during transit and surface feature tracking in lunar orbit. Two short range optical cameras (SROC) also made by Altasens will be used for the final stages of docking. Although the digital camera hardware is the same in both the SROC and LROC, the focal length of the lenses (16 mm-140 mm) is a specification under review in the CRC-3 trade space. One of these will be placed in LIDS, and one on the vehicle. Figures 8.1-2, 8.1-3, and 8.1-4 show the planned mounting locations for the sensors. To meet CEV SRD requirements for dissimilar redundancy and light independence, two infrared optical cameras (IROC) made by AST were selected. A short range illuminator array is also required to provide the light needed for the short range cameras. The cameras specifications are shown in Table 8.1-16. For viewing requirements a cut out of the vehicle will be required so that the camera will be able to see target.

2 Megapixel cameras (typical use 640x480 pixels) Camera spec is 1936x1090, pixel size – 5 microns
Rate – 1-5 frames per second
Lens – TBD focal lengths ranging from 16 mm to 180 mm
Requires Global Shutter
Lens focal length 16 mm-140 mm

Table 8.1-16 Camera Specifications

LIDAR Specifics

Two light detection and ranging (LIDAR, i.e., laser) sensors are included to provide range, bearing (azimuth and elevation) and relative attitude during various phases of rendezvous, prox ops, and docking. A trade study between several commercial off the shelf (COTS) and custom LIDAR designs was completed based upon Shuttle upgrade trades and HRV project experiences. The CSN010 LIDAR was chosen based on its accuracy, maximum operating range, and recent on-orbit flight testing. Depending on target material properties and size, the CSN010 has an operational range of 2 ft to 1.6 nmi. LIDAR CSN010 is technologically mature with considerable flight time and testing experience and would provide the navigation output needed with little modification required. A single LIDAR CSN010 sensor is composed of an optical unit and an avionics unit, with the latter performing the processing required for generating navigation measurements, thereby reducing the demands on the CEV flight computers. One disadvantage of the two-unit design is the increased mass, power, and volume specifications compared to a custom-developed unit or some of the other lower-TRL COTS options considered. The CSN010 would theoretically be easier to test since it is decoupled from the CEV flight computer; however, this introduces issues of code insight similar to that of GPS.

A concept was also developed for building a LIDAR from the ground up using existing space qualified parts and commercial technological capability. This sensor would have no flight time, and no testing experience but has mass, power, and volume benefits and could be easily modified for Mission Criteria, would have Flight Certified code. The drawbacks to this approach are that a fresh start sensor would take approximately 4 years to develop at a cost of approximately $20M. Developing a LIDAR this way would mean that the weight could drop to 5.8 lb, there would be power savings (30 W peak) and the size would be considerably smaller. Although the new development LIDAR realizes size and weight savings, the total volume is on par with the CSN010. The new development LIDAR processing code could be built into the CEV flight computer which gives NASA more access to code but will also make the box harder to test without an integrated avionics support platform.

Based on lack of flight experience, and technology development risk, and higher cost of new development LIDAR unit, the CSN010 was selected as the LIDAR sensor for the reference design in this analysis cycle. The new development and other potential COTS LIDAR units provide several alternatives should the need arise after the prime contractor has been chosen. Model performance and error parameters for the chosen LIDAR are shown in Tables 8.1-17 and 8.1-18.

LIDAR Model Performance	Value	Units
Max 3DOF Operating Range	5	km
Min 3DOF Operating Range	2	m
3DOF Meas Rate	1	Hz
Max 6DOF Operating Range	150	m
Min 6DOF Operating Range	2	m
6DOF Meas Rate	variable by range	

Table 8.1-17 LIDAR Model Performance Parameters

LIDAR 3DOF Model Parameter	Value (3σ)	Units
Range Noise	0.03	m
Range Bias	0.03	m
Range Bias Time Constant	1	orbit
Angle Noise	0.3	Deg
Angle Bias	0.3	Deg
Angle Bias Time Constant	1	Orbit

Table 8.1-18 LIDAR 3DOF Model Error Parameters

Sensor Placement Illustrations

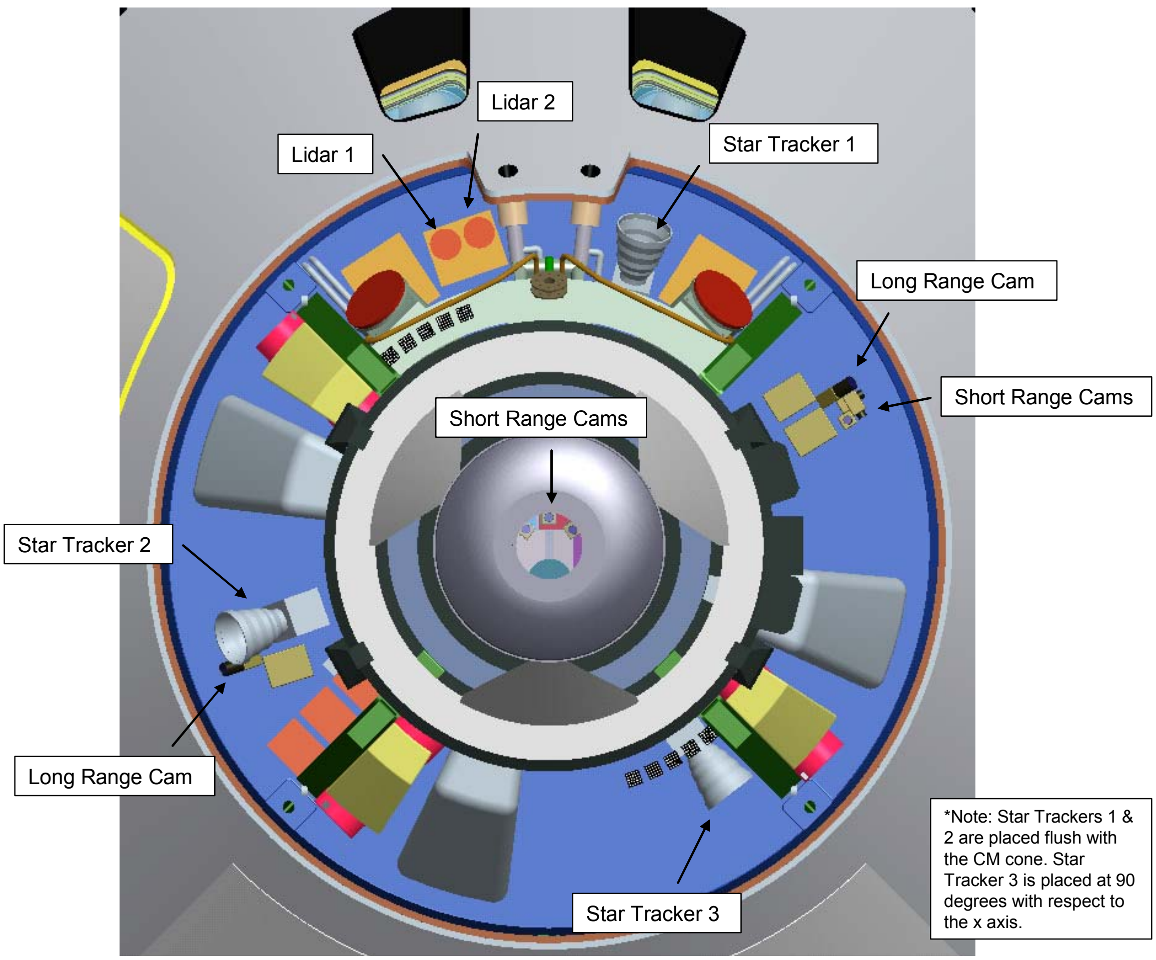

Figure 8.1-2 Sensor Placement Cone View

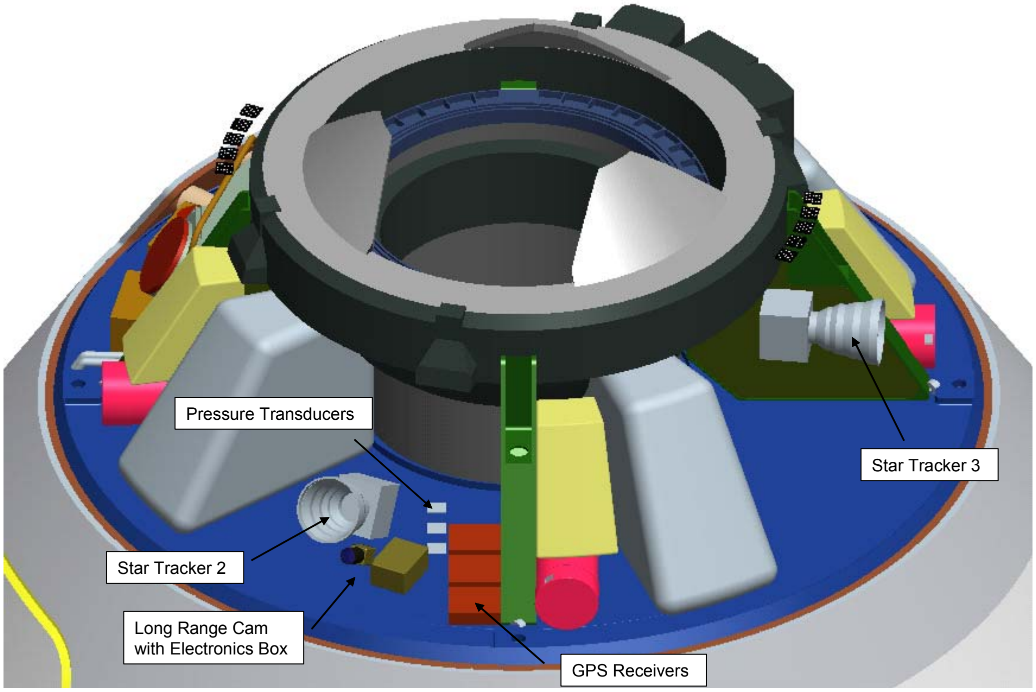

Figure 8.1-3 Sensor Placement Side View

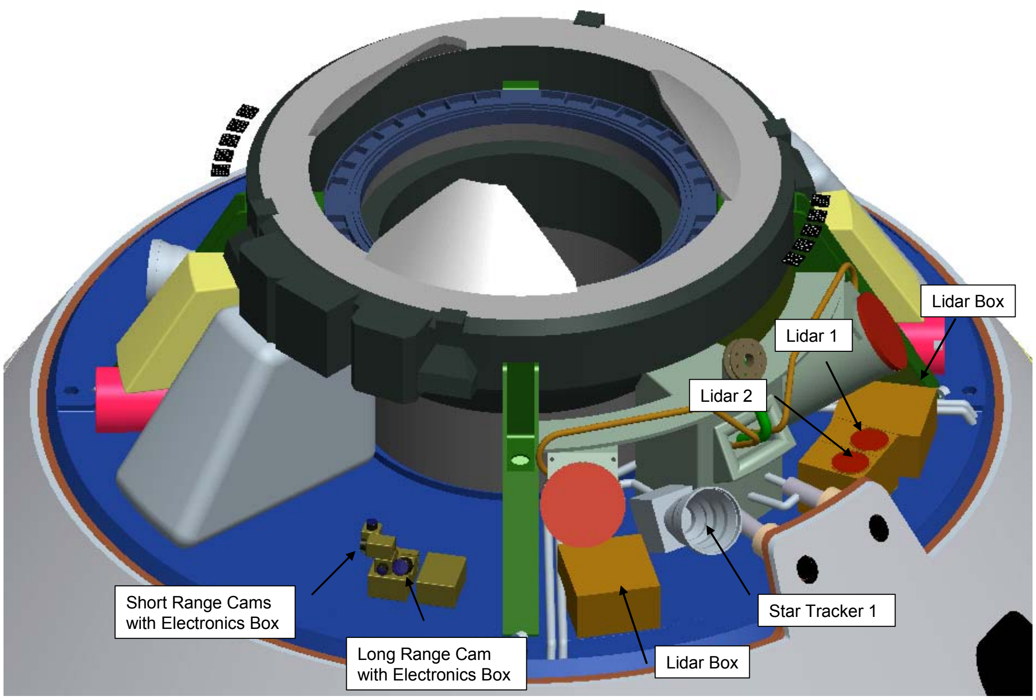

Figure 8.1-4 Sensor Placement Opposite Side View

Redundancy Management and Fault Tolerance Trades

To meet two fault tolerance and redundancy requirements, a preliminary study has been completed to select an RM scheme for the reference design. TDS 04-018 Subtask 1 addresses the options studied for FT&R. Refer to that report for more detailed information. Considerations for the different redundancy management options are as follows:

Should multiple sensor source data be screened to a single input prior to processing by the navigation algorithms? Examples of this screening include mid-value select, prime select, and weighted averaging.
Should multiple sensor source data be routed to isolated navigation processing algorithms? Examples include the Shuttle method of routing each of three IMUs data to a propagation routine. The final navigation solution is then a screened version of the independent navigation solutions.
Should separate and different filter instantiations be implemented (although each flight computer would carry identical copies of the multiple instantiations)? This allows for each flight computer to route varied combinations of sensor inputs as appropriate to flight phase.
Should the GN&C system implement a navigation backup flight software system on an isolated flight computer?
What is the specific sensor use strategy per flight phase? Refining this strategy will shape the RM considerations above as appropriate.

Table 8.1-19 Redundancy Considerations

Three options were designed as possible candidates for implementation. These options are based on a number of assumptions that were made. If these assumptions prove to be incorrect the design may have to be radically redesigned. The recommended design had the following features.

All sensors can be cross-strapped to all filters. Four string states are maintained, and flight modes dictate how, if, and when the separate states are used. Each filtered state is i-loadable and mode loadable (each flight phase could be a mode). FDIR occurs before sensors are input to the filter. One set of sensors is preselected as the Prime filter (the best measurements available will go to this filter depending on selection strategy). Two other filter strings maintain unique sensor outputs with quality rating flags for Prime filter assessment. One string is based on a clean propagated IMU that has no other sensors feeding it except for periodic state updates from the nav state output. All strings can be monitored/controlled by the ground or can run autonomously.

Figures 8.1-5 diagrams the selected option. This diagram is not detailed, rather is designed to give a basic flow.

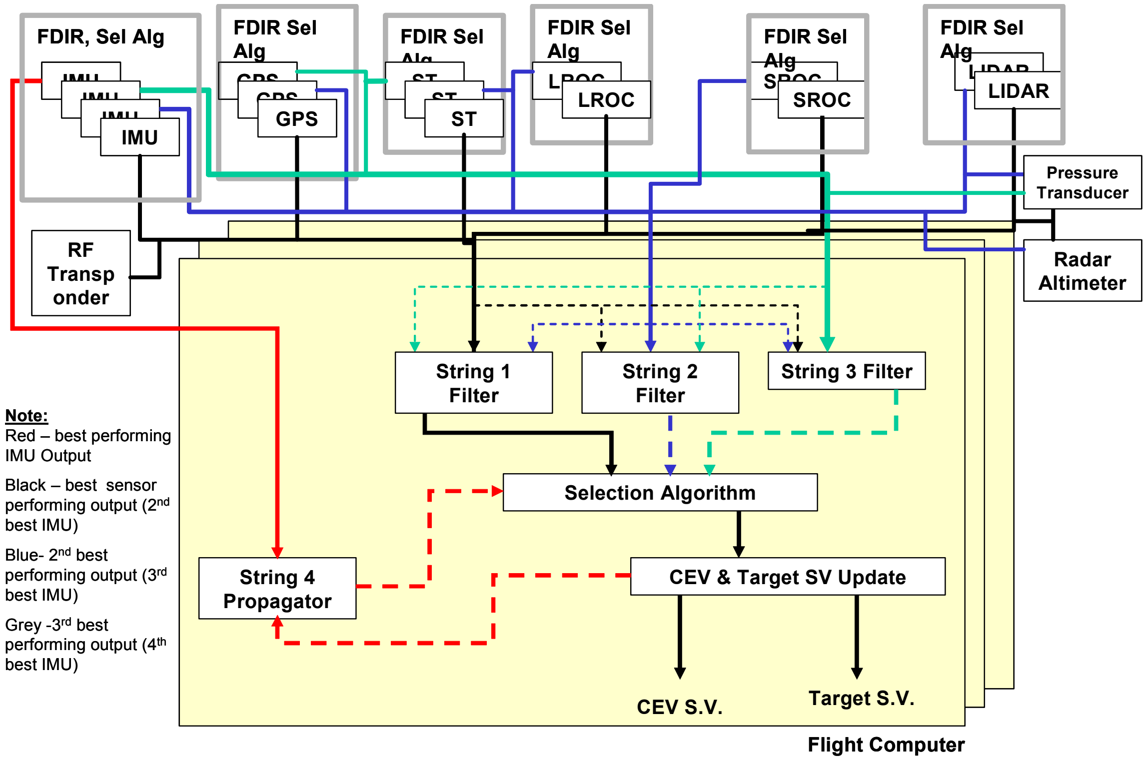

Figure 8.1-5 Fault Tolerance and Redundancy Option 1

Attitude Timeline

TDS 04-018 Subtask 3 CEV GN&C Attitude Timeline defines tools needed for future work in preparing a reference attitude timeline. Refer to TDS report for more detail. This attitude timeline GN&C work was also captured by the Integrated Analysis team and was completed in support of that team. Refer to the Integrated Analysis Charts for all the work completed under that effort. The analyses completed for this TDS are:

- Flight Modes
- Attitude Visualizations
- Clocking Visualizations
- Attitude Cost Estimation Worst Case Simulation
- Transient Attitude Descriptions and Assumptions
- Detailed Prox Ops Timeline
- Attitude Disturbance Listing

GN&C Flight Control Assessment

TDS 04-018 Subtask 4 CEV Flight Control Assessment analyzes flight control requirements for the CEV. Refer to the report for more detail. Analyses were completed to review Service Module

Candidate thruster configurations, analysis of docking / undocking from the tumbling LSAM, a CEV control analysis for mated CEV/LSAM, and an SM main engine trades and assessments study.

The Service Module candidate thruster configuration analysis determined that 100 lbf thrusters with 80 ms minimum on-time or greater are not recommended. Twenty-five lbf thrusters will provide adequate control authority based on the configurations that were assessed. The eighteen-thruster, six-pod configuration is not recommended due to poor efficiency and robustness characteristics. All configurations successfully provided control during typical proximity and docking operations in simulations completed.

Results from the analysis of docking / undocking from tumbling LSAM show that the centripetal acceleration dominates the action. The worst case magnitude in X is ~0.045 ft/s^2 at r = 150 ft and ~0.15 ft/s^2 at r = 500 ft. The worst case Y/Z component of centripetal acceleration is ~0.023 ft/s^2 at r = 150 ft and ~0.076 ft/s^2 at r = 150 ft. Coriolis disturbance is small for nominal closure rates: ~0.0009 ft/s^2 for 0.5 ft/s closure. Orbital mechanics disturbance acceleration is also small: <0.0025 ft/s^2. The transient velocity change at r = 150 ft is 2.6 ft/s, and 8.7 ft/s at 500 ft.

Based on this CEV RCS configuration analysis, the expected +X control acceleration for most of the configurations, firing four +X 25 lbf thrusters, is about 0.0672 ft/s^2. This leaves little control margin over worst case disturbances at 150 ft, and shows that the CEV cannot maintain station on the tumbling axis at 500 ft. Propellant usage for an approach to a tumbling target at 1 degree per second is expected to be very high. Analytical and simulation quantification of required propellant will be supplied in future versions of the TDS report.

The CEV control analysis for mated CEV/LSAM results are shown in Table 8.1-20, Table 8.1-21, and Table 8.1-22. The purpose of the mated CEV/LSAM control analysis was to determine the capability of the CEV to control the mated stack in lunar transit. This capability is desirable since the operational preference is to have the crew in the CEV during trajectory correction maneuvers (TCMs) since the CEV has the capability to return the crew in case of emergency.

	25 lbf ACS	*100 lbf ACS*
Roll	0.759	0.759
Pitch	3.247	3.247
Yaw	3.247	3.247

Table 8.1-20 Analytical Propellant Estimates for 0.2 deg/s Maneuvers

	25 lbf ACS		*100 lbf ACS*	
	$\frac{1}{2}T$ *Time between pulses [sec]*	$\dot{m}$ *Prop [lbm/hr]*	$\frac{1}{2}T$ *Time between pulses [sec]*	$\dot{m}$ *Prop [lbm/hr]*
Roll	3034.9	0.0297	758.7	0.475
Pitch	12987.0	0.0069	3246.8	0.111
Yaw	12987.0	0.0069	3246.8	0.111
Total		0.0435		0.697

Table 8.1-21 Analytical Attitude Hold Propellant Usage Rates for 5 deg Deadband

Rotate to Burn	Burn in Place
Rotate to and from burn attitude (0.1°/s)	
Average: 3.5 lbm per mnvr x 2 mnvrs = 7.0 lbm Max: ~5.23 lbm per mnvr x 2 mnvrs = 10.5 lbm Time: 0 to 180 deg mnvr 0 to 30 min	None
TCM Translation (1 ft/s)	
Fuel = ~24.1 lbm Time (8x100 lbf thrusters) = 6.0 sec Time (2x25 lbf thrusters) = 96 sec	Fuel (including attitude disturbance cancellation) ~24.1 lbm to ~105 lbm Time (8x100 lbf thrusters in X) = 6.0 sec Time (2x25 lbf thrusters in XZ) = 140 sec
Totals	
Fuel: 31 to 35 lbm Time: 6 sec to 30 min	Fuel: 24 lbm to 105 lbm Time: 6 sec to 140 sec

Table 8.1-22 Rotate to Burn Comparison with Burn in Place

The SM main engine trade and assessments results were not completed at time and the TDS report will be updated at a later date.

GN&C Roles and Responsibilities

TDS 04-018 Subtask 5 CEV GN&C Roles & Responsibilities defines the Roles and Responsibilities of the CEV GN&C with respect to its counterpart vehicles. Refer to the report for more detail. These roles and responsibilities were designed to help scope the level of fidelity needed for CEV's GN&C Algorithms, assist in writing requirements for the forthcoming Constellation vehicles (EDS and LSAM), and explore effector usage considerations.

GN&C Software Architecture

TDS 04-018 Subtask 6 CEV GN&C Software Architecture lays out and describes a candidate design architecture to meet the driving CARD and SRD requirements. Refer to report for more detail. The external interface is shown in Figure 8.1-6. The internal interface is shown in Figure 8.1-7. A targeting overview, a CEV Guidance overview, and a Navigation overview are shown in Figures 8.1-8, 8.1-9, and 8.1-10.

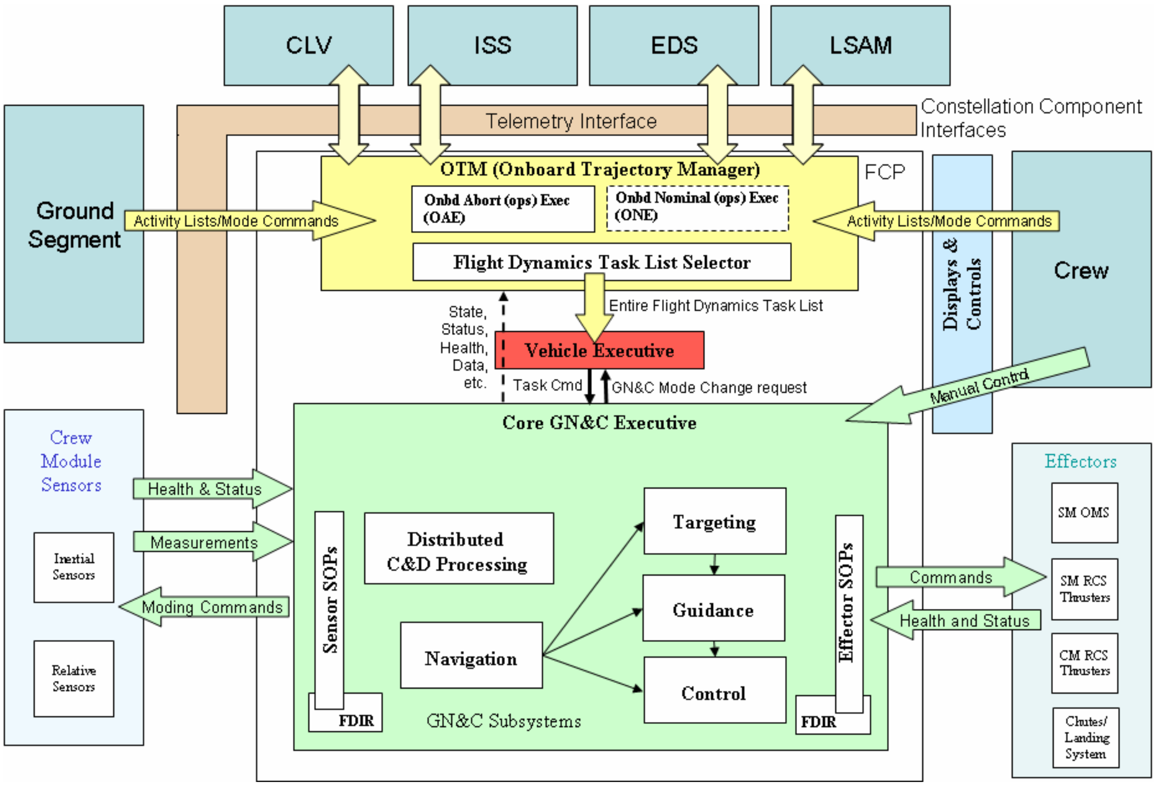

Figure 8.1-6 External Interface

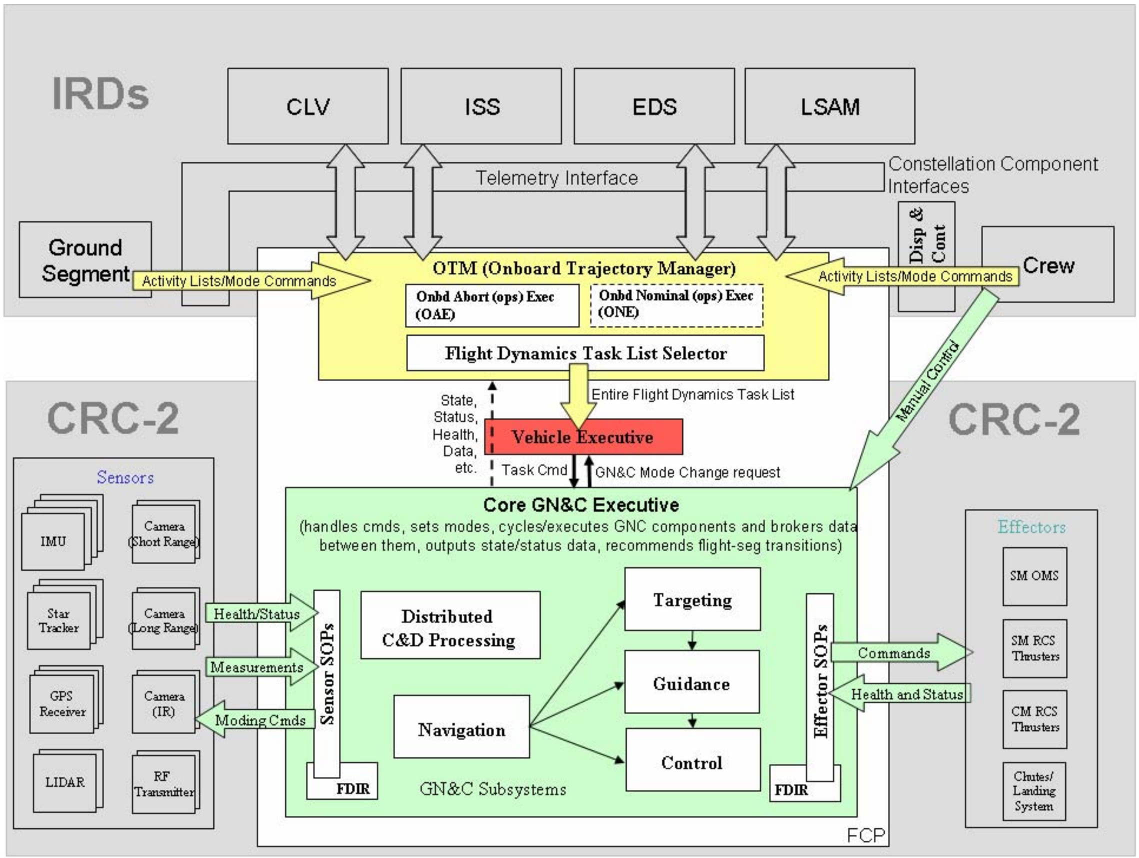

Figure 8.1-7 Internal Interface

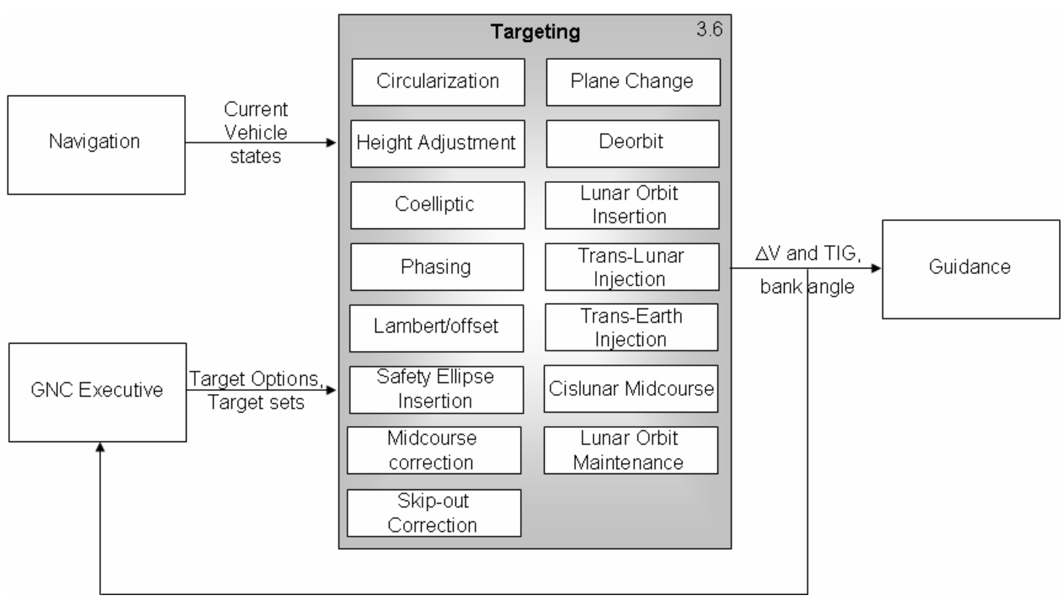

Figure 8.1-8 Targeting Overview

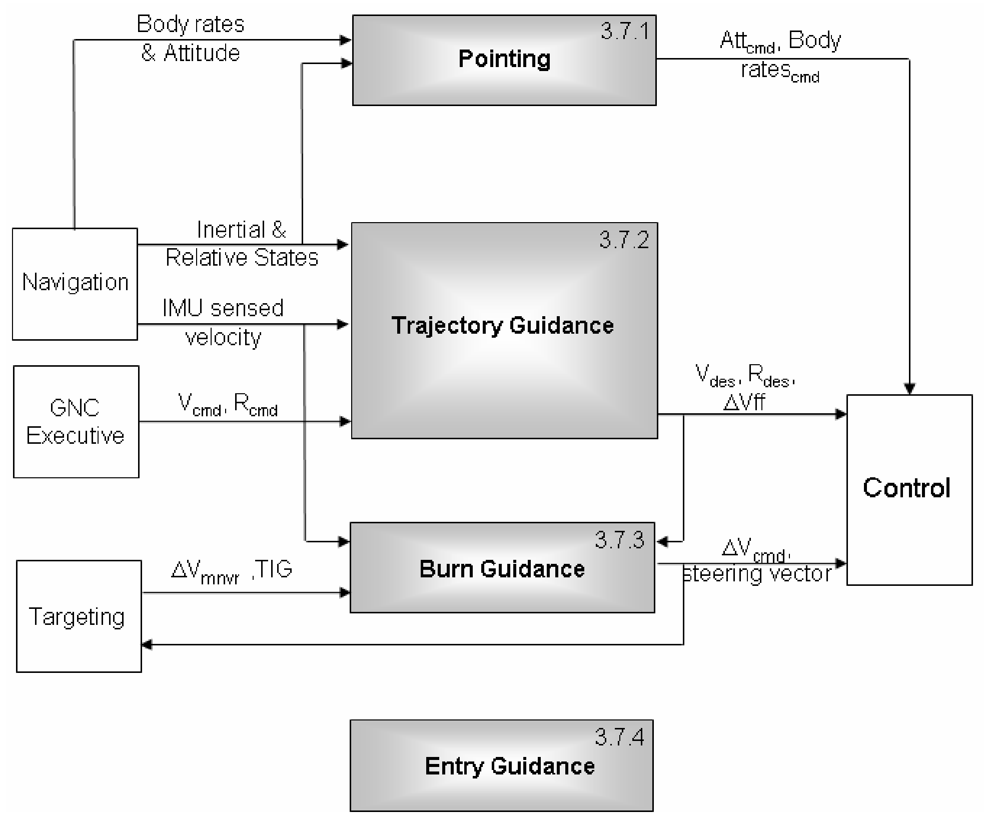

Figure 8.1-9 CEV Guidance Overview

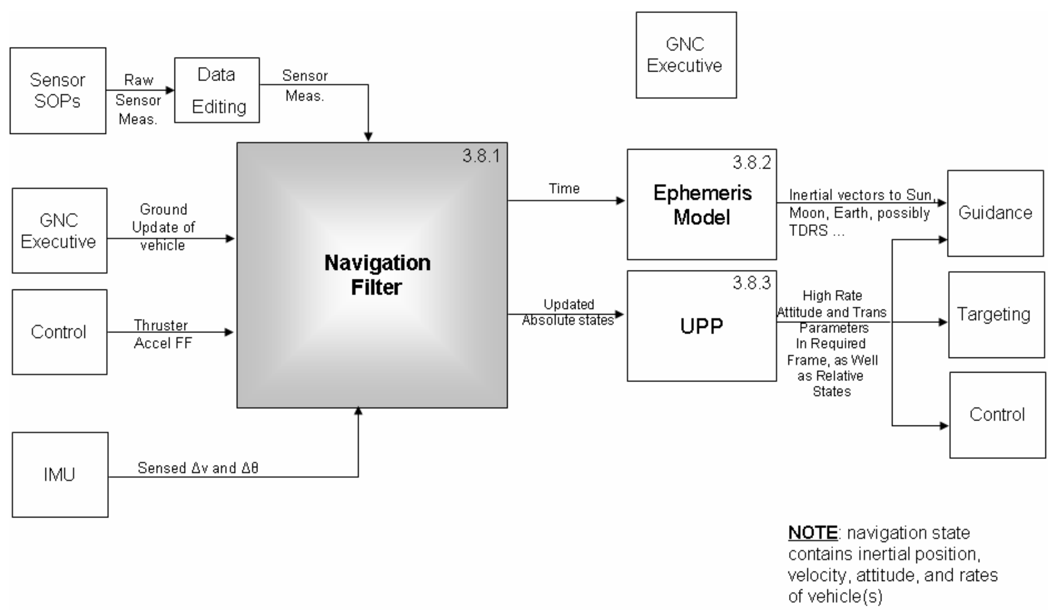

Figure 8.1-10 Navigation Overview

8.1.3 Mass Estimates and Design Maturity

Mass estimates for the GN&C sensor suite is based on the sensors selected with some approximations based on known modifications that will be required, such as, modifying the GPS boxes for 1553 communications. Mass properties are shown in Table 8.1-23.

Hardware Items	Quantity	Unit Mass (lbm)	Growth (%)	Total Mass (lbm)	CM Mass (lbm)	SM Mass (lbm)	Basis of Estimate
GN&C				**177**	**177**	**0**	
Inertial Measurement Unit	4	9	10%	39.8	39.8		Honeywell MIMU specifications
GPS Receiver	3	5	5%	15.8	15.8		HRSDM GNC-21 DRD
GPS Antenna	6	0.3	20%	2.2	2.2		Cory Micronics spec
Low Noise Amplifier	6	0.3	10%	2.0	2.0		MITEQ Spec.
Star Tracker	3	6	5%	18.8	18.8		Goodrich HD - 1005
Lidar Optical Unit	2	7	10%	15.8	15.8		HRVDM Peer Review
Lidar Avionics Processing Unit	2	14	10%	31.0	31.0		HRVDM Peer Review
Optical Camera: Short Range	4	2	10%	6.6	6.6		CSN006 Proprietary Briefing
Optical Camera: Long Range	2	5	10%	9.9	9.9		CSN007 Proprietary Briefing
Optical Camera Avionics	4	5	10%	19.8	19.8		
Optical Spotlight	1	4	5%	4.6	4.6		CSN008 Proprietary Briefing
Entry Phase Pressure Transducer	3	0.3	5%	0.8	0.8		LG-1237
Terminal Landing Velocimeter	2	3.0	5%	6.3	6.3		Honeywell HG8500 Series Spec
Terminal Landing Velocimeter Antennas	4	1.0	5%	4.2	4.2		MPL mission

Table 8.1-23 GN&C Mass Properties

8.1.4 Plan Forward

Common mode failure and single event upsets for the relative navigation LIDAR and camera sensors need to be protected against. A sensor protection strategy needs to be designed and implemented for ascent and orbital operations. Crew awareness needs during docking and maneuvers needs to be coordinated with the Cockpit Working Group. Determining the final number, placement, and lens focal length of the short and long range cameras to meet navigation requirements and meet crew awareness objectives need to be addressed. In general, all sensor accuracy numbers need to be refined for analysis support and consistency between the flight dynamics mode teams.

8.2 Trajectories

Entry trajectories were designed as part of DAC-2 for three different entry scenarios: ISS return, lunar direct entry, and lunar skip entry. The trajectories were generated using the Simulation and Optimization of Rocket Trajectories (SORT). Each trajectory was generated with a consistent set of constraints. Those constraints were:

- Guided entry must produce g-loads acceptable for de-conditioned crew

- Ballistic entry must produce g-loads acceptable for abort mode entry
- SM disposal footprint must be placed at least 25 nmi from U.S. border (200 nmi from international border)
- Must have sufficient entry flight path angle corridor (goal of $> 1.0°$)

The trajectories generated for DAC-2 were used in CRC-3 without modification.

Each trajectory also assumes a consistent parachute descent system that consists of two drogue chutes with a single dis-reef stage and three main chutes with two stage dis-reef. The drogue chutes are currently being deployed through an entry guidance flag that deploys when the vehicle is directly over the target. The main chutes are being deployed at an altitude of 10,000 ft above the surface. The parachute descent simulation is primarily based on the Apollo parachute system, with minor modifications.

In order to design the entry trajectories, assumptions had to be made about the aerodynamics of the vehicle, the dimensions of the vehicle, the mass of the vehicle, and the atmospheric environment the vehicle would fly through. There are many other models that go into the simulation, such as gravity models, flight control models, guidance routines, etc. and some of those will be specified later in the details of each entry scenario. The aerodynamics of the vehicle were provided by JSC/EG3 (Applied Aeroscience & CFD Branch) assuming a 16.5 ft aeroshell diameter or 213.8 ft^2 reference area. For these 3-DOF simulations, the angle-of-attack (alpha) was always assumed to be trimmed relative to the Mach number in the table below. The aerodynamic coefficients used for the entry trajectories are also provided in the following table.

#Mach	Alpha	CD	CL	L/D
0.5	162.35	0.86743	0.32535	0.37622
0.7	160.79	0.91428	0.28659	0.31402
0.9	154.74	0.97774	0.386	0.39506
1.1	149	1.1008	0.568	0.51652
1.2	147.31	1.13148	0.59228	0.52449
1.5	144.23	1.14083	0.59835	0.52494
2	144.11	1.08199	0.55493	0.51367
2.4	145.17	1.06284	0.53731	0.50573
3	146.55	1.04841	0.53153	0.50829
4	149.13	1.07064	0.52642	0.49284
6	149.41	1.07842	0.494	0.45885
9.26	149.6	1.09002	0.48856	0.44882
16.78	152.21	1.15235	0.47757	0.41631
23.84	153.3	1.18075	0.4707	0.40038
28.41	153.49	1.1867	0.47286	0.40009
33.7	153.74	1.18703	0.4613	0.39005

Table 8.2-1 DAC-2 CEV Entry Aerodynamics

The mass of the vehicle was assumed to be 16,354 lbm at entry interface. That mass is held constant throughout the entry trajectory. Currently, there is no modeling of fuel usage for attitude control or mass reductions due to jettison of vehicle components. This correlates to a ballistic number of the entry vehicle of 64.45 psf (314.7 kg/m^2) at Mach 28.4. A table summarizing the vehicle specific characteristics is included below.

Vehicle Mass at EI	16,354 lbm
Aeroshell Diameter	16.5 ft
Reference Area	213.8 ft^2
Ballistic Number at Mach 28.4	64.45 psf

Table 8.2-2 Crew Module Vehicle Characteristics

The Global Reference Atmosphere Model of 1999 (GRAM-99) was used to simulate atmospheric conditions throughout the trajectory. The atmosphere was assumed to be nominal (undispersed) for all of the nominal entry trajectory designs. The base date used to initialize the GRAM-99 software was May 8, 2012 at 14:00:0.0 for ISS return, and August 8, 2018 at 5:11:0.0 for lunar return.

Definition of the SM disposal footprint is typically done with Monte Carlo analysis. However, a quick assessment of the SM disposal footprint was needed in order to assess the impacts associated with different entry trajectory designs of the Crew Module (CM). In order to fly to a land landing target in the western CONtinental United States (CONUS), there must be a separation distance between the disposal footprint and the landing target. The greater the distance between the footprint and landing, the farther inland the vehicle can fly, and the potential for more landing sites. In order to simulate the SM disposal footprint, assumptions had to be made about the ballistic characteristics of the SM during entry, specifically the toe of the footprint. The SM disposal toe trajectory was simulated assuming a ballistic coefficient of 95 psf from entry interface (400,000 ft) down to 300,000 ft. At that point, the ballistic coefficient was changed to 123 psf, which was deemed the highest potential debris ballistic coefficient based on previous X-38 analysis, and would be used for definition of the SM disposal toe trajectory. A Lift-to-Drag (L/D) ratio of 0.075 was applied to the debris piece in order to account for dispersions in atmosphere, initial state, and aerodynamics associated with a Monte Carlo approach to defining the disposal footprint. The distance from the disposal toe to the landing point was used to satisfy the debris boundary constraint.

Evaluation of the entry corridor was consistent for the ISS return case and the lunar direct return case. Skip entry was a bit different and will be explained in detail in the skip trajectory section. ISS return and lunar direct corridor analysis begins with selection of the nominal trajectory and the guidance is designed around that nominal reference. Once the nominal trajectory is established, atmospheric dispersions are applied on the order of ±30% of the nominal density and the entry flight path angle is scanned on the shallow and steep side of the nominal. The corridor boundary is defined when the trajectory no longer satisfies a given constraint, typically a crew g-loads limit or range convergence tolerance. The ballistic entry trajectory must also be incorporated in the corridor analysis since it generally defines the steep side of the corridor relative to the crew g-load limits. The width of that corridor, shallow side plus steep side, is the acceptable entry corridor and is used in the entry design process to satisfy entry corridor constraints.

8.2.1 ISS Return Entry Trajectory

Return from the International Space Station is a requirement for the CEV. The nominal entry trajectory associated with return from ISS was generated as part of DAC-2. The constraints mentioned above all had to be met in order to have an acceptable entry design. The most difficult constraint to satisfy was the disposal of the SM 25 nmi off U.S. property and 200 nmi off international property. This is due to the low speed entry associated with return from Low Earth Orbit (LEO) and the flight path angle required to achieve an acceptable entry corridor. The current DAC-2 design assumes a flight path angle of -1.9° at entry interface. A more shallow flight path angle would increase the distance between the SM disposal footprint and the landing target, however, as the flight path angle becomes shallower, the entry corridor is reduced. Therefore the SM disposal constraint and entry corridor constraints are conflicting relative to entry flight path angle selection. However, even with the conflicting constraints, there are still solutions that satisfy both constraints.

The ISS return trajectory utilized closed-loop guidance in order to perform range convergence. The guidance routine used was the final phase or second entry Apollo guidance. This guidance phase is also called a terminal point controller. The guidance requires a stored reference trajectory and controller gains to achieve an end condition, or range target. Range is controlled by increasing or decreasing the drag experienced by the entry vehicle. The guidance cannot affect the vehicle drag coefficient, so drag control is accomplished by varying the vertical lift, to fly higher or lower in the atmosphere, as required. The vertical component of lift is varied by altering the vehicle bank angle, which is the primary output from the guidance routine. Through out the entry design process, nearly all entry design approaches were simulated nominally, as well as 3-sigma steep and 3-sigma shallow, in order to understand the guidance response to all dispersions.

The final design of the DAC-2 entry trajectory satisfied all constraints mentioned previously. The design for ISS return correlates to the following entry interface targets assuming an ascending approach from a 200 nmi ISS orbit.

Inertial Speed	25784.45 ft/s
Inertial Flight Path Angle	-1.9°
Inertial Azimuth	40.34°
Geodetic Altitude	400,000 ft
Longitude	-144.17°
Geodetic Latitude	16.45°

Table 8.2-3 Nominal ISS Return Entry Interface Conditions

The trajectory correlates to a range flown of ~1965 nmi and a maximum g-load during entry of 2.6 g. The following figures show plots that characterize the ISS return entry trajectory.

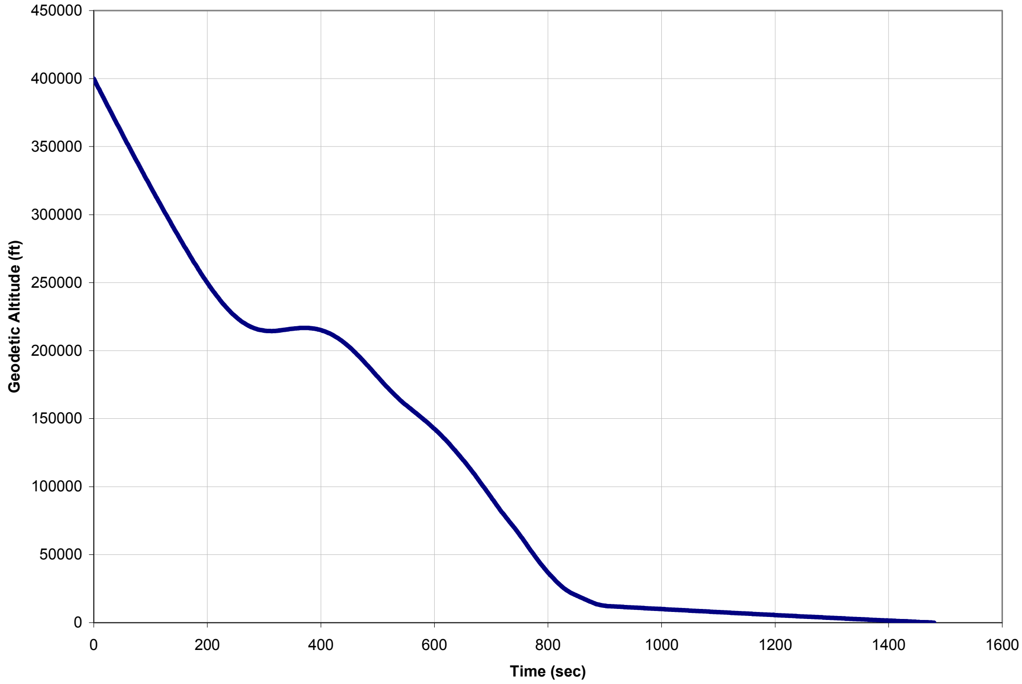

Figure 8.2-1 Geodetic Altitude Entry Profile (ISS Return)

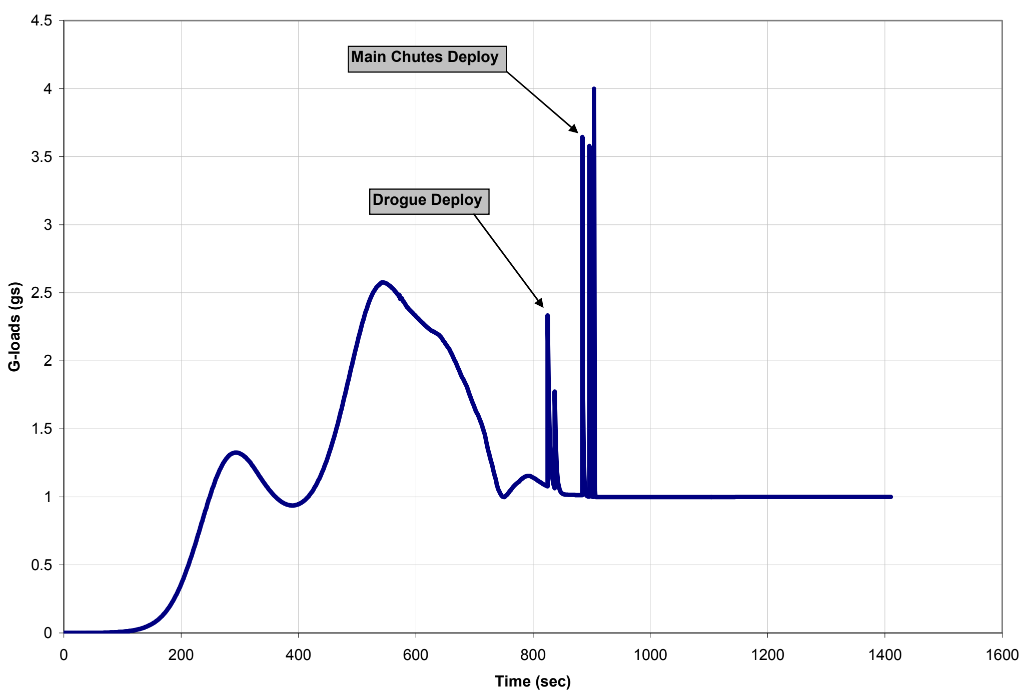

Figure 8.2-2 G-load Profile Entry (ISS Return)

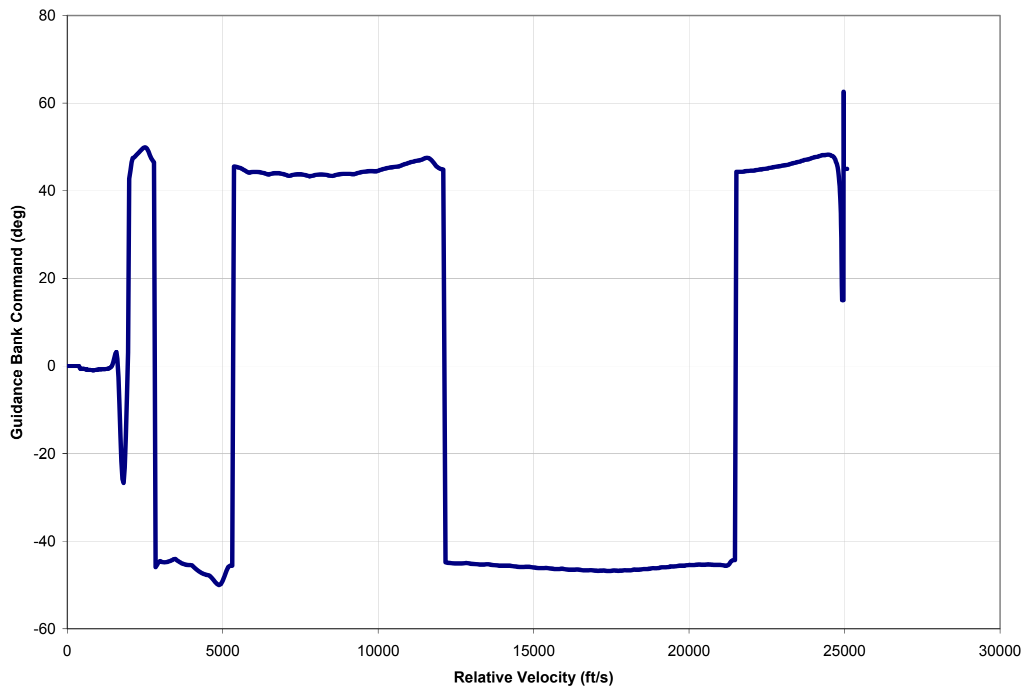

Figure 8.2-3 Guidance Bank Command Entry Profile (ISS Return)

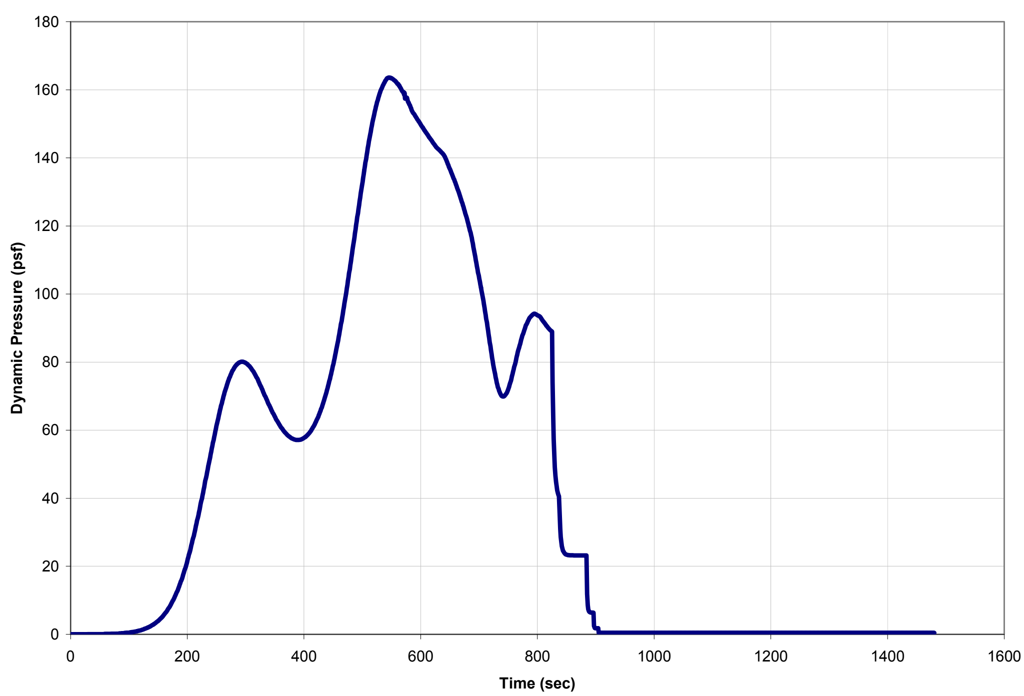

Figure 8.2-4 Dynamic Pressure Entry Profile (ISS Return)

The ballistic trajectory associated with each nominal trajectory design iteration had to be computed and compared to the abort mode g-load limits. This must be done in order to assess the impacts associated with each design relative to crew g-load limits. The ballistic trajectory associated with the final design of the nominal entry trajectory easily meets the abort mode crew limits. The following figures characterize the ballistic entry.

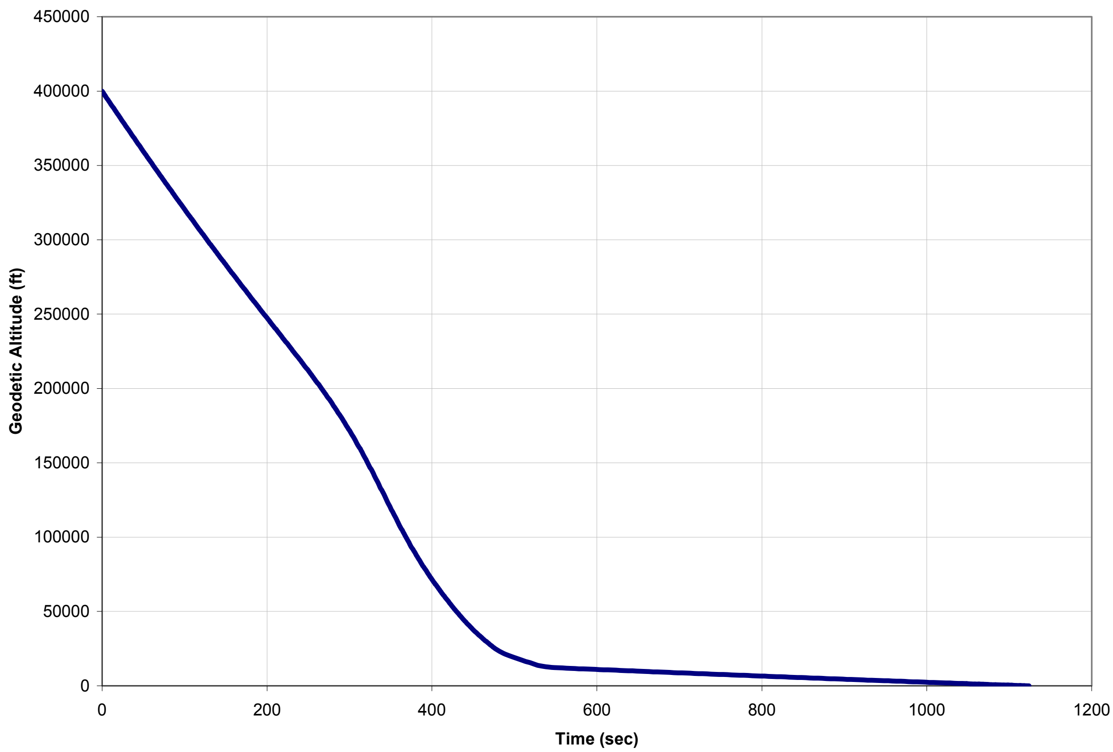

Figure 8.2-5 Geodetic Altitude Entry Profile (Ballistic ISS Return)

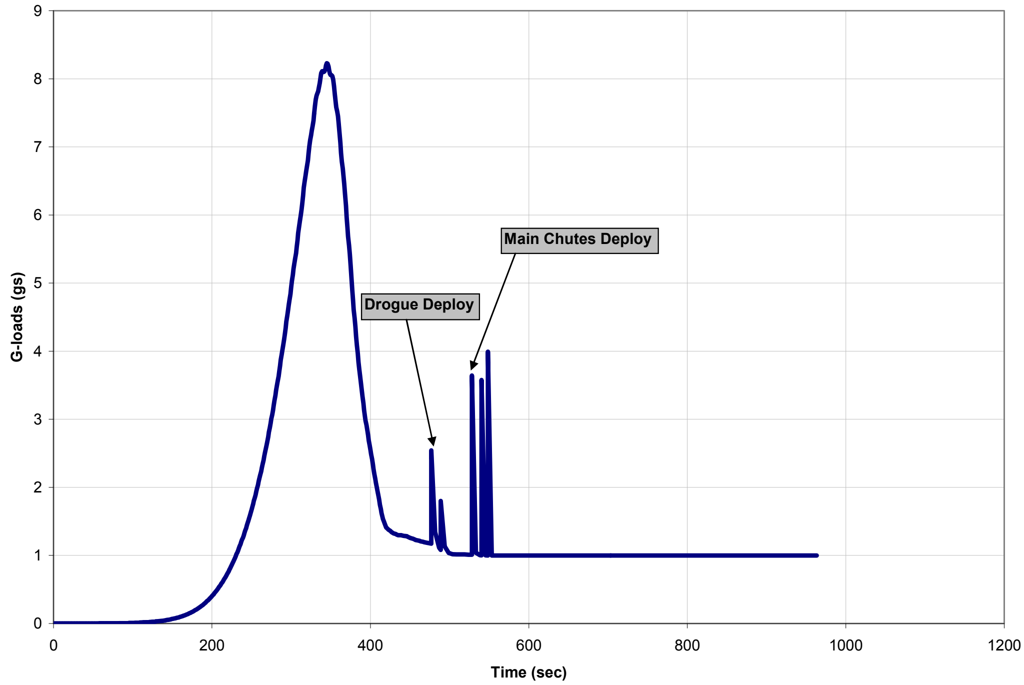

Figure 8.2-6 G-load Entry Profile (Ballistic ISS Return)

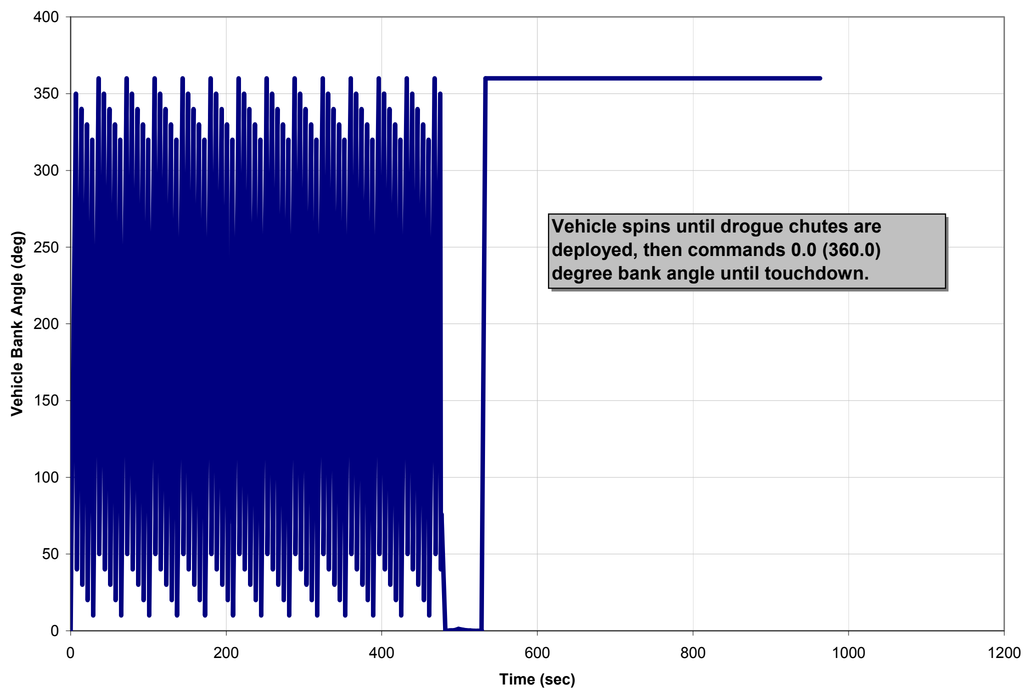

Figure 8.2-7 Bank Angle Entry Profile (Ballistic ISS Return)

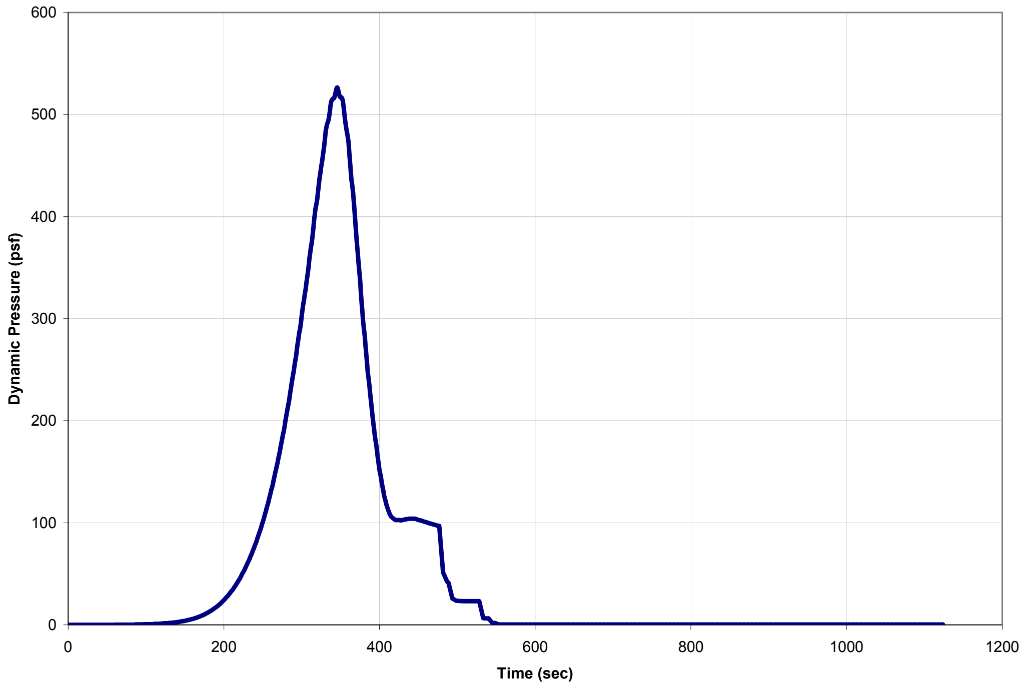

Figure 8.2-8 Dynamic Pressure Entry Profile (Ballistic ISS Return)

8.2.2 Lunar Direct Entry Trajectory

A direct entry from the Moon is also a requirement for the CEV. This is the same type of trajectory that all Apollo missions flew for Earth entry. The nominal entry trajectory for a direct return from the Moon was generated as part of DAC-2. All of the above constraints still apply to the lunar direct entry scenario. The major difference between an entry from LEO and a direct entry from the Moon is that the entry speed is greatly increased for lunar return. This generally means that the entry problem becomes more difficult since parameters like heating rate, heat load, g-loads, and dynamic pressure are all increased. The proper disposal of the SM still proved to be a difficult constraint to satisfy, however, not quite a constraining as in the ISS return case. With the increased entry speed, the ballistic entry g-load constraint also proved to be a challenge. However, an acceptable solution was achieved that met all constraints listed above.

The lunar direct entry was flown with closed-loop guidance, same as the ISS return cases. However, the guidance scheme chosen for the lunar direct entry was the full Apollo guidance algorithm. The only change from the original Apollo algorithm was that the up-control logic was inhibited, as this gets into the skip capability of the Apollo algorithm. Instead the guidance scheme is forced to use the constant drag logic until ~25,000 ft/s. At that point, the guidance switches to the final phase guidance algorithm. This approach also allows for easy selection of the desired range and speeds up the design process.

The final design of the DAC-2 lunar direct entry trajectory satisfied all constraints and correlates to the following entry interface targets.

Inertial Speed	36089.24 ft/s
Inertial Flight Path Angle	-6.1°
Inertial Azimuth	41.76°
Geodetic Altitude	400,000 ft
Longitude	-146.9°
Geodetic Latitude	3.519°

Table 8.2-4 Nominal Lunar Direct Return Entry Interface Conditions

The nominal trajectory correlates to a range flown of ~1865 nmi and a maximum g-load during entry of 4.4 g. The following figures characterize the lunar direct entry trajectory.

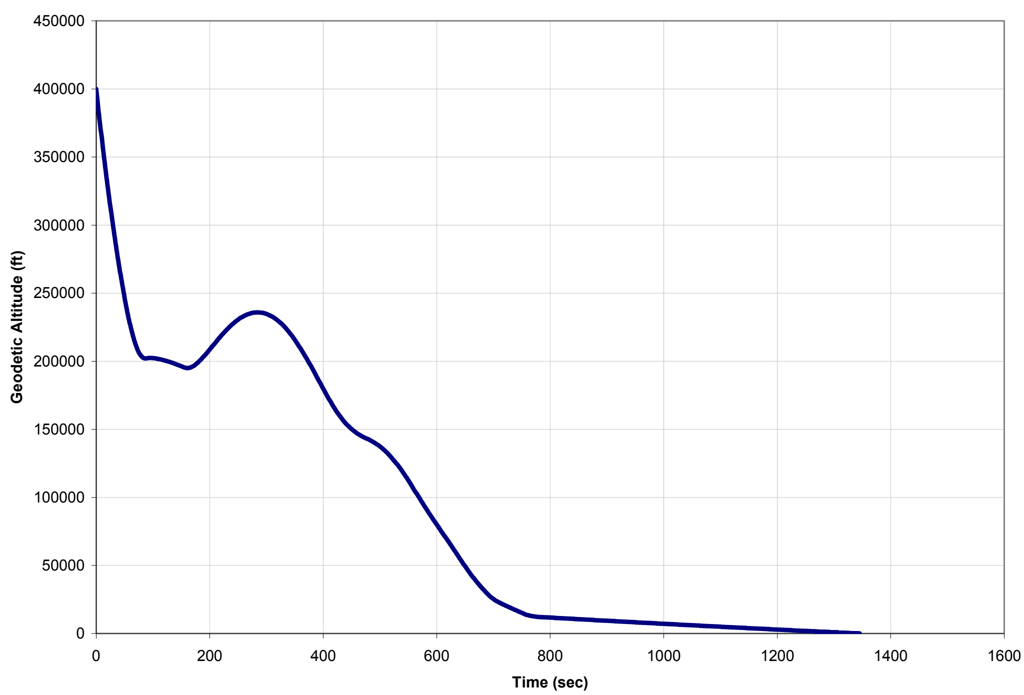

Figure 8.2-9 Geodetic Altitude Entry Profile (Lunar Direct)

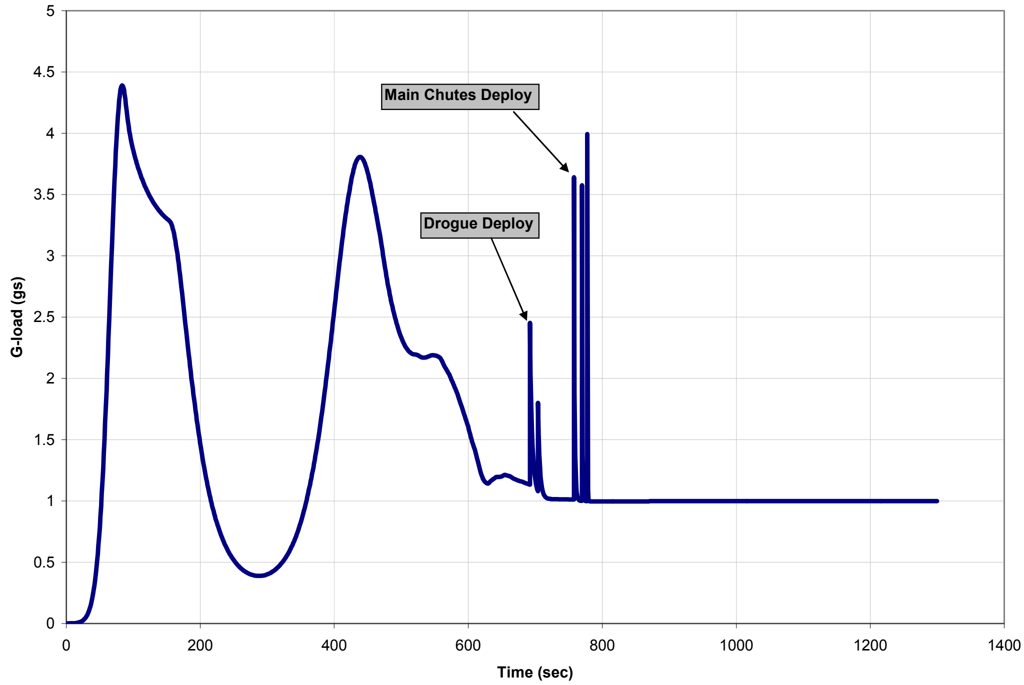

Figure 8.2-10 G-load Entry Profile (Lunar Direct)

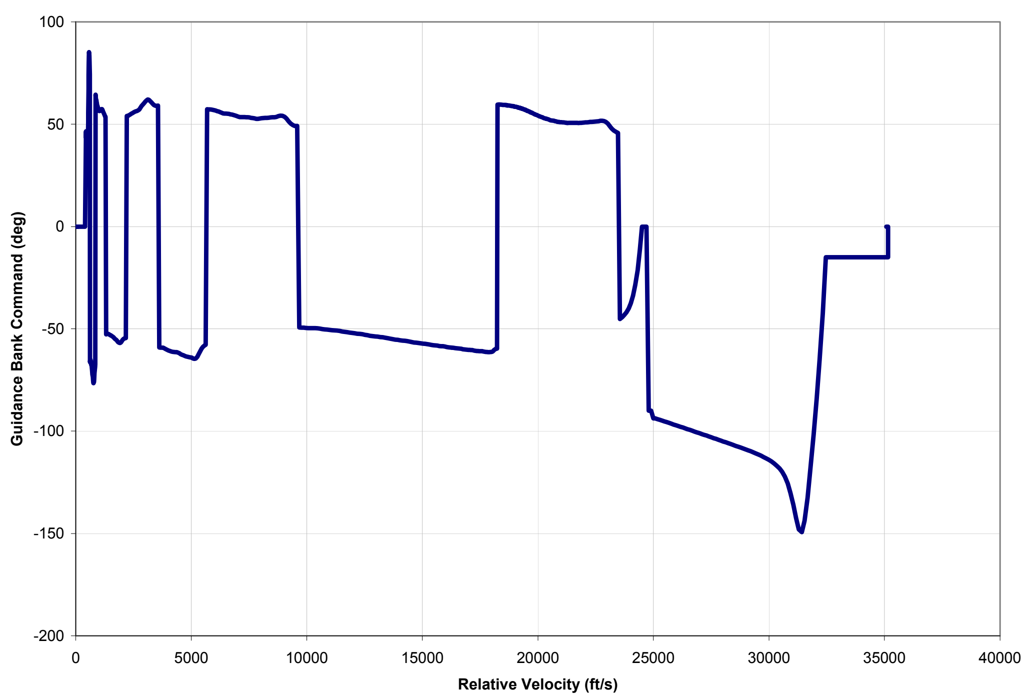

Figure 8.2-11 Guidance Bank Command Entry Profile (Lunar Direct)

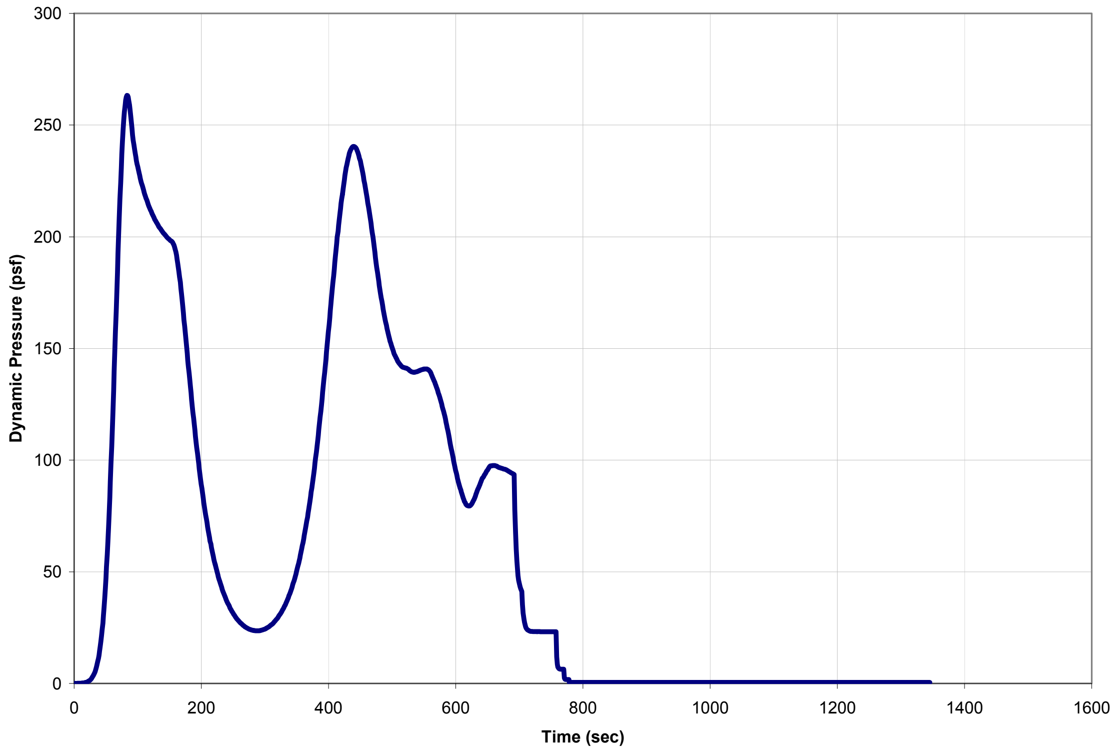

Figure 8.2-12 Dynamic Pressure Entry Profile (Lunar Direct)

The ballistic trajectory associated with each nominal trajectory design iteration was computed and compared to the abort mode g-load limits. The ballistic trajectory associated with the final design of the nominal entry trajectory meets the abort mode crew limits. The following figures characterize the ballistic entry.

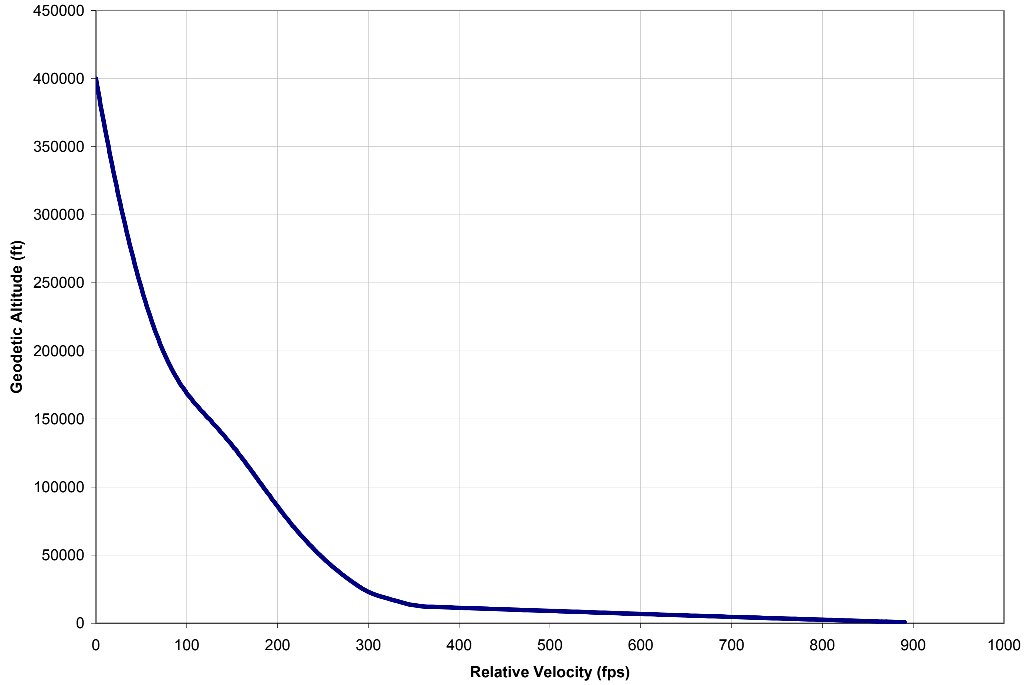

Figure 8.2-13 Geodetic Altitude Entry Profile (Ballistic Lunar Direct)

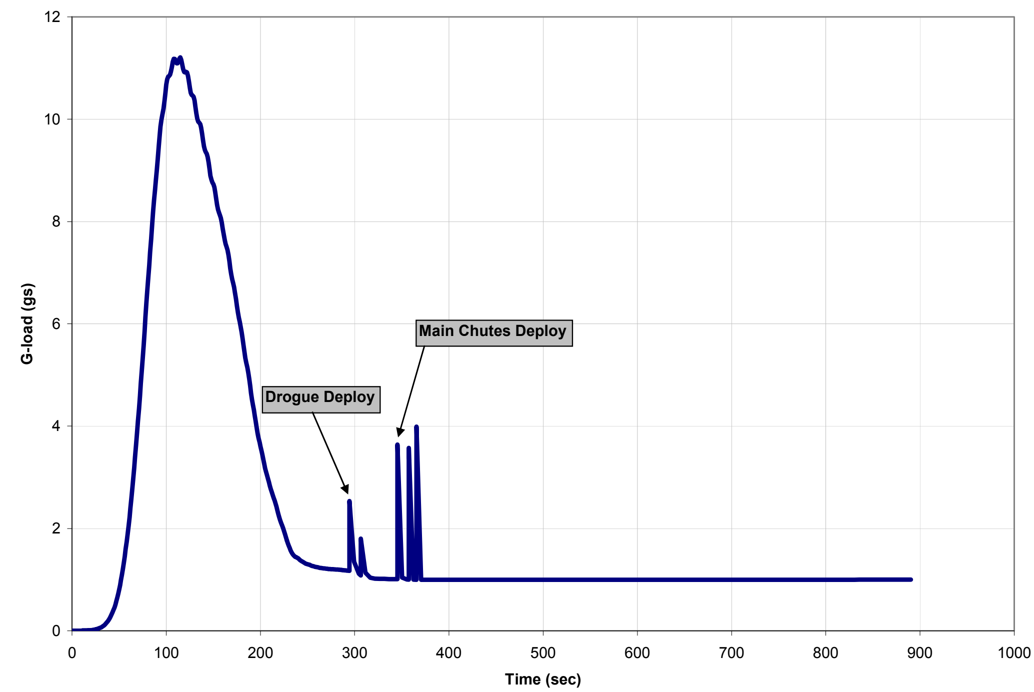

Figure 8.2-14 G-load Entry Profile (Ballistic Lunar Direct)

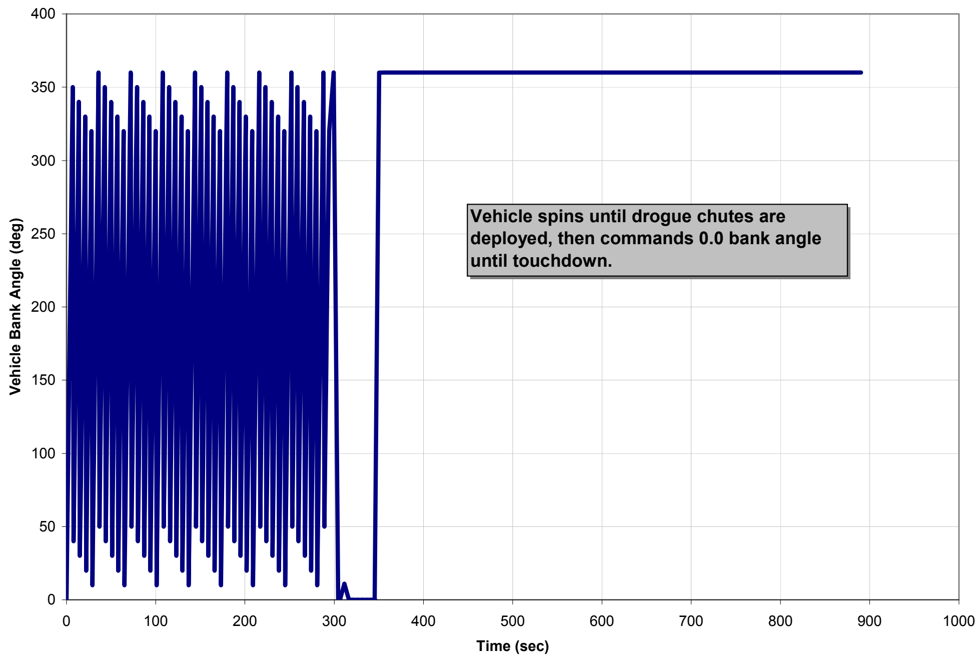

Figure 8.2-15 Vehicle Bank Angle Entry Profile (Ballistic Lunar Direct)

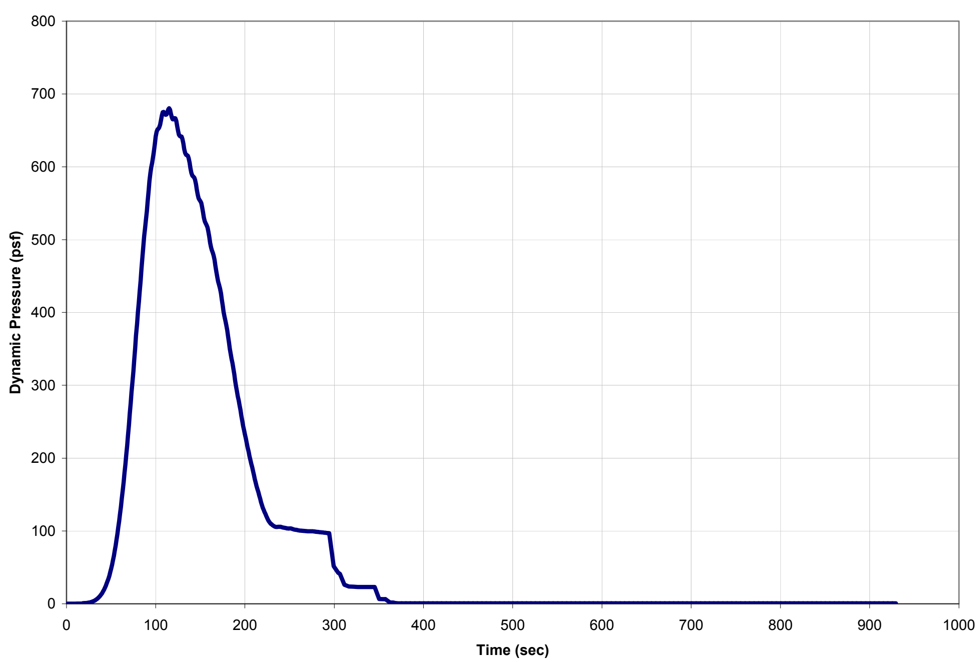

Figure 8.2-16 Dynamic Pressure Entry Profile (Ballistic Lunar Direct)

8.2.3 Lunar Return Skip Entry Trajectory

A skip entry trajectory for returning crew to Earth from the Moon is required to satisfy the CEV requirement for Continental United States (CONUS) landing site access throughout the lunar month. For example, a minimum skip range of 5000 nmi is required to access Vandenberg Air Force Base, Ca. when the Moon is at minimum declination during the maximum inclination cycle. Over the 18.6-year lunar nodal cycle the lunar inclination varies from 18.3° to 28.6°. We are currently approaching maximum lunar inclination in June of 2006, and a minimum lunar inclination will begin in October of 2015.

For cycle 1 and 2 of the DAC-2 trajectory deliveries, the skip entry trajectories were generated using a hybrid version of closed-loop guidance. This hybrid guidance cycled logic from three existing algorithms: the HYPAS (an aerocapture guidance), Shuttle Entry, and the Apollo Entry Guidance algorithms. Cycle-3 DAC-2 cycled logic using a numerical guidance algorithm. The purpose of the guidance algorithms is to compute the bank commands used by flight control to steer the vehicle lift during atmospheric flight, while satisfying all vehicle (thermal and structure loads), trajectory (Service Module disposal), and crew (acceleration magnitude, duration, and direction) constraints.

For a Crew Module with an L/D of 0.4, entry trajectories traversing ranges greater than about 2,500 nmi require significant trajectory lofting, or altitude increases, during entry flight. The phase of entry flight with increasing altitude is designated "Up-Control". If the drag acceleration drops below 6 ft/s^2 during the Up-Control phase of flight, the vehicle is classified as flying a skip trajectory. This exo-atmospheric phase of flight during the skip is called the Kepler phase. For DAC-2, the trajectory design utilized a skip range of 5,500 nmi to Carson Flats, Nevada and results in approximately 17 minutes of Kepler flight. The 5,500 nmi range was selected to provide adequate Service Module disposal in the Pacific Ocean for an ascending right, 49.5° inclination approach to the nominal landing site. The entry conditions are shown in Table 2.2-5.

Inertial Speed	36046 ft/s
Inertial Flight Path Angle	-6.06°
Inertial Azimuth	42.985°
Geodetic Altitude	400,000 ft
Longitude	165.09°
Geodetic Latitude	-17.8841°

Table 8.2-5 Nominal Skip Entry Interface (EI) Conditions

The flight corridor for a skip entry trajectory is currently being driven by the ballistic entry flight conditions. A ballistic flight results when the effect of lift acceleration on altitude rate is neutralized, either by spinning the vehicle or holding the lift vector at 90°. (Note: 0° bank directs the vehicle lift up and therefore accelerates the vehicle away from the planet, while 180° bank directs vehicle lift down and accelerates the vehicle towards the planet.) The ballistic flight requirement will enable the crew to safely enter and land in the event of a primary power loss or GN&C system failure.

The environment around a capsule during ballistic flight is extreme, and must be carefully designed in terms of the appropriate entry corridor. The entry flight path angle corridor must be designed nominally to insure that all dispersed flights will not exceed abort crew acceleration limits or excessive range deviations (Skip-out). The flight path angle corridor has a steep side (or Undershoot side) and a shallow side (or Overshoot side). The Undershoot side of the flight path angle corridor is defined using a +30% bias on a 76 Standard atmosphere and protects the crew from high accelerations, while the Overshoot side of the flight path angle corridor is defined with a -30% bias on a 76 Standard atmosphere and protects the crew from Skip-out. These two flights bound the maximum and minimum flight path angles and define the flight path angle corridor for skip entry. Using the Cycle-3 mass of 16,354 lbm the corridor width is ~1.1°, with the Undershoot (positive altitude rate) side of the corridor at ~-5.4° and the overshoot (max abort crew G-load) side of the corridor at -6.5°. The nominal flight path angle at EI was placed inside of this flight corridor at -6.06°, which is biased slightly to the undershoot side to protect against a skip-out.

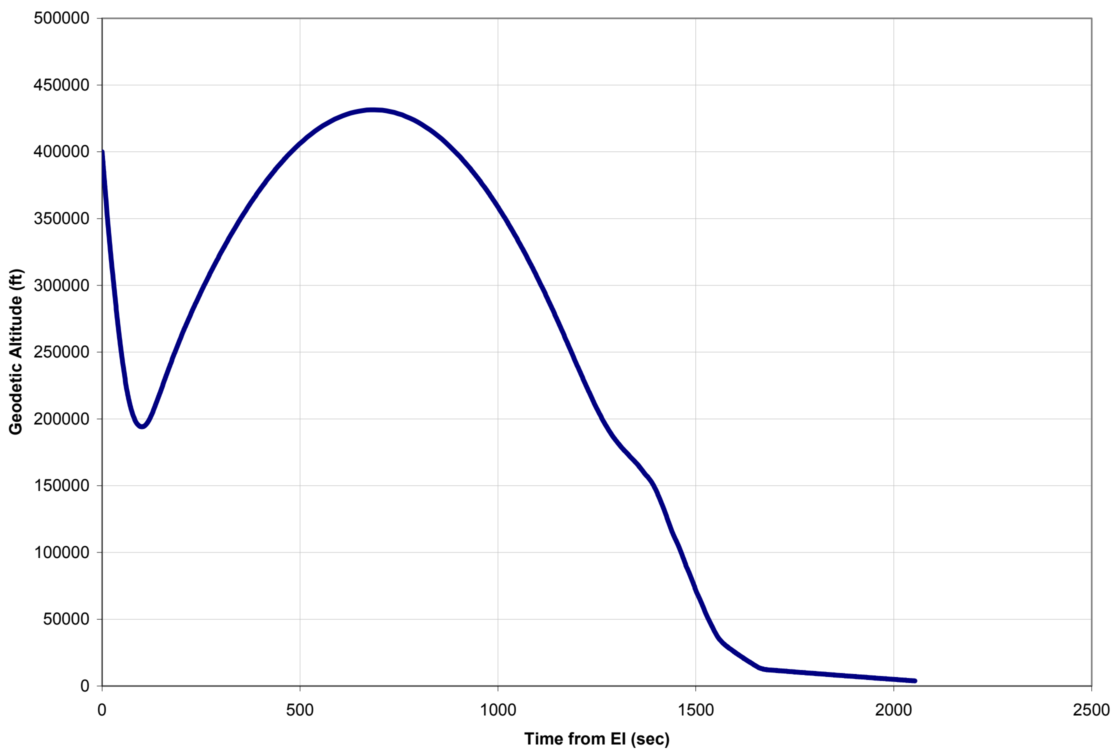

Figure 8.2-17 Geodetic Altitude (ft) vs Time (seconds)

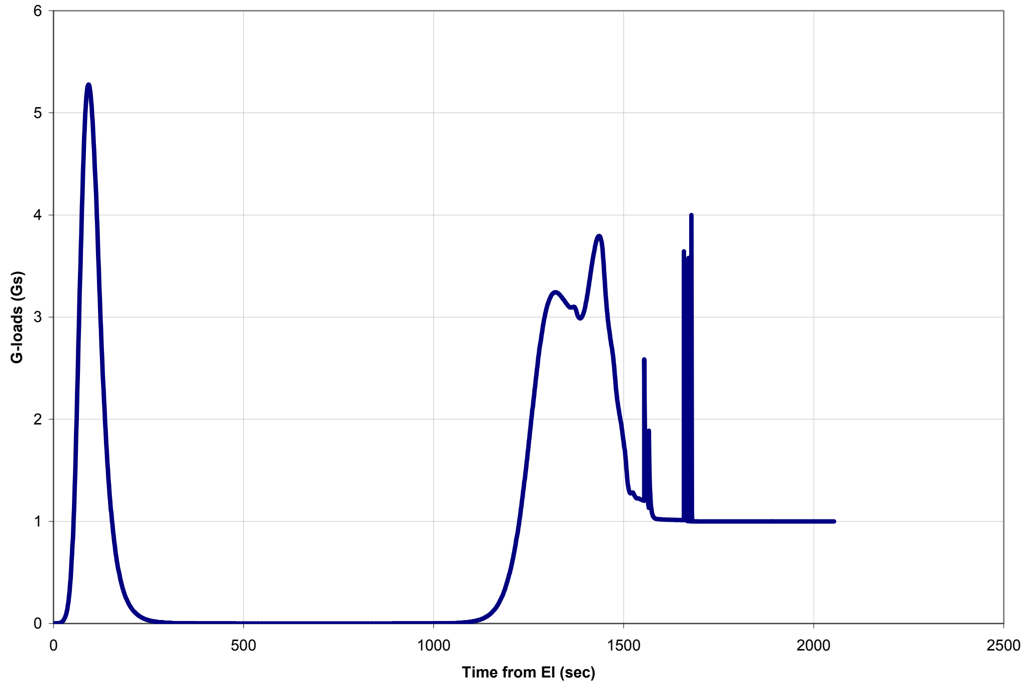

Figure 8.2-18 Total Sensed Acceleration Magnitude vs Time (seconds)

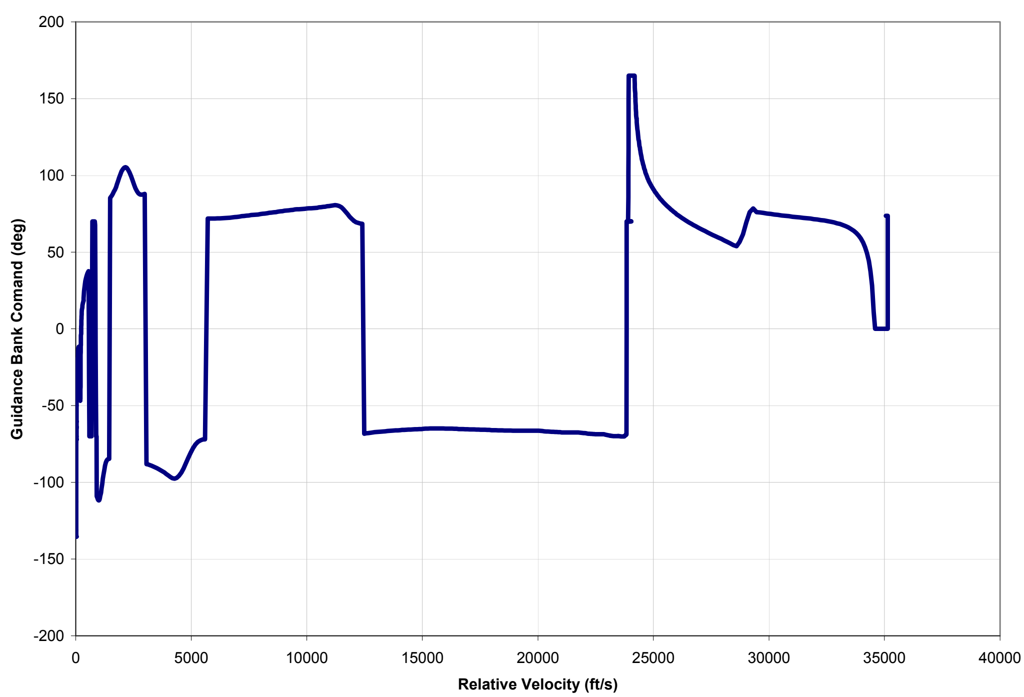

Figure 8.2-19 Bank vs Relative Velocity (ft/s)

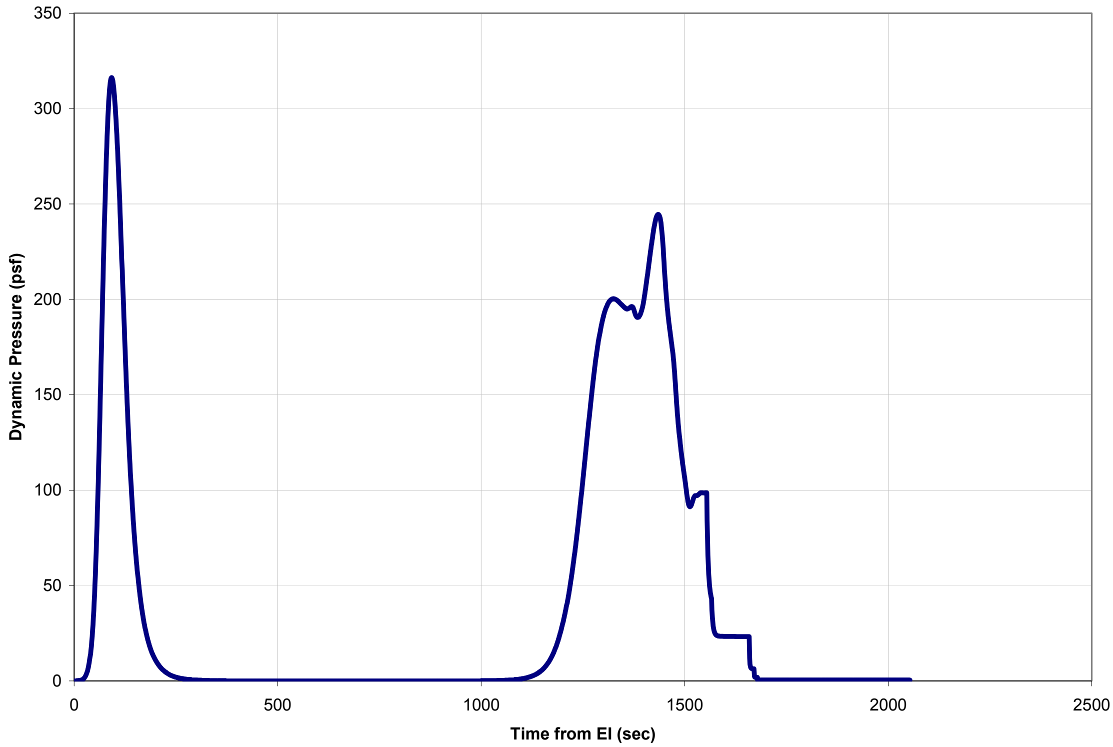

Figure 8.2-20 Dynamic Pressure (psf) vs Time (seconds)

Figures 8.2-21-24 provide the trajectory results for a ballistic entry simulation generated from the nominal entry conditions from Table 8.2-5. The vehicle spins at a constant rate until drogue chute deployment occurs at ~25,000 ft. Some small variability of the conditions shown in these plots is possible, depending on the initial bank angle chosen. An initial bank of 70° was chosen, which is close to the g-load peak for the given initial conditions.

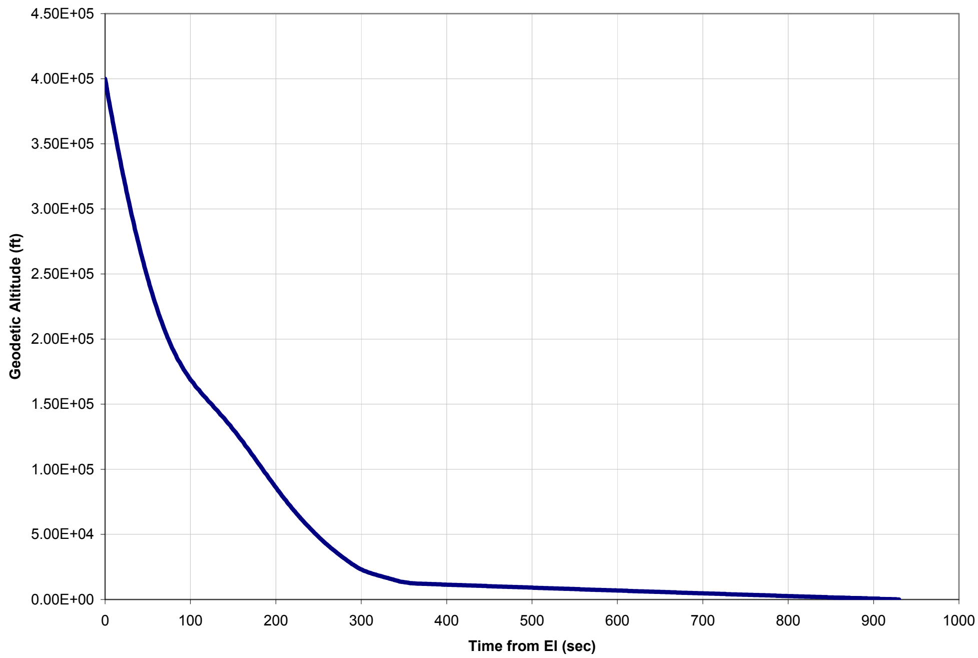

Figure 8.2-21 Ballistic Entry Geodetic Altitude (ft) vs Time from EI (seconds)

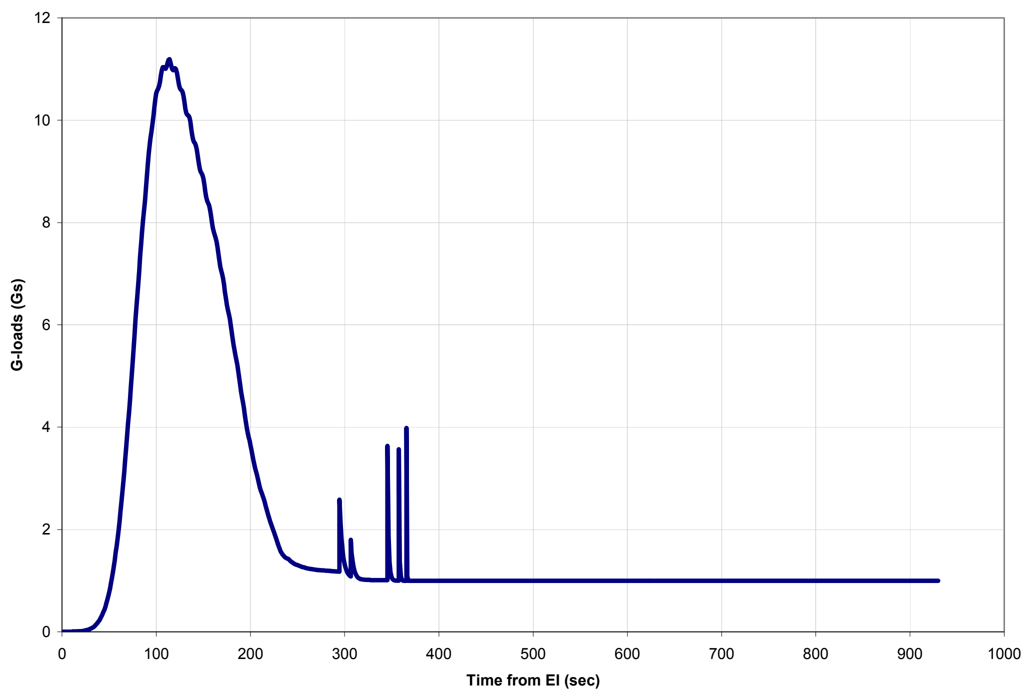

Figure 8.2-22 Ballistic Entry G-load (Gs) vs Time (seconds)

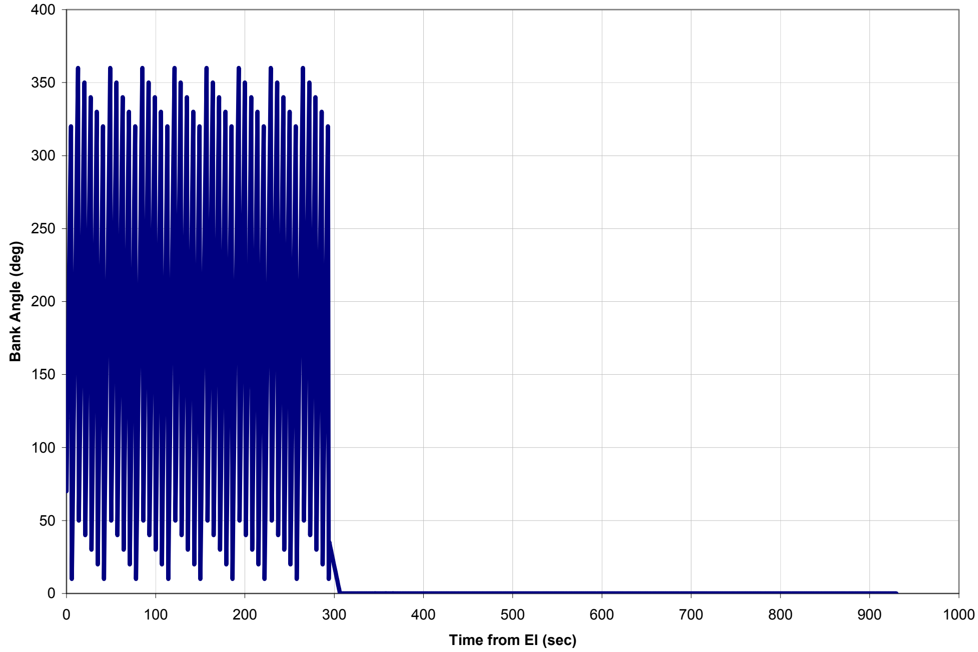

Figure 8.2-23 Ballistic Entry Bank Angle (deg) vs Time (seconds)

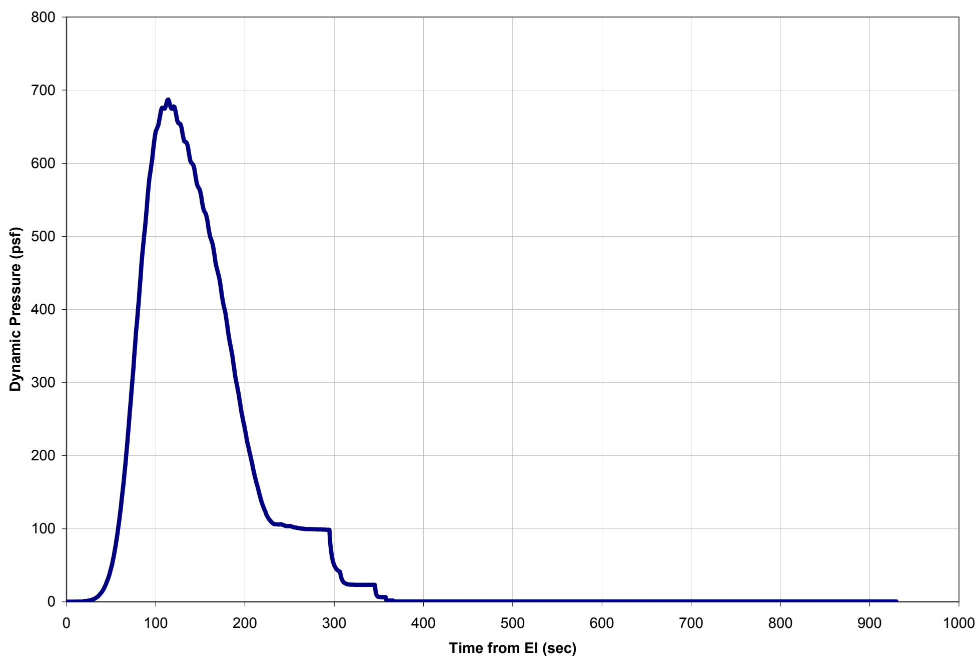

Figure 8.2-24 Ballistic Entry Dynamic Pressure (psf) vs Time (seconds)

8.3 Aerothermal

CEV aerodynamic and aerothermal analyses utilized in DAC-2 and CRC-3 are described in "CEV CM OML, Aerodynamic, and Aerothermal Database Background and Usage Information", Rev. 7, 01 March 2006. Primary points of contact for this document are Jim Greathouse/JSC/EG and Randy Lillard/JSC/EG.

9.0 Human and Cargo Systems

This section describes the trades, reference concepts, mass estimates, and analyses performed during CRC-3 as part of the Human and Cargo Systems functional area. Human and Cargo Systems for the purposes of this study includes the CEV Active Thermal Control System, Environmental Control and Life Support System, EVA and Crew Survival, and Flight Crew Equipment.

9.1 Active Thermal Control

The Active Thermal Control System (ATCS) collects and transports heat throughout the spacecraft and rejects heat from the spacecraft. This ensures that crew and equipment are maintained at acceptable temperatures during the entire mission from before launch to 60 minutes post-landing. Listed below are the requirements, ground rules, and assumptions that were used to design the ATCS. Then, a conceptual design overview is provided, followed by analysis results, mass estimates and recommendations for further study.

9.1.1 Driving Requirements, Groundrules, and Assumptions

This section lists the driving requirements, ground rules, and assumptions for the ATCS.

- The ATCS provides thermal control for a lunar mission. The design presented below can support crews of three to six people, but data for consumables are based on a lunar crew of four people. (i.e., larger crews may require more consumables.)
- The cabin air pressure varies from 14.7 psia at launch to 10.2 psia in lunar orbit.
- There are two thermal loops, and both loops are “on” during normal operations; one pump at a time is on in each loop.
- The cabin heat exchanger (HX) fan and evaporative heat sink are single-string except for controls and connection to both thermal loops.
- Radiators, cabin HX, suit HX, ground support equipment (GSE) HX, liquid cooling garment (LCG) HX, evaporative heat sink, and all cold plates have dual passages and both thermal control loops serve each device.
- Equipment on either thermal loop, A or B, is matched to different power strings, A, B or C.
- ECLSS controls cabin humidity, not the ATCS.
- Passive Thermal controls all cabin walls and surfaces to 68-77 °F, which is above the cabin dew point temperature.
- Cold plate areas are CM pressurized = 5,637 in^2, CM unpressurized = 1,260 in^2, SM = 4,287 in^2. Cold plate mass is computed based on the cold plate area times 1.8 lbm/ft^2, which is a factor derived from studying Shuttle cold plates.
- Quick disconnects on GSE HX pull apart based on mechanical systems; SM lines disconnect via pyrotechnics after closing TCS valves leading from the CM to the SM.

- Body-mounted radiators cover the SM cylinder (230 ft^2) and outwards-facing surface of aft torsion ring (165 ft^2). (That is 395 ft^2 or 37 m^2 total.) The fairing between the SM and CM (55 ft^2) is included, but not the area immediately around the RCS.
- The 395 ft^2 (37 m^2) radiator size is based on a nominal 4.3 kW long-term heat load. Worst case heat loads, such as during LSAM docking operations, will require use of the evaporative heat sink when the spacecraft is simultaneously in hot environments.
  - The four cylinder panels are actually two segments per panel due to removable fairing; four aft panels are not segmented. Radiator coating is Z93 on aluminum.
  - Original sizing was based on warm environment and orientation and 6 month end-of-life (EOL) properties (293 K (67 °F) radiator, 5.6 kW with 250 K sink temperature, λ=0.85, α=0.28, ε=0.91, 6 kg/m^2). Subsequent analysis of thermal environments showed that in lunar orbit the sink temperature can get much warmer than this.
  - Lunar orbit will be the worst case thermally and will require some water evaporative cooling on the hot day-side to maintain a design coolant set point temperature when heat load is high.
- Refrigerant tank sizing is based on crew of six, but quantity is based on crew of four to provide 60 minutes of post-landing cooling @ 1 kW. 36 lbm of Refrigerant 134a is carried for this event.
- Water evaporant quantity for supplemental on-orbit cooling is based on 18 kW-hr (63 lbm of water) of cooling (e.g., 9 hours @ 2 kW). A complete mission profile has not been analyzed to verify this water quantity. Both refrigerant and water tank masses were scaled from Shuttle water boiler tanks.
- Time from SM separation to CM touchdown is 44 minutes. The evaporative heat sink can be used with water until about 100,000 ft altitude. Below that, R134a must be used.
- Radiator Area vs. Heat Load issues will continue to be studied. Analysis to date is described below.
  - 395 ft^2 (37 m^2) is currently available per Structures, but the aft area must be used on the torsion ring since the DAC-2 "Short SM" reduced the cylinder area considerably. Impact: Adds complexity to ATCS plumbing and control.
  - Worst-case peak heat load is currently about 6 kW. Sustained maximum heat load is about 4.3 kW. (Per CEV_Ref_Power_Analysis_RevO2(2).xls Power/heat load profile)
  - Plumbing loop sizing reflects 6 kW maximum heat load with both loops flowing and 4.5 kW maximum heat load with one loop out. However, that does not mean the radiators, as currently sized, can reject this much heat in all environments.
- Loop flow and plumbing sizes are based on a working fluid flow rate of 250 lbm/hr on both TCS loops, designated "Loop A" and "Loop B," whether one or two loops are running. Maximum design load is 3 kW per loop when both loops are operating and 4.5 kW

when only one loop is operating. This could be increased by running a higher pump speed with the selected pump.

- Plumbing is stainless steel.

9.1.2 Conceptual Design Overview

Figure 9.1-1 presents the overall ATCS schematic. Major components, operational details, and rationale for their selection are presented below.

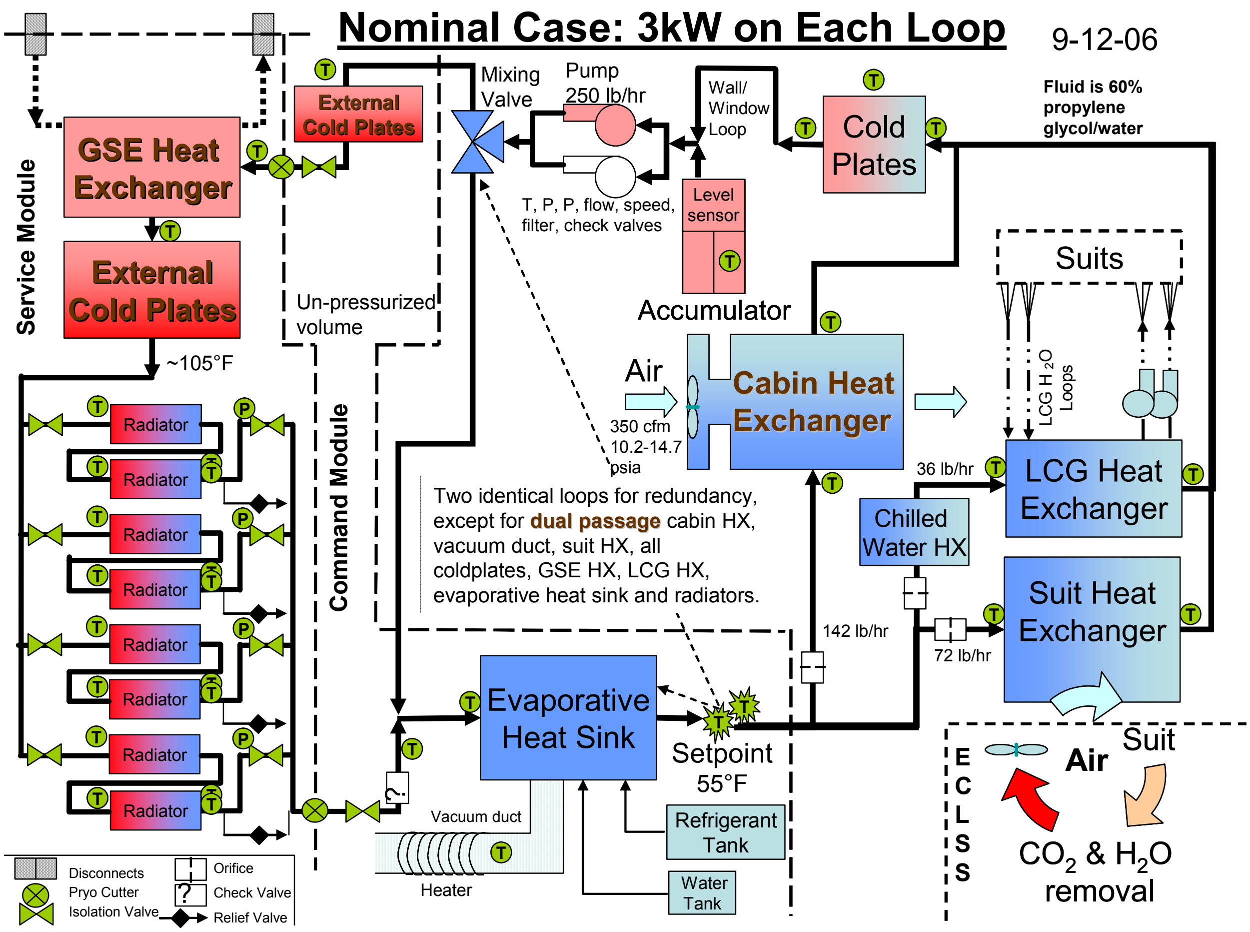

Figure 9.1-1 ATCS CEV Reference Design Schematic

First, note that the schematic shows only one coolant loop, but the design contains two such loops for redundancy, called “A” and “B”. Key components, such as radiators and heat exchangers, are dual-path components such that both coolant loops serve them. Both loops will run at the same time nominally, each carrying about half of the 6 kW maximum nominal heat load. Plumbing will also be sized to handle at least 4.5 kW on each loop in the case that one loop is out. Note that these sizing cases for the pump and plumbing do not imply that the radiators can always reject this much heat. Radiator heat rejection is discussed below.

The coolant will be a 60% propylene glycol / 40% water mixture. The pump package drives flow in the system. Two pumps are included for redundancy on each loop (four pumps total), but only one pump will be used on each loop nominally. Nominal working fluid flow rate is 250 lbm/hr per loop. Keeping this flow rate with one loop out would result in a maximum loop temperature of about 130 °F at 4.5 kW. If this is too hot or if more than 4.5 kW must be carried on one loop, the pump speed can be turned up to increase flow rate.

Flow passes from the pump package to the proportional mixing valve, which helps regulate the loop temperature downstream of the evaporative heat sink. When the loop control temperature is below set point, the valve will divert more flow through the bypass (and less through the radiators) to increase the temperature at the set point location. When the loop temperature is above set point, the valve will divert more flow through the radiators (and less through the bypass) to decrease the temperature at the set point location. The set point temperature will be 55 °F nominally. The evaporative heat sink outlet set point temperature will be a few degrees higher at 60 °F (TBR) to account for deadbands and to conserve evaporant water in lunar orbit.

Flow from the mixing valve splits to the external cold plates and to the radiator bypass and is recombined before entering the evaporative heat sink. A minimum flow may always need to be maintained in the radiator branch to service the external cold plate, but this value has not yet been determined. Also, analysis will need to show that loads on these cold plates can be cooled passively after the isolation valves are closed prior to SM separation. These external cold plates are contained within the unpressurized volume of the Crew Module and contain dual passages to allow both coolant loops to flow through them. Note the presence of an isolation valve and pyrotechnic cutter downstream of the external cold plates to allow separation of the Crew Module from the Service Module.

Flow passes from the external cold plates to the ground support equipment (GSE) heat exchanger, which provides cooling on the launch pad via a separate GSE fluid loop containing 60% propylene glycol/water solution. Combining the GSE heat exchanger and the evaporative heat sink was considered but was not favorable from a mass standpoint since a specifically designed liquid-to-liquid heat exchanger is more efficient than extra layers in the evaporative heat sink. Adding layers to the evaporative heat sink for ground cooling was estimated to add 19 lb vs. 13.5 lb for the separate GSE heat exchanger. From the GSE heat exchanger, fluid flows to additional cold plates on the SM. The cold plates and GSE heat exchanger contain dual passages to allow both coolant loops to flow through them.

Eight radiators are located downstream of the external cold plates. Four of these are curved and fit to the body of the Service Module cylinder, while the other four are fit to the aft torsion ring. Each quadrant's radiators (two panels together in series) have isolation valves upstream and downstream of them so that they can be isolated in the event of damage (as from MMOD). Also, flow can be stopped to a given quadrant by closing the inlet valve in the event that the radiator becomes exposed to a very hot environment condition that would adversely affect its performance. Each radiator contains dual passages to allow both coolant loops A and B to flow through each. The temperature and pressure instrumentation upstream and downstream of each radiator would be used to determine when each radiator should be valved off due to warm environment or a leak.

The flow passes downstream of the radiators to another pyrotechnic cutter that comes into play upon separation of the Service Module and Crew Module. Flow then combines with the bypass flow from the mixing valve and enters the evaporative heat sink.

The evaporative heat sink can be used whenever the radiators cannot be used (for example, post-landing), and it can be used to supplement the radiators during mission phases where the radiators are insufficient to provide needed cooling. This will occur when the CEV is exposed to a very hot environment and/or at higher heat loads. Note, however, that the evaporative heat sink makes use of a consumable to function and, thus, has a limited capacity. Both 63 lbm of water and 36 lbm of Refrigerant 134a are carried as "evaporants" to be used on-orbit through post-landing. These quantities allow for 18 kWh and 1 kWh of heat rejection, respectively.

The flow exiting the evaporative heat sink then passes through the loop temperature control point, which remains at a set point of 55 °F, except in lunar orbit when 60 °F set point will be used on the evaporative heat sink.

Coolant downstream of the control point reenters the pressurized volume and splits to service the cabin heat exchanger, the suit heat exchanger, and the liquid cooling garment (LCG) heat exchanger. The total flow in each loop is divided proportionally in accordance with expected nominal heat loads on each of these heat acquisition devices as follows: cabin heat exchanger 142 lbm/hr, suit heat exchanger 72 lbm/hr, and LCG heat exchanger 36 lbm/hr. The chilled water heat exchanger is located in series upstream of the LCG heat exchanger since these loads should not be active at the same time. Each of these heat acquisition devices contains dual passages to allow both coolant loops to pass through them.

The cabin heat exchanger cools the cabin air and is capable of maintaining the cabin air within a 70 °F – 80 °F range of temperatures, but it is not designed to dehumidify the air. Dehumidification will be accomplished by the ECLSS components via the suit loop. The cabin fan, which flows 350 cfm of air at any cabin pressure, is single-string and is part of the Thermal system rather than ECLSS. It may be integral with the cabin heat exchanger. Since the volumetric flow rate is held constant even when cabin pressure is reduced to 10.2 psia, air mass flow rate will decrease. Thermal design must account for this case.

Downstream of the cabin heat exchanger, LCG heat exchanger, and suit heat exchanger, the flows recombine and enter the internal cold plates. Components are cooled by dual passage cold plates. The use of single passage cold plates might reduce cold plate mass and volume, but it would result in degraded functionality in the event of a loop failure, and the mass savings is not expected to be significant.

An accumulator downstream of the cold plates maintains system pressure and accommodates fluid volume changes of 11.4 in^3 per loop due to temperature changes plus an additional TBD in^3 of fluid to account for leakage. Finally, the flow returns to the pump package.

9.1.2.1 Liquid Cooling Garment (LCG) Cooling Loop

Besides the ECLSS suit loop, which conditions the crewmember air while they are in their space suits, a liquid cooling loop is also necessary to keep them comfortable and in top condition for critical mission phases such as landing. Thus, the ATCS provides this function via a water cooling loop that transfers its heat to the main CEV propylene glycol loops. ATCS provides hardware and the cooling water only up to the Umbilical Interface Panels (UIP). UIPs are expected to be located at each seat for easy crew access. The UIP will have an interface for air or O_2 in, air or O_2 out, coolant water in, coolant water out, power and data bundle, and a tether hook. These umbilical connectors are expected to be the same at both the inlet and outlet. Two seats will have longer umbilicals allowing for contingency EVA from the CM cabin.

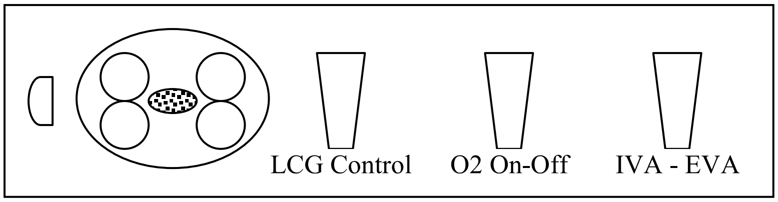

Figure 9.1-2 IVA-EVA Umbilical Interface Panel Concept

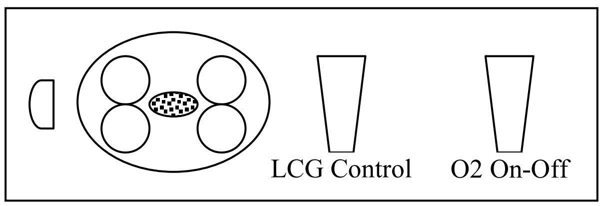

Figure 9.1-3 IVA Only Umbilical Interface Panel Concept

For the six-crewmember CEV design, seven slots are available. This provides single fault tolerance. It is assumed that when the crew is forced to rely on the umbilicals for life support, some failure has driven them to this off-nominal configuration; and, so, the first fault of two-fault tolerance has already occurred. Two-fault tolerance applies to the air function. Since the cooling water is for comfort and performance and not life critical, redundancy is a matter of smart design and not a requirement.

The coolant lines must have both an inlet and outlet from the suit to operate. There is no inlet only configuration like the high pressure oxygen option available for gas delivery. Each crewmember may have a different metabolic load on the system; and, so, individual control of the cooling water flow is provided to each crewmember through a restrictor valve. There is one heat exchanger with two liquid cooling water pumps to provide liquid cooling to the crew. Each of these pumps has three inlet and three outlet connections. Nominally, two crewmembers will use each pump for a lunar mission crew of four. In the event that a pump or heat exchanger fails, the two crewmembers using the failed resource will have their lines moved to the other pump. Because these two crewmembers do not have active cooling during this failed event, the moving of lines should be done by a crewmember who still does have active cooling. In a lunar mission, with enough heat exchangers available, ideally the person who moves the lines should neither be one of the crewmembers who is on the failed system, nor a crewmember who is about to have to share resources with three crewmembers on one pump.

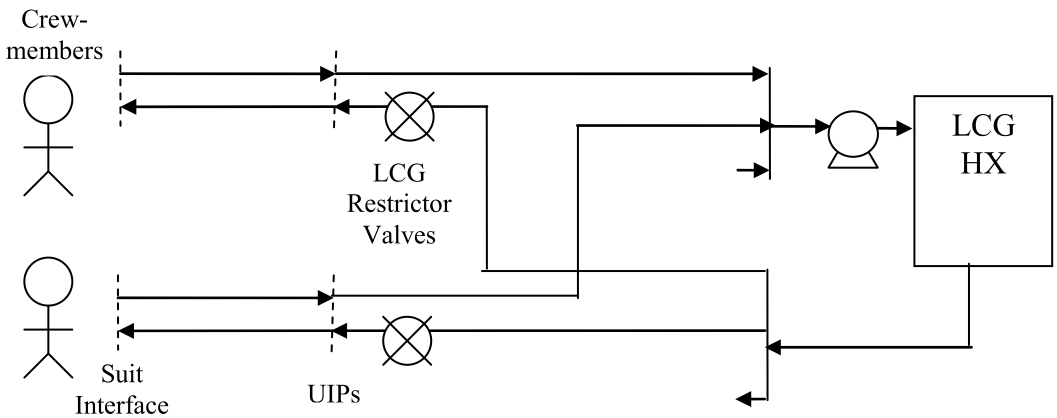

Figure 9.1-4 UIP to LCG heat exchanger concept

9.1.2.2 Analysis Results

CEV Heat Loads

Bottoms-up heat load estimates were made by the Power group during DAC-2 and their data found in the spreadsheet “CEV_Ref_Power_Analysis_RevO2(2).xls” was used for ATCS analysis in CRC-3. Total heat loads for on-orbit and entry mission phases are shown in Figures 9.1-5 and 9.1-6 below.

The general system sizing philosophy used for CRC-3 was to size the ATCS pumps, lines, etc. for 6 kW total nominal load. Radiator sizing, however, is based on a long term heat load level, which, according to Figure 9.1-5, is 4.3 kW. This means that the peaks in heat loads must be accommodated by the evaporative heat sink, at least in the worst case hot environments (low beta angles). The water tank size, however, is not sufficient for all these peaks to occur at the worst-case beta angles. Thus, a more-detailed, mission-specific analysis will still be required to determine exactly how much water evaporant will be required for each mission.

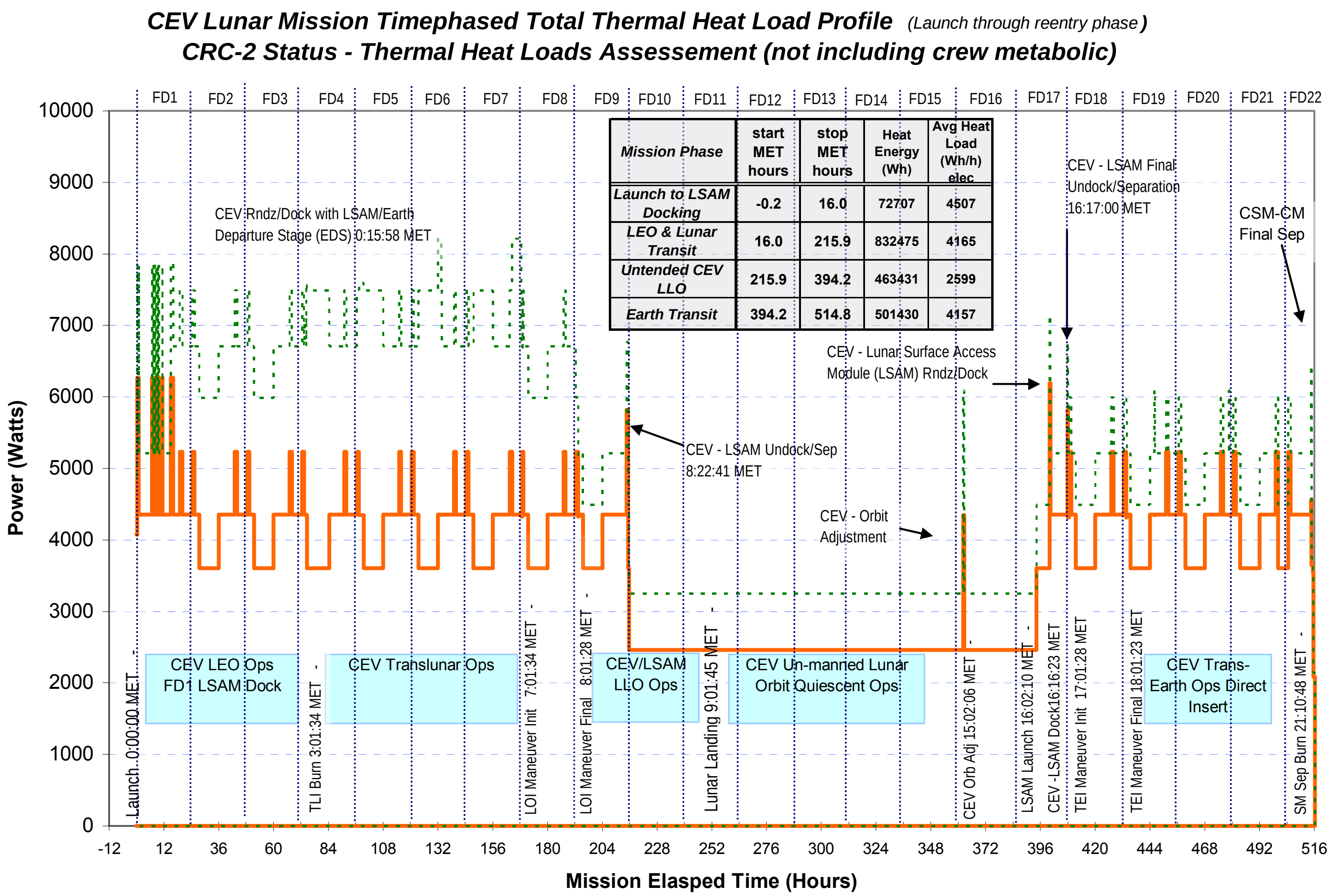

Mission Phase	start MET hours	stop MET hours	Heat Energy (Wh)	Avg Heat Load (Wh/h) elec
Launch to LSAM Docking	-0.2	16.0	72707	4507
LEO & Lunar Transit	16.0	215.9	832475	4165
Untended CEV LLO	215.9	394.2	463431	2599
Earth Transit	394.2	514.8	501430	4157

Figure 9.1-5 Thermal Heat Loads in Space for Lunar Mission

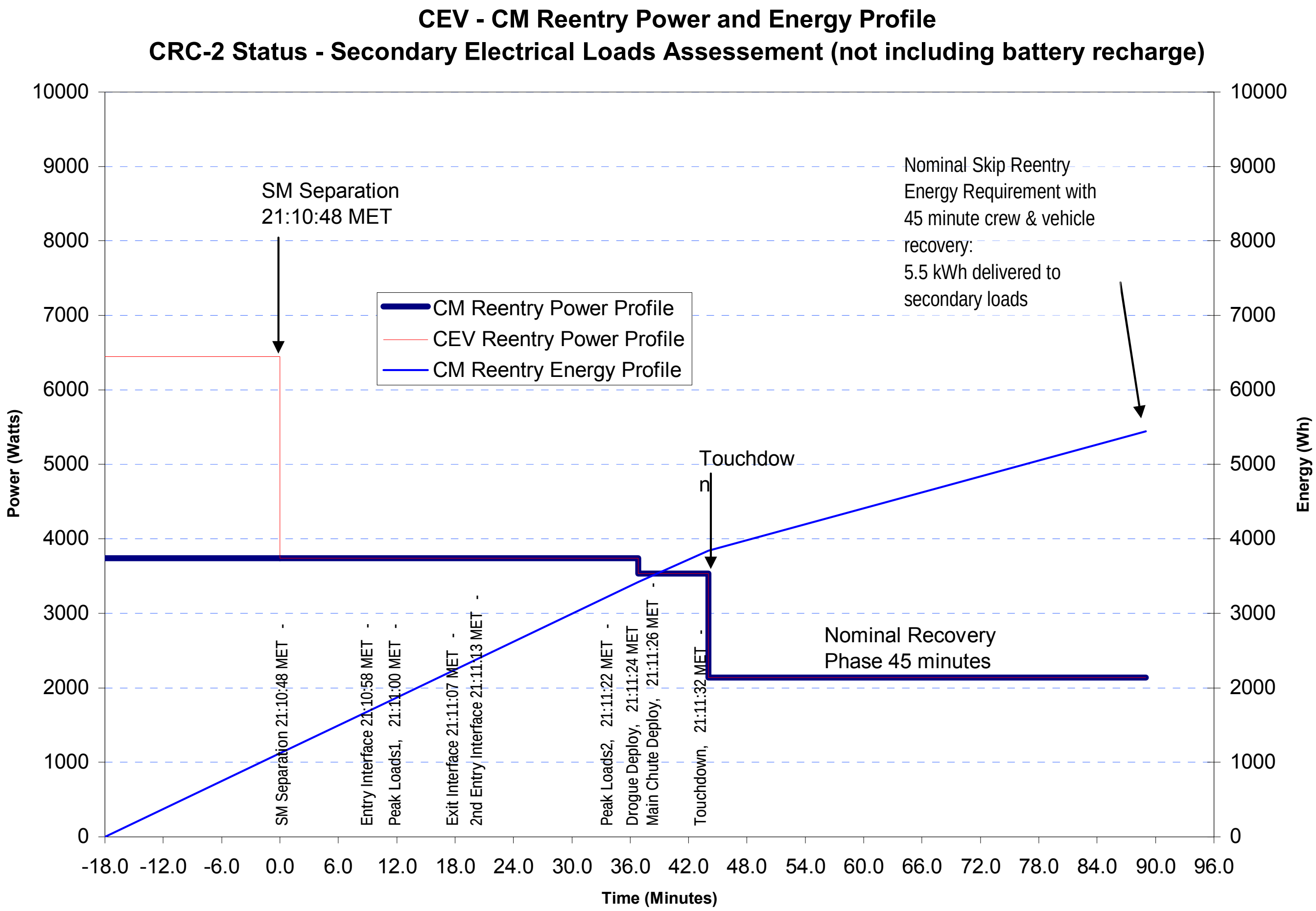

Figure 9.1-6 Thermal Heat Loads after Service Module Separation

Radiator Heat Rejection

Fairly detailed radiator environment analysis was completed during DAC-2. Figure 9.1-7 shows the coordinate system used. Table 9.1-1 shows the total predicted radiator heat rejection for a variety of beta angles and orientations at a lunar altitude of 100 km. Four cylindrical and four conical radiators were assumed with a total surface area of 21.4 m^2 + 15.3 m^2 = 36.7 m^2 = 395 ft^2. As seen from the table, some orientations yield 'acceptable' heat rejection rates (>4,700 Watts), whereas those cases highlighted in red are unable to meet the requirements. The preferred orientation (nose-to-moon or -XLV) heat rejection was somewhat below the required 4,700 W at low beta angles but above 4,700 W at all beta angles above 45°. The +/-YVV attitudes are better for ATCS; however, the +/-ZVV attitudes were preferred by other systems in the integrated analysis study. 'Acceptable' was defined in DAC-2 as >4,700 W, while CRC-3 heat loads would say >4,300 W is acceptable. However, we must recall that the analysis results in Table 9.1-1 are approximate, and some CRC-3 transient radiator analysis results discussed below show that they are not conservative.

The radiator heat rejection estimates in Table 9.1-1 are based on sun-side average thermal environments. "Sun-side average" was defined as -90° to +90° orbit angle even though the terminators will be somewhat beyond this. Radiators will reject more on the dark side of the orbit but less at the subsolar point, so "sun-side average" is a way of approximating the dampening effect of thermal capacitance in the loop. All eight radiator segments were assumed to be in parallel flow with no radiators valved off. That means that in some cases fluid in a radiator facing the hot lunar surface could come out warmer than it went in. A late design change in CRC-3 put the two radiators in a given quadrant in series flow rather than parallel, but this should only have a minor effect on heat rejection.

The heat rejection estimates in Table 9.1-2 assume a 'smart radiator' design, meaning that the inlet valves on each of the eight radiator segments can be closed independently and automatically when the outlet temperature of that segment is above the inlet temperature. It can be seen that in some attitudes at some beta angles, overall heat rejection is increased. However, in the preferred attitude of nose-to-moon (-XLV), there is no improvement.

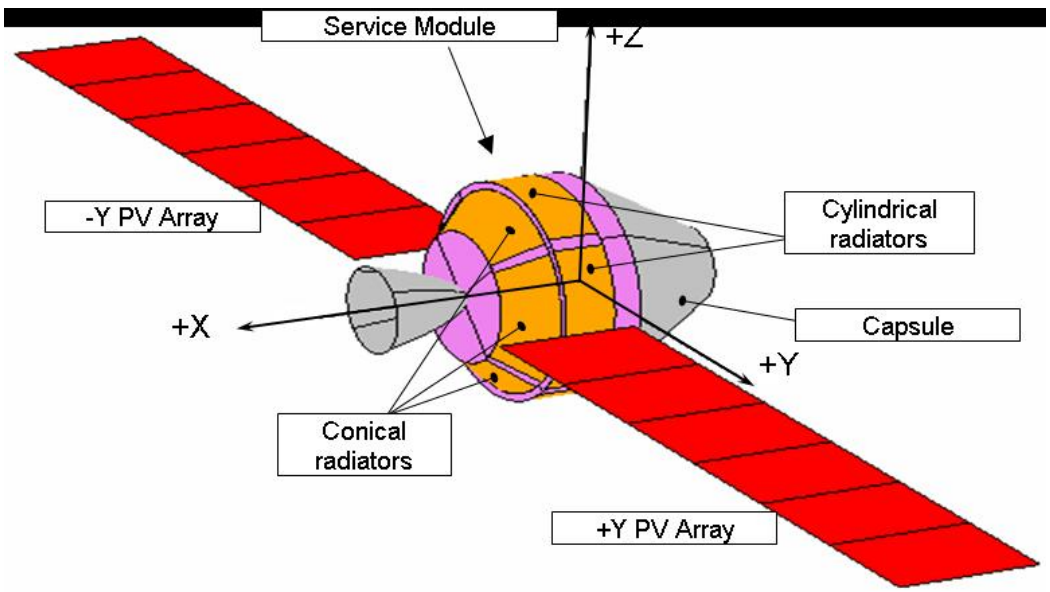

Figure 9.1-7 Coordinate System used for CRC-3 ATCS Analysis

CEV Dayside Average Total Heat Rejection (W) for CEV Alone in LLO and at 26.7°C Setpoint								
Beta Angle (°)		0	15	30	45	60	75	90
LV/SI Axis	**VV/NP Axis**	(W)	(W)	(W)	(W)	(W)	(W)	(W)
-XLV	-YVV	4463	4717	4978	5503	6489	8686	9190
-XLV	+YVV	4470	4715	4956	5526	6470	8680	9183
-XLV	-ZVV	3762	3850	4639	6027	7895	10497	10066
-XLV	+ZVV	3724	3826	4613	6046	7902	10490	10061
+XLV	-YVV	446	807	1407	2649	4446	7670	8968
+XLV	+YVV	493	830	1390	2675	4472	7678	8945
+XLV	-ZVV	-71	176	1185	3009	5361	9561	9818
+XLV	+ZVV	-95	171	1161	2977	5358	9551	9811
-YLV	-XVV	2326	2591	3087	4004	5398	8136	9074
-YLV	+XVV	2105	2399	2923	3849	5289	8158	9063
-YLV	-ZVV	1514	2373	3682	5590	7707	11150	12768
-YLV	+ZVV	1531	1583	1990	2966	4484	7140	8616
+YLV	-XVV	2333	2633	3055	3981	5409	8132	9085
+YLV	+XVV	2094	2408	2871	3812	5294	8139	9057
+YLV	-ZVV	1501	1628	2033	2955	4493	7139	8617
+YLV	+ZVV	1507	2345	3741	5607	7703	11159	12764
-ZLV	-XVV	1145	1406	2306	4066	6300	9920	9912
-ZLV	+XVV	991	1149	2156	3885	6211	9914	9915
-ZLV	-YVV	957	1043	1477	2503	4155	7039	8596
-ZLV	+YVV	992	1901	3395	5344	7501	11091	12725
+ZLV	-XVV	1152	1387	2367	4031	6295	9924	9914
+ZLV	+XVV	953	1155	2153	3915	6197	9908	9910
+ZLV	-YVV	983	2016	3473	5332	7506	11096	12741
+ZLV	+YVV	982	1012	1452	2496	4183	7057	8599
-XSI	+YNP	2269	2703	3958	5835	8211	11646	12774
+XSI	+YNP	2896	3105	3411	4211	5327	7671	8572
-YSI	+XNP	1578	1203	1605	2867	4816	8654	9930
-YSI	+ZNP	1847	2109	2911	4178	5846	8920	9923
+YSI	+XNP	1550	1193	1655	2875	4834	8656	9936
+YSI	+ZNP	1895	2187	2956	4171	5917	8917	9927
-ZSI	+YNP	716	975	1916	3355	5191	8111	9050
+ZSI	+YNP	600	922	1813	3311	5103	8078	9064

>4700	= meets pass criteria	surface area of single cylindrical radiator panel	
<3700	= meets fail (no go) criteria	5.343	m2
3700-4700	= marginal	surface area of single conical radiator panel	
Note: Run Categorize2 for this spreadsheet.		3.825	m2

Table 9.1-1 DAC-2 CEV Total Heat Rejection (Watts) (average design)

CEV Dayside Average Total Heat Rejection (W) for CEV Alone in LLO and at 26.7°C Setpoint								
Beta Angle (°)		0	15	30	45	60	75	90
LV/SI Axis	**VV/NP Axis**	(W)	(W)	(W)	(W)	(W)	(W)	(W)
-XLV	-YVV	4463	4717	4978	5532	6556	8686	9190
-XLV	+YVV	4470	4715	4956	5543	6550	8680	9183
-XLV	-ZVV	3762	3896	4702	6027	7895	10497	10066
-XLV	+ZVV	3724	3879	4691	6046	7902	10490	10061
+XLV	-YVV	2248	2308	2259	2712	4512	7670	8968
+XLV	+YVV	2248	2287	2265	2733	4541	7678	8945
+XLV	-ZVV	1802	1789	2090	3199	5363	9561	9818
+XLV	+ZVV	1789	1772	2085	3175	5359	9551	9811
-YLV	-XVV	3385	3576	3708	4243	5494	8136	9074
-YLV	+XVV	3211	3419	3577	4075	5386	8158	9063
-YLV	-ZVV	2611	3275	4246	5732	7707	11150	12768
-YLV	+ZVV	2601	2609	2712	3184	4484	7140	8616
+YLV	-XVV	3394	3601	3684	4241	5502	8132	9085
+YLV	+XVV	3207	3416	3556	4069	5387	8139	9057
+YLV	-ZVV	2609	2636	2723	3175	4493	7139	8617
+YLV	+ZVV	2594	3278	4272	5743	7703	11159	12764
-ZLV	-XVV	2573	2683	3268	4313	6300	9920	9912
-ZLV	+XVV	2471	2467	3129	4107	6211	9914	9915
-ZLV	-YVV	2403	2305	2351	2789	4155	7039	8596
-ZLV	+YVV	2405	3159	4142	5559	7501	11091	12725
+ZLV	-XVV	2567	2666	3296	4296	6295	9924	9914
+ZLV	+XVV	2409	2482	3125	4117	6197	9908	9910
+ZLV	-YVV	2388	3171	4170	5532	7506	11096	12741
+ZLV	+YVV	2373	2304	2371	2774	4183	7057	8599
-XSI	+YNP	2969	3170	4181	5835	8211	11646	12774
+XSI	+YNP	2896	3105	3470	4337	5452	7671	8572
-YSI	+XNP	1966	1593	1846	3093	4988	8654	9930
-YSI	+ZNP	2136	2284	3004	4317	5974	8920	9923
+YSI	+XNP	1964	1587	1893	3111	4998	8656	9936
+YSI	+ZNP	2165	2346	3042	4299	6050	8917	9927
-ZSI	+YNP	1384	1459	2095	3379	5232	8111	9050
+ZSI	+YNP	1306	1374	1992	3346	5158	8078	9064
>4700	= meets pass criteria				surface area of single cylindrical radiator panel 5.343 m2			
<3700	= meets fail (no go) criteria							
3700-4700	= marginal				surface area of single conical radiator panel 3.825 m2			
Note: Run Categorize2 for this spreadsheet.								

Table 9.1-2 DAC-2 CEV 'Smart Radiator' Total Heat Rejection (Watts)

Transient Radiator Heat Rejection Analysis

During CRC-3 some transient ATCS fluid loop models were run with the SINDA/FLUINT software tool. Results are still being analyzed and will be documented elsewhere, but an important observation can be made from Figures 9.1-8 and 9.1-9 below. These figures show the worst hot case transient thermal environment (Beta=0°, -XLV, +ZVV) results for 4 kW and 5 kW constant heat loads, respectively. Environmental heat sink temperatures were calculated for the worst of the 'nose to moon' attitudes assuming a radiator with optical properties of α=0.28, ε=0.91. This is a little bit worse case for ATCS than the –XLV, +/-YVV, but was preferred by other systems. In these plots, it can be seen that radiator outlet temperature exceeds set point temperature for almost an hour on the hot side of the orbit, thus requiring the water evaporator to turn on, even in the 4 kW case. Evaporator cooling rate shown in the graphs is for one of two loops, so it must be doubled for the total. Evaporated water usage would be prohibitive to fly in this condition for more than a few orbits. One thing that leaves room for improvement is the fact that the radiator inlet temperatures seen here (and thus the cold plate outlet temperatures) are 90-100 °F and actual flow rates in the model were about 290 lbm/hr per loop, higher than the 'design case'. Lower flow rates, and thus higher temperatures, are possible because they are not at the limit, which is considered to be 120 °F based on Shuttle experience.

It should also be noted that the model had to be 'tricked' by adjusting fluid viscosity to prevent flow stagnation and distribution problems going from the extreme hot to extreme cold environments encountered in one orbit. A 'stagnation radiator' design, similar to Apollo, should be feasible, but this is still an area of risk which is under investigation.

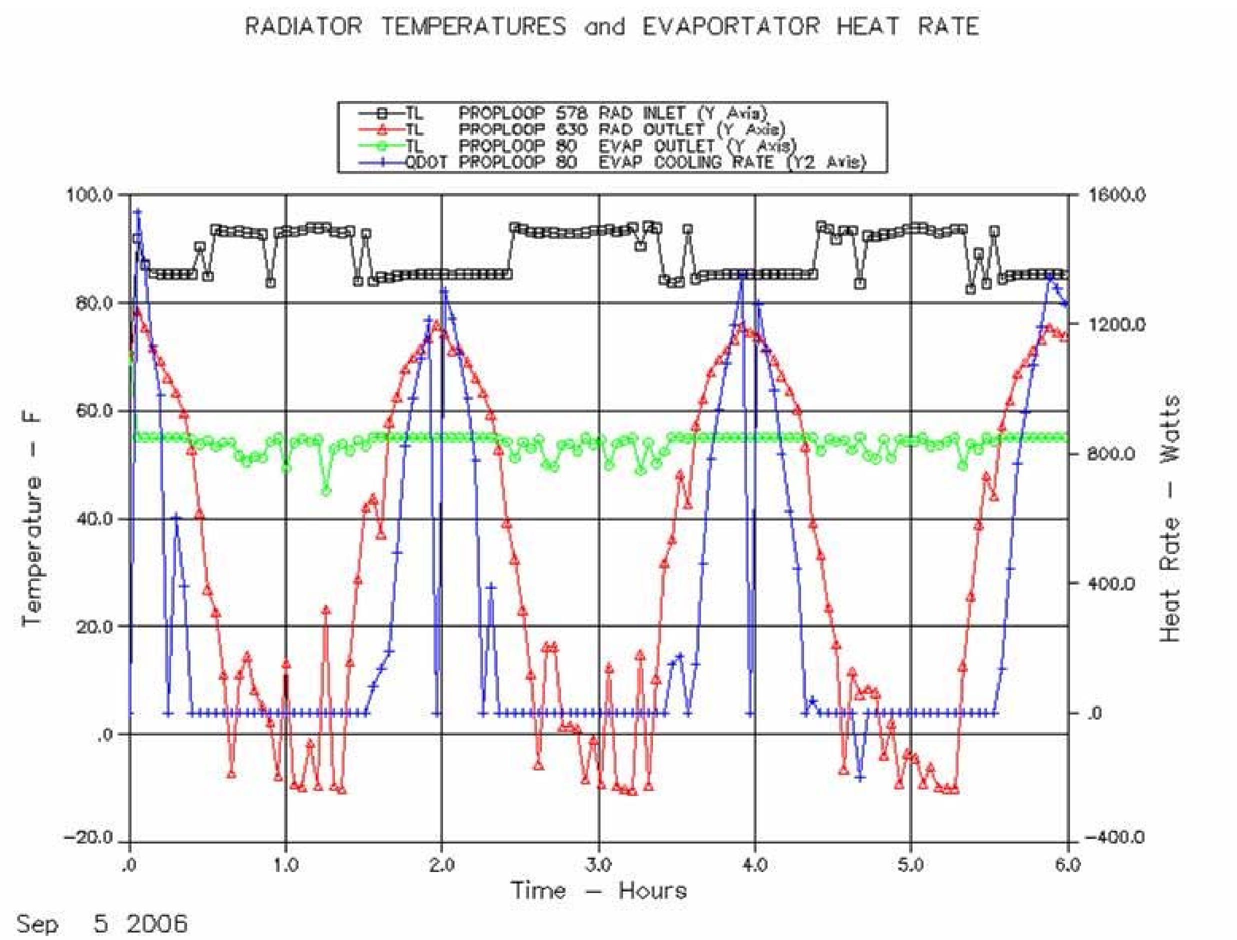

Figure 9.1-8 CRC-3 Transient Radiator Analysis for 4 kW Heat Load

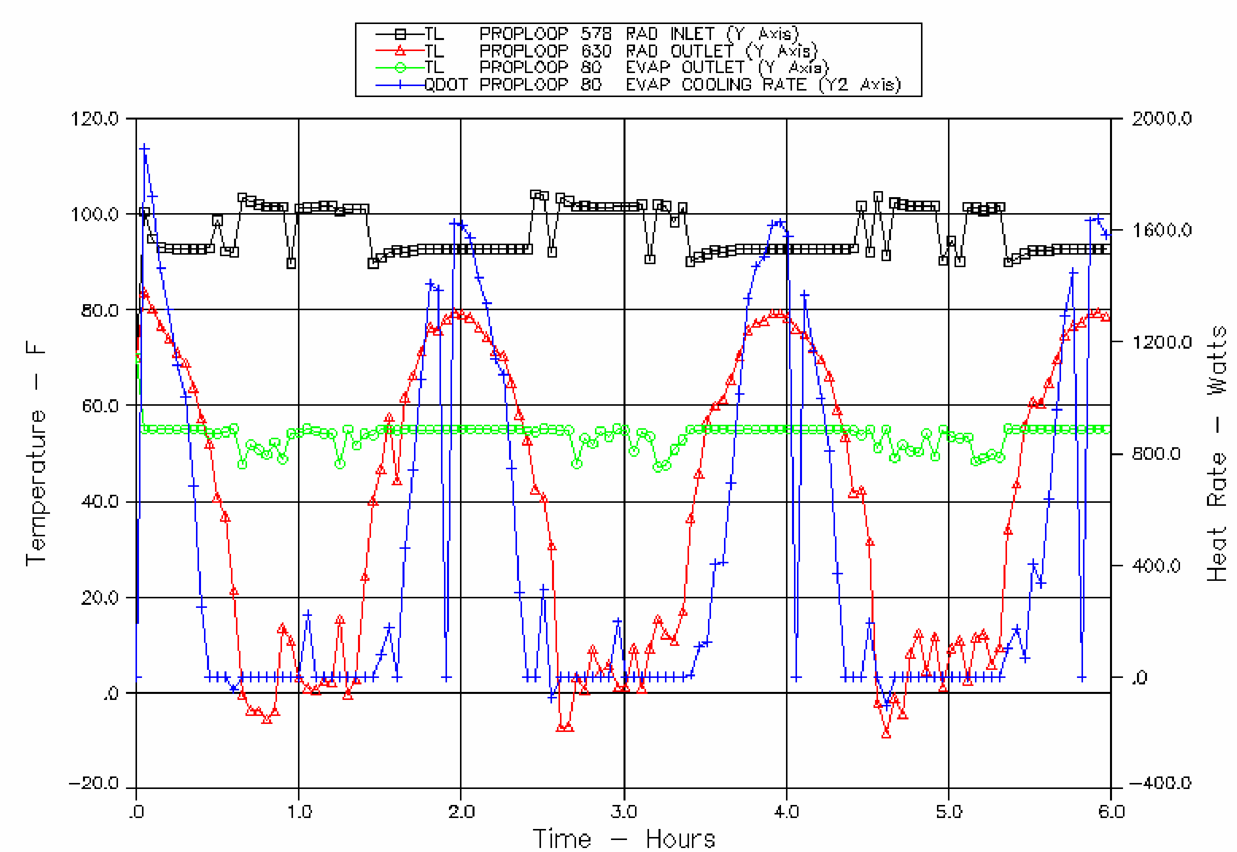

Figure 9.1-9 CRC-3 Transient Radiator Analysis for 5 kW Heat Load

A final transient thermal model case was run in CRC-3 and results are shown in Figures 9.1-10 and 9.1-11. In these cases, the artificial viscosity shift was still used but pump speed was reduced in order to lower flow rate to about 260 lb/hr (it varies throughout the orbit due to fluid properties). In Figure 9.1-10, evaporative heat sink load peaks at about 1 kW per loop. Heat loads in lunar orbit are predicted to be higher than this 3 kW case when the crew is on board, especially during operations such as docking. Thus, higher usage of the evaporative heat sink will be required in this worst case thermal environment. Note that all these analysis cases assumed a 55 °F set point for the evaporative heat sink rather than the 60 °F set point suggested above, so that will help a little.

Figure 9.1-11 shows results with a 3 kW total ATCS load just like Figure 9.1-10; however, in this case the evaporative heat sink was turned off and the loop temperatures were allowed to rise. It can be seen that the ATCS set point temperature peaks at about 90 °F at the hottest point and spends about 60% of the orbit at the desired value of 55 °F.

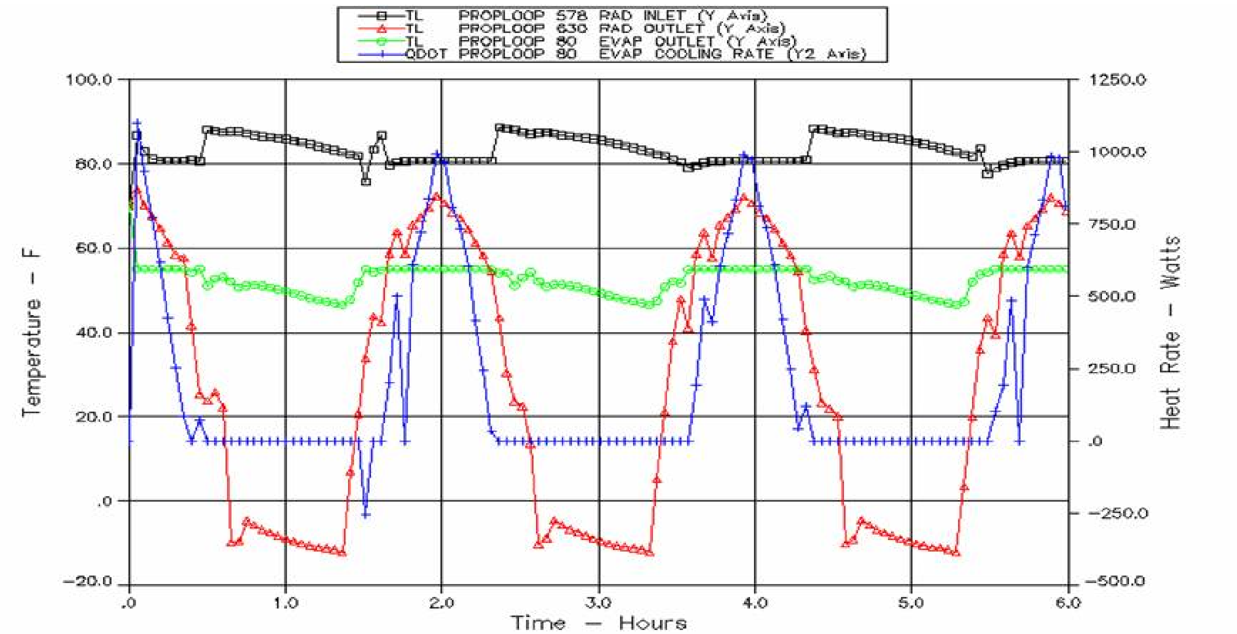

Figure 9.1-10 CRC-3 Transient Radiator Analysis for 3 kW Heat Load

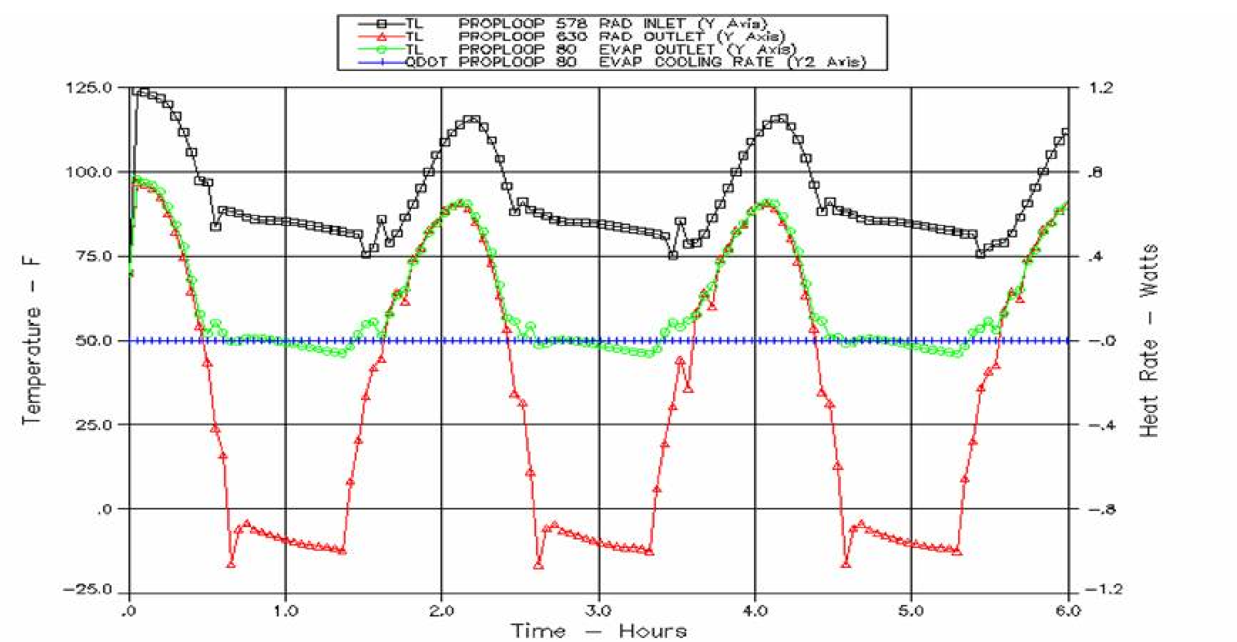

Figure 9.1-11 CRC-3 Transient Radiator Analysis for 3 kW Heat Load, Evaporator Off

Stagnation Radiator Evaluations

Apollo Block II SM radiators were studied. They were designed as a glycol-water selective-stagnation radiator. By taking advantage of the exponential viscosity increases of the glycol-water with decreasing temperatures, the Apollo radiator used different tube lengths to create uneven flow distribution across the radiator causing the tubes to stagnate sequentially. This resulted in a radiator that could change from having a high radiating-fin effectiveness to low radiating-fin effectiveness, essentially reducing the radiating area of a radiator panel and reducing the heat rejection in that panel. This was used to keep the radiator panel alive and turn down the heat rejection in the panel.

Recently a test of a stagnation radiator was performed. Stagnation flow manifolds were designed and built, a model of the radiator was made using Thermal Desktop, and the radiator was tested in Chamber E at JSC. The test used a 60/40 propylene glycol and water mixture and successfully demonstrated selective-stagnation and recovery with various heat loads and environment temperatures that ranged from 270 K to 180 K. Through the testing and data analysis, a successful turn down of the radiator with sink temperature was shown.

On the system level analysis described above, the stagnation manifold has not yet been implemented; however, stagnation was seen in the modeling. Due to the viscosity property of glycol-water mixtures, stagnation and total freezing was observed in the radiator panels as sink temperature decreased. The next step will be to apply the stagnation manifold to the system level model to prevent full shutoff of radiator panels.

9.1.2.3 Separate vs. Combined Cabin and Suit Loop Heat Exchangers

During the CRC-3 analysis cycle, the thermal team considered the possibility of combining the cabin non-condensing heat exchanger and the suit loop non-condensing heat exchanger (proposal 2 below). Also assessed was a related idea to move one ECLSS amine bed to the cabin air loop and eliminate one amine bed fan, a.k.a. ‘compressor’. Seth Alberts of S&MA wrote the assessment below, which discussed the options and captured the team’s conclusion on the matter – to keep the two separate heat exchangers. It is noted, however, that the single ‘combined’ heat exchanger approach is valid as well.

The S&MA assessment was not a comprehensive Preliminary Hazard Analysis. The goal was to look at failure types where the configurations provide differences in fault tolerance and/or redundancy. The conclusion reached by the team was that neither proposal appeared to provide significant savings in mass or volume or a significant increase in redundancy.

The first proposal appears to provide enhanced redundancy over the current configuration, but it is unclear if it will provide any mass or volume savings. The second proposal appears to provide a mass and volume savings but may result in a reduction in fault tolerance. The decision made was to retain the DAC-2 configuration.

Present Configuration:

- Cabin Loop contains Cabin Fan Package and 1,000 W Cabin Heat Exchanger.
- Suit Loop contains Amine Beds and 600 W Suit Air Loop Heat Exchanger.

Proposal 1

- Move one Amine Bed to Cabin Loop
- Eliminate One Amine Bed Compressor
- Replace 1,000 W Cabin Heat Exchanger with two 550 W Heat Exchangers.

- Replace 600 W Suit Heat Exchanger with one 550 W Suit Air Loop Heat Exchanger.
- Option: Use PLSS Amine Beds

Proposal 2

- Delete Cabin Fan Package and Cabin Heat Exchanger.
- Increase size of Suit Air Loop Fans and Heat Exchanger.

The tables below only include components that are changed in one of the proposals.

Current Configuration

Subsystem/Component Name	Basis of Estimate	Qty	Failure Type	Failure Effect	Fault Tolerance	Redundancy Provided By
"Cabin Loop" Air Recirculation						
HEPA Filter	Shuttle Filter and Debris Trap	1	Reduced or no Air Flow	Loss of Cabin Cooling	1	Suit Air Loop
Internal Cabin Ducting	Est. 25 ft polycarbonate, 4" diameter	1	Blockage or Leakage	Loss of Cabin Cooling	1	Suit Air Loop
Cabin Heat Exchanger fan assembly	1/2 X-38 mass(for 1 fan); Apollo power * 2	1	Reduced or No Flow	Loss of Cabin Cooling	1	Suit Air Loop
Cabin Heat Exchanger	Scaled STS IMU non-condensing HX	1	Reduced or no Air Flow	Loss of Cabin Cooling	1	Suit Air Loop DFMR
			Reduced or no Coolant Flow	Loss of Cabin Cooling	2	Redundant Coolant Loop Suit Air Loop
"Suit Loop" Air Revitalization						
HEPA Filter		1	Reduced or no Air Flow	Loss of Flow through Amine Bed		Spare HEPA Filter, IFM
Suit Air Loop Heat Exchanger	Scaled STS IMU non-condensing HX	1	Reduced or no Air Flow	Loss of Suit Air Loop Flow		DFMR
			Reduced or no Coolant Flow	Loss of Suit Loop Cooling	1	Redundant Coolant Loop
Guard Bed	Technology expert description of the guard bed size likely ending up "About the size of a LiOH canister"	1	Reduced or no Air Flow	Loss of Suit Air Loop Flow		DFMR
Compressors	Approximately 40cfm each. Based on Shuttle Avionics Cooling Fan. Pdrop will be higher, but flow less.	3	Reduced or no Air Flow	Loss of Suit Air Loop Flow	2	Redundant Compressors (on manifold?)
Amine Swing Bed Manual Shutoff Valves	Allows beds to seal line as third string after redundant seals in amine bed.	6	Fails Closed	Loss of Flow through Amine Bed	2	Redundant Amine Beds
			Fails Open	Inability to seal line	2	Redundant Seals in Amine Bed
Amine Swing Beds	Includes manifolds and swing valves. Number is latest estimate from technology developer.	3	Reduced or no Air Flow	Loss of Flow through Amine Bed	2	Redundant Amine Beds
			Failure of Amine Bed	Loss of CO2 Removal Capability	2	Redundant Amine Beds
Cabin Inlet Check Valve	Manual valve to isolate suit loop in depressurization	1	Fails Closed	Loss of CO2 Removal Capability	1	Suit Loop
Cabin Outlet shutoff valve	Manual valve to isolate suit loop in depressurization	1	Fails Closed	Loss of CO2 Removal Capability	1	Suit Loop

Table 9.1-3 Current Cabin & Suit Loop Configuration

Proposal 1 Configuration

Subsystem/Component Name	Basis of Estimate	Qty	Failure Type	Failure Effect	Fault Tolerance	Redundancy Provided By
"Cabin Loop" Air Recirculation						
HEPA Filter	Shuttle Filter and Debris Trap	1	Reduced or no Air Flow	Loss of Cabin Cooling	1	Suit Air Loop
Internal Cabin Ducting	Est. 25 ft polycarbonate, 4" diameter	1	Blockage or Leakage	Loss of Cabin Cooling	1	Suit Air Loop
Cabin Heat Exchanger fan assembly	1/2 X-38 mass(for 1 fan); Apollo power * 2	1	Reduced or No Flow	Loss of Cabin Cooling	1	Suit Air Loop
Cabin Heat Exchanger	Scaled STS IMU non-condensing HX	2	Reduced or no Air Flow	Loss of Cabin Cooling	2	Suit Air Loop Redundant Heat Exchanger (if installed in parallel)
			Reduced or no Coolant Flow	Loss of Cabin Cooling	2	Redundant Coolant Loop Redundant Heat Exchanger Suit Air Loop
Amine Swing Bed Manual Shutoff Valves	Allows beds to seal line as third string after redundant seals in amine bed.	2	Fails Closed	Loss of Flow through Amine Bed	2	Redundant Amine Beds
			Fails Open	Inability to seal line	2	Redundant Seals in Amine Bed
Amine Swing Bed	Includes manifolds and swing valves. Number is latest estimate from technology developer.	1	Reduced or no Air Flow	Loss of Flow through Amine Bed	2	Redundant Amine Beds
			Failure of Amine Bed	Loss of CO2 Removal Capability	2	Redundant Amine Beds
"Suit Loop" Air Revitalization						
HEPA Filter		1	Reduced or no Air Flow	Loss of Suit Air Loop Flow		Spare HEPA Filter, IFM
			Reduced or no Air Flow	Loss of Amine Bed flow	1	Redundant Amine Bed in "Cabin Loop"
Suit Air Loop Heat Exchanger	Scaled STS IMU non-condensing HX	1	Reduced or no Air Flow	Loss of Suit Air Loop Flow		DFMR
			Reduced or no Air Flow	Loss of Amine Bed flow	1	Redundant Amine Bed in "Cabin Loop"
			Reduced or no Coolant Flow	Loss of Suit Loop Cooling	1	Redundant Coolant Loop
Guard Bed	Technology expert description of the guard bed size likely ending up "About the size of a LiOH canister"	1	Reduced or no Air Flow	Loss of Suit Air Loop Flow		DFMR
			Reduced or no Air Flow	Loss of Amine Bed flow	1	Redundant Amine Bed in "Cabin Loop"
Compressors	Approximately 40cfm each. Based on Shuttle Avionics Cooling Fan. Pdrop will be higher, but flow less.	2	Reduced or no Air Flow	Loss of Suit Air Loop Flow	2	Redundant Compressors (on manifold?)
Amine Swing Bed Manual Shutoff Valves	Allows beds to seal line as third string after redundant seals in amine bed.	4	Fails Closed	Loss of Flow through Amine Bed	2	Redundant Amine Beds
			Fails Open	Inability to seal line	2	Redundant Seals in Amine Bed
Amine Swing Beds	Includes manifolds and swing valves. Number is latest estimate from technology developer.	2 (4 if PLSS Swing Beds used)	Reduced or no Air Flow	Loss of Flow through Amine Bed	2	Redundant Amine Beds
			Failure of Amine Bed	Loss of CO2 Removal Capability	2	Redundant Amine Beds
Cabin Inlet Check Valve	Manual valve to isolate suit loop in depressurization	1	Fails Closed	Loss of CO2 Removal Capability	1	Suit Loop
Cabin Outlet shutoff valve	Manual valve to isolate suit loop in depressurization	1	Fails Closed	Loss of CO2 Removal Capability	1	Suit Loop

Table 9.1-4 Proposal 1 Configuration

Proposal 2 Configuration

Subsystem/Component Name	Basis of Estimate	Qty	Failure Type	Failure Effect	Fault Tolerance	Redundancy Provided By
"Cabin Loop" Air Recirculation (eliminated)						
"Suit Loop" Air Revitalization						
HEPA Filter		1	Reduced or no Air Flow	Loss of Suit Air Loop Flow		Spare HEPA Filter, IFM
			Reduced or no Air Flow	Loss of Amine Bed flow		Suit Loop?
Suit Air Loop Heat Exchanger	Scaled STS IMU non-condensing HX	1	Reduced or no Air Flow	Loss of Suit Air Loop Flow		DFMR
			Reduced or no Air Flow	Loss of Amine Bed flow		DFMR
			Reduced or no Coolant Flow	Loss of Suit Loop Cooling	1	Redundant Coolant Loop
Guard Bed	Technology expert description of the guard bed size likely ending up "About the size of a LiOH canister"	1	Reduced or no Air Flow	Loss of Suit Air Loop Flow		DFMR
			Reduced or no Air Flow	Loss of Amine Bed flow	1	DFMR
Compressors	Approximately tbd cfm each. Based on Shuttle Avionics Cooling Fan. Pdrop will be higher, but flow less.	3	Reduced or no Air Flow	Loss of Suit Air Loop Flow	2	Redundant Compressors (on manifold?)
Amine Swing Bed Manual Shutoff Valves	Allows beds to seal line as third string after redundant seals in amine bed.	6	Fails Closed	Loss of Flow through Amine Bed	2	Redundant Amine Beds
			Fails Open	Inability to seal line	2	Redundant Seals in Amine Bed
Amine Swing Beds	Includes manifolds and swing valves. Number is latest estimate from technology developer.	3	Reduced or no Air Flow	Loss of Flow through Amine Bed	2	Redundant Amine Beds
			Failure of Amine Bed	Loss of CO2 Removal Capability	2	Redundant Amine Beds
Cabin Inlet Check Valve	Manual valve to isolate suit loop in depressurization	1	Fails Closed	Loss of CO2 Removal Capability	1	Suit Loop
Cabin Outlet shutoff valve	Manual valve to isolate suit loop in depressurization	1	Fails Closed	Loss of CO2 Removal Capability	1	Suit Loop

Table 9.1-5 Proposal 2 Configuration

9.1.3 Mass Estimates and Design Maturity

Table 9.1-6 gives a mass summary of the CEV ATCS design.

Hardware Items	Quantity	Unit Mass (lbm)	Growth (%)	Total Mass (lbm)	CM Mass (lbm)	SM Mass (lbm)	Basis of Estimate
ATCS - Heat Acquisition				**315**	**251**	**64**	
Cabin Heat Exchanger	1	52	5%	54.9	54.9		Scaled STS IMU non-condensing HX
Cabin Heat Exchanger Fan Assembly	1	36	5%	38.0	38.0		1/2 X-38 mass (for 1 fan)
Suit Air Loop Heat Exchanger	1	31	20%	37.4	37.4		Scaled STS IMU non-condensing HX
LCG Heat Exchanger	1	5	20%	5.8	5.8		STS multi-purpose HX
LCG Water Pump, Controls & QDs	2	4	20%	10.1	10.1		X38 w ater pump for mass
Coldplates - CM Internal	10	7	20%	85.2	85.2		Shuttle coldplate scaling
Coldplates - CM External	8	2	20%	19.2	19.2		Shuttle coldplate scaling
Coldplates - SM	3	18	20%	64.4		64.4	Shuttle coldplate scaling

Hardware Items	Quantity	Unit Mass (lbm)	Growth (%)	Total Mass (lbm)	CM Mass (lbm)	SM Mass (lbm)	Basis of Estimate
ATCS - Fluid Loop				**316**	**239**	**77**	
Accumulator (Passive)	2	5	5%	10.5	10.5		STS ITCS accumulator
Propylene Glycol Solution (60%) - CM	1	36	0%	36.0	36.0		3/4 total in CM; pipe vol.+25%
Propylene Glycol Solution (60%) - SM	1	12	0%	12.0		12.0	1/4 total in SM; pipe vol.+25%
Pump Package (2 Pumps)	2	27	5%	56.7	56.7		STS ITCS pri.H2O pump pkg.(970pph)(>>Apollo)
Isolation Valve (CM to SM)	4	4	5%	17.6	17.6		mass X38
Check Valve	2	2	5%	4.2	4.2		STS w ater pump check valve
Mixing Valve (Automatic & Manual)	2	14	5%	29.2	29.2		ISS ITCS 3-w ay mix valve
Set Point Temperature Sensors	4	0	20%	0.5	0.5		Shuttle thermistor
Temperature Sensors	80	0	20%	9.6	9.6		Shuttle thermistor
Pressure Sensors	8	1	20%	9.6	9.6		engineering judgement
Plumbing - CM	1	54	20%	64.8	64.8		Spreadsheet calc. - G. Tuan/EC2
Plumbing - SM	1	54	20%	64.8		64.8	Spreadsheet calc. - G. Tuan/EC2

Hardware Items	Quantity	Unit Mass (lbm)	Growth (%)	Total Mass (lbm)	CM Mass (lbm)	SM Mass (lbm)	Basis of Estimate
ATCS - Heat Rejection				**882**	**217**	**666**	
Evaporative Heat Sink	1	50	15%	57.5	57.5		Vendor est
Vacuum Duct	1	13	5%	13.2	13.2		STS FES high load duct
Vacuum Duct Heater	2	1	5%	1.3	1.3		STS FES nozzle heater
Water Supply Line	1	3	20%	3.6	3.6		engineering judgement
Water	1	63	0%	63.0	63.0		63 lbs for 18kWh of cooling
Water Tank	1	21	15%	24.2	24.2		scaled from STS w ater boiler tank
Refrigerant Supply Line	1	3	20%	3.6	3.6		engineering judgement
Refrigerant Tank	1	12	20%	14.4	14.4		scaled from STS w ater boiler tank
Refrigerant	1	36	0%	36.0	36.0		36 lbs R134a for 1kWh
GSE Heat Exchanger	1	14	5%	14.2		14.2	STS ETCS GSE HX
Quick Fluid Disconnect on GSE HX	2	2	20%	4.8		4.8	engineering judgement
Relief Valve	8	2	5%	16.8		16.8	engineering judgement
Radiator Isolation Valves	16	2	20%	38.4		38.4	guess based on Shuttle
Radiator Panels	8	62	20%	591.4		591.4	Spreadsheet calc.(9.33m^2,-10Fsink,shuttle derived mass)

Table 9.1-6 ATCS Mass Summary

More details of ATCS masses can be found on the master equipment list (MEL) (Table 9.1-7):

21-Jul-06

Active Thermal Control
Master Equipment List
Mike Ewert

		Component Quantity					*Component Properties*									*Component Totals*				
		Location					Mass/Power/Volume													
		Pressurized	Unpressurized				Unit Mass	Shape	Length	Width/Diam	Height/Thickness	Volume	Voltage	SS Power	Peak Power	Total	Unit Mass	Growth	Total Mass	Total Volume
Subsystem/Component Name	Basis of Estimate	CM	LAS	CM	SM	SA	(lb)		(in)	(in)	(in)	(in^3)	(V)	(W)	(W)	Quantity	(lb)	(%)	(lb)	(in^3)
Heat Acquisition																			**315.0**	
Cabin Heat Exchanger	Scaled STS IMU non-condensing HX	1					52.3	Box	15.11	15.11	15.11	3,450				1	52.3	5	54.9	3449.8
Cabin Heat Exchanger Fan Assembly	1/2 X-38 mass(for 1 fan); Apollo power * 2	1					36.2	Box	15.11	15.11	3	685	28DC	170	200	1	36.2	5	38.0	684.9
Suit Air Loop Heat Exchanger	Scaled STS IMU non-condensing HX	1					31.2	Box	12.74	12.74	12.74	2,068				1	31.2	20	37.4	2067.8
Liquid Cooling Garment (LCG) Heat Exchanger	STS multi-purpose HX	1					4.8	Box	12.33	7.74	3.5	334				1	4.8	20	5.8	334.0
LCG Water Pump, Controls & QDs	X38 water pump for mass	2					4.2	Cylinder				0	28DC	50	50	2	4.2	20	10.1	
Coldplates - CM Internal	Bufkin est. of area; shuttle density	10					7.1	Box	75	75.00	0.5	2,813				10	7.1	20	85.2	28125.0
Coldplates - CM External	Bufkin est. of quantity&area; shuttle density			8			2	Box	35	35.00	0.5	613				8	2.0	20	19.2	4900.0
Coldplates - SM	Bufkin est. of quantity&area; shuttle density				3		17.9	Box	65	65	0.5	2,113				3	17.9	20	64.4	6337.5
Fluid Loop																			**315.5**	
Accumulator(Passive);Vol.incl.w/pump pkg.	STS ITCS accumulator	2					5	Cylinder				0				2	5.0	5	10.5	
Propylene Glycol Solution (60%) - CM	3/4 total in CM; pipe vol.+25%	1					36	Other				0				1	36.0	0	36.0	
Pump Package (2 Pumps, Controls & Instr.)	STS ITCS pri.H2O pump pkg.(970pph)(>>Apollo)	2					27	Box	18.5	12.6	9.9	2,308	28DC	300	300	2	27.0	5	56.7	4615.4
Isolation Valve (CM to SM)	mass X38; power Apollo Ops Handbook	4					4.2	Cylinder				0	28DC	8	8	4	4.2	5	17.6	
Pyro Cutter (CM to SM Fluid Lines)	engineering judgment	0					5	Box				0	28DC				5.0	20		
Check Valve	STS water pump check valve	2					2	Box	5.54	3.54	1.52	30				2	2.0	5	4.2	59.6
Mixing Valve (Automatic & Manual)	ISS ITCS 3-way mix valve	2					13.9	Box	7	14	12.5	1,225	28DC	7.5	15	2	13.9	5	29.2	2450.0
Set Point Temperature Sensors	Shuttle thermistor	4					0.1	Box				0				4	0.1	20	0.5	
Temperature Sensors	Shuttle thermistor	80					0.1	Box				0				80	0.1	20	9.6	
Pressure Sensors	engineering judgment	8					1	Box				0				8	1.0	20	9.6	
Plumbing - CM	Spreadsheet calc. - plumbing X 2	1					54	Cylinder				0				1	54.0	20	64.8	
Plumbing - SM	Spreadsheet calc. - plumbing X 2				1		54	Cylinder				0				1	54.0	20	64.8	
Propylene Glycol Solution (60%) - SM	1/4 total in SM; pipe vol.+25%				1		12	Other				0				1	12.0	0	12.0	
Fluid Evaporator																			**216.1**	
Evaporative Heat Sink (inc. 5 lb for Redun. Cntrls)	Vendor est. for development hardware			1			50	Cylinder				0	28DC		100	1	50.0	15	57.5	
Vacuum Duct	STS FES high load duct	1					12.6	Cylinder				0				1	12.6	5	13.2	
Vacuum Duct Heater	STS FES nozzle heater	2					0.6	Other				0	28DC		200	2	0.6	5	1.3	
Water Supply Line	engineering judgment	1					3	Cylinder				0				1	3.0	20	3.6	
Water Tank	scaled from STS water boiler tank			1			21	Cylinder				0				1	21.0	15	24.2	
Refrigerant Supply Line	engineering judgment			1			3	Cylinder				0				1	3.0	20	3.6	
Refrigerant Tank	scaled from STS water boiler tank			1			12	Cylinder				0				1	12.0	15	13.8	
Refrigerant	36 lbs R134a for 1kWh post-land			1			36	Other				0				1	36.0	0	36.0	
Water for Heat Sink	63 lbs for 18kWh of cooling			1			63	Other								1	63.0		63.0	
GSE Heat Exchanger																			**19.0**	
GSE Heat Exchanger	STS ETCS GSE HX				1		13.5	Box	13.5	4.27	7.38	425				1	13.5	5	14.2	425.4
Quick Fluid Disconnect on GSE HX	engineering judgment				2		2	Cylinder				0				2	2.0	20	4.8	
Radiators																			**646.6**	
Relief Valve	engineering judgment				8		2	Box	3	2	1.5	9				8	2.0	5	16.8	72.0
Radiator Isolation Valves (Latching	guess based on Shuttle				16		2	Box				0	28DC			16	2.0	20	38.4	
Radiator Panels	Spreadsheet calc.(394.6ft^2 total area of 8 panels,-10Fsink,shuttle derived mass)				8		61.6	Other				0				8	61.6	20	591.4	

Table 9.1-7 ATCS Master Equipment List

9.1.4 Plan Forward

The NASA requirements cycles have verified the feasibility of a CEV ATCS design which can meet Constellation SRR requirements. There are two exceptions, depending on the outcome of post-landing and lunar orbit requirements discussions: 1) It does not appear feasible for the CEV to provide self-contained power and cooling for 36 hours after touchdown in all extreme environments; and 2) radiator sizing is based on a long term heat load level and peaks will be required for activities such as docking. These peaks in heat loads must be accommodated by the evaporative heat sink in the worst case hot environments (low beta angles in lunar orbit). The water evaporant tank size, however, is not sufficient for all these peaks to occur at the worst-case beta angles. Thus, a more-detailed, mission-specific analysis will be required to determine exactly how much water evaporant will be required for each mission. Other risk areas must continue to be studied as well, such as ascent heating of the radiators.

Recommendations for further ATCS studies in concert with the prime contractor are as follows:

- Future analysis should focus on the Lockheed vehicle and ATCS configuration while comparing to this NASA reference configuration, looking for the best features of both.
- Radiators:
    - More detailed radiator environment and fluid modeling will determine radiator heat rejection margin (or lack there of) for specific mission scenarios.
    - Consider leak scenarios & micrometeoroid and orbital debris (MMOD).
- Evaporative heat sink
    - Compare the evaporative heat sink technology used in this design to sublimators.
- Fluid loops and pumps
    - Further analyze redundancy in all mission scenarios
    - Determine if the propylene glycol/water coolant mixture used here is optimal.
    - Address glycol double containment issue which might be required when docking with ISS.
    - Determine accumulator volume needed to account for leaks.
    - Verify design flow rates, calculate pressure drop across each heat acquisition and rejection device, and determine the loop total pressure drop.

Alex Bengoa of the Ground Operations team at KSC pointed out that the radiators may gain or lose heat to the ambient while the ATCS is flowing on the launch pad prior to lift off. This may increase the capacity required of the ground service equipment (GSE) heat exchanger (see Figure 9.1-1), which is currently specified to be 6 kW and use a 60% propylene glycol fluid just like the CEV ATCS. An analysis of the launch pad thermal loads on the radiators has not been conducted; however, for KSC environmental loads (wind, thermal, humidity, etc.), the DSNE covers all of this in Section 3.1, Ground winds (3.1.3), Radiant energy (3.1.4), Air Temp (3.1.5), Humidity (3.1.7).

The cold plates in the unpressurized part of the Crew Module will not receive flow after the Service Module separates. Additional analysis needs to be done to ensure that thermal capacitance and/or passive cooling will be adequate for the equipment on those cold plates as long as it is required. Otherwise, the ATCS flow configuration and placement of the radiator mixing valve inside the pressurized area may need to be changed. It was placed inside the CEV CM in this design so that a manual over-ride feature could be included.

Analysis and design efforts should seek to improve thermal averaging between the hot and cold sides of the lunar orbit using either selective freezing of the radiators or dedicated thermal capacitance tanks or devices.

With the analytical tools soon available, a complete mission profile should be modeled to analyze ATCS performance, including transient system effects such as varying heat loads and environments. This analysis would also yield the exact quantity of evaporant water and refrigerant needed for a particular mission.

References:

"Umbilical Interfaces Concept" by Molly Anderson, Nicole Jordan, Grant Bue, Bruce Duffield, 7/13/06

"Preliminary Results from CEV ATCS S/F Transient Model for LLO Operation with Evaporative Cooling & Adjusted Coolant Viscosity", Quoc Nguyen, 08-31-2006.

"Preliminary Results from CEV ATCS S/F Transient Model for LLO Operation with Evaporative Cooling & Adjusted Coolant Viscosity", Quoc Nguyen, 09-14-2006.

"Preliminary Results from CEV ATCS S/F Transient Model for LLO Operation with Adjusted Coolant Viscosity & without Evaporative Cooling", Quoc Nguyen, 09-14-2006.

9.2 Environmental Control and Life Support System

The Environmental Control and Life Support System (ECLSS) scope for this study includes air revitalization systems, potable water systems, waste management systems, fire detection, and fire suppression systems. The system provides essentials and removes hazards to maintain a safe environment for the crew. The ECLSS system is highly integrated with the Active Thermal Control System (ATCS), Extravehicular Activity (EVA) and Crew Survival, Flight Crew Equipment and Human Factors concerns, and the vehicle seats.

9.2.1 Driving Requirements, Groundrules, and Assumptions

Environmental control and life support systems driving requirement is always to protect the health and safety of crewmembers by providing a habitable environment throughout the mission. The size of the system components are primarily driven by the number of crewmembers, for processing equipment, and the duration of the mission, for stored consumables. The complexity of the system is driven by the number of significantly different mission phases or types of operations during which the crew must be supported, such as pre-launch on the pad, powered flight that requires space suits to be worn, shirt-sleeve cabin environments in space, depressurized cabin events, and post-landing support. Each of these phases may have different functional requirements for the life support system, different environments that pose challenges or provide resources, or different interfaces with the crew and other vehicle systems.

The requirements for the CEV have been in revised several times throughout this study, and each design iteration helped demonstrate the impact of or need for new requirements. The requirements set used for the CEV Reference Configuration design was made of documents used for the Call for Improvement (CFI) release. Other document updates have not been baselined, but this study attempts to respond to the latest and best requirements available from several review cycles preparing for System Requirements Review (SRR). The primary documents that impact life support design are the Constellation Architecture Requirements Document (CARD) CXP-72000, the CEV System Requirements Document (SRD) CXP-72000, and the Human System Integration Requirements (HSIR) CXP-70024. Interface Requirements Documents (IRDs) between the CEV and the ISS (CXP-70031), LSAM (CXP-70034), and EVA (CXP-70033) also provide important requirements for the life support system, but at this stage often include many TBR values, so they give information about functions required rather than system sizing.

The CARD is the source of the most basic requirements that must be met by the ECLSS system. It states that crew sizes from zero to six must be launched to Low Earth Orbit in a single launch (LEO) (CA0447-PO), crew sizes from zero to six must be launched to the ISS (CA0388-HQ) and returned, and that crew sizes of two, three, and four must be delivered to the lunar surface and returned to Earth (CA0203-HQ). A duration of 18 days is defined for the lunar crew (CA3164-PO). For this study, 6 days is expected for ISS missions (TBD Reference).

Throughout the CARD are requirements that define the mission phases in which life support must be provided to support the crew. Overall, it includes the time from ingress on the launch pad through post-landing egress. This includes two hours while isolated from the ISS (CA0493-PO) to wait out transient hazardous conditions. The CARD also requires two EVA operations of up to four hours duration each (CA3166-PO) for emergencies or contingency response. The ECLSS within the CEV must provide support to enable the EVA system to meet that requirement. The CEV must provide support for the crew in a depressurized cabin for up to 120 hours, per several related requirements (CA0532-PO). Up to 36 hours of post-landing support is also called out (CA0194-PO) with the hatch closed after a landing in the water.

The CARD outlines a few details relevant to ECLSS. The CEV atmosphere is selectable to pressures between 14.9 and 9.4 psia with 0.1 psia increments (CA0288-PO) within +/-0.1 psia (CA3060-PO). Oxygen concentrations are limited to less than 30% oxygen (CA3061-PO), but oxygen partial pressure has to be maintained between 2.6 psia and 3.1 psia with 0.1 psia increments (CA3133-PO) with +/- 0.1 psia (CA3134-PO) for crew health. This allows the CEV to have a pressure of 14.7 nominally for ISS missions, and 10.2 psia for lunar missions.

Safety requirements apply to the whole vehicle, but impact the redundancy count and design of the ECLSS system. The CARD calls out requirements for single-fault tolerance for mission critical functions (CA0435-PO) and two-fault tolerance for catastrophic hazards (CA0436-PO) except those approved as Design for Minimum Risk (DFMR) areas. Also a single fault or event cannot eliminate more than one means of fault tolerance (CA0437-PO). The design to meet these fault tolerance requirements cannot require EVA or emergency systems . This prevents additional load being placed on the ECLSS consumables to support a large EVA load, but all redundancy strings must be part of the initial system design. The life support system will eventually play a role in the risk assessment that calculates loss of mission or loss of crew risks and must meet CARD requirements, but at this level, those requirements were not assessed for the life support system.

The CARD also calls some emergency responses, such as the ability to maintain cabin pressure at or above 8 psia in the event of a cabin leak equivalent to a 0.25 inch diameter hole size (CA3105-PO). This allows the crew time to don their suits before the cabin depressurizes. An hour is currently assumed as the time required (CA3058-PO). The CEV must also provide consumable gas and functionality to be able to repressurize the vehicle. Contingency gas stores are provided for two contingencies to meet two fault tolerance. The requirements state that these contingencies may be two cabin depress/repress events (such as following EVAs to respond to two failures), or one cabin depress/repress plus one cabin leak scenario as defined above (CA3140-PO). For CEV missions to ISS, only one cabin leak event at 14.7 psia is required

(CA3199-PO) because a quick return from Earth orbit is possible in this case, but not in the lunar mission cases.

The CEV SRD document includes many requirements that essentially repeat CARD requirements, such as crew size, but also some new requirements. The CEV SRD requirements have not been updated as frequently as the CARD, and may be slightly out of date in comparison. As of the ICPR review versions, some of the driving requirements for ECLSS are as follows. Safe haven requirements in the CEV SRD specify the speed at which the capability must be available (CV0014 and CV0015). Requirements related to attached operations require the CEV to be able to equalize pressure between the CEV and the vestibule (CV0063 and CV0493), monitor pressure (CV0064), include at least two vestibule pressurizations (CV0065), and depressurize the vestibule prior to demating (CV0068). The CEV must provide two repressurization cycles for its own cabin per mission (CV0080), but this will be updated to correspond to the contingency consumable requirements from CA3140-PO. The CEV must also equalize pressure between the CEV and Earths atmosphere prior to landing (CV0084), which is critical in cases where the cabin is depressurized.

The SRD provides the link to many sections of the HSIR document relevant to life support. It lists fire detection, isolation, and suppression requirements as per the HSIR Section 4.5 (CV0277), food storage and preparation per HSIR section 6.1 (CV0288), personal hygiene per the HSIR section 6.2 (CV0289), waste management per HSIR 6.3 (CV0290), internal atmosphere per HSIR Section 3.1 (CV0296), and potable water per HSIR Section 3.2 (CV0304). The atmospheric contaminant limits are per the Spacecraft Maximum Allowable Concentration (SMAC) levels (CV0297). The SRD also decomposes the atmospheric pressure requirements into high (CV0299) and low pressures (CV0301), maximum oxygen concentration at those pressures (CV0300 and CV0302), and overpressurization relief requirements (CV0303).

The Human System Integration Requirements (HSIR) requirements go in to much greater detail, and will be discussed as part of the subsystem driving requirements.

9.2.1.1 Air Revitalization System Driving Requirements, Groundrules, and Assumptions

The air revitalization system is design to remove constituents that would be harmful to the crew, such as CO_2 and trace contaminants like CH_4 and NH_3, and replace the constituents necessary to a habitable atmosphere, such as oxygen, and nitrogen to maintain total pressure. HSIR Section 3.1 lists the atmosphere related requirements for the quality that must be maintained. Determining the removal rates required is currently based on combining crew size requirements with historical data and assumptions or requirements used in other NASA missions to ensure the system design will maintain these levels. HSIR Section 6.4 on exercise requires the vehicle to support a crew that exercises during the mission, and the higher metabolic loads during these periods can significantly impact the size, and possibly the design concept, for the air revitalization system.

9.2.1.2 Pressure Control System Driving Requirements, Groundrules, and Assumptions

The pressure control system requirements are primarily based on mission information, such as docking, pressurization and depressurization of the cabin, and launch and re-entry. The atmospheric composition and requirement to operate in a depressurized cabin also drive the design.

9.2.1.3 Water and Waste Management Driving Requirements, Groundrules, and Assumptions

Other than defining crew size and duration in the CARD and SRD, the key requirements for the water and waste management systems come from the HSIR. HSIR Section 3.2 focuses on potable water. Potable water quality is called out in the HSIR, but for a primarily stored water system, it does not drive system costs. Potable water quantity, however, significantly drives the system size and cost. Since the CEV uses solar power and not fuel cells, all potable water required for the mission must be shipped directly. The HSIR also requires potable water to be available at specific temperature ranges, which drives vehicle design, since they are not all within the temperatures within the band expected in the thermal control loop. This requirement is also related to the food preparation requirements in Section 6.1.2.

The design of waste management system within life support is driven by HSIR Section 6.3, Body Waste Management. It provides baseline quantity information on urination and defecation and other bodily functions by the crew that sizes the toilet and supplies necessary as part of the Waste Management System (WMS). Odor control requirements in this section also drive the design of the WMS.

9.2.1.4 Fire Detection and Suppression Driving Requirements, Groundrules, and Assumptions

The HSIR Section 4.5 on fire protection is the source of driving requirements for this system. Fire detection and alarms are required, and portable fire suppression systems are required as well. The biggest driver in this section is the requirement that the fire suppression agents be non-toxic. These requirements have been updated between ICPR and the coming SRR to allow the possibility for fire management to be performed in avionics bays without sensors that detect fire byproducts or active fire suppressants through use of other methods of fire related faults, like over-current detection, and other means of fire suppression, like isolation from oxidizers. However, based on the CEV Reference Configuration avionics design, active fire suppressants are still required.

9.2.2 Conceptual Design Overview

The CEV ECLSS system proposed here is designed to try to provide all the necessary resources and functions in many different operating states. The air revitalization and pressure control system are highly integrated, and include the methods of providing oxygen and nitrogen, and removing airborne hazards from the cabin. A suit loop architecture enables all critical functions to be provided to the crew via the vehicle systems and resources while they are wearing pressure suits during depressurized cabin events. The same air revitalization hardware is used during nominal shirt sleeve environment operations. The pressure control systems are designed to control the total pressure and O_2 and N_2 concentrations in the cabin, in the vestibule for docking, and in the suit loop and space suits during depressurized cabin operations. The water and waste management system in the current design are the two components most able to stand alone. The fire detection and suppression system has both portable and integrated components. A top level schematic is provided in Figure 9.2-1 below.

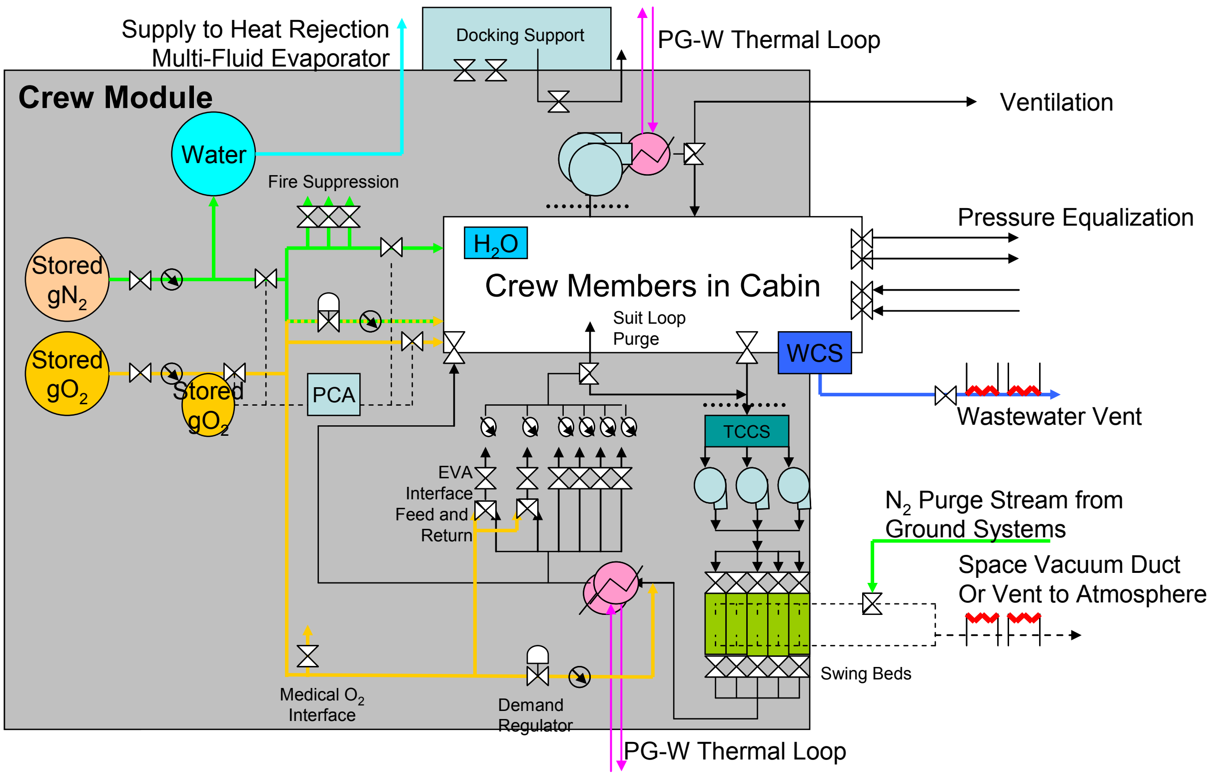

Figure 9.2-1 CRC-3 ECLSS Top-Level Schematic

9.2.2.1 Air Revitalization System

The air revitalization includes component for control of particulates, trace contaminants, carbon dioxide, and humidity, as well as the means to move air to and through the system. Cabin air can be directed through this system by opening the valves to the cabin for nominal operation. When in a suit loop mode, all valves to the cabin are closed, directing gases from the suited crewmembers to the air revitalization hardware, and then back to the crew members. While in this mode, the loop is filled with pure oxygen at a pressure appropriate for the EVA suits, either a small delta above cabin pressure when there is significant pressure in the cabin, or at a delta pressure above the cabin more suitable for operations in a depressurized cabin, such as 4.3 psi. A third option is to provide air to the crewmembers during times when they must wear their suits, such as on the pad or powered flight maneuvers, by allowing cabin air to be pulled into the loop. This is accomplished by closing the normal outlet and forcing the air through the suits and out the suit loop purge valve. Oxygen could be introduced into the line at a small delta above cabin pressure in this instance as well as added through the cabin. The purge valve is also critical for making the transition from shirt sleeve cabin operations to suit loop mode. During the transition, the nominal inlet and outlet from the cabin are closed, so that the only inlet is from the pure oxygen line, and nitrogen is purged out of the loop. The valves that close the nominal inlet and outlet will protect the crew from vacuum in an emergency, so redundancy would be desirable. However, the requirement for the crew to be in the suit loop on pure oxygen follows a failure of some sort, so only a single valve would be required by two-fault tolerance rules. If this design is selected, the suit loop can also provide atmosphere to fire fighting or toxic environment masks by purging the loop and using pure oxygen at a pressure slightly above cabin pressure. This would allow the crew to have pure oxygen in a recycling mode, which prevents increases in oxygen levels in the cabin during fire fighting emergency response activities.

The oxygen line that provides resources to the suit loop is also available to provide an interface for medical oxygen masks. Upstream of the regulator that reduces oxygen pressure to what is needed in the suit loop, a medical oxygen interface is provided to interface with oxygen ventilators potentially injured crewmembers who need assistance breathing.

In addition to the suit loop, the CEV Reference Configuration design includes a cabin loop, which contains a filter, a fan, and a heat exchanger. The filter is the only piece of hardware owned by the ECLSS system; the fan and heat exchanger are integrated and considered part of active thermal. However, they play an important role in the life support system. The fan processes a much higher flow rate than the suit loop, several hundred cubic feet per minute, and provides mixing of the CEV cabin. The fan also provides the air revitalization during post-landing periods. The fan is used to push air out of the CEV, drawing ambient air from the environment around the capsule into the cabin through open pressure equalization valves. It is important that the fan push air out rather than draw air in to prevent it from being flooded if the outside environment is a rough sea or storm. For lunar missions, if necessary, this loop could also be used to provide filtration of any lunar dust that is transferred to the CEV while the crewmembers are in their suits in the suit loop configuration at a pressure slightly above cabin pressure. The ducting for this loop is assumed to be a lightweight material, estimated here as polycarbonate, though it could be a metal foil similar to household dryer vent lines. The length of the ducting assumes that the hardware is located at the bottom of the CEV Crew Module, and the ducting allows flow to the top of the capsule to force mixing across the capsule volume. The outlet duct would likely be oriented at an angle to force a swirl of air, but further CFD analysis will be necessary when the cabin layout is known to establish those details.

The air revitalization hardware located in the suit loop includes filtration, trace contaminant control, combined CO_2 and H_2O removal. The ducting in this loop must be compatible with pure oxygen and designed to handle at least a 4.3 psi pressure differential between the inside and outside. All hardware in the loop must also be certified to operate in 100% oxygen environments.

The air revitalization hardware begins with a filter immediately downstream of the crewmembers to provide particulate control, whether they are in their suits in the suit loop, or in a shirt sleeve environment in the cabin. A coarse rock catcher filter followed by a HEPA filter is installed here.

Downstream of the filter is the trace contaminant control system (TCCS), referred to as a guard bed. The short duration of the mission, and the purge provided by venting of the amine swing bed means that many contaminants will never accumulate to dangerous levels. The baseline TCCS is primarily designed to remove ammonia with phosphoric acid coated charcoal and to oxidize volatile organic compounds (VOCs) with an ambient temperature catalytic oxidizer of platinum catalyst on charcoal. Because both of these technologies utilize charcoal as a support substrate, some bulk adsorption can also be expected. The system is referred to as the Guard Bed because it would help to protect the amine swing bed downstream from chemical releases or bulk release of water into the cabin that might create an upset in system performance.

The next components are the suit loop compressors and amine swing beds which control cabin CO_2 and humidity levels. In each case, enough units are included to provide two-fault tolerance for the critical function of CO_2 removal. For the fans, only one operational unit is required to maintain safe CO_2 levels. In initial designs, three swing beds were sized such that one bed would be sufficient for CO_2 control. In the most recent design, however, a new design paradigm was used. The beds are individually sized to be common with the amine swing bed size designed for EVA operations to provide commonality. As a result, two of these smaller beds are required to provide CO_2 control. Five beds are nominally included in this design, so two failures still leaves the system with sufficient removal capability. Humidity control is an important function, but high humidity in the cabin (assuming no electronics failures and continuing temperature control) is not life threatening, and only needs to be single fault tolerant. The three fans should have multiple speed set points to adjust for the varying metabolic rates of the crew during sleep, nominal daytime, and exercise periods, or failure cases. The gas flow is split to pass through each of the three fans. The gas flow is then mixed and split again to reach each of the amine swing beds. This allows any fan to provide air to any swing bed. Each fan and each swing bed are on separate power buses, so that the failure of one power bus does not cause failure of more than one fan or more than two swing beds at worst. The amine swing beds each have two internal volumes which alternate between being exposed to the cabin air or suit loop gases to remove CO_2 and H_2O, and being exposed to a source that is free of CO_2 and H_2O to allow them to vent the collected CO_2 and H_2O. On the launch pad, pure nitrogen from the ground systems is used to purge the swing bed. In space, they are exposed to vacuum to remove the load. The spool valve that controls the flow to each side has redundant seals, and cannot fail in position that allows cabin air to vent to vacuum. However, in the event of a cracked valve or other physical failure that allows the adsorbing and desorbing sides to mix, valves are placed at the inlet and outlet of each swing bed to isolate it from the ducting. To reduce losses of air to vacuum, at the end of each half-cycle the swing bed spool valve equalizes pressure between the vacuum side that is about to receive cabin air and the cabin air side that is about to vent to vacuum. A large vent line with a 4 inch diameter is desired to optimize the removal of the collected CO_2 and H_2O from the beds. The current design assumes that a vacuum utility will be available at the launch pad to draw vacuum on the duct line and allow the swing bed to operate before launch. Because water is the major component of the gases being vented to vacuum, heaters are placed on the vent line to mitigate risk of freezing the line closed and provide a way to recover from frozen water in the line.

9.2.2.2 Pressure Control System

The pressure control system regulates oxygen and nitrogen partial and total pressure in the cabin and vestibule and provides oxygen as a resource to other systems.

A Pressure Control Assembly (PCA) unit receives sensor data and provides signals and power to actuate valves to control the cabin pressure and oxygen and nitrogen concentrations. Most of the valves commanded by the PCA also have manual override capabilities as one string of fault tolerance. Because the CEV cabin is small, unlike the ISS, the power design will be more efficient if power to valves is distributed with the wiring that provides the signal. The PCA is packaged as one unit, but has redundant processors on separate power buses in the event of failure.

Positive and negative pressure relief valves are important during ascent and descent phases of the mission, as well as for deliberate cabin depressurization. Positive pressure relief valves open to release gas in the event of cabin over pressurization, or to transition to a lower total pressure atmosphere point. Negative pressure relief valves allow air back into the cabin during reentry to prevent the outside pressure from crushing the CEV. The negative pressure relief valves must be sized to return at cabin at vacuum to 14.7 psia at the maximum rate of re-entry. These valves are commanded automatically by the PCA, but should also have manual overrides.

The N_2 and O_2 resources are stored as high pressure gas in tanks in the Service Module. The lunar mission of four crewmembers for 18 days requires consumables for 72 crewmember-days (CM-d), while the ISS mission of six crewmembers for 6 days is only 36 CM-d, so the lunar case is the driver for tank sizing. In this design iteration, no additional consumables for contingency EVA were allotted. Additional gas to "Feed the Leak" to maintain cabin pressure while the crew dons their space suits is also not currently included in this design. The current allotment of O_2 and N_2 resources is shown in Table 9.2-1 below. Nitrogen is important for pressurized cabin operations, but other than as a solution for pressure maintenance, is but not critical for life. To provide additional redundancy, the oxygen system is linked to the CEV propulsion oxygen system. In addition, there is a small oxygen tank on the CEV CM to provide gas for the period after CM and SM separation.

Purpose	**CEV ISS Mission O_2 (lbm)**	**CEV ISS Mission N_2 (lbm)**	**CEV Lunar Mission O_2 (lbm)**	**CEV Lunar Mission N_2 (lbm)**
Crew Metabolism	66	-	133	-
Worst Case Emergency Consumables	12	30	21	50
Vehicle Leakage Makeup	0.1	0.4	0.3	1.1
Swing Bed Ullage Makeup	3	9	8	28
Total	**81**	**40**	**161**	**80**

Table 9.2-1 Consumable Quantities of O_2 and N_2 for CEV missions

Conveniently, the amount of oxygen required is almost exactly twice as much as the amount of nitrogen required. As a result, a common tank design was developed based on the assumption that there would be one nitrogen tank and two oxygen tanks. The approach was to limit the tank internal pressure to 3,000 psia, use a cylindrical design with hemispherical end-caps and set the height (h) to diameter (d) ratio, equal to two, h/d=2 shown in Figure 9.2-2.

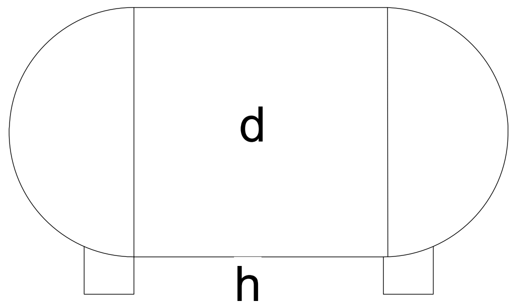

Figure 9.2-2 Pressure Vessel Shape for N_2 and O_2 Tank Properties Calculations

So if h/d = 2 then the volume is equal to:

$$V = \frac{4}{3}\pi\left(\frac{d}{2}\right)^3 + \frac{12}{3}\pi\left(\frac{d}{2}\right)^3$$

By first using the ideal gas law with temperature equal to 524 °R and pressure equal to 3,000 psia, the required volume was estimated for oxygen assuming two tanks and 161 lbm of oxygen and nitrogen assuming one tank and 80 lbm of nitrogen. An excess of 50 psia was assumed to be left in the tank at missions end. The volume was then reassessed using a Peng-Robinson equation of state to check for deviation from the ideality assumed by the ideal gas law. This deviation was roughly 15%. Calculation of the shell mass was done with a spreadsheet tool (COPV sizing.xls) developed by Jim Geffre. However the h/d ratio was still assumed to be two. There are three equally sized tanks proposed for commonality, two tanks for oxygen and one tank for nitrogen. The results of the tank mass, the tank volume and the tank diameter are given in Table 9.2-2 below.

Vol: 9,400 in^3 Diameter: 16.495 in	CRES 301 Polymer	Inconel 718 Polymer	AL 2219 Polymer	Proof & Minimum Burst Factors
Oxygen Tank 1	63 lb	68 lb	76 lb	1.5/2
Oxygen Tank 2	63 lb	68 lb	76 lb	1.5/2
Nitrogen Tank 1	63 lb	68 lb	76 lb	1.5/2
Oxygen Tank 1	136 lb	143 lb	166 lb	2/4
Oxygen Tank 2	136 lb	143 lb	166 lb	2/4
Nitrogen Tank 1	136 lb	143 lb	166 lb	2/4

Table 9.2-2 Table of Resultant Masses for Three Materials at the Given Gas Volume

Several delivery methods are possible for adding oxygen to the cabin. From the high pressure storage tanks at 3,000 psia, the pressure is stepped down to approximately 900 psia in the CM for storage in the accumulator tank. Downstream of the accumulator tank, the pressure is stepped down to 100 psia for distribution throughout the system. In shirt sleeve operations, a control valve closest to the cabin outlet would be used to add oxygen when the partial pressure is too low. If that valve fails, it can be manually opened and a valve upstream will be used for control. During depressurized cabin events, oxygen is added directly to the suit loop. A multiple setpoint regulator is used to control the oxygen flow. One setting should be only slightly above ambient cabin pressure. This setting is useful for prebreathe activities, and purging the suit loop to transition to depressurized cabin operations. The second setting would be 4.3 psi above cabin pressure to ensure that suited crewmembers are at an absolute pressure of at least 4.3 psia when the cabin depressurizes. In addition to flow to the suit loop, EVA umbilicals could also utilize the 100 psia oxygen distribution pressure to feed open-loop umbilicals during contingency EVAs.

Nitrogen is used to control total pressure in the vehicle. Similar to oxygen, there are two possible control valves, both with manual overrides. If the downstream control valve fails, it should be manually opened, and the upstream valve used to regulate nitrogen flow.

One important emergency response case, even though it is not explicitly called out in the current set of requirements, is feeding a leak. This critical capability maintains cabin pressure in the event of a leak so that the crew can remain conscious long enough to perform emergency response, such as putting on their suits, or initiating reentry from LEO. A large pressure regulator is included in the design to maintain cabin pressure at 8 psia. Control valves upstream of this regulator could be used to control the ratio of oxygen and nitrogen entering through the regulator. If the crew dons oxygen masks to begin prebreathe activities, these masks will already be releasing significant amounts of oxygen into the cabin, and the feed the leak response is best performed with pure nitrogen to keep oxygen partial pressures at a reasonable level. Also, nitrogen is a less critical consumable, and could be totally vented to maximize crewmember safety by maximizing prebreathe time at 8 psia to before depressurization of the cabin therefore reducing decompression sickness risks.

The final component of the pressure control system is a series of valves related to pressure equalization for docking. For simplicity and the lowest possible mass, the docking pressurization control valves are assumed to be manual. To add gas to a depressurized vestibule volume or equalize pressure between the CEV CM and the vestibule, the crew must open one of two redundant valves. To depressurize the vestibule to prepare for demating, plumbing must connect the vestibule to space, but the control valve must be on the CEV side so that the crewmembers can operate it, so the plumbing must also pass through the CEV CM cabin.

9.2.2.3 Water and Waste Management

The water and waste management system deal with the liquid resources required and liquid and solid wastes that are managed as part of the life support system.

<u>*Potable Water*</u>

Unlike Apollo and Shuttle missions, the CEV is not currently expected to use fuel cells as a power source. As a result, there will be no fuel cell product water for use as a potable water source and all potable water must be included as part of the vehicle manifest. The water must also be maintained at potable levels, because while a CEV mission may only be planned for 18 CM-d, the long dormancy periods between occupations to and from the Moon would provide significant time for microbial growth in the system. The potable water storage in this design iteration assumes that water is stored in soft sided containers in single use amounts. The final design for the system needs significant development, but these estimates should be conservative. Each crewmember is allocated 2.6 quarts per day for drinking and food rehydration, as well as 0.5 quarts per day for hygiene. In this conservative estimate, each container is sized like a current drink bag, shown in Figure 9.2-3, and assumed to hold 0.26 quarts of water. At this size, each crewmember would have a morning and evening hygiene water allocation, and multiple containers of water to split between hot and cold water for multiple meals, snacks and beverages throughout the day. Larger quantities of water, possibly 0.5 quarts or 1.06 quarts per bag, would reduce packaging costs, but would make the bags multi-use, possibly leading to the crew sharing bags for hygiene or food rehydration water. The bags are assumed to be constructed of layers of materials, such as polyethylene on the inside for food grade compatibility, foil for a permeability barrier, and polyester for strength. Each bag is 9.6 in. tall, 3.9 in. across, and 0.63 in. wide when full. Each bag weighs 0.0235 lb and would be packaged with a straw that weighs 0.0077 lb.

Figure 9.2-3 Astronaut George Low uses a Drink Bag

This design does result in many bags to meet the total mission requirements, and managing stowage would be quite a hassle if each 0.26 quart container were stowed separately. In this concept, twenty-four small bags are packed into a soft sided bag like a Cargo Transfer Bag (CTB) shown in Figure 9.2-4 for a total capacity of 6.3 quarts per bag, with an additional polycarbonate layer in the base for strength. A lunar mission crew of four would require two of these larger bags in a day, and an ISS crew of six would require three bags. Stowage of all of the bags must be accessible to the crew, but for each day two or three new bags can be removed from stowage and placed where they are readily accessible. Two designs were developed, one concept which is twelve drink bags long and two drink bags wide with a divider down the middle, and a second concept which is twenty-four drink bags long and only a single row. These different shapes provide packaging flexibility where necessary. The two-row design is the most mass efficient.

Figure 9.2-4 Cargo Transfer Bags

The water bag design achieves several goals. First, the lightweight materials save approximately 50% of the mass compared to metal bellows tanks, as well as reducing or removing plumbing hardware. The packaging estimates are currently conservative assuming that each bag takes up an envelope as large as its bottom width, and that the bags cannot be alternated upside down and right side up. This packaging results in a volumetric efficiency similar to metal bellows tanks. Microbial control is also improved with a single use design. It may be possible to use these bags without any residual disinfectant, though it currently violates requirements in HSIR. If the water is sterilized and degassed when it is packaged, there should be no microbial contamination possible until use. However, these bags would also be compatible with a silver based residual biocide. In addition, the boxes of water bags provide significant packaging flexibility. The flight heritage large metal bellows tanks initially considered for water storage had a length large enough that they had to be centrally located in the bottom of the CEV, and a diameter large enough that they protruded into spaces that were required for seats. These containers can be stowed in many places throughout the CEV until needed. And the used drink bag containers can be returned to their original bag, which can be folded down or used to stow other dry trash. These bags would also be compatible with the requirement to support the crew for 120 hours in a depressurized cabin. The crew would use a drinking tube interface into the suit, and change to a new bag when the last one had been consumed. The water in the bags will be degassed, so the bags should not expand in a cabin that is at vacuum.

Other options were examined, including moving the metal bellows tanks to the SM portion of the CEV. The cold environment would require at least 25 W heaters on each tank to maintain temperatures above freezing in the cold environment inside the SM. Additional insulation mass, plumbing, and line heaters would also be required. This location would also add more complexity to the CM-SM separation by adding more umbilicals which would have to be severed upon separation. As a result, this option was rejected.

Water heating and cooling requirements must still be met with these bags. Inline heaters are not likely to be a good choice, and they would provide a place for growth of microbial life. The bags would not provide significant resistance to heat transfer. To meet cold water requirements of 60 °F, a cold plate surface is needed shortly downstream of where the fluid returns to the inside of the CEV CM from the radiators. The water bags would be strapped onto this plate, possibly with an insulating cover, to be chilled. To heat the water to slightly above ambient, a similar technique can be used with a cold plate just before the fluid is returned to the radiators. However, hot water temperature requirements for potable water are higher than the maximum vehicle fluid loop temperature. As a result, an electric heater is necessary. To provide the most efficient heating, a conformal unit, like an electric blanket, would provide maximum heat transfer with the bags. A hot water bag will likely exceed touch temperature requirements, but so would hot food, or hot water dispensed from a galley into a drink bag filled with instant coffee to make coffee. The high temperature is a desired result of the process.

A metal bellows water tank is still included in the system to provide water to the thermal control system for use as a heat rejection consumable in the Multi-Fluid Evaporator.

Waste Management System

The Waste Collector System (WCS) for the CEV was defined as the hardware to collect urine, feces, emesis, and female menstrual waste and the consumables (wipes and bags). The WCS was sized based on the requirements of the HSIR and experience from the shuttle and ISS WCS systems. This section defines the general approach and assumptions used in sizing the WCS.

Waste Production and Frequency

The lunar sortie CEV mission (Block 2) assumed four crew for a total of 18 days (nominal + contingency). The total crew-days was 72. Similarly, the ISS CEV mission (Block A) assumed six crew for 6 days resulting in a total of 36 crew-days. The maximum uncrewed mission was defined by an assumed 210 days of docked ops to the ISS. Therefore the limiting condition is 72 crew-days of crew use with 210 days of uncrewed time between use after launch and before return.

STS-104 was the flight of the ISS Risk Mitigation Experiment (RME) WCS which provided detailed data on individual defecation and consumables usage. Frequency of crew use is an important parameter in determining the quantity of wipes and other consumables required to be stowed. The WCS hardware sizing is less dependent on the frequency of crew use but more dependent on maximum use mass/volume. The frequency of defecation was based on Shuttle historical and STS-104 data. There are some minor discrepancies of average/maximum parameters between HSIR requirements and the STS-104 data. However, the STS-104 data provides additional data on frequency and consumables usage so it was utilize in order to have a consistent data set. It was anticipated that the discrepancies between historical values, STS-104 data, and HSIR requirements would be resolved at a future date and the current analysis refined. However, it is anticipated that the refinements would not modify the proposed approach significantly.

The average defecation rate of STS-104 and ISS planning is 1.0 defecations/crew day but there is considerable variation among crew members. Historically, Shuttle has used 1.5 defecations per day for planning and this has always resulted in sufficient consumables and was used for the initial CEV design reference mission sizing. (A comment was recently included in review of the HSIR to establish a requirement of 1.2 defecations per crew-day for planning.)

Defecation values used in initial sizing:

- 1.5 defecations per crew-day.
- 108 defecations per Block 2 mission
- The average defecation mass was assumed to 0.25 lbm per use.
- 39 lbm of fecal and wipes per Block 2 mission

Urine parameters were based on historical values event though there are minor discrepancies with the HSIR. Urine frequency was not defined in the HSIR. (A comment was recently included in review of the HSIR to establish a requirement of six urinations per crew-day for planning.)

Urination values used in initial sizing:

- Seven urinations per crew-day (historical planning value)
- 504 urinations per Block 2 mission
- An average of 400 mL per crew use
- Average of 202 L of urine per Block 2 mission
- Average of 471 lbm mass for urine and wipes per Block 2 mission

Technology Selection Criteria

An analysis of previous WCS technologies was conducted to determine which technology components were best applicable to the CEV mission profile. Technology was broken into four categories:

- Urine pretreatment (stabilization and precipitation prevention)
- Air system (air movement and odor control for capture of urine and/or fecal)
- Urine collection (collection and separation)
- Fecal collection (collection and storage)

The analysis covered the following hardware systems:

- Gemini/Apollo (only IVA non-crew worn systems)
- Skylab (limited information available and not included in analysis. Did not appear to have any unique attributes applicable to CEV – primary focus was science collection.)
- Shuttle WCS (did not include Shuttle waste tanks, trash volumes, and venting hardware)
- Shuttle Extended Duration Orbiter (EDO)/RME WCS (did not include Shuttle waste tanks/volumes, trash volumes, venting hardware)
- Soyuz ACY
- ISS SM ACY (similar to late MIR ACY configuration)

The hardware configurations were scaled to the CEV Block 2 mission and compared on a total mass and volume basis and performance/crew parameters. The performance/crew parameters considered the following:

- Collection systems shall provide acceptable urine/fecal collection for both male and female crews
- Odor control is an essential requirement (i.e., air flow is required)
- Urine pretreatment should be avoided if possible to reduce change of chemical exposure in small crew volume
- Fecal material should be transportable to another vehicle
- System should be scaleable/adaptable to future vehicles

None of the hardware systems provided a clear advantage for CEV. Each system had a different technology or performance strength. The below chart in Figure 9.2-5 summarizes the lowest mass/volume parameters with green circles for each technology.

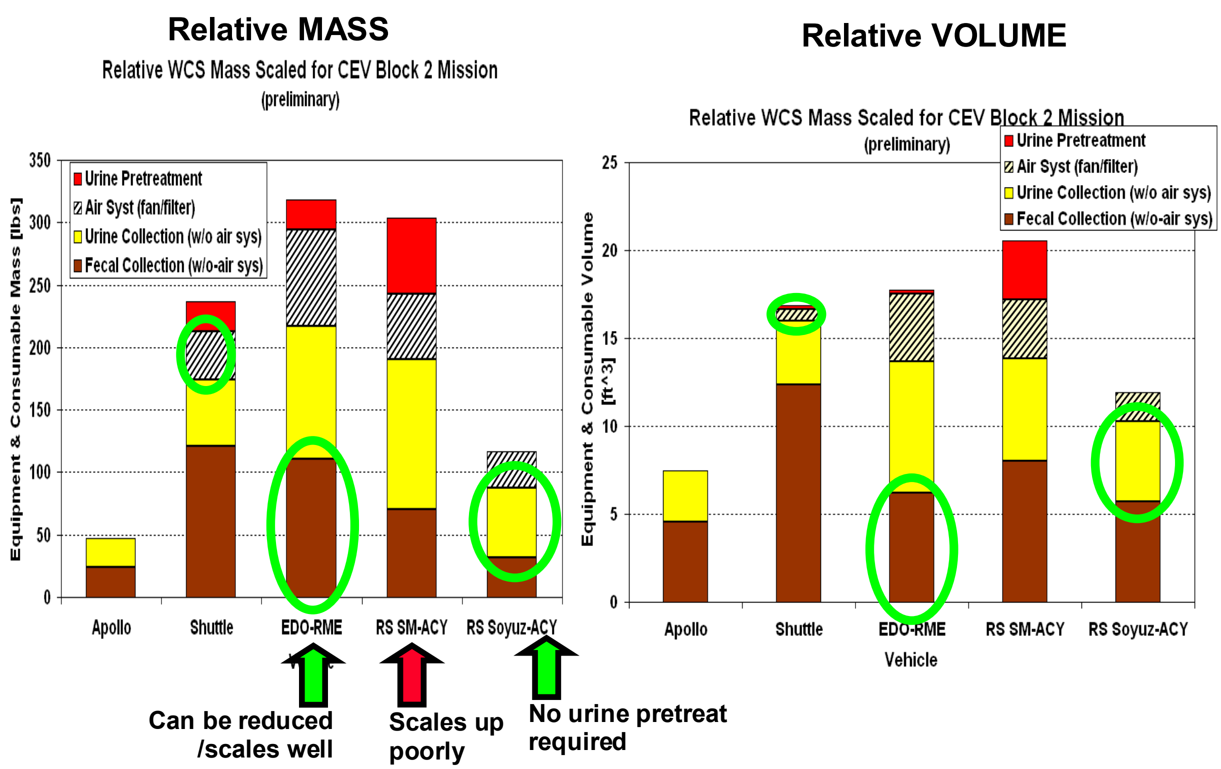

Figure 9.2-5: Relative WCS Technology Efficiency Scaled to CEV Mission

A similar analysis of fecal storage on a per defecation basis was performed because it separated the fecal collection from the fecal storage/capture systems. The results are shown in Figure 9.2-6.

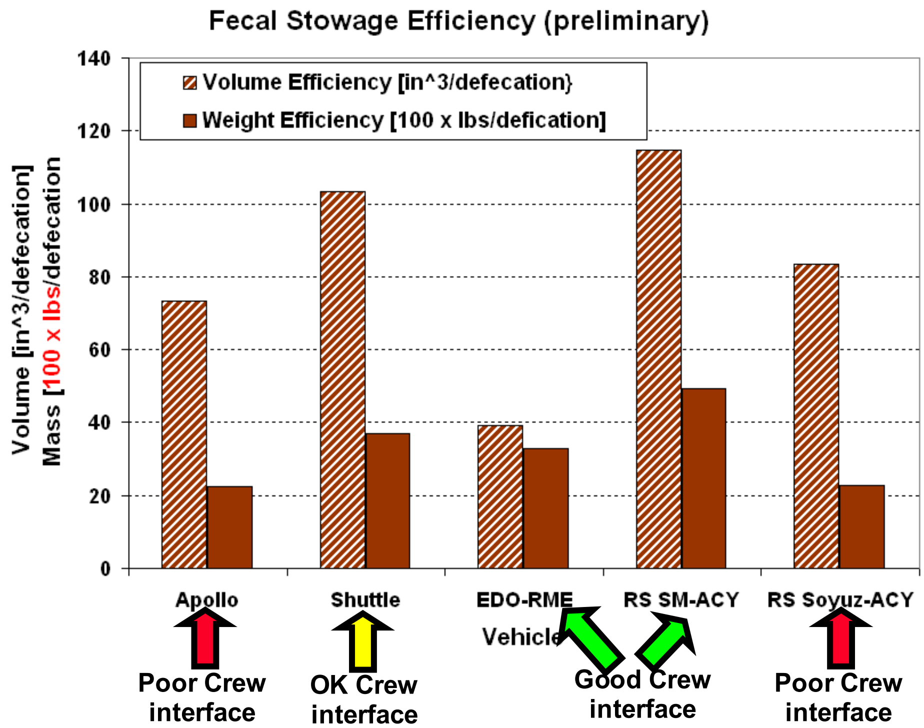

Figure 9.2-6 Relative Fecal Container Storage

Conceptual CEV WCS Configuration

Based on the above analysis results, a conceptual WCS configuration was developed utilizing the portions of several hardware configurations to utilize the technology and performance characteristics most advantageous to CEV. The concept was presented at a January 2006 CEV WCS brainstorming meeting with past WCS project managers and was agreed to with minor modifications. The rational in the current conceptual CEV WCS configuration are listed below.

- Apollo fecal bags were 'distasteful' to the crew. They required up to 45 minutes per use, were unhygienic because the fecal material often contacted the crew and surroundings, and provided no odor control.
- Apollo urine collection using the Urine Receptacle Assembly (UTA) worked well for male crew members but would not work well for female crew due to the reduced female velocity vector. The system did not require pretreatment and vented overboard.
- Shuttle fecal collection is volumetrically intensive because there is no compaction and wipes must be disposed of separately. The crew positioning on the seat can be challenging due to the relatively small opening and the single common tank is unhygienic. The shuttle fan and odor bacteria filter are relatively compact.
- The Shuttle, EDO-RME urine, and Russian SM-ACY collection require pretreatment because of the rotary separators and urine is stored for several days.

- The Shuttle EDO-RME fecal system has a good interface for the crew due to a larger opening, individual fecal collection bags. The system also has the good volume due to compaction but mass is larger due to automatic compaction feature.
- The Russian SM ACY is a fixed container system that does not scale well. It does have good crew interface due to individual fecal bags and large opening (similar to EDO-RME WCS openings).
- The Russian Soyuz system has an adequate urine interface for both male and females. The system does not require pretreatment because it uses a urine adsorber system that is particulate insensitive. The Russian urine system is not regenerable.
- The Russian Soyuz system has a fecal collection system that uses bags but requires extensive crew expertise for positioning, post use handling, and is considered unhygienic. The crew reportedly strongly avoids using it and no actual mission use data was available.

Based on the assessment the following system is conceptually proposed for CEV WCS. The following technology ration was used:

- It assumes a Shuttle/EDO-RME urine collection system with airflow. This provides acceptable urine capture and odor control for both male and female crew.
- It assumes static urine separator based on Apollo URA (capillary vent system but adapted for air flow) or Russian Soyuz urine adsorber (regenerable hydrogel but with vacuum exposure). The capillary and hydrogel systems could be used independently or in a combined mode to ensure separation. Both of these separator technologies hold a lot of promise because they remove the rotary separator and pretreatment hardware. EC3 is providing limited conceptual investigation in FY06 and is proposing additional effort in these areas for FY07-08.
- Assume urine venting overboard similar to Shuttle and Apollo.
- Assume EDO-RME style fans (quieter than Shuttle) and odor bacteria filters. Reduces redundancy from EDO-RME to closer to Shuttle configuration. Assume common air system for both urine and fecal collection.
- Assume EDO-RME fecal collection canister due to compaction efficiency, transportability of waste, odor control, hygienic concerns, and crew usability.

The conceptual CEV WCS uses a common air system for urine/fecal, a fecal collection system based on EDO/RME (except manual compaction), and a primary urine path with a static separator that can hold a limited quantity of urine for a short time (such as docked time) but vents overboard.

For contingency operations a direct urine vent overboard is provided (adoption of Apollo-like usage) with additional wipes/glove consumables for female use. The contingency fecal collection is with the EDO/RME canister but with additional wipes/gloves. During contingency operations odor control and crew usability will be degraded but hygienic capability will largely be maintained with minimal increase in consumables.

The technology would be expandable to future low gravity vehicles by replacing the static separator with a low gravity separator that could be plumbed to a water recovery system. The fecal system is expandable, and allows storage, odor control, and transport to future vehicles.

The estimated weight is 115 lb and 7.8 ft^3 for equipment. This represents a reduction of ~60 % in mass and 50% in volume for similar functionality with existing hardware solutions (EDO-RME WCS).

The proposed approach requires technology development in the following areas:

- Urine static separator with capillary forces.
- Urine adsorbing hydro gels that are reusable.
- Manual fecal compaction and compatibility with additional wet trash.

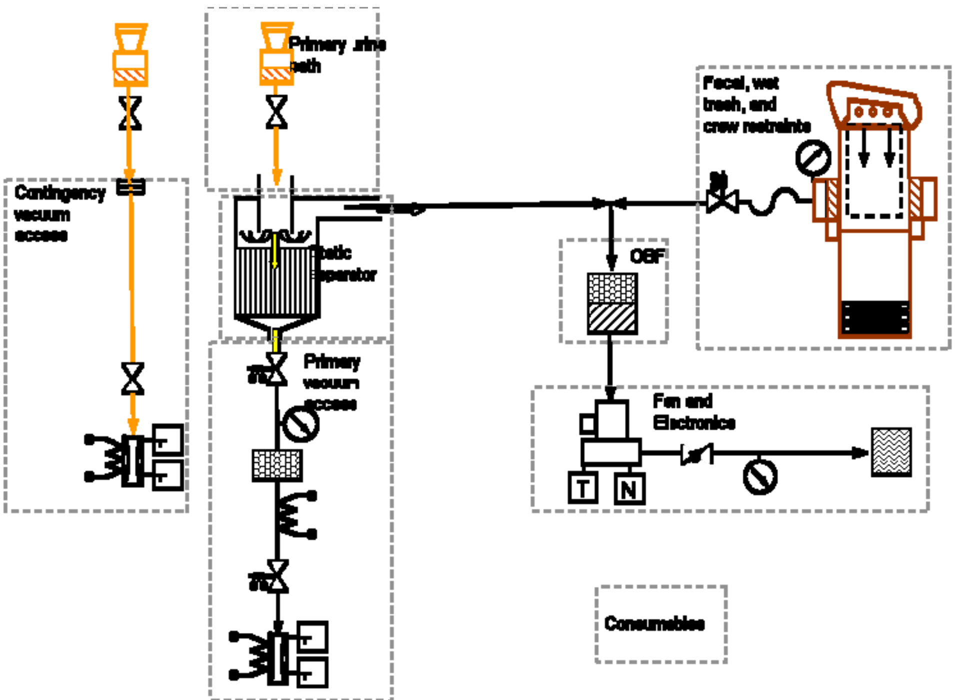

Figure 9.2-7 Waste Management System Schematic

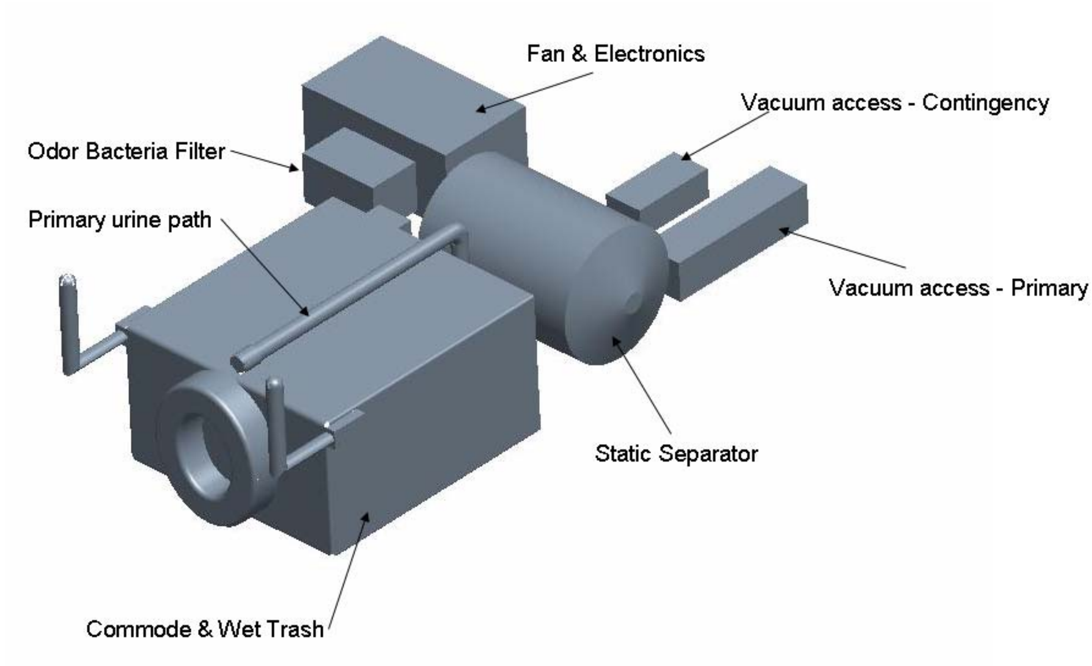

Figure 9.2-8 Conceptual Packaging of WCS Components

9.2.2.4 Fire Detection and Suppression

The fire detection and suppression approach is split depending on whether the event is in the primary crew cabin or inside an avionics bay or other piece of installed equipment segregated from the crew cabin. For events in the crew cabin, the air flow in the cabin can help bring the products of combustion reactions to the fire detector. The crew should be able to access fire extinguishers and the site of the fire and actively suppress it. For events in an avionics bay or other similar location, the air flow required to bring the evidence of a fire to a detector would actually create greater risk by moving oxygen to the fire. In this case, temperature sensors, over-current sensors, and other signals of malfunctioning equipment provide the evidence that there is a fire or fire risk such as a short circuit. The crew most likely will not be able to quickly or easily access the location of the fire. In many cases, removing power to the area, and keeping the bays closed so that more oxygen is not provided to the fire will suppress it. If not, automated or remotely controlled systems are necessary to provide active suppression.

In the crew cabin, design choices had to be made to select fire detectors and a fire suppression agent. In previous flight experiences, having sensors based on a single type of measurement for fire detection created issues with false alarms. For the CEV, the proposed system would use multiple measurement types within each fire detection unit to prevent false alarm events, and provide redundancy. The sensors proposed are being developed at Glenn Research Center, and provide measurements of CO, CO_2, HC, H_2, and H_2O, as well as particulate levels. The proposed fire suppression agent for cabin emergencies is a water foam fire extinguisher, similar to what is currently used in Russian designs on the ISS. The CEV power bus level is set at 28 Vdc, which reduces some risk of using water in the cabin. Water can also be removed from the cabin by the amine swing beds, and does not pose a great health threat if the humidity levels are raised after fire suppression activities.

In the avionics bays, three valves are currently allocated to provide a release of nitrogen from the vehicle stores to suppress fires. In segregated bays, many avionics fires will quickly consume the available oxygen and be suppressed naturally. If this is not sufficient, the nitrogen flood would flush any remaining oxygen. These valves must be automated since by definition they are installed in areas the crew cannot access.

9.2.3 Mass Estimates and Design Maturity

Most of the mass and dimension data for the ECLSS system design come from several sources. Where possible, they are based on flight components from Shuttle or ISS design, though the components may be scaled to estimate the size of a similar design for a different performance requirement. In some subsystems, the design concept utilizes existing flight equipment in new ways or new combinations. And finally, some data comes from prototype technologies being developed for the CEV.

9.2.3.1 Air Revitalization Mass Estimates and Design Maturity

The mass properties for the air revitalization components are shown in Table 9.2-3. The air revitalization hardware has a broad range of data sources. The amine swing bed information is based on high fidelity prototype data from the technology developer, Hamilton Sundstrand, and is related to the design of the Shuttle Regenerable Carbon Dioxide Removal System (RCRS) design, and is considered fairly mature. The TCCS bed design has been developed through analysis of flight material performance, but the design is immature. Most of the other components are based on scaling existing flight hardware. The technology for these components is mature, but there is some risk that the final sizes may change.

Hardware Items	Quantity	Unit Mass (lbm)	Growth (%)	Total Mass (lbm)	CM Mass (lbm)	SM Mass (lbm)	Basis of Estimate
ECLSS - Air Revitalization System				**235**	**233**	**2**	
HEPA Filters	2	1	5%	2.1	2.1		
Internal Cabin Ducting	1	9	5%	9.4	9.4		
Post Landing Ventilation Valves	2	2	5%	4.2	4.2		
Guard Bed	1	33	20%	39.7	39.7		
Compressors	3	4	15%	14.1	14.1		
Amine Swing Bed Manual Shutoff Valves	10	1	15%	11.5	11.5		
Amine Swing Beds	5	16	15%	91.4	91.4		
Cabin Inlet Valve	1	2	15%	2.3	2.3		
Valves to Select Nitrogen Sweep	3	1	15%	3.5	3.5		
Cabin Outlet shutoff valve	1	2	15%	2.3	2.3		
Humidity Vent Line Heater	1	1	15%	1.5	1.5		
Vent Line	1	11	15%	13.1	13.1		
Internal Cabin Ducting	1	30	15%	34.7	34.7		
Nitrogen Sweep Lines - CM	2	2	15%	3.5	3.5		
Nitrogen Sweep Lines - SM	1	2	15%	1.7		1.7	

Table 9.2-3 Air Revitalization System Mass Estimates

9.2.3.2 Pressure Control Mass Estimates and Design Maturity

Almost all of the components of the pressure control system, listed in Table 9.2-4 are sized by taking comparable components from Shuttle Orbiter designs. The CEV design is required to operate at multiple pressures and oxygen concentrations, so there is some risk that the component design might have to be changed.

Hardware Items	Quantity	Unit Mass (lbm)	Growth (%)	Total Mass (lbm)	CM Mass (lbm)	SM Mass (lbm)	Basis of Estimate
ECLSS - Pressure Control System				**734**	**205**	**529**	
Gas in Cabin at Launch	1	51	0%	50.5	50.5		
CM Oxygen	1	0.5	0%	0.5	0.5		
Oxygen Surge Tank	1	5	20%	5.6	5.6		
SM Oxygen	1	165	0%	164.5		164.5	
Oxygen Storage Tank	2	63	20%	151.2		151.2	
Insulation, Valves, and TPS - O2	1	23	15%	26.5		26.5	
Nitrogen	1	84	0%	84.1		84.1	
Nitrogen Tank	1	63	20%	75.6		75.6	
Insulation, Valves, and TPS - N2	1	23	20%	27.6		27.6	
Pressure Controller	1	15	20%	18.0	18.0		
Negative Pressure Relief Valve	2	1	15%	2.3	2.3		
Positive Pressure Relief Valve	2	1	15%	2.3	2.3		
Vent Valve	1	2	15%	2.3	2.3		
Controlled N2 Valves	3	4	15%	13.8	13.8		
Controlled O2 Valves	3	4	15%	13.8	13.8		
Check Valves	4	1	15%	2.3	2.3		
Emergency Feed Pressure Regulator Valve	1	4	15%	4.6	4.6		
Demand Regulator	2	1	15%	2.3	2.3		
Suit Loop Purge Valve	2	4	15%	9.2	9.2		
Docking Vent Valve	1	1	15%	1.2	1.2		
Docking Pressure Equalization Valve	2	1	15%	2.3	2.3		
Docking Pressure Equalization Tubing	1	0	15%	0.3	0.3		
Umbilical Interface Panel (EVA Spots)	2	12	15%	27.6	27.6		
Umbilical Interface Panel (IVA Only Spots)	4	8	15%	36.8	36.8		
Umbilical Interface Panel (Contingency Lines)	1	4	15%	4.6	4.6		
Medical Oxygen Interface	2	2	15%	4.6	4.6		

Table 9.2-4 Pressure Control System Mass Estimates

9.2.3.3 Water and Waste Management Mass Estimates and Design Maturity

The water and waste management system, shown in Table 9.2-5, both are new design concepts with mass estimates based on existing flight technology. For the water system, the bag mass estimates are based on flight certified ISS drink bags and the materials used to create Cargo Transfer Bags. In the waste components, flight data on usage was combined with flight components from various systems to create a concept optimized for CEV applications. As a result, the confidence in these design estimates is high.

Hardware Items	Quantity	Unit Mass (lbm)	Growth (%)	Total Mass (lbm)	CM Mass (lbm)	SM Mass (lbm)	Basis of Estimate
ECLSS - Water and Waste Management				**719**	**719**	**0**	
Potable Water	1	485	0%	485.0	485.0		
Water Boxes	37	3	0%	96.0	96.0		
Water Heater and Accumulator	1	15	0%	15.0	15.0		
Toilet and Urinal System	1	115	5%	120.5	120.5		
Wastewater Vent Line	1	2	15%	1.7	1.7		
Wastewater Vent Line Heater	1	1	15%	1.2	1.2		

Table 9.2-5 Water and Waste Management Systems Mass Estimates

9.2.3.4 Fire Detection and Suppression Mass Estimates and Design Maturity

Mass estimates for the components of the fire detection and suppression system are listed in Table 9.2-6. The fire detectors proposed for the CEV here are still in development, but the mass estimates included are intended to be conservative. The water foam fire extinguishers are based on flight manifested Russian designs. A design certified for Exploration missions would still need to be developed. The fire suppression mass estimates for the avionics bays are based on powered flight valves to release the N_2 gas.

Hardware Items	Quantity	Unit Mass (lbm)	Growth (%)	Total Mass (lbm)	CM Mass (lbm)	SM Mass (lbm)	Basis of Estimate
ECLSS - Fire Detection & Suppression				**52**	**52**	**0**	
Fire Detectors	4	4	5%	18.5	18.5		
Water Foam Fire Extinguishers	2	9	5%	19.4	19.4		
Nitrogen Release Valves	3	4	15%	13.8	13.8		

Table 9.2-6 Fire Detection and Suppression Mass Estimates

9.2.4 Plan Forward

The CEV Reference Configuration design work is drawing to a close after prime contractor selection. Regardless of the designer, forward work for ECLSS design will primarily be in three categories. The first category will be work to update the design to include requirements changes. The second category of work will be updating the design to respond to changes in interfacing subsystems. And finally, future work will include maturation and further trade studies to optimize the CEV ECLSS design.

Emergency and contingency related requirements have undergone significant changes between the second and third design cycles of this study. Fire, feed the leak, and repressurization requirements seem to be stable and met in this design. Current activity is focused on determining the best way to meet emergency mask requirements to provide crewmembers breathing air during fire or toxic release events.

The CEV ECLSS design must respond to changes in the other vehicle designs. One important example of this is the maturation of space suit and crew survival system designs for the CEV. Manifolds, regulators, and other components may be impacted by development of space suit design concepts, or maturation of the concept of operations for EVA or crew survival activities. Major trade studies are still ongoing to determine whether EVA umbilicals should be high pressure or low pressure, and whether they are open or closed loop.

Future work to optimize the CEV design primarily focuses on mass and volume savings. Many of the highest priority trades were already performed and included in this design. Current trade studies include examining advanced trace contaminant control methods. Further refinement of water storage issues may also be conducted to optimize the CEV ECLSS design.

9.3 EVA and Crew Survival

This document is being provided to capture the current NASA conceptual design for the Constellation Program's Crew Exploration Vehicle (CEV) with respect to vehicular interfaces and hardware provided to support the Extravehicular Activity (EVA) System. This document is intended to give the CEV Prime contractor insight into NASA's CEV conceptual design in this area. Note that this information is not being provided nor should be used as CEV prime contract direction, but should be used as an aid during the prime contractor's design development process. For questions on the content of this document or to check for updated information, please contact the NASA CEV Project Office and/or EVA points of contact - J. Marmolejo (281-483-9233) or J. Davis (281-244-9070).

The Extravehicular Activity (EVA) System provides both crewmember protection and mobility to work effectively in the CEV pressurized/unpressurized and thermal environments which include contingency and unscheduled extravehicular excursions and unplanned vehicular depressurizations. The EVA System currently consists of the following:

- Launch/entry/abort and EVA pressure suits and corresponding life support equipment
- Suit donning and other crew aids
- EVA tools and crew mobility hardware
- Vehicle support systems
- Crew survival equipment (only that integrated to the pressure suit)
- Ground support systems

The purpose of this document is to capture NASA's conceptual design in the following areas:

- Section 9.3.1 – Driving Requirements, Groundrules, and Assumptions
- Section 9.3.2 – Conceptual Design Overview
- Section 9.3.3 – CEV Master Equipment Listing (MEL)
- Section 9.3.4 – Forward Plan and Possible Design/Capability Changes

9.3.1 Driving Requirements, Groundrules, and Assumptions

9.3.1.1 Driving Requirements

Driving requirements for the EVA and Crew Survival System are captured in Table 9.3-1. Note that these requirements are the Interim Constellation Program Review (ICPR) version and have been modified since then (e.g., requirements combined, updated, etc.). The latest version will be those released for the Constellation SRR.

Doc + No.	Requirement	Rationale
CARD 3.2.2.2	Crew Survival Probabilities The Constellation Architecture System shall ensure that no combination of two failures, except for areas approved to use Design for Minimum Risk Criteria, or two operator errors, or one of each can cause a critical hazard. [CA0214-PO]	Two Fault Tolerance protects against catastrophic failures and is dictated by programmatic decision to ensure mission safety. The Constellation Program Office will define levels of fault tolerance that are satisfied by multiple elements and the allocations to those elements. This does not preclude more than the minimum level of fault tolerance.
CARD 3.3.4 [CA0355-PO]	Human Engineering The Constellation Architecture shall provide flight and ground crew human interfaces in accordance with the CXP-01000 Human-Systems Integration Requirements (HSIR). [CA0355-PO] Note: New Document # CxP 70024	Capabilities and limitations of the flight and ground crew should be considered in designing Constellation Architecture elements to give the greatest chance of achieving mission objectives.
CEV SRD 3.3.8.3 [CV0286]	Crew Anthropometric, Biomechanical, and Strength Constraints The CEV shall accommodate the crew anthropometric, biomechanical, and strength constraints in accordance with the CXP01000, Human Systems Integration Requirements (HSIR), section 2. [CV0286]	This requirement presents the CEV-relevant design requirements on human physical dimensions, ranges of motion, and strength.
CARD 3.7.1.6 CA0060-HQ	Mission Rates and Durations The CEV shall remain at the ISS during a nominal 180 day ISS crew increment with the capability to support up to 210 days at the ISS for contingency situations. [CA0060-HQ]	This requirement reflects the crew to ISS mission mode decision. The CEV is used to transport the crew to ISS, remains with the crew during their stay at the ISS, and returns the crew from the ISS either at the end of the nominal mission, or early for contingency situations. The CEV may not be attached to the ISS during the entire crew increment due to ISS mission operations (such as CEV relocation to another port).
CEV SRD 3.4.6 [CV0379]	Suit, EVA and Survival Crew Equipment Interface The CEV shall meet interface requirements defined in CXP-01009, CEV to Suits, Extra Vehicular Activity (EVA) and Survival Crew Equipment Interface Requirements Document (IRD). Note: New Document # CxP 70033	The CEV will need to interface with the launch/entry and EVA suit (s) by providing suit/umbilical interfaces for providing power, oxygen, water, cooling, contaminant control and communications, airlock or vehicle depressurization/repressurization system interfaces, support of EVA hatch design and mechanisms, specialized CEV-specific EVA tools, internal seat and control interfaces, and external devices, restraints and mobility aids.

Doc + No.	Requirement	Rationale
CARD 3.2.2 [CA0107-HQ]	Crew Survival The Constellation Architecture shall provide crew survival capabilities through each mission phase.	The CA uses robust designs (i.e. ballistic entry), safe haven, emergency egress, and aborts as techniques to provide for crew survival. Each mission phase will utilize different techniques. For example, while on the pad, emergency egress to a safe haven or a pad abort may be used. During ascent, the CEV may perform an ascent abort or an abort to orbit. The CEV may also perform and early return/abort from LEO and during lunar transit. For lunar landings, the LSAM may perform an abort back to orbit. After TEI, there is no abort because you are already on way home. During Entry, Descent, & Landing there is no abort but a ballistic entry in the event of loss of primary power or attitude control.
CARD 3.2.2.1	Crew Survival Probabilities The Constellation Architecture shall support suited crew in an unpressurized cabin for return to Earth from any point in the mission. [CA0530-PO] The CEV shall support suited crew in an unpressurized cabin for return to Earth from any point in the mission. [CA0532-PO] The CEV shall support a suited crew in an unpressurized cabin to return safely from any point in mission. [CA0495-PO]	Supports contingency EVA operations for cabin leaks during ascent or orbit operations. The maximum duration required for return to Earth from any point in a lunar mission is 120 hours (TBR-001-005). Allocation of CA0352-HQ. Also protects for adequate consumables needed for potential contingency EVA scenarios. The number and length of EVA will be determined as vehicle design matures. The number of crewmembers required to perform an EVA is usually dependent on the contingency scenario; however all crewmembers will need to be in pressure suits.
CEV SRD 3.2.2.6.1.9 [CV0081]	Unpressurized Operations The CEV shall operate in flight in an unpressurized state for not less than 120 (TBR-002-036) hours.	Supports contingency EVA operations. Also includes contingency operations for cabin leaks during ascent or on orbit. 120 hours supports maximum duration required for any point return to Earth. Crew members will be suited during this 120 hours so power, communications, & life support will be provided for suited operations.
CEV SRD 3.2.2.6.1.9.1 [CV0448]	Unpressurized Crew Survival The CEV shall provide hydration, oxygen, atmospheric conditioning, power and communication to the suited crew in an unpressurized environment state for not less than 120 hours (TBR-002-036). [CV0448]	This emergency capability is necessary to support contingency operations for cabin leaks during ascent or on orbit to enable the survival of four crewmembers. 120 hours supports maximum duration required for any point return to Earth during a lunar mission. This capability may also be used to support contingency EVA operations.
CEV SRD 3.2.2.2.3 [CV0029]	Suited Crew Emergency Egress The CEV shall provide for unassisted pre-launch emergency egress for 6 (TBR-002-030) suited crewmembers in not greater than 120 seconds (TBR-002-157) starting from egress initiation to complete crew egress from vehicle.	Flow down from NPR 8705.2 requirements 3.9.1. For contingency situations, where no ground crew is immediately available, the crew will need the capability to egress the vehicle for safety reasons. This should drive design of seat restraints and hatch mechanisms and egress paths in the pre-launch orientation to allow the crew to egress without ground crew assistance. On the launch pad there may be hazardous conditions that preclude return of ground crew to the launch pad in a timely enough fashion to assist the crew in egress, but that do not in fact warrant use of the launch abort system, which is in itself a hazardous operation with its own inherent safety risks to crew survival.

Doc + No.	Requirement	Rationale
CARD 3.7.1.8.7 [CA0194-PO]	CEV Return and Recovery The CEV shall provide for crew survival for at least 36 hours (TBR-001-045) following landing. [CA0194-PO]	This capability represents an estimate of the maximum reasonable time the crew would spend in the CEV post-landing in water. It is presumed the CEV power requirements for this phase would be a fraction of that required for the active mission and would probably only provide basic ventilation and emergency systems. The requirement was developed for water landing to address the design case for the developers. The crew survival capabilities will also be available for land based touchdowns but that is not the driving case for design.
CEV SRD 3.2.2.9.1.6 [CV0093]	Crew Survival Following Landing The CEV shall provide for crew survival for at least 36 hours (TBR-002-009) with the hatch closed following landing.	This capability represents an estimate of the maximum reasonable time the crew would spend in the CEV post-landing in water. It is presumed the CEV power requirements for this phase would be a fraction of that required for the active mission and would probably only provide basic ventilation and emergency systems. The requirement was developed for water landing to address the design case for the developers. Crew survival includes emergency gear such as life raft, clothing, water survival equipment, radios, signal devices, tracking/homing devices, food and water. The crew survival capabilities will also be availability for land based landings but that is not the driving case for design.
CARD 3.2.12 [CA0181-PO]	EVA The Constellation Architecture shall provide the capability for contingency EVA operations. [CA0181-PO].	Contingency EVA capability was specifically identified by the Operations Advisory Group (OAG) as a high priority capability. For example, contingency EVA is considered for situations where the vehicles have achieved a sufficient structural attachment during docking but the pressure in the vestibule between vehicles cannot be maintained.
CEV SRD 3.2.2.6.1 [CV0072]	Contingency EVA The CEV shall provide for contingency EVA operations. [CV0072]	This capability is required for contingency scenarios to ensure safety and mission success.
CEV SRD 3.2.2.6.1.8 [CV0080]	CEV Cabin Repressurization Cycles The CEV shall provide not less than two (TBR-002-088) repressurization cycles, from unpressurized state, per mission.	CEV needs to support Contingency activities for LEO operations, Earth-Moon Transit operations, and lunar orbit operations.

Doc + No.	Requirement	Rationale
CEV SRD 3.2.1.1.1.8 [CV0446]	Scientific Cargo The CEV shall provide 20 (TBR-002-169) cubic feet of volume for accommodating science, engineering demonstrations, development test objectives, and deployment of lunar infrastructure elements during the cruise and lunar orbit phases of lunar missions. [CV0446]	This capability would be similar to the capability provided by the Apollo Service Module Scientific Instrument Module (SIM) Bay. The goal would be to provide a flexible capability to support a myriad of scientific and engineering activities that may vary from mission to mission. Fields of study that may leverage this capability include: lunar surface mapping, lunar gravity field mapping, space environment measurements, evaluation of environmental exposure of materials and/or components planned for future missions, and infrastructure elements such as navigation or communication satellites that could be deployed from the CEV. The support of cargo capability is secondary in priority to design and layout of propulsion systems.
CARD 3.2.12 [CA0202-HQ]	EVA The Constellation Architecture shall support the capability to perform lunar surface EVAs. [CA0202-HQ]	Identifies the need for lunar sortie and outpost crews to have the capability to leave the lander to perform activities related to accomplishing mission objectives. The number of EVA crew-hours and the distance that the EVA crewmembers need to traverse will be established through analysis of specific mission objectives.
CARD 3.2.12 [CA0022-PO]	EVA The Constellation Architecture shall support the capability to perform lunar surface EVAs with all crewmembers or a partial set of crewmembers.	Lunar EVAs may typically be performed in teams of 2 crewmembers. However, the lunar architecture must be capable of supporting lunar surface EVAs with all crewmembers.
CARD 3.2.12 [CA0287-PO]	EVA The Constellation Architecture shall provide the capability for the astronauts to traverse distances on the lunar surface of at least 5.4 nmi (10 km) from the landing point for lunar sortie missions.	Traverse capability needed to satisfy exploration and operational objectives
CARD 3.2.12 [CA0407-PO]	EVA The Constellation Architecture shall provide the capability for the astronauts to traverse distances on the lunar surface of at least TBD-001-013 nmi from the outpost for Lunar Outpost missions.	Exploration of the surface of the Moon is an essential element of the Vision for Space Exploration. The surface mobility strategy for outpost missions is still in development and will probably include combinations of EVA suits, unpressurized rovers, and pressurized rovers. In addition, the hub and spoke outpost strategy (see DRM description for lunar outpost) can extend the effective exploration range for the astronauts while still satisfying safety (walk back) requirements, thus the range for outpost missions is currently undefined.
CARD 3.7.1.6 CA0082-P0	Mission Rates and Durations The CEV shall operate without a crew in LLO for up to 210 days.	The Lunar Outpost Crew missions call for the CEV to loiter in LLO while the crew goes to the lunar surface. In addition, the Lunar Outpost Crew DRM calls for providing the capability for continuous human presence and mission intervals of two per year. Overlapping of crews will be required for handoff activities. An operational capability of 210 days provides additional overlap and contingency time.

Doc + No.	Requirement	Rationale
CARD 3.7.3.6 CA0842-PO	Mission Rates and Durations The LSAM shall remain on the lunar surface from up to 210 days during outpost missions. [CA0842-PO] The LSAM shall loiter up to 95 days (TBR-001-030) prior to TLI. [CA0839-PO]	LSAM needs to be able to survive on lunar surface for duration of outpost missions LSAM needs to be able to survive on-orbit for a sufficient period of time to allow launch attempt of CEV for two monthly windows following initial launch attempt.
CARD 3.2.2 [CA0203-HQ]	Crew Size The Constellation Architecture shall provide the capability to deliver 2, 3 and 4 crew to the lunar surface and return them safely to Earth. [CA0203-HQ]	Establishes a baseline crew size for both sortie and outpost lunar operations. A four-person crew delivered to the lunar surface is the minimum number required to demonstrate operations concepts for exploring more distant destinations such as Mars. A four-person crew allows two surface EVA teams (two crew per team) to operate simultaneously or in series while providing the capability for operational assistance from the non-EVA crew. There may be excursions from normal operations where fewer (test flights) crewmembers are flown.
CARD 3.2.4 [CA0020-HQ]	Crew Size The Constellation Architecture shall support at least 4 (TBR-001-010) crewmembers per rotation at the Lunar Outpost . [CA0020-HQ]	A four-person crew is the minimum number required to demonstrate operations concepts for exploring more distant destinations such as Mars. A four-person crew allows two EVA teams (two crew per team) to operate simultaneously or in series while providing the capability for operational assistance from the non-EVA crew. Total crew size at the Lunar Outpost could be 8 during operational handover periods.
CARD 3.2.13 [CA0208-HQ]	Destination Surface Support The Constellation Architecture shall provide the capability to perform Lunar Sortie missions without the aid of pre-deployed lunar surface infrastructure. [CA0208-HQ]	Independence from pre-positioned infrastructure will allow for early mission execution and enhanced flexibility in selecting landing sites and executing sortie missions. This requirement does not prohibit the execution of sortie missions which may utilize landing near assets previously deployed by either robotic or human missions. In some cases, landing nearby to previously deployed assets may be utilized to fulfill specific mission objectives.
CARD [CA0005-HQ]	Destination Surface Support The Constellation Architecture shall provide the capability to establish and support a permanently habitable outpost on the lunar surface. [CA0005-HQ]	Required to achieve Constellation Program Goal CxP-G11: "Develop the capability for a sustainable and extensible permanent human presence on the Moon for commercial, national pre-eminence and scientific purposes leading to future exploration of Mars and beyond."
CARD [CA0014-HQ]	Destination Surface Support The Constellation Architecture shall establish a lunar outpost located within 5 degrees latitude of the lunar South Pole (TBR-001-009). [CA0014-HQ]	Polar regions of the moon present unique opportunities for lunar resource utilization, scientific investigations, advantages for transportation system flexibility, efficiency. Specific outpost site selection criteria will be developed and documented in a separate TBD-001-009 HQ controlled document as was done during Apollo.

Table 9.3.1 EVA System Driving Requirements

9.3.1.2 Groundrules

1) All EVA System equipment is provided as government-furnished equipment (GFE). A contractor response to a single suit system architecture has been requested by the Constellation Program (see Section 9.3.2.1).
2) All «personal» crew survival hardware is provided as GFE.
3) CEV suit resources (e.g., oxygen/breathing gas, cooling, communications, etc.) are provided via an umbilical interface for each crewmember.
4) The umbilicals are provided as GFE. Seat (i.e., «short») umbilicals are utilized for launch/entry/abort operations; while, EVA (i.e., «long») umbilicals are provided for contingency EVA.
5) EVAs are performed via umbilical by two crewmembers, excluding transfer events.
6) Radio Frequency (RF) communications to the EVA crewmembers is not provided by the CEV.
7) For ISS missions, ISS EVA suits and resources are utilized for conducting an EVA for CEV contingencies.
8) For Lunar missions, a known contingency EVA is the crew transfer from the Lunar Surface Ascent Module (LSAM) to the CEV.

9.3.1.3 Assumptions

The government reference configuration assumes that an umbilical interface assembly (UIA) is provided as GFE and provides access to the CEV resources and controls to support suited operations. It is envisioned that this assembly will be common to all vehicles and will provide the desired feature to be able to utilize the same quick disconnect feature on both the vehicle and suit sides of the umbilical (important for the LSAM return to the CEV EVA scenario). This UIA will physically mount to the CEV-provided umbilical interface panel (UIP). A sketch of the UIP/UIA interfaces is provided in Figure 9.3-1.

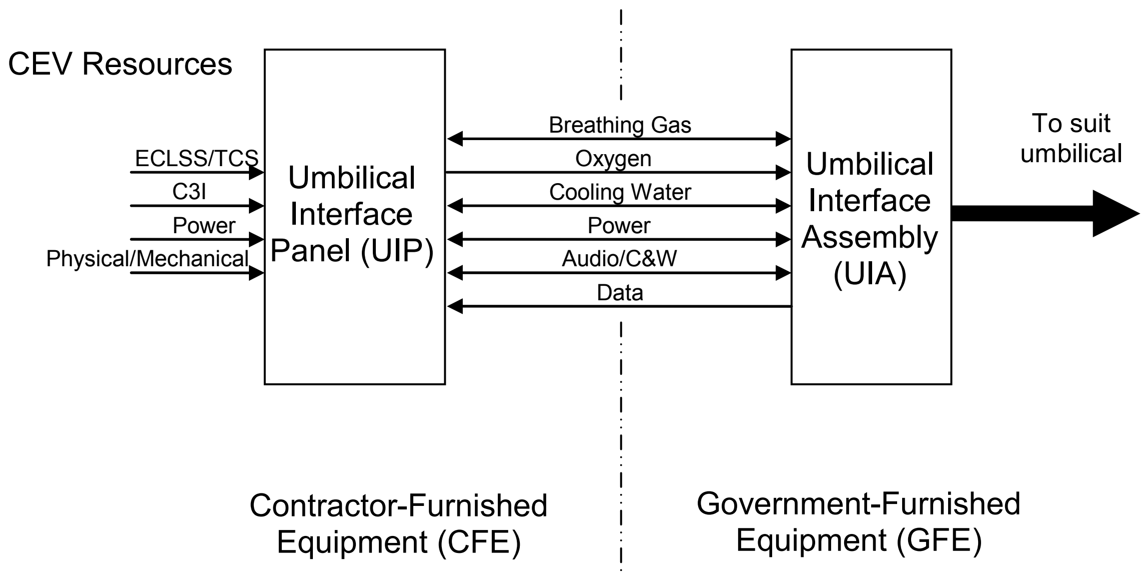

Figure 9.3-1 Umbilical Interface Panel - Umbilical Interface Assembly Interfaces

9.3.2 Conceptual Design Overview

9.3.2.1 Suit Architecture

A contractor response to a “Single Suit System” architecture has been requested by the Constellation Program. The details for that architecture strategy and suit development activity are currently underway and will not be discussed in this paper. The data contained in this package will focus on the interfaces necessary to implement the single suit system architecture.

9.3.2.2 Vehicular Interfaces

The EVA System contains several key CEV interfaces. The sections below describe these interfaces and some offer a NASA concept. Requirements for these interfaces are documented in the CEV to EVA System Interface Requirements Document (IRD), CXP-70033.

Pre-Launch

The suited crewmembers will be assisted into the CEV prior to launch by ground operations personnel. While seated in the CEV, the crewmembers will be wearing their spacesuits. Personal floatation and other survival gear provided as GFE are envisioned; however, these items may be integrated into the vehicle for access upon egress or be provided by the Prime as crew (i.e., non-individual) hardware. The crew will be connected to the CEV via an umbilical in order to receive critical life support and other functions. Requirements for both pre-launch and post-landing EVA and suit-integrated Crew Survival equipment are documented in the EVA System-to-Ground Operations Interface Requirements Document (IRD), CXP-70104. Note that EVA and Crew Survival pre-launch ground operations end (for requirements purposes) when the CEV hatch is closed prior to launch.

Cockpit

The suited crewmember will need to reach and manipulate certain controls and view displays depending on the specific mission phase (e.g., pre-launch, launch, ascent, rendezvous/docking, etc.). As a result, both unpressurized and pressurized suit mobility are key drivers for the suit design for successful CEV operation. An equally important driver for the suit design is the suit-to-seat interface during launch and landing operations. Due to CEV volume limitations, mechanical loading, anthropometry ranges to be accommodated, suit system architecture, etc., this interface will be a very tightly coupled development effort.

Stowage

Standard stowage provisions for the EVA and Crew Rescue System are envisioned for the CEV except for temporarily stowed items. Temporarily-stowed items include the pressure suits and umbilicals used for launch/entry, and, perhaps, personal floatation and rescue gear. Specific requirements for stowage volume, access, etc., are captured in the CEV-to-EVA IRD. It is assumed that any hardware necessary to support a contingency EVA crew transfer from the LSAM to the CEV (e.g., EVA umbilicals) is stowed in the LSAM itself.

Translation Paths (Internal)

Pre-Launch: The CEV will need to provide provisions for normal and emergency egress from the vehicle while at the pad and post-landing. Special attention must be made on disconnecting the suit umbilicals and retrieving survival gear in order to facilitate the egress.

In-Flight: The CEV will need to provide provisions for suited crewmembers to easily maneuver about the vehicle and to access and operate the CEV side hatch. In order to operate the side hatch, the suited crewmember will require sufficient lighting, sufficient swept volume, a means for body restraint, handholds, equalization valves, pressure gages, instruction placards, etc. Note that these items are not provided by the EVA System. Special attention should be made by CEV to prevent hatch seals or mechanisms from becoming damaged and becoming inoperable. An EVA umbilical guide roller or other concept may be necessary near the hatch to fend the umbilicals off the hatch seals. Should the hatch become difficult to operate or close, hatch support tools may be required. These tools could be existing dual-use intravehicular activity (IVA) tools. Note that during an EVA, it is envisioned that only one crewmember will exit the vehicle. A second EVA crewmember will tend to the first EVA crewmember's umbilical, assist with tool transfer, and be available for safety purposes. In order for this crewmember to adequately support umbilical tending operations, adequate restraints need to be provided. During this EVA time, the other crewmembers will be connected to their seat umbilicals.

Safety Considerations

Both external and internal CEV hardware that may come in contact with a suited crewmember will need to be designed to accommodate induced loads (e.g., kick loads). In addition, sharp edges for any CEV hardware that may come in contact with a suited crewmember must meet EVA sharp edge requirements. It is anticipated that EVA sharp edge and other requirements will be levied on the CEV via the Human Systems Integration Requirements (HSIR) document, CXP-70024 and EVA Design and Construction Specification, CxP-70130.

Umbilical - Fluids

A GFE-provided umbilical interface assembly (UIA) is expected to be located at or near each seat for easy crew access. It is envisioned that the UIA will have an interface for air or O2 IN, air or O2 OUT, coolant water IN, coolant water OUT, power, data bundle, and a tether hook. The UIA umbilical-side connectors will be designed to be quickly installed or removed via a common multiple gang connector. This gang connector is expected to be the same at both ends of the umbilical. This allows simpler contingency EVA operations and provides commonality opportunities for connection between suit system components, other Constellation vehicle elements, and Constellation mission operations. The panels will also contain an oxygen isolation valve, two oxygen check valves, and a liquid cooling garment flow control valve. For the EVA-designated UIAs, an IVA-EVA selector valve would also be included. It may be necessary to recess or provide guards for the O2 ON/OFF and IVA-EVA selector switches so they cannot be activated by accident. The surface area for each of these items will be such so as to ensure that they can be operated by crewmembers in an inflated space suit.

Breathing Gas & Oxygen Interface:

Refer to Figure 9.3-2. For IVA operations, each umbilical needs to be connected to the vehicle suit loop. There are some possible designs that will use this loop as a feed to the EVA crewmembers also. If the suit loop resources are provided to the EVA crewmembers, a booster fan might be integrated as part of the EVA umbilical to overcome pressure drop along the long umbilical. If not, then the EVA crewmembers may require high pressure oxygen to be provided through their O_2 interface. For each crewmember, the UIA will have an inlet oxygen line which can be controlled to ON or OFF with an isolation valve. For the two UIAs that support EVA, a three-way valve selects whether this oxygen IN comes from a high pressure (~100 psia) source, or from the suit loop source (~4.3 psia).

Note for unsuited IVA operations, it is possible to add a by-pass valve and diffuser at each of the UIAs to provide supplemental flow to the CEV or to a crewmember.

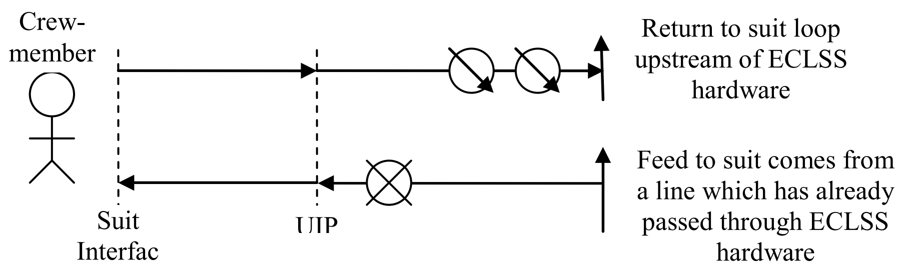

Figure 9.3-2 Concept for UIP-to-Vehicle for the Panels with IVA-only Capability

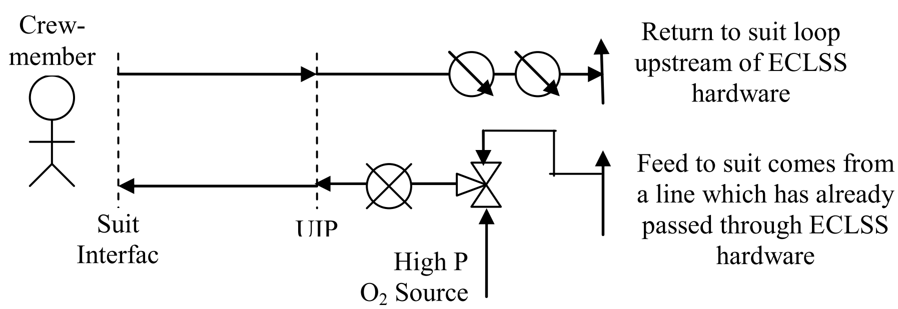

Figure 9.3-3 Concept for UIP-to-Vehicle for the Two Panels with IVA-EVA Capability

Refer to Figure 9.3-4. For the six-crewmember CEV design, seven slots are made available. This concept provides single-fault tolerance. It is assumed that when the crew is forced to rely on the umbilicals for life support, some failure has driven them to this off-nominal configuration; and so, the first fault of two-fault tolerance has already occurred. This does create a requirement that the connections from the UIP outlet port to the interface with the air lines be accessible and use quick disconnects (QDs); so that, if a check valve fails closed, the crewmember has an alternate path. If the check valve fails open, there is another check valve in line. On the feed side, there must be seven ports with lines than can feed UIP inlet ports; but, nominally, only six are connected. If a control valve on the oxygen feed line fails closed, the crewmember would have to have an alternate line to connect. It could be possible to unplug a QD that has a valve elsewhere on the line and replace it with the QD interface of another line; but, it is not feasible to install the control valve on the new line in the panel. As a result, if there is a valve on the replacement valve to protect for a leaking QD when it is not plugged in, that valve would have to be opened before the line is connected to the UIP inlet port and located in a place where it does not cause interference with the existing valve and failed, but disconnected line.

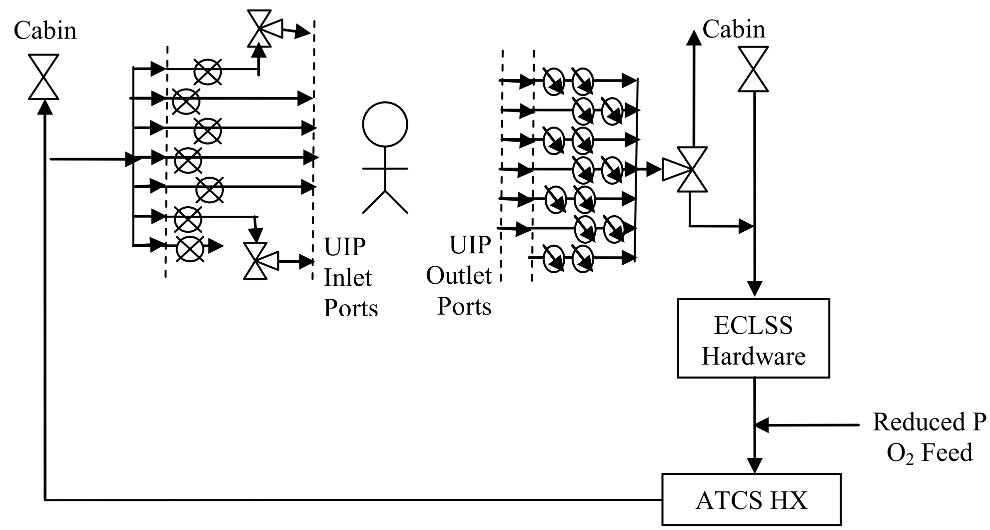

Figure 9.3-4 Overall UIP-to-Vehicle Concept with Required Interfaces and Manifolds

Cooling Water Interface:

Refer to Figure 9.3-5. The coolant lines must have both an inlet and outlet from the suit to operate. There is no inlet only configuration like the high pressure oxygen option available for gas delivery. Each crewmember may have a different metabolic load on the system; and, so, individual control of the cooling water flow is provided to each crewmember through a restrictor valve. In the NASA concept, there are assumed to be three heat exchangers, each with liquid cooling water pumps to provide liquid cooling to the crew. Each of these pump-heat exchanger assemblies should have three inlet and three outlet connections. Normally, two crewmembers will share one LCG heat exchanger. In the event that a pump or heat exchanger fails, the two crewmembers using the failed resource will have their lines moved to one of the other pump-heat exchanger combinations. Because these two crewmembers do not have active cooling during this failed event, the moving of lines should be done by a crewmember that still does have active cooling. For lunar missions with only four crewmembers, additional heat exchanger resources will be available. As a result, for a failed system, the crewmember with active cooling attached to the heat exchanger that will not be receiving new loads should be the one to move the lines for a failed system.

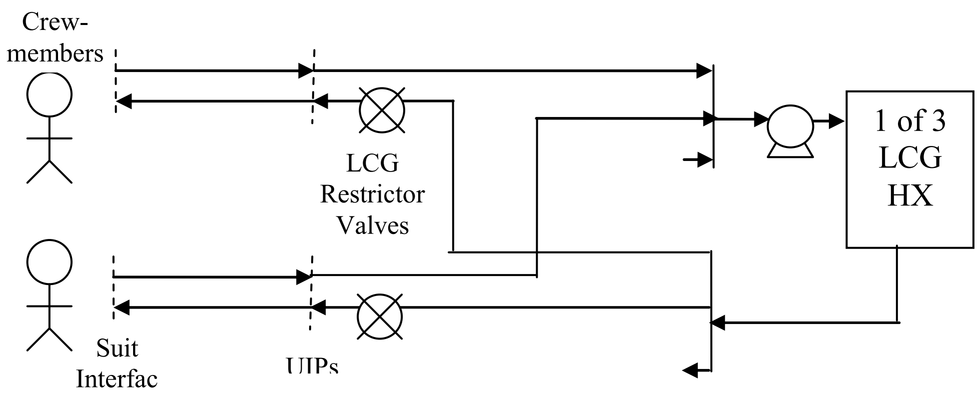

Figure 9.3-5 UIP-to-LCG Heat Exchanger Concept (1 of 3 required)

Umbilical - Electrical

The electrical umbilical interface provides the following key functions between the CEV and the EVA System:

CEV to EVA:

- Power
- Audio (voice and caution and warning tones)

EVA to CEV:

- Audio (transmitted voice from microphones)
- Data (Crew health information (e.g., biomedical data))
- Data (Suit health information (e.g., pressure, cooling water temp, etc.))

Audio: The voice and audio interface between CEV and EVA System should include redundant lines for each crewmember. It is recommended that the interface boundary between CEV and EVA should be drawn at the electrical analog signal level to give maximum implementation flexibility to the Prime CEV contractor (see Data section below). Unlike current ACES and EMU headsets, which have different electrical analog signal characteristics, the CEV to EVA audio interface will have a single voice communications electrical interface. An EVA headset could also be usable with the UIA/UIP for voice communications during unsuited (i.e., IVA) operations.

Data: The CEV will need to process and display crew and suit health information as well as relay this information to the Mission System.

There are two approaches for interfacing with the CEV for suit and crew health information. The selection will depend on the quantity of parameters needing to be monitored. NASA will work with the Prime contractor to determine the most efficient means for implementing.

- The first approach is to send/receive digital packets of data to/from CEV for distribution. In this approach, the CEV would not need to perform the analog-to-digital conversion and much of the data processing.
- The second approach would be to provide the analog/discrete signals directly to CEV for processing and distribution.

An additional auxiliary data path may be desirable (possibly required) for relaying inspection video or photography during a contingency EVA. This would only be needed for the EVA UIAs, but could require display of information on CEV resources.

Note: Currently, Command, Control, Communications and Information (C3I) requirements for the EVA & System are rather vague. However, command & control functions are not envisioned at this time. Either of the above audio/data approaches would constitute real-time hard-line communications and would not need to invoke the C3I interoperability specification over the interface. Data parameters from the suit system will probably be few in number; since, many parameters for measuring suit performance can be obtained from the CEV ECLSS system. Medical data may consist of heart rate, and an electrocardiogram (EKG) parameter. While EKG needs are yet to be defined, monitoring EKG during non-EVA events, including launch and landing, will probably not be a requirement. This is primarily a result of the time required to install and verify proper performance of the EKG instrumentation. For an unplanned cabin depressurization event, the time necessary to install the EKG instrumentation would probably prohibit its use.

Power: Redundant power is envisioned to be provided by the CEV System to the EVA System at a single voltage (15 – 28 Vdc (TBR)). Appropriate grounding and shielding will be provided per standard CEV specifications.

Translation Paths (External)

Two (2) recognized scenarios will drive the placement of external EVA translation aids (e.g., handholds): EVA support from ISS (using ISS resources) and contingency EVA crew transfer from the LSAM. Exact placement for these translation and possible work aids will be documented in the CEV-to-EVA Systems IRD. An EVA Design and Construction Specification, CxP-70130, that will be levied on any Constellation system that will interface with EVA is in work for the Constellation Program and should be utilized by all participants.

Suit Donning

At this time, it is unknown whether suit donning aids will be required or whether existing equipment/structure will be sufficient.

CEV Depressurized Operation

Requirements exist to support the contingency case in which the CEV cabin becomes depressurized. In this scenario, while troubleshooting is being conducted to determine the severity of the leak, the suits will be unstowed by the other crewmembers. Therefore, access to the temporarily-stowed suits must be rapid (on the order of 2 minutes). Since all crewmembers will not be able to don their suits at the same time (due to CEV internal volumetric limitations), each crewmember will take turns donning their suits. The total time currently required for the entire crew to don their suits is approximately 1 hour. As a result of the time required to allow all crewmembers to don their suits, the CEV is requiring the Environmental Control and Life Support System (ECLSS) to provide sufficient gas to feed-the-leak for 1 hour minimum (assuming a 1/4-inch diameter equivalent penetration).

EVA Tools

For information only, below is a listing and flow chart illustrating the types of tools that may be needed for various zero-g EVA scenarios. Quantities for a two-person EVA are shown in Figure 9.3-6. It is envisioned that the EVA crewmember will utilize an EVA tool bag or a suit-mounted harness/utility belt for tool transfer.

Proposed Inspection EVA Tool Set:	**Proposed Repair EVA Tool Set:**
Portable Helmet lights	EVA transfer bag w/ retractable equipment tethers (RETs)
Television (TV) Camera & bracket	Vice Grips
Safety tethers (55 ft.)	Needle-Nose Pliers
Translation handholds	Screwdriver Set/Caddy
EVA scissors	Probe
Load Alleviating Worksite Tether	Pry Bar
Adjustable Equipment Tether	Adjustable Wrench
Retractable Equipment Tether (RET)	Cable Cutter
EVA transfer bag w/ RETs	Mechanical Fingers
Camera & Bracket	Tie Wraps
	Wire Ties (short)
	Wire Ties (long)
	Small-Small (hook) Tether
	Large-Large (hook) Tether
	Retractable Equipment Tether
	Small Trash Bag
	Intravehicular Activity (IVA) Stowage Bag
INSPECTION EVA TOOL SET Total Volume: 8392 in^3 ; *Total Weight: 85.5 lb	***REPAIR EVA TOOL SET Total Volume: 3400 in^3; *Total Weight: 86 lb***

*NOTE: The EVA Tools sets listed above were NOT included in the Stowage Assessment nor do they appear in the CAD models or stowage-provided spreadsheets.

Table 9.3-2 Proposed EVA Tool Sets

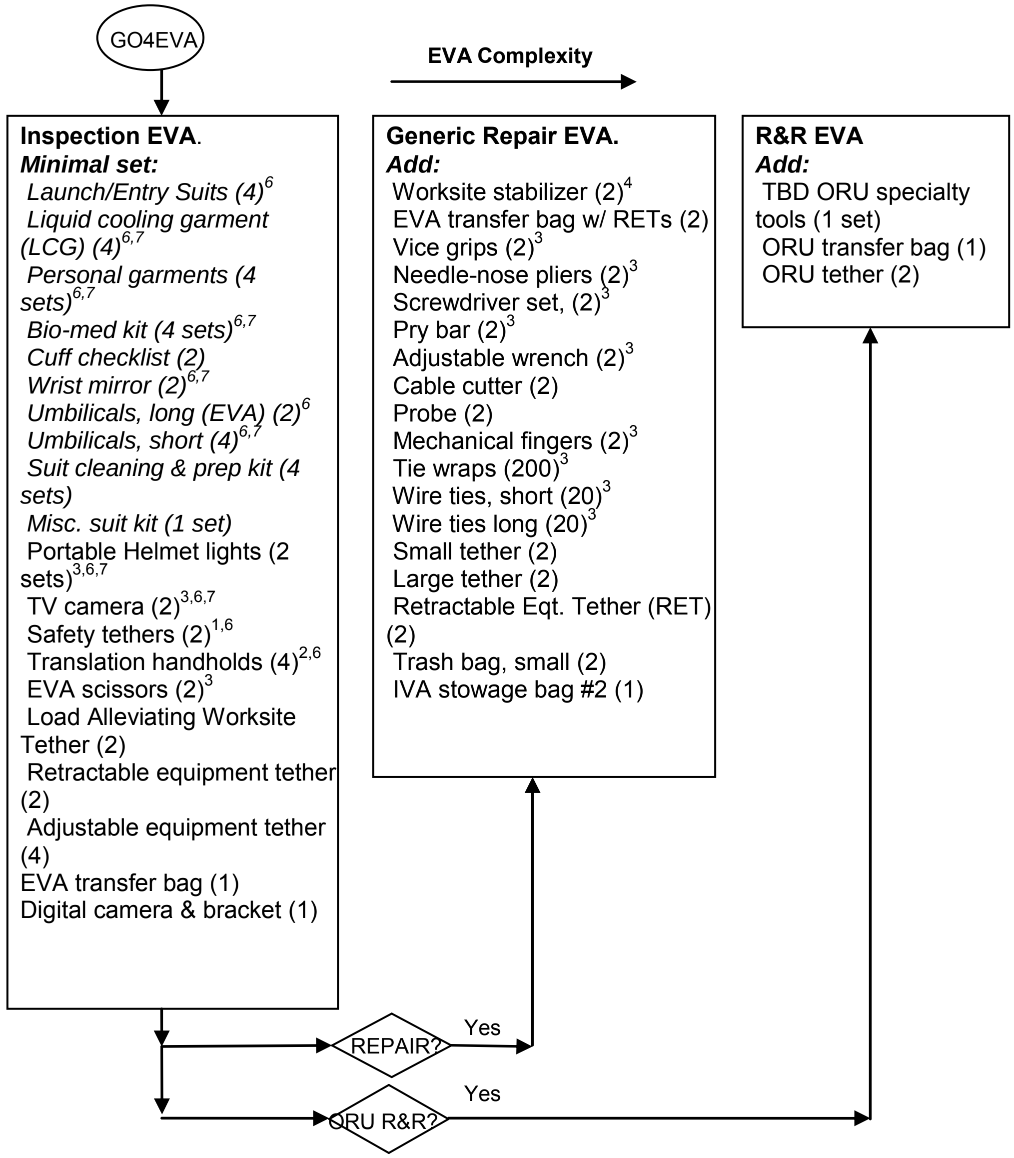

Notes:

1 – unless safety tether feature built into umbilical
2 – necessary if translation aids are not available; also assumes melt adhesive (no tools needed); On-Orbit Installed (OIH) type require tools for installation
3 – may be common to IVA toolset
4 – may require suit modification
5 – handheld provisioning only
6 – Block 2 LSAM-to-CEV scenario only: suit (4), LCG (4), personal garments (4 sets), biomed kit (4), portable lights (4 sets), wrist mirrors (4 sets), long umbilical (2), short umbilical (4), safety tether (2), translation handholds (2 sets)
7 – common element between launch/entry & surface suit?

Figure 9.3-6 Minimal Tool Requirements to Support a Contingency Zero-g EVA

Post-Landing

Following landing (either land or water), the crewmembers may remain in their suits for a rather lengthy time (36 hours) until they are recovered. During this time period, it is unclear just how many life support resources will be made available to the suited crewmember. Provisions must be available for safe and efficient hatch operation and for crew survival gear access and deployment. Post-landing EVA and suit-integrated crew survival equipment requirements are documented in the EVA System-to-Ground Operations Interface Requirements Document (IRD), CXP-70104.

9.3.3 Mass Estimates and Design Maturity

Some preliminary mass and volume estimates of EVA System equipment needs for both ISS and Lunar missions are provided in Tables 9.3-3 and 9.3-4. The mass and volume of the crew pressure suits for launch, entry, abort, survival, and contingency EVA were based on several assumptions. Estimates were derived from a JSC Engineering Directorate study. The volume assessment was derived from an I-suit (9326 in^3), a soft planetary-based EVA suit with minimal hard bearings minus a Thermal Micrometeoroid Garment (TMG). The TMG was added by estimating an additional 10% in volume.

Several EVA System line items are not considered stowed for launch because they are worn by the crewmember. These items include the pressure suit, umbilicals, helmet, and, possibly, personal flotation and other survival gear. The mass values for crew-worn items should be accounted for in the total launch mass, but not in the stowed mass. The volumes for all crew-worn items were accounted for in the on-orbit stowage assessments (see below).

All mass and volume allocations for EVA support items (e.g., EVA umbilicals and EVA tools) were deleted from the stowage list during the Design Analysis Cycle - 1 (DAC1) review based on the assumption that there would be no contingency or unscheduled EVAs from the CEV on ISS missions. The general consensus was that if there were an emergency en route to the ISS, the spacecraft would either return to Earth or dock to the ISS to effect repairs. In this scenario, the EVA repair tools could be stowed on board ISS.

For Lunar missions, the Constellation Program has stipulated that CEV will have the capability to perform contingency or unscheduled EVAs independent of other vehicles.

Hardware Items	Quantity	Unit Mass (lbm)	Growth (%)	Total Mass (lbm)	CM Mass (lbm)	SM Mass (lbm)	Basis of Estimate
EVA and Survival Gear - ISS				**822**	**822**	**0**	
Pressure Suits	6	80	0%	480.0	480.0		EC Suit Study
Suit Flight Support Equipment	6	5	0%	30.0	30.0		Based on EMU FSE
Personal Flotation	6	4	0%	24.0	24.0		Based on Shuttle life preserver
Crew Survival Gear (inc. 4.5 L Water)	6	19	0%	114.0	114.0		Shuttle + HSIR
Umbilicals (Seated/Suited)	6	14	0%	84.0	84.0		8-10 ft umbilical length
Umbilical Interface Assembly	6	15	0%	90.0	90.0		Based on ISS UIA

Table 9.3-3 EVA and Crew Survival Mass Estimates – ISS Mission

Hardware Items	Quantity	Unit Mass (lbm)	Growth (%)	Total Mass (lbm)	CM Mass (lbm)	SM Mass (lbm)	Basis of Estimate
EVA and Survival Gear - Lunar				**799**	**799**	**0**	
Pressure Suits	4	80	0%	320.0	320.0		EC Suit Study
Suit Flight Support Equipment	4	5	0%	20.0	20.0		Based on EMU FSE
Personal Flotation	4	4	0%	16.0	16.0		Based on Shuttle life preserver
Crew Survival Gear (inc. 4.5 L Water)	4	19	0%	76.0	76.0		Shuttle + HSIR
Umbilicals (Seated/Suited)	4	14	0%	56.0	56.0		8-10 ft umbilical length
Umbilical Interface Assembly	4	15	0%	60.0	60.0		Based on ISS UIA
Secondary Oxygen Pack*	4	30	0%	120.0	120.0		
Umbilicals (EVA)*	2	30	0%	60.0	60.0		
Contingency EVA Tools/Aids*	1	71	0%	70.5	70.5		Minimum tool set estimate

** Not included in CRC-3 Final Masses*

Table 9.3-4 EVA and Crew Survival Mass Estimates – Lunar Mission

9.3.4 Plan Forward

The EVA System team will continue to provide inputs to the CEV Master Equipment List (MEL) as the suit architecture and suit design mature.

Possible CEV Modifications:

- Currently, the only agreed-to EVA scenario for CEV Lunar missions is the contingency transfer of the crew from the LSAM to the CEV. However, as the CEV design matures, the need to develop additional EVA tasks will continually be evaluated. If it is deemed by the program that EVA could offer a significant improvement in either crew safety or mission success, the additional tasks and their associated EVA translation paths and worksites will be documented in the CEV-to-EVA Systems IRD. Associated hardware design considerations and stowage for additional tools (if any) will be coordinated with CEV as well.
- An RF EVA video interface is under consideration. This would be an especially valuable tool during contingency or unplanned EVA events.
- Discussions are being held between the CEV and EVA Systems projects to consider making the CEV seats GFE due their intimate interface with the launch/entry/EVA suit.

9.4 Flight Crew Equipment

CEV Flight Crew Equipment is provided for the following subsystems: Personal Hygiene, Sleeping, Housekeeping, Crew Provisions/Clothing, Maintenance, Operational Supplies, Food Preparation, Food, Trash Volumes, Medical Equipment, and Exercise.

9.4.1 *Driving Requirements, Groundrules, and Assumptions*

Driving Requirements for CEV Flight Crew Equipment are from the SRD and HSIR:

Lunar Mission Crew Transport Capacity Requirements

The CEV shall transport crews of 2, 3, and 4 crew members between Earth and lunar orbit in accordance with Table 1, Total Lunar DRM Crew, Destination Cargo, and Equipment Definition. [CV0001]

Rationale: …"Equipment" values are provided for an example 15 day lunar mission and include the following: Food System, EVA & Crew Survival, Exercise Countermeasure, Medical, Personal Hygiene, Sleeping, Photography, Housekeeping, Clothing & Crew Preferences, Maintenance, Operational Supplies, Trash Stowage, and Cargo Support Equipment. Equipment does not include vehicle specific spares.

ISS Crew and Cargo Mission Transport Capacity Requirements

The CEV shall be configurable to deliver crewmembers and pressurized cargo to ISS for the crew to ISS missions and return them to Earth in accordance with Table 3, Total ISS DRM Crew, Destination Cargo, and Equipment Definition. [CV0011]

Rationale: …"Equipment" values are provided for an example ISS crew mission and include the following: Food System, EVA & Crew Survival, Medical, Personal Hygiene, Sleeping, Photography, Housekeeping, Clothing & Crew Preferences, Maintenance, Operational Supplies, and Trash Stowage. Equipment does not include vehicle specific spares.

Personal Hygiene Requirements

The CEV shall provide for crew personal hygiene in accordance with the CXP01000, Human Systems Integration Requirements (HSIR), section 6.2. [CV0289]

Rationale: Personal hygiene has significant impact to overall crew health. It is necessary for CEV to provide the capabilities such as shower, etc. to maintain crew health.

The CEV shall provide for body waste management in accordance with the CXP01000, Human Systems Integration Requirements (HSIR), section 6.3 [CV0290]

Rationale: Waste will be created during the mission and support is needed in the CEV to collect and store the waste products and prevent the introduction of those products or byproducts of the waste (such as odors) in the crew habitable volume.

The vehicle shall provide for the collection and containment of 2 L of vomitus per crewmember per mission. [HS6013]

Rationale: Space Adaptation Syndrome (SAS) occurs in up to 70% of first time fliers (up to 30% of who may experience vomiting) during the first 48-72 hours of microgravity. Vomiting and its associated odor, mainly produced by the compound putrescene, in enclosed space and close proximity may trigger a bystander nausea and vomiting reaction, in adjacent crewmembers. Regurgitation of the entire stomach contents will result on average of 0.2 to 0.5 L of vomitus. The average number of vomiting episodes per crewmember will vary from 1 to 6 per day, over a 2- to

3- day period. A stowage and disposal capacity of 2 L per crewmember per mission should be adequate for a worse case number of involved crew, severity and duration of symptoms, and volume of gastrointestinal contents regurgitated.

<u>*Sleeping Requirements*</u>

No further design driving requirements exist for this subsystem.

<u>*Housekeeping Requirements*</u>

Reusable air filters shall be cleanable within 1 (TBR-006-8008) minute. [HS8044]

Rationale: Flight crew time is at a premium during flight. Preliminary studies based on ISS operation indicate that 3 minutes per filter is reasonable and balances overhead without incurring detrimental effects on primary mission activities.

Materials used for interior cabin surfaces shall be smooth and nonporous. [HS8039]

Rationale: This is intended to prevent film, particulate, and microbial contamination on spacecraft internal surfaces to mitigate the crew health risk of such contamination.

Materials used for all interior surfaces shall allow the cleaning of chemical contamination to a Visually Clean (TBR-006-8004) level. [HS8040]

Rationale: This is intended to ensure that chemical contamination on spacecraft internal surfaces can be removed to mitigate the risk of such contamination to the crew.

Materials used for all interior surfaces shall allow the cleaning of microbial contamination to a level of 500 (TBR-006-8005) CFU per 100 cm^2 or less. [HS8041]

Rationale: This is intended to ensure that microbial contamination on spacecraft internal surfaces can be removed to mitigate the risk of such contamination to the crew. The limit is from the ISS MORD, Rev. B.

Materials used for all interior surfaces shall allow the cleaning of fungal contamination to a level of 10 (TBR-006-8006) CFU per 100 cm^2 or less. [HS8042]

Rationale: This is intended to ensure that microbial contamination on spacecraft internal surfaces can be removed to mitigate the risk of such contamination to the crew. The limit is from the ISS MORD, Rev. B.

<u>*Crew Provisions/Clothing Requirements*</u>

No further driving requirements exist for this subsystem.

<u>*Maintenance Requirements*</u>

Equipment intended to be removed, disassembled, repaired, reassembled, or replaced shall be capable of being removed, disassembled, repaired, reassembled, and replaced (as appropriate) in its operational environment by personnel wearing clothing and safety equipment appropriate to the environment and phase of flight (including prelaunch and postlanding phases). [HS8001]

Rationale: Varying environmental conditions require the use of protective clothing and equipment. Equipment must be maintainable by personnel wearing such clothing. Examples of protective clothing and equipment include flight suits, and Self Contained Atmosphere Protective Ensemble (SCAPE) suites. Equipment includes everything that is planned to be maintained in flight, from the LRU down to the component level. Components may include computer cards, power supplies, or in some cases individual electronic components.

The vehicle shall allow maintenance in flight with only those tools in the Common Inflight Toolset defined in Table 9.4-1. [HS8037]

Rationale: Tools add to the weight, volume, and training requirements of a mission. Using a standard tool set for all equipment eliminates the proliferation of unique tools and reduces the training and support requirements for the system.

Description	Sizes
Combination Wrenches	1/4”, 5/16”, 3/8”, 7/16”, 1/2”, 9/16”, 5/8”, 3/4”, 7/8”, 1”
Sockets, 3/8” drive, 6 point	1/4”, 5/16”, 3/8”, 7/16”, 1/2”, 9/16”, 5/8”, 3/4”, 7/8”, 1”
Hex Head Driver, 3/8” drive	1/8”, 5/32”, 3/16”, 1/4”, 3/8”, 1/2”
Ratchets	1/4” drive, 3/8” drive
Extensions, 3/8” drive	6”, 11”
Adapter	1/4” drive to 3/8” drive
Torque Wrench, 3/8” drive	40-200 in-lb
Torque Wrench, 1/4” drive	10-50 in-lb
Screwdrivers	--
Adjustable Pliers	--
Dial Calipers	--
Digital Multimeter	--
Static Wrist Tether	--

Table 9.4-1 Common Inflight Tool Set

Each item that may require inflight maintenance should be maintainable with the smallest possible subset of the tools listed in Table 9.4-1. [HS8038]

Rationale: Minimizing the tool set reduces the training and support requirements for the entire system (flight and ground) and reduces the mass, volume and supply requirements for the flight portions of the mission.

<u>*Operational Supplies Requirements*</u>

The vehicle shall provide restraints for stowed items sufficient to prevent them from coming loose under the expected acceleration and vibration environments. [HS6050]

Rationale: Stowed items must be restrained so that they are not free to move during vehicle motion, under the influence of internal air movement, or after inadvertent contact.

<u>*Food Preparation Requirements*</u>

The CEV shall provide for food stowage and food preparation in accordance with CXP01000, Human Systems Integration Requirements (HSIR), Section 6.1. [CV0288]

Rationale: Food currently designed for long term space usage required that it is to be hydrated and heated prior to consumption.

The vehicle should provide readily accessible stowage volume for eating utensils and any required food and drink preparation equipment. [HS6006]

Rationale: When laying out the stowage and food preparation areas, consideration must be given to minimizing the time and effort involved in food and drink preparation.

The vehicle shall provide restraints for food, drink, and preparation utensils. [HS6007]

Rationale: Food, drink, and associated utensils often need to be restrained while they are unstowed for use, for example by the use of hook-and-loop tape, bungee cords, or some other quick and simple device.

The vehicle shall heat food and drinks to between 155 °F and 175 °F, and maintain them within that temperature range. [HS6003]

Rationale: Heating is required for subjective quality of food. Maintaining the temperature of rehydrated food above 150 °F helps prevent microbial growth.

The vehicle shall allow the crew to rehydrate food and drinks with hot or cold potable water. [HS6004]

Rationale: Many foods must be rehydrated prior to consumption because (i) the water content of food is an important component of daily water intake, and (ii) people are used to the taste and texture of hydrated foods. Some foods must be rehydrated with hot water to ensure activation of certain chemical processes.

The vehicle should allow the crew to prepare a meal for all crewmembers within a single 30-minute period. [HS6005]

Rationale: The food heating facility, and the delivery and heating system for the rehydration water must support the full crew, if the mission schedule requires that they eat some meals together.

The vehicle shall prevent cross-contamination between food preparation and personal hygiene areas, and between food preparation and body waste management areas. [HS6001]

Rationale: This requirement helps protect crew health, by limiting the transfer of microorganisms to the food preparation area.

The distance between food preparation and body waste management areas should be as large as possible. [HS6002]

Rationale: This requirement is designed to prevent interference of body waste management functions with food preparation. Shuttle and ISS designs both put the waste management facilities unnecessarily close to the food preparation areas. It is a design goal, because the other constraints on the layout of the spacecraft interior may preclude meeting any specific separation between the food preparation area and, for example, the body waste management area.

The vehicle shall heat food and drinks to between 155 °F and 175 °F, and maintain them within that temperature range. [HS6003]

Rationale: Heating is required for subjective quality of food. Maintaining the temperature of rehydrated food above 150 °F helps prevent microbial growth.

The vehicle should allow the crew to prepare a meal for all crewmembers within a single 30-minute period. [HS6005]

Rationale: The food heating facility, and the delivery and heating system for the rehydration water must support the full crew, if the mission schedule requires that they eat some meals together.

<u>Food Requirements</u>

The food provided shall meet the minimum nutritional requirements, including fluid requirements, as required by JSC 28038, Nutritional Requirements for International Space Station Missions up To 360 Days.

Rationale: Proper nutrition is required for crew health and performance during and after the mission.

The food provided shall remain safe to eat when stored at room temperature.

Rationale: There are no refrigerators or freezers on board the CEV for food stowage.

The food provided shall be packaged as individual menu items.

Rationale: It is too difficult to transfer food to a plate or other serving device.

<u>Food Preparation Requirements</u>

The vehicle should provide readily accessible stowage volume for eating utensils and any required food and drink preparation equipment. [HS6006]

Rationale: When laying out the stowage and food preparation areas, consideration must be given to minimizing the time and effort involved in food and drink preparation.

The vehicle shall provide restraints for food, drink, and preparation utensils. [HS6007]

Rationale: Food, drink, and associated utensils often need to be restrained while they are unstowed for use, for example by the use of hook-and-loop tape, bungee cords, or some other quick and simple device.

The vehicle shall heat food and drinks to between 155 °F and 175 °F, and maintain them within that temperature range. [HS6003]

Rationale: Heating is required for subjective quality of food. Maintaining the temperature of re-hydrated food above 150 °F helps prevent microbial growth.

The vehicle shall allow the crew to rehydrate food and drinks with hot or cold potable water. [HS6004]

Rationale: Many foods must be rehydrated prior to consumption because (i) the water content of food is an important component of daily water intake, and (ii) people are used to the taste and texture of hydrated foods. Some foods must be rehydrated with hot water to ensure activation of certain chemical processes.

The vehicle should allow the crew to prepare a meal for all crewmembers within a single 30-minute period. [HS6005]

Rationale: The food heating facility, and the delivery and heating system for the rehydration water must support the full crew, if the mission schedule requires that they eat some meals together.

The vehicle shall prevent cross-contamination between food preparation and personal hygiene areas, and between food preparation and body waste management areas. [HS6001]

Rationale: This requirement helps protect crew health, by limiting the transfer of microorganisms to the food preparation area.

The distance between food preparation and body waste management areas should be as large as possible. [HS6002]

Rationale: This requirement is designed to prevent interference of body waste management functions with food preparation. Shuttle and ISS designs both put the waste management facilities unnecessarily close to the food preparation areas. It is a design goal, because the other constraints on the layout of the spacecraft interior may preclude meeting any specific separation between the food preparation area and, for example, the body waste management area.

Trash Volumes Requirements

The CEV shall provide for trash management in accordance with the CXP01000, Human Systems Integration Requirements (HSIR), Section 6.8 [CV0498]

Rationale: Trash will be created during the mission and support is needed in the CEV to collect and store the trash products and prevent the introduction of those products or byproducts of the trash (such as odors) in the crew habitable volume.

The vehicle should provide readily accessible trash collection for food- and drink-related waste. [HS6008]

Rationale: Sufficient trash volume for disposable food and drink preparation supplies (e.g., drink bags and food packets) must be readily accessible after their use.

The vehicle should provide readily accessible trash collection for disposable personal hygiene supplies. [HS6012]

Rationale: Sufficient trash volume for disposable hygiene supplies such as tissues and wipes must be readily accessible after their use.

The vehicle should provide readily accessible trash collection, with odor control, for waste management items. [HS6031]

Rationale: Waste management items that cannot be collected and contained with human waste must be put in the trash immediately after use.

Stowage should be reconfigurable during the mission. [HS6049]

Rationale: Any stowage system must be flexible enough to accommodate the changes and evolution expected in the stowage plan over the length of a mission. For example, (i) as food is consumed during a mission, food stowage may need to be reallocated for trash, and (ii) during lunar return, lunar samples might be stowed in space originally allocated for water storage.

Trash stowage should not interfere with normal crew operations. [HS6054]

Rationale: This requirement is intended to prevent the trash system from interfering with normal operations such as translation and vehicle control. A "should" is used because constraints on the placement of other items may prevent the design from completely satisfying this requirement.

Trash stowage shall not interfere with emergency crew operations. [HS6055]

Rationale: This requirement is intended to prevent the trash system from interfering in any way with emergency operations such as egress, hatch closure, and fire fighting.

The trash management system should provide odor control for wet trash. [HS6056]

Rationale: Uncontrolled odors can have an adverse affect on crew performance, and can exacerbate pre-existing symptoms of SAS.

The trash management system shall prevent contamination of other parts of the vehicle from microorganisms within the trash. [HS6057]

Rationale: Many microorganisms present a risk to the crew, and should not be allowed to spread.

The trash management system shall safely contain sharp items, harmful chemicals, and biological wastes in accordance with OSHA guidelines. [HS6058]

Rationale: If not properly contained, sharp items can damage equipment, injure crewmembers, and transmit disease. Chemical or biological waste can also cause injury and transmit disease.

<u>Note</u>: This requirement has been challenged through the ICPR process. No harmful chemicals should be allowed to fly that would require disposal into the Trash Management System. This requirement puts hazard control responsibility on the vehicle trash management system rather than in the design control of the item with the hazard. If hazardous chemicals or sharp items require disposal, it should be the responsibility of the hardware provider to design in and/or provide controls (proper levels of containment) for the hazard during use and prior to disposal into the Trash Management System.

Photography Requirements

Digital still imagery shall be captured both IVA and EVA.

Digital still imagery shall be capable of being downlinked to the ground the C&T systems.

Digital video images shall be recorded during IVA operations.

Digital video images shall be capable of being downlinked to the ground the C&T systems.

Medical Equipment Requirements

The Constellation Architecture shall provide the capabilities necessary to comply with NASA crew health and medical standards for levels of care, crew selection, and exposure/operating limits. [CA0126-PO]

Rationale: Crew health and medical standards will ensure that exploration missions are not impacted by crew medical issues, and that long term astronaut health risks are managed within acceptable limits.

The CEV shall provide the capabilities necessary to comply with NASA crew health and medical standards as defined in TBD for levels of care and exposure/operating limits. [CA0375-PO]

Rationale: Allocation of CA0126.

The CEV shall meet portable equipment interface requirements defined in the CXP-01006 Crew Exploration Vehicle (CEV) to Portable Equipment Interface Requirements Document (IRD). [CV0483]

Rationale: Some Government provided portable equipment (including medical equipment) will require power and data interfaces. The interface may be established via utility panels distributed through out the cabin.

The CEV shall downlink (TBD-002-076) medical equipment data to the (MPTFO) Element (TBR-002-031). [CV0376]

Rationale: The flight surgeon will reside in the Mission Control Center (MCC) and available crew medical equipment data that can be downlinked in the event of crew illness or injury needs to be transmitted to the ground and the flight surgeon.

9.4.2 Conceptual Design Overview

Personal Hygiene Concept

Community Hygiene Kit: A similar Community Hygiene Kit is proposed for CEV which will include items such as No-rinse shampoo, toothpaste, No-Rinse body wash, cotton swabs, dental floss, hair conditioner, hand lotion, and shaving cream. A large ziplock may be used to take the place of the nomex modifiable compartmentalized kit shown.

Figure 9.4-1 Shuttle Personal Hygiene Kit

Emesis Bags: The Emesis Bag is composed of a commercially manufactured material of a Poly-tetrafluorethylene (PTFE) membrane with a non-woven polyethylene support, cotton fabric, thread, tape, safety wire, and a polyethylene zipper bag. A ziplock bag is included to facilitate disposal. The emesis bag is gas permeable so that off-gassing of the emesis does not cause the bag to expand and possibly rupture. Emesis Bag is discarded in a wet trash container.

Figure 9.4-2 Emesis Bag (left); Emesis Bag in Ziplock Ready for Disposal (right)

Sleeping Concept

Sleep Restraint: The shuttle sleep restraint weighs about 10 lb and was designed for shuttle interfaces including the sleep compartment. Due to more recent advances in lightweight fabrics a lighter sleep restraint is proposed for CEV. The current shuttle sleep restraint includes a head pad, back support, and liners with multiple straps. Russian ISS sleeping bags consist of three layers. The outer layer is made of synthetic material, the middle layer is made of camel wool, and the inner layer is a cotton sheet/liner. The crew suggested reducing the shuttle restraint to a simpler version w/o pad and accessories or use a new lightweight commercially available off-the-shelf bag such as the Bivisack made from Gortex. If architecture allows, the seats may be a location to which the restraints can attach.

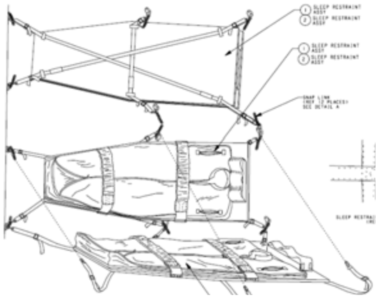

Figure 9.4-3 Shuttle Sleeping Bag (left); STS-112 Crew in Sleeping Bags (right)

Figure 9.4-4 ISS Russian Sleep Restraint (left); COTS Bivisack (right)

<u>*Housekeeping Concept*</u>

Vacuum Cleaner: The design was based on the STS wet/dry vacuum cleaner (STS requires 3-phase 110 Vac for dry only capability, 28 Vdc for wet/dry capability, and ISS requires 120 Vdc for wet/dry capability). The Vacuum Cleaner will not be required for the ISS missions which have the shorter duration. For lunar missions, the Vacuum may play a more important role for general clean-up, fluid containment and for filter cleaning as an alternate to grey tape. The Vacuum Cleaner can be used for filter cleaning, removal of free floating and collected debris, and collection of up to 48 fluid ounces per disposable bag. Accessories may include a suction hose, surface attachment and crevice tool.

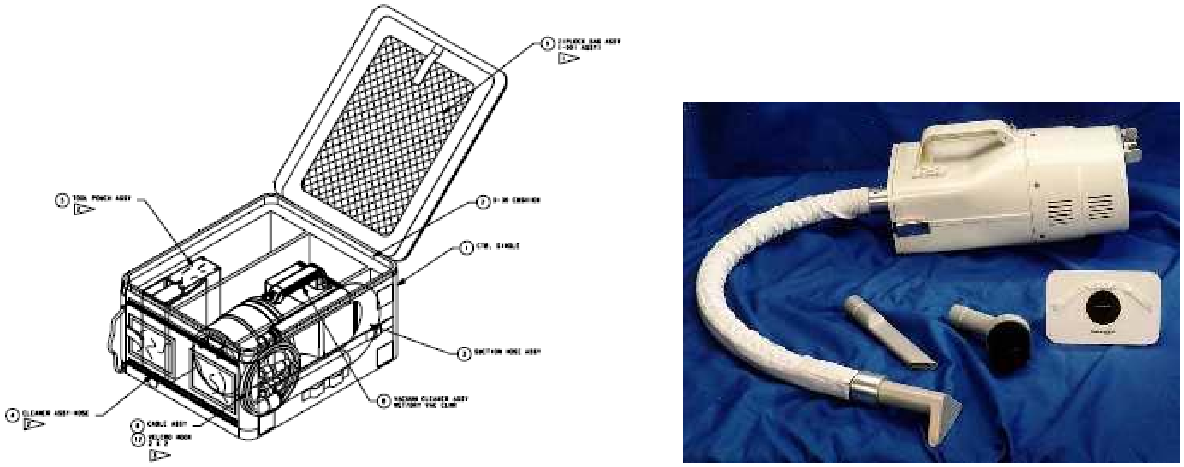

Figure 9.4-5 Vacuum Cleaner as Stowed in CTB (left); Vacuum Cleaner Assembly (right)

Wet Wipes: Commercially available off-the-shelf products currently flown on Shuttle. Bookkeeping of all wet wipes was consolidated under the housekeeping subsystem to eliminate duplications or omissions. Wet wipes are used for pre-meal personal hygiene, post-meal personal hygiene, WMC facility clean-up, Waste Hygiene, utensil cleaning, and food preparation and clean-up. A supply will be located near the commode. Resupply packs can be stowed elsewhere and relocated to commode as necessary.

Figure 9.4-6 Shuttle Wet Wipe Package

Dry Wipes: Commercially available off-the-shelf product currently flown on Shuttle. Bookkeeping of all dry wipes was consolidated under the housekeeping subsystem to eliminate duplications or omissions. Dry wipes are used for WMC facility clean-up, Waste Hygiene, and utensil cleaning. Locate supply near commode. Resupply packs can be stowed elsewhere and relocated to potty if necessary.

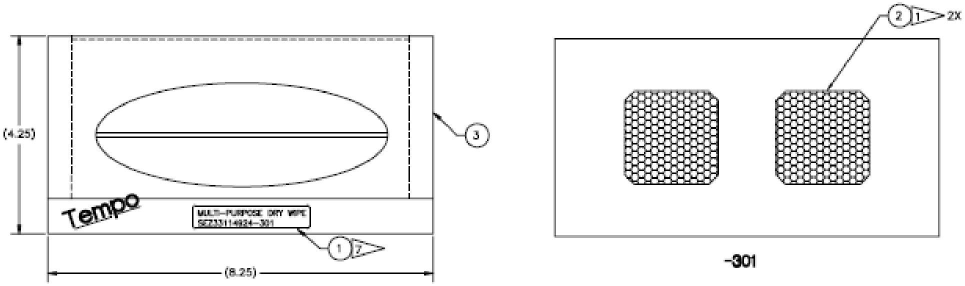

Figure 9.4-7 Front and Back Views of a Shuttle Dry Wipe Package

Sanitation Wipe Kit: For larger scale interior wipe-downs, this Russian type kit contains dry wipes that are dampened with a premixed evaporative detergent/biocidal solution to support moderate cleaning.

Towels: Russian type of large towel preferred over smaller STS towel with washcloth. Larger towel can be stretched across the back. US towels are comparatively small and do not provide the extended coverage. Crewmembers expressed how well they liked pre-wet towels. On flight day 1, the crewmember receives one wet and one dry towel. On flight day 2, the crewmember receives one new wet towel and uses yesterday's wet towel as today's dry towel and the pattern continues through the duration of the flight. CEV ventilation will be used to dry the used wet towels. On Mir, wet towels were placed close to ventilation so facilitate drying. Towels are pre-wet prior to flight.

Figure 9.4-8 Russian Wet Towels

Crew Provisioning /Clothing Concept

Clothing and Crew Preference: This is a crewmember's personal CTB (or proportional equivalent for shorter ISS Mission duration) that includes clothing, watches, glasses, personal electronic devices, personal items, fanny pack, and diapers or thermal underwear (if required in the suit).

Figure 9.4-9 Typical CTB with Clothing and Personal Preference Items

Tablet PC: The crew has indicated a preference for a tablet-type PC that has fully integrated, wireless display and control functions.

Figure 9.4-10 COTS Tablet PC

Maintenance Concept

IFM Standard Tool Kit: The HSIR specifies a minimal tool set for CEV. The Engineering In-Flight Maintenance (IFM) team/EC concurs with this tool set and agrees that the HSIR minimal tool set be considered the “design to” list and be distributed to all hardware providers. The intent of the tool set is to limit the numbers of tools required to perform ground and flight maintenance activities on the IVA systems including ORU/LRU changeout. The tools are also shown in Figure 9.4-10.The Engineering IFM team/EC recommends providing a supplemental set of tools intended for unplanned repairs consistent with the type of repairs seen previously on-orbit. The supplemental set also includes fastening tapes and safety accessories. Table 9.4-2 shows the comparison of the Shuttle Tool Kit, HSIR Tool List, and EC’s proposed tool set. Below the table are pictorial representations of the STS Tools (Figure 9.4-11) which are stowed in trays compatible with Shuttle locker stowage and the ISS Drawer type tool chest (Figure 9.4-12). Stowage design for the CEV tool set has not been addressed although “jelly-roll” type options that provide greatest stowage efficiency will also be considered.

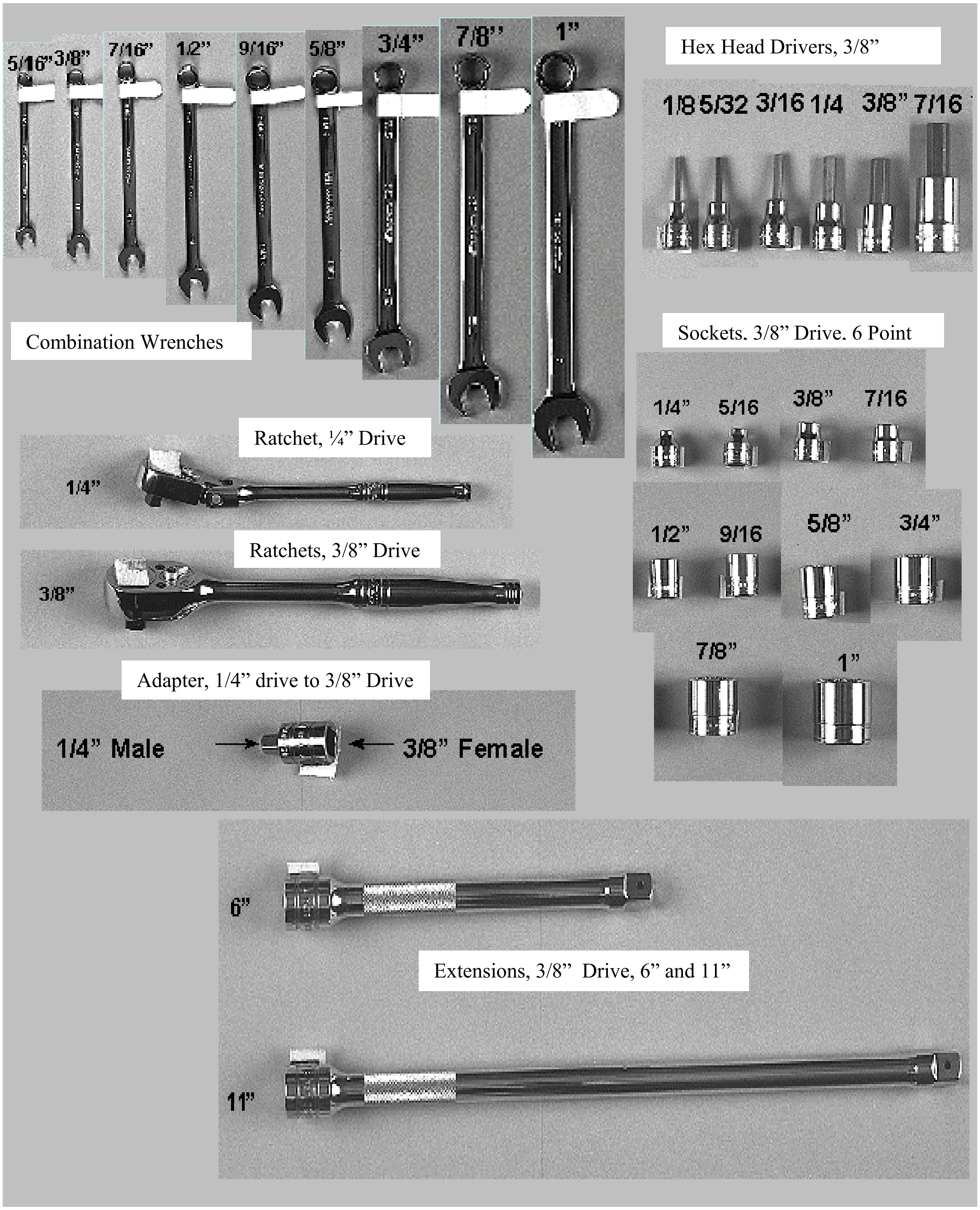

Figure 9.4-11 HSIR Tool Set

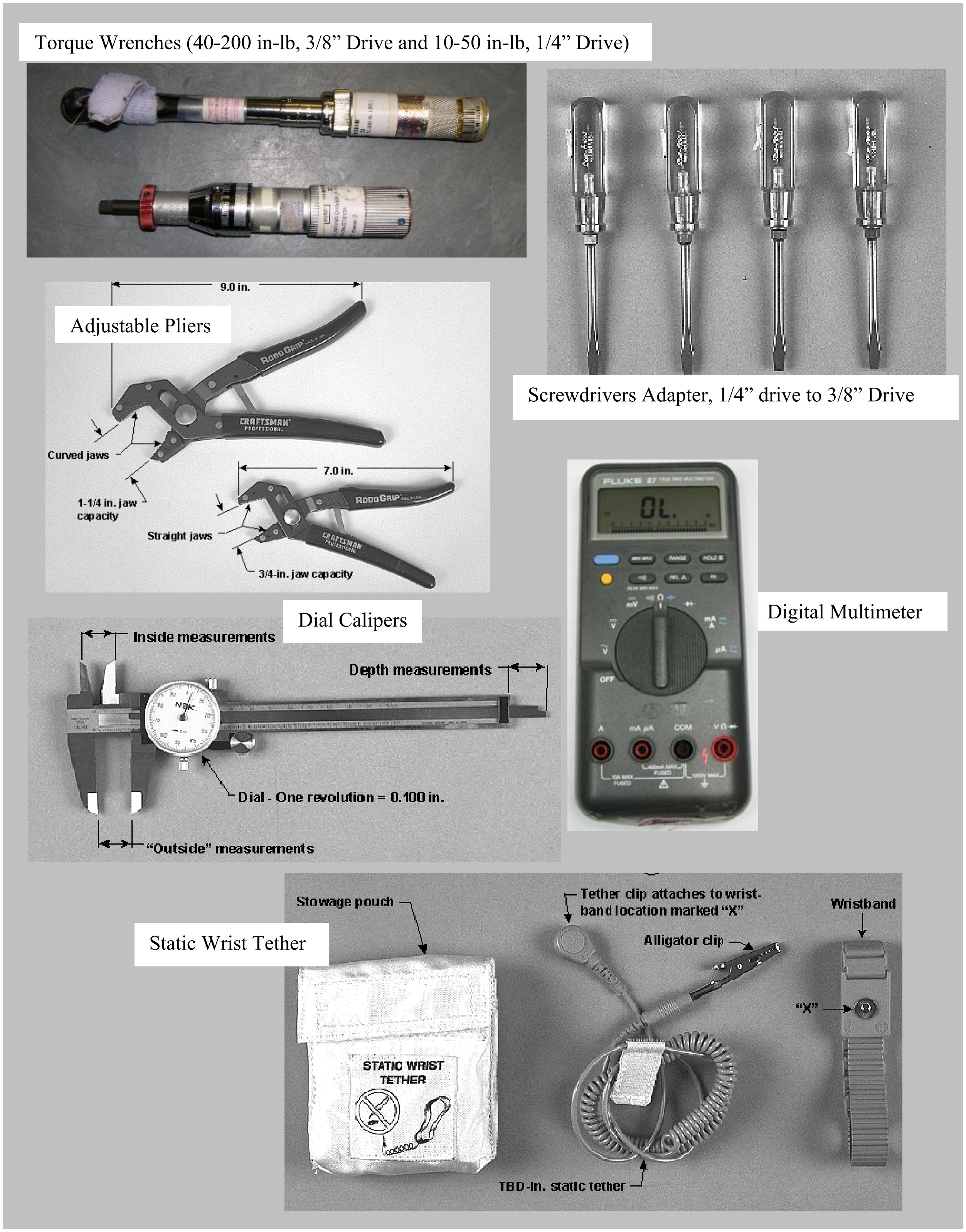

Figure 9.4-11 HSIR Tool Set, Concluded

Tool Set Comparisons	Maintenance and Repair		
	STS	HSIR	EC Proposed
Adapters			
Torque Adapter, 7/16"	YES	NO	NO
1/4" to 3/8"	YES	YES	YES
3/8" to 1/4"	YES	NO	NO
3/8" Universal Joint	YES	NO	NO
Allen Head Drivers			
Drivers, Allen Head	YES	NO	NO
Cutting Tools			
File, Set, Small	YES	NO	YES
File, Set, Large	YES	NO	NO
Hacksaw/Blades	YES	NO	YES
Hand Saw, Flexible (Bone Saw)	YES	NO	NO
Leatherman Tool	YES	NO	NO
Punch	YES	NO	YES
Scissors	YES	NO	YES
Wire Cutters	YES	NO	YES
Extensions			
1/4" Drive, 4" L.	YES	NO	NO
1/4" Drive, 6" L.	YES	NO	NO
1/4" Drive, 11" L.	YES	NO	NO
3/8" Drive, 6" L.	NO	YES	YES
3/8" Drive, 11" L.	NO	YES	YES
Hammers			
Hammer, Ball Peen	NO	NO	NO
Hammer, Dead Blow	YES	NO	YES
Handles			
Driver, Handle, 1/4"	YES	NO	NO
Driver, Handle, 3/8"	YES	NO	YES
Hardware Protection			
Tool Table Cloth	YES	NO	NO
Switch Guards	YES	NO	NO
Hex Drivers			
3/8" Drive, Set	YES	YES	YES
Hex Ball, 3/16"	YES	NO	NO
Hex Ball, 5/32"	YES	NO	NO
Hex Key, Metric, Set	NO	NO	YES
Hose and Cable Repair			
Hose and Cable Kit	YES	NO	NO
Leak Repair Tools			
Leak Patch Kit	YES	NO	YES
Measurement/Inspection			
Calipers	NO	YES	YES
Feeler Gage Set	YES	NO	NO
Magnifying glass (5X)	YES	NO	YES
Mirror, Inspection	YES	NO	NO
Tape Measure	YES	NO	YES
Phillips Drivers			

Drivers, Phillips, Set	YES	NO	NO
Pliers			
Pliers, Adjustable	NO	YES	YES
Pliers, Combination	NO	NO	NO
Pliers, Connector	YES	NO	YES
Pliers, Needle Nose, Large	YES	NO	NO
Pliers, Needle Nose, Small	YES	NO	NO
Vise Grips	YES	NO	YES
Pry Bar			
Pinch/Pry Bar	YES	NO	YES
Safety			
Goggles	YES	NO	NO
Sockets			
1/4" Drive, Standard, Set	YES	NO	NO
3/8" Drive, Standard, Set	YES	YES	YES
1/4" Drive, Deepwell, Set	YES	NO	NO
Metric, Set	YES	NO	NO
Screw Drivers w/Handles			
Screw Driver, Phillips, Set	YES	YES	YES
Screw Driver, Flat, Set	YES	YES	YES
Screw Driver, Jewelers, Standard, Set	YES	NO	NO
Screw Driver, Jewelers, Phillips, Set	YES	NO	NO
Screw Driver, Torque Tip	YES	NO	NO
Screw Driver, Powered	YES	NO	NO
Screw Driver, Powered, Allen Driver, Set	YES	NO	NO
Screw Driver, Powered, Flat Driver and Phillips Driver, Set	YES	NO	NO
Screw Driver, Powered, 1/4" to 3/8" Adapter	YES	NO	NO
Tape/Fastening/Retaining			
Dyna Band	YES	NO	NO
Mechanical Fingers	YES	NO	NO
PBI Cord	YES	NO	NO
Sewing Kit	YES	NO	NO
Tape, Aluminum	YES	NO	YES
Tape, Grey	YES	NO	YES
Tape, Kapton	YES	NO	YES
Tie Wraps	YES	NO	YES
Velcro	YES	NO	NO
Velcro Cable Strap	YES	NO	YES
Wire Spool	YES	NO	NO
Torque Tip Drivers			
Torque Tips	YES	NO	NO
Wrenches			
Wrench, Adjustable, 4"	YES	NO	NO
Wrench, Adjustable, 10"	YES	NO	YES
Wrench, Combination, Standard, Set	YES	YES	YES
Wrench, Combination, Metric, Set	NO	NO	NO
Wrench, L-Wrench/Allen, Set	YES	NO	YES
Wrench, Ratchet, 1/4" Drive	YES	YES	YES
Wrench, Ratchet, 3/8" Drive	NO	YES	YES

Wrench, Robbins	YES	NO	NO
Wrench, Strap, Connector	YES	NO	NO
Wrench, Torque, 1/4" Drive, 10-50 in-lb	YES	YES	YES
Wrench, Torque, 1/4" Drive, 40-200 in-lb	YES	NO	NO
Wrench, Torque, 3/8" Drive, 40-200 in-lb	NO	YES	YES
Electrical			
Contingency Power Cables	YES	NO	NO
Pin Kit	YES	NO	YES
Power Supply, IFM Breakout Box	YES	NO	NO
Scopemeter/Multimeter w/ Voltage, Current, Temp, & Pressure Probes	YES	YES	YES
Soldering Iron Kit	NO	NO	YES
Splice Crimp Tool	(Pin Kit)	NO	(Pin Kit)
Static Wrist Tether	YES	YES	YES

Table 9.4-2 Tool Set Comparison Chart

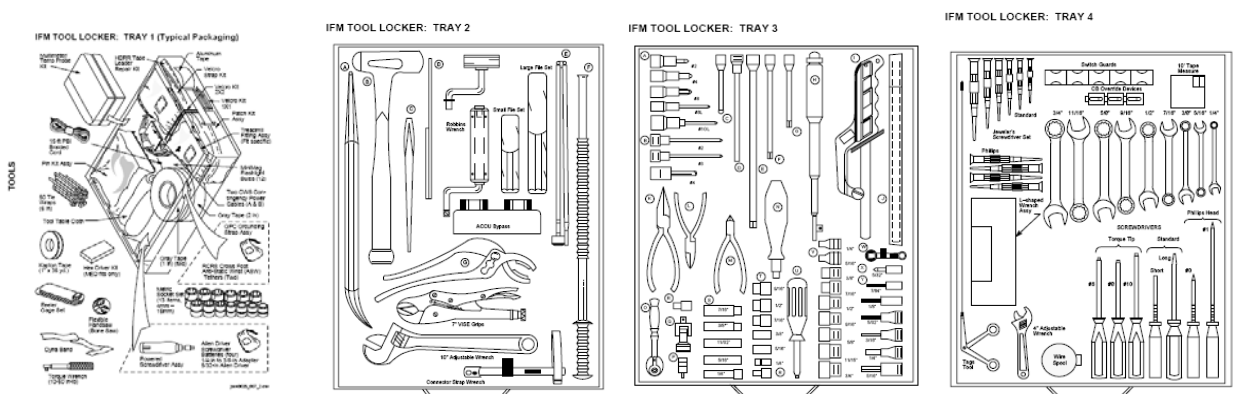

Figure 9.4-12 STS Tool Trays

Figure 9.4-13 ISS Tool Drawer Design

Operational Supplies Concept

Bungees: The Crew Office suggested adding multiple bungee cords for on-orbit restraint of hardware such as the launch/entry suit, sleep restraints, and loose crew equipment.

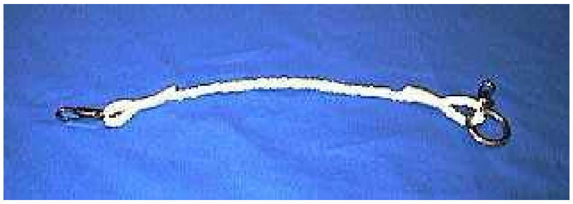

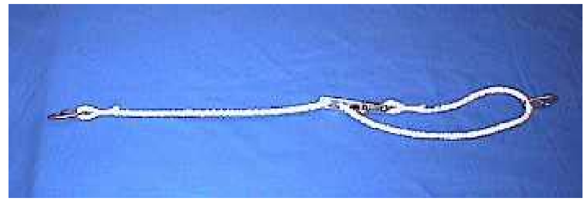

Figure 9.4-14 Bungees

Multiuse Bracket: Mounting brackets, commonly known as Bogan Arms, are included to provide a camera shoe interface or seat track interface to secondary structure of the vehicle.

Figure 9.4-15 Bogan Arm

Food Preparation Concept

Food Warmer: The food warmer is based on conduction heating (Hot water for food preparation is supplied by ECLSS). Per crew input, Block 1A ISS missions will not require a food warmer for such a short duration mission. Future technology improvements will allow us to decrease the size of the Block 2 food warmer.

Figure 9.4-16 Current ISS Food Warmer

Food Concept

Food Types: Food is kept shelf stable by thermal processing, thermostabilized and irradiated, by removing water from the food, freeze dried and intermediate moisture, and through formulation, natural form foods. Beverages are dried powders and are packaged in metalized material. Each individual menu item is packaged separately. The irradiated and thermostabilized are packaged in a multi-layer, metalized film and the other food items are packaged in a multilayer poly material. A vacuum is pulled on the freeze dried, intermediate moisture, beverages, and natural form foods to remove oxygen and moisture.

Figure 9.4-17 Thermostabilized and Irradiated Food (left); Freeze-Dried Food (right)

Figure 9.4-18 Natural Form Food (left); Intermediate Moisture Food (right)

Utensils and Straws: Utensils, including scissors, are required to eat out of the food packages. Straws are stowed separately and used for the beverages.

Food Container: The packaged foods are stowed in a container to protect the food packages from damage. Any damage to the metalized food packaging will result in unsafe food.

Figure 9.4-19 Current ISS Food Container

Trash Volumes Concept

Food Trash Volume Compartment: Wet Trash is predominantly food waste products with possibly some safely contained medical and personal hygiene wastes. The proposed food containers flatten out for increased packing efficiency. Not as much wet trash is expected to be generated as compared to shuttle and ISS. Trash is expected to be stored in multiple locations due to lack of available sufficiently sized single volumes. The Crew Office recommended Russian type trash containers with a valve added to prevent leakage due to contingency depress.

Dry Trash Volume Compartment: Dry Trash is predominantly used wipes, excess ziplocks/dry packages, little paper, with possibly some safely contained medical and personal hygiene wastes. Not as much dry trash is expected to be generated as compared to shuttle and ISS. Trash is expected to be stored in multiple locations due top lack of available sufficiently sized single volumes. The Crew Office recommended Russian type trash containers with a valve added to prevent leakage due to contingency depress.

Photography Concept

Digital Still Imaging capability is provided by a professional quality Commercial off the Shelf (COTS) digital camera modified for flight. It will have the capability of being used either IVA or EVA with minimal reconfiguration to reduce the number of cameras required. The camera will have interchangeable lenses giving the crew the ability of changing the capability of the camera. It shall be capable of storing the images in solid state storage that can be downlinked to the ground using vehicle C&T systems. By storing the images in solid state storage, this allows the camera to be used EVA as well as minimizes potential damage to the storage media.

Digital Video Imaging capability will be provided by a either a professional or a consumer quality COTS camcorder modified for flight. The camcorder can be used inside the cabin and record on its own internal media, which can be downloaded to the ground at a later time. No interchangeable lenses will be provided and the camcorder will be all self-contained with only interface cables for downlinking.

Both the Digital Still and Digital Video Imagers will receive power from batteries internal to the units that can be charged with chargers using vehicle power.

Medical Equipment Concept

Medical Kit: The medical kit is based on an EDOMP style and capable kit to include ambulatory care and toxic release containment PPE.

Figure 9.4-20 Medical Kit

Medical Interface Items: The medical interface items include an adapter for pressurized gas, power connections for electrical hardware, accommodation for portable medical hardware items, etc brought from LSAM in case of medical contingency for Earth return.

Contaminant Cleanup Kit: The contaminant cleanup kit is based on the current Shuttle kit containing mittens, bags, goggles, supplies for biological and chemical spills, broken glass, and eyewash goggles.

Environment Health: The environment health equipment is based on shuttle/ISS fire detection capabilities. No in-flight trace organic compound measurements will be required; only combustion products will be monitored, on a contingency basis, in-flight.

9.4.3 Mass Estimates and Design Maturity

Table 9.4-3 lists the mass properties for the CEV Block 2 (lunar) flight crew equipment.

Hardware Items	Quantity	Unit Mass (lbm)	Growth (%)	Total Mass (lbm)	CM Mass (lbm)	SM Mass (lbm)	Basis of Estimate
Flight Crew Equipment				**647**	**647**	**0**	
Personal Hygiene	1		10%	13.1	13.1		See below
Community Hygiene Kit	1	8	10%				
Emesis Bags	30	0.1	10%				
Sleeping Restraints	4	4	10%	15.4	15.4		
Housekeeping	1		10%	51.6	51.6		
Vacuum Cleaner	1	15	10%				
Wet Wipes	18	0.4	10%				
Dry Wipes	29	0.2	10%				
Sanitary Wipe Kit	1	1	10%				
Towels	60	0.3	10%				
Crew Provisions / Clothing	1		10%	123.2	123.2		
Personal Stowage	4	24	10%				
Tablet PC	4	4	10%				
IFM Standard Tool Kit	1	46	10%	50.3	50.3		
Restraints & Mobility Aids	1		10%	10.5	10.5		
Bungees	18	0.3	10%				
Multiuse Bracket (Bogen Arm)	2	3	10%				
Food & Food Preparation	1		10%	324.1	324.1		
Food with packaging	60	4	10%				
Container that holds food	60	1	10%				
Utensils	4	0.4	10%				
Food Warmer	1	20	10%				
Trash Volumes	1		10%	4.3	4.3		
Food Trash Volume Compartment	60	0.04	10%				
Dry Trash Volume Compartment	60	0.03	10%				
Medical Equipment	1		10%	30.8	30.8		
Medical Kit	1	10	10%				
Contaminant Cleanup Kit	1	10	10%				
Environment Health Monitoring	1	8	10%				
Exercise Equipment	1	22	10%	24.2	24.2		

Table 9.4-3 Flight Crew Equipment Mass Properties

Hardware Items	Quantity	Unit Mass (lbm)	Growth (%)	Total Mass (lbm)	CM Mass (lbm)	SM Mass (lbm)	Basis of Estimate
Flight Crew Equipment				**113**	**113**	**0**	
WCS Supplies	1		10%	52.3	52.3		See below
WCS Supplies	1	42	10%				
Contingency Urine Collection	60	0.1	10%				
Digital Video Camcorder	1		10%	11.8	11.8		
Digital Video Camcorder	1	2	10%				
Rechargeable Batteries	2	1	10%				
Battery Charger & Pow er Supply	1	5	10%				
Pow er Cables	1	1	10%				
Video Interface Cables	1	1	10%				
Digital Video Storage Media	7	0.1	10%				
Digital Still Camera	1		10%	14.1	14.1		
Digital Still Camera	1	4	10%				
Rechargeable Battery	1	1	10%				
28V Battery Charger and Pow er Supply	1	5	10%				
28V Input Pow er Cables	1	1	10%				
Camera Pow er Cables	1	1	10%				
Memory Storage Device	30	0.1	10%				
Camera Flash	1	1	10%				
Photo / TV Accessories	1		10%	15.7	15.7		
Camcorder Accessory Light	1	1	10%				
Mounting Brackets	2	3	10%				
Binoculars, 8 X 20	1	0.4	10%				
Lens Cleaning Kit	1	0.1	10%				
Common Video Interface Unit	1	3	10%				
CVIU pow er cables	2	1	10%				
Video Monitor	1	4	10%				
Lenses	1		10%	19.1	19.1		
Wide Angle Lens	1	1	10%				
Lens Kit	1	16	10%				

Table 9.4-3 Flight Crew Equipment Mass Properties, Concluded

Personal Hygiene

Community Hygiene Kit:

Heritage: STS

Maturity: Concept. New CEV item will be developed and certified for CEV.

Basis of Estimate: STS has an individual Personal Hygiene Kit for each crewmember. In July, 2003, a change proposal was submitted to the Shuttle FCE CCB to develop a single community shared kit based on a CB recommendation. CEV will have single community shared kit. Use rates of individual items within the kit are based on Shuttle use rates. For Block 2 Lunar Missions and Block 1A ISS Missions, the same standard kit will be provided.

Emesis Bags:

Heritage: STS

Maturity: Flight certified for STS and ISS. Similar item will be re-certified for CEV.

Basis of Estimate: Shuttle stows an average of 40-70 per mission, depending on crew size and experience. Bag use is predominantly at the beginning of a mission when sickness is more prevalent. For Block 2 lunar missions, six emesis bags per crew member plus six additional due to extended duration over ISS missions. For Block 1A ISS missions, six emesis bags per crew member will be provided.

Sleeping

Sleep Restraint:

Heritage: STS and Commercial of-the-shelf

Maturity: Concept. New CEV modified commercial off-the-shelf or modified shuttle item will be developed and certified for CEV.

Basis of Estimate: For Block 2 Lunar Missions and Block 1A ISS Missions, each crewmember will have his/her own sleep restraint.

Housekeeping

Vacuum Cleaner:

Heritage: The design was based on the STS wet/dry vacuum cleaner (STS requires 3-phase 110 Vac for dry only capability, 28 Vdc for wet/dry capability, and ISS requires 120 Vdc for wet/dry capability). The Vacuum Cleaner will not be required for the ISS missions which have the shorter duration.

Maturity: The current flight certified configuration will require a follow-up recertification.

Basis of Estimate: For Block 2 lunar missions, the Vacuum may play a more important role for general clean-up, fluid containment and for filter cleaning as an alternate to grey tape. One Vacuum Cleaner will be required similar to STS and ISS versions. The Vacuum Cleaner will not be required for the Block 1A ISS missions which have the shorter duration.

Wet Wipes:

Heritage: STS and ISS

Maturity: Flight certified for STS and ISS. Similar item will be re-certified for CEV.

Basis of Estimate: Assuming 40 wipes per pack. Each crew member/day: 1 pre-meal personal hygiene, 1 post-meal personal hygiene, 3 WMC facility clean-up, 3 Waste Hygiene, 2 other housekeeping, 2 other personal hygiene=12/crew member/day. 12/40=0.3 pack/crew member/day. WMC facility clean-up for minor cleansing. WMC sanitation kit being bookkept with WMC commode.

Dry Wipes:

Heritage: STS and ISS

Maturity: Flight certified for STS and ISS. Similar items will be re-certified for CEV.

Basis of Estimate: Assuming 40 wipes per pack. Each crew member/day: 3 WMC facility clean-up, 12 Waste Hygiene, 2 other housekeeping, 2 other personal hygiene=19 wipes/crew member /day. 19/40=0.475 pack/crew member/day.

Sanitation Wipe Kit:

Heritage: Mir and ISS

Maturity: Russian certified for ISS. Similar item will be re-certified for CEV.

Basis of Estimate: Quantity packaged as kit for ISS will suffice for CEV duration. CB provided data from ISS logs.

Towels:

Heritage: ISS

Maturity: Russian certified for ISS. Similar item will be re-certified for CEV.

Basis of Estimate: New use rate is 1+ (1/crew member/1 Day). First day - need 1 wet + 1 dry each. For future days, the former wet towels will become the future dry towels. CB provided data from ISS logs.

Crew Provisioning /Clothing

Clothing and Crew Preference:

Heritage: STS and ISS

Maturity: Flight certified for STS and ISS. Similar items will be re-certified for CEV.

Basis of Estimate: Start with ½ CTB as a base and add 1/15 of ½ CTB mass and volume for each day of mission. CB provided data.

Tablet PC:

Heritage: New item.

Maturity: Concept.

Basis of Estimate: 1 per crew member.

Maintenance

IFM Standard Tool Kit:

Heritage: STS

Maturity: Flight certified for STS and ISS. Similar items will be re-certified for CEV.

Basis of Estimate: The HSIR specifies a minimal tool set. The Engineering In-Flight Maintenance (IFM) team concurs with this tool set but suggests we supply several components not contained in HSIR. Engineering suggests that the HSIR minimal tool set be considered the “design to” list and be distributed to all hardware providers. In addition, EC recommends the addition of a supplemental set of tools intended for unplanned repairs consistent with the type of repairs seen on-orbit.

<u>*Operational Supplies*</u>

Bungees:

Heritage: STS and ISS

Maturity: Flight certified for STS and ISS. Similar items will be re-certified for CEV.

Basis of Estimate: Bungee estimates based on small item restraints used in STS and ISS.

Multiuse Bracket:

Heritage: STS and ISS

Maturity: Flight certified for STS and ISS. Similar items will be re-certified for CEV.

Basis of Estimate: Based on STS and ISS use, 2 are being proposed to support FCE (2 units are also being flown by Photo/TV).

<u>*Food Preparation*</u>

Food Warmer:

Heritage: STS and ISS

Maturity: New development based on STS and ISS units incorporating advanced technology to decrease the weight and maximize warming efficiency.

Basis of Estimate: Based on CB input, Block 1A will not require a food warmer for such a short duration mission. Block 2 Lunar mission, one food warmer is proposed. Original estimates for the food warmer sizes were based on doubling the capacity of existing ISS food. New unit will attempt to reduce the mass and volume of the ISS unit by 15%-30% and increase warming capacity by 15%-30%.

<u>*Food*</u>

Food:

Heritage: ISS and Shuttle

Maturity: New development based on ISS units in incorporating advanced food technology in food packaging to decrease overall mass of packaged food.

Basis of Estimate: Based on ISS food system averages, one crewmember uses 1.83 kg of packaged food per day. The volume of that food is 0.00472 m^3.

Food Container:

Heritage: ISS collapsible food container

Maturity: New development based on ISS units in incorporating advanced technology in food packaging to decrease overall mass of container while still protecting the food packages from damage.

Basis of Estimate: Each food container has a volume of 0.0137 m^3 and a mass of 0.705 kg.

<u>*Trash Volumes*</u>

Food Trash Volume Compartment:

Heritage: ISS

Maturity: Russian certified for ISS. Similar item will be re-certified for CEV.

Basis of Estimate: 0.67 L / day/ crewmember based on Don Pettit's ISS data. 6 L / 3 days/ 3 crewmembers. 0.5 Kg for 23 L is Russian Bag estimate for mass. 15% margin added to trash generation estimate.

Dry Trash Volume Compartment:

Heritage: STS and ISS

Maturity: Russian certified for ISS. Similar item will be re-certified for CEV.

Basis of Estimate: Based on Don Pettit's ISS data. 46 L / 30 days/ 3 crewmembers. This equals 0.51 L / day/ crewmember. 0.5 kg for 23 L is Russian Bag estimate for mass.15% margin added to trash generation estimate. 1 bag was allocated for Dry Trash based on CB estimate.

Photography

Heritage: STS and ISS

Maturity: U.S. certified for SSP and ISS. Similar items will be re-certified for CEV if possible. All still and video hardware is upgraded as it becomes obsolete and higher capability hardware becomes available

Basis of Estimate: All estimates are based on the existing SSP/ISS hardware.

Medical Equipment

Heritage: STS and ISS

Maturity: Still in requirements definition phase. Large experience base with shuttle missions. Biggest risk is returning ill/injured crewmember from ISS/LSAM.

Basis of Estimate: Single kit shared by entire crew.

9.4.4 Plan Forward

- EC FCE
    - Update trash volumes required per crew use rates instead of using volumes based on 23 L Russian Bag. (One volume will be given instead of bag quantities.)
    - Determine personal hygiene water required to be provided by ECLSS. Since towels are pre-wet prior to packaging on the ground for use on-orbit, ECLSS water numbers need to be reassessed.
    - Determine if food warmer will be required based on input from the Food System.
    - Better define restraints required for hardware and stowage.
    - Track changes to SRD, HSIR, and IRDs and re-assess provisioning based on changes or proposed changes to baselines.

- Document changes due to Cockpit Working Group studies reflecting various crew sizes, mission durations, and mission cargo requirements

- Photography
  - Investigate the use of vehicle power to directly power both the digital still and digital video imagers during IVA operations eliminating the need for batteries and battery chargers.
  - Investigate the use of EMU power to directly power the digital still imager for use in IVA operations
- Medical
  - Performing requirements traceability in FY06. Working with HF/HR SIG to find homes for our requirements that will affect vehicle and operations designs.

10.0 Mechanical Systems

Trades, reference concepts, mass estimates, and analyses performed during CRC-3 as part of the Mechanical Systems functional area are detailed in this section. Mechanical Systems for the purposes of the CEV Reference Configuration study encompasses the CEV Structure, Thermal Protection System, Passive Thermal Control System, Mechanisms, Pyrotechnics, Recovery Systems, and Landing Systems.

10.1 Structures

This section describes the design of the CEV primary structure, including the Crew Module, Service Module, Spacecraft Adapter, and associated mechanical interfaces (Figure 10.1-1). A structures summary of the Launch Abort System (LAS) is contained in separate section describing all subsystems of the LAS.

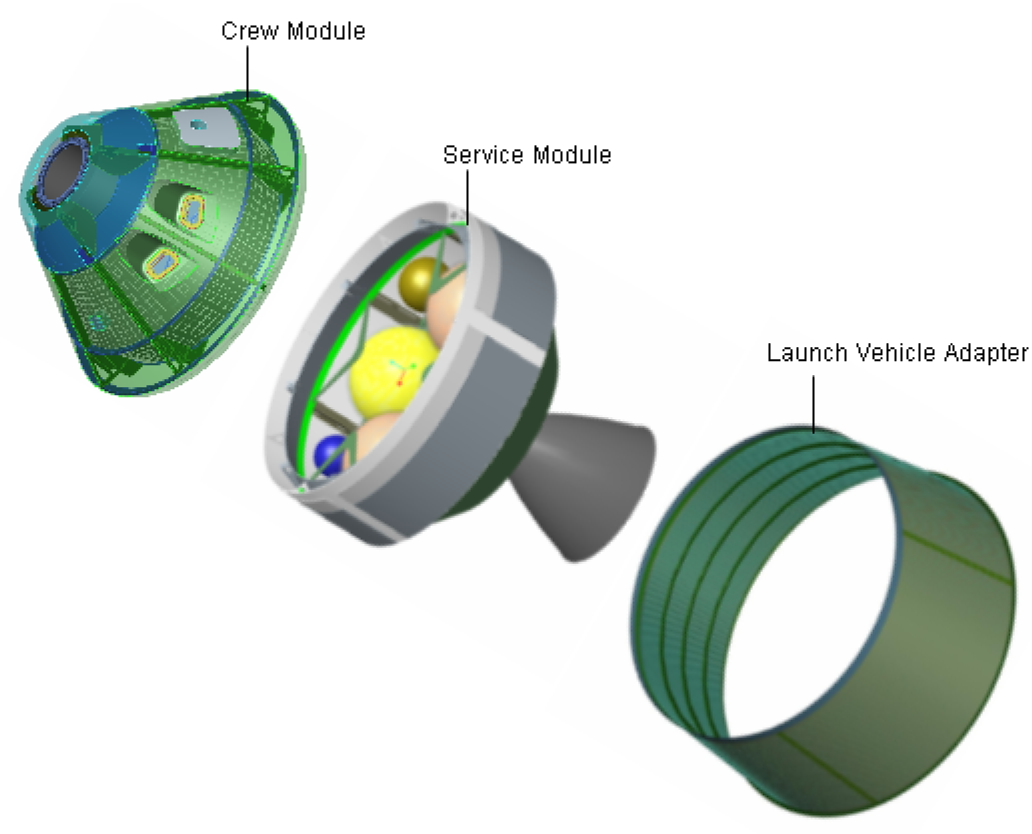

Figure 10.1-1 CEV Primary Structure

10.1.1 Driving Requirements, Groundrules, and Assumptions

The design and analysis of the primary structure for this study was performed assuming a Block II configuration (lunar mission) and an airbag landing system. During the CRC-3 design cycle the decision was made to switch to a vehicle-mounted retrorocket concept with crushable structure to provide landing attenuation in favor of airbags. This will clearly affect the design and sizing of the primary structure, and the effects of this change have not been thoroughly assessed. As such, the majority of the results described in this section still reflect the airbag option with the understanding that further work will be required to assess the retrorocket option.

The coordinate system utilized for the primary structure featured the origin located at the theoretical apex of the back shell cone, with +X pointing aft along the axis of the stack, +Y pointing to starboard, and +Z pointing up (with respect to crew seat orientation).

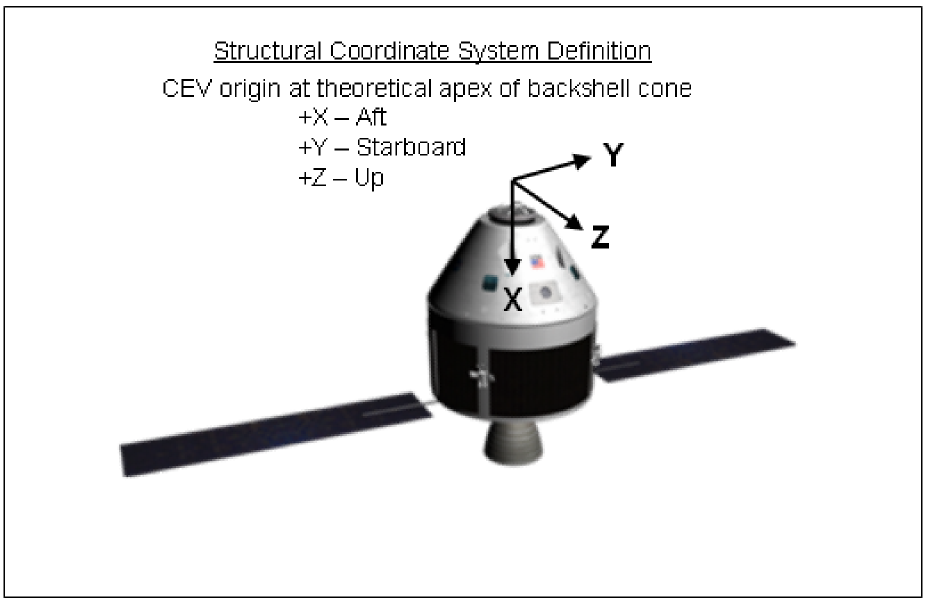

Figure 10.1-2 CEV Coordinate System

There are many CEV Project and Constellation Program requirements relevant to the design, a subset of which is listed below:

CEV System Requirements Document (CXP-10001)

- The CEV Launch Abort System shall provide a thrust of not less than 15 times (TBR-002-12) the combined weight of the CM+LAS for a duration of 2 seconds (TBR-002-149). [CV0042]
- The CEV shall withstand a maximum blast overpressure of 20 psid (TBR-002-150) over ambient conditions for crew survival. [CV0043]
- The CEV design shall comply with Section 5 of NASA-STD-5001, Structural Design and Test Factors of Safety for Spaceflight Hardware. [CV0254]

- The CEV safety or mission critical mechanisms shall in accordance with Section 1- 4 of NASA-STD-5017, Design and Development Requirements for Mechanisms. [CV0255]
- The CEV pressure vessels, pressurized structures, and pressure components shall comply with ANSI/AIAA S-80-1998, Space Systems - Metallic Pressure Vessels, Pressurized Structures, and Pressure Components. [CV0256]
- The CEV composite overwrapped pressure vessels shall comply with ANSI/AIAA S-081-2000, Space Systems – Composite Overwrapped Pressure Vessels (COPVs). [CV0257]
- The CEV structural design and verification requirements for windows, glass, and ceramic structure shall be in accordance with JSC-62550, Structural Design and Verification Criteria for Glass, Ceramics and Windows in Human Space Flight Applications. [CV0258]
- The CEV shall meet its requirements during and after being exposed to the environment defined in the Document Number (TBD-002-110), CEV Loads Data Book. [CV0259]
- The CEV joint design for preloaded joints shall be in accordance with NSTS 08307, Criteria for Preloaded Bolts. [CV0451]
- The CEV shall comply with provisions of JSC 49774A, Standard Manned Spacecraft Requirements for Materials and Processes. [CV0260]
- The CEV shall not automatically relieve cabin pressure volume overboard at a pressure lower than 15.05 psia (778 mmHg) (TBR-002-071). [CV0303]

CEV/CLV Interface Requirements Document (CXP-01001)

- The interface structure shall accommodate the loads defined in the CEV/CLV Loads Requirements Databooks (TBR).
- The CEV shall provide minimum cantilevered natural frequencies of 5 Hz (TBR) laterally and 25 Hz (TBR) axially.

The Design Specification for Natural Environments (CXP-00102) contains requirements for landing conditions (winds, terrain) and MMOD probability of no penetration. In addition, the Human Systems Integration Requirements document (CXP-01000) contains requirements defining the allowable crew loading and acceleration limits as a function of time of exposure.

These requirements have been in a state of flux as the Program refines and updates these documents in preparation for the System Requirements Review (SRR) scheduled to begin in October, 2006. The requirements assumed for this study are consistent with the requirements document versions at the time of the Interim Constellation Program Requirements (ICPR) review in May, 2006. Several additional requirements documents are expected to be included as a part of the SRR process that will also directly affect the primary structure in future design and analysis cycles (Structural Design and Verification Requirements, Fracture Requirements, others). For example, the clean pad ground processing strategy requires a vehicle capable of being lifted and stacked while fully loaded.

Finally, the CEV SRD requirement number CV0259 refers to the CEV Loads Data Book, which contains the derived requirements for vehicle loads. There will actually be two separate loads data books, 1) a Constellation loads data book developed by NASA containing integrated loads while CEV is attached to the CLV or in other mated configurations (LSAM, ISS), and 2) a CEV loads data book developed by the prime contractor containing CEV specific loads (unmated). Neither of these books existed at the time of this design study, so a set of load cases were developed internally by gathering data from numerous sources and trade studies. The following table and figures show the load cases initially applied to size the structure:

Mission Phase	Load Case	Description	Magnitude	CM	SM	LVA
Lift Off	Lift Off	Inertial load factors	Axial = 3.3/-2.0g's Lateral = 1.5g's (RSS)	X	X	X
1st Stage Ascent	Max Accel with Q-bar	Inertial loads and dynamic pressure	2.6g's, 350 psf	X	X	X
	Max Q-bar with Accel	Inertial loads and dynamic pressure	1.75g's, 832 psf	X	X	X
	Max Load	Inertial loads and dynamic pressure	2.5g's, 510 psf	X	X	X
2nd Stage Ascent	Max Accel	Inertial load factor	Axial = 5.0g's	X	X	X
Pad Abort	LAS Thrust	Acceleration	15 g's	X		
	Blast Overpressure	Quasi-static pressure (0° symmetric blast & 45° oblique blast assessed)	20 psi	X		
	Combined LAS Thrust and Blast	Acceleration and applied pressure	15 g's, 20 psi	X		
On-Orbit Ops	Cabin Pressure	Applied internal pressure	15.2 psi (ISS)	X		
	TLI Burn (EDS Thrust)	Eyeballs-out acceleration and cabin pressure	1.4 g's (burnout), 9.5 psi	X	X	
	LOI Burn (LSAM Thrust)	Eyeballs-out acceleration and cabin pressure	0.53 g's (burnout), 9.5 psi	X	X	
	TEI Burn (SM Thrust)	Eyeballs-in acceleration and cabin pressure	0.49 g's (burnout), 9.5 psi	X	X	
Atmospheric Entry	ISS Nominal Direct	Applied dynamic pressure with inertia relief	272 psf	X		
	ISS Ballistic	Applied dynamic pressure with inertia relief	836 psf	X		
	Lunar Skip	Applied dynamic pressure with inertia relief	366 psf	X		
	Lunar Ballistic	Applied dynamic pressure with inertia relief	1001 psf	X		
	Unpressurized Entry	Cabin crush pressure due to venting lag	1 psi	X		
Recovery and Landing	Drogue Chute Line Loads	Acceleration	5g's in 40° cone about X-axis	X		
	Main Chute Line Loads	Acceleration	5g's in 20° cone about X-axis	X		
	Landing	Nominal attenuation at 25 ft/sec (acceleration)	8g's reacted at CM pressure vessel	X		

Table 10.1-1 Load Cases Assessed for Structural Sizing

Integrated stack analyses were performed which generated a series of enveloping design loads (axial, shear, bending) as a function of CLV X-station (see Figures 10.1-3 through 10.1-6). These loads represent the maximum values for all ascent flight phases and uncertainty factors have been included since fully dispersed Monte Carlo dispersions were not yet available for all cases (described in CxP 72067 "Ares-I System Structural Dynamics, Loads, and Model Data Book", draft dated August 31, 2006). These loads include both inertial and aerodynamic loading.

The majority of the structural sizing was performed using the blue curves labeled "CFI". An updated set of loads became available at the end of this study which is shown in red, labeled "DAC1A". Note that although the axial loads were significantly reduced in this update, the bending moments increased dramatically. There was insufficient time to fully resize the structure with these updated loads in this design cycle and the affect on the vehicle structural mass estimates has not been quantified. It should be noted, however, that the interface forces and joint preload estimates at the LAS-CM and CM-SM interfaces are consistent with the updated DAC1A loads.

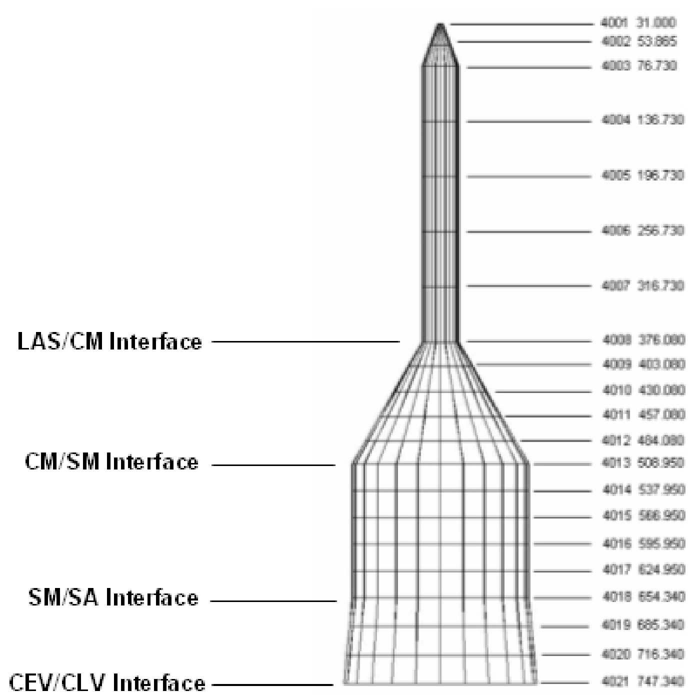

Figure 10.1-3 CLV X-Station Coordinates in Integrated Coupled Loads Model

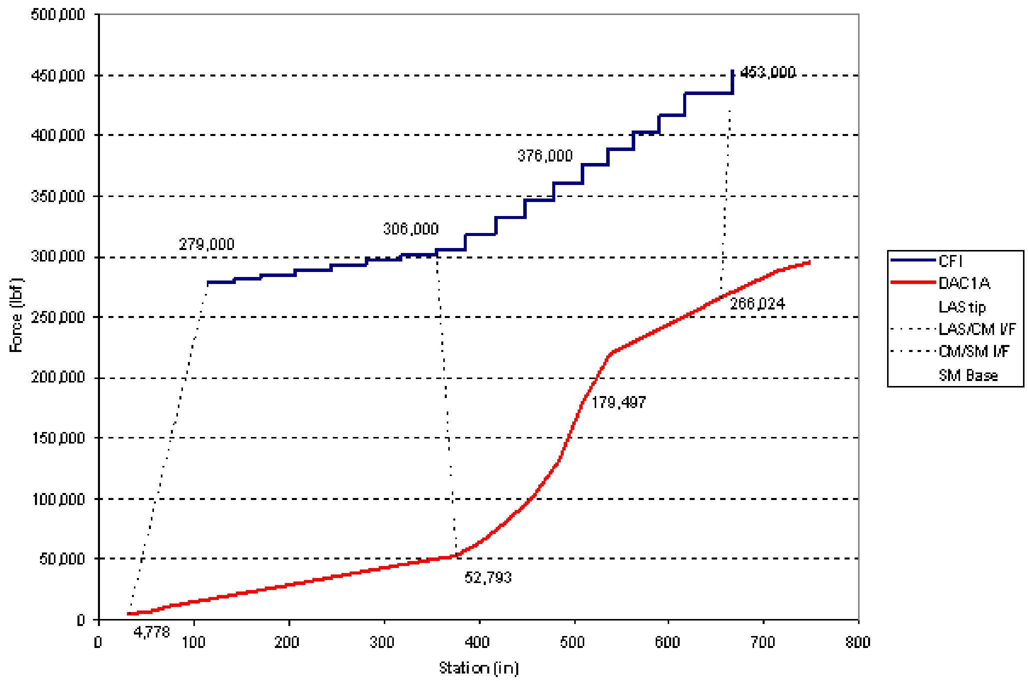

Figure 10.1-4 Axial Force in CEV vs. CLV Stack X-Station

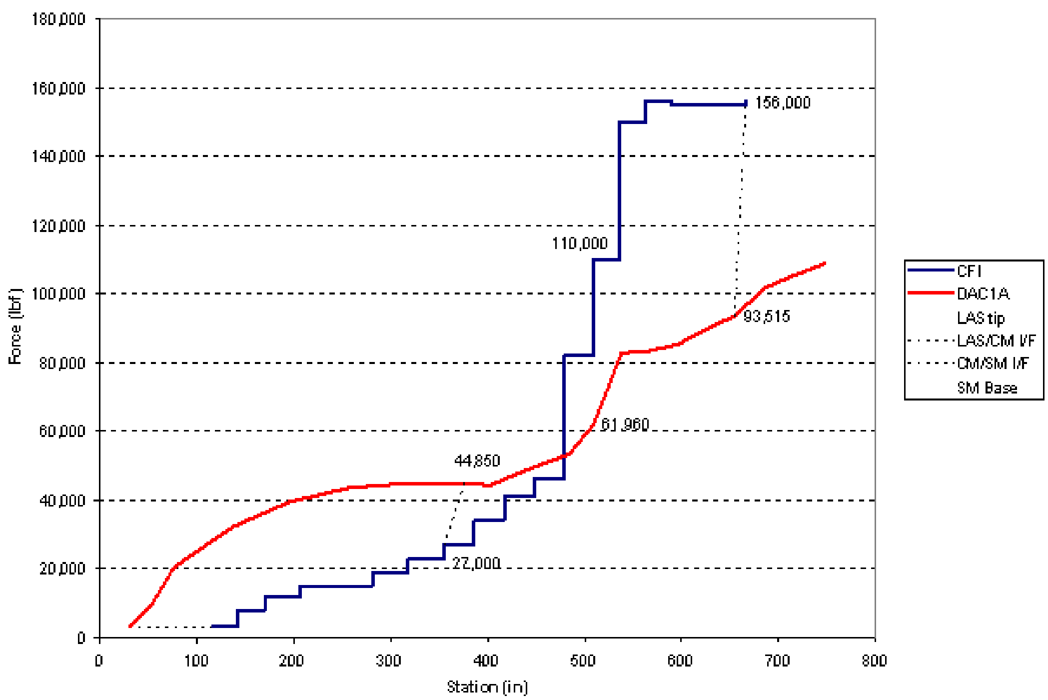

Figure 10.1-5 Shear Force in CEV vs. CLV Stack X-Station

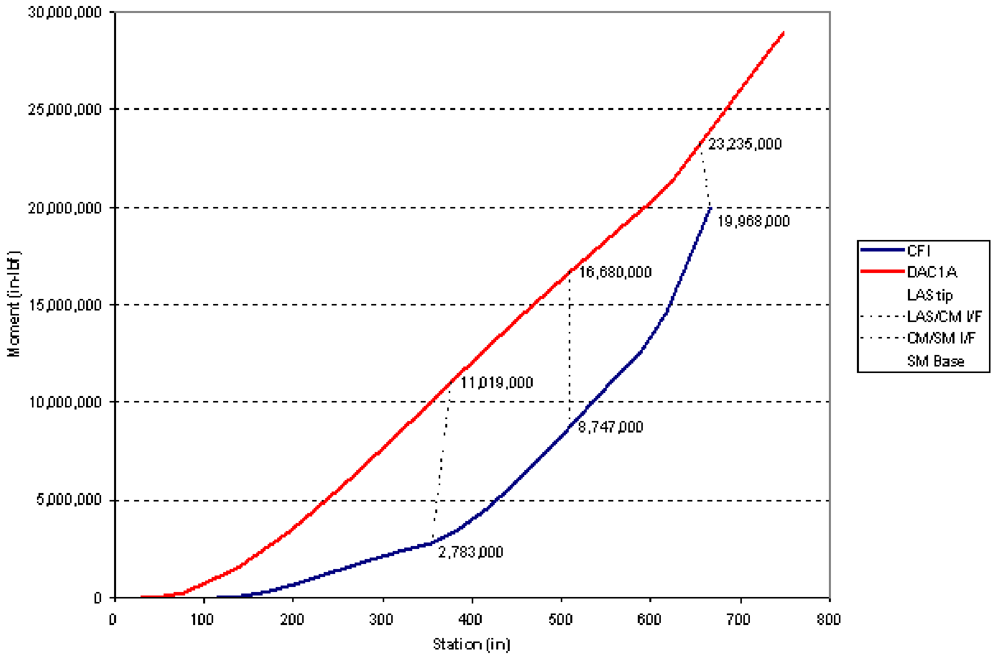

Figure 10.1-6 Bending Moment in CEV vs. CLV Stack X-Station

10.1.2 Conceptual Design Overview

10.1.2.1 Crew Module

The Crew Module structure consists primarily of a pressurized compartment for crew habitation and an outer aeroshell, which is used to react aerodynamic loading and provide the structural interface for the thermal protection system.

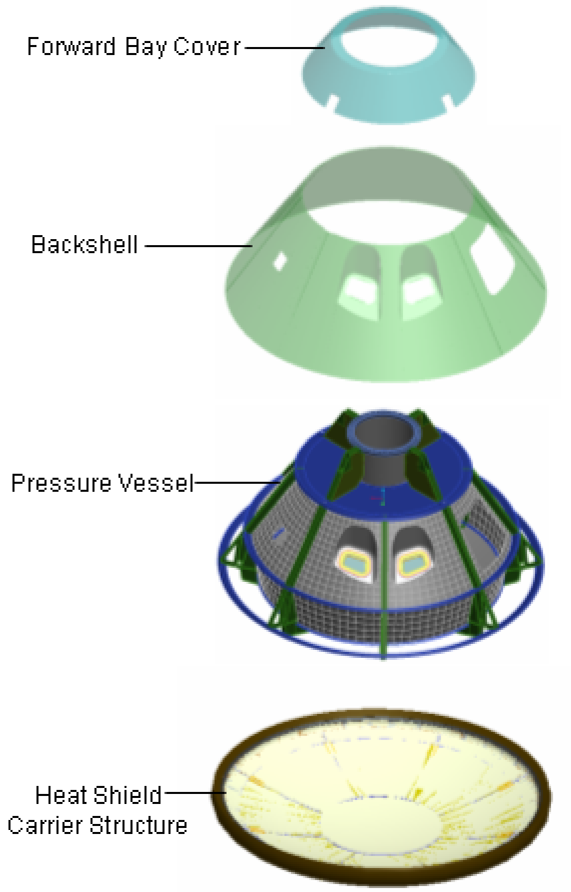

Figure 10.1-7 Crew Module Primary Structural Components

The pressurized crew compartment, shown in Figures 10.1-8 and 10.1-9, features ring frames, longerons, and skin panels machined from 2195-T8 aluminum-lithium alloy. There are eight longitudinal beams, or longerons, that carry the axial loads through the capsule. Four of the longerons are considered to be primary longerons in that they react the LAS loads, the crew seat pallet strut X-loads, the CM/SM interface forces during liftoff and ascent, and landing loads. There are also four intermediate, or secondary, longerons that are primarily designed to react CM/SM interface and landing loads but also help react internal cabin pressure and support the back shell. There are eight interface points between the CM and SM in the form of tension ties and compression pads. Four hardpoints at the forward bulkhead serve as the structural interface with the LAS tower.

The cabin side walls are a machined orthogrid configuration, with roll-formed or bump-formed skin panels. The aft bulkhead dome features a spin-formed aft dome cap surrounded by 8 stretch-formed gore sections. The forward bulkhead is an integrally machined flat plate. The skin panels are attached to ring frames and longerons using the friction stir welding process.

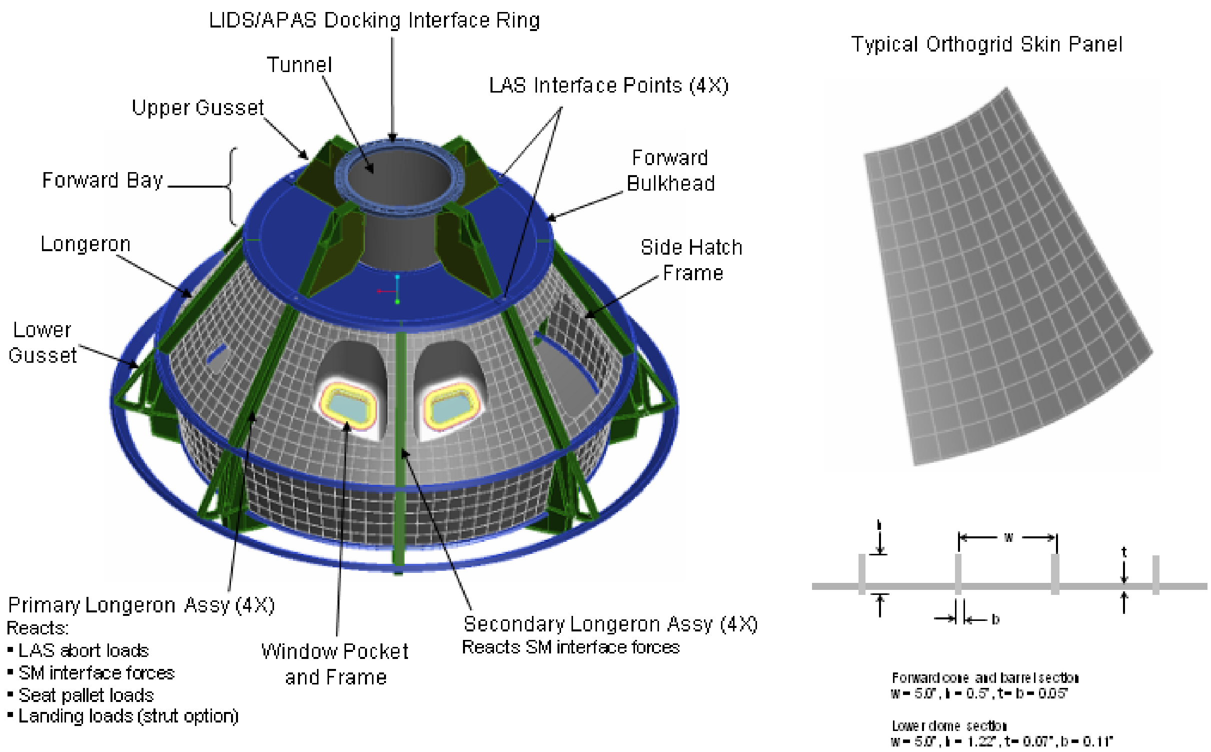

Figure 10.1-8 Crew Module Pressure Vessel - Upper Iso View

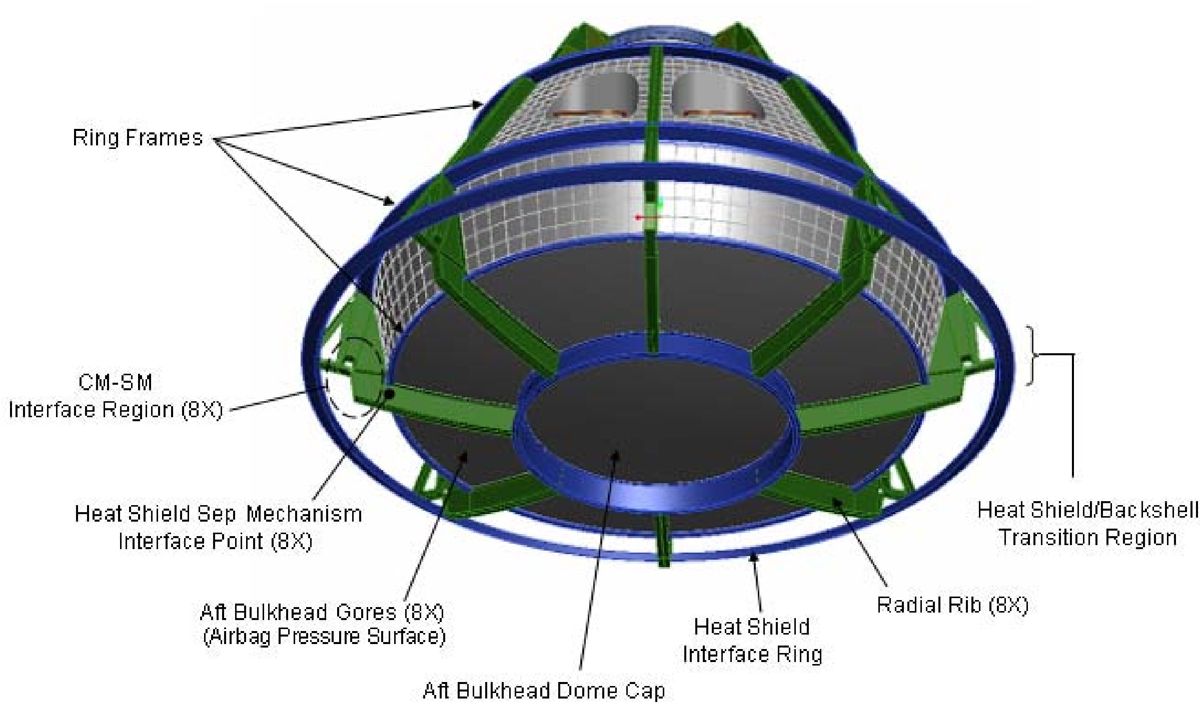

Figure 10.1-9 Crew Module Pressure Vessel - Lower Iso View

Initial studies assumed a fusion welded approach for the pressurized portion of the Crew Module using 2219-T87 aluminum alloy due to extensive flight heritage in launch vehicle propellant tanks as well as the Space Shuttle crew compartment. However, due to the importance of minimizing vehicle dry mass, numerous other alloys were considered. These include aluminum alloys 2124, 7475, and 7050, as well as aluminum-lithium 2195 and titanium 6Al-4V.

Figure 10.1-10 shows how the specific strength (i.e., strength/weight ratio) for these alloys compare. Although titanium offers superior strength per unit density, it was eliminated from consideration based on expected fabrication and machining challenges which could significantly drive the cost and schedule. The 2195 aluminum-lithium alloy ultimately selected offers a mass savings of approximately 15% compared to Al 2219. This alloy is currently certified for use in the barrel sections of the Shuttle External Tank (ET) and is compatible with both friction-stir and fusion weld processes (although the fusion weld strength is significantly lower than that of the friction-stir weld). The intent with this design is to leverage off of the design and material allowable development efforts already invested for the certification of the super-lightweight ET to the greatest possible extent (i.e., usage of plate thicknesses and weld lands for which design allowables already exist).

Although there are obvious mass advantages with the use of aluminum-lithium, there are also a number of technical issues to be addressed when using this material for the CEV pressure vessel. In particular, fatigue data for friction-stir welded joints is somewhat limited and may require some expansion of the existing database in order to qualify the vehicle for multiple flights. Also, this alloy is aged to final temper at around 300 °F and strength degradation could occur if there is prolonged exposure at temperatures above this value during thermal soak-back after landing (could also affect reusability). It is not anticipated that the material will exceed these thermal limits given the additional requirement that the crew compartment walls not exceed a touch temperature limit of 110 °F, although this must be verified by analysis (particularly for the outer flanges of the ring frames and longerons). Additional material property characterization will be required for any product forms not already developed for ET (such as forgings potentially used for ring frames). Finally, the highly directional grain structure in this alloy can result in a delamination failure mode if not appropriately accounted for in the design, particularly in regions of triaxial stress.

Composite materials were not initially considered for the pressurized crew compartment design for a number of reasons, including concerns about permeability, handling risk (sensitivity of thin facesheets to out-of-plane bump loads causing delamination or cracking), questionable mass benefit (after including ply buildups, potting, or metallic inserts around pressure vessel penetrations with higher factor of safety required), low ductility (low strain energy to failure and sudden load redistribution post-failure in a load overshoot scenario), crashworthiness and reusability concerns, as well as development cost/schedule risks to achieve flight certification in time to meet project milestones.

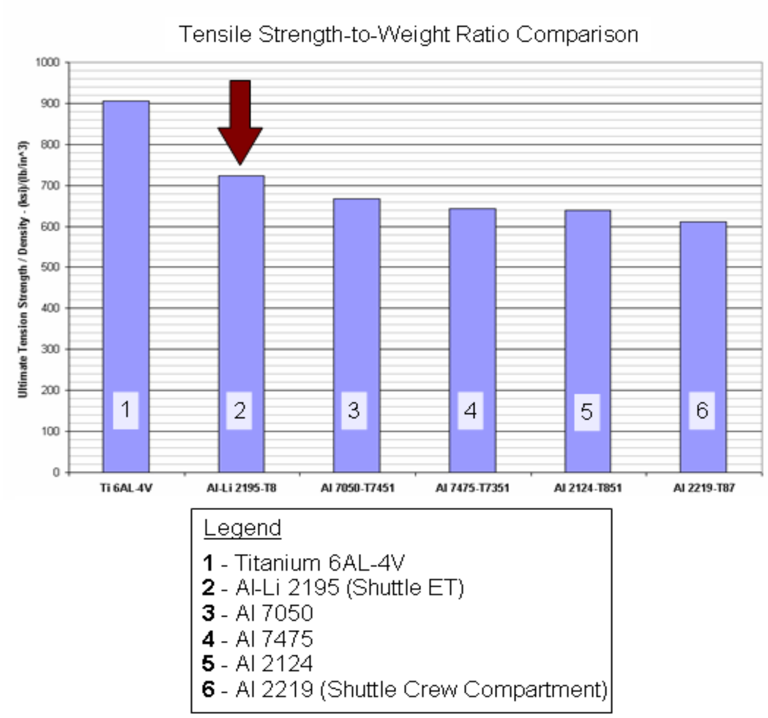

Figure 10.1-10 Specific Strength Comparison for CM Pressure Vessel Alloy Candidates

The Crew Module aeroshell, shown in Figure 10.1-11, is a honeycomb sandwich panel construction. The back shell and forward bay cover are made of graphite/bismalimide (BMI) composite facesheets that are 0.04 inches thick each (eight plies of unidirectional tape in a quasi-isotropic layup) with a 0.75 inches thick aluminum honeycomb core. The back shell is comprised of eight removable panels that are rigidly attached to the pressure vessel for load sharing and structural efficiency. Lightning protection is provided by a layer of copper mesh screen that is integrated into the outer facesheet of the back shell and grounding straps are included to provide electrical continuity (may be integrated into the boost protective cover (BPC) instead, depending upon final BPC configuration).

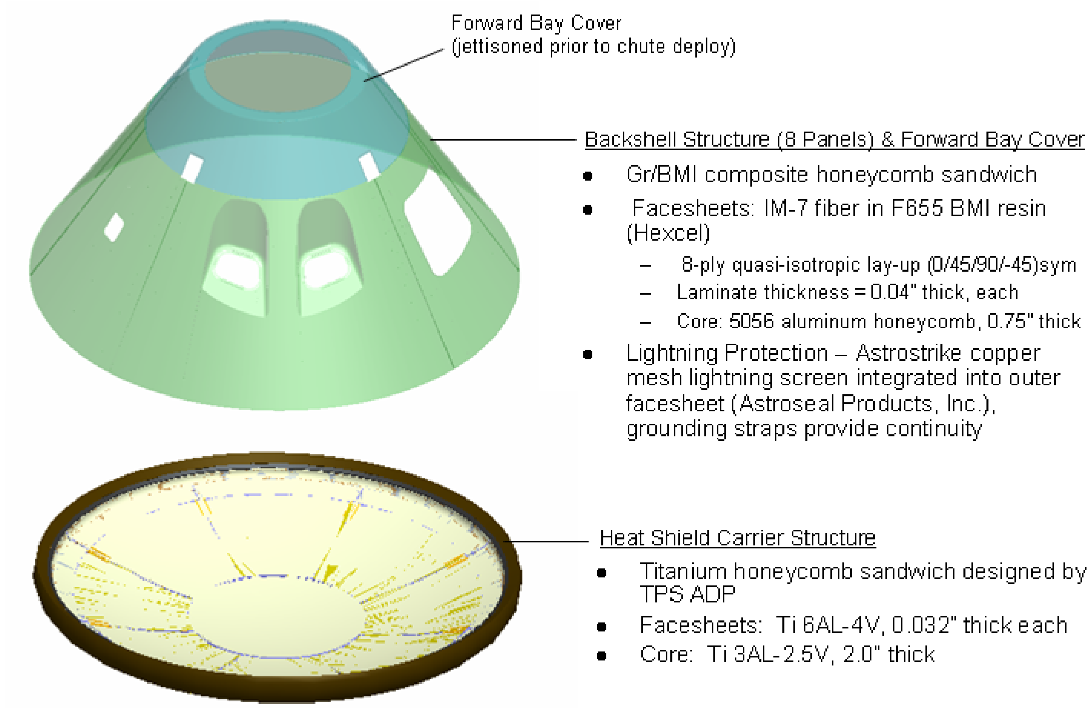

Figure 10.1-11 Crew Module Aeroshell

Figures 10.1-12 and 10.1-13 show additional design details of the back shell. These panels are designed to be removable to provide access to subsystem components and facilitate TPS processing and installation onto the back shell in a separate location. These panels are mechanically attached to the longeron and ring frame flanges using 0.25 inch diameter A-286 fasteners around the panel perimeter. The panel edges are closed out with separate perimeter carrier panels that cover the back shell fastener pattern and provide a continuous TPS surface at the OML. These carrier panels are attached to the structure with a smaller number of fasteners, with carrier panel fastener access provided by threaded tile insert plugs.

The TPS Advanced Development Project team has selected BRI tile as the TPS back shell material for this study (although TPS material trades are still in work). Low density BRI-8 tile covers the majority of the back shell (panels 1 through 3 and 6 through 8) and the higher density BRI-18 is located on panels 4 and 5 where the back shell heating is higher. Since the thickness of the TPS was assumed to be constant for each tile type in this design cycle, the longeron and ring frame flanges were required to be offset at the boundary between the BRI-8 and BRI-18 tile zones to maintain a continuous OML. While this simplifies the mold lines of the underlying structure, this stepped offset is not ideal for load transfer between panels so it is recommended that a continuously variable thickness back shell TPS be assessed as an alternate approach. There is a nominal gap of approximately 4 inches between the inner surface of the back shell structure and the crew compartment pressure wall to enhance MMOD protection. The thermal insulation blankets on the outer surface of the crew compartment panels will provide some additional MMOD mitigation, and additional layers of Nextel and Kevlar can also be included if required.

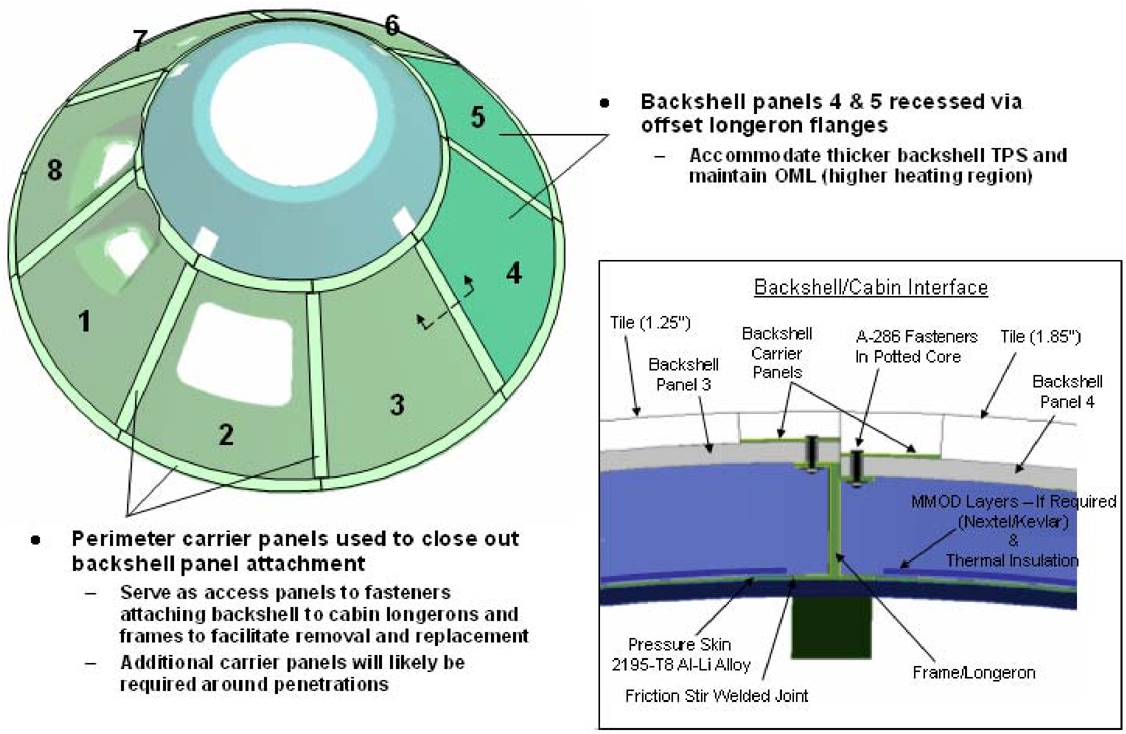

Figure 10.1-12 Back Shell Design Details

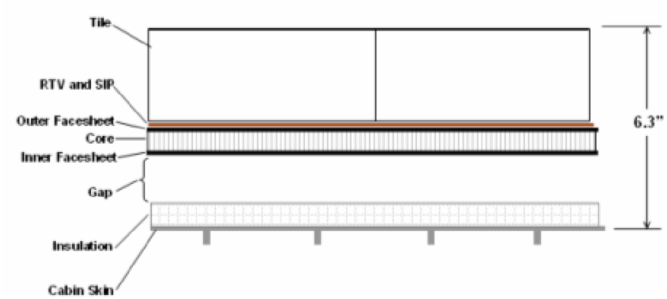

Layer	Thickness (inches)
Tile	1.25"
RTV	.0075"
SIP	.016"
RTV	.0075"
Outer Facesheet (Graphite/BMI Laminate)	0.04"
Core	0.75"
Inner Facesheet (Graphite/BMI Laminate)	0.04"
Gap	3.45"
Thermal Insulation	0.5"
Cabin Skin (2195-T8 Aluminum)	.05"

Figure 10.1-13 Typical Back Shell Section Thicknesses

As shown in Figure 10.1-14, the graphite/BMI composite material utilized for the back shell panels offers excellent specific strength properties. This material has a maximum temperature limit of 450 °F dry and 350 °F – 375 °F with absorbed moisture. The maximum TPS bond line temperature limit on the back shell is therefore assumed to be 350 °F. The RP46 polyimide composite offers higher temperature capability (600 °F dry, temperature limit unknown with absorbed moisture), however a large material allowables program is required to develop design strength properties (TRL ~6). The high temperature RP46 material was not selected for the back shell since initial thermal analysis has shown that the back shell TPS does not realize significant mass savings with a higher bond line temperature in this area (plus the fact that higher temperatures pose additional challenges around penetrations and for surface mounted components such as antennas). Higher bond line temperatures may also threaten the temper and mechanical properties of the underlying aluminum-lithium frames. Although graphite/BMI composites were selected as the baseline back shell material in this design cycle, titanium is a possible weight-competitive alternate material for the back shell if sufficiently thin facesheet thicknesses can be implemented (see base heat shield discussion below).

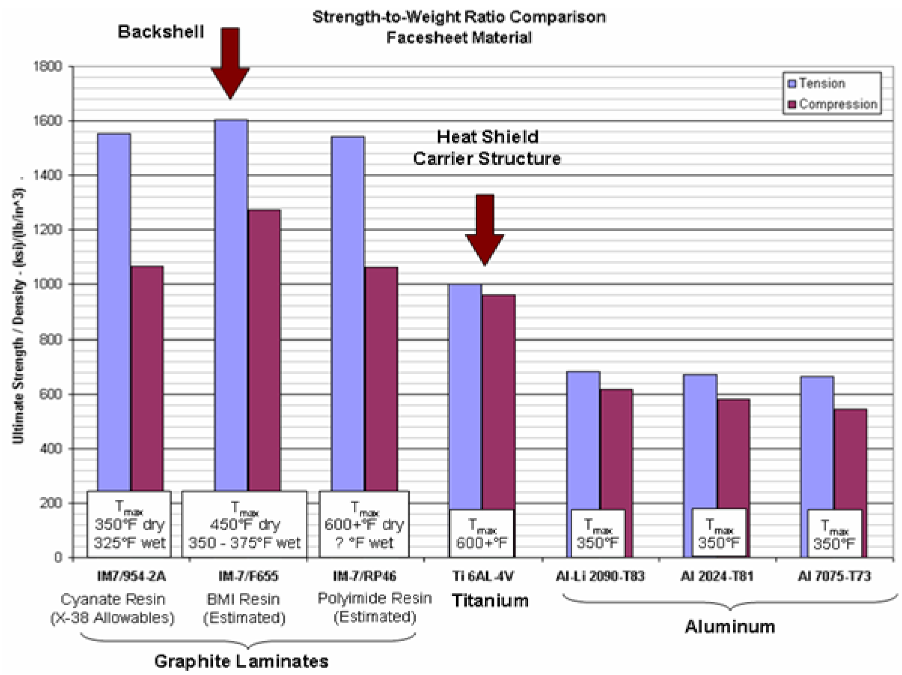

Figure 10.1-14 Specific Strength Comparison, Back Shell Material Options

The base heat shield carrier structure is a Ti 6AL-4V titanium sandwich panel with 0.032 inch facesheets and a 2.0 inch core and is jettisoned prior to deployment of the landing system. Titanium allows for a higher TPS bond line temperature for significant ablator mass savings on the base heat shield (limited by ablator temperature limits at the bond line). The availability of titanium in thinner gages makes it an appealing alternative to composite laminates for facesheets (which are restricted by ply lay-up rules to maintain quasi-isotropy). Figure 10.1-15 shows the specific strength comparison normalized by material minimum gage (~0.04 inches assumed for composite laminates, ~0.02 inches for sheet metal). This plot shows how the metallic facesheet options become weight competitive at thicknesses less than the minimum gage allowed for composites.

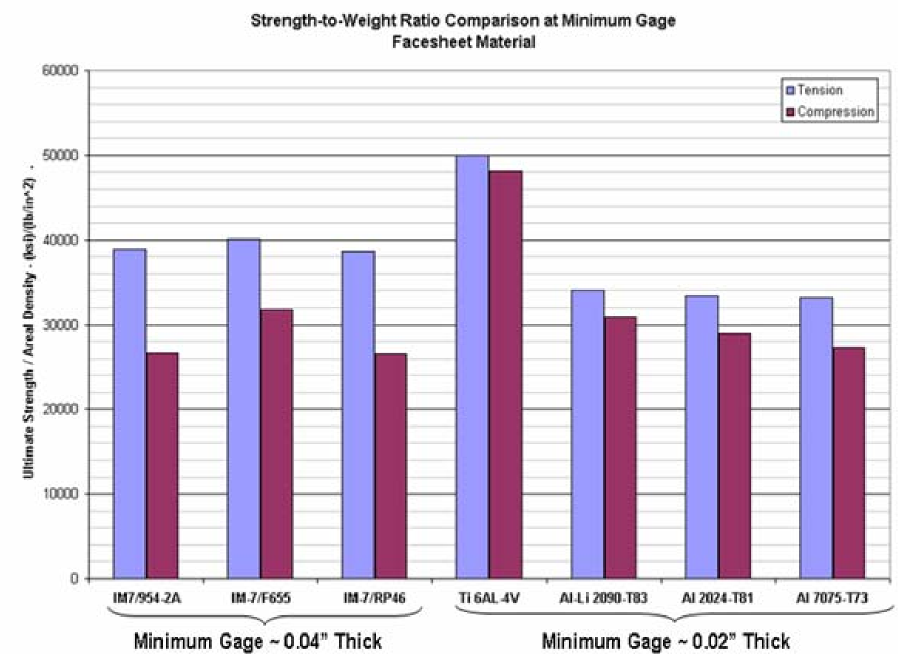

Figure 10.1-15 Specific Strength Comparison, Normalized by Minimum Gage

Windows

The rendezvous and side windows in the Crew Module incorporate features from both the ISS and Space Shuttle window designs (Figure 10.1-16). The window design is comprised of an inner pressure pane assembly and an outer thermal pane assembly which float relative to one another (structurally decoupled to prevent load transfer between the two assemblies). A flexible contamination and moisture barrier is used to close out the volume between the thermal pane and the outer pressure pane. The thermal pane assembly consists of a single thermal pane, a thermal panel retainer and an outer frame that is attached to the back shell structural panels. The pressure pane assembly consists of two pressure panes (for redundancy), two pressure pane retainers and an inner frame that is welded around the perimeter to the aluminum orthogrid pressure skin. In addition, a non-structural scratch pane is in place to protect the inner pressure pane from inadvertent damage during ground processing or flight. This scratch pane is removable for operations that may require optimum optical properties of the windows (cameras, range finders, or other hand-held instruments). This design also allows for an inner protective cover (IPC) to be installed in the event of a pressure pane fracture (the IPC would replace the scratch pane in this case). All critical pressure and contamination seals have at least one backup seal for redundancy.

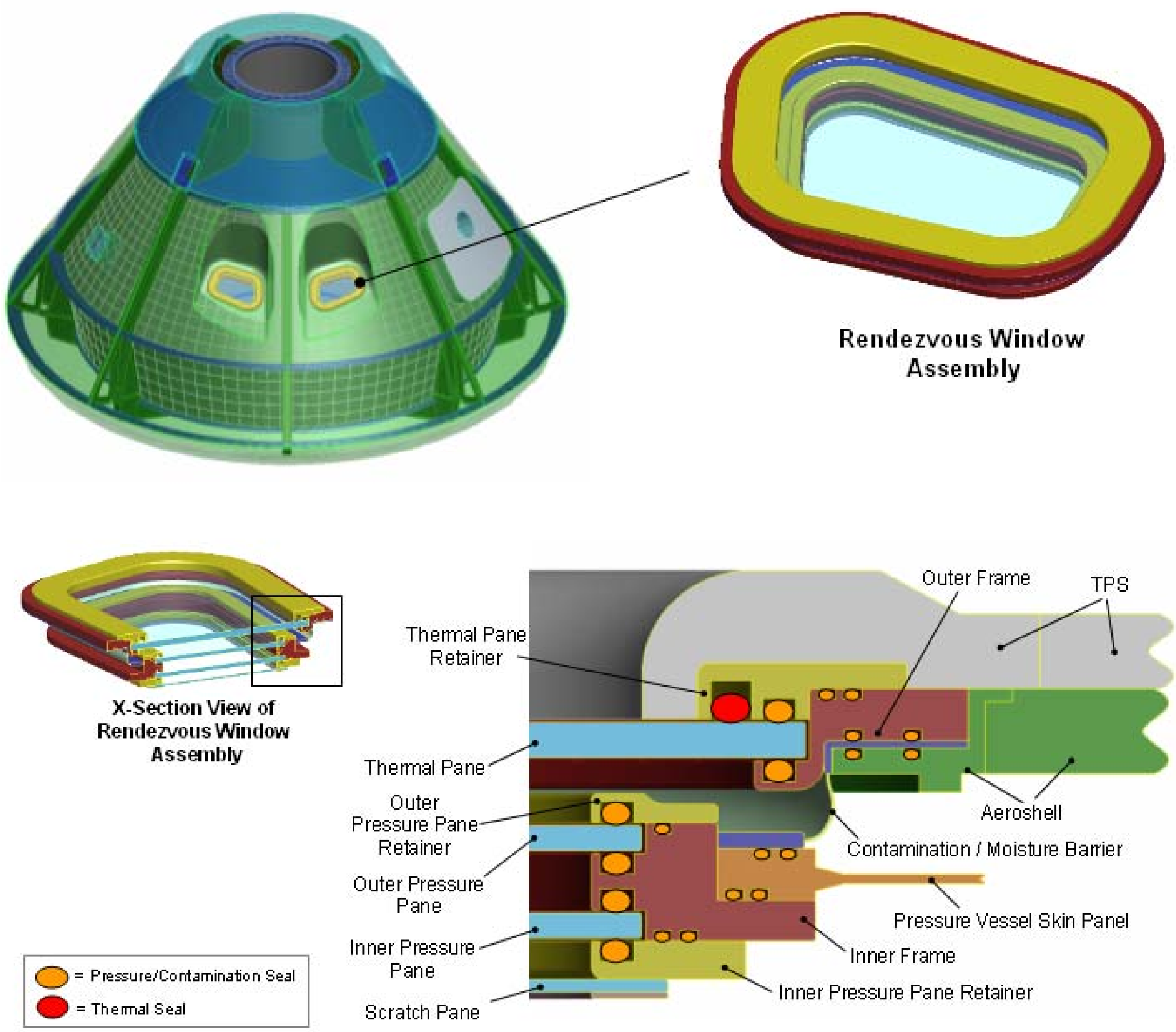

Figure 10.1-16 Crew Module Window Design Details

Crew Module Structural Interfaces

The Crew Module must provide a structural interface with numerous vehicle systems and components, including the Launch Abort System (LAS), docking system, seat pallet struts, heat shield attachment mechanism, and the Service Module (Figure 10.1-17).

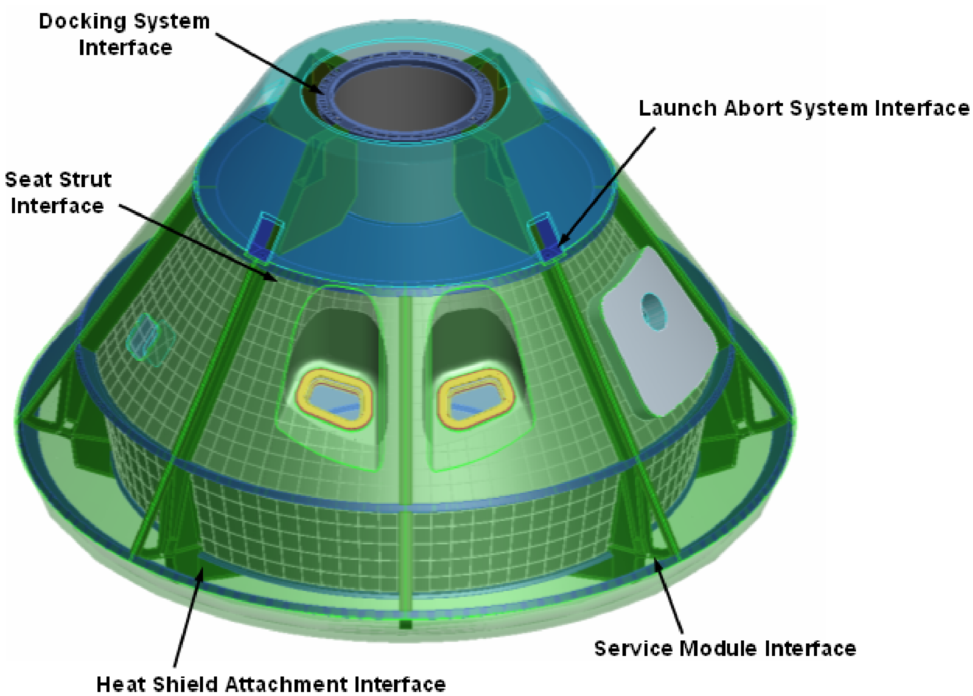

Figure 10.1-17 Crew Module Structural Interfaces

The LAS interface consists of four 1.21 inch diameter threaded steel studs protruding from the forward bulkhead of the Crew Module which are secured to the aft skirt of the LAS adapter with pyro-actuated frangible nuts. These studs are located at a 50 inch radial distance from the vehicle centerline on the forward bulkhead. The LAS loads from the longerons in the aft skirt are transmitted across this interface and into the four primary longerons of the Crew Module (Figure 10.1-18). The overall interface loads and individual hardpoint loads are shown in the tables below. Note that the pad abort loads in these tables do not include dynamic amplification due to ignition and separation transients. If a dynamic amplification factor of 1.5 is assumed, the joint preload at each location would increase from 156,940 lbf to 235,340 lbf, with a required stud diameter of 1.5 inches. A transient analysis of is required to quantify the appropriate factor to be applied.

Load Case	Axial Tension (lbf)	Axial Compression (lbf)	Shear (lbf)	Moment (in-lbf)
Nominal Liftoff/Ascent	0	-52,790	44,850	11,019,000
Pad Abort	258,780	0	17,300	4,738,120

Table 10.1-2 Peak Stack Loads at CM/LAS Interface

Load Case	Axial Tension (lbf)	Axial Compression (lbf)	Shear (lbf)
Nominal Liftoff/Ascent	110,200	-123,400	11,210
Pad Abort	112,100	0	4,325

Joint preload = 156,940 lbf (including 1.4 factor of safety for gapping)

Table 10.1-3 Maximum Interface Forces at Each LAS Hardpoint Location

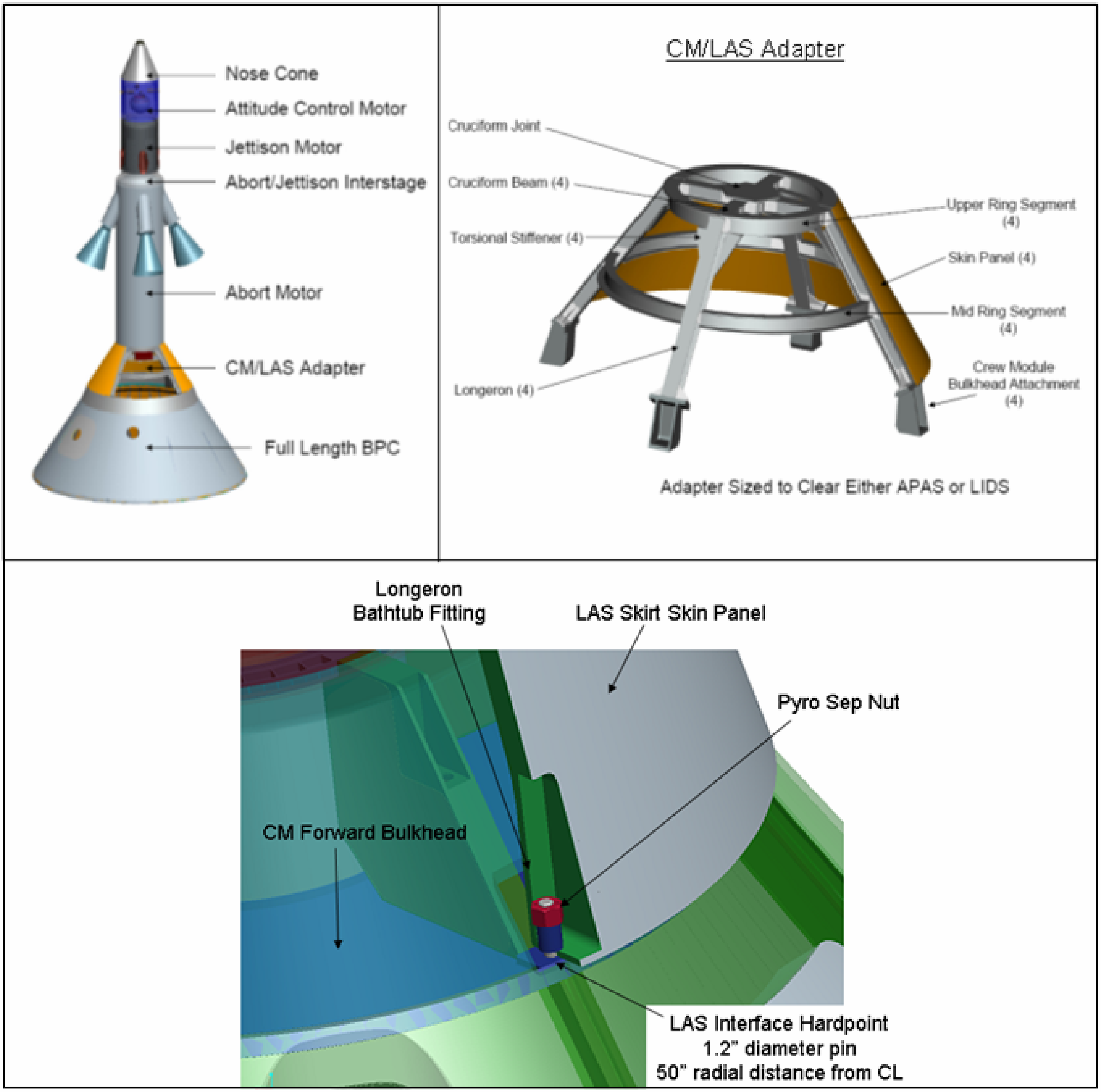

Figure 10.1-18 Launch Abort System (LAS) Adapter Interface

The primary structural interface with the docking system is provided at a ring at the top of the Crew Module tunnel. This ring includes a pyro line charge to separate the docking system prior to atmospheric re-entry (Figures 10.1-19 and 10.1-20). Loads imparted while mated to the LSAM or the ISS are transmitted through the docking system and out to the upper longeron gussets. The Low Impact Docking System (LIDS) is shown, however this design will also accommodate the APAS docking option.

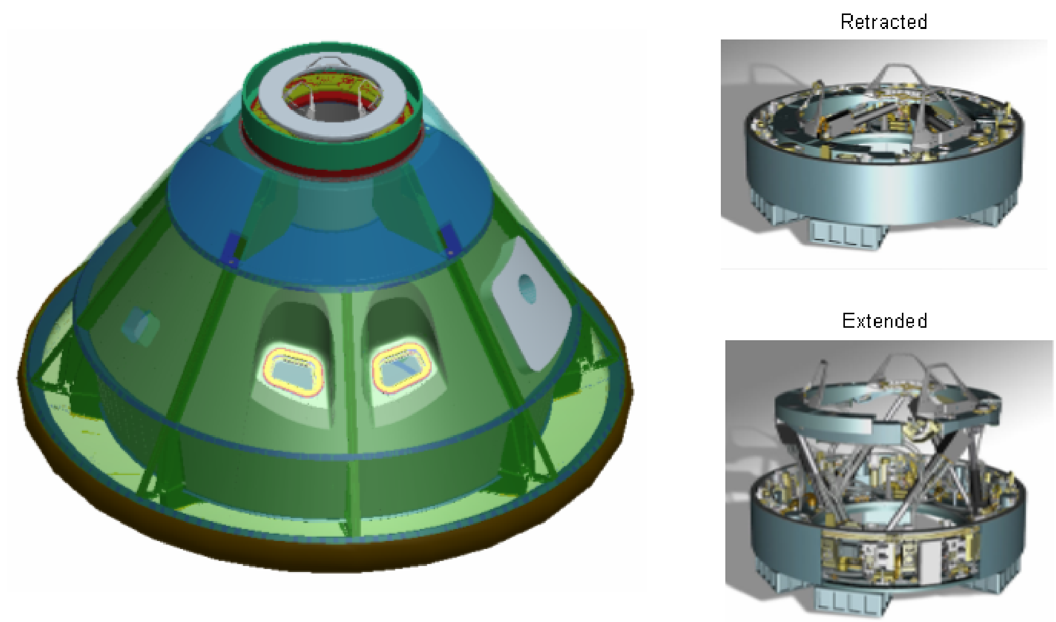

Figure 10.1-19 Low Impact Docking System (LIDS)

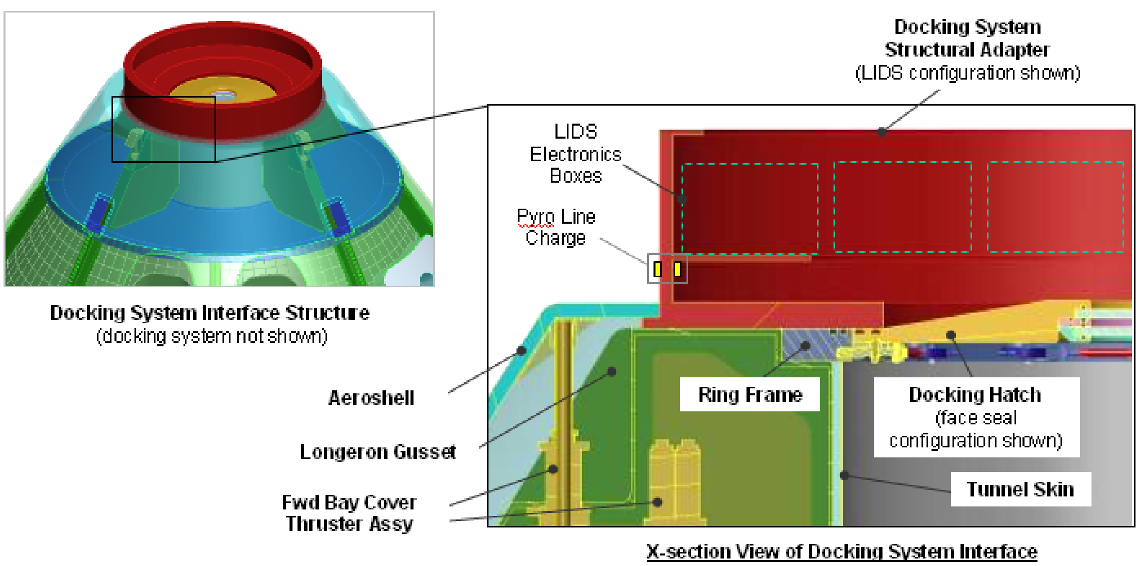

Figure 10.1-20 Docking System Interface Detail

The seat pallet is supported in the Crew Module by a total of eight struts. Four struts are used to attach the pallet to the forward bulkhead (adjacent to the primary longerons for a direct load path) and react the launch and landing loads in the X direction. Lateral loads are reacted by two struts each in the Y and Z directions which attach either to the lower ring frame or the lower longerons in the barrel section of crew compartment.

An alternate strut arrangement was assessed featuring the X-direction struts mounted to the aft bulkhead to provide increased unimpeded habitable volume. Seat pallet stability issues were encountered with this concept, however, as well as problematic out-of-plane point loading into the aft bulkhead. Since additional development will be required to address these issues and establish the feasibility of this approach, forward mounting X-direction struts remain the baseline at this time. Implementation of quick-release pins at the strut attachment location could facilitate removal of a subset of the struts in orbit to provide additional unimpeded habitable volume (Figures 10.1-21 and 10.1-22).

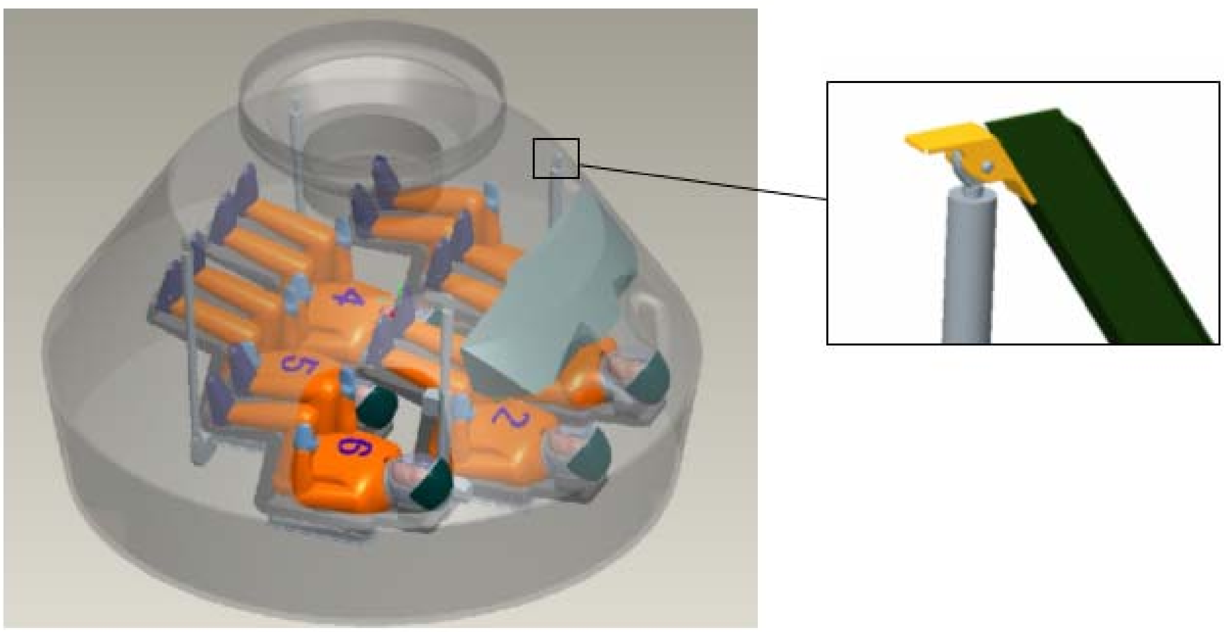

Figure 10.1-21 Seat Pallet Attachment (ISS Configuration Shown)

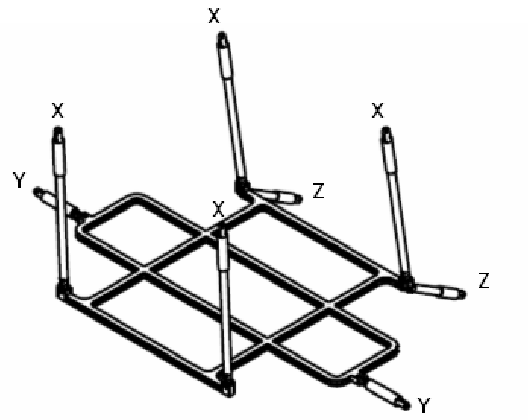

STRUT	LENGTH (INCH)	ANGLE (DEG) (SEE DWG FOR DEF)	FORCE (LBS AXIAL IN STRUT)	QTY	STROKE (INCH)
X (HEAD)	56.25	8.5	9,739	2	6.0 TENSION 3.0 COMP
X (FOOT)	55.69	2.6	10,377	2	6.0 TENSION 3.0 COMP
Y	17.84	0.0	9,954	2	4.0 TENSION 4.0 COMP
Z	26.43	31.9	11,725	2	4.0 TENSION 4.0 COMP

Figure 10.1-22 Stroke and Peak Loads in Each Seat Pallet Strut

The primary structural interface between the Crew Module and the Service Module is provided at eight locations featuring a tension tie and a heat shield compression pad at each point. Each tension tie is preloaded to 72,520 lbf to insure that no gapping occurs at the mating surfaces between the Service Module compression pad and the Crew Module heat shield during the mission (with launch and ascent loading being the most critical). The tension tie is pyrotechnically severed just outside of the heat shield to allow the Service Module to be jettisoned prior to re-entry. Shortly thereafter, the other end of the tension tie is also cut to eliminate a thermal conduction path into the Crew Module. The remaining tension tie segment remains mechanically captive with the heat shield carrier structure during re-entry and is jettisoned with the heat shield prior to the deployment of the landing system.

One concept for this interface is shown in Figure 10.1-23 featuring a non-coaxial tension tie and heat shield compression pad assembly similar to the Apollo design. The centers of the compression pads in the heat shield are located at a radial distance of 80 inches from the vehicle centerline while the tension tie penetrations are located at a radial distance of 89.5 inches. The tension tie diameter is 0.82 inches.

A coaxial tension tie and compression pad concept was also evaluated, however geometric clearance problems were noted between the tension tie remnant and the Crew Module lower gusset structure that would interfere with heat shield separation. An alternate tension tie concept featuring a pin retraction mechanism instead of an additional pyro cutter may be more compatible with the coaxial design concept and is recommended for further study. An assessment of the optimum number of tension ties and compression pads is also recommended. The current design assumes a tension tie at each of the eight compression pad locations in order to more evenly distribute the interface forces around the vehicle. However, concerns about system reliability during Service Module separations as well as heat shield penetrations near the flow stagnation region may warrant a reduction in the number of tension ties to four, although this will result in a significant increase in the local interface forces and tension tie preload (see Table 10.1-5).

Load Case	Axial Tension (lbf)	Axial Compression (lbf)	Shear (lbf)	Moment (in-lbf)
Nominal Liftoff/Ascent	0	-179,500	61,960	16,680,000

Table 10.1-4 Peak Stack Loads at CM/SM Interface

Configuration	Tension (lbf)	Compression (lbf)	Shear (lbf)	Tension Tie Preload (lbf)*	Peak Compression Pad Force (lbf)**
Baseline 8 Tension Ties 8 Comp Pads 8 Shear Cones	51,800	68,740	7,750	72,520 tension tie dia. = 0.82 in.	141,260
Option 1 4 Tension Ties 8 Comp Pads 4 Shear Cones	71,740	86,560	15,490	100,436 tension tie dia. = 0.97 in.	186,996
Option 2 4 Tension Ties 4 Comp Pads 4 Shear Cones	103,600	137,500	15,490	145,040 tension tie dia. = 1.17 in.	282,540

*Tension tie preload includes 1.4 factor of safety for gapping

**Peak load on compression pad includes tension tie preload reaction plus compressive flight loads

Table 10.1-5 Maximum Interface Forces at Each Joint Location

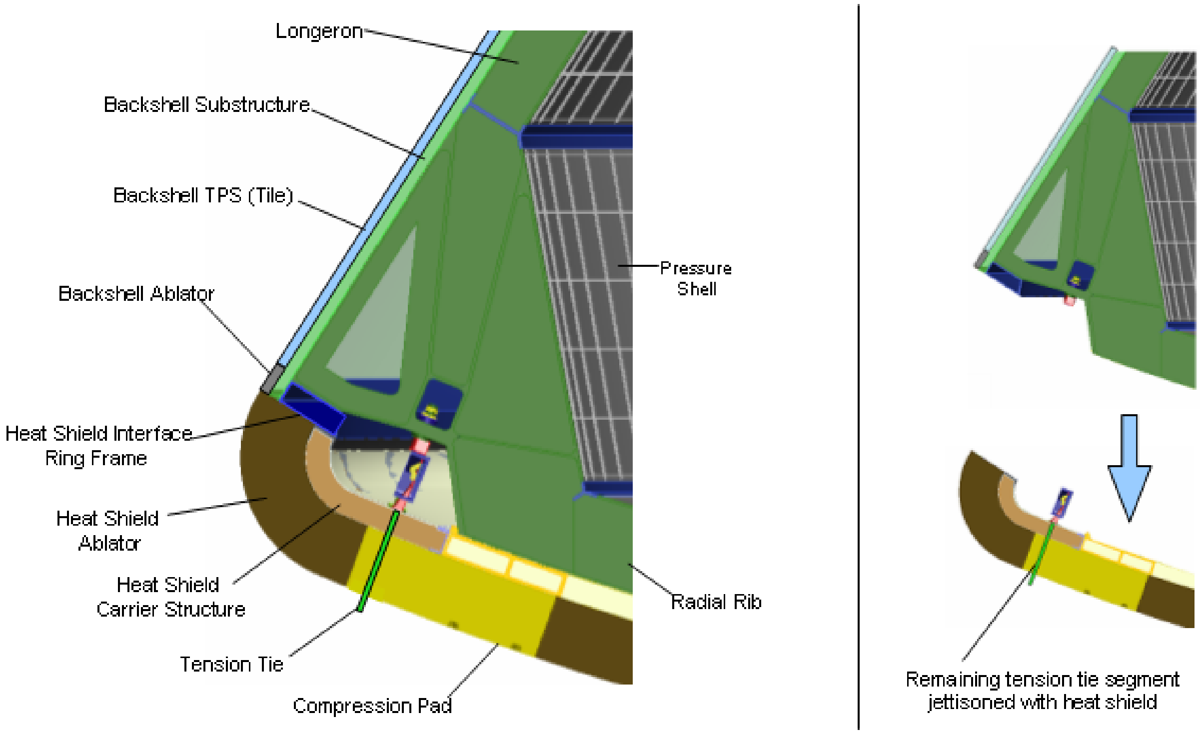

Figure 10.1-23 CM/SM Structural Interface Concept

10.1.2.2 Service Module

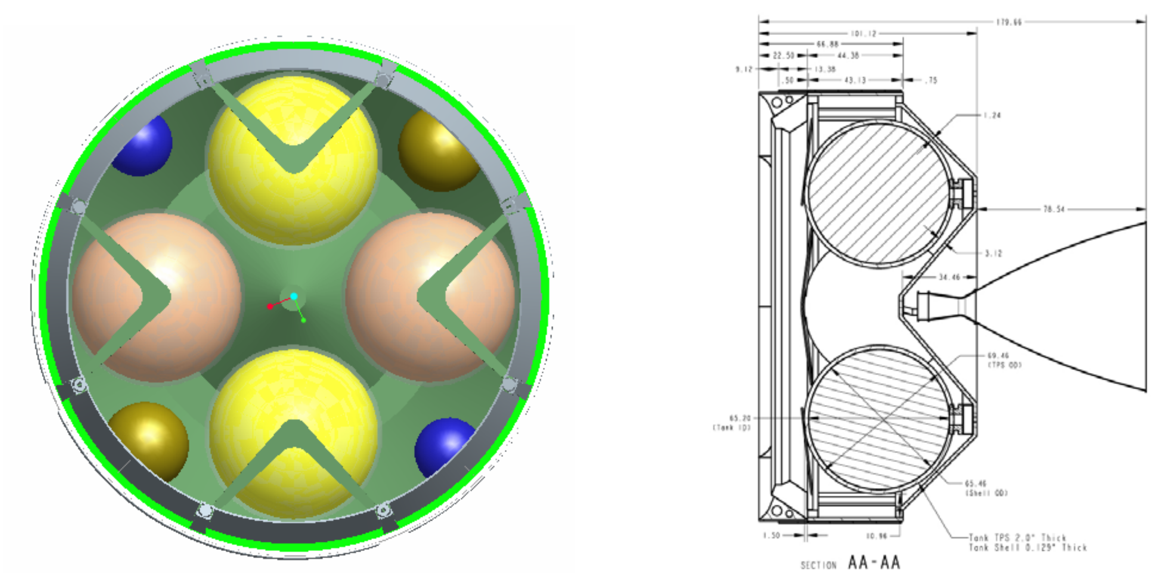

Figure 10.1-24 Service Module

The Service Module structural configuration features a graphite/BMI composite outer shell that transmits primary launch loads into the Crew Module through the eight structural interface points at the CM heat shield. The Service Module longerons function primarily to join adjacent outer shell panels together so that the assembly performs as a monocoque structure. Point loads from the CM are sheared into the outer shell through the conical torque box at the CM/SM interface. The mass of the SM propellant and tanks is reacted by a lower tank support ring which is attached to the launch vehicle adapter ring with a tension cone at the base of the Service Module. Each tank is also supported by two horizontal struts at the top of the tank to react lateral inertial loads. See Figures 10.1-24 through 10.1-26 for these details. The outer shell and tank support tension cone are graphite/BMI composite sandwich panels with 0.08 inch facesheets and an aluminum honeycomb core. The primary ring frames are machined from 7050-T7451 aluminum alloy. Note that in this design, the body-mounted radiators are nonstructural.

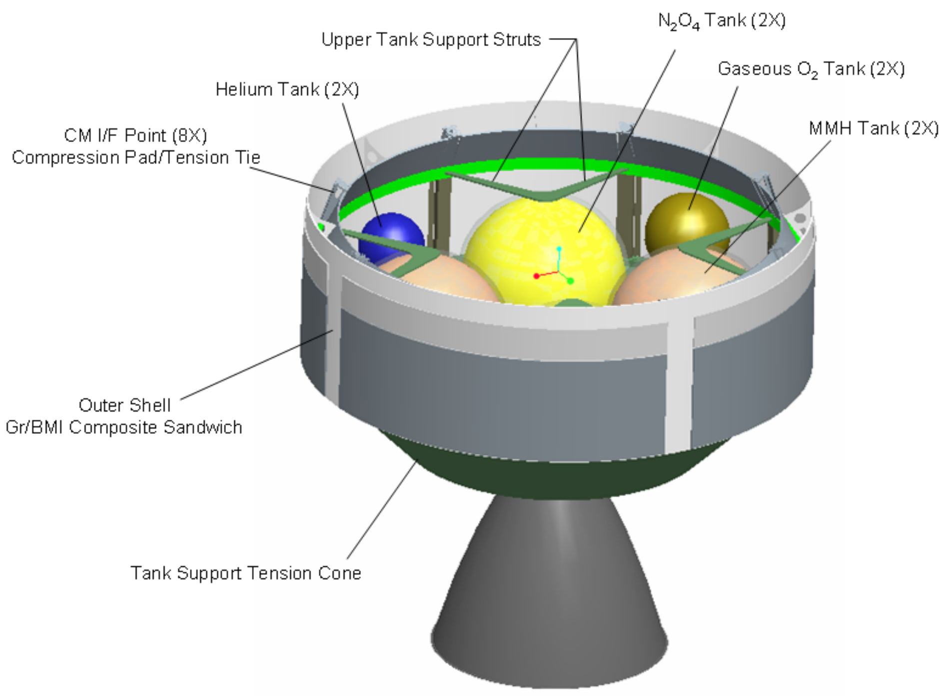

Figure 10.1-25 Service Module – Upper Iso View

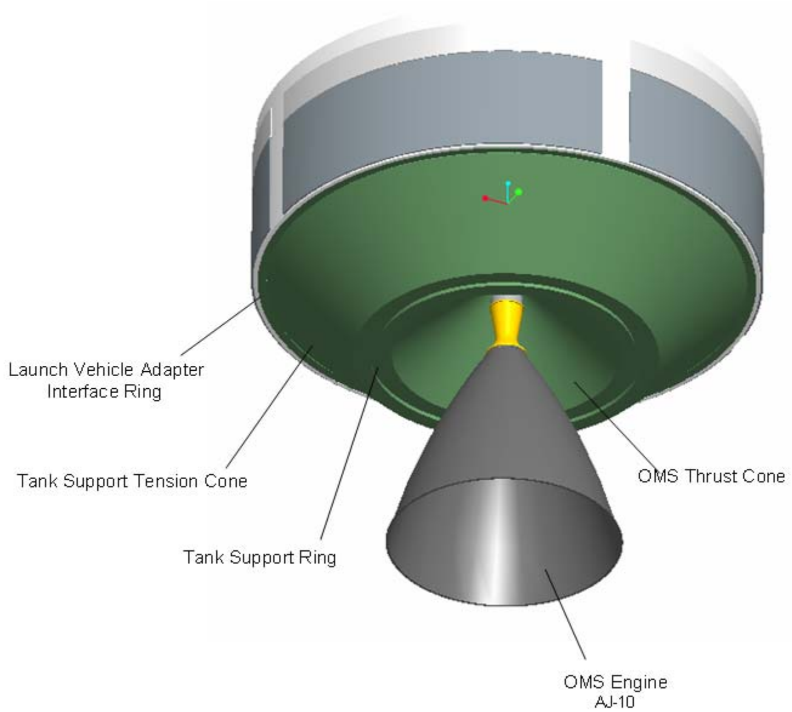

Figure 10.1.26 Service Module – Lower Iso View

One issue not fully resolved in this design cycle was the load path from the Crew Module into the Service Module. The inboard radial location of the compression pad on the CM heat shield results in a significant kick load in the SM interface structure that must be reacted in some fashion (with either a conical torque box or additional struts at each interface location). One potential alternate solution to this issue is to straighten the load path through the SM by implementing longitudinal struts that connect the compression pad down to the lower ring frame (see figure below). These struts would transfer the large CM/SM interface loads directly to the aft ring frame and hence into the Spacecraft Adapter. These changes are not reflected in the structural analysis described in later sections but are considered to be mass-neutral.

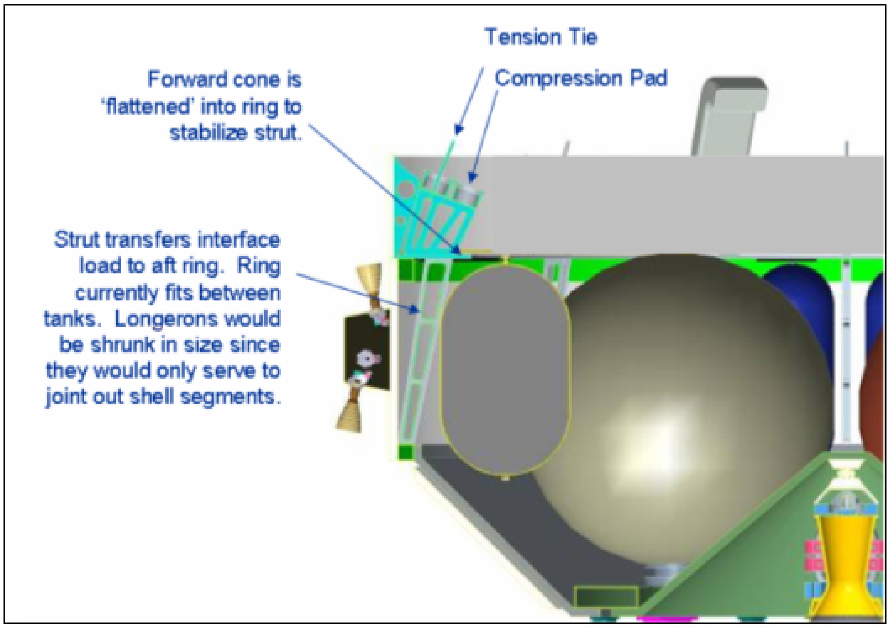

Figure 10.1-27 Potential SM Modification to Straighten Load Path to CM Interface

An alternate approach to transmitting loads through the Service Module was examined as part of a trade study performed to determine the weight impact of different structural configurations that offer increased axial stiffness (described further in the Modal Analysis discussion in Section 10.1.2.4). This analysis showed that structural efficiency improvements could be achieved with little mass penalty by including four internal vertical shear panels and altering the tank support from a polar mount approach to equatorial tank support rings that react the load at the Service Module aft ring frame (the polar mount concept was a carry-over from the cryogenic propulsion system that was later changed to hypergolic). It should be noted that the addition of these internal shear panels will likely affect subsystem packaging in the Service Module and the impact of this has not been quantified at this point.

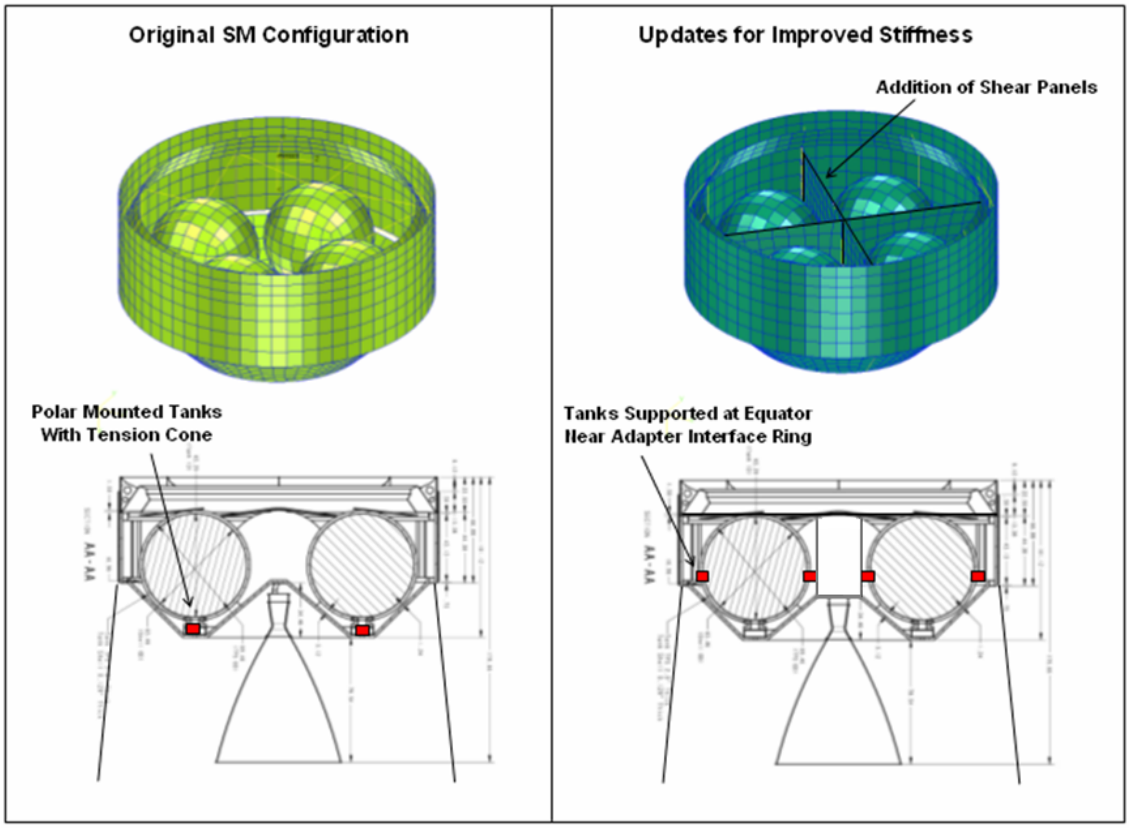

Figure 10.1-28 Service Module Design Changes for Improved Structural Efficiency

10.1.2.3 Spacecraft Adapter

The initial spacecraft adapter design concept featured an aluminum skin-stringer design with 240 internal longitudinal hat stiffeners and three intermediate rings. In an effort to reduce part count and minimize mass, an updated design featuring stiffened graphite composite outer shell panels was baselined for this design cycle (with an estimated mass savings of approximately 110 lb). The upper Service Module interface ring is integrated with a pyro line charge to facilitate vehicle separation from the booster at second stage burnout. The lower CLV interface ring is a mechanical connection to the booster upper stage that remains attached during CEV separation (Figure 10.1-29).

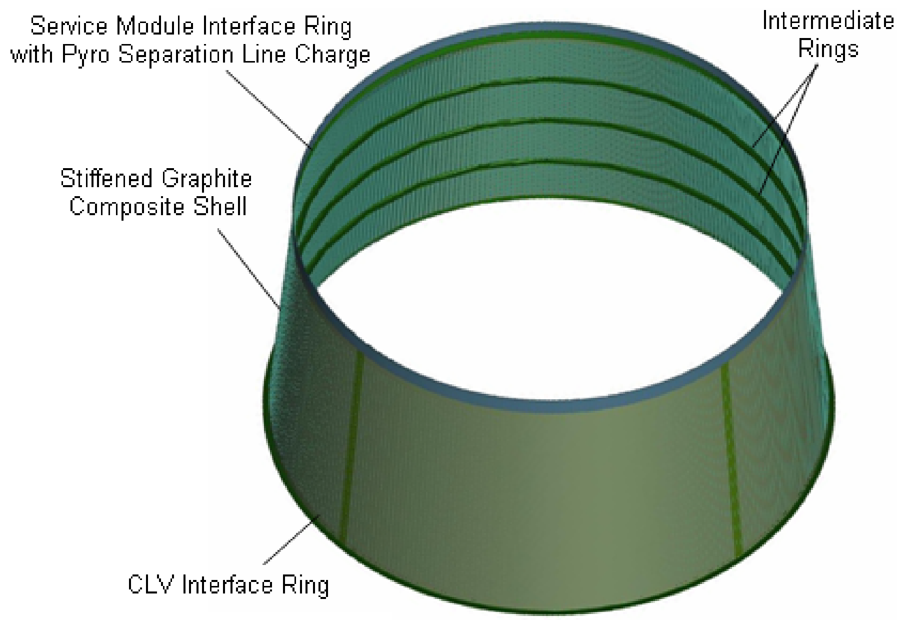

Figure 10.1-29 Spacecraft Adapter

10.1.2.4 Structural Analysis

Structural finite element models were developed to perform CEV component sizing and to facilitate coupled loads analysis with the CLV (Figures 10.1-30 and 10.1-31). The structure was analyzed for static stress, buckling, and modal frequencies using MSC/NASTRAN with pre- and post-processing performed with MSC/Patran. The CEV finite element model is primarily shell and beam element construction, with 9488 elements and 9758 nodes. Nonstructural mass is represented with distributed mass as well as point masses to match overall vehicle mass and CG targets (TPS mass was distributed onto the aeroshell elements, CM subsystem mass was smeared into frames/longerons as required to achieve CG location, point masses were used to represent the LIDS docking system, crew members on seat pallet, SM propellant and tanks, and SM engine). Numerous analysis iteration cycles were performed to optimize the structure for strength and stability and to minimize mass. Once the structure was sized for strength and stability, a modal analysis was performed to determine the fundamental structural frequencies.

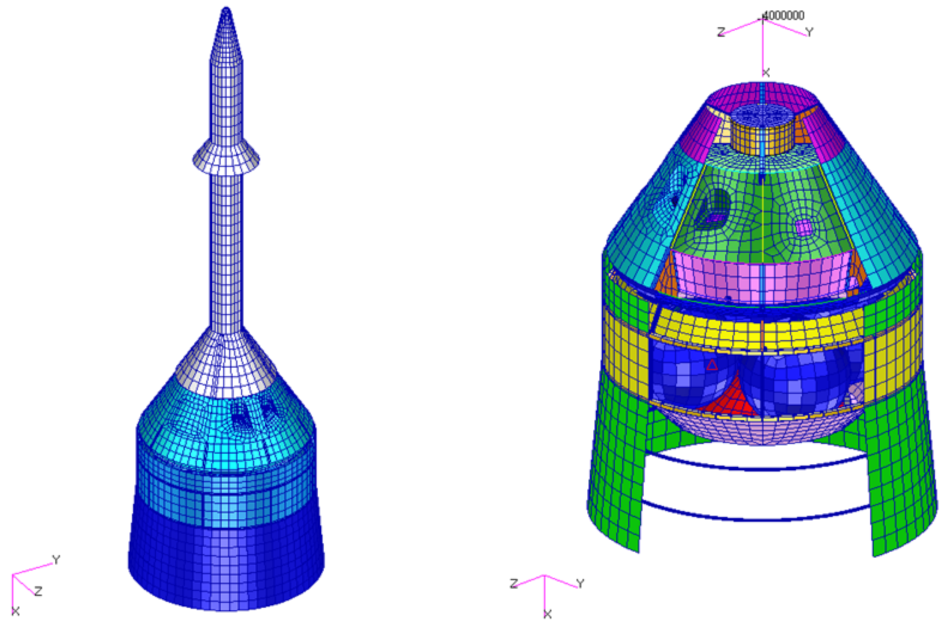

Figure 10.1-30 CEV Structural Finite Element Model

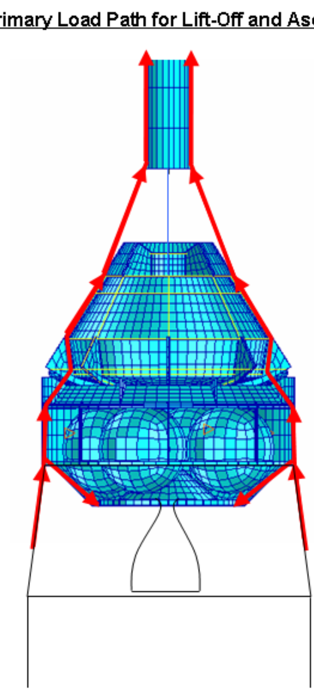

Figure 10.1-31 Primary Load Path

Sample analysis results are shown in Figures 10.1-32 and 10.1-33. Examination of the Crew Module results shows that the abort cases generate the majority of the driving loads that size the structure. The back shell and heat shield is driven by the 20 psid blast overpressure while the primary longerons and local areas of the forward bulkhead are sized by the LAS thrust case. Internal cabin pressure sizes the pressure skins, although the overall sensitivity of operating pressure on vehicle mass is relatively low. An assessment of a nominal landing scenario with the load limited to an assumed 8 g attenuation level shows that nominal landing is not the driving load case for the aft bulkhead (sized by internal pressure), although this will likely not be the case for contingency landing scenarios with a single chute out or high crosswinds. It should also be noted that this preliminary assessment was a quasi-static analysis with vertical velocity only and that a nonlinear dynamic analysis simulating the contact event (using LS-Dyna or equivalent) will be required to more accurately assess the landing cases.

The outer shell of the Service Module is sized by the lift-off inertial loads, which have the highest lateral loads and stack bending moments. The tension cone supporting the propellant tanks is driven by the late ascent axial acceleration, while the inner cone supporting the main engine is sized by the engine thrust loads imparted during the trans-earth injection burn.

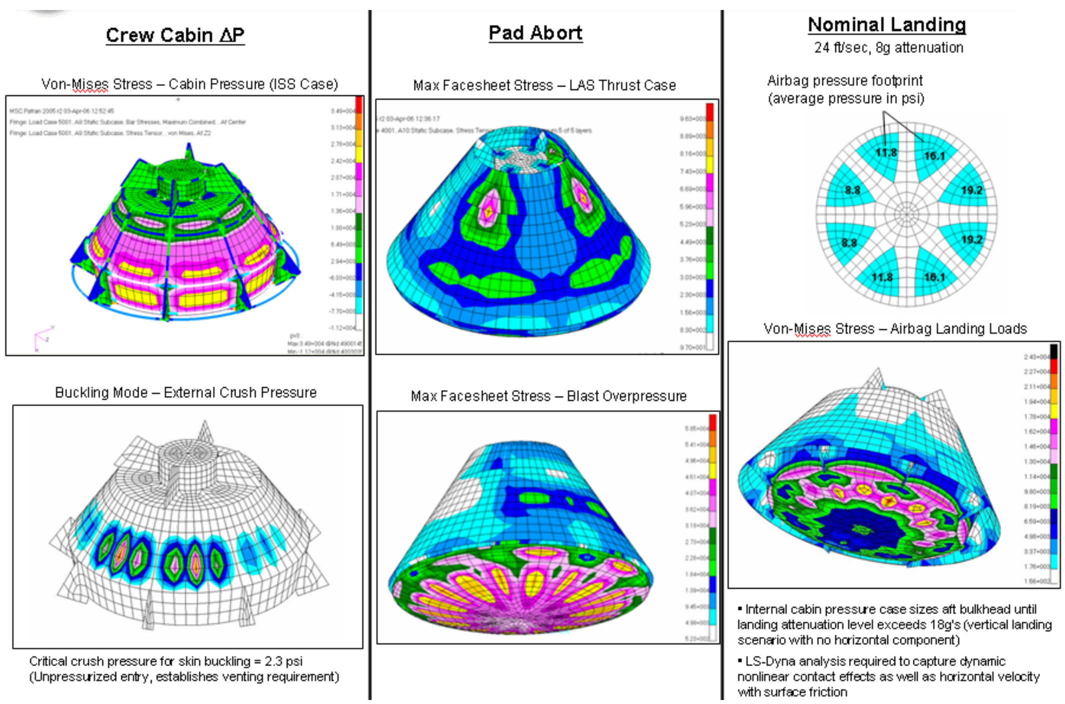

Figure 10.1-32 Crew Module Sample Analysis Results

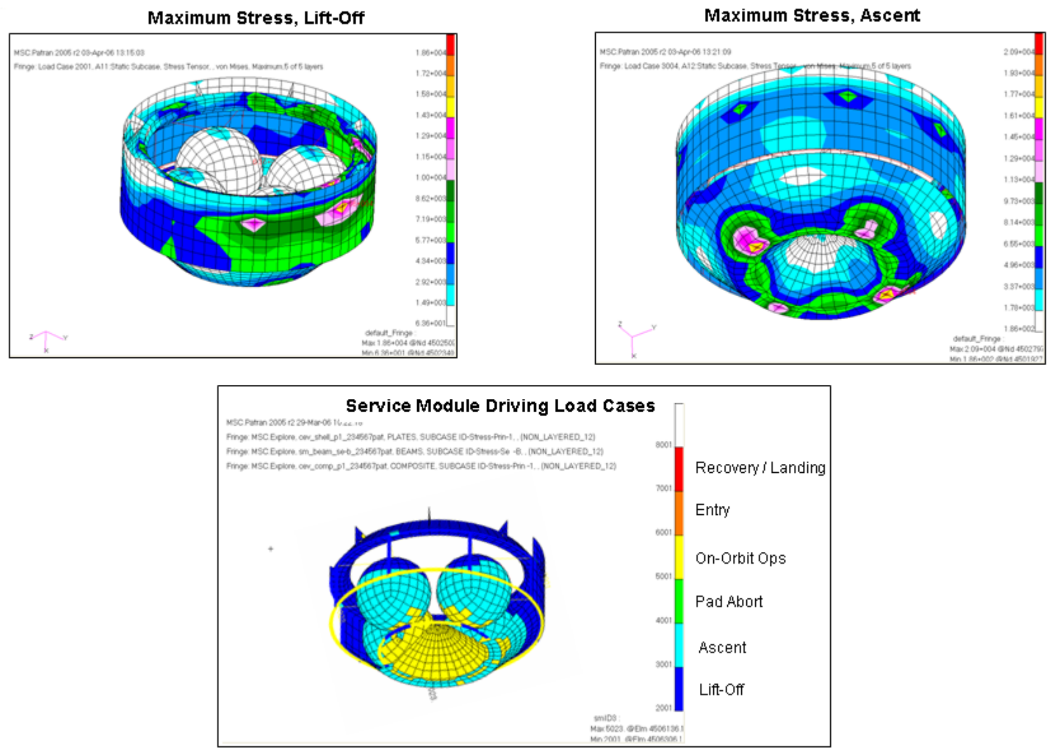

Figure 10.1-33 Service Module Sample Analysis Results

An initial modal analysis performed in the previous design cycle with the model fixed at the base of the Spacecraft Adapter showed a first lateral frequency of 2.6 Hz. This is a LAS bending mode and is driven by the compliance of the LAS aft skirt at the CM interface and the long moment arm to the LAS center of gravity. The first axial frequency was at 11.0 Hz and was predominantly a propellant tank mode driven by the concentrated propellant mass and the compliance of the lower tension cone, with the compliance of the spacecraft adapter a secondary contributor (Figure 10.1-34). Since these frequencies were well short of the requirements specified in the ICPR version of the CEV/CLV IRD (5 Hz lateral, 25 Hz axial), a sensitivity analysis was performed to optimize the structure for increased stiffness and quantify the associated mass penalty incurred. The results of this analysis showed that 3 Hz lateral and 17 Hz axial is achievable with little mass penalty by making several structural changes to the LAS and the Service Module, however significant mass increases were noted to occur for frequencies above these values.

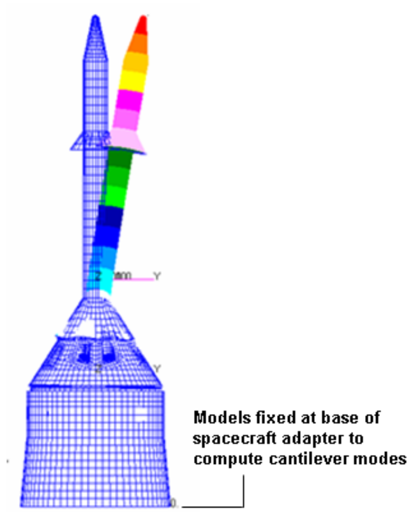

Lateral: 2.6 Hz (LAS Bending Mode)
Improved to 3 Hz with negligible mass penalty
(mass increases rapidly beyond this value)

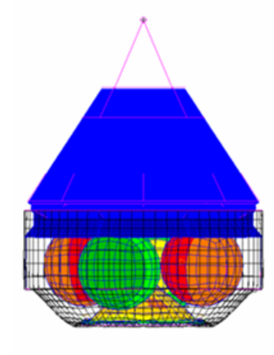

Axial: 11.0 Hz (Tank Support Mode)
Improved to 17 Hz with negligible mass penalty
(mass increases rapidly beyond this value)

Figure 10.1-34 Modal Analysis Results

The primary factor affecting frequency and stiffness of the LAS is the length to diameter aspect ratio, with the shorter and wider abort motors offering increased stiffness as well as reduced aerodynamic drag. Based on this and other factors, the LAS abort motor diameter was increased from 36 inches to 45 inches (with the appropriate reduction in length, see Figure 10.1-35).

Numerous structural configurations were developed for the Service Module to assess alternate methods of supporting the propellant tanks and transmitting the primary loads. Figure 10.1-36 shows several of these concepts with different structural component arrangements featuring a combination of shear panels, bulkheads and truss members. As shown in Figure 10.1-37, each configuration option required large mass increases to achieve small increases in axial frequency (achieved by increasing shell thicknesses and beam section properties in the structure). However, more dramatic improvements were noted between the different configurations with alternate arrangements of internal structural elements.

The addition of four vertical shear panels to the Service Module in a cruciform configuration provided significant axial stiffness and support for the propellant tanks (which was previously supported solely by the lower tension cone). Structural efficiency was also improved by changing the tank supports from a polar to an equatorial support scheme (corresponding to Configuration 3 in Figures 10.1-36 and 10.1-37). This change effectively eliminates the lower tension cone from the load path and provides direct support of the tanks at the adjacent lower ring frame that serves as the interface to the spacecraft adapter. Compressive loading on the lower tank dome is also eliminated. The mass increase associated with the addition of internal shear panels is essentially negated by the reduction in mass of the lower tension cone due to its removal from the primary load path, thereby achieving a significant stiffness increase with negligible mass penalty.

While these design changes represent improvements in structural efficiency and are recommended on their own merits, it is clear that the stated frequency requirements are not feasible and will result in a prohibitively high mass penalty to achieve (1000+ lb). Based on this analysis and numerous requirements working group meetings, this requirement is expected to be deleted from the CEV/CLV IRD prior to the System Requirements Review. The structural response of the integrated launch stack will be tracked by the appropriate Constellation System Integration Group (Integrated Loads, Structures, and Mechanisms) via numerous coupled loads analysis iterations to verify that undesirable structural coupling does not occur between the CEV and CLV during flight.

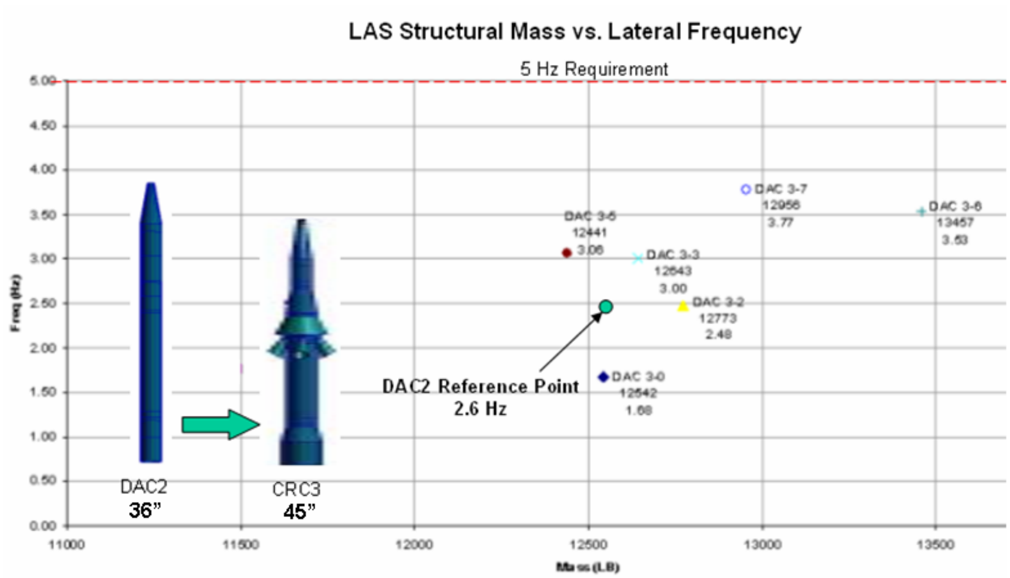

Figure 10.1-35 Lateral Frequency of Alternate LAS Configurations

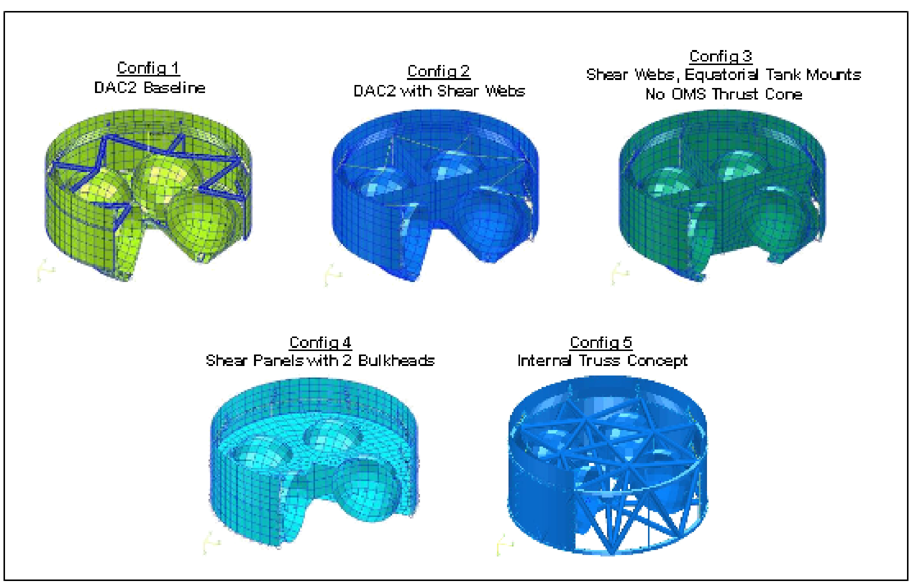

Figure 10.1-36 Service Module Structural Configuration Options

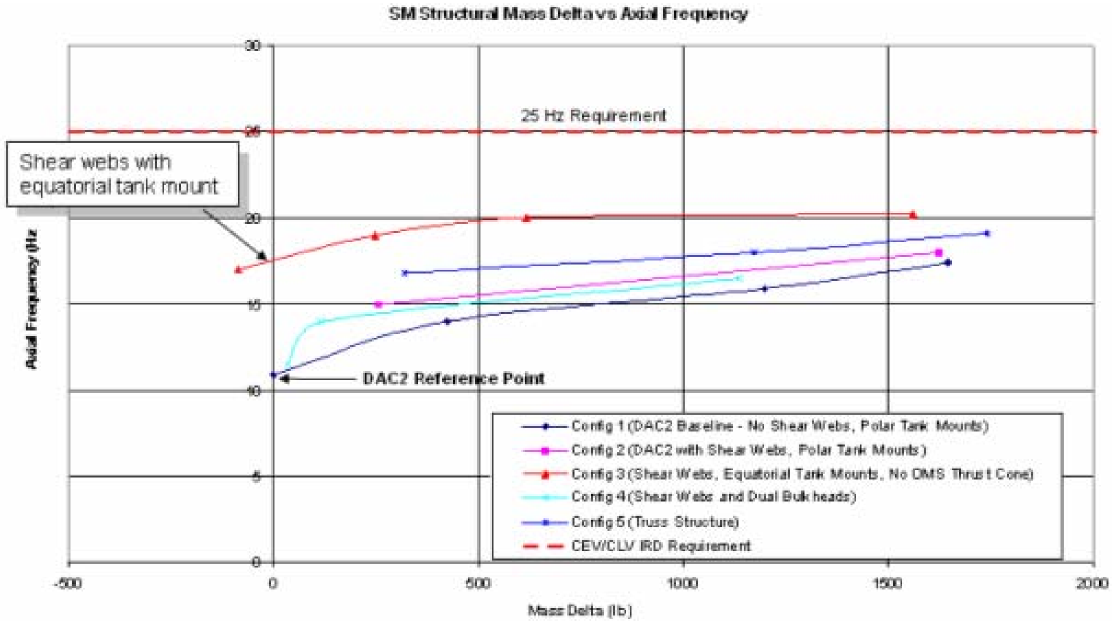

Figure 10.1-37 Axial Frequency of Alternate Service Module Configurations

MMOD Assessment

A preliminary assessment of the micrometeoroid and orbital debris (MMOD) threat was also performed with this vehicle design configuration. A detailed finite element model of the vehicle was created and integrated into the BUMPER code for orbital debris impact assessment (the standard tool used for Space Shuttle and ISS orbital debris threat assessments). The ISS case was initially assessed using the SSP30425 and ORDEM2000 environment definitions and generated an overall Probability of No Penetration (PNP) value of 0.811 (compared to the requirement of 0.993 over 5 years, minimum).

As shown in the following figure, the probability of impacts is dominated by the Service Module (significant Crew Module shadowing is provided by the Service Module and ISS). Even though the Service Module is predicted to take the majority of the impacts, however, the total risk is almost evenly shared between the Crew Module and the Service Module. This is due primarily to the sensitivity of the Crew Module TPS to damage (the exposed heat shield ablator near the Service Module in particular). MMOD blankets can be added in critical locations on the Service Module to improve performance, however the Crew Module will likely need to address MMOD from a damage tolerance perspective for the heat shield ablator to determine the level of damage that is acceptable and still be able to withstand atmospheric re-entry. Note that these results are very preliminary and quite sensitive to numerous assumptions regarding the degree of allowable damage for each zone on the vehicle. A significant amount further analysis and testing will be required to fully assess the MMOD PNP requirements.

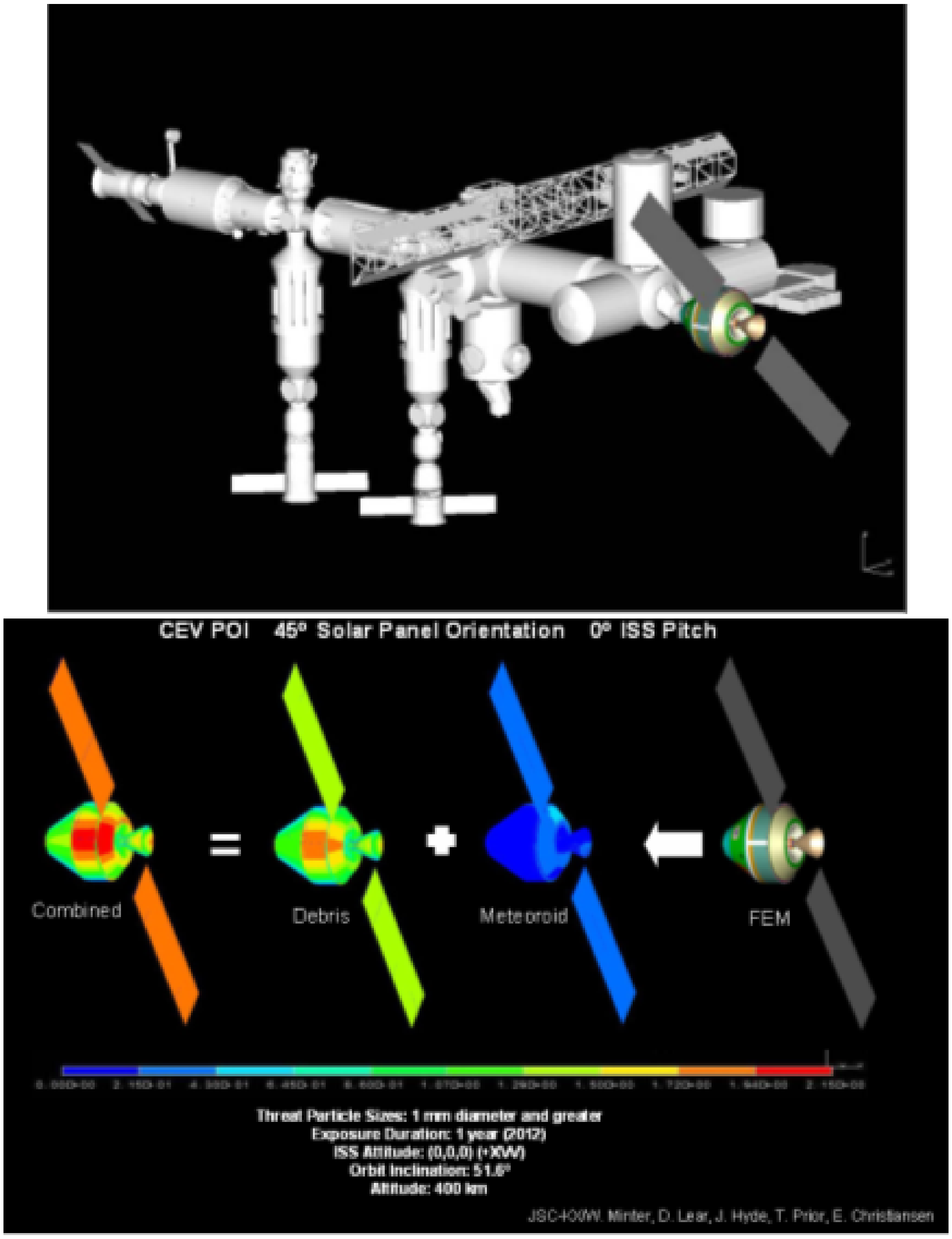

Figure 10.1-38 MMOD Probability of Impact for ISS

10.1.3 Mass Estimates and Design Maturity

The mass breakdown for the primary and secondary structure is shown in Table 10.1-6. The mass estimates for the Crew Module and Service Module were based on the mass reported by the finite element model after the initial round of sizing was performed. A 1.2 factor was applied to this value to cover secondary features not explicitly modeled such as fasteners, fillets, and local reinforcement around penetrations. An additional 25% was then applied to cover expected growth due to preliminary design maturity and uncertainties in the loading environment. Secondary structure estimates for the Crew Module and Service Module were based on an assumed percentage of the primary structure mass (CM = 20%, SM = 10%). The spacecraft adapter mass estimate was based on the mass properties from the Pro-E assembly CAD model with a 25% growth factor applied as before.

Hardware Items	Quantity	Unit Mass (lbm)	Growth (%)	Total Mass (lbm)	CM Mass (lbm)	SM Mass (lbm)	SA Mass (lbm)	Basis of Estimate
Structures				**7,163**	**3,963**	**2,274**	**926**	
Cabin Skin (Cone And Barrel)	1	256	25%	320.0	320.0			CM Finite Element Model * 1.2
Fwd And Aft Bulkheads	1	317	25%	395.6	395.6			CM Finite Element Model * 1.2
Ring Frames	1	492	25%	615.5	615.5			CM Finite Element Model * 1.2
Longerons	1	210	25%	262.5	262.5			CM Finite Element Model * 1.2
Base Heat Shield Carrier Structure	1	730	25%	912.5	912.5			TPS ADP
Backshell Structure	1	313	25%	391.5	391.5			FEM mass x 1.2
Backshell Lightning Screen	1	14	0%	14.1	14.1			based on 0.04 lb/ft^2 areal density
Upper/Lower Gussets	1	264	25%	330.0	330.0			FEM mass x 1.2
Tunnel Shell And Cap	1	48	25%	60.0	60.0			FEM mass x 1.2
Secondary Structure	1	529	25%	661.1	661.1			20% of Primary Structure
Outer Shell	1	319	25%	398.4		398.4		SM Finite Element Model * 1.2
Ring Frames/Longerons	1	319	25%	398.8		398.8		SM Finite Element Model * 1.2
CM I/F (8 Hardpoints & Torque Box)	1	443	25%	553.8		553.8		SM Finite Element Model * 1.2
Prop Tank Support Cone	1	336	25%	420.0		420.0		SM Finite Element Model * 1.2
OMS Thrust Cone	1	140	25%	175.5		175.5		SM Finite Element Model * 1.2
Prop Tank Struts	1	97	25%	121.5		121.5		SM Finite Element Model * 1.2
Secondary Structure	1	165	25%	206.3		206.3		10% of Primary Structure
Skin Panels (Composite)	1	137	25%	171.2			171.2	Pro-E Assembly Model x 1.1
Hat Stringers (Composite)	1	221	25%	276.3			276.3	Pro-E Assembly Model x 1.1
Intermediate Rings	1	97	25%	121.3			121.3	Pro-E Assembly Model x 1.1
Fwd Attach Ring	1	69	25%	86.3			86.3	Pro-E Assembly Model x 1.1
Seperation Ring (SM Interface)	1	121	25%	151.3			151.3	Pro-E Assembly Model x 1.1
Aft Attach Ring (CLV Interface)	1	96	25%	120.0			120.0	Pro-E Assembly Model x 1.1

Table 10.1.6 Mass Estimate Breakdown

10.1.4 Structural Issues, Risks, and Forward Work

A CEV structural design concept has been developed and sized to generate mass estimates based on vehicle requirements and loads. However, there are numerous issues that will require focused attention as this project transitions into the next phase after the prime contract is awarded:

- One of the primary risks to the listed mass estimates is uncertainty in the CLV loads. Recent updates to lift-off and ascent loads from CLV coupled loads analysis show significant increases in stack shear forces and bending moments (by a factor of two in some cases, see TDS CEV-08-004) and the impact on structural mass has not been quantified. Frequent integrated stack analyses will be required to verify that booster loads are well characterized and that no undesirable structural coupling is present.
- Numerous load cases were not assessed that are likely to be design drivers in specific regions of the structure and represent a threat to the current mass estimates. Future analyses should include the following loads not initially considered:

   - Assess acoustic and associated vibe environment during nominal ascent and abort.
   - Perform transient analysis to quantify appropriate dynamic amplification factors to be applied to LAS load cases to account for rapid thrust rise rate or tail-off (can be a significant component of the total load).
   - Include effects of temperature and other dispersions not included in LAS load cases (vehicle structure initially sized for a minimum T/W of 15, however the T/W ratio may approach 20 with LAS dispersions).
   - Assess max-Q abort scenario: Abrupt LAS thrust termination generates acceleration step function from +8 g to -7 g, resulting in large dynamic loading.
   - Assess credible booster failure scenarios for prior ascent abort (e.g., hard-over gimbal generating maximum stack bending prior to CM separation and abort motor ignition).
   - Perform integrated thermoelastic stress assessment of back shell and heat shield by mapping the structural temperature distribution onto the aeroshell at numerous points in the entry profile.
- Blast overpressure loading environment should be refined. Blast is currently idealized as a 20 psi static pressure, however detailed blast modeling may generate more realistic loading scenarios (magnitude and shape of blast loading curve assessed with a transient analysis).
- The bird strike requirement has not been assessed at this point and could be a design driver for the boost protective cover and the back shell TPS.
- Landing analysis is currently at a low level of maturity. A detailed integrated analysis (with LS-Dyna or equivalent) and testing plan is required to assess the nonlinear contact dynamics and generate internal structural loads for various nominal and contingency landing scenarios on land and water (sink rate, crosswinds, ground slope, wave state, etc.)
- Continued MMOD assessment is required to determine vehicle capability and shielding requirements. Development of allowable TPS damage states is of particular importance.
- Aluminum-Lithium 2195 development:
   - Although the approach in the design of the CM pressure vessel is to leverage off of the existing ET database for Al-Li 2195-T8 as much as possible, there will likely be some additional material property development required (additional fatigue data for friction stir welds, material property characterization of large diameter spin-formed domes (T6 properties), and material property development for extrusions or forgings required for frames).
   - Thermal soak back after landing could affect the T8 temper if temperatures exceed 300 °F for a prolonged period of time (could affect reuse).
   - Some manufacturing development may be required to demonstrate that roll-forming and bump-forming of orthogrid panels is feasible with external ribs in tension (roll-formed orthogrid panels have typically featured internal ribs rather than external ribs).

    - A material acquisition strategy is required at the agency level to ensure availability of this alloy for both CEV and CLV as the Space Shuttle External Tank production contracts are phased out.
- The current Service Module concept does not facilitate internal cargo options. Integration of a cargo door results in a significant impact to load distribution, with implications for primary structure mass and the separation joint with the Spacecraft Adapter.
- Access for LRUs and umbilicals may require lengthening the Service Module and the associated mass penalty has not been quantified.
- Finally, several trade studies have been identified for the next design/analysis cycle as the various contractor and government design concepts are consolidated:
    - Assessment of design impact of retro-rocket landing attenuation option (trade capsule mounted vs confluence fitting mounted options).
    - Trade six vs eight longerons in the Crew Module and Service Module.
    - Refine design fidelity at key structural interfaces (LAS/CM, CM/heat shield, CM/SM) and perform trade study to determine optimum number of tension ties/compression pads. Heat shield penetration location considerations (clocking and radial distance) should be included in this trade.
    - Perform a trade between the fixed and floating back shell attachment design options (benefits of thermal isolation and thermoelastic stress relief vs. uncertain load path and structural inefficiency associated with floating joints with friction).

10.2 Thermal Protection System

The primary function of the Thermal Protection System (TPS) is to protect the vehicle, crew and payload from the intense heat associated with atmospheric entry. This function is achieved with materials applied or attached to the exterior of the CM primary structure. The TPS must also interface appropriately with other subsystems, by accommodating load transfer between the Service Module and Crew Module, and by providing access to other subsystems as needed. To achieve these additional functions, the TPS may include carrier structure, seals, heat shield attachment mechanisms to the CM, heat shield penetrations in the form of compressive load bearing materials, and bonding materials. Discontinuities in the TPS, including seals, penetrations, steps, and gaps, will be part of the TPS Advanced Development Project (ADP) design scope. Tension ties, which secure the CM to the SM, pass through the heat shield but are outside the TPS design scope.

The heat shield and back shell TPS, shown conceptually in Figure 10.2-1, will likely be constituted with different materials due to the significant differences in induced (aerothermodynamic) environments experienced by the CEV during atmospheric passage. As a result, the requirements will be different for each component of the TPS.

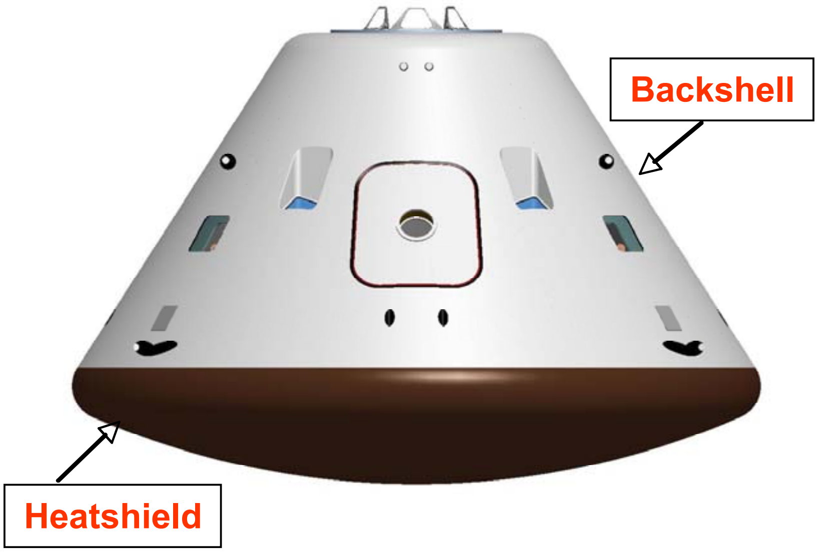

Figure 10.2-1 TPS Reference Locations on CEV CM

The key objectives of the TPS design for CRC-3 included:

1) Mass and volume sizing estimates for the five Phase 1 TPS candidate heat shield ablator materials (AVCOAT, CC-CalCarb, PhenCarb28, PICA, Textron 3DQP) for Block II conditions.
2) Mass and volume sizing estimates for Shuttle tile and SLA-561V materials for Block I conditions.
3) Back shell TPS mass and volume sizing estimates for current back shell carrier panel configuration.
4) Conceptual design detail heat shield penetration (compression pad).
5) Update TPS Margins Policy including adjustments for different ablator classes; i.e., monolithic vs. multi-layer.
6) Perform trade and sensitivity studies for carrier structure core thickness.
7) Initiate assessment of OML dimensional sensitivity due to TPS initial variable thickness, recession, and structural deformation.

The analyses for CRC-3 were performed in close coordination with the existing CEV operational mission scenario, entry trajectories and associated induced environments, and all subsystems requiring close monitoring of interfaces and systems-level impacts. The TPS system was designed consistent with the CFI (SRD) requirements set.

The results of the Thermal Protection System (TPS) subsystem presented for CRC-3 contain the additional or significantly changed design results from the previous design cycle, DAC-2, which concluded in May, 2006. As such, where little or no differences in assumptions, constraints, loads, or design features from DAC-2 occur, the text will refer the reader to the TPS DAC-2 report.

The Thermal Protection System allocated target mass for CRC-3 was assumed to be unchanged from the DAC-2 value of 2300 lbm. Modifications of the margins policy, adoption of a five Block II candidate material average of a variable thickness heat shield design, and an updated (higher) virgin PICA material density were prime contributors to the CRC-3 MEL. Updates to the MEL were delivered on Aug 11. Carrier structure mass is book-kept with Structures, and heat shield separation mass is book-kept with Mechanisms.

	DAC-2 MEL (3/34)	CRC-3 MEL (8/11)	DAC-2	CRC-3
Block II Heat Shield TPS	1630 lb	1800 lb	4.8 in.	4.8 in. max thickness
Back Shell TPS	630 lb	560 lb	1.9 in.	1.6 in. max thickness
Block II Total	2260 lb	2360 lb		
Block I Heat Shield TPS		1350 lb	.	2.2 in. max thick-ness
Back Shell TPS		560 lb		1.6 in. max thickness
Block I Total		1910 lb		

Table 10.2-1 CRC-3 TPS Mass Summary

10.2.1 Driving Requirements, Groundrules, and Assumptions

An overview of the key requirements, groundrules, and assumptions is described below. More details of the TPS Assumptions used for CRC-3 can be found in Appendix A. The objective of the assumptions document is to have a single location for all assumptions made in order to perform trade studies, simulations, analyses, CAD modeling, etc. As the work performed using these assumptions matures, design requirements will be created and documented.

The TPS shall maintain the attachment between itself and the rest of the CEV at or below specified temperature limits against aerothermodynamic loads for all mission phases including ascent, on-orbit, trans-Earth departure and return, Earth entry, descent, landing and recovery including nominal and abort cases. During ascent, liftoff loads will be transferred from the SM into the CM at several discrete attachment points located on the heat shield carrier structure. During ascent the back shell and heat shield will be required to withstand mechanical liftoff loads, thermal loads, acoustic, vibration, and aerodynamic loads. On orbit, the TPS must withstand temperature cycles, the solar radiation environment and micro meteoroid debris flux. On re-entry the TPS needs to withstand thermal loads, vibration and aerodynamic loads experienced throughout atmospheric deceleration. Prior to landing, the heat shield may be separated from the CM prior to landing system deployment. After landing the back shell TPS will be reused or refurbished as needed and the heat shield will be discarded.

Mass Assumptions

1) Heat shield (Carrier Structure and TPS Material) target weight for CRC-3 is assumed to be 2,160 lbm (980 kg). From DAC-2 Assumptions & Mass Targets
2) TPS material target weight (including heat shield and back shell) for CRC-3 is assumed to be 2,300 lbm (1,045 kg). From DAC-2 Assumptions & Mass Targets
3) Crew Module mass assumed to be 17,300 lbm (7,850 kg) at Earth launch. From DAC-2 Assumptions & Mass Targets
4) Crew Module Mass assumed to be 16,700 lbm (7,570 kg) at Earth entry. From DAC-2 Assumptions & Mass Targets. Rationale: 600 lbm LIDS is jettisoned during LSAM un-docking.
5) Crew Module Mass assumed to be 15,500 lbm (7030 kg) hanging below parachutes after parachutes deployed. (Used in DAC-1A analysis assumptions – Rationale: 17,300 – 600 (LIDS jettison) – 1,200 (Recovery System Mass) = 15,500 lbm. From DAC-2 Assumptions & Mass Targets.

Safety Factors

1) Structural design and analysis will be performed assuming standard practices according to NASA-STD-5001.
2) The TPS Ablator thermal and thickness factors of safety will be specified in Interim TPS Margin Process Version 5d – July, 2006.

Geometric Constraints

The inner mold line (IML) and outer mold line (OML) is described in Figure 10.2-2. This comes from 198_OML_IML_C in the Reference Configuration Project on Windchill.

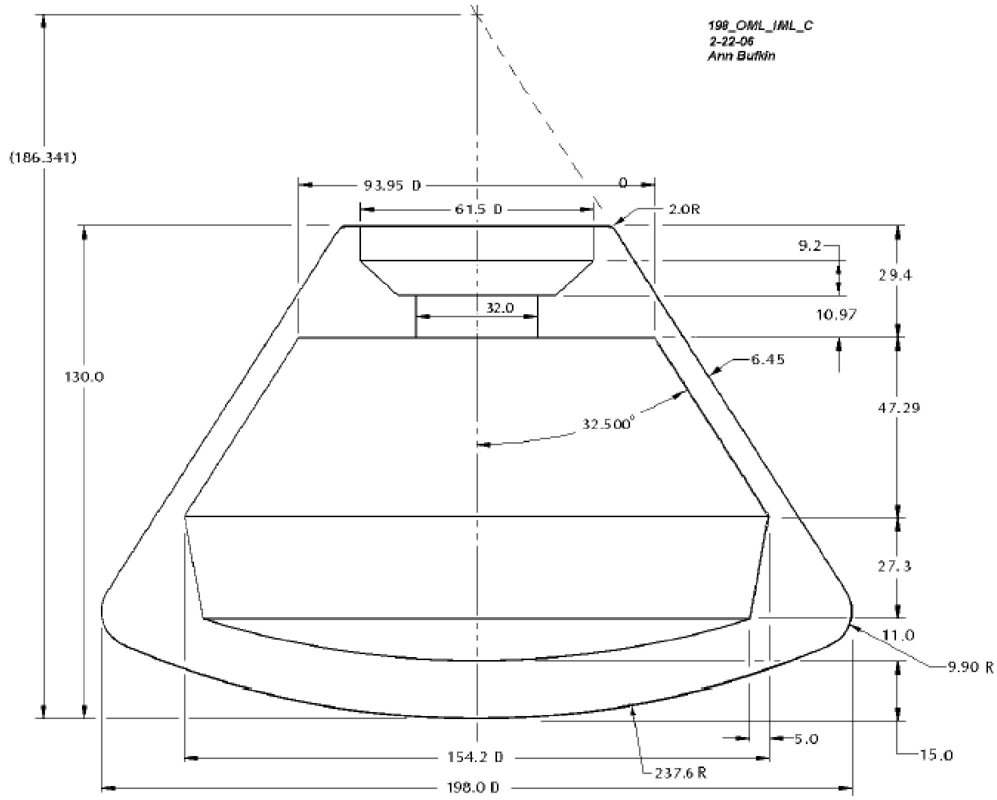

Figure 10.2-2 Reference Dimensions of CEV CM

Water Floatation System

Assume no floatation accommodation is needed in the heat shield.

Environmental Loads

1) Lift off and ascent structural loads are provided in the Crew Exploration Vehicle (CEV) Loads Data Book.
2) Lift off and ascent thermal loads will be provided in a CLV Ascent Aerothermodynamics Loads Data Book. Thermal loads are not evaluated in CRC-3.
3) LAS acceleration loads are provided in the Crew Exploration Vehicle (CEV) Loads Data Book.
4) Blast overpressure loads are provided in the Crew Exploration Vehicle (CEV) Loads Data Book.
5) Entry structure loads are provided in the Crew Exploration Vehicle (CEV) Loads Data Book.
6) Thermal Entry loads will be provided in LEO Entry Environments - Current and Lunar Entry Environments - Current Documents. The entry loads were based on JSC Cycle 3 (3/15/06) Lunar Return Trajectory Set. The set included Block I and Block II entry trajectories shown in Figure 10.2-3.

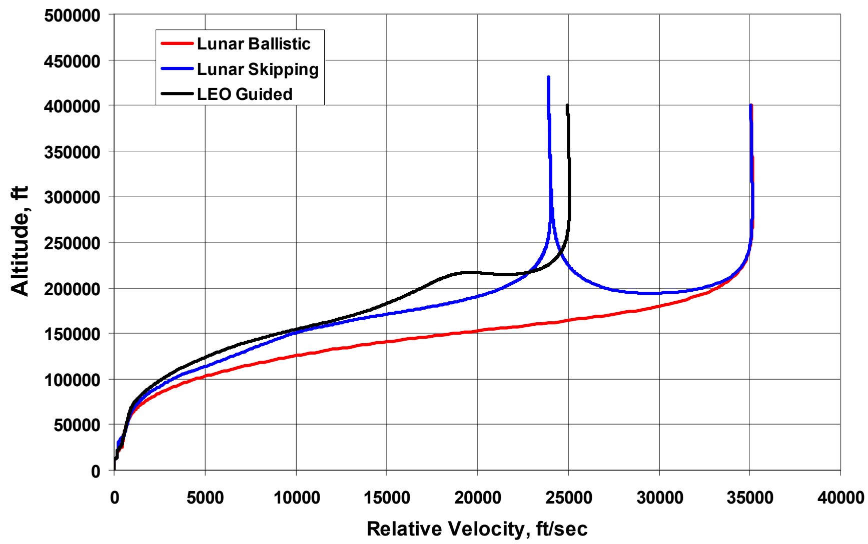

Figure 10.2-3 CEV Block I and Block II Return Conditions, Altitude vs. Velocity

Carrier Structure Deflection Limit

The Carrier Structure cannot mechanically deflect more than +/- 0.5 inches over the entire diameter during earth entry. This is a guideline and not a hard limit. The deflection limit will be updated once test data is available.

Heat Shield

No additional mass is assigned for penetrations, closeouts or non-ideal thickness variation. Heat shield results are for analysis using a 2.0 inch titanium sub-structure system (two 0.032 inch face sheets and 6.0 lb/ft^3 honeycomb core). The predicted savings for variable thickness heat shields are based on a 1-D thermal model applied at several discrete locations on the heat shield. The heat shield was sized for Block I conditions using FIAT (LI-2200, RCG-coated LI-2200, and SLA-561V), SINDA (RCG-coated TUFI/BRI-18), and AESOP-STAB (SLA-561V). The heat shield was sized for Block II conditions using either FIAT (PICA, CC/Calcarb, and 3DQP) or AESOP-STAB (AVCOAT, PhenCarb28) thermal analysis programs. More detail on heat shield design assumptions are given in Appendix C and Appendix D.

Back Shell

For the CRC-3 analysis cycle, the CEV geometry, TPS support structure, trajectory set, and resulting aerothermal environments are as per the DAC-2 data set. For CRC-3, the candidate TPS material selection was extended to include: 1) Uncoated LI-2200 ceramic tile, 2) RCG-coated LI-2200 tile, 3) BRI-18 tile with both a TUFI diffusion layer and RCG coating, and 4) SLA-561V ablator system. The back shell results are for analysis using a baseline back shell TPS support structure consisting of a composite honeycomb carrier panel using 0.040 inch Graphite/BMI-IM7 face sheets with a 0.75 inch height aluminum core with a density of 4.4 lb/ft^3. Cell size is 3/16 inches with cell wall thickness of 0.0015 inches. More detail on back shell design assumptions are given in Appendix E.

Carrier Structure

The CRC-3 trade studies modeled the structure only with the 5 inch ablator being considered as parasitic mass at 30 lb/ft^3. Only mechanical loads were applied to the structure. Thermal loads have not yet been included in the sizing study. All designs used a 35,000 square inch surface area. Eight radial ribs on the bottom of the CEV pressure vessel provide intermediate bearing support to the carrier structure for external pressure. These ribs are part of the structure baseline design for CRC-3.

The heat shield must separate from the CEV prior to landing with the heat shield to pressure vessel separation/attach points located on the ribs at a radius of about 85 inches. A separate inertial load case of 15 g's down is associated with accelerations from the Launch Abort System (LAS). This loading pulls the heat shield away from the radial ribs and is only resisted by the eight separation/attach points.

All load cases were assumed to quasi-static including the postulated blast pressure. A uniform pressure distribution was used on a symmetry model for the shell even though reentry at an angle of attack produces vehicle pressure variations between the windward and leeward sides of the vehicle. A uniform pressure of 15 psi over the heat shield results in an integrated force of about 450,000 lb. This force would produce a deceleration of about 26 g's to a 17,000 lb CEV.

The initial sizing of metallic face sheets was based on material strength limits. The initial sizing of composites assumed strain-limited laminate behavior (4000 microstrain). Biased ply as well as quasi-isotropic lay ups were used. Tailoring the composite lay up to the main load-carrying direction can reduce the composite weight. All composite thicknesses were changed in increments.

A safety factor of 1.4 was applied to all loads and a joint factor of 1.3 was added to account for doublers, inserts, and fasteners. The honeycomb core was sized by shear strength using equations from Bruhn's *Analysis and Design of Flight Vehicle Structures*. Local stability equations for core and face sheet were also based on Bruhn's equations.

Launch Abort System

Under abort scenario, assume the maximum altitude is low enough so that entry heating is insignificant and any degradation of heat shield from LAS plume does not affect TPS performance.

The CRC-3 cycle assumed a boost protective cover that fully shielded the CM back shell during ascent. This assumption resulted in a lower priority given to ascent induced environments impacting TPS design, especially back shell TPS. As a result, entry conditions were the driving thermal environment in sizing the TPS.

Separation System

The assumptions and requirements for designing the heat shield separation system are listed below:

1) The heat shield will be separated after the CM has reached terminal velocity on the parachute: nominal 25 ft/s, worst case 29 ft/s.
2) The heat shield will separate at ≤ 7,000 ft.
3) Heat shield drag coefficient will be estimated using Viking data.
4) The tension tie will be designed such that it does not affect heat shield separation (i.e., the CM/SM separation includes an interior separation device of the tension tie that allows the heat shield to separate freely).
5) Access will be provided through the back shell to assemble separation mechanism and attach the heat shield to primary structure.
6) Heat shield is retained for water landing.
7) The pressure in the cavity between the carrier structure and pressure cabin is equal to atmospheric pressure at separation.

Seals

The assumptions and requirements for designing the seals are listed below:

1) The seals cannot adhere to both surfaces of the heat shield and back shell in order to allow for separation.
2) The seal will be used for only one mission.
3) The seals need to be able to be installed and reinstalled during ground operations prior to flight.
4) The seals do not need to be water-tight in the event of a water landing.
5) The seals need to keep moisture from the heat shield cavity area while on the launch pad.

Penetrations

The assumptions and requirements for designing the penetrations are listed below:

1) Eight compression pads equally spaced 45° apart.
2) All compression pads shall be located under the radial ribs.
3) The center of the compression pads shall be located at 0.9*R (TBR) from the vehicle centerline.
4) Compression pad must not (TBR) protrude with respect to the acreage TPS material.

There will be eight tension ties consistent with the number of compression pads.

Interim TPS Margin Policy

The current CRC-3 TPS margin policy (Appendix B) is based primarily on heritage techniques employed for prior planetary and earth entry missions of ablating TPS. The policy concentrates on thermal margin (e.g., the insulative requirement of the TPS material), and arrives at a final design thickness by using a root-sum-square (RSS) analysis of the various uncertainties and factors of safety on applied loads (aeroheating uncertainties), as well as the material thermal response (due to material property variability and other uncertainties in the thermal response model employed). Uncertainties due to trajectory dispersions are not RSS'd, but rather are stacked in the final analysis due primarily to the relative immaturity of the dispersed trajectory analysis at this time. The uncertainty in recession of the ablating materials, which is one of the largest uncertainties in current material response models, is incorporated using an RSS process. The intent of this part of the margin process is to protect against incipient failures resulting from excessive removal of TPS material; a failure mode for which the predicted bondline temperature is very insensitive. For the dual layer materials a minimum face sheet thickness, including the expected recession, is derived based on thermostructural stress requirements. Not to exceed bondline temperature limits are chosen on a material-by-material basis by determining the weakest link in the stackup, including the requirement that pyrolysis should not occur at the TPS bondline for phenolic impregnated materials. Issues such as thermal stress limits of the TPS material or underlying substructure are not considered currently due to immaturity of the required analytical models, but will be included in future analyses. The policy for CRC-3 is nearly identical to that employed for DAC-2, except that face sheet minimum thicknesses and thermal margins for the various materials are analysis-based. In addition, a policy for Block-1 TPS options is included. Table 10.2-2 lists important values from the process.

OML Sensitivity Analysis

PICA has relatively high recession, so it is used to define the bounds on the anticipated range of shapes for Block II heat shields. The CG is assumed fixed throughout trajectory (apart from change due to recession), so trim angle of attack will vary as shape changes. The CAP team required an assumption that the initial shape of the heat shield shoulder should not deviate from the nominal shape.

	Version 5d Employed for CRC-3 Analysis
HS Aerothermal Uncertainty Factors	
Laminar Convective Heating	LEO: 1.15 ; LDR: 1.2
Turbulent Convective Heating	LEO: 1.25 ; LDR: 1.35
Radiative Heating	2.0
BS Aerothermal Uncertainty Factors	
Convective Heating	LEO: 1.3 ; LDR: 1.5
Radiative Heating	3.0
Atmospheric/Trajectory Dispersion Factors	
Heating Rate	1.10
Heat Load	1.35
Global Assumptions:	
TPM Thickness Distribution	Variable
Growth Margin (mass)	1.25
Manufacturing Tolerance	0.0 inches
Bondline Temperature	Variable HS ; 350 °F BS
Cold Soak Temperature Assumptions:	
Block-I (HS & BS)	100 °F HS ; 100 °F BS
Block-II	40 °F HS ; 70 °F BS
Thermal Margin	
Block I HS (tile)	130 °F
Block II HS & Block I (SLA)	108 °F
Back Shell (tile)	50 °F
Back Shell (SLA)	108 °F
TPS Factor of Safety	
Recession	1.5
Default (Back Shell and Block I)	1.1
TPS Margin Application:	
Load FOS and Thermal Margin	RSS (details are different for different materials)
Recession FOS	RSS
Minimum Face Sheet Thickness	
ACC	0.15 inches
3DQP	0.10 inches

Table 10.2-2 Interim TPS Margin Process

10.2.2 Conceptual Design Overview

TPS sizing activity in CRC-3 uses an updated margins policy and considers more candidate materials for the heat shield with the inclusion of design for a Block I-only heat shield. Analysis of the carrier structure was performed in this design cycle, and the combined mass of thermal material and support structure was investigated. To complete the component level conceptual design from DAC-2, details of the recent penetration (compression pad) analysis is contained in this report. Figure 10.2-4 gives a graphic view of the TPS component break out.

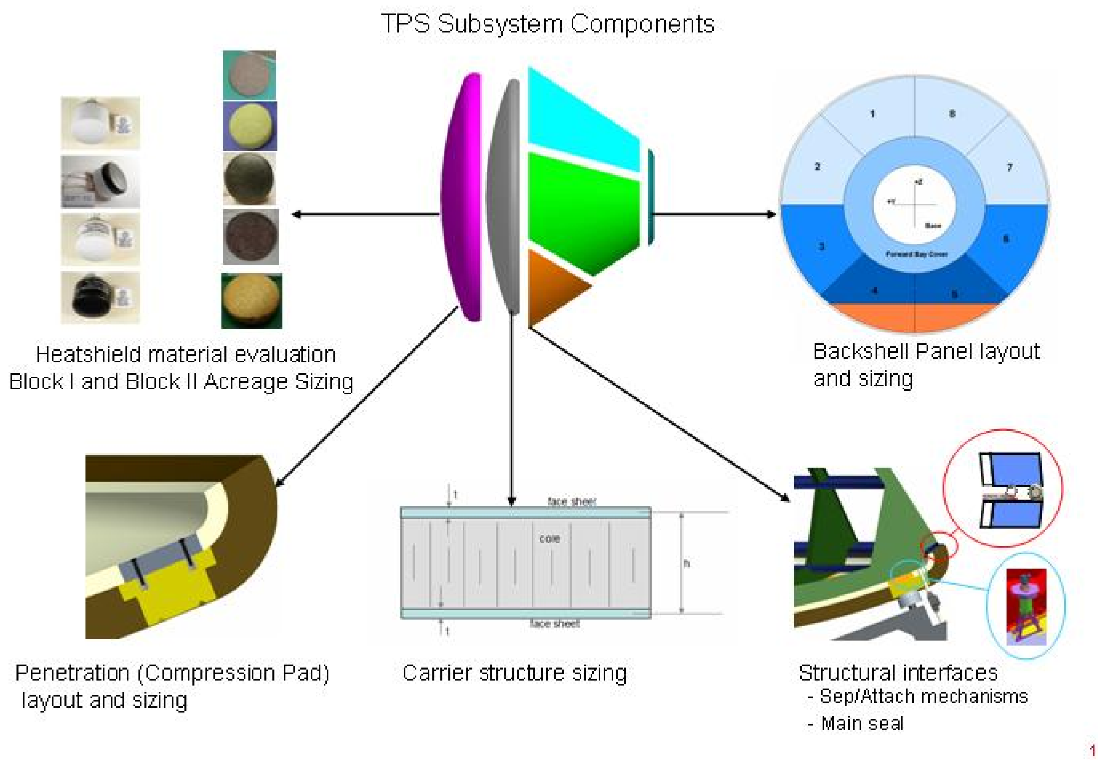

Figure 10.2-4 Progress from DAC-2 Concept to Current Concept

<u>Heat Shield (Block I)</u>

The TPS sizing analysis was performed using two programs, TPSSizer version 2.0 and AESOP-STAB version 7. TPSSizer uses FIAT for the thermal analysis of ablative TPS materials (SLA-561V and PICA) and SINDA/FLUINT 4.7 to analyze non-ablative materials (LI-2200 and BRI-18 ceramic tile systems). AESOP-STAB was used to analyze SLA-561V, AVCOAT and Phen-Carb. More details on assumptions, modeling limits, and trade study results are given in Appendix C.

For the MEL deliverable, the uncoated LI-2200 option was chosen since it was the slightly highest mass option, and still fell within the mass allocation. Figure 10.2-5 summarizes the Block I heat shield TPS sizing results for the various candidate material concepts and shows the impact of the current Margin Policy on the weight for each material. For the tiled-based TPS systems, the resulting TPS system weights are very similar. The SLA-561V ablator system offers a measurable reduction in TPS system weight. All the TPS materials exhibit approximately the same relative sensitivity to the various margin requirements.

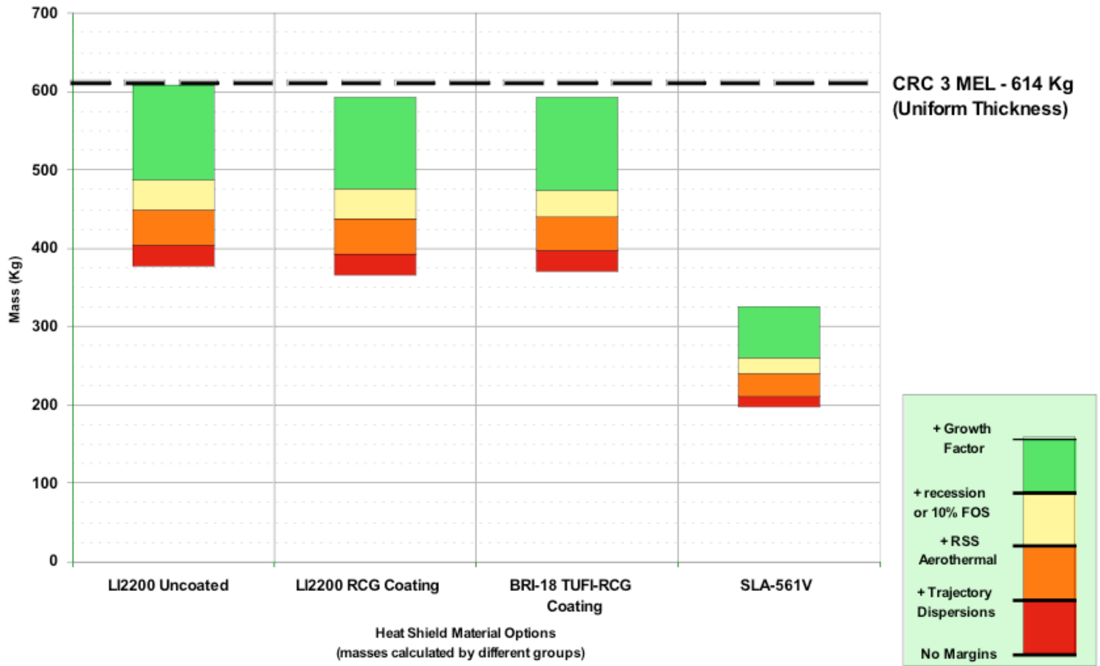

Figure 10.2-5 Block I Heat Shield Mass Estimates for Different Materials

For the candidate Block I materials, there exist some key concerns with the fidelity of the modeling tools that will need to be improved. For the Tile Response Models, the material property data for the tile systems does not include values for the high temperatures seen in the analysis. For example, the LI-2200 data goes to 3,460 °F but the analysis predicts temperatures around 4,000 °F. The melting temperature of LI2200 is also less than 4,000 °F. Therefore, the accuracy of these models is uncertain. For RCG material properties, there are two data sets available for RCG emissivity. A determination needs to be made on which is the more accurate set. For SLA Response Models, the SLA models are being evaluated and compared to Arc-Jet data.

Heat Shield (Block II)

The TPS sizing analysis was performed using two programs, TPSSizer version 2.0 and AESOP-STAB version 7. TPSSizer uses FIAT for the thermal analysis of ablative TPS materials (PICA, CC/Calcarb, and 3DQP) and SINDA/FLUINT 4.7 to analyze non-ablative materials. AESOP-STAB was used for AVCOAT and PhenCarb28. Excel spreadsheets were used to RSS the thermal analysis results according to the Interim TPS Margin Process. A model of the heat shield TPS and support structure was created in ProE Wildfire to calculate the mass of a uniform thickness heat shield for the various resulting thicknesses. The heat shield TPS analysis used the

DAC-2 baseline 2 inch titanium honeycomb support structure consisting of two Ti face sheets, each 0.032 in, with a 1.936 inch, 6.0 lb/ft^3 Ti honeycomb core. The cell size was 0.375 inches with a foil gauge of 0.0025 inches. More details on assumptions, modeling limits, and trade study results are given in Appendix D.

Much of the heat shield endures heat loads that are substantially lower than the maximum, so the ablator material could be less thick in those areas. Figure 10.2-6 maps regions of the heat shield that have different levels of heat load, from 90-100% of the maximum heat load down to the region with 0-10% of the heat load. In each region, the location with the highest heat load for that region is used to calculate the required ablator thickness. Notice that the heating changes rapidly around the shoulder, but much of the acreage sees heat loads between 40 and 70% of the maximum. Substantial thickness reductions are possible in these regions.

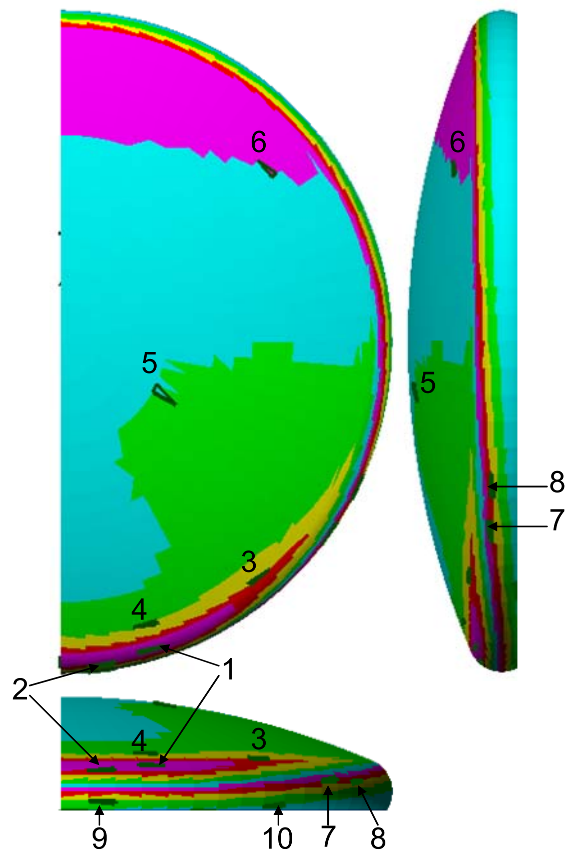

Figure 10.2-6 Heat Load Distribution on the CEV Heat Shield

Figure 10.2-7 summarizes the Block II heat shield TPS sizing results for the various candidate material concepts and shows the impact the current margin policy on the weight for each material. The different material properties and responses to the heating environments result in observable variations in sensitivity to the various margin requirements.

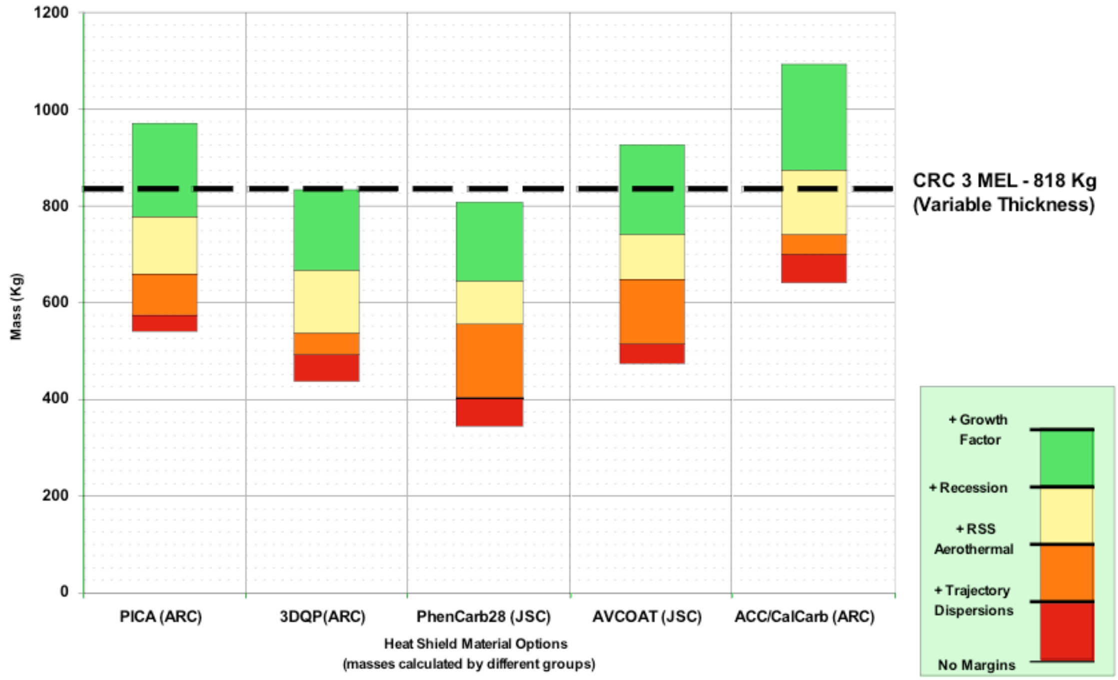

Figure 10.2-7 Block II Heat Shield Mass Estimates for Different Materials

Back Shell TPS

For the back shell TPS, the approach taken was to allow a uniform TPS thicknesses for each panel, and not tailor the thickness on the back shell. On each panel, the surface point with the highest integrated heat load usually determines the maximum insulation thickness, and this occurs for the skipping lunar return trajectory. Referring to Figure 10.2-8, the windward panels (#4, #5) will have one uniform insulation thickness, sized by the most critical point on the windward centerline at the aft tangency point. All the remaining panels and the Forward Bay Cover will have different uniform thicknesses, also sized by the most critical point for these panels. Panels #1, #2, #7 and #8 are all minimum gauge TPS thickness for the tile systems.

Figure 10.2-8 presents the area breakdown for the baseline BRI-18/8 tile system, and Figure 10.2-9 shows the tile system thickness distribution. The choice of the BRI tile with TUFI/RCG for the CRC-3 back shell TPS reference design is based on operability and robustness considerations. The higher density BRI-18 represents 18% of the total back shell surface area. Over 40% of the area is minimum gauge tile. Panels #4 and #5 are a mixture of both BRI-18 and BRI-8 tile, but all have the same thickness of 1.57 inches.

Panel #	Area (ft^2)
1	34.531
2	34.531
3	34.531
4: BRI-18 BRI-8 SubTotal	13.080 21.451 34.531
5: BRI-18 BRI-8 SubTotal	13.080 21.451 34.531
6	34.531
7	34.531
8	34.531
Forward Bay Cover	63.42
Total	339.67

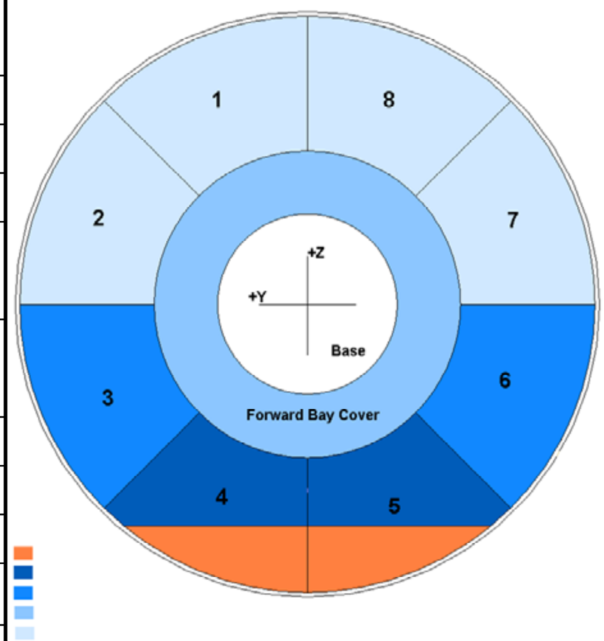

Figure 10-2.8 CEV Back Shell TPS Panel Naming Convention and Area Distribution

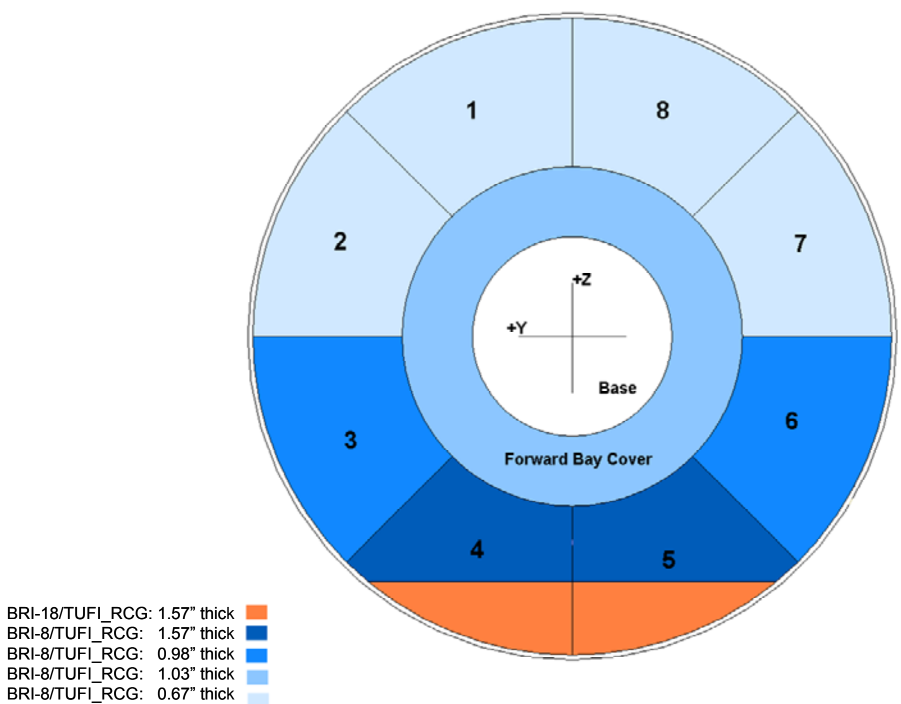

Figure 10-2.9 BRI-18/BRI-8 Tile Thickness Distribution

Carrier Structure

The carrier structural system was designed to meet strength and stiffness requirements for a limited set of flight-like pressure and inertial loads. Design variables investigated were pressure range (10-20 psi) and honeycomb core height (1.5-3.0 inch) and face sheet thickness. For composite face sheets, bias ply lay ups were investigated in addition to quasi isotropic lay ups. The extra plies in the circumferential direction resulted in a circumferential modulus that was roughly twice the radial modulus. A lay up biased toward the load-carrying direction results in a more efficient structure. Additional details on the structural sizing analysis are provided in Appendix F.

Design variables investigated were material systems, core height, face sheet thickness, lay up, and external pressure. The objective was to minimize structure weight while satisfying strength and stiffness requirements for the applied loads. A formal optimization procedure was not used. A simple model was first developed to size the structure using conservative methods. The baseline designs resulting from the simple models were then validated and refined using detailed finite element analysis. Pressure loadings for the trade study were set at 10, 15, and 20 psi. This range covers a wide set of conditions for reentry and even a postulated blast load following a lift off abort. Weights were calculated as a function of pressure.

Facing	Core	Weight	Facing Thickness	Core Height
Ti 6Al 4V	Ti 3Al 2.5V	730 lbs	.025 in.	2.5 in.
Gr/BMI bias ply	Ti 3Al 2.5V	785 lbs	.0936 in.	2.0 in.
Gr/BMI quasi-isotropic	Ti 3Al 2.5V	876 lbs.	.083 in.	3.0 in.
17-4 SS	17-4 SS	916 lbs.	.0189 in.	2.5 in.

Table 10.2-3 Carrier Structure Mass Estimates for Different Materials and Configurations

Table 10.2-3 indicates that the Ti 6-4 honeycomb structure design with a 2.5 inch core height had the minimum weight for the pressure loadings. Inertia loadings did not govern any of the designs. The beam model equations used for preliminary strength sizing were reasonably accurate and produced slightly conservative designs. Displacements were calculated for all options and were not excessive. Curvature and strain limits were used to evaluate the various design options.

A separate study of loads associated with water impact was performed under CRC-3. The complete report of this loads study is presented in Appendix G.

Seals

The relatively complete concept design and trades for seals analysis performed for DAC-2 did not need to be updated for CRC-3. For more information, refer to the DAC-2 Seals Appendix.

Heat Shield Penetrations (Compression Pad)

Presently, the CEV reference configuration is proposing a tension tie/compression pad system similar to the Apollo design. Like Apollo, this system will require penetrations in the heat shield as shown in Figure 10-2.10. Trade studies were proposed by the CEV Thermal Protection System (TPS) Advanced Development Program (ADP) Penetrations Team to identify leading designs for the heat shield compression pads. In consideration of multiple heat shield ablator systems, these trade studies identified compatible compression pad material candidates, viable compression pad configurations, and methods of attachment of the compression pads to the heat shield carrier structure. This CRC-3 design report summarizes the results of the trade studies to identify the leading compression pad designs. This report also recommends methods of attaching the compression pads to the heat shield carrier structure. For more information, refer to Appendix I.

Trade studies to determine the best compression pad material for each candidate acreage TPS material were performed. Trade studies to determine the best compression pad mechanical design and attachment scheme to the carrier structure were performed. The trade study results showed that differential recession is of very high importance to the PICA heat shield design and that a monolithic piece of ACC4 becomes prohibitively thick as a compression pad. The results showed that there is no universal compression pad material that can serve as a compression pad for every candidate acreage TPS material. The leading mechanical design is tailored for "machineable" materials such as PICA, FM5055, FM5504, and ACC4/Calcarb. The trade focused on the current baseline which was the coaxial configuration; however, each mechanical design and attachment concept can be applied to the off-axis Apollo style compression pad.

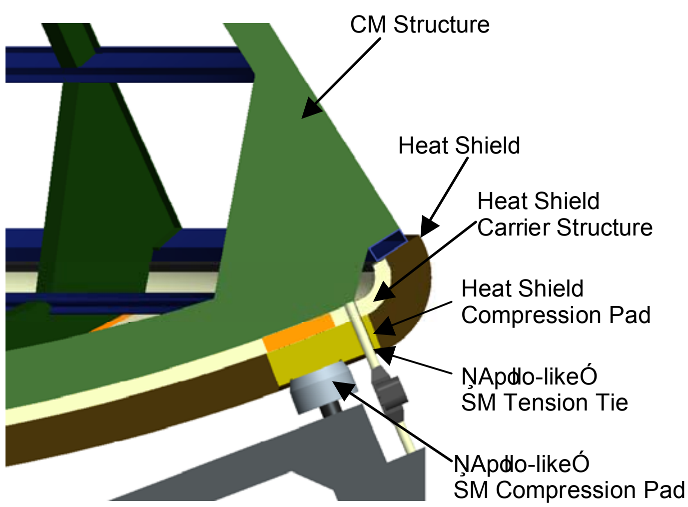

Figure 10.2-10 Penetration Design Integration with Heat Shield

Heat Shield Separation System

The relatively complete concept design and trades for the heat shield separation system performed for DAC-2 did not need to be updated significantly for CRC-3. For more information, refer to the DAC-2 Separation Systems Appendix.

OML Sensitivity Analysis

The initial shape was constrained to match the nominal shoulder shape. With this restriction, an efficient variable thickness heat shield can conform to the nominal OML, with an axisymmetric carrier structure that is offset from the surface by a varying amount in the radial direction.

For the fully ablated heat shield shape, hypersonic aerodynamics is only slightly affected. The ablated shape should trim at slightly higher angle of attack and therefore generate slightly higher L/D. Further investigation of transonic performance is required from the CAP team.

The thinnest Block I heat shield candidate on the carrier structure for the thickest Block II candidate produced a significant deviation from the nominal shoulder shape. It is anticipated that separate carrier structures may be required for the two heat shields, although more detailed aerodynamic analysis, particularly for stability in the transonic regime prior to parachute deployment, would be required to make a definitive determination.

An axisymmetric heat shield can deliver most of the potential benefits from thickness tailoring while respecting the nominal OML, provided that the associated axisymmetric carrier structure shape is manufacturable. Heat shield ablation does not have a strong influence on hypersonic aerodynamics. The influence of structural deformation on trim angle of attack needs to be analyzed. Transonic aerodynamics should be evaluated for all shapes considered in this study.

For more information, refer to the OML Sensitivity Report in Appendix H.

Boost Protective Cover TPS Sensitivity

As a continuation of the DAC-2 effort, further analysis was desired for CRC-3 to better understand whether the TPS subsystem presented driving requirements for the need of a Boost Protective Cover. The LAS team delivered abort motor plume thermal environments to support analysis of any effects on the back shell TPS. Workforce resource limitations prevented this analysis from being implemented until late in the CRC-3 schedule.

The fully margined ascent heating profile was augmented by the inclusion of the abort motor heating and was supplied to the back shell TPS and windows teams for their assessment. Neither team found any deleterious effects from the thermal environments of the abort motor plume. However, both teams are still concerned about the potential for damage from the abort motor and/or jettison motor particulate ejecta (alumina) which is still being characterized. Consequently, we find no thermal driver for the BPC, but other environmental aspects need to be considered before the decision can be finalized.

Back Shell Refurbishment

For CRC-3, an evaluation was initiated of a conceptual design of back shell TPS with removable panels to enable off-vehicle check-out. In order to accurately evaluate the work-flow benefits of a removable (off-line processed) back shell, the vehicle access time that TPS might expect access to the CM must be known (as a baseline). No vehicle processing plans of sufficient detail to provide this access time were available for CRC-3.

In conversation with Structures lead Ronny Baccus, no rationale could be developed for non-removable back shell panels (TPS and supporting structure). From a TPS perspective, the perimeter seals that would be required around each of these removable panels do not present a problem and the TPS refurbishment/replacement time-line becomes irrelevant to vehicle turn-around. Both Structures and TPS teams agree that the back shell panels should be made removable and the TPS processed off-line.

Risk Support for Water versus Land Trade

As part of the NESC and Constellation Water vs. Land studies, the TPS ADP provided reliability estimates for the CEV TPS system. TPS reliability is broken out between skip and ballistic entries for ISS and Lunar missions resulting in four different cases. At the time of CRC-3, only two different sources of TPS failure were considered. These are TPS failure based on 1) proximity to operating margins for re-entry environments and material response and 2) micrometeoroid and orbital debris (MMOD) damage. Failure based on proximity to operating margins captures the environment and material response uncertainty of TPS systems due to the inability to recreate entry environments in ground testing. MMOD damage captures the risk of TPS damage on orbit due to micrometeoroids and debris. Further analysis of other failure types is underway.

Based on the DSNE specification of the MMOD environments for ISS and Lunar missions, it is clear that a TPS system meeting ISS MMOD probability of no penetration (PNP) requirements exceeds Lunar PNP requirements. ISS re-entry environments are more benign than Lunar re-entry environments. Thus, ISS mission reliability is driven by MMOD and Lunar mission reliability was assumed to be driven by entry environment and material response uncertainties.

Preliminary analysis indicates that a TPS meeting ISS PNP requirements demonstrates a probability of 2.0e-4 of MMOD causing subsequent TPS failure on re-entry. This is based on the known MMOD flux at the ISS orbit, and the exposed area of the TPS. The feasibility of providing such a TPS is a forward goal of the TPS ADP. Basic margin analysis indicates a TPS reliability of 0.9998 for lunar ballistic returns where heat flux, pressure and shear are maximized. The proximity of these numbers is coincidence.

The major TPS discriminator in the question of water vs. land landing is the contribution of heat shield ejection risk to the land landing case. Otherwise, TPS is simply a contributor to the overall risk of vehicle breakup – independent of water vs. land.

Important considerations in this analysis are the probability of ballistic missions being flown, the availability of on-orbit inspection and the different types of failures resulting from TPS local burn-through vs. general bondline overheat. Further analysis along all of these lines remains to be done.

TPS Instrumentation

To obtain time-history data concerning the aerothermal and material response performance of the TPS material in the heat shield, carrier structure, and back shell of the vehicle, a mixture of different types of instrumentation will be used. The suite of instruments include thermocouples for temperature measurement, Hollow aErothermal Ablation Temperature (HEAT) sensors for char-depth measurements, pressure ports, different types of slug calorimeters for heat flux measurement, spectrometers for radiative heating measurements, and strain gages for measuring the carrier structure strain. Each instrument has been tested in representative ground-test facilities and/or is commercially readily available to minimize development risk.

Many of these instruments will be co-located in the TPS to minimize the number of penetrations required for instrumentation of the vehicle. Thermocouples, HEAT sensors, and pressure ports can generally be combined into a single penetration on the heat shield. The use of a spectrometer requires a special window on the exterior of the vehicle that allows for the spectrometer instrument an unobstructed view of the external aerothermal flow field. Slug calorimeters, appropriate for the back shell, will consist of monitoring the temperature of a piece of well-characterized material located flush with the TPS surface.

Vehicle Location	Sensor	Physical Property	Electric Property
Heatshield	**Standard Thermocouples**	Temp	V
	HEAT Sensor	Char Interface Level	R
	Forebody Pressure Sensor	Pressure	V
	Triaxial Strain Gage	Strain	V
Backshell	**Standard Thermocouples**	Temp	V
	ISP Thermal Sensor	Catalytic Heating	R
	Slug Calorimeter	Heat Flux	V
	HEAT Sensor	Char Interface Level	R
	Backshell Pressure Sensor	Pressure	V
TBD	**Spectrometer**	Radiative Heating	Serial

Table 10.2-4 Table of Possible Instruments for TPS

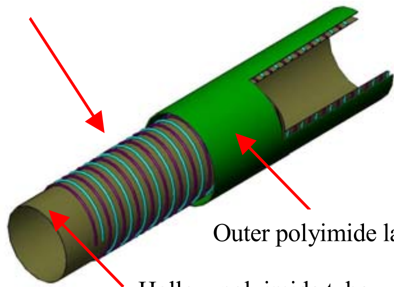

Figure 10-2.11 Schematic of HEAT Sensor

10.2.3 Mass Estimates and Design Maturity

Block I Heat Shield TPS

Table 10.2-5 gives a summary of maximum TPS system thickness and system weight for the four candidate TPS concepts for the CRC-3 analysis results using the DAC-2 TPS carrier structure. The TPS system weights are presented for the uniform TPS thickness distribution. The uncoated LI-2200 ceramic tile system was selected as the baseline Block I heat shield TPS material, with a resulting maximum TPS system thickness of 2.2 inches and a system weight of 1,350 lb (615 kg). For the final CRC-3 carrier structure design, Table 10.2-6 presents the TPS system thicknesses and weights for the baselined uncoated LI-2200 tile and the various candidate carrier structure concepts. Table 10.7-6 summarizes the TPS sizing results for the Block II candidate materials sized for the Block I ISS-LEO entry. Results presented in all three tables include a TPS system growth allocation of 25%. The results also include the margins and factors of safety specified in version 5d of the Interim TPS Margin Process.

TPS Concept	Max Thickness (inches)	TPS System Weight (lb)	TPS Support Structure Weight (lb)	Total System Weight (lb)
LI2200/Uncoated	2.21	1348.5	765.7	2114.1
LI2200/RCG Coated	2.10	1310.5	767.9	2078.4
BRI-18/TUFI/RCG Coated	2.36	1307.9	762.8	2020.9
SLA-561V (FIAT)	1.50	707.5	780.4	1487.9
SLA-561V (STAB)	2.046	944.1	769.0	1713.1

Table 10.2-5 Block I TPS Thicknesses and System Weights (Uniform Thickness)

Carrier Support Concept	Maximum Thickness (inches)	TPS System Weight (lb)	Carrier Structure Weight (lb)	Total Weight (lb)
2.5 in. Ti_Ti_HC	2.204	1315.0	740.0	2055.0
2.0 in. GrBMI_Ti_HC	2.345	1353.8	767.2	2121.0
3.0 in. GrBMI_Ti_HC	2.356	1349.0	870.1	2219.0
2.5 in. SS_SS_HC	2.197	1330	904.3	2234.0

Notes

There is a small difference in the TPS thickness and system weight for the uncoated LI-2200 tile between the DAC-2 and the CRC-3 TPS carrier structure. The CRC-3 carrier structure design has slightly less thermal mass in the face sheet compared to the DAC-2 configuration, however this is offset by the higher thermal conductivity of the CRC-3 0.25 in. honeycomb core design, resulting in slightly lower required TPS thickness.

Table 10.2-6 Uncoated LI-2200 for Candidate CRC-3 Carrier Structures

TPS Concept	Max Thickness (inches)	TPS System Weight (lb)	TPS Support Structure Weight (lb)	Total System Weight (lb)
PICA	3.8	1730	730	2460
Avcoat	1.8	1830	770	2600
PhenCarb	1.3	1020	790	1810

Table 10.2-7 Summary of Block II TPS materials Sized for ISS-LEO Entry

Block II Heat Shield TPS

The updated heat shield TPS mass estimations are shown in Table 10.2-8. As for the DAC-2 analysis cycle the estimates are given for PICA, ACC/Calcarb, AVCOAT and PhenCarb. In addition, estimates are included for 3DQP. All results are for analysis run using the DAC-2 baseline carrier structure as specified in the CRC-3 assumptions document.

For the MEL update on August 11, 2006, an average of the five candidates was computed and the savings for a variable thickness configuration was estimated to be 13%. This resulted in the MEL estimate of 1,800 lb. The thickness of PICA was used (4.8 inches). This MEL update is slightly heavier than the DAC-2 MEL update due to updates to the PICA density, updates to the variable thickness calculations and updates to the margin process.

TPS Candidate	Max Thickness cm [inches]	Uniform Thickness (includes 25% growth)		Variable Thickness with Heat Load Binning (includes 25% growth)			Variable Thickness with Radial Binning (includes 25% growth)		
		Mass kg [lb]	Z-axis CG Offset cm [in]	Reduction from Uniform Thickness	Mass kg [lb]	Z-axis CG Offset cm [in]	Reduction from Uniform Thickness	Mass kg [lb]	Z-axis CG Offset cm [in]
PICA	12.1 [4.8]	980 [2150]	0	13%	850 [1870]	-6.0 [-2.4]	10.0%	880 [1940]	0
ACC-Calcarb	11.9 [4.7]	1070 [2370]	0	14%	920 [2040]	-6.7 [-2.6]	10.4%	960 [2120]	0
3DQP	6.7 [2.6]	820 [1810]	0	17%	680 [1510]	-5.9 [-2.3]	11.8%	730 [1600]	0
AVCOAT	5.8 [2.3]	1020 [2250]	0	15%	870 [1920]	-7.4 [-2.9]	10.4%	920 [2020]	0
PhenCarb	5.8 [2.3]	810 [1790]	0	18%	670 [1470]	-8.3 [-3.3]	11.4%	720 [1590]	0

Table 10.2-8 Summary of Block II TPS Thicknesses and System Weights

Back Shell TPS

The predicted mass for the baseline back shell TPS weight is 560 lb (255 kg), with a maximum thickness of 1.6 inches using a BRI-18 and BRI-8 ceramic tile with a TUFI diffusion layer and RCG coating. The choice of the BRI tile with TUFI/RCG is based on operability and robustness considerations. The LI-2200-based tile systems have approximately 20% lower TPS mass, while the SLA-461V ablator represents about a 50% TPS mass penalty compared to the BRI-based system. Table 10.2-9 summarizes the required TPS thicknesses and system masses.

Compared to DAC-2, there is an overall decrease in TPS mass for the baseline system. This decrease is primarily due to increased detail in the margin process. The current panel configuration consists for four distinct panel/bay cover thicknesses, compared to only two for the DAC-2 design.

TPS Type	**Max Required System Thickness (inches [cm])**	**TPS System Weight (Including 25% Growth) (lb [kg])**
LI2200/RCG + LI900/RCG & LRSI Tile		
LI2200	1.36	86.0 [38.8]
LI900	1.36/0.83/0.75/0.67	340.0 [154.2]
Total		426.0 [195.0]
LI2200/Uncoated + LI900/RCG & LRSI Tile		
LI2200	1.70	05.0 [47.6]
LI900	1.70/0.83/0.75/0.67	350.0 [158.8]
Total		450.0 [204.0]
BRI-18/TUFI/RCG + BRI-8/TUFI/RCG Tile		
BRI-18	**1.57**	**95.0 [43]**
BRI-8	**1.57/1.03/0.98/0.67**	**465.0 [210]**
Total		**560.0 [255]**
SLA-561V Ablator	1.86 {STAB Code} 1.84 {FIAT Code}	856.0 [388] 842.0 [382]

Table 10.2-9 Summary of Back Shell TPS Thicknesses and System Mass

Carrier Structure

The titanium honeycomb structure with a 2.5-inch core height produced the lightest weight design at 735 pounds for the 20 psi external pressure (without safety factor). For 2.0-inch core height and similar loading, the bias ply Gr/BMI design weight was 785 pounds and the 2.5-inch stainless steel design weighed 916 pounds. The recommendation for carrier structure material following CRC-3 analysis and design is either the 2.5-inch titanium honeycomb or the 2.0-inch bias ply Gr/BMI. Further study and comparison to other requirements, such as thermal performance, will lead to a final selection before PDR. These results should be viewed in light of the groundrules and assumptions discussed earlier. The carrier structure mass is carried under Mechanical Systems-Structures MEL.

Seals

From the DAC-2 study results, a best estimate mass is based on a bulb-based pressure seal design and a single-bulb thermal barrier. Bulb-based seals provide higher compression ratios, apply minimal loads to the surrounding structures, weigh less, and better conform to the sealing surface than gaskets, O-rings, or Gask-O-seals. The single-bulb thermal barrier geometry looks to be the best choice from the thermal barrier trade study. The combined mass of the seal system is 20 lb with growth.

Penetrations

An examination of competing compression pad configurations and material was performed for the CEV heat shield. Comparisons were made between each candidate compression pad and the acreage TPS according to thermal and mechanical performance criteria, as well as material specific characteristics such as availability, and model fidelity. Comparisons between each of the mechanical designs and attachment methods were made and ranked according to their respective design factors. Table 10.2-10 summarizes the results of the material trade study and lists the most compatible and second most compatible compression pad material for each of the five candidate TPS materials.

Acreage TPS Candidate	Best Compression Pad	Best Alternative Compression Pad
PICA	FM5504	FM5055 (MX4926)
ACC4/Calcarb	FM5055 (MX4926)	FM5504
3DQP	FM5504	3DQP (HD layer)
Avocoat 5026†	FM5504	FM5055 (MX4926)
Phencarb †	FM5055 (MX4926)	FM5504

Table 10.2-10 Leading Candidate Compression Pad Materials

Compression Pad Material	Lunar Skip Thickness (unmargined)	Mass, lb (based on Eight 8-inch pads)
FM5055 carbon phenolic	2.71	127
FM5504 silica phenolic	2.28	129

Table 10.2-11 Leading Candidate Compression Pad Materials Mass Estimates

<u>*Separation System*</u>

The current best estimate for the baseline separation system is given in DAC-2 final report. A 25% growth allocation was added to the mass of each part to come up with a final mass for each separation mechanism. The total weight (with growth) of the entire separation system is about 40.3 pounds, corresponding to a weight of just over 5 pounds per separation mechanism.

An estimate was made on how much the separation system would weigh if it also had to cut the tension tie. For the purposes of cutting the tension tie, it was assumed that a Mega Cutter would be used. Taking this entire system into account, the total separation system weight (with growth) becomes 56.8 pounds.

10.2.4 Plan Forward

<u>*Heat Shield and Back Shell TPS Sizing*</u>

1) Update TPS sizing for CRC-3 TPS support structure configurations.

2) Assess impact of heat shield ejection at altitudes lower than 7,000 ft.
3) Update back shell TPS sizing for RCG emissivity (Bouslog & Cunnington data).
4) Improve uncoated LI-2200 tile thermal response model and update Block I heat shield TPS sizing.
5) Improve SLA-561V response models and update Block I heat shield TPS sizing for SLA-561V.
6) Continue monitoring studies on how to implement a variable thickness heat shield.

Carrier Structure

The carrier structure analysis requires investigation of more load cases. In particular, the time-varying pressure and thermal loads, throughout the trajectory, need to be applied for analysis of the thermostructural response. More detailed study of the shoulder region is required. Investigation of the sensitivity to attachment and support details will also be conducted. Additional cases such as water landing abort and separation loads also need to be included in the analyses conducted thru PDR.

OML Sensitivity Analysis

Additional aerodynamic analysis is planned by the CAP team for the shapes defined in this study. In particular, evaluation of transonic behavior is required.

A CAD part that is suitable for representing structural deformations has been developed, but aerodynamic analysis has not been performed for these shapes. The influence of structural deformation on trim angle of attack needs to be analyzed.

Analysis of the manufacturability of carrier structure that is axisymmetric by not a constant offset from the nominal OML is in progress.

Transonic aerodynamics should be evaluated for all shapes considered in this study.

Penetrations

Future work will focus on refining the mechanical design and delving deeper into the thermal stress issue. The full margin policy will be applied to all future thermal response calculations. The thermal environments specific to each of the eight compression pads will be used instead of assuming the compression pads are located at the point of peak heating. A thickened ACC4/Calcarb compression pad will be evaluated. The Block I compression pad design will be brought to the level of Block II, which was the focus in this study.

Instrumentation

The major outstanding engineering issue concerning the instrumentation suite and layout involves tailoring the instruments to the particular TPS materials chosen for the vehicle. For example, in a charring ablator material, penetrations may be made to the material surface whereas in a dual-layer material, penetrations might only be made to a single layer. Once installed, the instrumentation wiring will be routed to an electronics interface box that will process the instrumentation signals and store it for post-flight analysis.

Interface Requirements and Design

The CEV reference design cycles have served to improve understanding on the interactions between the TPS and the CEV and other subsystems. Future work will be needed to better refine design decisions on the landing system, LAS boost protective cover, carrier structure attachment and separation to the CM prime structure, OML definition, CAP environment refinements, thermal constraints of maintaining pressure vessel temperature on TPS sizing, and others.

Note: Additional future work still pending is identified in the DAC-2 final report and not reported in this report.

The following is a listing of TPS-related appendices to the CRC-3 Design Definition Document, available upon request.

Appendix A	Assumptions	Davis
Appendix B	ITMP-v5d	Wright
Appendix C	Block I Heat shield Sizing	Rezin/Bowles/Coughlin
Appendix D	Block II Heat shield Sizing	McGuire/Coughlin
Appendix E	Back Shell Sizing	Rezin/Bowles/Rodriguez
Appendix F	Carrier Structure	Vause/Hamm
Appendix G	Water Impact Loads Study	Vause/Hamm
Appendix H	OML Sensitivity	Gage/Hawke
Appendix I	Penetrations	Dec

10.3 Passive Thermal Control

This section describes the Passive Thermal Control Subsystem of the CEV Reference Configuration design. The main function of the PTCS is to maintain equipment within its defined temperature limits. This is accomplished through the use of bulk insulation, multi-layer insulation, thermal optical coatings, and heater systems. The summary below details the PTCS changes and analyses performed as part of the CRC-3 design cycle. For a review of requirements and previous work, please see the PTCS section from the CEV Reference Configuration Study Design Analysis Cycle 2 Design Definition Document, CxP 72103.

10.3.1 Driving Requirements, Groundrules, and Assumptions

There were no major changes to the PTCS driving requirements or groundrules for the CRC-3 design cycle. Therefore, no additional data is presented here. However, progress was made on the PTCS thermal models. This includes the addition of structural members to the CM as well as components and equipment located within the CM's unpressurized region. Due to the lack of design maturity, several assumptions about how these components are located and how they interact thermally with the CEV needed to be made. These design/analysis assumptions are documented in section 10.3.2 Conceptual Design Overview.

10.3.2 Conceptual Design Overview

10.3.2.1 CM PTCS Thermal Model

The major components of the CM remained unchanged from the DAC-2 model. These include the TPS back shell and support structure, the TPS heat shield and support structure, the LIDS, the pressure vessel, and the shell heater components. A full description of these items is available in the DAC-2 report and they are shown in Figure 10.3-1, Unchanged PTCS CM Thermal Model Elements. The only exception is that an additional layer of MLI was modeled on the underside of the TPS support structure. This was added at the recommendation of experienced personnel in an attempt to minimize the radiation heat loss from the pressure vessel to the TPS.

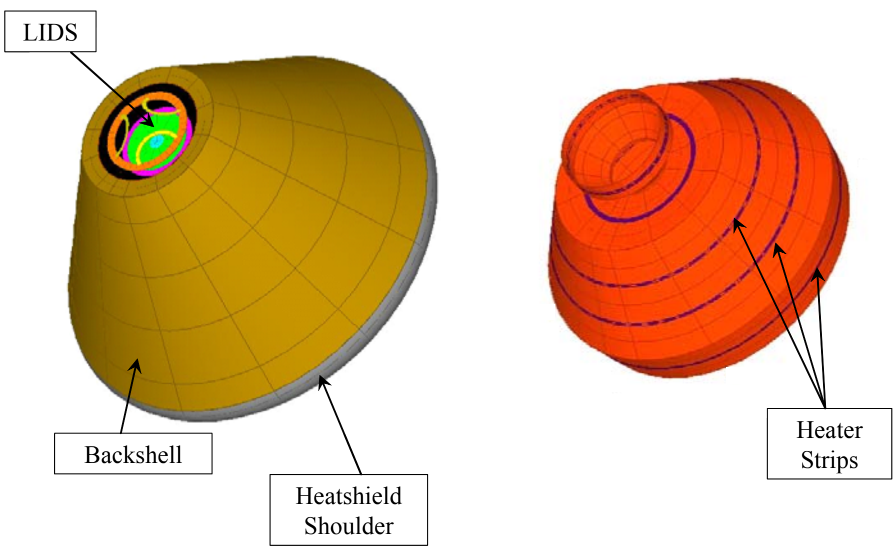

Figure 10.3-1 Unchanged PTCS CM Thermal Model Elements

The DAC-2 CAD layout (16 June 2006 version) was used to size and locate several components within the unpressurized segment of the CM. Additionally, the PTCS team met with other System Managers to discuss these components in an attempt to accurately create a thermal model. Table 10.3-1, New CM PTCS Thermal Components, lists the components that were added to the model, as well as several key assumptions, such as the material and optical property. Note that during the design cycle, several different configurations were run to determine differences in thermal performance. In some instances, the optical coating assumptions may seem odd, such as having a Silver Teflon tape covered by MLI. Further refinement of the model would be done to eliminate these types of inconsistencies. Figure 10.3-2, New CM PTCS Model Elements, illustrates the size and location of these new components.

It should be noted that none of these components have any internal heat dissipation or heaters at this time. Therefore, they are responding purely to the thermal environment and pressure vessel shell heaters. Developing an accurate power dissipation profile for these components is also future work.

Component Name	Location in Model	Material	Optical Coating
Structural Members	Throughout	Aluminum	Clear Anodized, no MLI
Star Trackers	Top of CM, Unpressurized	Aluminum	Blackbody, with MLI on avionics
Main Chutes	Top of CM, Unpressurized	Aluminum	Blackbody, no MLI
Flotation bags	Top of CM, Unpressurized	Aluminum	Silver Teflon tape, no MLI
Drogue Mortars	Top of CM, Unpressurized	Aluminum	Clear Anodized, no MLI
O2 Prop Tanks	Base of CM, Unpressurized	Titanium	Silver Teflon tape, with MLI
Ethanol Tanks	Base of CM, Unpressurized	Titanium	Silver Teflon tape, with MLI
He Tanks	Base of CM, Unpressurized	Titanium	Silver Teflon tape, with MLI
N2 ECLSS Tanks	Base of CM, Unpressurized	Titanium	Silver Teflon tape, with MLI
O2 ECLSS Tanks	Base of CM, Unpressurized	Titanium	Silver Teflon tape, with MLI
ATCS Freon Tank	Base of CM, Unpressurized	Titanium	Silver Teflon tape, with MLI
ATCS Water Tank	Base of CM, Unpressurized	Titanium	Silver Teflon tape, with MLI
ATCS Evaporator	Base of CM, Unpressurized	Aluminum	Clear Anodized, with MLI
S-Band Avionics	Base of CM, Unpressurized, mounted on ATCS Cold Plates	Aluminum	Clear Anodized, with MLI
ATCS Cold Plates	Base of CM	N/A	N/A
Internal Avionics*	Inside CM Pressure Vessel	N/A	N/A
Internal ECLSS*	Inside CM Pressure Vessel	N/A	N/A
Internal ATCS*	Inside CM Pressure Vessel	N/A	N/A

* - These components are treated as boundary nodes set to the ATCS fluid temperature.

Table 10.3-1 New CM PTCS Thermal Components

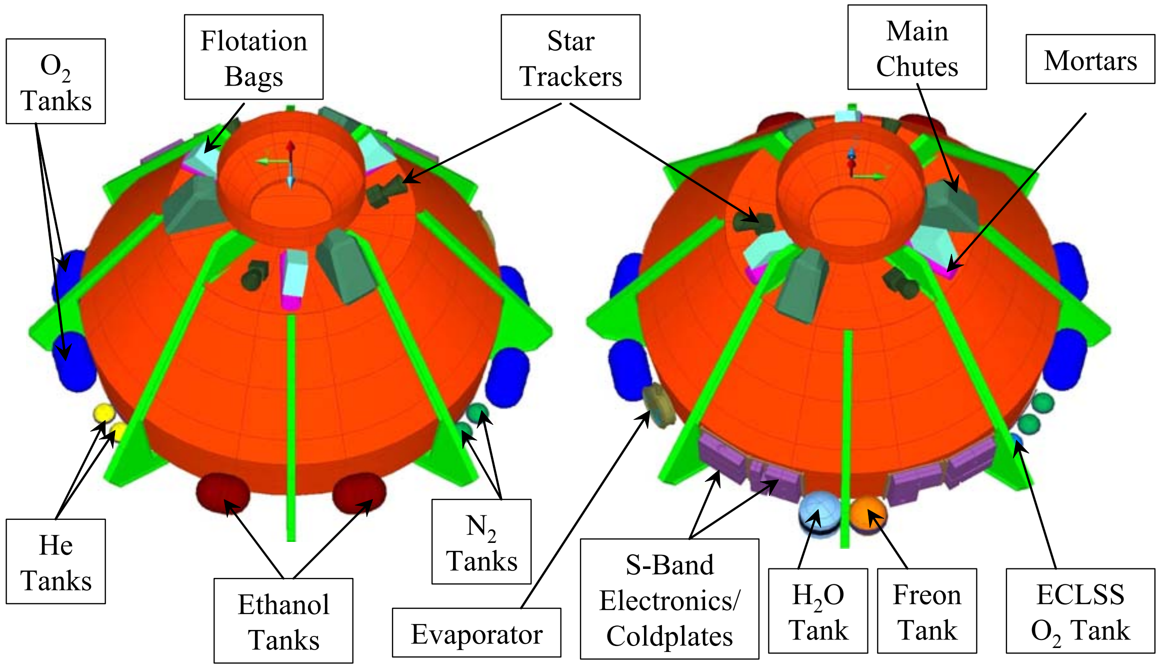

Figure 10.3-2 New CM PTCS Model Elements

The DAC-2 CM thermal model employed only radiation heat transfer between the pressure vessel and the aeroshell. However, with the addition of the structural members and other components, conduction heat transfer was included in the CRC-3 CM PTCS model. Estimating the thermal conductance between the pressure shell and other components is difficult because the conduction path is highly dependant on factors such as contact area, contact pressure, surface finishes, the presence or absence of a thermal gap filler, etc. With the attachment mechanisms for components still largely conceptual at this time, calculations including the parameters previously listed are not possible. Therefore, an engineering estimate of conductance was made for values between components and the pressure vessel. Future work will include studies on the sensitivity of the model to the conductances and how those values effect the heater power and component temperatures. Unless otherwise noted, the absolute conductance between components and the pressure vessel is assumed to be 1.0 BTU/hr/°F. This value represents a relatively small heat leak that can be achieved through the use of thermal isolation pads and other techniques. Notable exceptions to this value are listed in Table 10.3-2, Component to PV Conductance Values, along with rationale for the deviation.

Contactor	Conductance (BTU/hr/°F)	Rationale
LIDS to PV	5	Assumed a higher conductance value due to the larger contact area.
Ethanol Tank 2 to PV	25	Allows comparison of heat leak with other Ethanol Tank still at 1 BTU/hr/°F.

Table 10.3-2 Component to PV Conductance Values

Of particular interest is the heat leak path from the Pressure Vessel to the TPS aeroshell via the CM structural members. Figure 10.3-3, Proposed CM Structural Attachment, shows the method of attachment proposed by the structural community. In this configuration, the support structure is welded to the Pressure Vessel as an integral part of the assembly. As such, the thermal model assumes a perfect thermal conduction path from the Pressure Vessel into the structural member. The upper flange of the structural member would be bolted to the TPS carrier structure. For thermal isolation, a 0.2 inch layer of G-10 is assumed to separate the metal components. Additionally, it is assumed that the G-10 runs the entire length of the structural member. Using these assumptions, a conductance-per-area of 10 BTU/hr/ft^2/°F was calculated and used in the thermal model. As with the other conductance assumptions, a sensitivity study to this parameter should be performed in the future to determine if any requirements or design limitations need to be imposed on this thermal joint.

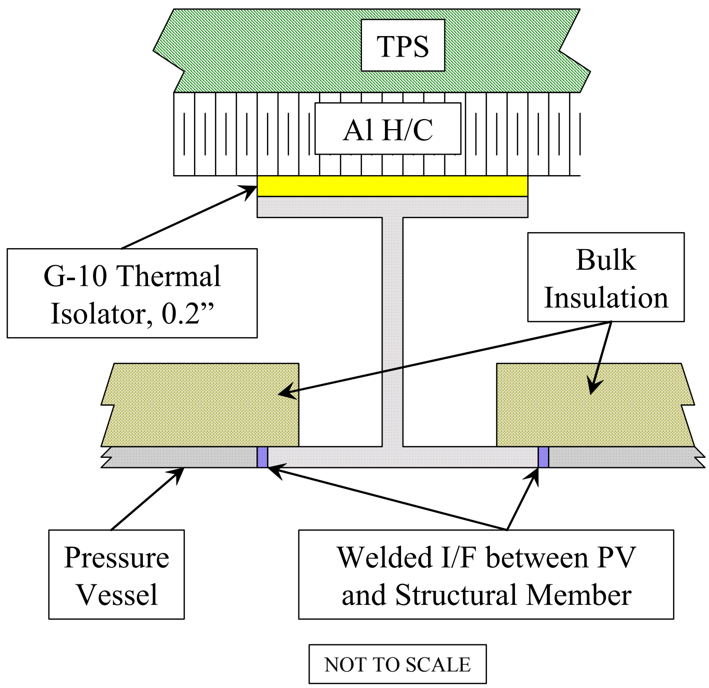

Figure 10.3-3 Proposed CM Structural Attachment

10.3.2.2 CM Analysis Cases and Results for the Integrated Analysis Team Assessment

For CRC-3, the Integrated Analysis Team convened to focus on LEO attitudes that would be acceptable to a wide range of disciplines. In addition to the LEO attitudes, a select subset of LLO and Transit attitudes were analyzed for comparison against DAC-2 results. The attitudes considered are described in Table 10.3-3, Integrated Analysis Vehicle Attitudes.

Case Designation	Reference Frame	+X-Axis on the …	Array Orientation
+XLV AIP	LVLH	Local Vertical	In the orbital plane
+XLV AOP	LVLH	Local Vertical	Out of the orbital plane
+XVV AIP	LVLH	Velocity Vector	In the orbital plane
+XVV AOP	LVLH	Velocity Vector	Out of the orbital plane
PTC 3RPH	Transit/SI	Velocity Vector, Slow roll of 3 rev/hr	N/A
Aft Sun	Transit/SI	SM Engine facing the sun	
+XLV AIP	LVLH	Local Vertical	In the orbital plane
+XLV AOP	LVLH	Local Vertical	Out of the orbital plane

Table 10.3-3 Integrated Analysis Vehicle Attitudes

For LEO attitudes, beta angles of 0°, -30°, -45°, -60° and -75° were analyzed (the thermal response is assumed to be symmetric about Beta = 0°). For the low lunar orbit cases, beta angles from 0° to -90° were analyzed in 15° increments. The environmental parameters used in the analyses are defined in Table 10.3-4, Thermal Environments for Integrated Analysis. All analysis cases were performed using a steady state solution routine.

Orbital Case	Environment	Solar Flux (W/m^2)	Albedo* (W/m^2)	Planetshine† (W/m^2)	Altitude (km)
LEO	Hot	1414	0.28	258	460
	Cold	1322	0.17	217	350
LLO	Hot	1422	0.20	11.8/1208*cos(*i*)	90
	Cold	1315	0.07	2.3/1118*cos(*i*)	400
Transit	Hot	1422	N/A	N/A	N/A
	Cold	1315	N/A	N/A	N/A

* - The LEO albedo is a function of the solar zenith angle, which varies with the Beta angle and true anomaly. The uncorrected factor is listed in the table. The correction can be found in the NEDD.

† - The Lunar planetshine flux, also known as Outbound Longwave Radiation (OLR) or Lunar IR, varies dramatically between the sunlit and dark portions of the moon. The first number given is the dark-side Lunar IR value. The sunlit Lunar IR value varies with the spacecraft's solar incidence angle, *i*, as shown in the table above.

Table 10.3-4 Thermal Environments for Integrated Analysis

The first case run was the Transit Aft Sun case in order to verify that the new thermal model provided consistent results with the DAC-2 model (recall that in DAC-2, an estimated 1200 W of heater power was needed to maintain the pressure vessel at 22.5 °C). Much to the analyst's surprise, the CRC-3 model predicted that over 3700 W of shell heater power were required. This far exceeds a reasonable amount of power that PTCS can expect to receive for shell heaters. After much research and many model runs, analysts discovered that the heat leak from the pressure shell to the TPS carrier structure via the structural members was the cause of this increased power estimate. If the conductances for the members are zeroed out (reverting to radiation heat transfer only), then the CRC-3 model predicts a heater power of 1000 W is needed (the difference from the DAC-2 result is due to the addition of MLI blankets on the underside of the TPS carrier structure and a reduction in the LIDS-to-PV conductance).

The fact that the heat loss through the structural members was so large is an important finding. It points to the need for cooperation between the thermal, structural, and power community to develop a structurally sound joint that limits the heat leak from the pressure shell such that shell heater power requirements are maintained at a reasonable value. This is the most important conclusion reached during CRC-3 for the CM PTCS.

Rather than speculate on different conductance values for the structural members, the PTCS team left the existing conductances in the model and compared the trends of the predicted heater power. Knowing that the Transit Aft Sun case requires the most heater power, the LLO and LEO cold cases should all show considerably less power draw, indicating a reduced shell heater duty cycle in these attitudes. Figure 10.3-4, Predicted LEO and LLO Shell Heater Power, shows precisely that trend. This figure plots results for the cold biased environmental parameters over the range of beta angles considered. Note that for LEO, AOP attitudes tend to require less power at lower beta angles. This is due to the fact that the solar arrays do not shade the CM at various points in the orbit. However, as beta angle increase, the AIP attitudes use less heater power for precisely the same reason. As the beta angle increases, the AOP array position begins to shade the CM back shell during longer portions of the orbit, while the AIP arrays become less of an obstruction.

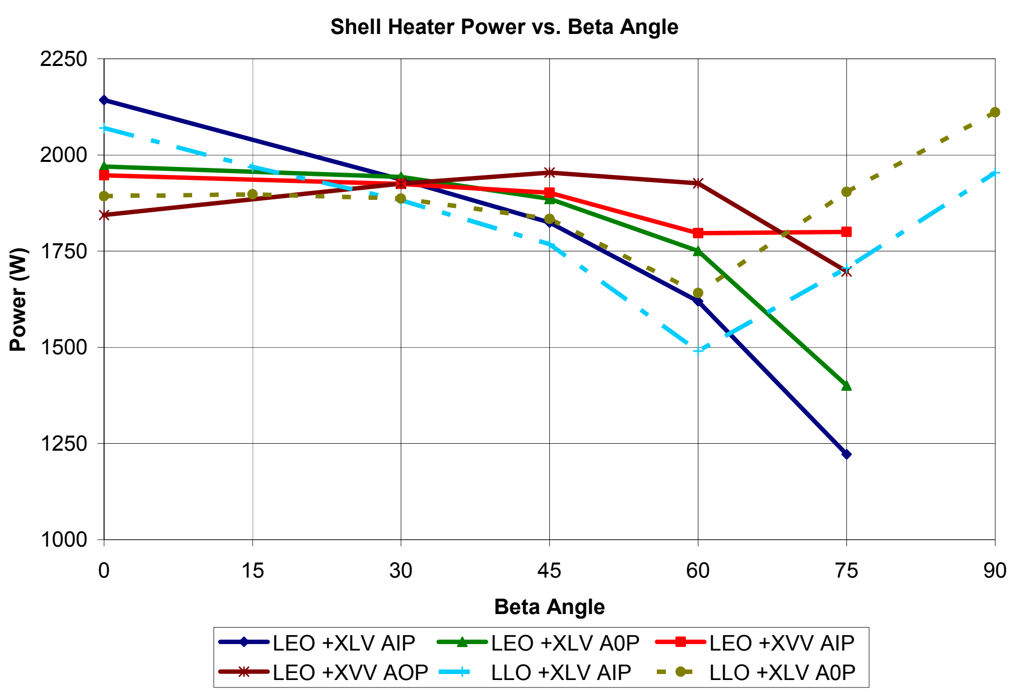

Figure 10.3-4 Predicted LEO and LLO Shell Heater Power

It is also worthwhile to note the LLO shell heater response. In LLO, the lower beta angles are generally considered the hottest due to the large amount of planetary IR. However, in the cold cases with the high orbital altitude (400 km), this appears not to be the case. As the beta angle increase, and more time is spent in the sun, the LLO shell heater power demand decreases (the demand at beta = 90° increases due to the near complete lack of albedo and lunar IR). However, as seen in Figure 10.3-5, Hot Case LLO Shell Heater Power, the predicted heater powers mostly follow the assumed trend. Although, there is still a marked decrease in the required heater power once a full sunlit orbit is achieved. Further investigation is required to verify these results. It could be that the steady-state results and vehicle attitude are masking the effects of the very hot LLO low beta cases.

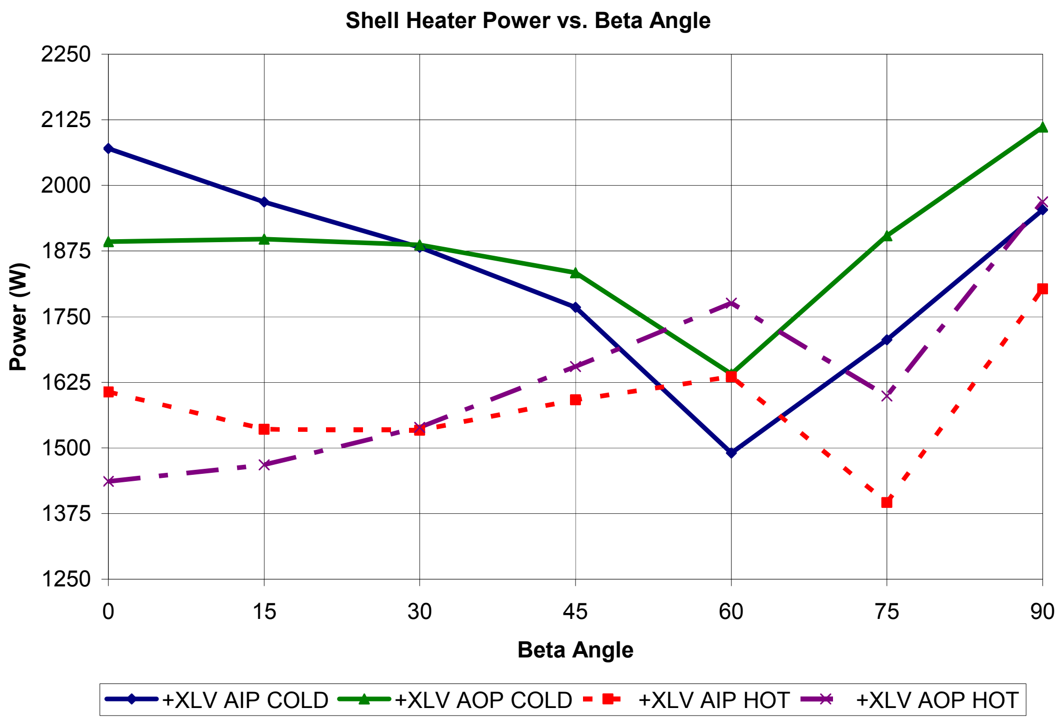

Figure 10.3-5 Hot Case LLO Shell Heater Power

A final observation from the CM PTCS analysis is that thermally sinking components in the unpressurized volume to the pressure vessel and covering them with MLI appears to be an effective method or eliminating the need for individual heaters on these components. For instance, no heater power was required to keep the star trackers, tanks, or recovery components above 10 °F, even in the extreme cold case of Transit Aft sun. This could vastly simplify the wiring and power needs of many subsystems by tying their thermal performance to that of the pressure shell, which is kept at a relatively constant and benign temperature. The penalty for this implementation could be the increased shell heater power required due to the additional thermal mass. There may also be some redundancy issues to address. Further, temperature insight into all components would still be desired. Finally, the hot cases with component heat dissipation would need to be evaluated to ensure that hot temp limits are not violated. Nevertheless, this is an intriguing option that deserves further investigation.

10.3.2.3 PTCS SM Thermal Model

The CRC-3 PTCS thermal model of the SM did not change much from the DAC-2 version. The most significant change was adding fidelity to the solar arrays, the solar array drive assemblies and the addition of a thermal insulation blanket between the stowed solar arrays and the engine nozzle. The thermal blankets are needed to protect the stowed solar arrays while the SM engine is firing. This occurs during a circularization burn or contingency abort-to-orbit burn. The SM engine is based upon the Aerojet AJ10-118K Delta II second stage engine. The cooling method utilizes an ablative chamber, and radiative skirt. The engine is not regeneratively cooled. It uses an ablative chamber made from rubber modified silica phenolic at the combustion flame front.

Another configuration change to the CRC-3 SM model is the clocking of the solar arrays by 45° to accommodate placement of the CEV RCS thruster pods on the coordinate axes and referenced to crew head ups. The SM docked to Node 2 on the ISS is shown in Figure 10.3-6.

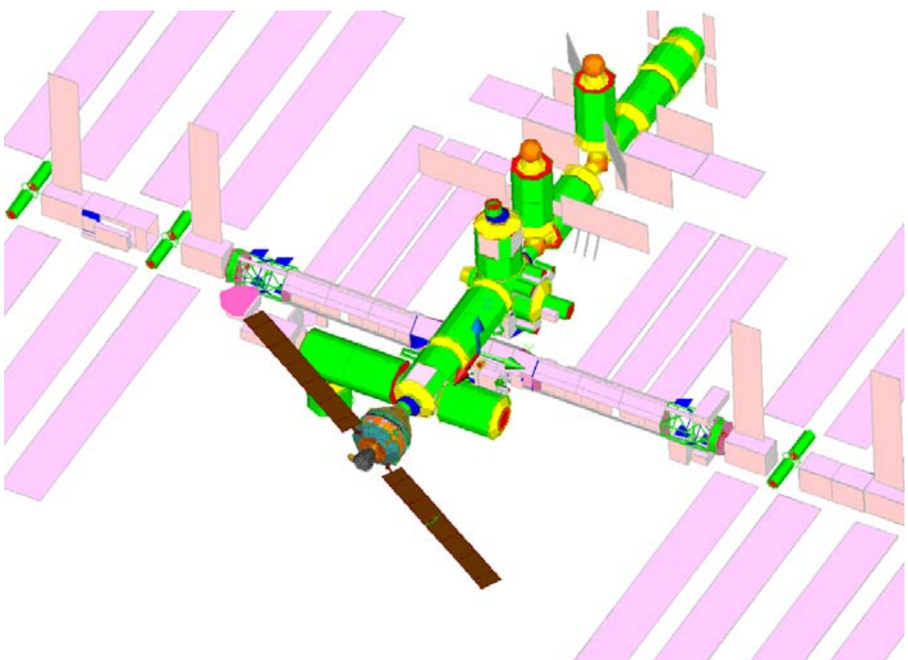

Figure 10.3-6 SM Docked to ISS

The high temperature insulation used to protect the stowed solar arrays is a five-layer blanket comprised of two layers of a nickel alloy 0.005 inches thick and three layers of Double Aluminized Mylar. An effective emissivity for the five-layer blanket was calculated to be 0.031. The sizing condition for the blankets was to keep the layer of the solar arrays closest to the engine nozzle below their 302 °F non-operating high temperature limit. The heat radiating from the nozzle and from the hot exhaust plume was calculated for the analysis.

Analysts also looked at cases to determine the radiator heat rejection capability of the SM in the ISS/CEV configuration. Due to time constraints, it was not feasible to perform a detailed thermal analysis for all the combinations of attitude (yaw, pitch, roll), beta angle (ranges from -75° to +75°), and the thermal environments (hot/cold). Therefore, analysts used results from the NESC Smart Buyer Study to narrow the number of orientations to analyze. The Smart Buyer Team used the ISS Flux Cube Database to show the hottest environments were at the higher beta angles. Using the hot biased environmental properties from the Natural Environment Definition Document (NEDD), only the high beta angles were analyzed. The ISS/CEV docked cases were only run for the configuration where the CEV is docked to Node 2. The ISS configuration is assumed to be in the Assembly Complete Configuration at the time the CEV is ready to be launched. Figure 10.3-7 shows the ISS/CEV docked at Node 2 configuration in orbit around the Earth. The Node 3 location is considered future work.

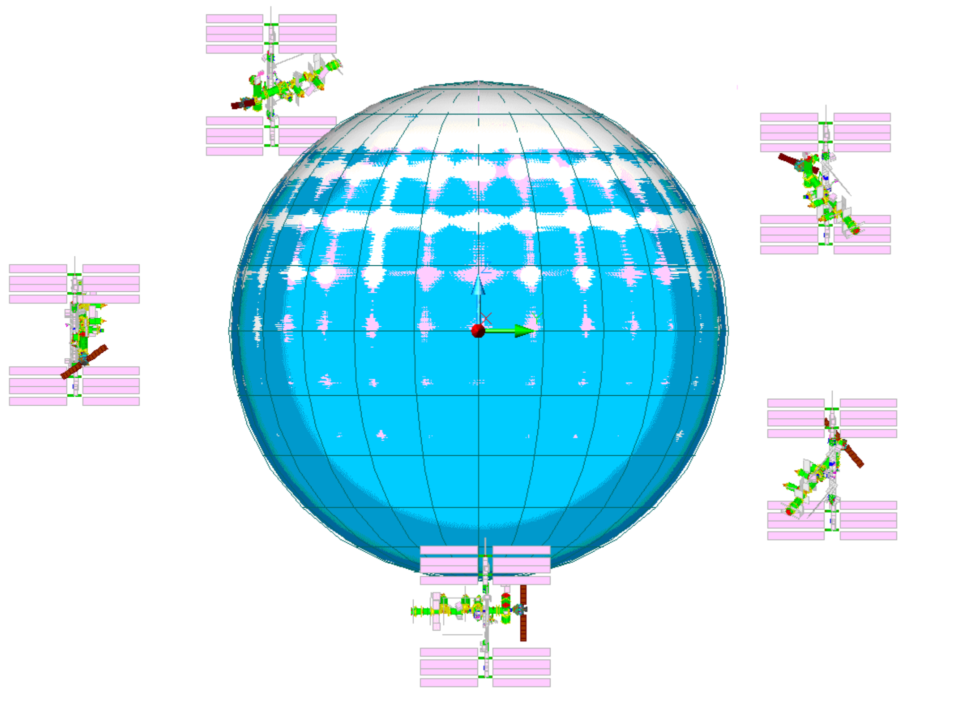

Figure 10.3-7 CEV Docked to ISS at Node 2 at High Beta Angle

The CEV-only configuration in LEO was also analyzed. The orientations of the CEV were performed for Local Vertical and Solar Inertial configurations. The Local Vertical and Solar Inertial orientations considered were +/- X, +Y, and +Z. The variation of the axis on the velocity vector would be the other two axes (i.e., +XLV ±YVV; +XLV ±ZVV; etc.).

10.3.2.3.1 SM Analysis Cases and Results

For the solar array heating from the rocket engine analysis case, a CFD code was used to calculate the hot gas temperatures inside the rocket engine and in the expanding plume. The thermal analysis used the total heat produced by the plume and the calculated exterior wall temperature of the engine nozzle to provide the heat sources to the vehicle. The exhaust plume was modeled as a series of connected parabolas with the total heat produced from that section of the exhaust plume applied to that section of geometry. The total heat radiated from the exhaust plume was

6.6 kW of heat. Thermal Desktop was used to calculate the view factors from the geometry and calculate the resulting temperatures. The heating from the exhaust plume did not apply any significant heating to the SM in the solar arrays deployed configuration. However, in the stowed configuration, see Figure 10.3-8, the stowed solar arrays extend beyond the exit plane of the engine nozzle.

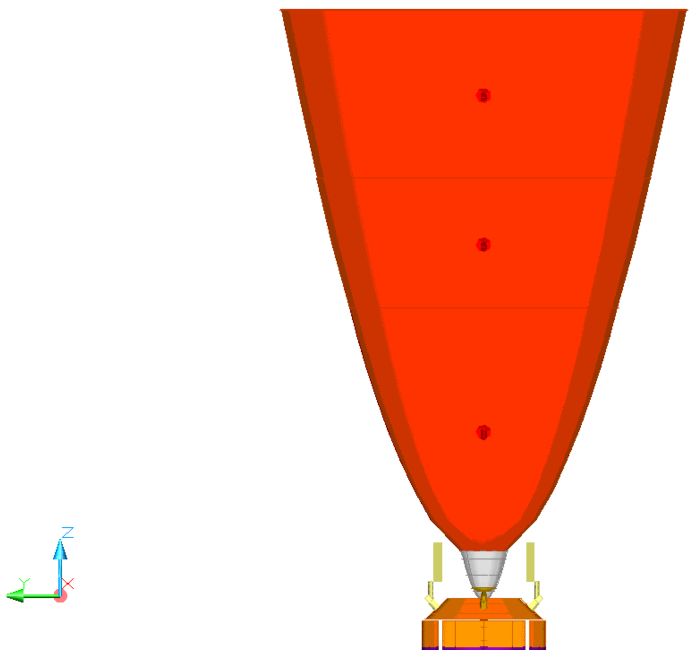

Figure 10.3-8 Engine Exhaust Plume and Stowed Solar Arrays

The resulting temperature of the solar array segment closest to the engine nozzle was 290 °F, which is less than the 302 °F non-operational hot temperature limit. The surrounding structure will require MLI on it to shield it from the radiating engine nozzle. Temperatures up to 984 °F were calculated for the outer surface. See Figure 10.3-9 for a temperature contour plot of the analysis case. The ablative engine nozzle approached temperatures up to 1600 °F.

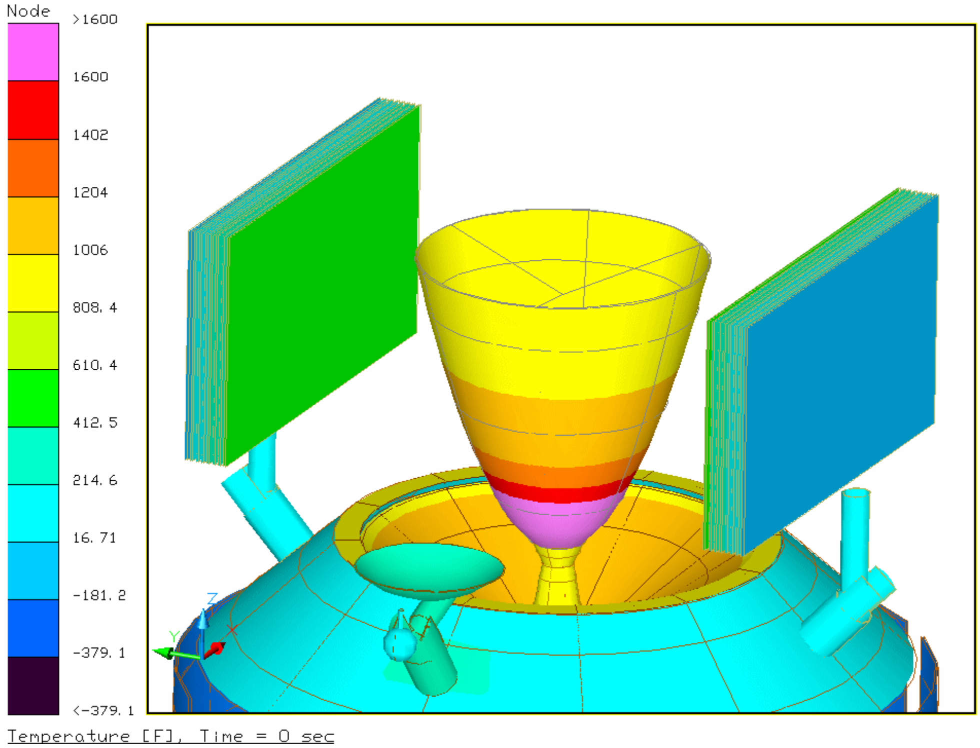

Figure 10.3-9 Stowed Solar Array Temperatures During an Engine Burn.

Due to the MMOD requirements, a shield is being considered to be placed around the rocket injector head and combustion section. A parabolic shield was input in the model and the resulting calculated shield temperature was 1489 °F. This high temperature is due to the view factor the inside of the parabola had to the hot section of the radiatively cooled nozzle. The radiation trapped inside the shield was then re-radiated onto itself resulting in higher temperatures.

For on-orbit cases where the solar arrays are deployed in LEO, the radiators can reject the nominal 4 kW of heat for any orientation and beta angle. For the case where the power load increases during docking to almost 7 kW, the flash evaporator may be needed to compensate for short duration of the docking maneuver.

While docked to the ISS, the CEV is only required to reject up to 1.2 kW of heat. With the 340 ft^2 of radiator area, there will be no issues of rejecting heat while docked at Node 2 location. The Node 3 location has been identified as forward work.

10.3.3 Mass Estimates and Design Maturity

The components tracked on the PTCS MEL include only the PTCS materials used by the subsystem. The PTCS MEL does not contain MLI or heater/temperature sensor information for other subsystems. Note that the SM solar array engine heat shield mass is bookkept in the Power System MEL. The PTCS MEL contains estimates for the CM MLI, bulk insulation, shell heaters, temperatures sensors, and the SM MLI. The CM bulk insulation mass is based on a 0.5 inch thickness of Pyrogel AR5223 covering the entire pressure vessel. It is assumed that an MLI blanket covers the bulk insulation and the underside of the TPS support structure. In the SM, an MLI blanket is modeled around the interior of the OML to prevent heat leak/gain from the internal components. Table 10.3-5, PTCS CRC-3 MEL, is the PTCS MEL.

Hardware Items	Quantity	Unit Mass (lbm)	Growth (%)	Total Mass (lbm)	CM Mass (lbm)	SM Mass (lbm)	Basis of Estimate
PTCS				**384**	**275**	**109**	
CM Bulk Insulation	1	126	15%	144.9	144.9		Assume 0.5" of insulation over the CM pressure shell surface area.
CM MLI Insulation	1	100	20%	120.0	120.0		Assumed 10-layer blanket to cover bulk insulation as a radiation shield and another 10-layer blanket on the underside of the TPS structure
Pressure Shell Heaters	52	0.1	25%	8.3	8.3		Generic density of silicon rubber and estimated heater dimensions
Pressure Shell Temp Sensors	28	0.1	20%	1.7	1.7		
SM MLI Insulation	1	91	20%	109.2		109.2	Assumed 15-Layer MLI buildup

Table 10.3-5 PTCS CRC-3 MEL

10.3.4 Plan Forward

With the completion of the above work through CRC-3, PTCS has examined numerous attitudes and environments for a wide range of beta angles. The following list of forward works items represents tasks to be accomplished should additional development work be performed.

- Update PTCS models to latest SM and CM layout configurations
  - Expand model detail to include additional components and heat dissipation
- Run sensitivity studies for the following thermal parameters:
  - Conductance between components and CM pressure vessel
  - Sensitivity of TPS temperatures and heater power to TPS optical coatings
  - Quantify the shell heater power increase caused by thermally sinking components to the pressure vessel (also examine hot case effects)
  - Trade study for the use of MLI vs bulk insulation for the CM
- Perform thermal analysis to support he following:
  - Ascent thermal performance
  - Re-entry/Post-Landing
  - Perform a full thermal analysis mission simulation

10.4 Mechanisms

The systems currently bookkept under Mechanisms include the docking mechanism, docking mechanism jettison, docking hatch, ingress/egress hatch, launch restraint release, deployment and gimbaling of the high gain antenna, launch restraint release, deployment and gimbaling of the solar array stack, LAS/CM separation, heat shield separation, CM/SM separation, SM/SA separation, forward bay aeroshell jettison, crew seat attenuation, structural vents, and umbilicals. The panel deployment and gimbaling of the solar arrays is currently bookkept under EPS.

10.4.1 Driving Requirements, Groundrules, and Assumptions

Driving requirements are based upon the initial ICPR release of the requirements documents. Driving requirements are considered to be those whose application results in a design that is significantly different from the design that would be chosen if the requirement were not applicable. The following requirements have been identified as driving requirements for mechanisms:

- CEV SRD: The CEV shall be single-fault tolerant for critical hazards except for areas approved to use Design for Minimum Risk criteria. [CV0270]

  This requirement drives the architecture of nearly all mechanisms on the vehicle.

- CEV SRD: The CEV shall be two-fault tolerant for catastrophic hazards, except for areas approved to use Design for Minimum Risk Criteria. [CV0271]

  This requirement drives the architecture of nearly all mechanisms on the vehicle.

- CEV SRD: The CEV Crew Module shall have an outer mold line that is derived from the Apollo Command Module design as defined in CXP-15000, Crew Exploration Vehicle (CEV) Crew Module Outer Mold Line. [CV0186]

  This requirement itself is not a driver, however the mold line defined in CXP-15000 is a driver. The use of a 16.5 ft diameter CM with the Apollo mold line drives the need to jettison the docking system.

- CEV-ISS IRD: The CEV shall dock with the ISS at PMA-2 (Node 2 Forward port) and PMA-3 (Node 3 Nadir port) via an ISS Androgynous Peripheral Assembly System (APAS). [CV0602]

  This requirement drives the use of a modified APAS system that would not be required otherwise.

- CARD: The Constellation Architecture's primary landing mode for return to Earth shall be on land at CONUS locations. [CA0044-PO]

  This requirement increases the amount of energy that needs to be absorbed by the crew seat attenuation system.

- DSNE: Landing Site wind speeds, landing site ground slope, and abort landing site sea state requirements

  These requirements also increase the amount of energy that needs to be absorbed by the crew seat attenuation system.

10.4.2 Conceptual Design Overview

Docking Mechanism

As specified by requirement CV0602, the Block 1 CEV uses a modified Russian APAS docking mechanism. The APAS has flight heritage as the Space Shuttle Orbiter docking system used to dock with the International Space Station. The extent and nature of the modifications required are currently unknown and will depend on the outcome of detailed approach and capture simulations and negotiations with RSC/Energia. At a minimum the avionics will need to be redesigned to allow vacuum operation, and it is likely that changes to mechanical components governing the response of the capture ring will also be required. Figure 10.4-1 shows an unmodified APAS system as utilized on the Space Shuttle Orbiter.

Figure 10.4-1 The APAS System Utilized in the Orbiter Docking System

As specified by requirement CV0315, the Block 2 CEV uses an American LIDS docking system. This docking system is still in the development stage, but provides a fully androgynous, load-sensing force feedback system that allows docking between any two units with impact forces greatly reduced over other docking systems. Figure 10.4-2 shows a detailed CAD model of the LIDS risk reduction unit.

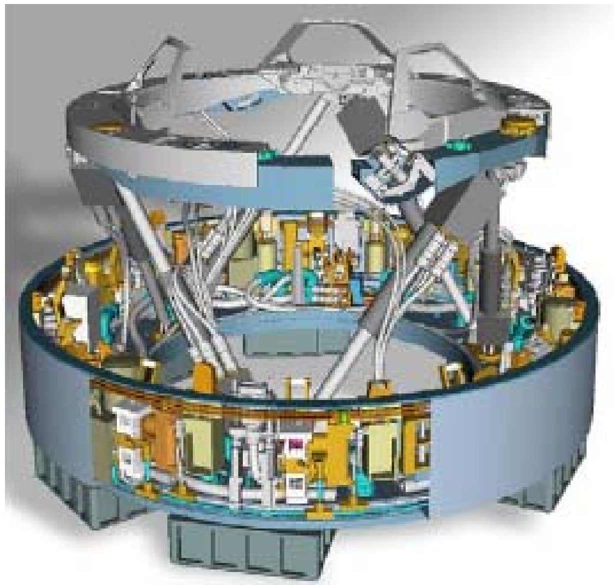

Figure 10.4-2 A Detailed CAD Model of the LIDS Risk Reduction Unit

Docking Mechanism Jettison

The docking system is jettisoned for several reasons, the biggest of which is that in the 16.5 ft configuration it blocks extraction of the parachutes. However, jettison has other benefits as well: it lowers the cg of the CM, it reduces the landing mass of the CM, and it simplifies the thermal protection scheme at the forward end of the CM. Preliminary results indicate that without significant thermal protection, the docking mechanism would be heated beyond its capability during atmospheric entry.

The current baseline for the docking system jettison is a linear shaped charge to sever the structural connection combined with a set of springs to achieve separation velocity between the docking system and CEV. In the case of the LIDS, the electronic boxes are jettisoned along with the mechanism. Currently the spring system utilized 28 total springs to provide 5 ft/s ΔV with force margin meeting the requirements of NASA-STD-5017 (see Figure 10.4-3). The linear shaped charge was chosen as the separation system because of the reduction in critical functions it affords over discrete attachment points and separation systems such as separation nuts.

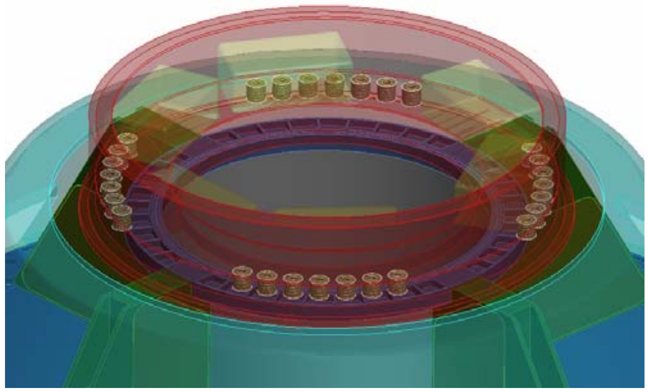

Figure 10.4-3 The Docking Mechanism Separation System

Docking Hatch

The docking hatch design is currently undefined beyond assumption of a LIDS-like or Apollo-like docking hatch. The hatch is required to have a window for viewing of the environment on the other side. It will be covered with TPS on the external surface to protect against entry heating and will feature a removable scuff guard to protect the TPS during crew and cargo translation. This hatch will also serve as a backup path for post-landing crew egress in the event of malfunction of the ingress/egress hatch or blockage due to rollover. A pressurized suited crew member must be able to pass through the hatch.

Ingress/Egress Hatch

The ingress/egress hatch is located on the conical portion of the CM structure. It is an outward-opening trapezoidal hatch of approximately 34 inches tall by 35 inches at the base with a viewing window, similar to the Apollo hatch (Figure 10.4-4). The ingress/egress hatch has stored-gas assisted opening in the event of an emergency situation, and a pyro capability provided by a linear shaped charge in the hatch frame to allow for escape in the event of a latch mechanism failure. This hatch also interfaces with a BPC hatch to allow concurrent access through both the BPC and CM structure. A pressurized suited crew member must be able to pass through the hatch during an EVA. The dimensions of a pressurized suited crew member are not yet known, since the suit requirements and design have not been developed yet.

Figure 10.4-4 The Apollo Command Module Hatch

High Gain Antenna Launch Restraint Release, Deployment, and Gimbaling

The launch restraint release for the high gain antenna is baselined as a paraffin-actuated pin puller, an example of which is shown in Figure 10.4-5, selected for its low-shock characteristics desirable near sensitive electronic equipment where the release is not time-critical. The deployment mechanism is currently baselined as a passive spring-driven, damped hinge with a passive lock for the deployed position. Gimbaling and pointing of the antenna is to be accomplished with a two-axis gimbal and controller, similar to the example depicted in Figure 10.4-6.

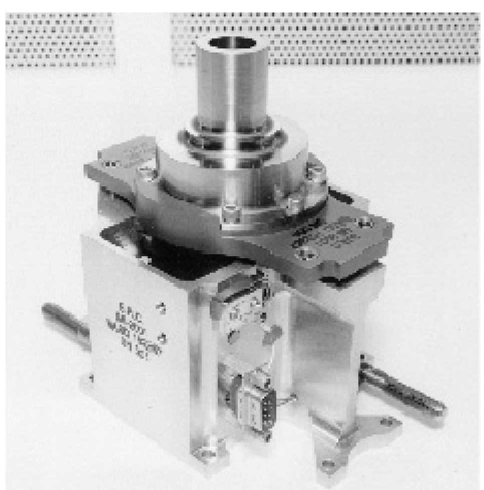

Figure 10.4-5 An Example Paraffin Launch Latch (Starsys Research)

Figure 10.4-6 A Typical 2-Axis Gimbal

Solar Array Stack Launch Restraint Release, Deployment, and Gimbaling

The launch restraint release for the stowed solar array stack is baselined also as a paraffin-actuated pin puller, similar to the device used for the high gain antenna and the example in Figure 10.4-5 above. The deployment mechanism is also similar to that of the high gain antenna, currently baselined as a passive spring-driven, damped hinge with a passive lock for the deployed position. The release of the array panels is accomplished with non-explosive actuation. The solar arrays utilize a single axis SADA for tracking.

LAS-CM Separation

The baseline design for the LAS separation is a four-point interface with the Crew Module longerons and forward bulkhead with redundantly-initiated frangible nuts within a surrounding debris shield. Current implementation has the nut on the LAS side. This option was chosen for its light weight, its simplicity, and its mechanical reliability, though a desire to reduce the quantity of power lines that must cross the CM/LAS interface may result in the frangible nut being retained on the CM.

Heat Shield Separation and CM/SM Separation

As the design currently stands, the CM and SM are connected with eight offset compression pads and tension ties that connect the primary structure of the SM and CM (see Figure 10.4-7). These tension ties pass through the heat shield but are made captive by the heat shield structure. To separate the CM from the SM, redundant linear shaped charges are fired on a flattened section of the tension tie external to the heat shield, leaving a tension tie remnant that extends beyond the heat shield and is still connected to the CM primary structure. After this separation, another set of linear shaped charges separates the tension time remnant from the primary structure, mechanically and thermally isolating the primary structure from the tension tie remnant during entry while keeping the portion of the remnant that does not ablate away during entry captured by the heat shield structure. The heat shield separation is then achieved by a system similar to that used on the Mars Exploration Rovers (MER), shown in Figure 10.4-8. The system consists of eight pyrotechnic separation nuts with mechanical springs for initial separation impulse. This allows the heat shield and tension tie remnants to be carried away by gravity after separation.

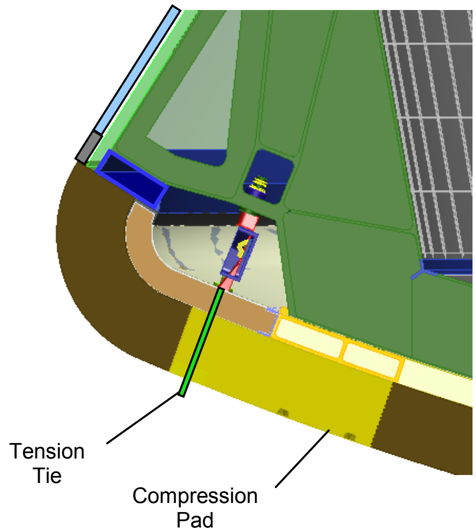

Figure 10.4-7 The CM/SM Separation Interface

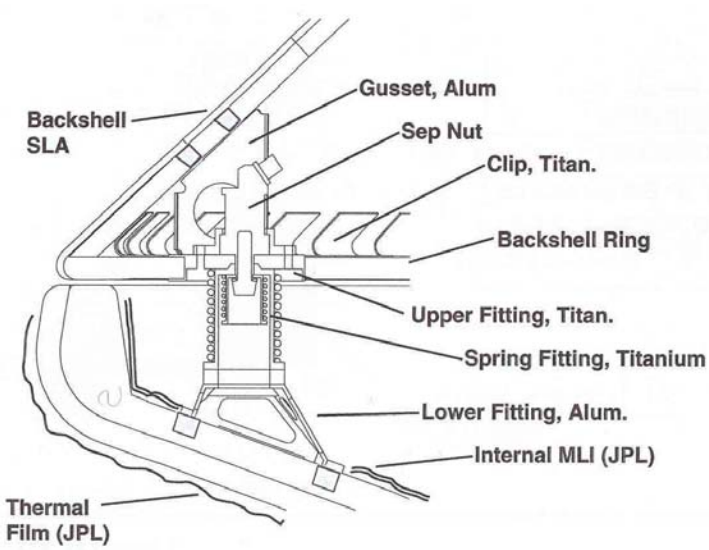

Figure 10.4-8 The MER Heat shield Separation System

SM/SA Separation

The SM/SA separation is achieved with redundant linear shaped charges that run the circumference of the spacecraft adapter. This joint is designed to host as much of the separation system mass possible on the spacecraft adapter. An example architecture is shown in Figure 10.4-9.

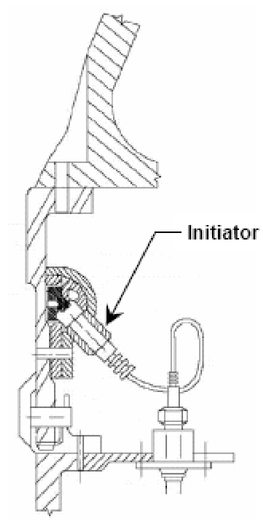

Figure 10.4-9 A Circumferential Linear Shaped Charge Device

Forward Bay Aeroshell Jettison

The forward bay aeroshell jettison system is similar to that used by Apollo. Shear pins restraining mechanical preload springs are severed by pyro-initiated manifolded gas generator. The energy of expanding gas provides initial separation of the aeroshell and a small drogue connected to the aeroshell is released to prevent recontact with the entering CM. Figure 10.4-10 shows the system Apollo used for the forward aeroshell jettison.

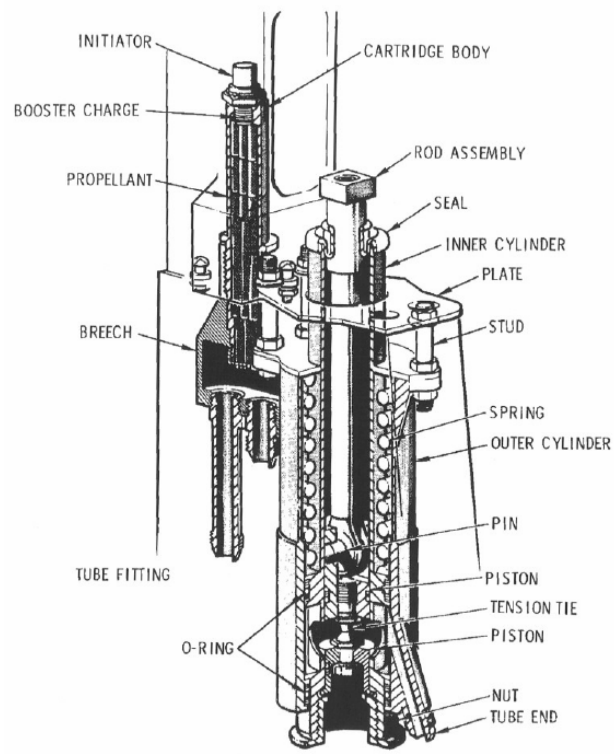

Figure 10.4-10 The Apollo Forward Aeroshell Jettison Mechanism

Crew Seat Attenuation

The crew seat attenuation system is designed to actuate only in failure scenarios where touchdown energies higher than those the CM landing system can fully absorb exist. The crew seats are all mounted to a single seat pallet structure that spans the CM, connected to the primary structure via multiuse attenuators. The baseline attenuators extend upward to a primary structure ringframe in the vehicle X direction, and outward to primary structural members in the Y and Z directions. The residual impact energies and therefore the stroke lengths are based on a retro deceleration system with horizontal rockets that produce 17.2 ft/s and 7 ft/s axial and lateral residual velocities, respectively. Six inches of stroke are required in the +X direction, three inches in the –X direction, and 4 inches in the Y and Z directions to provide g-limits of 24 g in +X and 6 g in –X, ±Y and ±Z. Figure 10.4-11 illustrates the baseline seat attenuation design.

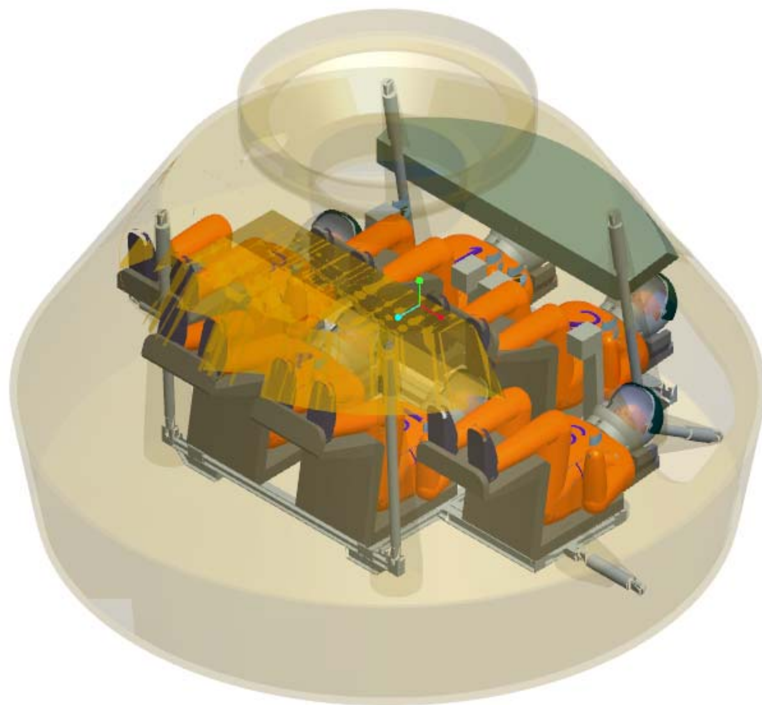

Figure 10.4-11 The Crew Seat Attenuation Layout

<u>*Structural Vents*</u>

There are currently no passive structural vents identified as being required. However, the vestibule pressurization equalization device is currently being bookkept under this category in the mechanisms mass estimate.

<u>*Umbilicals*</u>

The only umbilical currently requiring a mechanism is the CM/SM umbilical. Because it reaches around the shoulder of the CM, a mechanism will be required to rotate the umbilical arm away from the structure. The current concept consists of a passively actuated spring mechanism that rotates the umbilical arm at the base on the SM after the umbilicals are separated.

10.4.3 Mass Estimates and Design Maturity

The mass estimates for the mechanisms subsystems and corresponding bases of estimate are provided in the following tables. Table 10.4-1 provides the Block 1 mass estimate, while Table 10.4-2 provides the Block 2 estimate.

Hardware Items	Quantity	Unit Mass (lbm)	Growth (%)	Total Mass (lbm)	CM Mass (lbm)	SM Mass (lbm)	SA Mass (lbm)	Basis of Estimate
Mechanisms - Block 1				**2,270**	**1,813**	**344**	**113**	
APAS	1		11%	815.7	815.7			APAS IDD
APAS Mechanical Components	1	662	10%					
Avionics Suite	2	35	25%					
Docking Hatch	1		35%	128.4	128.4			LIDS Whitepaper Estimate
Hatch Mounting/Guide Hardw are	1	15	20%					
Hatch	1	80	38%					
Ingress/Egress Hatch	1	230	10%	253.0	253.0			Scaled Apollo Design
Seat Attenuators	1	148	25%	185.0	185.0			Conceptual CAD Model
Seat Frame	1	140	25%	175.0	175.0			Conceptual CAD Model
High Gain Antenna Mechanisms	1		25%	25.0		25.0		Scaled Similar Systems
Launch Restraint Release	1	2	25%					
Deployment Actuation	1	3	25%					
Gimbal + Controller	1	15	25%					
Solar Array Wing Deployment	1		25%	47.5		47.5		Scaled Similar Systems
Launch Restraint Release	2	4	25%					
Gimbal + Controller	2	15	25%					
Solar Array Stack Deployment	1		25%	111.7		111.7		Scaled Similar Systems
Array Stack Restraint/Release	2	14	25%					
Array Deployment Synchronization	2	12	25%					
Sw ival Hinge Mechanism	2	9	25%					
Saddle Capture Mechanism	2	10	25%					
Solar Array Drive Assembly	1		25%	60.7		60.7		Scaled Similar Systems
Gimbal	2	20	25%					
Drive Stepper Motor	2	2	25%					
Electronic Control Unit	2	2	25%					
Heatshield Retention Hardware/Guides	8	4	25%	40.0	40.0			Engineering Estimate
LAS Retention Hardware	4	2	25%	10.0	10.0			Engineering Estimate
CM Tension Ties	8	5	25%	50.0	50.0			Engineering Estimate
CM Compression Pads	8	3	25%	30.0	30.0			Engineering Estimate
SM Compression Pads	8	3	25%	30.0		30.0		Engineering Estimate
SA Separation - SM Retained Hardware	1	30	25%	37.5		37.5		Engineering Estimate
SA Separation - Pyro Line Charge	1	90	25%	112.5			112.5	Engineering Estimate
Passive Vents	3	4	25%	15.0	15.0			Engineering Estimate
CM-SM Umbilical Connectors	1	1	25%	1.3	1.3			Engineering Estimate
SM-CM Umbilicals	1	20	25%	25.0		25.0		Engineering Estimate
CM-LAS Umbilical Connectors	2	0.25	25%	0.6	0.6			Engineering Estimate
SM-Pad Umbilicals	1	5	25%	6.3		6.3		Engineering Estimate
Forward Bay Aeroshell Jettison	1		25%	40.0	40.0			Scaled Apollo Design
Retention Hardw are/Guides	8	3	25%					
Separation Springs	4	2	25%					
APAS Jettison System	1		25%	69.5	69.5			Engineering Estimate
Charge Holder	1	20	25%					
Springs and Housings	1	36	25%					

Table 10.4-1 CEV Block 1 Mechanisms Mass Estimates and Bases of Estimate

Hardware Items	Quantity	Unit Mass (lbm)	Growth (%)	Total Mass (lbm)	CM Mass (lbm)	SM Mass (lbm)	SA Mass (lbm)	Basis of Estimate
Mechanisms - Block 2				**2,226**	**1,770**	**344**	**113**	
Low Impact Docking System	1		18%	900.5	900.5			LIDS Whitepaper
LIDS Mechanical Components	1	600	12%					
LIDS Electronics Boxes	6	12	43%					
LIDS Hatch	1	80	38%					
Hatch Mounting/Guide Hardw are	1	15	20%					
Ingress/Egress Hatch	1	230	10%	253.0	253.0			Scaled Apollo Design
Seat Attenuators	1	148	25%	185.0	185.0			Conceptual CAD Model
Seat Frame	1	140	25%	175.0	175.0			Conceptual CAD Model
High Gain Antenna Mechanisms	1		25%	25.0		25.0		Scaled Similar Systems
Launch Restraint Release	1	2	25%					
Deployment Actuation	1	3	25%					
Gimbal + Controller	1	15	25%					
Solar Array Deployment Mechanisms	1		25%	47.5		47.5		Scaled Similar Systems
Launch Restraint Release	2	4	25%					
Gimbal + Controller	2	15	25%					
Solar Array Stack Deployment	1		25%	111.7		111.7		Scaled Similar Systems
Array Stack Restraint/Release	2	14	25%					
Array Deployment Synchronization	2	12	25%					
Sw ival Hinge Mechanism	2	9	25%					
Saddle Capture Mechanism	2	10	25%					
Solar Array Drive Assembly	1		25%	60.7		60.7		Scaled Similar Systems
Gimbal	2	20	25%					
Drive Stepper Motor	2	2	25%					
Electronic Control Unit	2	2	25%					
Heatshield Retention Hardware/Guides	8	4	25%	40.0	40.0			Engineering Estimate
LAS Retention Hardware	4	2	25%	10.0	10.0			Engineering Estimate
CM Tension Ties	8	5	25%	50.0	50.0			Engineering Estimate
CM Compression Pads	8	3	25%	30.0	30.0			Engineering Estimate
SM Compression Pads	8	3	25%	30.0		30.0		Engineering Estimate
SA Separation - SM Retained Hardware	1	30	25%	37.5		37.5		Engineering Estimate
SA Separation - Pyro Line Charge	1	90	25%	112.5			112.5	Engineering Estimate
Passive Vents	3	4	25%	15.0	15.0			Engineering Estimate
CM-SM Umbilical Connectors	1	1	25%	1.3	1.3			Engineering Estimate
SM-CM Umbilicals	1	20	25%	25.0		25.0		Engineering Estimate
CM-LAS Umbilical Connectors	2	0.25	25%	0.6	0.6			Engineering Estimate
SM-Pad Umbilicals	1	5	25%	6.3		6.3		Engineering Estimate
Forward Bay Aeroshell Jettison	1		25%	40.0	40.0			Scaled Apollo Design
Retention Hardw are/Guides	8	3	25%					
Separation Springs	4	2	25%					
LIDS Jettison System	1		25%	69.5	69.5			Engineering Estimate
Charge Holder	1	20	25%					
Springs and Housings	1	36	25%					

Table 10.4-2 CEV Block 2 Mechanisms Mass Estimates and Bases of Estimate

10.4.4 Plan Forward

Forward work includes:

- Continued docking hatch definition to work out structural interface issues
- Seat attenuation trade to determine mass impact of compression X-direction attenuators

- Continued docking system structural adapter definition to work out differences in mechanism packaging and interface issues with the CM structure and LAS
- Ingress/Egress hatch definition to refine mass estimates
- CM/SM attachment design refinement
- Heat shield separation mechanism design refinement
- Design refinement of other mechanisms

10.5 Pyrotechnics

The pyrotechnics system consists primarily of separation systems, mortars and cutters. A complete list of the pyrotechnic devices in the system is listed in Table 10.5-1. Pyrotechnics offer a light-weight, highly reliable means of generating energy or performing work.

The pyrotechnics system design did not change between CRC-2 and CRC-3.

Application	Device	Location
LAS Umbilical	Gas Generator Panel	LAS
LAS Docking Separation	Cutter/ Mild Detonating Fuse	CM
LAS Motor Initiators	Initiators/S&A Devices	LAS
LAS Umbilical Separation	Gas Generator Panel	LAS/CM
LAS to CM Separation	Mild Detonating Fuse	LAS/CM
Deploy Forward Heat Shield	Thruster	CM
Fwd Heat Shield Mortar	Small Mortar	CM
Deploy Drogue Mortars	Mortars	CM
Deploy Pilot Mortars	Mortars	CM
Drogue/Main Release	Strap Cutters	CM
Reefing Line Release	Reefing Line Cutters	CM
Hatch Release	Mild Detonating Fuse	CM
Heat Shield Jettison	Linear Shaped Charge	CM
Air Bag Initiation	Initiators	CM
Up-righting Bag Gas Gen	Initiators	CM
CLV Adapter Separation	Linear Shaped Charge	SM
CM/SM Umbilical	Gas Generator Panel	CM/SM
SM/CM Separation	Linear Shaped Charge	CM/SM
SM/CM Arm Release	Guillotine Cutter	CM/SM
Crew Personal Pyros	Flares, Seawars, RLC’s	CM

Table 10.5-1 CEV Pyrotechnic Devices

10.5.1 Driving Requirements, Groundrules, and Assumptions

The requirements that drive the pyrotechnics subsystem are the dual fault tolerant requirement, The JSC 62809 Constellation Pyrotechnics Specification and the AFSPCMAN 91-710 Eastern and Western Test Range Safety User Requirements.

The assumptions that were made prior to developing the pyrotechnics subsystem were the following:

- The CEV will use NASA Standard Initiators (NSIs) and NASA Standard Detonators (NSDs) wherever possible to ensure safe reliable initiation and to limit development and qualification costs.
- The firing system architecture will consist of modular capacitive discharge firing cards similar to the Shuttle Pyrotechnics Initiator Controllers (PICs).
- The firing system components shall be considered a part of the electrical power system and the weights and volumes for the firing circuitry and wiring will be listed in the Electrical Power Systems Master Equipment List (MEL).
- Firing leads will be made of twisted shielded pair running to each initiator.
- The power supply for the firing circuitry will require a backup or redundant source for emergency crew return due to an electrical failure.
- The fault tolerance plan is to make the pyrotechnic devices dual fault tolerant to premature firing and single fault tolerant / Design for Minimum Risk (DFMR) for failure to fire. This convention is the same method used on both the Shuttle and Apollo programs.
- Separate Safe and Arm devices are not required for parachute devices.

10.5.2 Conceptual Design Overview

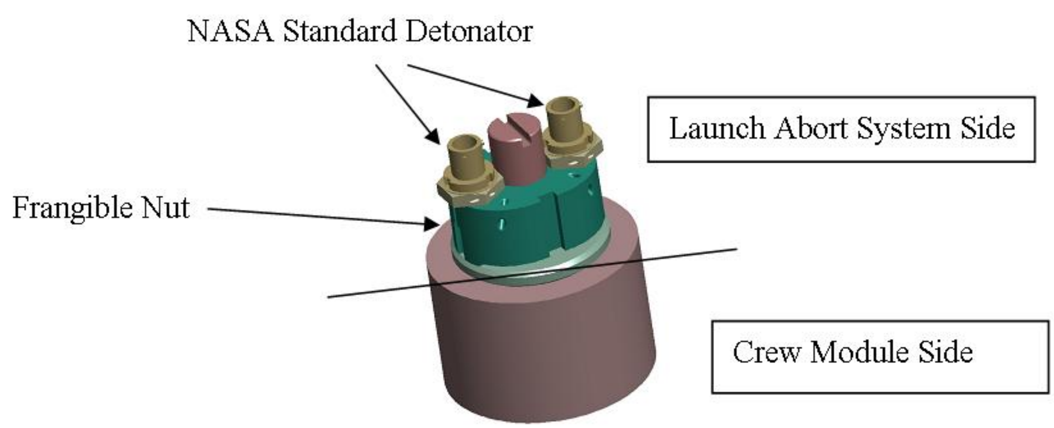

Figure 10.5-1 Launch Abort System Frangible Nut Release

The frangible nut design displayed in Figure 10.5-1 is the design selected to release the LAS from the CM for both nominal and abort scenarios. The LAS is attached to the CM at four attach points and at each of the four attach points is a frangible nut. The bolt and mounting structure both remain with the Crew Module. The frangible nut has two NASA Standard Detonators (NSDs) that are designed to break the nut when the firing pulse is received. The frangible nut is designed with enough margin to break completely and release when only one NSD receives the firing pulse.

The frangible nut was selected for this application based on its simplicity and its proven flight history on NASA programs. The Apollo design for this application was also a frangible nut, and frangible nuts have flown in multiple locations on the Shuttle Orbiter for many years. On the Shuttle frangible nuts attach the SRBs to the launch pad and the external tank to the orbiter.

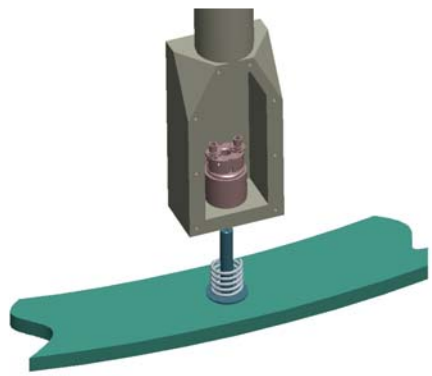

Figure 10.5-2 Launch Abort System Frangible Nut, Released View

The interface between the CM and SM consists of eight compression pads and four tension ties at four of the eight compression pads. The compression pads are integrated into the heat shield on the CM side and are structurally supported on the SM side.

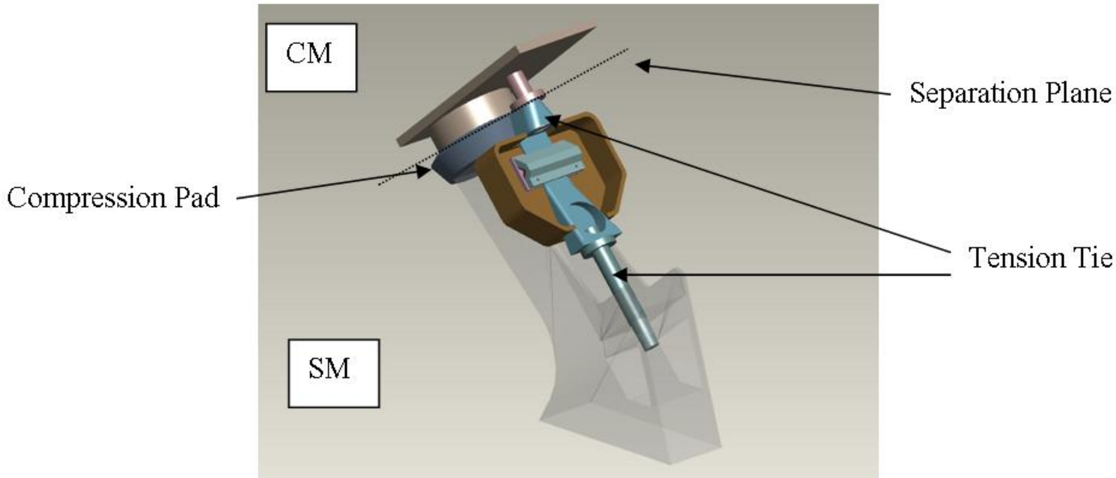

Figure 10.5-3 CM/SM Compression Pad with Tension Tie

Each tension tie has a portion of the tie that flattens out to reduce the thickness of the part for separation. On top of the flattened section a piece of linear shaped charge is placed with a NASA Standard Detonator (NSD) at each end to ensure reliable initiation.

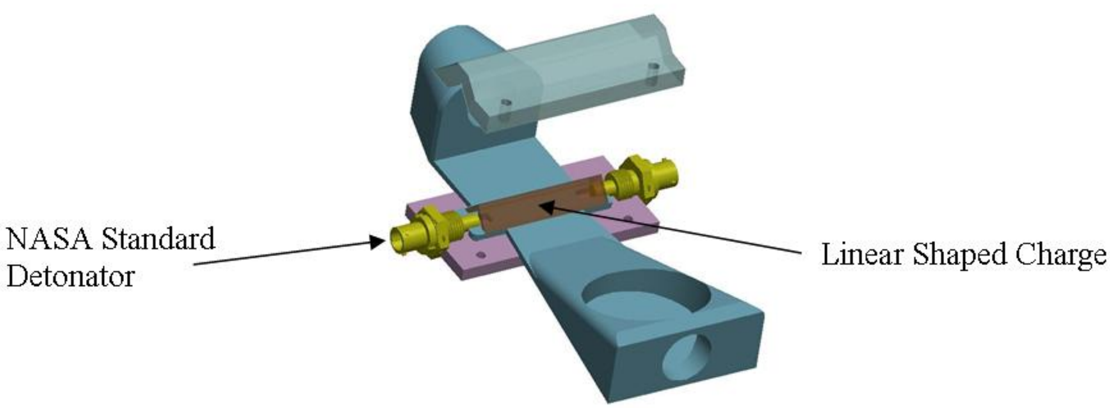

Figure 10.5-4 CM/SM Tension Tie Separation Details

10.5.3 Mass Estimates and Design Maturity

The pyrotechnics subsystem is heavily dependant on the overall design of the vehicle. Changes in structure, landing attenuation methods, and location of components will greatly affect the weight and volume required by the pyrotechnics subsystem. The current estimates for weight and mass are believed to be conservative estimates based on NASA heritage hardware on both the Shuttle and Apollo programs.

Hardware Items	Quantity	Unit Mass (lbm)	Growth (%)	Total Mass (lbm)	CM Mass (lbm)	SM Mass (lbm)	SA Mass (lbm)	Basis of Estimate
Pyrotechnics				**536**	**301**	**149**	**85**	
Forward Heatshield Thrusters	4	6	10%	26.4	26.4			Shuttle MLG Thruster
Pilot Chute Mortars	3	12	10%	40.8	40.8			Shuttle Mortar Estimate
Drogue Mortars	2	22	10%	47.6	47.6			Shuttle Mortar Estimate
Drogue/Main Release	12	4	10%	52.8	52.8			X-38 Strap Cutters
Reefing Line Cutters	20	0	15%	0.9	0.9			Shuttle H5-3.4 Second Delay (RRL)
Side Hatch Emergency Release	1	22	25%	27.5	27.5			2 MDF Cords with Charge holder
Heat shield Jettison	4	10	25%	50.0	50.0			LSC at four attach points
Air Bag Initiation	12	1	25%	18.0	18.0			Engineering Estimate
Uprighting Bag Gas Generators	4	8	25%	37.5	37.5			Engineering Estimate
Spacecraft Adapter Separation - SM Side	2	30	25%	75.0		75.0		Engineering Estimate
Spacecraft Adapter Separation - SA Side	2	34	25%	85.0			85.0	Engineering Estimate
CM/SM Umbilical Cutters	2	11	25%	28.1		28.1		Engineering Estimate
Umbilical Arm Release	1	2	10%	2.2		2.2		Engineering Estimate
SM/CM Separation	4	10	10%	44.0		44.0		Apollo Design

Table 10.5-1 CEV Pyrotechnics Mass Estimates and Bases of Estimate

10.5.4 Plan Forward

Forward work includes a more detailed analysis of the separation methods for the docking mechanism (APAS, LIDS, or both) and how to adequately include this in LAS separation for abort scenarios. The future plans also include a more detailed stress analysis of each part with its predicted loads to ensure the sizing and design assumptions are correct.

10.6 Parachute System

The CEV parachute system consists of the drogue and main parachutes needed to slow the Crew Module during Earth entry, descent, and landing from a terminal velocity of several hundred miles per hour to a safe operational speed for the landing system. The parachute system configuration defined for CRC-2 is a scaled-up version of the Apollo parachutes where two parallel, mortar-deployed drogue parachutes are simultaneously deployed to stabilize and slow the vehicle, followed by three mortar-deployed pilot parachutes that extract the main parachutes once the drogues have been released. An alternate parachute architecture has also been sized in this design cycle and is included for comparison – one in which two serial, mortar-deployed drogue parachutes (one primary, one backup) directly deploy four main parachutes.

The parachute system also consists of a small, mortar-deployed drag parachute mounted on the forward heat shield. When the forward heat shield is jettisoned prior to drogue deployment, this parachute helps to drag the heat shield out of the wake created by the descending CM and prevent the heat shield from recontacting the vehicle. Parachute system mortars, strap cutters, and reefing line cutters are bookkept with the CEV pyrotechnics system.

There were no designs changes made to the parachute system between CRC-2 and CRC-3.

10.6.1 Driving Requirements, Groundrules, and Assumptions

The key driving requirements for the parachute system are listed in Table 10.6-1.

Document	Req. #	Requirement	Rationale/Comments
SRD	CV0044	The CEV shall provide for pad abort.	This requirement meets the intent of paragraphs 3.9.3 (Requirements 34471) of NPR 8705.2. Catastrophic failures could occur on the launch pad. In addition to pad emergency egress, the CEV must also provide pad abort to ensure crew survival from pad failure scenarios, in which there is not enough time for the crew to get out of the vehicle and off the launch pad.
SRD	CV0088	The CEV shall perform land landing.	Land landing to a designated site or zone is preferred since it generally offers easier crew pickup and spacecraft recovery. The environment for land landing is typically less hazardous than ocean landing and crew survival probability is higher, particularly for the case of abort or early return landings when rescue forces may not be pre-positioned.
SRD	CV0089	The CEV shall perform water landings in the event return to land is not possible.	Land landing to a designated site or zone is preferred since it generally offers easier crew pickup and spacecraft recovery. The environment for land landing is typically less hazardous than ocean landing and crew survival probability is higher, particularly for the case of abort or early return landings when rescue forces may not be pre-positioned. Water landing is required to achieve 100% ascent abort coverage. Sufficient clearance between the water line and the bottom of the vehicle hatch should prevent flooding should the crew need to open the hatch before rescue personnel could reach the vehicle to stabilize it.
SRD	CV0092	The CEV shall perform nominal and abort landing independent of ambient lighting conditions.	Landing site lighting will be governed by earth-moon-sun geometry resulting in earth landings which may occur in darkness as well as daylight. Lighting for an ascent abort landing is determined by the liftoff time. Restricting launches to only times that allow for lighted abort landings would severely constrain mission planning. Early return cases are generally time critical and should also not be constrained by daylight landing requirements.

Document	Req. #	Requirement	Rationale/Comments
SRD DSNE	CV0220 Sect 3.5	The CEV shall meet all functional and performance requirements for nominal landing in the environment conditions as defined in the CXP-00102, Constellation Program Design Specification for Natural Environments (DSNE), Section 3.5.	The CEV must be able to operate in the natural environments that it will be exposed to during normal landing operations.
SRD DSNE	CV0228 Sect 3.6	The CEV shall meet its functional and performance requirements for abort landing during and after exposure to the environment conditions as defined in the CXP-00102, Constellation Program Design Specification for Natural Environments (DSNE), Section 3.6.	The CEV must be able to operate and land in the natural environments that it will be exposed to during a mission abort.

Table 10.6-1 Parachute System Driving Requirements

The following assumptions were made for parachute system sizing. All assumptions were made for a nominal entry case.

- The Crew Module suspended mass for the drogue parachutes is 15,850 lbm.
- Drogue parachute(s) are deployed at a maximum dynamic pressure of 113 psf.
- Main parachutes deployment is initiated at 8,000 ft mean sea level (MSL) and a dynamic pressure of 30 psf.
- The main parachutes slow the Crew Module to a sink rate of 24.2 ft/s with all parachutes fully deployed, and 29.0 ft/s with one failed parachute.
- Nominal land landing occurs at 4,000 ft MSL and main parachutes full open no less than 1,000 ft AGL.
- The base heat shield is jettisoned after the main parachutes have fully opened and has an assumed mass of 2,600 lbm.

10.6.2 Conceptual Design Overview

10.6.2.1 Baseline Architecture (Scaled-Up Apollo)

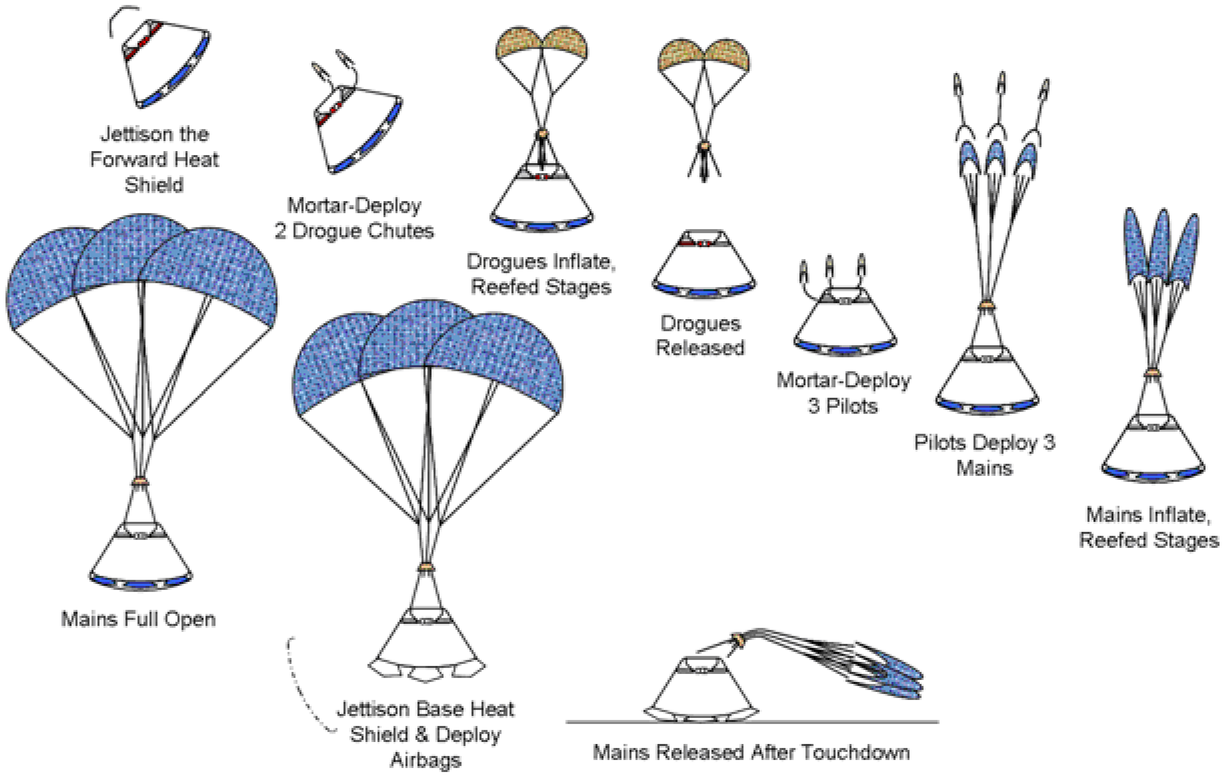

Figure 10.6-1 Parachute System Sequence of Events

The nominal sequence of events for the CRC-2 parachute system is illustrated in Figure 10.6-1. Two parallel, mortar-deployed drogue parachutes are simultaneously deployed to stabilize and slow the vehicle, followed by three mortar-deployed pilot parachutes that extract the main parachutes once the drogues have been released. Under nominal conditions, the CM lands with a vertical sink rate of 24.2 ft/s.

There are two 22.8-ft diameter circular drogue parachutes in the parachute system. Each drogue parachute consists of a deployment bag, a 408 ft^2 canopy, seventy-two 27-ft suspension lines, and a 71-ft riser line. Attachment of the riser lines to the vehicle is accomplished with a "flower-pot"-like structure similar to the system used on the Block II Apollo Command Module. The drogue has a mass of 55 lbm without mass growth allowance and is packed with to an average density of 35 lbm/ft^3. The packed drogue parachutes are installed in pyrotechnic mortars in the Crew Module forward compartment. The mortar system mass is carried in pyrotechnics.

The main parachute system includes three 98-ft diameter circular ring sail parachutes. Unlike the mortar-deployed drogues, each main parachute is deployed by a separate mortar-deployed pilot parachute. Pilot parachutes are deployed following release of the drogues at approximately 11,000 ft MSL and the pilots pull the three main parachute assemblies away from the CM. The main parachutes are extracted from their deployment bags, are inflated, and then disreefed in multiple stages until reaching their fully-open state. Once fully open, the base heat shield is jettisoned and the landing airbags are inflated. After landing, the main parachutes are manually released.

Each main parachute assembly includes a deployment bag, bridle line, canopy, suspension lines, and riser line packed with a pack density of 35 lbm/ft^3 (Apollo main chute packs were 43 lbm/ft^3). The main parachute riser lines are connected to the CM primary structure via four harness lines which rise above the CM and meet the three riser lines at a seven-point confluence fitting. The entire main parachute system has a mass of 525 lbm and the pilot parachutes are 22 lbm each with the mass of the mortars included in pyrotechnics.

10.6.2.2 Alternate Architecture

An alternate parachute system architecture is described in Figure 10.6-2. In this approach, a single primary drogue parachute is deployed with a spare drogue nominally left undeployed. If the primary drogue fails, it is released and the backup drogue is mortar-deployed. This architecture also differs from the baseline in the technique used for main parachute deployment. Whereas the scaled-up Apollo architecture deployed the mains with pilot parachutes, this system uses the drogue to deploy directly the mains as it is released. Finally, this architecture assumes four slightly smaller 85-ft main parachutes rather than three 98-ft mains in the baseline.

Both parachute architectures considered in DAC-2 have advantages and disadvantages that will be weighed in future design cycles.

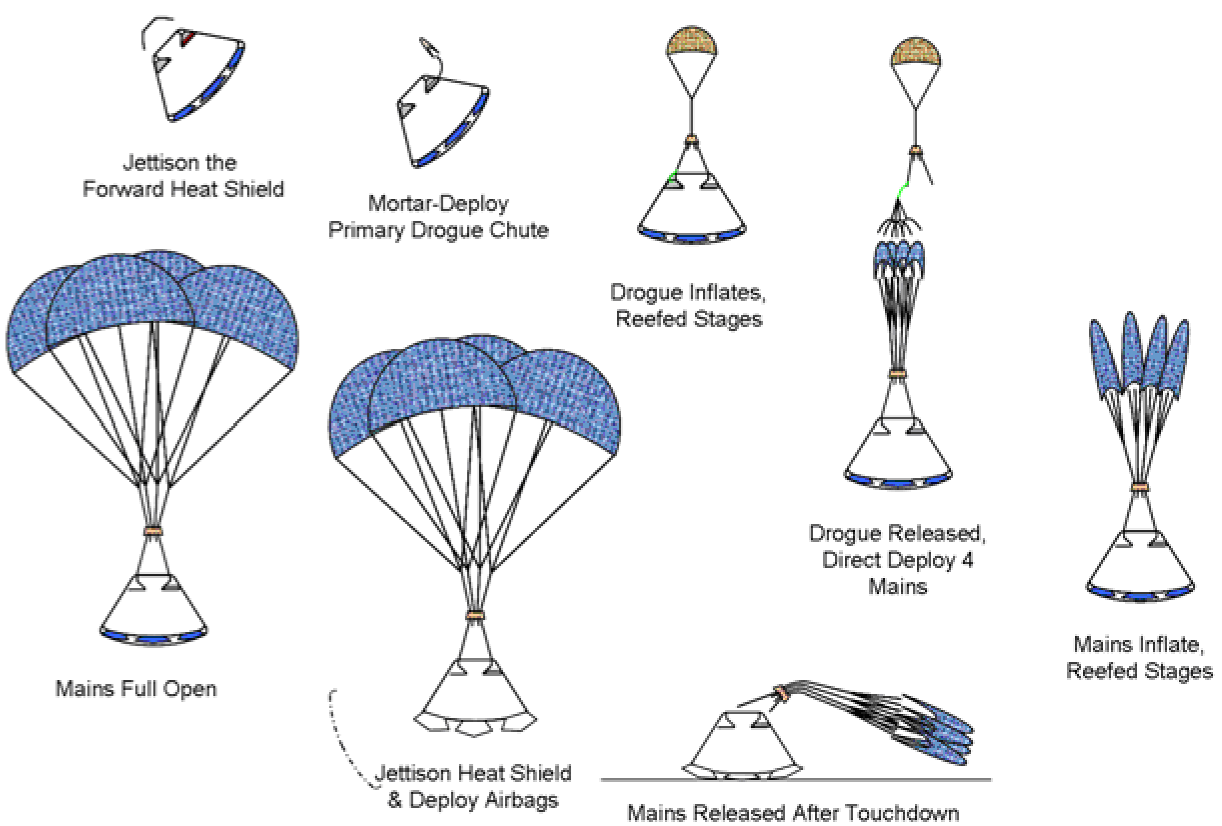

Figure 10.6-2 Alternate Parachute Architecture Sequence of Events

10.6.3 Mass Estimates and Design Maturity

The CRC-2 parachute system masses and bases of estimate are shown in Table 10.6-2. Masses for the alternate parachute architecture are given in Table 10.6-3 for comparison.

Hardware Items	Quantity	Unit Mass (lbm)	Growth (%)	Total Mass (lbm)	CM Mass (lbm)	SM Mass (lbm)	Basis of Estimate
Parachute System				**846**	**846**	**0**	
Drogue Parachutes*	1		17%	129.5	129.5		
Canopy	2	16	17%				
Suspension Lines	1	10	17%				
Riser Line	2	32	17%				
Deployment Bag	2	2	17%				
Main Parachutes	1		17%	614.1	614.1		
Canopy	3	46	17%				
Suspension Lines	1	176	17%				
Riser Line	3	17	17%				
Harness Line	4	25	17%				
Deployment Bag	3	9	17%				
Confluence Fitting	1	31	17%				
Pilot Parachutes*	3	22	17%	77.2	77.2		
Forward Heat Shield Parachute	1	20	25%	25.0	25.0		

** Drogue and Pilot Mortar Mass Included in Pyrotechnics System*

Table 10.6-2 CRC-2 Parachute System Masses and Bases of Estimate

Hardware Items	Quantity	Unit Mass (lbm)	Growth (%)	Total Mass (lbm)	CM Mass (lbm)	SM Mass (lbm)	Basis of Estimate
Parachute System				**925**	**925**	**0**	
Drogue Parachutes	1		17%	191.1	191.1		
Canopy	2	16	17%				
Suspension Lines	1	10	17%				
Riser Line	2	32	17%				
Harness Line	1	44	17%				
Deployment Bag	2	1	17%				
Confluence Fitting	2	5	17%				
Main Parachutes	1		17%	708.7	708.7		
Canopy	4	34	17%				
Suspension Lines	1	174	17%				
Riser Line	4	35	17%				
Harness Line	4	22	17%				
Deployment Bag	4	9	17%				
Confluence Fitting	1	31	17%				
Forward Heat Shield Parachute	1	20	25%	25.0	25.0		

Table 10.6-3 Mass of Alternate Architecture

10.6.4 Plan Forward

The following list of forward work items represents planned tasks during the next design phase of the parachute system:

- Continue analysis of nominal entry and pad/ascent abort parachute system performance.
- Continue trade of baseline (scaled-up Apollo) and alternate parachute system architectures.
- Select a parachute system vender (CEV parachutes are government-furnished equipment).
- Choose a parachute architecture that best suits the CEV requirements including how the parachute system interacts with the landing system design.
- Work with the CEV prime contractor to integrate the chosen parachute architecture.

10.7 Landing System

This section describes the landing system (LS) of the CEV Crew Module reference configuration design. The main function of the landing system is to provide attenuation of the residual energy in the CM during the landing sequence resulting from the vertical and horizontal landing velocities imposed by the CM parachute system.

10.7.1 Driving Requirements, Groundrules, and Assumptions

The key driving requirements for the landing system are listed in Table 10.7-1.

Document	Req. #	Requirement	Rationale/Comments
SRD	CV0044	The CEV shall provide for pad abort.	This requirement meets the intent of paragraphs 3.9.3 (Requirements 34471) of NPR 8705.2. Catastrophic failures could occur on the launch pad. In addition to pad emergency egress, the CEV must also provide pad abort to ensure crew survival from pad failure scenarios, in which there is not enough time for the crew to get out of the vehicle and off the launch pad.
SRD	CV0088	The CEV shall perform land landing.	Land landing to a designated site or zone is preferred since it generally offers easier crew pickup and spacecraft recovery. The environment for land landing is typically less hazardous than ocean landing and crew survival probability is higher, particularly for the case of abort or early return landings when rescue forces may not be pre-positioned.

Document	Req. #	Requirement	Rationale/Comments
SRD	CV0089	The CEV shall perform water landings in the event return to land is not possible.	Land landing to a designated site or zone is preferred since it generally offers easier crew pickup and spacecraft recovery. The environment for land landing is typically less hazardous than ocean landing and crew survival probability is higher, particularly for the case of abort or early return landings when rescue forces may not be pre-positioned. Water landing is required to achieve 100% ascent abort coverage. Sufficient clearance between the water line and the bottom of the vehicle hatch should prevent flooding should the crew need to open the hatch before rescue personnel could reach the vehicle to stabilize it.
SRD	CV0092	The CEV shall perform nominal and abort landing independent of ambient lighting conditions.	Landing site lighting will be governed by earth-moon-sun geometry resulting in earth landings which may occur in darkness as well as daylight. Lighting for an ascent abort landing is determined by the liftoff time. Restricting launches to only times that allow for lighted abort landings would severely constrain mission planning. Early return cases are generally time critical and should also not be constrained by daylight landing requirements.
SRD DSNE	CV0220 Sect 3.5	The CEV shall meet all functional and performance requirements for nominal landing in the environment conditions as defined in the CXP-00102, Constellation Program Design Specification for Natural Environments (DSNE), Section 3.5.	The CEV must be able to operate in the natural environments that it will be exposed to during normal landing operations.
SRD DSNE	CV0228 Sect 3.6	The CEV shall meet its functional and performance requirements for abort landing during and after exposure to the environment conditions as defined in the CXP-00102, Constellation Program Design Specification for Natural Environments (DSNE), Section 3.6.	The CEV must be able to operate and land in the natural environments that it will be exposed to during a mission abort.
HSIR	HS3059	The vehicle shall limit the rate of change of acceleration to 500 g/s.	Acceleration onset rates greater than 500 g/s significantly increase the risk of crew incapacitation, thereby threatening crew survival.

Document	Req. #	Requirement	Rationale/Comments
HSIR	HS3060	The vehicle shall not subject crew-members to accelerations greater than those depicted by the dotted (green) lines in Figures 3.2.4-1 through 3.2.4-5 during nominal entry.	The dotted (green) lines in Figures 3.2.4-1 through 3.2.4-5 represent the maximum level of sustained acceleration allowed on a crewmember after being in a continuous microgravity environment for greater than 30 days. These crew-members could have degraded capabilities because of the pathophysiology of being deconditioned and therefore should not be exposed to higher acceleration limits depicted in the charts. This could significantly affect human performance and safety.
HSIR	HS3064	The vehicle shall limit the injury risk criterion, β, to 1.0: $$\beta=\sqrt{\left(\frac{DR_x(t)}{DR_x^{\lim}}\right)^2+\left(\frac{DR_y(t)}{DR_y^{\lim}}\right)^2+\left(\frac{DR_z(t)}{DR_z^{\lim}}\right)^2}$$ where DR(t)'s are calculated using the Brinkley Dynamic Response model from AGARD-CP-472 "Development of Acceleration Exposure Limits for Advanced Escape Systems", where, under nominal conditions, limits, DRlim, are those given in the "Very low" row of Table 3.2.4-1, and where, under off-nominal conditions, limits are those given in the "Low" row of Table 3.2.4-1 for transient accelerations during parachute deployment and landing touchdown on land or water.	Utilizing the above Dynamic Response Model limits for parachute deployment and landing impacts provides the proper margins of safety (a risk of sustaining a serious or incapacitating injury of no greater than 0.5%) for a healthy deconditioned and/or an Ill/Injured crewmember. The Dynamic Response Model will provide a medical risk assessment in the event of either a CEV nominal and off-nominal failure or multiple failures. The desired Dynamic Response limits are very low (less than 0.5%) for all cases. Multiple off-nominal failures could impart risks in the medium risk and high risk categories (5% and 50% risk of sustaining a serious or incapacitating injury). These limit values are based on data from experiments in which the seat occupant was restrained to the seat and seat back by a lap belt, shoulder straps, and a strap or straps to prevent submarining of the pelvis. The restraint system was adequately pre-tensioned to eliminate slack. The +z axis limits assume that the seat cushion materials do not amplify the acceleration transmitted to the seat occupant. The +x axis limits presume that the seat occupant's head is protected by a flight helmet with a liner adequate to pass the test requirements of ANSI Z-90 (latest edition) or equivalent. These requirements assume that the crew will be similarly restrained during all events that might require application of the Brinkley model. Examples of off-nominal conditions are (i) a landing with one parachute failed, and (ii) a landing with a component failure in the landing system.
HSIR	HS3065	The vehicle shall limit rotational accelerations to 115 degrees/s^2.	Crewmembers are not expected to be able to tolerate rotational accelerations in excess of 115 degrees/s^2 without significant discomfort and disorientation.

Document	Req. #	Requirement	Rationale/Comments
HSIR	HS3066	The vehicle shall not subject crew-members to a yaw rate that produces centripetal accelerations resulting in a violation of the linear acceleration limits depicted by the dotted (green) line in Figure 3.2.4-1 to Figure 3.2.4-5 during nominal entry.	Yaw rate is rotation about the body's z-axis, as shown in Figure C-2. The maximum yaw rate a body can withstand is very high, and the limiting factor is the centripetal forces induced by the yaw rate based on crew position and orientation relative to the spin axis. The dotted (green) lines in Figures 3.2.4.1-1 through 3.2.4.1-5 represent the maximum level of sustained accelerations allowed on a crewmember after being in a continuous microgravity environment for greater than 30 days. These crewmembers could have degraded capabilities because of the pathophysiology of being deconditioned and therefore should not be exposed to higher acceleration limits depicted in the charts. This could significantly affect human performance and safety.
HSIR	HS3069	The vehicle shall not subject crew-members to pitch or roll rates greater than those depicted by the dotted (green) line in Figure 3.2.4-6 during nominal entry.	Pitch and roll rates are rotations about the body's y- and x-axes respectively, as shown in Figure C-2. Deconditioned, ill, or injured crewmembers are not expected to be able to tolerate sustained spin rates in excess of 5 to 8 RPM for extended periods of time. In addition, crewmembers outside the spin axis may experience large undesirable centripetal forces in several vectors dependent upon the spin rate, orientation, and distance from the axis of rotation. Therefore crewmembers should not be exposed to higher rotational limits depicted in the chart. This could significantly affect human performance on entry and landing.
-	-	Landing System retro rockets shall be capable of installation after the CM has been integrated with the SM and SA.	The installation of retro rockets into the CM is limited by the facility due to explosive safety requirements. Therefore, the retro rockets need to be installable after the CM has been integrated with the SM.

Table 10.7-1 LS Driving Requirements

Due to its dependence on the vehicle configuration and layout, a number of assumptions must be made in order to provide preliminary landing system results for the program to use. Table 10.7-2, LS Assumptions, lists the major assumptions made for the current study.

Variable	Baseline Landing Conditions	Comments
CEV Landed Mass	12,004 lbm	From DAC-2 Initial Mass Targets
Acceptable Decelerations	Brinkley Dynamic Response Model & Injury Charts	From HSIR
Landing System Mass Budget	458 lbm	From DAC-2 Summary
Landing System Volume	Based on DAC-2 CAD models	From DAC-2
Initial Vertical Velocity	25 ft/s +/- 3 ft/s	From Parachute System group
Vertical Landing Velocity	5 ft/s +3/-5 ft/s	Following vertical propulsive pulse
Initial Horizontal Velocity	58 ft/s	From DSNE
Horizontal Landing Velocity	15 ft/s +5/-15 ft/s	Following horizontal propulsive pulse
Crew Module Pitch Attitude	-10° to +10° (Negative angle is pitch down or "toe-in," Positive angle is pitch up or "heel-in")	From Apollo historical data
Crew Module Yaw Attitude	-10° to +10°	From Apollo historical data
Landing Surface Slope Angle	0° to 5° (At any orientation with respect to the horizontal velocity vector)	From DSNE

Table 10.7-2 LS Assumptions

10.7.2 Conceptual Design Overview

10.7.2.1 Landing System Layout

The CEV CM landing system consists of the following subsystems:

- Vertically-oriented propulsive units.
- Horizontally-oriented propulsive units.
- Passive crushable honeycomb structure.

10.7.2.2 Vertically-Oriented propulsive units

The vertical propulsive units of the CM landing system are used to reduce the vertical landing speed of the CM from the nominal value of 25 ft/s under a fully deployed parachute system to 5 ft/s + 3/- 5 ft/s. This subsystem consists of four fixed-thrust solid motor assemblies mounted in the "shoulder" region of the CM (see Figure 10.7-1). Each motor assembly has a nominal thrust of 6970 lbf. The mounting configuration consists of two groups of two motor assemblies (one group is shown in Figure 10.7-1). This grouping allows the adverse roll that would result from a failed motor assembly to be predominately in the yaw direction where it is less detrimental to the CM landing stability.

The operational sequence for the vertical propulsive units is envisioned as follows:

- CM stable under the parachute system.
- The CM heat shield is jettisoned.

- Ground sensing begins with a high-resolution altimeter.
- All vertical propulsive units (four) are fired at an altitude calculated to bring the vertical landing speed of the CM within the requirements stated in Table 10.7-2.

The future work includes determination of an altimeter system with a suitable ground resolution. The assumption is that this altimeter system would be charged against the GN&C budget and is not reflected in the landing system master equipment list.

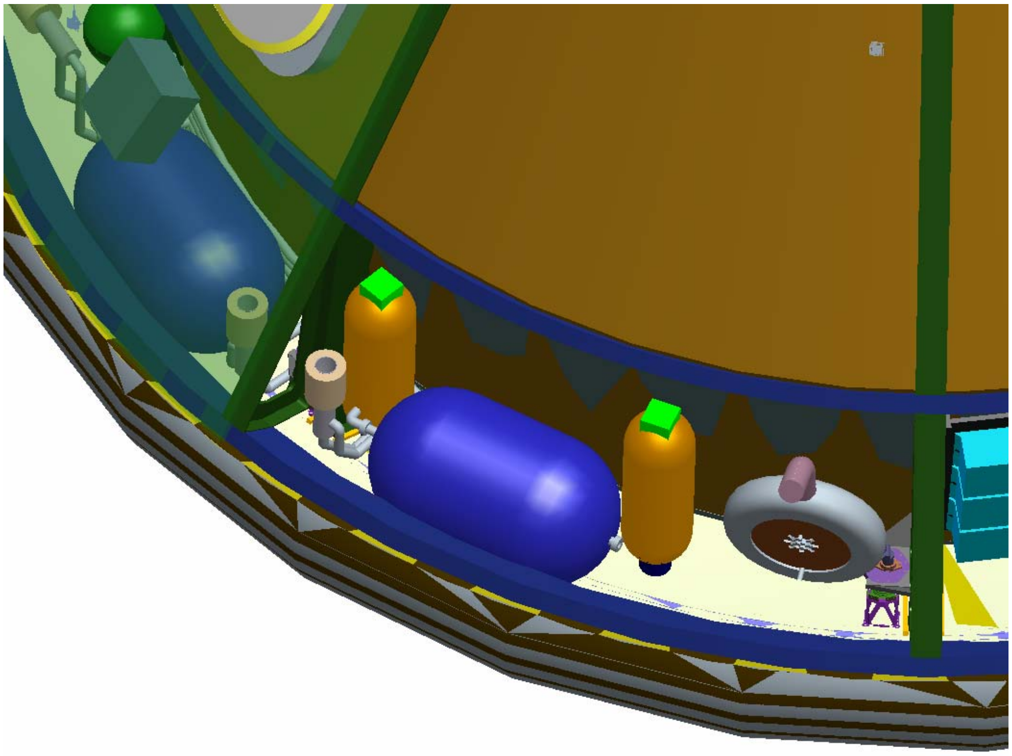

Figure 10.7-1 Vertical Propulsive Units (2 shown, 2 opposite side)

10.7.2.3 Horizontally-Oriented Propulsive Units

The horizontal propulsive units of the CM landing system are used to reduce the horizontal landing speed of the CM from the nominal value of 58 ft/s during maximum wind conditions to 15 ft/s + 5/- 15 ft/s. This subsystem consists of four fixed-thrust solid motor assemblies mounted in the "shoulder" region of the CM (see Figure 10.7-2). Each motor assembly has a nominal thrust of 9400 lbf. The mounting of these motor assemblies are more challenging since they are grouped together at one CM rib assembly.

The operational sequence for the horizontal propulsive units is envisioned as follows:

- CM stable under the parachute system.
- The CM heat shield is jettisoned.

- Horizontal ground speed is determined from the CM GN&C systems.
- The required number of horizontal propulsive units (0, 1, 2, 3 or 4) is fired that are calculated to bring the horizontal landing speed of the CM within the requirements stated in Table 10.7-2.

The thrust vectors of the horizontal propulsive units pass through the CM center-of-gravity and are required to be fired along the CM horizontal velocity vector. The current landing system configuration assumes the CM RCS will be active until the end of the landing sequence and would be used for directional control of the horizontal propulsive units. The future work includes a determination of the additional RCS consumables required for the landing system, but are not currently reflected in the master equipment list.

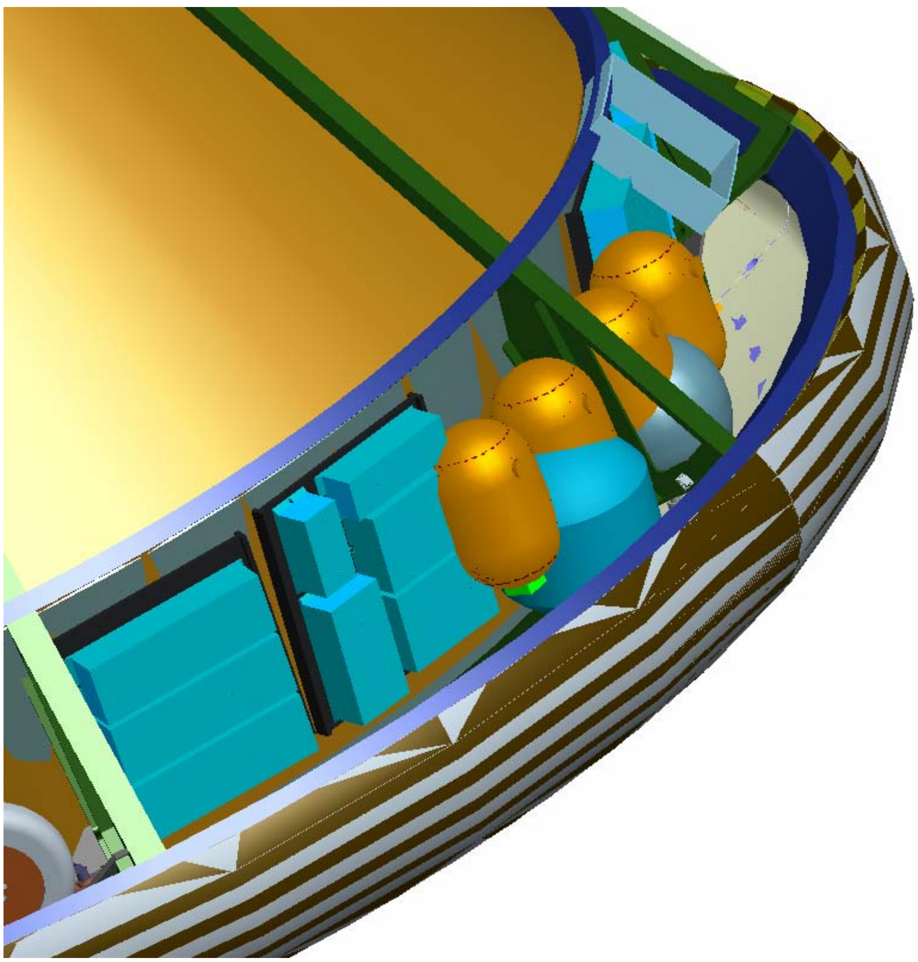

Figure 10.7-2 Horizontal Propulsive Units

10.7.2.4 Passive Crushable Honeycomb Structure

A passive crushable honeycomb structure is mounted to the outer mold line of the CM pressure vessel and is used to attenuate the residual vertical landing speed during the landing sequence. It consists of a 4-inch thick honeycomb layer covering the entire lower surface of the CM pressure vessel. It will perform its attenuation functions following heat shield jettison and is calculated to attenuate a vertical landing speed of approximately 9 ft/s while maintaining the 8-g CM structural limit.

10.7.2.5 Analysis Results

LS-DYNA results indicate that stable landings occur (no overturning) at the requirement ranges shown in Table 10.7-2. These analyses were conducted using a soil model developed by the Landing System ADP from on-site surveys of the candidate landing sites at Edwards AFB and NAS Fallon.

10.7.3 Mass Estimates and Design Maturity

The landing system CRC-3 master equipment list (MEL) is shown in Table 10.7-3.

Hardware Items	Quantity	Unit Mass (lbm)	Growth (%)	Total Mass (lbm)	CM Mass (lbm)	SM Mass (lbm)	Basis of Estimate
Landing System				**445**	**445**	**0**	
Vertical Propulsive Subsystem	1		16%	155.6	155.6		
SRM Propellant	4	14	10%				Pro/E Model
SRM Burnout	4	9	20%				Pro/E Model
SRM Safe & Arm Box	12	2	20%				Vendor Specifications
SRM Cable/Wiring	4	1	20%				Estimate
SRM Structure	4	6	20%				Pro/E Model
Horizontal Propulsive Subsystem	1		15%	188.7	188.7		
SRM Propellant	4	19	10%				Pro/E Model
SRM Burnout	4	10	20%				Pro/E Model
SRM Safe & Arm Box	12	2	20%				Vendor Specifications
SRM Cable/Wiring	4	1	20%				Estimate
SRM Structure	4	7	20%				Pro/E Model
Miscellaneous Propulsive Subsystems	1		3%	100.9	100.9		
Crushable Honeycomb Attenuation	1	84	0%				Pro/E Model
Ordnance Controller/Driver Box	3	4	20%				Vendor Specifications
Ordnance Box Cable/Wiring	3	0	20%				Estimate
Ordnance Box Structure	3	1	20%				Estimate

Table 10.7-3 Landing System CRC-3 Master Equipment List

10.7.4 Plan Forward

The following list of forward work items represents planned tasks during the next design phase of the landing system:

- Update landing system models to latest CM layout configurations:
  - Elimination of subsystem interferences.

- Meet with other subsystem personnel to better define component architecture including:
    - Attachment methods to CM support structure.
    - Protection panels for subsystems in CM "shoulder" region.
    - Integration of the landing system/TPS/parachute system into a more unified design.
- Run analyses using LS-DYNA software:
    - Landing sequence following landing system propulsive burns.
    - Monte Carlo simulations to capture 3-sigma variations.
- Results from the above analyses will be used to:
    - Refine propulsive unit sizes.
    - Refine CM RCS usage during the landing sequence.
- Investigate alternate landing system propulsive configurations:
    - Variable thrust motor assemblies.
    - Retained heatshield with blowout plugs.
    - Propulsive system at the parachute confluence.
- Investigate altimeter designs for inclusion in the landing system.

11.0 Propulsion

This section describes the trades, reference concepts, mass estimates, and analyses performed during CRC-3 as part of the Propulsion functional area. Propulsion for the purposes of the CEV Reference Configuration study includes the Crew Module Reaction Control System and Service Module Propulsion System.

11.1 Crew Module Reaction Control System

The Crew Module (CM) Reaction Control System (RCS) consists of the necessary tanks, valves, regulators, thrusters, tubing, sensors for RCS health monitoring, and fluids to perform the maneuvers and attitude control as required by the Guidance, Navigation, and Control (GN&C) after Service Module (SM) separation and entry, through parachute deploy.

11.1.1 Driving Requirements, Groundrules, and Assumptions

These are the requirements as outlined in the Constellation Architecture Requirements Document (CARD) and CEV Systems Requirement Document (SRD).

CARD

For atmospheric entry, the Constellation Architecture shall provide a backup mode to a guided entry. [CA0313-PO]

Constellation Architecture flight elements shall be capable of remaining at the launch pad for up to 70 days (TBR-001-023) after the initially scheduled launch date without the need for vehicle destack or return of the vehicle to the vehicle integration facility. [CA0408-PO]

The CEV shall limit turnaround ground processing to less than 45 workdays. (TBR-002-151). [CV0023]

SRD

3.2.2.7.1 Earth Entry Attitude

The CEV shall establish and then passively maintain, within the sensible atmosphere, an entry attitude aligning the CEV windward TPS with the Earth entry velocity vector. [CV0082]

3.2.2.7.2 Earth Entry Trajectory Options

The CEV shall be designed to execute both direct entry and skip entry trajectories. [CV0083]

3.2.2.8.2 Emergency Entry Mode without Primary Systems

The CEV shall provide emergency entry mode, terminal descent and landing without the use of primary systems for either power or attitude control. [CV0087]

3.3.1.4 Composite Overwrapped Pressure Vessels

The CEV composite overwrapped pressure vessels shall comply with ANSI/AIAA S-081-2000, Space Systems – Composite Overwrapped Pressure Vessels (COPVs). [CV0257]

3.3.7.3 Two Fault Tolerance for Catastrophic Hazards

The CEV shall be two-fault tolerant for catastrophic hazards, except for areas approved to use Design for Minimum Risk Criteria. [CV0271]

3.3.7.4 Fault Tolerant Restrictions

The CEV shall not use emergency systems or emergency operations, to satisfy the fault tolerance requirements. [CV0272]

3.3.7.13 Ground Recovery Environment

The CEV shall be recoverable by ground personnel without inducing hazardous work environments to the ground crew. [CV0282]

3.3.8.4.7 Acoustic Noise

The CEV shall limit noise levels within the habitable volume in accordance with CXP01000, Human Systems Integration Requirements (HSIR), Section 3.6. [CV0295]

In addition to the items outlined above, the system design was driven to the following parameters: ΔV of 164 ft/s, vehicle mass at start of descent of 16,354 lbm, and a thrust level per thruster of 160 lbf.

11.1.2 Conceptual Design Overview

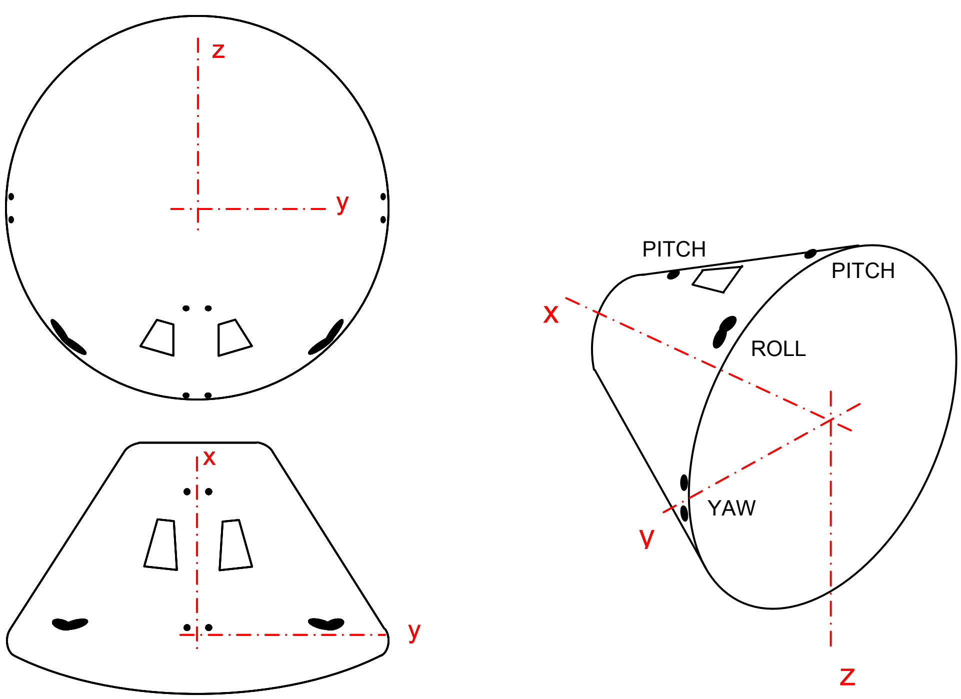

Figure 11.1-1 CM Translation and Rotation Axes

The CM RCS will provide attitude control after SM separation. They can be pulse fired to a minimum impulse bit of 80 milliseconds or fired continuously to provide a maximum of 160 lbf thrust each. The system consists of two identical, independent systems of six thrusters and propellant tanks. A single system can perform the full skip entry maneuver, provided the propellant cross-over valves are open. However, a single system has enough propellant to perform a limited range skip entry maneuver, a direct entry, or a ballistic entry.

The propellant is pressurized gaseous oxygen (GOX) and pressurized gaseous Methane. The propellants are stored as a gas to accommodate the long term storage requirements and the oxygen also serves as a back-up to the ELCS breathing oxygen supply.

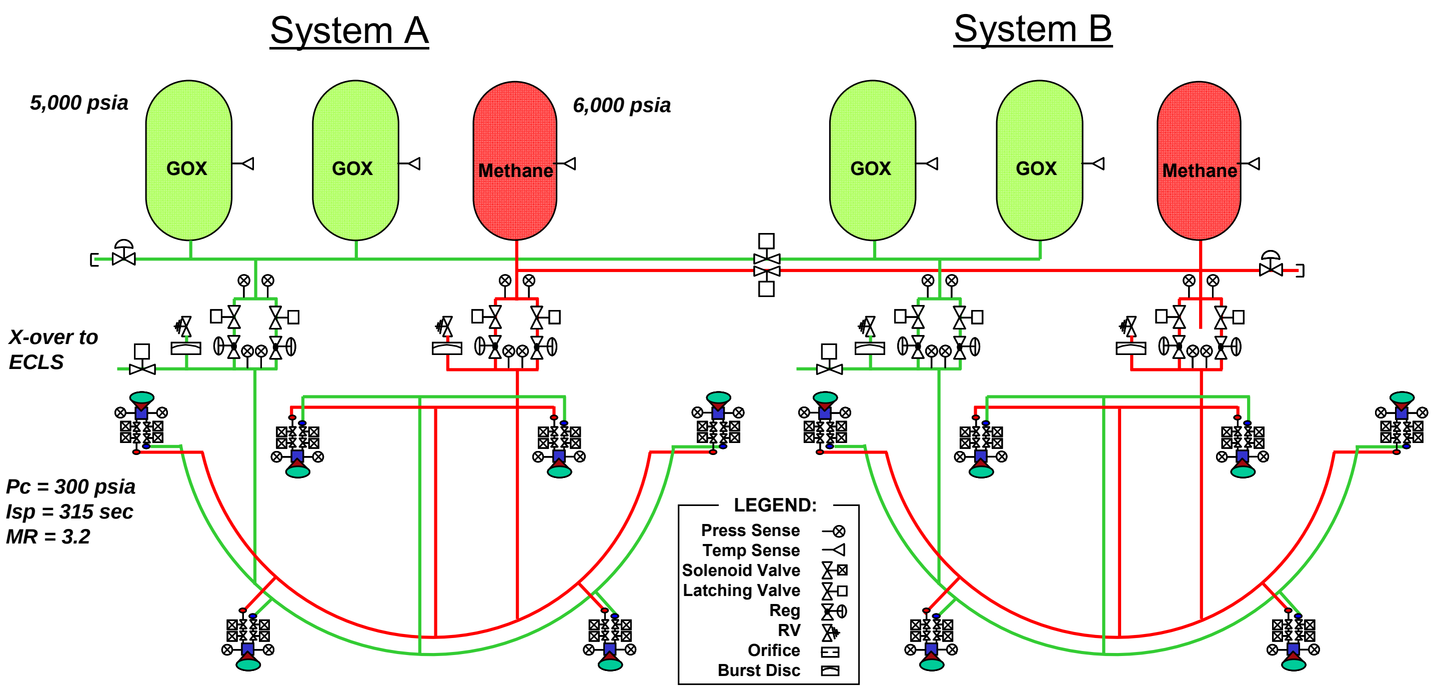

Figure 11.1-2 CM RCS Schematic

Propellants are fed up to the twelve engines by parallel manifolds. The engines are designed with a redundant solenoid coil to provide additional fault tolerance, without adding another string of thrusters. The propellant tank isolation valves work off of a piezoelectric technology, that allows it to operated fast enough and accurately enough to function as a back-up to the regulator. In the event of a complete electrical and computer system failure, either one or both of the gaseous systems can operate in a manual “cold-gas” mode to perform a ballistic entry. The schematic is being presented as a “notional” schematic, since the number and shape of the tanks are representative of the actual system and the semicircular layout of the propellant lines that feed the thrusters are close to how the lines on the vehicle are visualized to be laid out.

11.1.3 Mass Estimates and Design Maturity

The mass estimates for the CM RCS subsystems and corresponding bases of estimate are provided in the following table.

Hardware Items	Quantity	Unit Mass (lbm)	Growth (%)	Total Mass (lbm)	CM Mass (lbm)	SM Mass (lbm)	Basis of Estimate
CM RCS				**925**	**925**	**0**	
CM RCS Engine (160 lbf)	12	11	15%	154.6	154.6		Historical
Igniter	12	1	15%	13.8	13.8		Similar to existing test article
Valve Panel	1	12	15%	13.9	13.9		math model
Oxygen tanks	4	32	10%	140.8	140.8		Similar to Arde 4500 psia COPV
Fuel tanks	2	45	10%	99.0	99.0		math model
Ox high press feed lines	2	4	10%	8.1	8.1		200" of .375" x .065 wall ss tubing
Ox low press feed lines	2	9	10%	20.2	20.2		300" of 1" x .035 wall ss tubing
Fuel high press feed lines	2	4	10%	8.1	8.1		200" of .375" x .065 wall ss tubing
Fuel low press feed lines	2	9	10%	20.2	20.2		300" of 1" x .035 wall ss tubing
Fittings	36	0.4	10%	13.9	13.9		~11 ea dynatube fitting connections
Oxidizer Isolation Valves	4	8	10%	35.2	35.2		Similar to X-38 iso valves
Oxidizer Regulators	4	6	10%	26.4	26.4		Similar to X-38 iso valves
Oxidizer Crossover Latching valves	1	2	10%	2.2	2.2		est
Oxygen ELCS interconnect valve	2	2	10%	4.4	4.4		est
Fuel Isolation Valves	4	8	10%	35.2	35.2		Similar to CEV SM valves
Fuel Regulators	4	6	10%	26.4	26.4		Similar to X-38 iso valves
Fuel Crossover Latching Valves	1	2	10%	2.2	2.2		est
Fill Valves	2	1	10%	2.2	2.2		est
Burst Discs and Relief Valves	4	1	10%	4.4	4.4		est
High Pressure Sensors	8	0.5	10%	4.4	4.4		est
Low Pressure Sensors	8	0.1	10%	0.9	0.9		est
Temperature Sensors	8	0.1	10%	0.4	0.4		est
Oxygen	1	221	0%	221.0	221.0		
Methane	1	67	0%	67.4	67.4		

Table 11.1-1 CM RCS Mass Estimates and Bases of Estimate

11.1.4 Plan Forward

The system is designed to operate in a manual over-ride "cold gas" mode, in the event all computing power is lost to the CM after SM separation. The current cold-gas thrust level, as designed, is calculated to be about 50 lbf. Simulations need to be run to see if that is sufficient to perform the spin-up maneuver to stabilize the CM in order to do a ballistic re-entry.

11.2 SM Propulsion

The SM propulsion system consists of:

- Helium propellant pressurization system

  - Pressurant tanks
  - Isolation valves
  - Pressure regulation valves
  - Pressure relief devices
  - Instrumentation
  - Lines, fittings, test and service ports
- Propellant feed system
  - Fuel and oxidizer tanks
  - Isolation valves
  - Instrumentation
  - Lines, fittings, test and service ports
- Engines and related hardware
  - Main engine (including quad-redundant bi-prop valves and necessary manifolds)
  - Reaction control engines
  - Backup engines
  - Main engine gimbals (exclusive of controllers)
  - Engine heaters
  - Instrumentation
- Fluids
  - Fuel (MMH)
  - Oxidizer (NTO)
  - Pressurant (He)

It does not include:

- Tank and line heaters
- Secondary structure and mounting hardware

11.2.1 Driving Requirements, Groundrules, and Assumptions

SM propulsion system driving requirements and ground rules (largely summarized in Fig 11.2-1):

- Lunar mission
- Useable propellant is 20,500 lbm
- Allowable propulsion system dry mass is 4,050 lbm

- Initial CEV (CM+SM) inserted mass of 47,170 lbm
- Reaction control engine Isp of 280 seconds
- Reaction control engine thrust of 25 lbf
- Reaction control engine ΔV of 237 ft/s
- Main engine Isp of 323 seconds
- Main engine thrust of 10,000 lbf
- Main engine Delta-V of 5,849 ft/s

SM propulsion system assumptions:

- Helium tanks to be COPV
- Line failures not considered
- T/W = 0.2 (or better)
- Propellant tanks:
    - Ullage is 3%
    - Propellant management device (PMD) occupies 2% of tank volume
    - Are oversized by 0.3% to account for manufacturing tolerances
    - Permit 3% propellant margin to account for loading inaccuracy, Isp losses, etc
- Burst factor is 1.5 for metallic, 2.0 for composite overwrapped
- Maximum number of simultaneously firing RCE's is 8
- Required pressurant is calculated for an isothermal case, plus an additional 20%
- Service Module length is driven by propellant tank height and not other factors, such as radiator surface area (i.e., tank height will be minimized, irrespective of the void fraction, to achieve lowest SM mass)

Jim Geffre
Updated 26 Feb 2005
Updated 8/25/2006 (Bryan Fraser)

	Isp	Thrust (lbf)
OMS	323.0	10,000
RCS*	280.0	25

Propulsive Maneuver	OMS ΔV (ft/s)	RCS ΔV (ft/s)	Initial CEV Mass (lbm)	OMS Prop Used (lbm)	RCS Prop Used (lbm)	Usable Prop Remaining (lbm)	Initial OMS T/W	Final OMS T/W
Insertion			47,170			20,507		
Rendezvous w/ LSAM	504.9	106.1	47,170	2,237	552	17,717	0.21	0.23
Lunar Orbit Maneuvering	590.6	49.2	43,121	2,382	235	15,100	0.23	0.25
Trans-Earth Injection	4,753.9		40,749	14,959		141	0.25	0.39
Mid-Course Correction(s)		32.8	25,790		94	47		
SM Disposal		49.2	8,711		47	0		
Totals	5,849	237		19,578	928			

* RCS Isp is an average of thruster Isp for short and long impulses (assumed to be 275 and 300 s)

CEV Mass Gained or Lost During the Mission	Crew	Suits	Lunar Samples	Food Trash	Water	Water Tanks	LIDS Mech
	820	440	280	163	371	89	672

Pre-LO Maneuvering Mass Gains/Losses	Crew, Suits (Losses)
Pre-Trans-Earth Injection Mass Gains/Losses	Crew, Suits, Lunar Samples (Gains); Food Trash, Water, Water Tanks, LIDS Mechanism (Losses)
Pre-SM Disposal Mass Gains/Losses	Crew Module (Losses)

EPW	50,785	lbm
LAS	13,290	lbm
SA	1,400	lbm
Insertion Mass	47,170	lbm

Figure 11.2-1 SM Propulsion System Requirements and Ground Rules Summary

11.2.2 Conceptual Design Overview

11.2.2.1 System Piping and Instrumentation Diagram (P&ID)

The following diagram is the SM propulsion system P&ID, some key aspects of which are:

- Single AJ10-118 main engine
- Parallel-plumbed propellant tanks
- Heat exchangers on propellant feed lines to help minimize the helium required by "en-forcing" an isothermal condition
- Separate helium pressurization system for fuel and oxidizer, which can be made common in the vent of certain failure modes
- Direct-acting helium pressure regulators
- Three seats to leakage
- Eight strings of three R-1E reaction control thrusters to maximize propellant efficiency, maximize system reliability, and minimize fabrication/maintenance complexity
- Ability to isolate individual tanks for failure, diagnostic, or operational purposes
- Four aft-firing R-40B engines serve as main engine backup

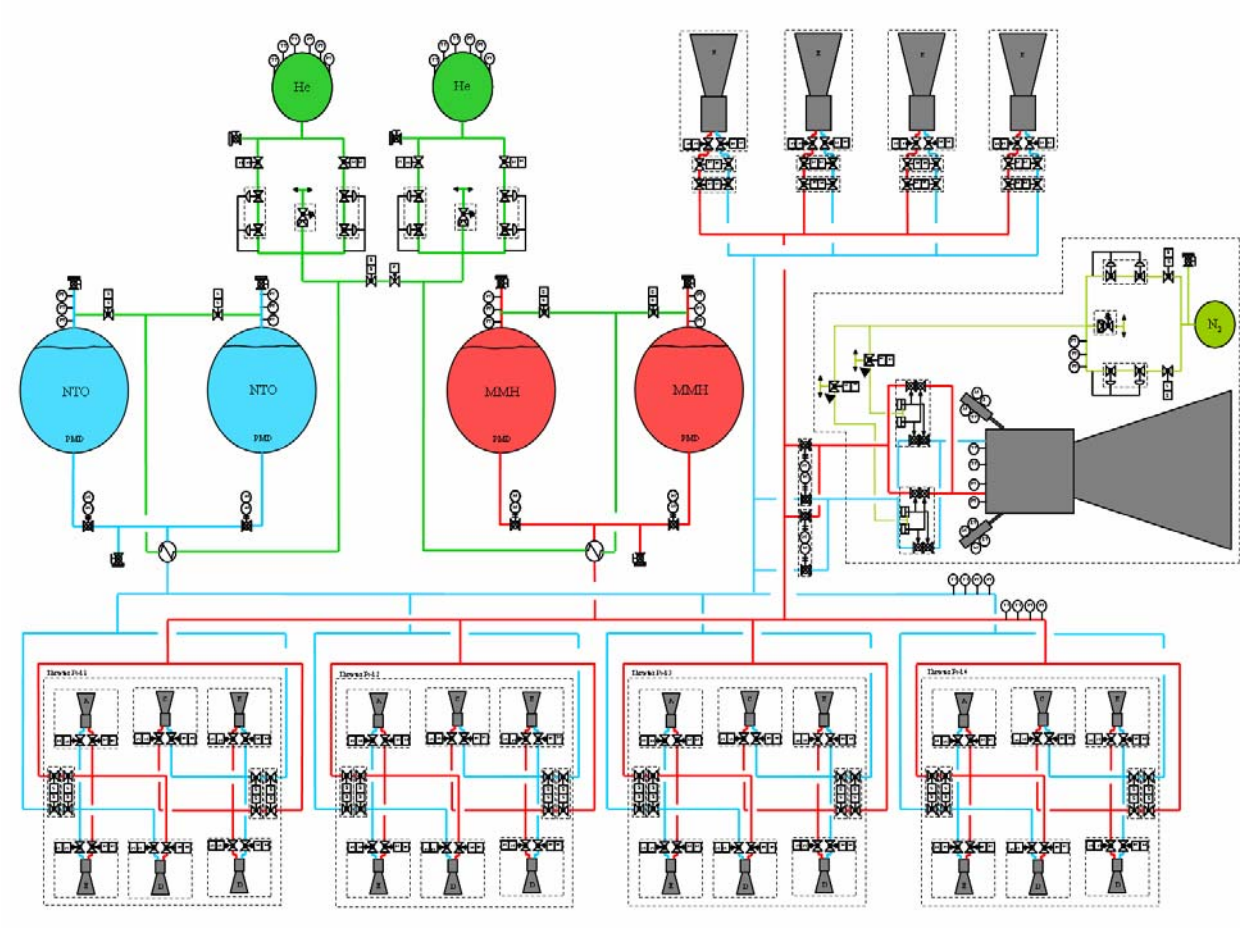

Figure 11.2-2 SM Propulsion P&ID

11.2.2.2 Main Engine

- Assessed pressure-fed engines that had been produced, are being produced, or have undergone some development
- Focused on engines with thrusts between 3,500 and 15,000 lbf
- Focused on U.S. and European suppliers
- Shuttle OME and Delta II rose to the top of the list

Ranking	Engine Name/ Designation	Notes, Issues, and Downselect Criteria	Engine Designer/ Manufacturer	Launch Vehicles or Mission Application	Rated Duration (sec)	No. of Restarts	Production Status	Man Rated	Thrust in Vacuum (lbf)	Oxidizer	Fuel
1	AJ10-190	designed for reusibitliaty (not currently required)	Aerojet	Shuttle - OME	1250	150	Recent Production	yes	6,000	N2O4	MMH
2	AJ10-118K	not currently man rated	Aerojet	Delta II, Delta IV (small)	500	10	In Production	no	9,753	N2O4	Aerozine-50
3	Aestus	foreign supplier (?)	Astrium	Ariane 5 Upper Stage			In Production		6,504	N2O4	MMH
NA	SE-10	development engine only (no flight heritage)	Rocketdyne	Developed for LEM Descent	730	20	Never Produced	yes	10,500	N2O4	Aerozine-50
NA	TR-201	out of production for a long time (since early 80's?)	TRW	Fixed thrust variant of LEM Descent, Delta upper stage (replaced by AJ10-118K)	500	5	Out of Production	no	9,900	N2O4	Aerozine-50
NA	XLR 66-AJ-2	development engine only (no flight heritage), very short rated duration	Aerojet	Development Engine for Space Missions	95	unlimited	Never Produced	prob. no	9,000	N2O4	Aerozine-50
NA	AJ10-138	out of production for a long time (last flight in the early 80's?)	Aerojet	Titan III Transtage	500	prop lmtd	Out of Production	prob. no	8,000	N2O4	Aerozine-50
NA	XLR-132 (RS-47)	pump fed	Rocketdyne	Upper Stage	4000	10	Never Produced	prob. no	3,750	N2O4	MMH
NA	Transtar	pump fed	Aerojet	pump fed version of the OMS engine		15	Out of Production		3,748	N2O4	MMH
NA	RS-18	out of production for a long time, low thrust	Rocketdyne	LEM Ascent	460	35	Out of Production	yes	3,500	N2O4	Aerozine-50
NA	AJ10-131	development engine only (no flight heritage)	Aerojet	Apollo Service Module - Subscale	1000	prop lmtd	Out of Production	yes?	2,200	N2O4	Aerozine-50

Figure 11.2-3 Hypergolic Main Engine Survey

- Aerojet-provided data compares present Shuttle and Delta II engines, to uprated versions that would:
  - Maintain existing engine heritage
  - Minimize re-qualification (and thus schedule)
  - Be deliverable within 24 – 36 months

Parameter	SPS	Delta (AJ10-118)	Man Rated Delta	SS OMS-E	High PC OME
Thrust (lbf)	20,500	9,800	10,000	6,000	10,000
Performance --Isp (sec)	314	320	323	316	331
Chamber Pressure (psia)	97	125	125	125	205
Nozzle Area Ratio	62.5:1	65:1	110:1	55:1	177:1
Injector OD (in)	18	12	12	8	8
Nozzle Length	112	74	100	50	100
Valve	Quad Red.	No Red.	Quad Red	Series Red.	Quad Red
Gimbal	Throat	Head End	Throat	Throat	Throat
ERE	0.96	0.99	0.99	0.98	0.98
Propellant	A50	A50	MMH	MMH	MMH
Mixture Ratio	1.6	1.9	1.9	1.65	1.9
Life (seconds)	750	450	1000	54,000	<54000
Number of Restarts	50	Unl (duration)	Unl (duration)	500	<500
Man Rated	yes	no Red.	yes	yes	yes
Chamber Construction	ablative	ablative	ablative	regen	regen

Figure 11.2-4 Shuttle OME and Delta II Engine Comparison

- Based upon this data, a Delta II engine is recommended for this effort
- Additional, more current data for the Delta II engine (which may differ from the previous chart):

- Isp = 323 seconds at a MR of 1.65, with no reduction in Isp at end-of-life for our application
- Use Shuttle quad-redundant valves (which would require modification to the present P&ID) to "man-rate"
- Area ratio = 110
- Overall length = 128 inches (including valves)
- Bi-prop valve inlet pressure = 225 psia
- A replacement for the asbestos ablative is presently undergoing re-qualification with Boeing
- Presently, about 3 flights/year (25 engines presently scheduled to be flown)
- Throat gimbaled

▪ GRC analysis suggests that the Isp and overall engine length reported by Aerojet are reasonable

11.2.2.3 Propellant and Main Engine

Goals

It was desired to understand the performance variations between several potential propellant combinations for use on the main propulsion system of the CEV Service Module. The propellant combinations of interest were NTO/MMH, LOX/LCH4, and LOX/Ethanol. In addition to these propellant combinations, LOX/LH2 was also investigated. Since there are a significant number of flight engines that use LOX/LH2 it provides a useful reference point to anchor the analysis approach.

For each propellant combination, it was desired to understand:

1) How specific impulse (Isp) varies with oxidizer to fuel ratio (O/F) for a fixed chamber pressure (Pc) and expansion area ratio (AR).
2) How Isp varies with Pc and AR for a fixed O/F.
3) How engine length would vary for a fixed Isp over a range of Pc's and thrust levels.

Analysis Approach

Theoretical performance numbers were obtained using a one-dimensional equilibrium chemistry code (CEA). CEA cases were run as an infinite area combustor. To provide a more complete picture, theoretical values of Isp were obtained using full equilibrium chemistry as well as equilibrium chemistry with a freeze point at the throat. The theoretical value of Isp will fall somewhere between these two scenarios depending on the specifics of the engine design (Pc, thrust, AR, O/F, et cetera) and the resulting kinetic losses. A more sophisticated tool that takes into account two-dimensional and kinetic effects could be used to provide a more accurate assessment of specific point designs.

For data on Isp vs O/F, a reference condition of Pc = 125 psia and AR = 55 was selected. These values come from the Shuttle OME (AJ10-190) operating point. Figure 11.2-5 shows the theoretical performance of NTO/MMH as a function of O/F at the reference condition. The actual Isp of the Shuttle OME is also shown. Actual Isp can be related to either the equilibrium or the frozen at the throat curve. For the case of the OME, the Isp is 93.7% of the equilibrium value and 96.5% of the frozen at the throat value.

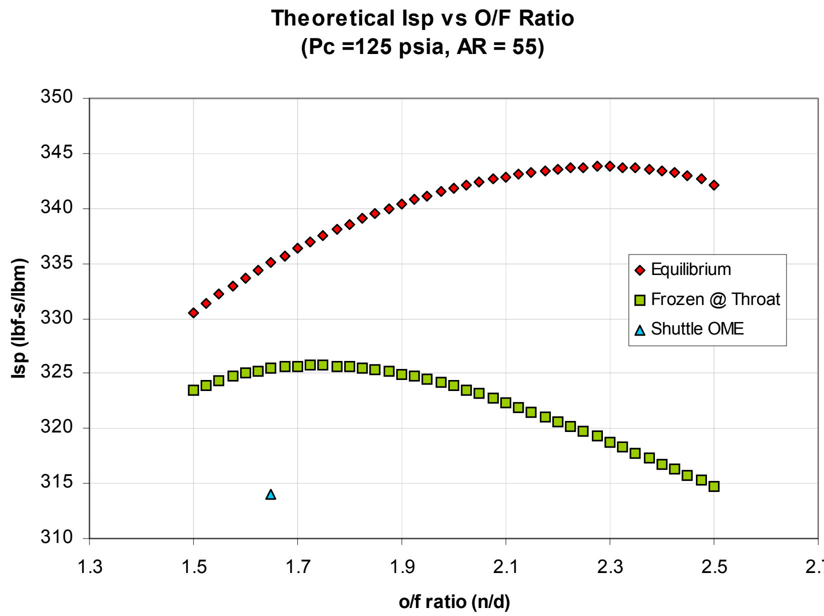

Figure 11.2-5 Theoretical Values of Isp for NTO/MMH as a Function of O/F Ratio

Theoretical values of Isp were also investigated as a function of Pc and AR. The range of Pc's investigated was 100 psia to 250 psia. The range of AR's investigated was 50 to 250. The results of these investigations for NTO/MMH can be seen in Figures 2 and 3 for equilibrium and frozen at the throat chemistry respectively. For the NTO/MMH propellant combination, an O/F ratio of 1.65 was selected (again from Shuttle OME design point).

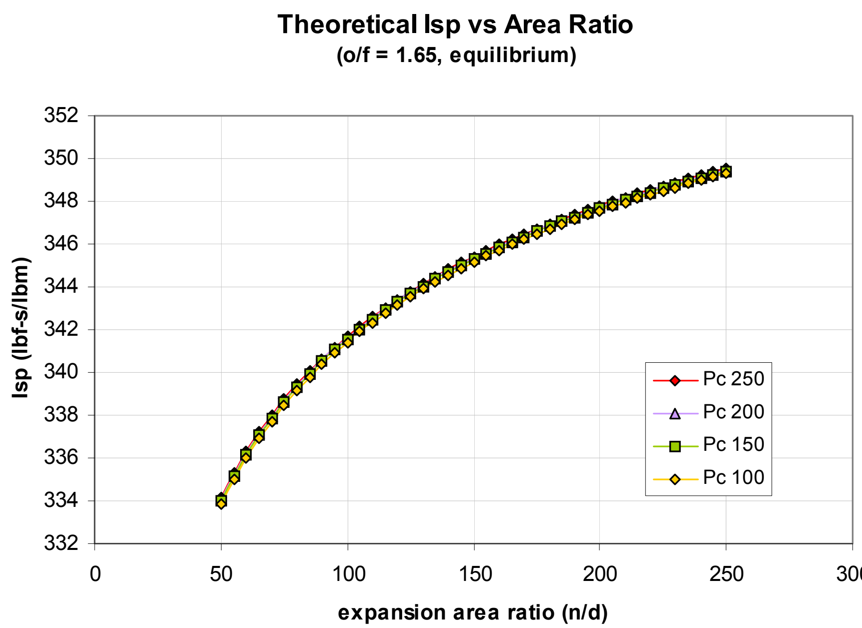

Figure 11.2-6 Theoretical Isp as a Function of Pc and AR – Equilibrium Chemistry

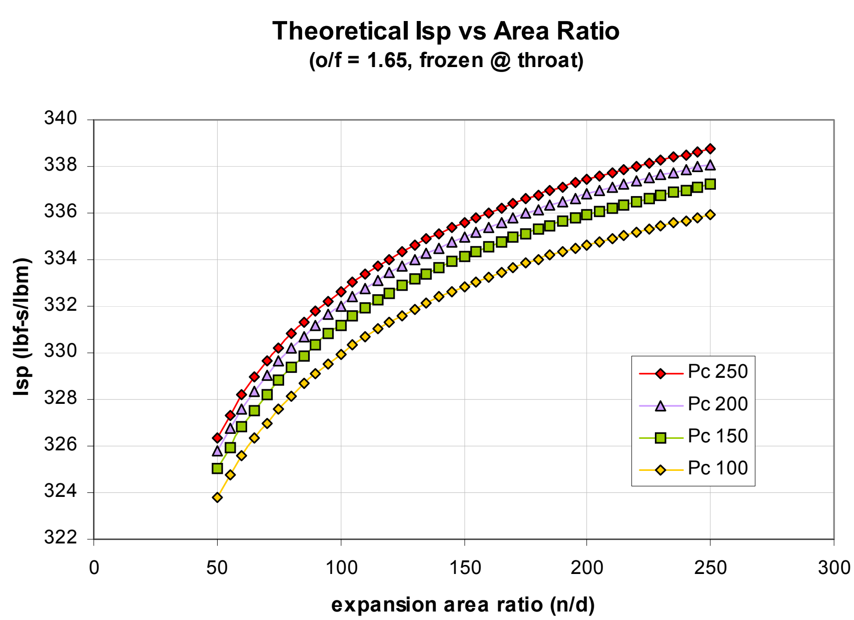

Figure 11.2-7 Theoretical Isp as a Function of Pc and AR – Frozen Throat Chemistry

For each of the propellant combinations investigated, any real engine performance data that was available was compared to theoretical predictions in an effort to provide guidance on how much the theoretical performance should be reduced. Table 11.2-1 shows a survey of NTO/MMH engines and how the actual performance compares to the theoretical values (for both equilibrium and frozen at the throat). The table covers a range of Pc's, O/F ratios, and thrust levels. The low Isp on the R-40-A is a reflection of the low AR and the film cooling of the radiatively cooled RCS thruster. All of the remaining engines investigated performed between 96.5% - 98.9% of the theoretical value (when referencing frozen at the throat performance predictions).

	Pc (psia)	O/F (n/d)	SUPAR (n/d)	Thrust (lbf)	Actual Isp (lbf-s/lbm)	Equil Isp (lbf-s/lbm)	Froz @ Th Isp (lbf-s/lbm)	Equil Delta (% of theo)	Froz @ Th Delta (% of theo)
AJ10-190	125	1.65	55	6,000	314.0	335.1	325.4	93.7	96.5
XLR-132 (RS-47)	1,500	2.00	441	3,750	340.0	363.3	349.5	93.6	97.3
R-40-A	152	1.60	22	870	281.0	321.5	314.8	87.4	89.3
Transtar	345	1.80	132	3,748	328.0	348.5	336.8	94.1	97.4
Aestus	145	2.05	83	6,504	324.0	347.8	327.7	93.2	98.9

Table 11.2-1 NTO/MMH Engine Performance Survey

The final parameter of interest was the length of the engine as a function of Pc and thrust level. The range of Pc's investigated was again 100 psia to 250 psia. The thrust levels investigated were from 5,000 lbf to 15,000 lbf. For this analysis, Isp values were based on frozen at the throat results adjusted according to the results of the previously discussed engine survey. Values of C* were adjusted in the same manner, by anchoring to available real engine data. Two values of Isp were selected for the engine length investigation. A low and a high value where selected which represented an "easy" Isp target and a more "challenging" Isp target. Engine throat and exit diameters were calculated based on standard rocket engine equations and adjusted performance values from CEA. An engine L/D ratio (overall length divided by exit diameter) was calculated based on thrust level from trends of real engines. Knowing the exit diameter and the L/D ratio allowed the engine length to be estimated. Figure 11.2-8 shows the results of estimated engine length as a function of Pc and thrust level for NTO/MMH. The target Isp for this data was 314.0 lbf-s/lbm and the O/F ratio was 1.65. This allows a comparison of predicted engine length to the actual length of the Shuttle OME. Figure 11.2-8 shows the Shuttle OME actual length (72 inches). This analysis predicted the length to be 71 inches, a difference of about 1 percent. This level of accuracy at the Shuttle OME design point is somewhat expected since the performance efficiencies are tied to Shuttle OME data. This level of accuracy will not be maintained over the full operating range of the data, but does indicate that the predicted values are reasonable and that the trends should be valid for rough engineering purposes.

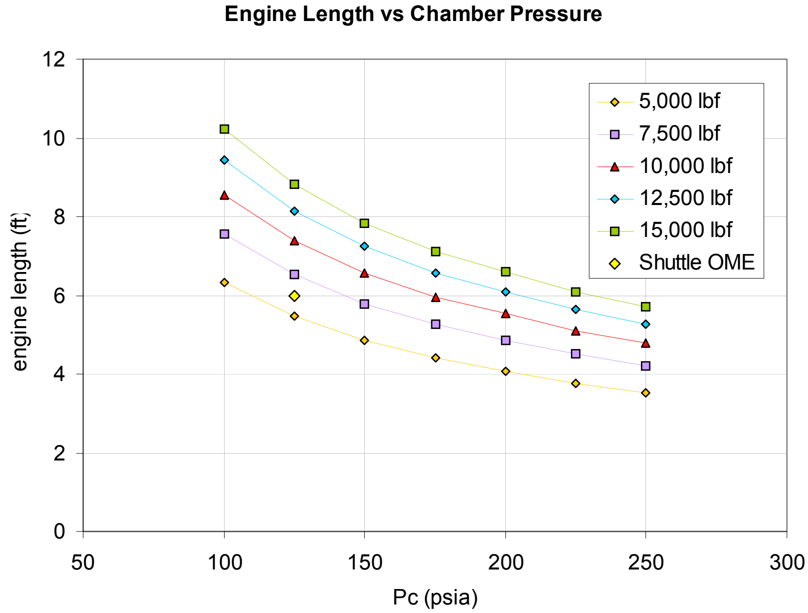

Figure 11.2-8 Estimated Engine Length for NTO/MMH as a Function of Pc and Thrust

The AR required to achieve the desired Isp is independent of the thrust level. For a given target Isp and O/F ratio, the AR required can be plotted as a function of Pc alone. Figure 11.2-9 shows this plot for NTO/MMH with a target Isp of 323 lbf-s/lbm and an O/F ratio of 1.65.

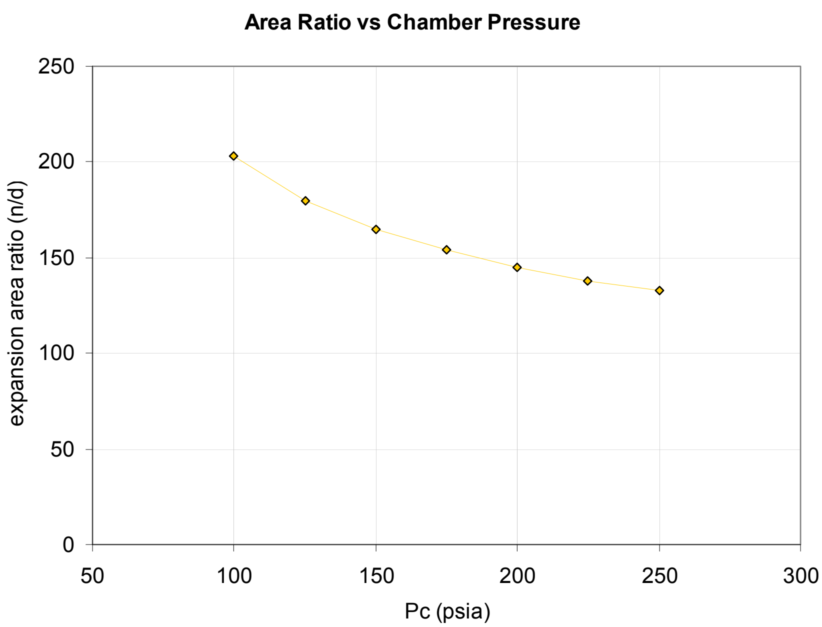

Figure 11.2-9 AR as a Function of Pc for NTO/MMH

Results

The analysis approach outlined above was performed for the three propellant combinations of interest as well as LOX/LH2 for reference. Table 11.2-2 shows the target Isp values that were used for each propellant combination when estimating engine length as well as the Pc and AR used when predicting Isp. Most of the cases were evaluated at Shuttle OME operating conditions (Pc = 125 psia, AR = 55). LOX/Ethanol was investigated at a second design point using a higher Pc and a larger AR. LOX/LCH4 was also investigated at a second design point using a higher Pc, larger AR, and a lower O/F. For both of these alternative cases, more aggressive Isp values were selected when evaluating engine length.

Appendix	Propellant Combination	Pc (psia)	AR (n/d)	O/F Ratio (n/d)	Low Isp (lbf-s/lbm)	High Isp (lbf-s/lbm)
A-1	NTO/MMH	125	55	1.65	315	323
A-2	LOX/LCH4	125	55	3.60	335	344
A-3	LOX/Ethanol	125	55	1.50	320	330
A-4	LOX/LH2	125	55	5.50	430	443
A-5	LOX/LCH4	225	150	2.80	-	355
A-6	LOX/Ethanol	225	150	1.50	-	333

Table 11.2-2 Propellant Combinations and Design Points Investigated

Discussion of Selected Results

It should be noted that the range of target Isp's for each propellant combination were selected such that a similar range of engine lengths resulted. Figure 11.2-10 shows the relative performance range of each propellant combination of interest. It can be seen that for similarly sized engines (engine length) LOX/Ethanol only offers a slight increase in performance over NTO/MMH (about 5 lbf-s/lbm), while LOX/LCH4 offers a somewhat more significant performance increase (about 20 lbf-s/lbm). For contrast, Figure 11.2-11 shows the same data but also includes LOX/LH2. This highlights the much larger potential benefit of LOX/LH2 with respect to Isp (about 110 lbf-s/lbm).

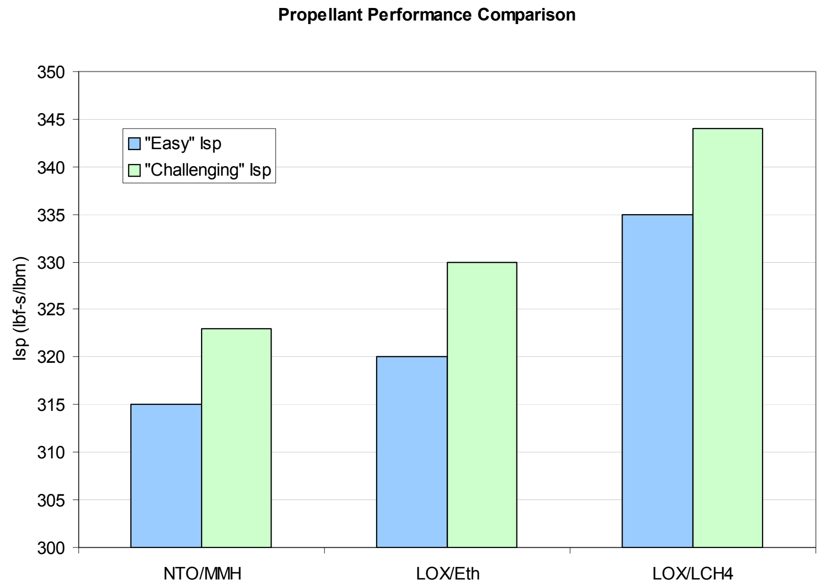

Figure 11.2-10 Propellant Performance Comparison

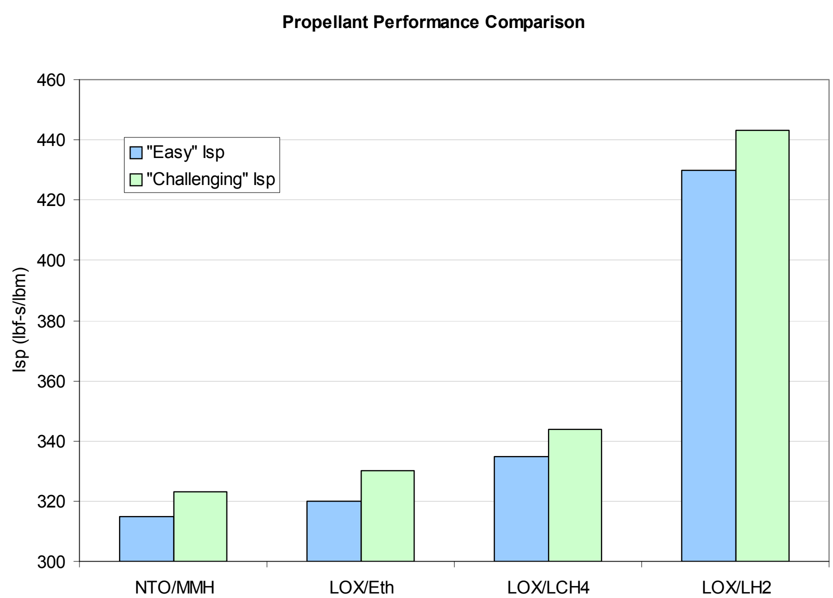

Figure 11.2-11 Propellant Performance Comparison – Including LOX/LH2

The data plots generated in this effort can be used as a "look up table" of sorts for different cases of interest. For example if a single engine operating at 10,000 lbf of thrust was desired for the Service Module main engine, the resulting engine lengths for each of the propellant combinations can be obtained at the bounded Isp values. Figure 11.2-12 shows two-dimensional line drawings of largest and smallest engines that fit this thrust class. As expected, each propellant combination provides a similar engine length but at different performance levels. The small, “easy” Isp engines are roughly 8 feet long while the large, “challenging” Isp engines are roughly 13 feet long (for reference, the Shuttle OME is about 6 feet long and the Apollo Service Propulsion System main engine was just under 13 feet long). Depending on the tolerable engine length for the CEV Service Module (based on engine manufacturing limits, interstage adapter length, et cetera) the resulting Isp would fall somewhere between those bounded limits.

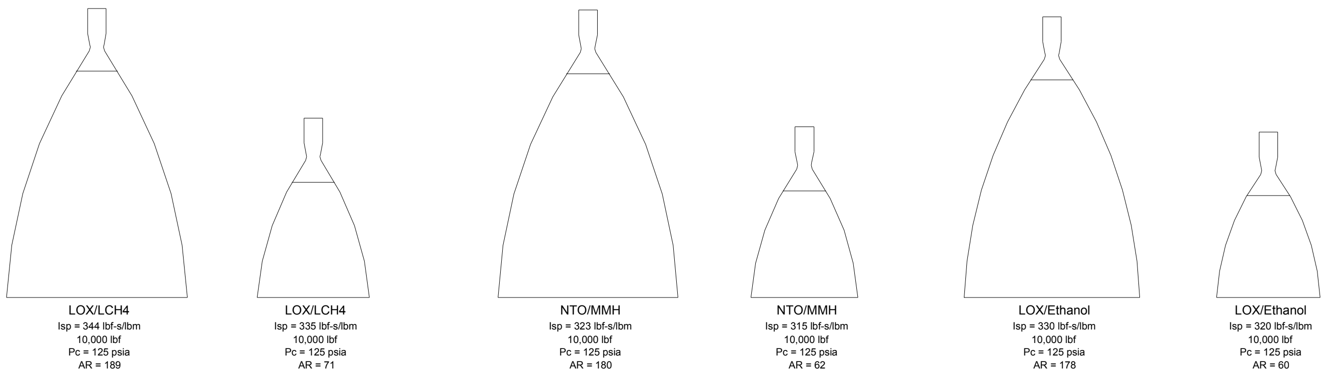

Figure 11.2-12 2-D Line Drawings of 10,000 lbf Engines

11.2.2.4 Reaction Control System

Glenn Research Center performed a number of analyses for the CEV SM RCS as a part of CRC-3. The goal of these analyses was to understand the performance differences between various RCS layouts and main engine augmentation schemes, as well as to develop a baseline system design to meet the Constellation and CEV program requirements. Analyses included:

- RCS configuration vs. propellant consumption for two fault scenarios
- Vehicle control dynamics vs. thruster size
- Main engine thrust vector control vs. thruster attitude control for main engine burns and late ascent abort maneuvering
- RCS leak detection capabilities

RCS Baseline Design

The baseline RCS developed as a result of these analyses consists of four RCS pods evenly distributed on the Y and Z vehicle axes, with six 25 lbf thrusters on each pod. A set of four 900 lbf thrusters configured in a ring around the main engine is included to provide a backup to the main engine. Alternative configurations could have 100 lbf thrusters on RCS pods rather than 25 lbf thrusters, or 200 lbf thrusters for main engine backup rather than 900 lbf thrusters. The configuration baselined is shown in 11.2-13.

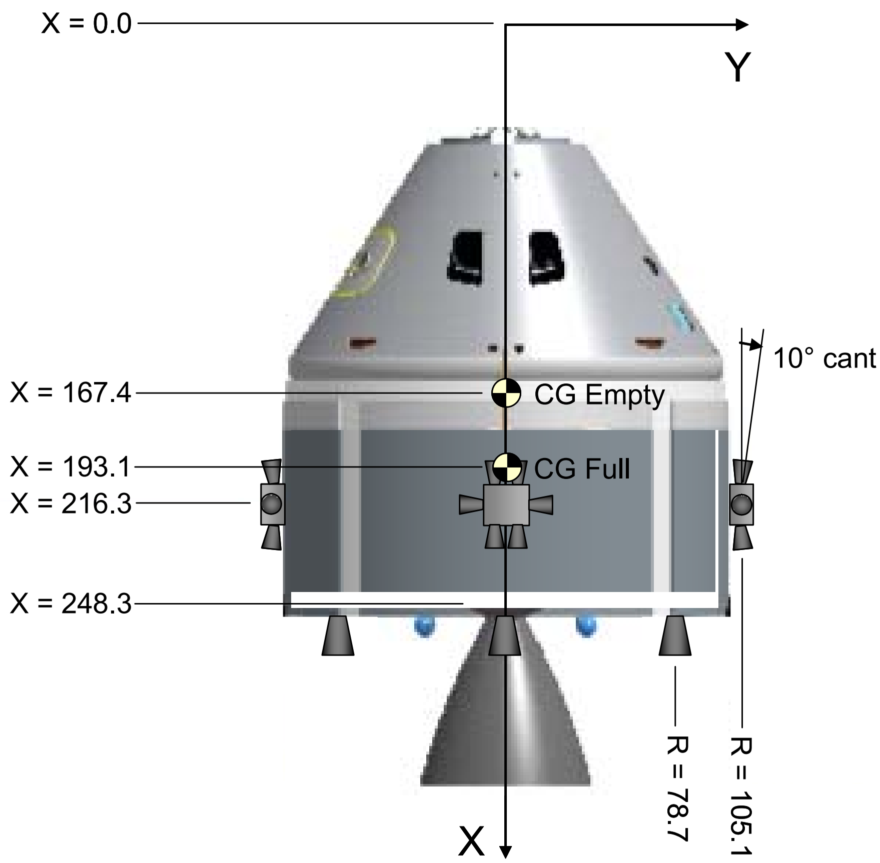

Figure 11.2-13 Baseline CRC-3 SM RCS Layout

<u>*Summary of RCS Analyses*</u>

A number of the RCS analyses were performed in support of various TDS's for CRC-3. For those analyses, only a summary is provided here, with a reference to the more complete TDS report.

Thruster Configuration

A study of various RCS thruster and plumbing configurations was performed to determine the relative efficiency of propellant consumption between each. Propellant use efficiency was calculated assuming different spacecraft center of gravity (CG) locations, which bounded the worst case CG movement over the course of the mission. This was done for both fully operational scenarios and various two fault scenarios, from which the worst was chosen for comparison. The primary requirement was that all thruster configurations must be able to continue with 6 Degree of Freedom (6DOF) operations after two faults.

Thruster configurations analyzed are shown in Figure 11.2-14, with relative propellant consumption shown in Table 11.2-3.

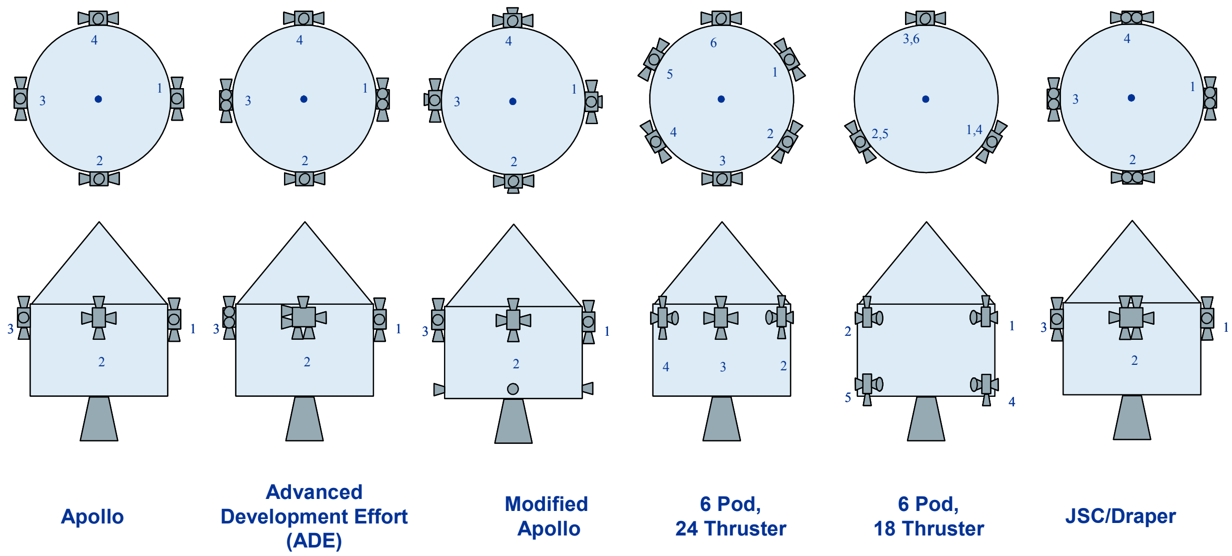

Figure 11.2-14 SM RCS Configurations Studied for DAC-2

Configuration	Propellant Consumption*	
	No Fault (Nominal)	Two Faults
Apollo	1.07	n/a***
ADE, 3 strings	1.06	1.86
ADE, 8 strings	1.06	1.47
ADE, individual thrusters	1.06	1.20
Modified Apollo	1.07	1.91
24 Thruster, 6 Pod	1.13	1.62
18 Thruster, 6 Pod	1.59	2.06
JSC/Draper**	1.10	2.70

*Relative to Apollo configuration with thrusters aligned to vehicle CG
** JSC/Draper has thruster canted 10 degrees outboard, all others 0 degrees

Table 11.2-3 Relative Propellant Consumption of Different RCS Layouts

While the Advanced Development Effort (ADE) configurations provided the best propellant consumption in worst case two fault scenarios, they were not chosen for the RCS thruster layout. The JSC/Draper configuration was instead chosen, primarily as it was the thruster configuration most extensively analyzed. Ongoing analysis of the RCS thruster configuration and its effects on various requirements should continue before a final decision is made.

Control Dynamics vs. Thruster Size (TDS 04-018)

A study of CEV vehicle (SM+CM) control dynamics vs. thruster size was performed by Draper Labs/JSC as a part of TDS 04-18. Results of this analysis indicate that with an 80 ms minimum firing time, 25 lbf thrusters are required to provide increased control precision and to minimize propellant consumption during attitude hold maneuvers.

100 lbf thrusters with a smaller minimum firing time (25 ms) could provide similar control and propellant consumption characteristics, but operation of the 100 lbf thrusters at this low firing time is not recommended, primarily to prevent buildup of FORP (fuel-oxidizer reaction products) due to incomplete combustion of propellants. FORP can lead to either inter-manifold explosions (known in the industry as Zots) or engine chamber explosions, either of which may result in loss of the thruster for future use. Other control schemes are currently being evaluated, which may allow for re-inclusion of the 100 lbf thrusters.

Control during Main Engine Firing (TDS 04-018 and TDS 09-003)

The goal of this work is to assess CEV control methods during firings of the Service Module (SM) main engine (ME). Three different control schemes were assessed for their ability to counter disturbance torques on the CEV during the ME burns:

- Reaction Control System (RCS) thrusters
- ME thrust vector control (TVC) via gimbal
- Dedicated aft-firing thrusters

In this study, both thrust level and duty cycle of the RCS thrusters were varied to determine the maximum CG offset and maximum ME angular misalignment that could be corrected for by the RCS. These results were compared to the maximum CG offset that was corrected for by the TVC, and it was found that the TVC configuration was able to correct for 2.5-3.5 times larger CG offsets than could the RCS thrusters, even when 100 lbf RCS thrusters were used. The thruster configuration used for this study is that shown in Figure 11.2-13.

RCS thrusters showed the ability to correct for the anticipated CG offset due to propellant tank drainage, although the configuration required two aft-firing and two forward-firing thrusters, each at 100 lbf thrust and operating at 70% duty cycle to make this correction. Therefore, the configuration resulted in large propellant losses for marginal control. The 900 lbf, aft-firing thrusters have the ability to correct for CG offsets anticipated during propellant tank drainage when they are operating at only 50% duty cycle. However, neither the RCS nor aft-firing engines are single-fault tolerant in this operating mode, since they are not capable of performing attitude control during a main engine burn with a single thruster failure.

Figure 11.2-15 shows the control capability of different thruster configurations as well as the gimbal. While the RCS and aft-firing thrusters are able to manage the predicted propellant shifts, they are not fault tolerant in doing so, and also provide less control margin. Additionally, Table 11.2-4 shows the propellant consumption required to control the vehicle during a main engine burn and it is comparable to the additional mass of the gimbal system (86 lbm), in some cases considerably more.

Based on the results of this study it is recommended that a gimbal system be added to the main engine for CRC-3. Analysis shows that the maximum range of motion needed by the gimbal to overcome worst case CG shift due to propellant depletion is 3 degrees, but margin should be added to this to account for uncertainties in the CG location and motion.

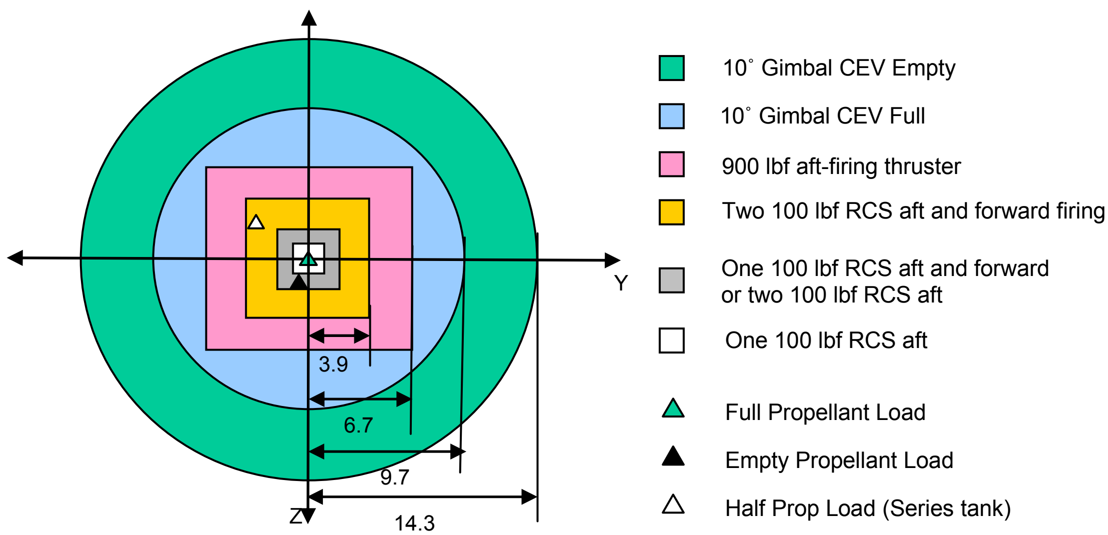

Figure 11.2-15 Lateral Cross-Section of SM Showing Range of CG Offsets

Thrusters Firing 100% Duty Cycle	CG Offset in Y and Z (ME Misalignment)		Propellant Consumed		Control Capability*
	Full Tanks	Empty Tanks	Single axis (Y only)	Two axis (Y and Z)	
One 25 lbf Aft	0.3 in (0.3°)	0.3 in (0.2°)	4 lbm	8 lbm	No
Two 25 lbf Aft	0.5 in (0.5°)	0.5 in (0.3°)	8 lbm	16 lbm	No
One 25 lbf Aft, One 25 lbf Forward	0.5 in (0.5°)	0.5 in (0.3°)	55 lbm	110 lbm	No
Two 25 lbf Aft, Two 25 lbf Forward	1.0 in (1.0°)	0.9 in (0.7°)	110 lbm	220 lbm	No
One 100 lbf Aft	1.0 in (1.1°)	0.9 in (0.7°)	16 lbm	32 lbm	No
Two 100 lbf Aft	1.9 in (2.0°)	1.9 in (1.3°)	32 lbm	64 lbm	Parallel Tank
One 100 lbf Aft, One 100 lbf Forward	2.0 in (2.1°)	1.9 in (1.3°)	220 lbm	440 lbm	Parallel Tank
Two 100 lbf Aft, Two 100 lbf Forward	3.9 in (4.1°)	3.8 in (2.7°)	440 lbm	880lbm	Parallel or Serial Tank

One 900 lbf Aft	6.5 in (6.7°)	6.5 in (4.6°)	135 lbm	270 lbm	Parallel or Serial Tank

*whether or not control can be maintained for parallel or serial tank drain, assuming good ME alignment

Table 11.2-4 Maximum CG Offsets that a Given Thruster Configuration can Correct

Control during Late-Ascent Abort (TDS 09-003)

A study of CEV flight dynamics during a late ascent abort where the Main Engine is fired to perform an abort maneuver was undertaken by GRC. The goal of this study was to determine whether RCS thrusters could be used to re-orient the CEV for proper burn attitude or if a Main Engine gimbal would be more effective.

The study performed assumed a 15 degree initial pitch angle as the CEV separates from the CLV, and tip-off rates of 0, 5, and 10 deg/s were included to determine their effect on thruster size and gimbal range of motion required. Analysis was performed using a GRC 4-DOF simulation model. Both analyses (gimbal and RCS) assumed only rotation about the pitch axis.

Results of the study indicate that a maximum gimbal range of motion of 3.5 degrees was required to control the CEV during late ascent abort with 10 deg/s tip-off rate. For RCS control of the CEV under the same conditions, two 100 lbf thrusters must be fired forward and aft (four total) to provide adequate control torque. For lesser tip-off rates, less thrust is required. Table 11.2-5 shows the required gimbal angle and total control thrust needed to perform CEV maneuvers during late ascent abort. Figures 11.2-16 and 11.2-17 show the gimbal and RCS control response for CEV flight during late ascent abort.

Total control thrust can be provided by combination of forward and aft-firing thrusters. Only in the 0 deg/s tip-off rate case are 25 lbf thrusters able to provide sufficient control torque to perform the abort maneuver.

Initial Tip-off Rate	Max Gimbal Angle	Total Thrust Required
0 deg/s	2.4°	25 lbf
5 deg/s	2.7°	150 lbf
10 deg/s	3.5°	375 lbf

Table 11.2-5 Gimbal Motion and RCS Thrust for Abort Maneuver Reorientation

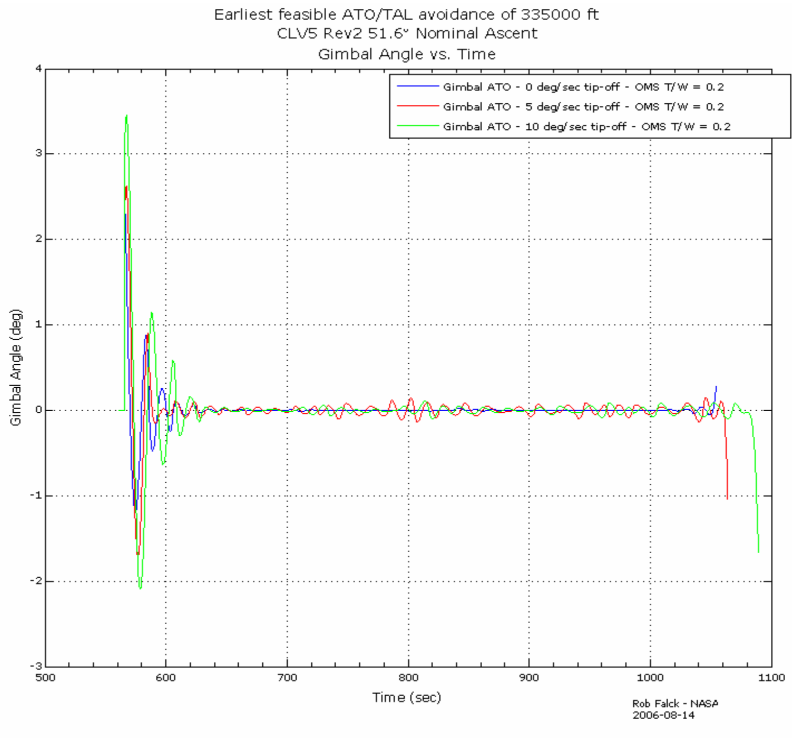

Figure 11.2-16 Gimbal Control Response for CEV Late Ascent Abort

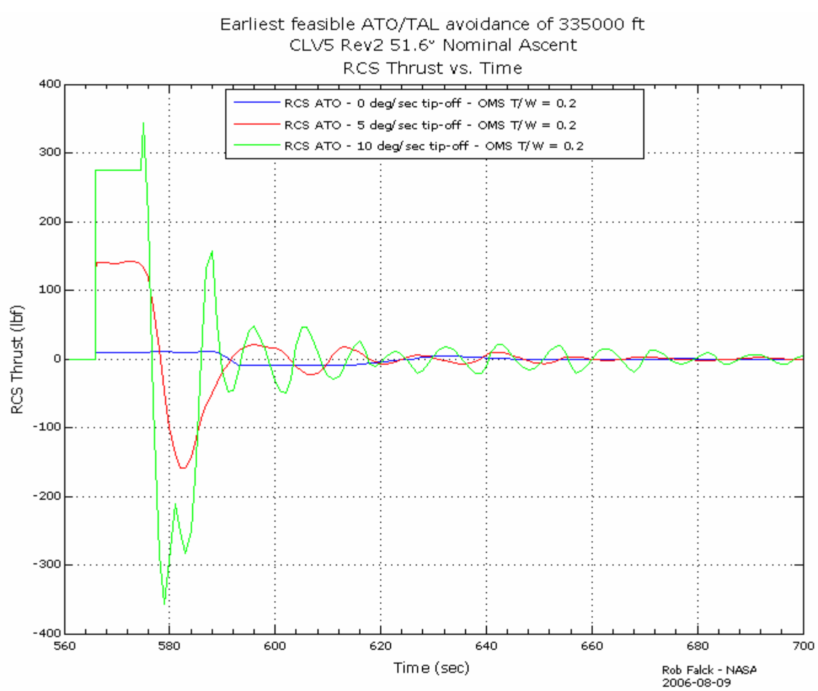

Figure 11.2-17 RCS Thrust Control Response for CEV Late Ascent Abort

RCS Leak Detection Study

There are currently no explicit requirements for the CEV to have a leak detection capability. A study was performed to determine design criteria for leak detection two different methods, both of which are currently employed in manned and unmanned spaceflight:

- Thermal detection of evaporating propellant as used in the space shuttle reaction control system (RCS)
- Detection of off-nominal torques on the spacecraft as is done with commercial satellite attitude control systems (ACS)

The maximum acceptable leak rate was defined as the maximum acceptable propellant loss for a given mission scenario. Two mission scenarios were examined:

- Case I - a 14-day lunar sortie
- Case II - a 210-day lunar outpost or ISS mission

Because no requirement explicitly states the amount of propellant which can be acceptably lost due to a thruster leak, a range of fuel/oxidizer losses was examined: 0.25%, 0.5%, 1%, 2%, and 3% of total mass of fuel or oxidizer. Three percent is the current margin carried on propellant load and it is expected that leaks which consume more than this amount would not be acceptable. The SM propulsion system total fuel and oxidizer weights are 12,764 lb of NTO and 7,736 lb of MMH (20,500 lb total).

Tables 11.2-6 and 11.2-7 list the leak rates which correspond to the total propellant loss values studied for Case I and Case II, respectively. The calculations assume that only one thruster is the source of either a fuel leak or an oxidizer leak. In order for a leak detection method to be considered feasible, it should be sensitive enough to detect leaks larger than the maximum acceptable leak rate.

% prop loss	NTO leak rate (lb/min)	MMH leak rate (lb/min)	NTO leak rate (cc/hr)	MMH leak rate (cc/hr)
0.25	1.6E-03	9.6E-04	30	32
0.5	3.2E-03	1.9E-03	60	65
1	6.3E-03	3.8E-03	120	129
2	1.3E-02	7.7E-03	240	259
3	1.9E-02	1.2E-02	360	388

Table 11.2-6 Maximum Acceptable Leak Rates for Case I (14-day lunar sortie)

% prop loss	NTO leak rate (lb/min)	MMH leak rate (lb/min)	NTO leak rate (cc/hr)	MMH leak rate (cc/hr)
0.25	1.1E-04	6.4E-05	2.0	2.2
0.5	2.1E-04	1.3E-04	4.0	4.3
1	4.2E-04	2.6E-04	8.0	8.6
2	8.4E-04	5.1E-04	16	17
3	1.3E-03	7.7E-04	24	26

Table 11.2-7 Maximum Acceptable Leak Rates for Case II (210-day lunar outpost)

Leak Detection by Temperature Change

Detection of propellant leakage through the valve by detecting temperature changes resulting from evaporation of the propellant is currently in use on the Space Shuttle Primary RCS and Vernier thrusters (the 900 lbf R-40A and 25 lbf R-1E, respectively). The leak detection systems on these thrusters can detect leaks as small as 30 cc/hr for the Vernier thruster and 100 cc/hr for the Primary RCS thrusters (Pfeifer, G. "Space Shuttle RCS Thruster Propellant Leak Detection" AIAA Paper No. 80-1131). Maximum leak rates of 4000 cc/hr (Vernier) and 40,000 cc/hr (PRCS) can be detected. It is assumed that this demonstrated range is independent of propellant type.

Based on the state of the art capability of the Shuttle RCS thrusters, it appears that leaks on a lunar sortie mission should be easily detectable down to loss of just less than 1% of the total propellant load (less for the 25 lbf Vernier engine leaks). However, for the 210 day outpost or ISS mission, the detectable leak rates are too high to prevent loss of more than 3% of the propellant load, due to the long duration over which the leak can act. Application of this methodology to the SM RCS thrusters without any design modifications and/or demonstration testing could result in total propellant losses up to 3.7 % of MMH (290 lb) and 3.7 % of NTO (470 lb) in the case of a leak through the 25 lbf R-1E thrusters, and up to 11.6% of MMH (900 lb) and 12.5% of NTO (1600 lb) in the case of a leak through the 900 lbf R-40 thruster.

Leak Detection by Attitude Disturbance

Small leaks that are discharged through the thrust chamber create small amounts of propulsive force, which create a steady-state disturbance torque on the spacecraft. Although the disturbance force may be small, if the duration is sufficiently long, the total impulse imparted on the spacecraft may be detectable by the SM ACS. In order to evaluate the feasibility of this option a cold-gas, ideal thrust was calculated at some of the representative leak rates derived in Tables 11.2-6 and 11.2-7.

The calculation of cold gas requires several assumptions that need to be evaluated, including the location of the liquid-gas phase change and flow choking. The propellant will vaporize as long as the local pressure is below the vapor pressure. For extremely small leak rates (below $\dot{m}_{crit}$) the propellant will vaporize in the injector tube. The gas would then expand into the combustion chamber. As the leak rate exceeds the $\dot{m}_{crit}$, the pressure in the injector tube would exceed the vapor pressure, so the propellant would stay in its liquid phase and begin to dribble into the combustion chamber and vaporize during its expansion in the combustion chamber. The $\dot{m}_{crit}$ was calculated for MMH and NTO for both the R-1E (25 lbf) thruster geometry and the R-4D (100 lbf) thruster geometry and are shown in Table 11.2-8. The injector area was estimated with an equivalent total hole diameter of 1 mm and 2 mm for the R-1E and R-4D geometries, respectively.

Propellant	$\dot{m}_{crit}$ for R-1E	$\dot{m}_{crit}$ for R-4D
MMH	16 cc/hr	62 cc/hr
NTO	110 cc/hr	450 cc/hr

Table 11.2-8 $\dot{m}_{crit}$ for R-1E and R-4D Thrusters

A calculation of the flow rates required to choke the flow at the R-1E nozzle throat indicates that a flow rate of 2,300 cc/hr (for MMH) or 13,000 cc/hr (for NTO) would be required, far greater than the leak rates of interest in this study. This confirms that the flow should be subsonic at the nozzle exit, and that the thrusts should be small.

As expected, the thrust produced by these small leak rates is also quite small, on the order of 1-85 millipounds, as shown in Figure 11.2-18. In order to implement this leak detection method, the ACS for SM would need to be adequately responsive to thrust on this order.

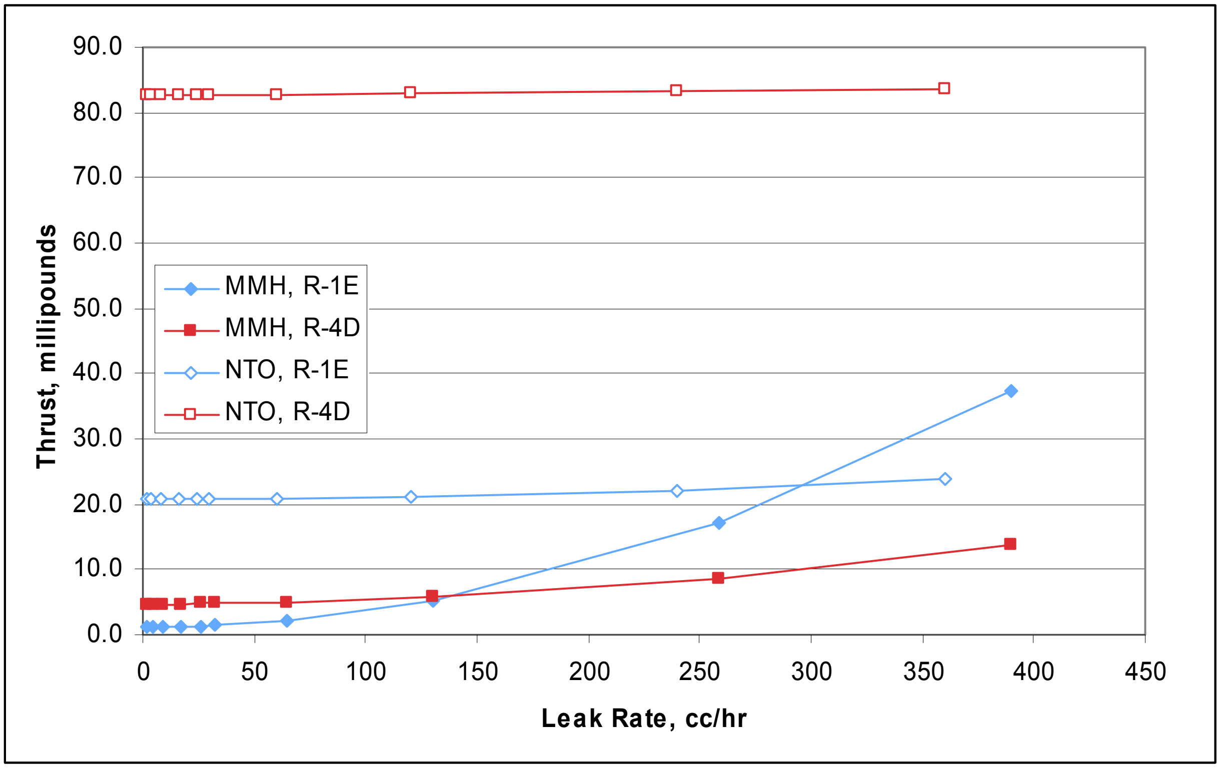

Figure 11.2-18 Thrust Developed by Leaks through 25 lbf and 100 lbf Thrusters

Leak Detection Summary

The primary points of the evaluation of various leak detection methods are:

- Given the longer duration missions of interest, relatively small leak rates can result in substantial propellant losses.
- The sensitivity of existing temperature sensor used on space shuttle is not adequate to detect finer leaks. Design modification and demonstration tests are likely required.
- A range of ideal thrusts was calculated as the ACS detection threshold for disturbance forces. In order to complete the feasibility study, an evaluation of ACS capabilities will need to be completed.
- The sensitivity of the thrust leak detection method can be significantly decreased if multiple leaks develop in a single engine pod. The disturbance forces could oppose and cancel each other out.

A meeting was held during CRC-3 to determine current methods of managing leaking thrusters on the Shuttle. It was determined from this meeting that a multi-step approach is used. If a thruster is determined to be leaking, the following is done (simplified of course):

1) The thruster is removed from the selection table, preventing its use (this is to minimize the likelihood of additional thruster damage due to FORP buildup).

2) If the thruster leak is determined to be significant enough to affect the propellant remaining for the mission, the thruster manifold is closed to prevent further loss of propellant.

While the final methodology for diagnosing and managing a leaking thruster on the SM RCS has not been decided, it will likely be performed similar to the Shuttle procedures.

Overall, it was determined that requirements regarding propellant leakage need to be determined before detection and mitigation processes and procedures can be developed. It may not be necessary, for example, to include costly temperature sensing capability if control system disturbances can provide necessary detection capability.

11.2.2.5 Pressurization System Architecture

"Bang-bang" pressurization:

- Pros:
  - Component commonality – i.e., valves for regulation the same as those for isolation
  - Likely to be less prone to seat contamination than direct-acting regulators
- Cons:
  - Increased probability of valves failing closed (may increase overall valve count, but further work required)
  - Overall system weight a bit higher than a mechanically regulated system, because valve weights are slightly greater.
  - Less flight history

Conclusion: A "bang-bang" pressurization system is a viable approach, but a direct-acting system is recommended because of its flight heritage and lesser probability of failing closed.

6,000 psia pressurization system:

- Pros:
  - Better packaging (smaller tank)
- Cons:
  - Overall system cost higher (it is more difficult and time-consuming to design, qualify, and build higher pressure components)
  - Overall system weight may be a bit higher (tank weight and valve weights are slightly greater than their lower pressure counterparts)
  - Less flight history

Conclusion: A 6,000 psia pressurization system is a viable approach, but a 4,500 psia system is recommended because of its flight heritage.

11.2.2.6 COPV vs all metal propellant tanks

On low pressure liquid tanks, a composite wrap might be added for a multitude of reasons, a couple of which are structural stiffness and cost. However, the resulting tank will never be lighter than its all metal counterpart. Considering the following tank geometries:

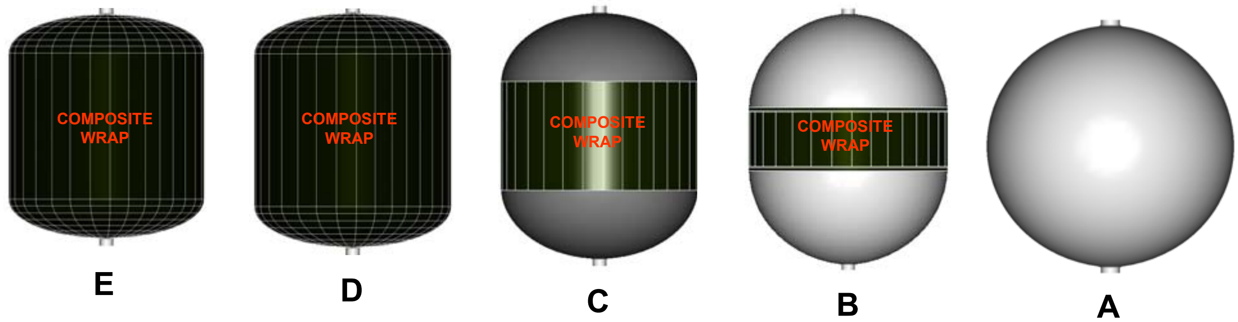

Figure 11.2-19 Tank Geometry Alternatives

Assuming all tanks to be equal volume and pressure, and mounted identically:

Tank A (sphere): Most efficient (i.e., lightest). A composite wrap would add cost and weight with no benefit.

Tank B (spherical ends, short cylindrical mid-section): Composite wrap of cylindrical portion added for cost reasons, only. Resulting tank is less expensive, but heavier than all-metal counterpart.

Tank C (slightly flattened ends, longer cylindrical section): Composite wrap of cylindrical portion added for stiffness. The flatter heads, although heavier than spherical ends, are not prone to buckling and do not warrant a composite wrap.

Tanks D and E (flatter ends, longer cylindrical section): The flat heads are prone to buckling, and the long cylindrical section requires stiffening. The weight of these configurations is prohibitive for flight applications.

Conclusion: For low pressure liquid tanks, composites wraps always add weight. Because of the myriad factors that play into the decision to wrap a vessel, higher fidelity (i.e., quantitative) results for our application (and variations in approach) can only be obtained by engaging the vendor as part of the design effort. Since we can fit spherical tanks within our vehicle, it is recommended that all-metal tanks be used to minimize mass.

11.2.2.7 Service Module Orbital Maneuvering Engine Start Time Analysis

Background

The purpose of this task is to determine if the Service Module (SM) Orbital Maneuvering Engine (OME) start time requirement is driven by CEV abort mode criteria.

This task will determine if a requirement for SM OME "start time to 90% thrust" is needed based on anticipated CEV abort mode performance requirements. This activity will include identification of state-of-the-art engine start times, identification of operational abort modes that require OME firing, and comparison of the flight-performance-driven start time needs with the state-of-the-art values. If better than state-of-the-art start-up performance is needed from the OME and propulsion subsystem, a vehicle-level requirement to document the need and rationale is necessary.

Assumptions

1) The original requirement read as follows: "The CEV shall provide a latency of less than 300 milliseconds from abort command initiation receipt until abort engine start." It was assumed that the maximum latency of 300 ms is from the time the SM OME receives the engine command until the SM OME achieves 90% full thrust (includes valve response, engine priming and rise in engine chamber).
2) Shuttle OME is representative of state-of-the-art performance for SM OME class engines.
3) Start-time performance of regeneratively cooled OME "worst-case" compared to ablative options.

Initialization Data

Shuttle OMS data, provided by Bryan Evans of White Sands Test Facility. Data was dated July 25, 2006.

Discussion

This task was comprised exclusively of data collection exercises. Sources for Shuttle OME and CEV abort data were identified and used to address specific TDS elements.

A recommendation regarding a requirement for SM OME start-time performance was made based on state-of-the-art engine performance data and abort scenario analysis.

Analytical Models and Tools

The trajectory design tool, OTIS was used to perform the abort scenario analysis that was used in this task.

Summary of Results

Analysis of abort modes, which require SM main engine firing performed assuming 5, 15, or 40 seconds between abort initiation and SM OME firing. The requirement for SM OME start time is related to CEV/CLV separation. Separation time on the order of "seconds" and state-of-the-art SM class engine time to 90% thrust is approximately 420 ms (significantly less than CEV/CLV separation time).

Requirement (CV0058) was likely originally conceived for the LAS and the SRD has been modified to clarify applicability to the LAS motor.

Conclusion and Issues

A vehicle level, abort-related requirement for SM OME to 90% thrust is not recommended. State-of-the-art SM class engine time to 90% thrust is significantly less than CEV/CLV separation time (~400 ms compared to multiple seconds).

SM OME start performance will be addressed in the engine specification.

Recommendations

Requirement (CV0058) was likely originally conceived for the LAS and the SRD has been modified to clarify applicability to the LAS motor.

Follow-on Analysis

A systems level analysis that evaluates the time duration from fault detection to 90% thrust is recommended. This analysis would include the time for determining and commanding the abort in addition to the time required for valve response, engine priming and rise in engine chamber pressure evaluated herein.

11.2.3 Mass Estimates and Design Maturity

The mass estimates for the SM Propulsion subsystems and corresponding bases of estimate are provided in the following table.

Hardware Items	Quantity	Unit Mass (lbm)	Growth (%)	Total Mass (lbm)	CM Mass (lbm)	SM Mass (lbm)	Basis of Estimate
SM Propulsion				**24,116**	**0**	**24,116**	
Helium System	1		18%	580.2		580.2	
Isolation Valves	9	8	10%				Similar to Valvetech p/n 12178
Regulators (proportional)	4	5	10%				Similar to shuttle oms regulators
Relief Valves	2	5	10%				Similar to Shuttle OMS burst disk/relief valve combos
Tanks	2	195	20%				4500 psi COPV
Propellant Feed System	1		19%	1258.4		1258.4	
Main Engine Isolation Valves	2	8	10%				Similar to Shuttle OMS iso valves
RCS Cluster Isolation Valves	16	4	10%				Scaled from similar Moog 53-145
900 lbf Engine Isolation Valves	8	4	10%				Scaled from similar Moog 53-145
Propellant Tank Isolation Valves	4	6	10%				Scaled from Shuttle OMS biprop
Tanks With PMD	4	231	20%				Titanium
Engines and Related Hardware	1		21%	737.4		737.4	
25 lbf Reaction Control	24	9	10%				Aerojet R-1E including valves
900 lbf Reaction Control	4	15	15%				Aerojet R-40B including valves
Main Engine Gimbal Actuators	2	17	20%				Centaur-like
Main Engine	1	300	30%				Human-rated delta-2; a/r = 110; throat gimbal; pc =125 psia
Miscellaneous	1	321	10%	352.8		352.8	15% of dry mass
Usable Oxidizer	1	12764	0%	12764.0		12764.0	NTO, rocket equation
Usable Fuel	1	7736	0%	7736.0		7736.0	MMH, rocket equation
Residual Oxidizer	1	383	0%	383.0		383.0	3% (2% trapped, 0.5% performance margin, 0.5% load inaccuracies)
Residual Fuel	1	232	0%	232.0		232.0	3%
Helium	1	72	0%	72.0		72.0	Isothermal + 20% + initial ullage and lines + what is needed to assure 500 psi final pressure

Table 11.2-9 SM Propulsion Mass Estimates and Bases of Estimate

Shuttle Analog

Part of the validation of system sizing was done using a Shuttle heritage. This Shuttle analogy consisted of using the mass properties of the OMS Pod in a CEV configuration. The Shuttle OMS is very similar in size and capability to the CEV design so it provides a very good baseline for representative component masses. The Shuttle OMS propellant and pressurization tanks were linearly scaled from 90 cubic feet to the CEV requirements of 80 cubic feet. The same was done with the pressurization system. A configuration equivalent to the DAC-2 layout resulted in a dry mass of 2700 lbm with an additional 830 lbm for MLI/thermal blankets, heaters, instrumentation, EPD&C, purge and vent which is not specifically assigned to the propulsion system mass. This compares favorably to the CEV mass estimate generated during DAC-2. The detail can be seen in Table 11.2-10.

Component	Current Shuttle OMS POD Weight (lbs)	Pod Quantity	Total Mass		Pseudo CEV Weight (lbs)	Pod Quantity	Total Mass
Pressurization			**394**				**634**
HE tank	289	1	289	reduce vol	216.8	2	434
LV High Pressure	2.85	2	5.7		2.9	4	11
HE regulator	4.4	2	8.8		4.4	4	18
LV Low Pressure	2.4	2	4.8		2.4	4	10
Check Valve	2.9	2	5.8		2.9	4	12
Fill and Vent lines	4.8	1	4.8			2	
Relief Valve and Burst Disk	5.1	2	10.2		5.1	4	20
Manual Valve	2.3	2	4.6		2.3	4	9
Lines hi press	4.7	1	4.7		4.7	2	9
Lines Low Press	6.8	1	6.8		6.8	2	14
Couplings	5.7	1	5.7		5.7	2	11
RV lines	9.2	1	9.2		9.2	2	18
Test ports and Lines	5.9	1	5.9		5.9	2	12
Installation	28	1	28		28.0	2	56
Propellant Storage			**647**				**1183**
OX/FU tank, Shell, Penetrations and support	260	2	520	reduce vol	232.0	4	928
OX/FU tank, PAD	36.9	2	73.8		36.9	4	148
Gaging System	17.9	2	35.75		17.9	4	72
LV Tank Isolation	4.35	4	17.4		4.5	8	36
Propellant Distribution			**162**				**314**
Lines OME	20	2	40		20	4	80
Lines RCS- Distribution/Crossfeeds	18.5	1	18.5		18.5	2	37
Lines RCS- Manifolds	19.1	1	19.1		19.1	2	38
couplings OME	14.7	2	29.4		14.7	2	29
couplings RCS	8.6	2	17.2		8.6	2	17
Purge&drain	3.1	2	6.2		3.1	4	12
Filll&vent	3.8	2	7.6		3.8	4	15
Installation	12	2	24		12	4	48
Manifold Isolation	4.35	8	34.8		2.3	16	37

Table 11.2-10 Shuttle OMS Analogy

11.2.4 Plan Forward

- Evaluate the main engine isolation and bi-prop valves which are presently shown as motor-operated. Fail-last position valves must be avoided, and "pneumatic" valves may be, all things considered, a better fit for the program.
- Perform duty cycle analysis on RCEs
- R-4D rated for duty cycles in 5%-100% range, some study results have duty cycles less than 5%
- Identify "hard working" thrusters and optimize configuration to distribute thruster work
- Perform analysis of vehicle rates vs. thruster thrust
- May find 100 lbf thrusters are not best size for maneuvering (25 lbf and 200 lbf thrusters are available as well)
- Perform analysis accounting for 900 lbf aft thrusters and effect on RCE duty cycle and controllability
- Integrate efforts with related GN&C and cockpit efforts to develop optimal 6 DOF thruster layout
- Directly support the solid modeling design effort
- Continue refinement of P&ID (e.g., – line sizing and "minor" components), as well as associated hazards analysis

- Refine helium needs analysis
- Continue to develop skills and techniques which will permit the assessment and validation of proposed vendor tank, engine, and valve data
- A higher fidelity look at main engine performance using a two dimensional kinetics code. Those results may provide more insight into what a realistic performance number would be (especially with respect to film cooling requirements).
- A sensitivity study of Isp on the Service Module would also be helpful. If an Isp efficiency of 94.3% is not achievable, the reduced Isp might be offset by the down side of the larger engine required to hit the target Isp.
    - A larger area ratio nozzle (such as an AR = 150) would result in a longer (and heavier) engine, a longer (and heavier) interstage adapter, and may exceed the current tooling limits of the vendor (driving up development time and engine cost)
    - For reference, at an area ratio of 110 and an Isp efficiency of 93.6%, the Isp would be 320.5 lbf-s/lbm

12.0 Team Listing

Discipline	Name	Center Affiliation	Discipline	Name	Center Affiliation
Study Lead	**Jim Geffre**	**JSC**	Electrical Power	Tom Goodnight	GRC
Aerodynamics	**Jim Greathouse**	**JSC**	Electrical Power	Chuck Haynes	JSC
Aerothermal	**Randy Lillard**	**JSC**	Electrical Power & Integrated Analysis Lead	Jeff Hojnicki	GRC
ATCS	**Mike Ewert**	**JSC**	Electrical Power	Tom Kerslake	GRC
ATCS	Seth Alberts	JSC	Electrical Power	Ramon Lebron-Velilla	GRC
ATCS	Alex Bengoa	KSC	Electrical Power	Dan Mayes	JSC
ATCS	A. J. Hanford	JSC	Electrical Power	Dave McCurdy	GRC
ATCS	Eric Malroy	JSC	Electrical Power	Nelson Morales	GRC
ATCS	Brian Motil	GRC	Electrical Power	David Nawrocki	GRC
ATCS	Quoc Nguyen	JSC	Integrated Analysis	Terrian Nowden	GRC
ATCS	Ryan Stephan	JSC	Electrical Power	Mike Politi	GRC
ATCS	George Tuan	JSC	Integrated Analysis	Carlos Rodriguez	GRC
ATCS	Matt Vogel	JSC	Electrical Power	Lizalyn Smith	GRC
ATCS	Xiao-Yen Wang	GRC	Electrical Power	Scott Woodard	JSC
ATCS	Gregg Weaver	JSC	Electrical Power	Reza Zinolabedini	GRC
ATCS	David Westheimer	JSC	**EVA & Crew Survival**	**Joey Marmolejo**	**JSC**
ATCS	Jim Yuko	GRC	EVA & Crew Survival	Brian Daniel	JSC
Avionics	**Helen Neighbors**	**JSC**	EVA & Crew Survival	Tammie Mcgrath	JSC
Avionics	David Allega	JSC	**FCE**	**Larry Spector**	**JSC**
Avionics	Joel Busa	JSC	FCE	Jennifer Villarreal	JSC
Avionics	Colleen Crawford	JSC	**GN&C**	**David Saley**	**JSC**
Avionics	Ralph David	JSC	GN&C	Tim Crain	JSC
Avionics	Jason Gibson	JSC	GN&C	Susan Gomez	JSC
Avionics	Coy Kouba	JSC	GN&C	Rodolfo Gonzalez	JSC
Avionics	Jonathan Lapin	JSC	GN&C	Scott Tamblyn	JSC
Avionics	David Miller	JSC	**LAS**	**Mike Lindell**	**LaRC**
Avionics	Hai Nguyen	JSC	**LAS**	**Ben Neighbors**	**MSFC**
Avionics	Sharada Vitalpur	JSC	LAS	Jeff Adams	MSFC
Avionics	Randy Wade	JSC	LAS	Byron Bartlow	MSFC
CAD/Vehicle Layout	**Ann Bufkin**	**JSC**	LAS	Marlon Batey	LaRC
CAD/Vehicle Layout	Jason Haratyk	JSC	LAS	Sherry Cantrell	MSFC
CAD/Vehicle Layout	Liana Rodriggs	JSC	LAS	Garfield Creary	LaRC
CM RCS	**Victor Spencer**	**JSC**	LAS	Mark Davis	MSFC
CM RCS	Mike Baine	JSC	LAS	Joe Gasbarre	MSFC
Cockpit Working Group	**Jim Ratliff**	**JSC**	LAS	Steve Harvison	MSFC
Cockpit Working Group	Jeff Fox	JSC	LAS	Jim Hawkins	MSFC
Cockpit Working Group	Lee Morin	JSC	LAS	Mark Kearney	MSFC
Cockpit Working Group	Christie Sauers	JSC	LAS	Doug Kramer	MSFC
ECLSS	**Molly Anderson**	**JSC**	LAS	Robert Kwas	MSFC
ECLSS	Jim Broyan	JSC	LAS	Melvin Lucy	LaRC
ECLSS	Bruce Duffield	JSC	LAS	Rumaasha Maasha	MSFC
Electrical Power	**Karla Bradley**	**JSC**	LAS	Noah Rhys	MSFC
Electrical Power	Rob Button	GRC	LAS	Darron Rice	MSFC
Electrical Power	Dan Catalano	GRC	LAS	Joe Ruf	MSFC
Electrical Power	Tom Cressman	GRC	LAS	Todd Steadman	MSFC
Electrical Power	Eric Darcy	JSC	LAS	Josh Wilson	MSFC

Team Discipline Lead
CEV Functional Area/Subsystem Manager
Team Member

Table 12.0-1 CRC-3 Team Listing

Discipline	Name	Center Affiliation	Discipline	Name	Center Affiliation
Landing System	**Robin Tutterow**	**LaRC**	Structures	Wayne Jermstad	JSC
Landing System	Frank Boyer	LaRC	Structures	Chip McCann	JSC
Landing System	Garfield Creary	LaRC	Structures	Dave McCurdy	GRC
Landing System	Robert Frisbee	JPL	Structures	Jim McMichael	JSC
Landing System	Ravi Prakash	JPL	Structures	Jim Meehan	JSC
Landing System	Gurkirpal Singh	JPL	Structures	Nelson Morales	GRC
Landing System	Josh St. Vaughn	JPL	Structures	Marshall Neipert	JSC
Mechanisms	**Brandan Robertson**	**JSC**	Structures	Galen Overstreet	JSC
Mechanisms	Dan Catalano	GRC	Structures	Ross Patterson	JSC
Mechanisms	Alison Dinsel	JSC	Structures	Katy Powell	JSC
Mechanisms	Brent Evernden	JSC	Structures	Ben Quasius	JSC
Mechanisms	Ross Patterson	JSC	Structures	Tim Roach	GRC
Mechanisms	Jeff Polack	GRC	Structures	Lizalyn Smith	GRC
Mechanisms	Paul Solano	GRC	Structures	Ted Tsai	JSC
Parachute System	**Koki Machin**	**JSC**	Structures	Warren Tyree	JSC
Parachute System	Pete Cuthbert	JSC	Structures	C. J. Walthall	JSC
Parachute System	Chris Madsen	JSC	Structures	Reza Zinolabedini	GRC
PTCS	**Stephen Miller**	**JSC**	**TPS**	**Paul Wercinski**	**ARC**
PTCS	Angel Alvarez-Hernandez	JSC	TPS	Jeff Bowles	ARC
PTCS	Scott Coughlin	JSC	TPS	Lynn Bowman	LaRC
PTCS	Brian Motil	GRC	TPS	Y-K Chen	ARC
PTCS	Xiao-Yen Wang	GRC	TPS	Scott Coughlin	ARC
PTCS	Jim Yuko	GRC	TPS	Keith Davis	LaRC
Pyrotechnics	**Matt Maples**	**JSC**	TPS	Todd Denkins	LaRC
Pyrotechnics	Frank Salazar	JSC	TPS	Pat Dunlap	GRC
Requirements Validation	**Christie Sauers**	**JSC**	TPS	Josh Feinkbeiner	GRC
SM Propulsion	**Rex Delventhal**	**GRC**	TPS	Peter Gage	ARC
SM Propulsion	Mike Baine	JSC	TPS	Steve Gayle	LaRC
SM Propulsion	Kevin Dickens	GRC	TPS	Dave Hahne	JPL
SM Propulsion	Bryan Fraser	GRC	TPS	Chip Holloway	LaRC
SM Propulsion	Julie Grantier	GRC	TPS	Loc Huynh	ARC
SM Propulsion	Tyler Hickman	GRC	TPS	John Kowal	JSC
SM Propulsion	David Jacobson	GRC	TPS	Chris Lang	LaRC
SM Propulsion	Shane Malone	GRC	TPS	Ron Lewis	JSC
SM Propulsion	Dave McCurdy	GRC	TPS	Kathy McGuire	ARC
SM Propulsion	Leah McIntyre	GRC	TPS	Mike Meachum	JPL
SM Propulsion	Eric Pencil	GRC	TPS	Frank Milos	ARC
SM Propulsion	Chuck Pierce	MSFC	TPS	Carl Poteet	LaRC
SM Propulsion	Frank Quinn	GRC	TPS	Ravi Prakash	JPL
SM Propulsion	Al Seigneur	GRC	TPS	Marc Rezin	ARC
Structures - CM	**Ronny Baccus**	**JSC**	TPS	Alvaro Rodriguez	JSC
Structures - SM/SA	**Tom Cressman**	**GRC**	TPS	Tom Squire	ARC
Structures	Tom Anderson	JSC	TPS	Josh St. Vaughn	JPL
Structures	Alison Dinsel	JSC	TPS	Bruce Steinetz	GRC
Structures	Brent Evernden	JSC	TPS	Frank Vause	LaRC
Structures	Josh Figuered	JSC	TPS	Mike Wright	ARC
Structures	Tom Goodnight	GRC	**Trajectories**	**Joey Broome**	**JSC**
Structures	Jeff Hagen	JSC	Trajectories	Mike Tigges	JSC
Structures	Nick Jensen	JSC			

Team Discipline Lead
CEV Functional Area/Subsystem Manager
Team Member

Table 12.0-1 CRC-3 Team Listing, Concluded

13.0 CRC-3 Master Equipment List

Table 13.0-1 Crew Module Detailed Mass Properties

CEV CREW MODULE - CRC-3 FINAL CONFIGURATION - 4 CREW LUNAR SORTIE - LAUNCH CONFIGURATION - MASS PROPERTIES REPORT

DESCRIPTION	Unit Mass (lbm)	Qty	CBE Mass (lbm)	Growth %	Growth Mass (lbm)	Predicted Mass (lbm)	Center of Gravity X (in)	Center of Gravity Y (in)	Center of Gravity Z (in)	Moments of Inertia Ixx ($slug\text{-}ft^2$)	Moments of Inertia Iyy ($slug\text{-}ft^2$)	Moments of Inertia Izz ($slug\text{-}ft^2$)	Products of Inertia Ixy ($slug\text{-}ft^2$)	Products of Inertia Ixz ($slug\text{-}ft^2$)	Products of Inertia Iyz ($slug\text{-}ft^2$)
AVIONICS			552.9	11.7%	64.7	617.6	118.4	0.7	-18.6	471	402	166	6	-46	45
Command & Data Handling			214.0	10.0%	21.4	235.4									
FCC (Flight Critical Computer)	49.00	3	147.0	10.0%	14.7	161.7	138.9	-14.4	-59.3	123	100	30	-4	-14	24
Data Storage Unit	22.00	1	22.0	10.0%	2.2	24.2	158.0	34.5	-38.5	11	9	10	5	-4	-5
DAU (Data Acquisition Unit)	15.00	3	45.0	10.0%	4.5	49.5	134.1	16.9	-56.8	38	29	13	3	-1	-7
Comm & Tracking			225.1	13.2%	29.8	254.9									
Video Panel	6.00	1	6.0	20.0%	1.2	7.2	130.9	0.5	-68.5	6	6	0	0	0	0
Crew Audio Interface			16.5	20.0%	3.3	19.8									
Headsets (6 Hardline And 4 Wireless)	0.25	10	2.5	20.0%	0.5	3.0	130.1	1.1	-0.5	0	0	0	0	0	0
Headset Control Unit (2)	3.00	2	6.0	20.0%	1.2	7.2	130.1	1.1	-0.5	0	0	0	0	0	0
Speakers (2)	4.00	2	8.0	20.0%	1.6	9.6	130.1	1.1	-0.5	0	0	0	0	0	0
Comm Equipment			192.6	12.6%	24.3	216.9									
S-band Transponder	12.00	2	24.0	5.0%	1.2	25.2	104.2	-34.3	-41.7	13	11	11	5	5	7
Ka-band Transceiver	12.00	1	12.0	5.0%	0.6	12.6	108.4	34.9	-44.8	7	5	5	-2	2	-3
S-band Low Gain Antenna + Mount	2.00	3	6.0	20.0%	1.2	7.2	100.9	0.0	0.0	6	4	4	0	0	0
S-band Antenna Electronics	6.00	3	18.0	20.0%	3.6	21.6	147.2	46.5	-63.4	24	16	11	3	-4	-12
S-band Medium Gain Antenna	25.00	2	50.0	12.0%	6.0	56.0	136.5	0.0	0.0	86	74	13	0	0	30
S-band MGA Electronics	18.00	2	36.0	12.0%	4.3	40.3	120.1	-6.7	-51.1	33	24	20	-7	2	8
S-band Prox Ops Antenna + Mount	2.00	2	4.0	20.0%	0.8	4.8	83.5	0.0	-0.4	2	3	4	0	0	-1
S-band Prox Ops Antenna Electronics	10.00	2	20.0	12.0%	2.4	22.4	129.9	-45.4	-48.9	20	12	13	0	-1	10
SARSAT Xmit Beacon	3.60	1	3.6	20.0%	0.7	4.3	95.0	-31.3	-37.0	2	2	2	1	1	1
SARSAT Xmit Beacon Antenna and Cable	0.50	1	0.5	20.0%	0.1	0.6	63.0	0.0	0.0	0	1	1	0	0	0
UHF/VHF ATC Antenna	3.00	2	6.0	20.0%	1.2	7.2	72.7	0.0	0.0	0	5	5	0	-1	0
UHF/VHF ATC Antenna Electronics	1.25	2	2.5	5.0%	0.1	2.6	124.9	-40.0	-49.3	2	2	1	0	0	1
UHF/VHF ATC Comm	10.00	1	10.0	20.0%	2.0	12.0	142.8	23.5	-65.0	10	9	2	1	-2	-3
Crash-Survivable Flight Data Recorder	10.00	1	10.0	10.0%	1.0	11.0	131.0	12.2	-69.5	9	9	0	0	0	-2
Displays & Controls			113.8	11.9%	13.5	127.3									
Display w/ Edge Keys - Center	7.00	2	14.0	20.0%	2.8	16.8	107.1	0.0	48.3	11	13	2	0	-5	0
Display w/ Edge Keys - CDR/PLT	6.00	4	24.0	20.0%	4.8	28.8	107.3	0.0	47.7	20	22	5	0	-8	0
Translational Hand Controller	5.60	2	11.2	5.0%	0.6	11.8	114.9	-9.5	41.9	7	7	2	0	-2	-1
Rotational Hand Controller	10.30	2	20.6	5.0%	1.0	21.6	118.7	14.0	30.5	9	7	3	-1	-2	2
Keypad	5.00	2	10.0	5.0%	0.5	10.5	112.6	-0.5	42.1	6	6	1	0	-2	0
Switch Panel	10.00	2	20.0	5.0%	1.0	21.0	134.6	2.5	57.6	17	15	5	0	-5	0
Peripheral Bus Bridge	2.00	2	4.0	20.0%	0.8	4.8	105.1	11.0	45.1	3	4	1	0	-1	1
C&W Panel	10.00	1	10.0	20.0%	2.0	12.0	111.8	-7.9	41.2	6	7	1	0	-2	-1
GN&C			163.3	8.6%	14.1	177.4	86.8	9.0	8.6	75	127	126	-18	-32	2
Inertial Navigation Sensors			72.6	8.0%	5.8	78.4									
Inertial Measurement Unit	9.04	4	36.2	10.0%	3.6	39.8	89.0	38.0	3.6	14	17	27	-13	-4	3
GPS Receiver	5.00	3	15.0	5.0%	0.8	15.8	84.2	29.9	-22.9	4	8	10	-5	2	-2
GPS Antenna	0.30	6	1.8	20.0%	0.4	2.2	116.6	0.1	0.1	3	2	1	0	0	0
Low Noise Amplifier	0.30	6	1.8	10.0%	0.2	2.0	116.6	0.1	0.1	2	2	1	0	0	0
Star Tracker	5.95	3	17.9	5.0%	0.9	18.7	76.6	1.8	-0.2	5	15	14	0	-1	0
Relative Navigation Sensors			80.0	9.7%	7.8	87.7									
Lidar Optical Unit	7.17	2	14.3	10.0%	1.4	15.8	80.8	11.3	40.3	8	16	9	-2	-8	2
Lidar Avionics Processing Unit	14.11	2	28.2	10.0%	2.8	31.0	82.2	0.0	35.5	15	28	19	0	-14	0
Optical Camera: Short Range	1.50	4	6.0	10.0%	0.6	6.6	65.6	-10.2	6.6	1	7	7	1	-1	0
Optical Camera Avionics: Short Range	4.50	2	9.0	10.0%	0.9	9.9	85.4	-16.4	25.3	4	7	6	2	-3	-1
Optical Camera: Long Range	4.50	2	9.0	10.0%	0.9	9.9	78.5	1.4	2.4	4	7	9	0	-1	-2
Optical Camera Avionics: Long Range	4.50	2	9.0	10.0%	0.9	9.9	83.5	0.0	-0.4	3	5	8	0	-1	-1
Optical Spotlight	4.40	1	4.4	5.0%	0.2	4.6	56.2	0.0	0.0	0	6	6	0	-1	0
Recovery System Sensors			10.8	5.0%	0.5	11.3									
Terminal Landing Velocimeter	3.00	2	6.0	5.0%	0.3	6.3	141.8	-65.1	-46.2	8	2	6	-1	-1	3
Terminal Landing Velocimeter Antennas	1.00	4	4.0	5.0%	0.2	4.2	164.9	0.0	0.0	3	3	3	0	0	0
Entry Phase Pressure Transducer	0.25	3	0.8	5.0%	0.0	0.8	84.2	26.5	-13.3	0	0	0	0	0	0

CEV CREW MODULE - CRC-3 FINAL CONFIGURATION - 4 CREW LUNAR SORTIE - LAUNCH CONFIGURATION - MASS PROPERTIES REPORT

DESCRIPTION	Unit Mass (lbm)	Qty	CBE Mass (lbm)	Growth %	Growth Mass (lbm)	Predicted Mass (lbm)	Center of Gravity X (in)	Center of Gravity Y (in)	Center of Gravity Z (in)	Moments of Inertia Ixx (slug-ft^2)	Moments of Inertia Iyy (slug-ft^2)	Moments of Inertia Izz (slug-ft^2)	Products of Inertia Ixy (slug-ft^2)	Products of Inertia Ixz (slug-ft^2)	Products of Inertia Iyz (slug-ft^2)
ACTIVE THERMAL CONTROL			505.7	12.8%	64.8	570.5	139.6	-4.4	-49.4	456	284	257	13	-47	2
Heat Acquisition			219.9	14.0%	30.7	250.6									
Cabin Heat Exchanger	52.30	1	52.3	5.0%	2.6	54.9	142.9	-58.1	-31.6	49	9	44	-8	-3	17
Cabin Heat Exchanger Fan Assembly	36.20	1	36.2	5.0%	1.8	38.0	131.9	-58.9	-32.1	35	5	30	0	0	12
Suit Air Loop Heat Exchanger	31.20	1	31.2	20.0%	6.2	37.4	122.5	-37.2	-42.9	22	11	13	3	2	11
Liquid Cooling Garment (LCG) Heat Exchanger	4.80	1	4.8	20.0%	1.0	5.8	122.4	-38.2	-50.7	4	2	2	0	0	2
LCG Water Pump, Controls & QDs	4.20	2	8.4	20.0%	1.7	10.1	147.7	-3.1	-50.3	8	5	5	0	-2	0
Cold Plates - Flight Computer (large)	7.10	1	13.0	20.0%	2.6	15.6	139.1	0.0	-71.1	14	15	1	0	-2	0
Cold Plates - Flight Computer (small)		1	5.7	20.0%	1.1	6.8	140.3	-48.0	-56.5	7	4	4	-1	-1	4
Cold Plates - SPDU		1	18.6	20.0%	3.7	22.3	157.4	2.0	-40.5	5	10	4	0	-4	0
Cold Plates - DAU #1		1	2.4	20.0%	0.5	2.9	153.8	47.5	-53.5	3	2	2	1	-1	-1
Cold Plates - DAU #2		1	2.4	20.0%	0.5	2.9	122.9	29.3	-61.6	2	2	1	0	0	-1
Cold Plates - DAU #3		1	2.4	20.0%	0.5	2.9	122.9	-22.8	-64.3	2	2	0	0	0	1
Cold Plates - PTCU		1	3.5	20.0%	0.7	4.2	78.8	-7.9	-35.1	1	3	3	0	1	0
Cold Plates - Comm Electronics #1	4.00	1	10.1	20.0%	2.0	12.1	101.9	36.8	-41.1	6	5	6	-3	3	-3
Cold Plates - Comm Electronics #2	4.00	1	9.6	20.0%	1.9	11.6	146.0	-45.1	-61.9	13	8	6	-2	-2	6
Cold Plates - Comm Electronics #3	4.00	1	10.1	20.0%	2.0	12.1	101.9	-37.8	-40.3	7	5	6	3	2	3
Cold Plates - Comm Electronics #4	4.00	1	9.2	20.0%	1.8	11.1	146.0	45.3	-61.7	12	8	5	2	-2	-6
Fluid Loop			183.0	10.8%	19.7	202.7									
Pump Package	32.00	2	64.0	5.0%	3.2	67.2	145.3	-3.1	-50.3	56	31	33	-5	-8	0
Isolation Valve (CM to SM)	4.20	4	16.8	5.0%	0.8	17.6	132.7	1.5	-78.7	19	19	0	0	0	0
Check Valve	2.00	2	4.0	5.0%	0.2	4.2	132.7	1.5	-78.7	5	5	0	0	0	0
Mixing Valve (Automatic & Manual)	13.90	2	27.8	5.0%	1.4	29.2	106.0	0.0	-53.0	13	17	4	0	7	0
Set Point Temperature Sensor	0.10	4	0.4	20.0%	0.1	0.5	154.9	0.0	-37.3	0	0	0	0	0	0
Temperature Sensors	0.10	80	8.0	20.0%	1.6	9.6	154.9	0.0	-37.0	2	3	1	0	-1	0
Pressure Sensors	1.00	8	8.0	20.0%	1.6	9.6	154.9	0.0	-38.0	2	3	1	0	-2	0
Plumbing	54.00	1	54.0	20.0%	10.8	64.8	145.3	-3.1	-50.3	26	29	3	-1	-9	2
Fluid Evaporator			102.8	13.9%	14.3	117.1									
Evaporative Heat Sink (inc. Controls)	50.00	1	50.0	15.0%	7.5	57.5	152.8	63.7	-47.0	69	26	55	17	-11	-31
Vacuum Duct	12.60	1	12.6	5.0%	0.6	13.2	152.8	63.7	-47.0	16	6	13	4	-2	-7
Vacuum Duct Heater	0.60	2	1.2	5.0%	0.1	1.3	152.8	63.7	-47.0	1	1	1	0	0	-1
Water Supply Line	3.00	1	3.0	20.0%	0.6	3.6	152.7	48.2	-61.6	4	3	2	1	-1	-2
Water Tank	21.00	1	21.0	15.0%	3.2	24.2	152.6	32.8	-76.2	31	28	8	4	-8	-11
Refrigerant Supply Line	3.00	1	3.0	20.0%	0.6	3.6	152.2	15.6	-61.6	2	3	1	0	-1	-1
Refrigerant Tank	12.00	1	12.0	15.0%	1.8	13.8	151.7	-32.4	-76.2	18	16	5	-2	-4	7
ENVIRONMENTAL CONTROL & LIFE SUPPORT			516.0	11.9%	61.2	577.2	132.5	13.6	-30.4	444	260	253	30	29	-15
Cabin Loop Air Recirculation			13.9	5.0%	0.7	14.6									
HEPA Filter	1.00	1	1.0	5.0%	0.1	1.1	131.9	-58.9	-32.1	1	0	1	0	0	0
Internal Cabin Ducting	8.90	1	8.9	5.0%	0.4	9.3	159.6	0.0	-30.8	8	1	7	0	0	3
Post Landing Ventilation Valves	2.00	2	4.0	5.0%	0.2	4.2	159.6	-15.2	-30.8	4	4	2	1	-2	-2
Suit Loop Air Revitalization			188.7	15.8%	29.9	218.6									
HEPA Filter	1.00	1	1.0	5.0%	0.1	1.1	123.2	38.0	-48.3	1	0	0	0	0	0
Guard Bed	33.10	1	33.1	20.0%	6.6	39.7	123.2	38.0	-48.3	26	15	12	-2	3	-13
Swing Bed Compressor	4.10	3	12.3	15.0%	1.8	14.1	116.7	0.0	-59.8	9	9	1	0	2	0
Amine Swing Bed + Two Manual Valves	17.90	5	89.5	15.0%	13.4	102.9	124.2	0.0	-60.0	63	64	3	0	8	1
Cabin Inlet Valve	2.00	1	2.0	15.0%	0.3	2.3	116.7	0.0	-59.8	1	1	0	0	0	0
Nitrogen Sweep Valves	1.00	3	3.0	15.0%	0.5	3.5	116.7	0.0	-59.8	2	2	0	0	1	0
Nitrogen Sweep Lines	1.50	2	3.0	15.0%	0.5	3.5	124.7	0.0	-69.2	3	3	0	0	0	0
Cabin Outlet Shutoff Valve	2.00	1	2.0	15.0%	0.3	2.3	116.7	0.0	-59.8	1	1	0	0	0	0
Humidity Vent Line Heater	1.30	1	1.3	15.0%	0.2	1.5	124.7	0.0	-69.2	1	1	0	0	0	0
Vent Line	11.40	1	11.4	15.0%	1.7	13.1	124.7	0.0	-69.2	11	11	0	0	1	0
Internal Cabin Ducting	30.10	1	30.1	15.0%	4.5	34.6	125.1	-6.1	-54.0	20	17	4	0	2	2
Water Management			15.0	0.0%	0.0	15.0									
Water Heater and Accumulator	15.00	1	15.0	0.0%	0.0	15.0	137.6	-66.1	-17.1	15	1	15	-1	0	2
Gas Management & Pressure Control			133.0	15.7%	20.9	153.9									
Oxygen Surge Tank	4.70	1	4.7	20.0%	0.9	5.6	155.0	-59.3	-52.5	7	3	5	-2	-1	3

CEV CREW MODULE - CRC-3 FINAL CONFIGURATION - 4 CREW LUNAR SORTIE - LAUNCH CONFIGURATION - MASS PROPERTIES REPORT															
	Unit		CBE	Growth	Growth	Predicted	Center of Gravity			Moments of Inertia			Products of Inertia		
DESCRIPTION	Mass	Qty	Mass	%	Mass	Mass	X	Y	Z	Ixx	Iyy	Izz	Ixy	Ixz	Iyz
	(lbm)		(lbm)		(lbm)	(lbm)	(in)	(in)	(in)	(slug-ft^2)	(slug-ft^2)	(slug-ft^2)	(slug-ft^2)	(slug-ft^2)	(slug-ft^2)
Pressure Controller	15.00	1	15.0	20.0%	3.0	18.0	106.0	0.0	-53.0	8	11	2	0	4	0
Negative Pressure Relief Valve	1.00	2	2.0	15.0%	0.3	2.3	106.0	0.0	-53.0	1	1	0	0	1	0
Positive Pressure Relief Valve	1.00	2	2.0	15.0%	0.3	2.3	106.0	0.0	-53.0	1	1	0	0	1	0
Vent Valve	2.00	1	2.0	15.0%	0.3	2.3	106.0	0.0	-53.0	1	1	0	0	1	0
Controlled N2 Valves	4.00	3	12.0	15.0%	1.8	13.8	106.0	0.0	-53.0	6	8	2	0	3	0
Controlled O2 Valves	4.00	3	12.0	15.0%	1.8	13.8	106.0	0.0	-53.0	6	8	2	0	3	0
Check Valves	0.50	4	2.0	15.0%	0.3	2.3	106.0	0.0	-53.0	1	1	0	0	1	0
Emergency Feed Pressure Regulator Valve	4.00	1	4.0	15.0%	0.6	4.6	106.0	0.0	-53.0	2	3	1	0	1	0
Demand Regulator	1.00	2	2.0	15.0%	0.3	2.3	124.7	0.0	-69.2	2	2	0	0	0	0
Suit Loop Purge Valve	4.00	2	8.0	15.0%	1.2	9.2	124.7	0.0	-69.2	8	8	0	0	1	0
Docking Vent Valve	1.00	1	1.0	15.0%	0.2	1.2	58.5	0.0	0.0	0	1	1	0	0	0
Docking Pressure Equalization Valve	1.00	2	2.0	15.0%	0.3	2.3	58.5	0.0	0.0	0	3	3	0	0	0
Docking Pressure Equalization Tubing	0.26	1	0.3	15.0%	0.0	0.3	58.5	0.0	0.0	0	0	0	0	0	0
Umbilical Interface Panel (EVA Spots)	12.00	2	24.0	15.0%	3.6	27.6	145.1	68.4	25.3	33	7	28	6	3	13
Umbilical Interface Panel (IVA Only Spots)	8.00	4	32.0	15.0%	4.8	36.8	145.1	0.0	25.3	46	10	39	0	4	0
Umbilical Interface Panel (Contingency Lines)	4.00	1	4.0	15.0%	0.6	4.6	145.1	-68.4	25.3	6	1	5	-1	0	-2
Medical Oxygen Interface	2.00	2	4.0	15.0%	0.6	4.6	145.1	-68.4	25.3	6	1	5	-1	0	-2
Fire Detection & Suppression			48.1	7.5%	3.6	51.7									
Fire Detectors	4.41	4	17.6	5.0%	0.9	18.5	140.1	-6.7	41.1	21	10	12	0	2	-1
Water Foam Fire Extinguisher	9.25	2	18.5	5.0%	0.9	19.4	123.1	0.1	50.4	22	14	9	0	-2	0
Nitrogen Release Valves	4.00	3	12.0	15.0%	1.8	13.8	138.0	0.0	-64.0	10	10	0	0	-1	0
Waste Collection System			117.3	5.2%	6.1	123.4									
Toilet and Urinal System	114.80	1	114.8	5.0%	5.7	120.5	151.9	55.1	-22.3	87	22	89	29	-8	-20
Wastewater Vent Line	1.50	1	1.5	15.0%	0.2	1.7	151.9	55.1	-22.3	1	0	1	0	0	0
Wastewater Vent Line Heater	1.00	1	1.0	15.0%	0.2	1.2	151.9	55.1	-22.3	1	0	1	0	0	0
SEATS			100.0	25.0%	25.0	125.0	130.2	0.0	10.1	42	36	12	0	3	-1
Basic Seat Structure - CDR	30.00	1	30.0	25.0%	7.5	37.5	129.5	-17.1	30.7	17	15	4	0	1	-6
Basic Seat Structure - PLT	30.00	1	30.0	25.0%	7.5	37.5	129.5	16.9	30.7	16	15	4	0	1	5
Basic Seat Structure - MS#1	20.00	1	20.0	25.0%	5.0	25.0	131.1	-16.0	-20.7	4	3	2	0	1	1
Basic Seat Structure - MS#2	20.00	1	20.0	25.0%	5.0	25.0	131.1	16.0	-20.7	4	3	2	0	1	-1
PROPULSION			571.9	11.4%	65.1	637.0	145.6	-2.6	42.6	1,008	576	574	-6	94	-14
CM RCS Engine + Igniter	12.20	12	146.4	15.0%	22.0	168.4	136.4	0.0	42.3	272	155	166	0	9	-2
Valve Panels	4.03	3	12.1	15.0%	1.8	13.9	142.1	19.3	48.2	22	10	13	1	2	2
Propellant Feed			413.4	10.0%	41.3	454.7									
Oxygen Tank	32.00	4	128.0	10.0%	12.8	140.8	154.3	0.0	0.0	213	34	213	-1	5	0
Methane Tank	45.00	2	90.0	10.0%	9.0	99.0	154.3	0.0	80.2	175	176	23	-1	43	-2
Lines and Fittings	64.20	1	64.2	10.0%	6.4	70.6	144.7	-1.3	45.2	93	65	53	-1	12	0
Oxidizer Isolation Valves	8.00	4	32.0	10.0%	3.2	35.2	142.4	-10.6	57.8	57	34	25	-1	6	-2
Oxidizer Regulators	6.00	4	24.0	10.0%	2.4	26.4	142.4	-10.6	57.8	43	25	19	-1	4	-1
Oxidizer Crossover Latching Valve	2.00	1	2.0	10.0%	0.2	2.2	142.4	-65.5	47.8	4	2	2	0	0	-2
Oxidizer ECLSS Interconnect Valves	2.00	2	4.0	10.0%	0.4	4.4	142.4	-65.5	47.8	7	3	4	-1	1	-3
Fuel Isolation Valves	8.00	4	32.0	10.0%	3.2	35.2	142.4	-10.6	57.8	57	34	25	-1	6	-2
Fuel Crossover Latching Valve	2.00	1	2.0	10.0%	0.2	2.2	142.4	-65.5	47.8	4	2	2	0	0	-2
Fuel Regulators	6.00	4	24.0	10.0%	2.4	26.4	142.4	-10.6	57.8	43	25	19	-1	4	-1
Oxidizer Fill Valve	1.00	1	1.0	10.0%	0.1	1.1	141.5	79.2	28.8	2	0	1	0	0	1
Fuel Fill Valve	1.00	1	1.0	10.0%	0.1	1.1	141.5	79.2	28.8	2	0	1	0	0	1
Oxidizer Burst Disc & RV	1.00	2	2.0	10.0%	0.2	2.2	142.4	-10.6	57.8	4	2	2	0	0	0
Fuel Burst Disc & RV	1.00	2	2.0	10.0%	0.2	2.2	142.4	-10.6	57.8	4	2	2	0	0	0
Oxidizer Temp Sensor	0.05	4	0.2	10.0%	0.0	0.2	142.4	-10.6	57.8	0	0	0	0	0	0
Fuel Temp Sensor	0.05	4	0.2	10.0%	0.0	0.2	142.4	-10.6	57.8	0	0	0	0	0	0
Oxidizer High Pressure Sensor	0.50	4	2.0	10.0%	0.2	2.2	142.4	-10.6	57.8	4	2	2	0	0	0
Oxidizer Low Pressure Sensor	0.10	4	0.4	10.0%	0.0	0.4	142.4	-10.6	57.8	1	0	0	0	0	0
Fuel High Pressure Sensor	0.50	4	2.0	10.0%	0.2	2.2	142.4	-10.6	57.8	4	2	2	0	0	0
Fuel Low Pressure Sensor	0.10	4	0.4	10.0%	0.0	0.4	142.4	-10.6	57.8	1	0	0	0	0	0

CEV CREW MODULE - CRC-3 FINAL CONFIGURATION - 4 CREW LUNAR SORTIE - LAUNCH CONFIGURATION - MASS PROPERTIES REPORT

DESCRIPTION	Unit Mass (lbm)	Qty	CBE Mass (lbm)	Growth %	Growth Mass (lbm)	Predicted Mass (lbm)	Center of Gravity X (in)	Center of Gravity Y (in)	Center of Gravity Z (in)	Moments of Inertia Ixx (slug-ft^2)	Moments of Inertia Iyy (slug-ft^2)	Moments of Inertia Izz (slug-ft^2)	Products of Inertia Ixy (slug-ft^2)	Products of Inertia Ixz (slug-ft^2)	Products of Inertia Iyz (slug-ft^2)
POWER & WIRING			1,529.0	13.7%	209.5	1,738.4	149.8	0.1	-34.9	681	719	333	-9	-217	36
LithiumIon Rechargeable Battery	55.00	8	440.0	17.0%	74.8	514.8	151.8	0.2	-60.4	378	366	111	-2	-122	5
Lighting			22.0	20.0%	4.4	26.4									
General Internal Lighting	4.40	3	13.2	20.0%	2.6	15.8	125.0	0.0	0.0	0	0	0	0	0	0
Tunnel Adapter Light Assy	4.40	1	4.4	20.0%	0.9	5.3	75.0	0.0	-10.0	0	4	4	0	0	0
External Floodlight	4.40	1	4.4	20.0%	0.9	5.3	150.0	0.0	79.6	9	9	0	0	2	0
Power Management & Distribution			420.8	13.4%	56.4	477.2									
Power Distribution Units (PDUs)	45.00	2	90.0	12.0%	10.8	100.8	156.4	-30.5	-40.3	46	38	36	-17	-18	23
Secondary Power Distribution Units (SPDUs)-Int	74.00	2	148.0	10.0%	14.8	162.8	157.1	13.8	-40.5	45	64	31	12	-30	-15
Secondary Power Distribution Units (SPDUs)-Ext	44.00	2	88.0	10.0%	8.8	96.8	157.1	-10.3	-40.5	26	38	18	-6	-18	8
Power Transfer Converter Unit	13.00	2	26.0	30.0%	7.8	33.8	79.1	-7.9	-35.1	6	26	21	3	11	2
Thruster Controller Unit	16.00	2	32.0	20.0%	6.4	38.4	144.7	8.7	55.9	60	36	28	1	7	0
Utility Outlet Panels	0.40	12	4.8	30.0%	1.4	6.2	135.0	0.0	0.0	0	0	0	0	0	0
Pyro Controller	16.00	2	32.0	20.0%	6.4	38.4	141.4	48.6	45.1	60	34	28	4	4	11
Wiring			646.2	11.4%	73.8	720.0									
Primary Power Wiring Harness	106.00	1	106.0	30.0%	31.8	137.8	150.0	0.0	-25.0	9	20	11	-1	-10	1
Secondary Power Wiring Harness	140.16	1	140.2	30.0%	42.0	182.2	150.0	0.0	-25.0	12	26	14	-1	-13	1
Instrumentation & Avionics Wiring	400.00	1	400.0	0.0%	0.0	400.0	150.0	0.0	-25.0	27	58	31	-2	-29	2
STRUCTURE			3,199.1	24.9%	796.3	3,995.4	132.8	-0.3	-3.0	3,256	2,686	2,586	4	10	-13
Cabin Skin (Cone and Barrel)	256.00	1	256.0	25.0%	64.0	320.0	124.1	-2.1	-1.4	320	198	190	3	-1	-5
Forward Bulkheads	211.10	1	211.1	25.0%	52.8	263.9	85.0	0.0	0.0	101	173	170	3	-19	0
Aft Bulkhead	105.40	1	105.4	25.0%	26.4	131.8	166.6	0.0	0.0	74	74	72	-1	7	0
Ring Frames	492.40	1	492.4	25.0%	123.1	615.5	151.0	0.0	0.0	883	524	517	-3	19	-1
Longerons	210.00	1	210.0	25.0%	52.5	262.5	142.2	0.0	0.0	289	188	185	-1	5	0
Base Heat Shield Carrier Structure	730.00	1	730.0	25.0%	182.5	912.5	168.4	0.0	0.0	1,000	787	777	-8	53	-1
Back Shell Structure	313.20	1	313.2	25.0%	78.3	391.5	111.8	-1.6	-0.5	440	324	312	4	-11	-5
Back Shell Lightning Screen	14.10	1	14.1	0.0%	0.0	14.1	111.8	-1.6	-0.5	16	12	11	0	0	0
Upper/Lower Gussets	264.00	1	264.0	25.0%	66.0	330.0	72.7	0.0	0.0	72	286	282	4	-30	-1
Tunnel Shell and Cap	48.00	1	48.0	25.0%	12.0	60.0	62.7	0.0	0.0	6	64	64	1	-6	0
Forward Windows (panes only)	13.03	2	26.1	25.0%	6.5	32.6	113.0	0.0	58.1	32	32	4	0	-8	0
Secondary Structure	528.84	1	528.8	25.0%	132.2	661.1	129.8	0.0	-20.0	23	23	0	0	2	2
TPS			1,888.0	25.0%	472.0	2,360.0	157.9	-0.3	-3.2	2,790	2,214	2,114	-11	96	-8
Heat Shield Ablator	1,440.00	1	1,440.0	25.0%	360.0	1,800.0	171.2	0.0	0.0	2,135	1,726	1,706	-16	113	-3
Back Shell BRI-18 Panel 4 (1.566")	38.00	1	38.0	25.0%	9.5	47.5	139.9	23.4	-83.7	68	62	9	3	-7	-17
Back Shell BRI-18 Panel 5 (1.566")	38.00	1	38.0	25.0%	9.5	47.5	139.9	-23.4	-83.7	69	62	10	-3	-7	19
Back Shell BRI-8 Forward Bay Cover (0.895")	76.00	1	76.0	25.0%	19.0	95.0	69.9	0.0	-1.1	41	99	99	1	-8	0
Back Shell BRI-8 Panel 4 (1.566")	35.20	1	35.2	25.0%	8.8	44.0	113.0	31.9	-61.6	40	34	17	-4	8	-16
Back Shell BRI-8 Panel 5 (1.566")	35.20	1	35.2	25.0%	8.8	44.0	113.0	-31.9	-61.6	42	34	19	4	8	17
Back Shell BRI-8 Panel 3 (0.98")	42.40	1	42.4	25.0%	10.6	53.0	122.7	69.8	-28.9	65	14	61	-4	1	-16
Back Shell BRI-8 Panel 6 (0.98")	42.40	1	42.4	25.0%	10.6	53.0	122.7	-69.8	-28.9	68	14	64	4	1	17
Back Shell BRI-8 Panels 1, 2, 7, 8 (0.776")	140.80	1	140.8	25.0%	35.2	176.0	122.6	-4.3	51.0	263	170	128	3	-14	-8
PASSIVE THERMAL CONTROL			234.1	17.5%	40.8	274.9	136.5	-1.5	-0.9	231	160	154	1	4	-3
Bulk Insulation	126.00	1	126.0	15.0%	18.9	144.9	136.5	-1.5	-1.0	126	87	84	1	2	-2
Pressure Shell Heater Patch (50 W)	0.14	20	2.7	25.0%	0.7	3.4	136.5	0.0	0.0	0	0	0	0	0	0
Pressure Shell Heater Patch (25 W)	0.07	10	0.7	25.0%	0.2	0.8	136.5	0.0	0.0	0	0	0	0	0	0
Pressure Shell Heater Patch (30 W)	0.08	14	1.1	25.0%	0.3	1.4	136.5	0.0	0.0	0	0	0	0	0	0
Pressure Shell Heater Patch (100 W)	0.27	8	2.2	25.0%	0.5	2.7	136.5	0.0	0.0	0	0	0	0	0	0
Pressure Shell Temp Sensors	0.05	28	1.4	20.0%	0.3	1.7	136.5	0.0	0.0	0	0	0	0	0	0
MLI	100.00	1	100.0	20.0%	20.0	120.0	136.5	-1.5	-1.0	105	72	70	1	2	-1
LANDING SYSTEM			263.7	13.6%	35.9	299.6	154.4	0.0	-40.1	322	220	181	-2	-35	2
Vertical Propulsive System			78.0	20.0%	15.6	93.6									
Rocket #1	19.50	1	19.5	20.0%	3.9	23.4	151.1	80.0	-5.0	32	2	34	8	0	1

CEV CREW MODULE - CRC-3 FINAL CONFIGURATION - 4 CREW LUNAR SORTIE - LAUNCH CONFIGURATION - MASS PROPERTIES REPORT

DESCRIPTION	Unit Mass (lbm)	Qty	CBE Mass (lbm)	Growth %	Growth Mass (lbm)	Predicted Mass (lbm)	Center of Gravity X (in)	Center of Gravity Y (in)	Center of Gravity Z (in)	Moments of Inertia Ixx (slug-ft^2)	Moments of Inertia Iyy (slug-ft^2)	Moments of Inertia Izz (slug-ft^2)	Products of Inertia Ixy (slug-ft^2)	Products of Inertia Ixz (slug-ft^2)	Products of Inertia Iyz (slug-ft^2)
Rocket #2	19.50	1	19.5	20.0%	3.9	23.4	151.1	70.4	-38.3	29	7	26	7	-3	-11
Rocket #3	19.50	1	19.5	20.0%	3.9	23.4	151.1	-80.0	-5.0	33	2	35	-8	0	-1
Rocket #4	19.50	1	19.5	20.0%	3.9	23.4	151.1	-70.4	-38.3	31	7	28	-7	-3	11
Horizontal Propulsive System			87.6	20.0%	17.5	105.1									
Rocket #1	21.90	1	21.9	20.0%	4.4	26.3	148.5	6.5	-82.8	33	34	2	1	-7	-2
Rocket #2	21.90	1	21.9	20.0%	4.4	26.3	148.5	17.3	-81.2	33	33	3	2	-7	-7
Rocket #3	21.90	1	21.9	20.0%	4.4	26.3	148.5	-17.3	-81.2	33	33	4	-2	-7	8
Rocket #4	21.90	1	21.9	20.0%	4.4	26.3	148.5	-6.5	-82.8	33	34	2	-1	-7	3
Miscellaneous Propulsive Subsystems			98.1	2.9%	2.8	100.9									
Crushable Honeycomb Attenuation	84.00	1	84.0	0.0%	0.0	84.0	166.6	0.0	0.0	47	47	46	-1	5	0
Ordnance Controller/Driver Box	3.60	3	10.8	20.0%	2.2	13.0	148.5	0.0	-81.2	15	16	1	0	-4	0
Ordnance Box Cable/Wiring	0.40	3	1.2	20.0%	0.2	1.4	148.5	0.0	-81.2	2	2	0	0	0	0
Ordnance Box Structure	0.70	3	2.1	20.0%	0.4	2.5	148.5	0.0	-81.2	3	3	0	0	-1	0
PARACHUTE SYSTEM			764.0	17.2%	131.5	895.5	75.7	3.7	-5.4	232	694	737	-28	-21	20
Uprighting Airbag	14.00	3	42.0	17.0%	7.1	49.1	71.2	7.3	-10.0	14	44	46	-4	2	3
Forward Aeroshell Jettison Parachute	20.00	1	20.0	25.0%	5.0	25.0	71.5	28.2	-19.3	5	20	23	-9	4	-2
Drogue Parachute	55.50	2	111.0	17.0%	18.9	129.9	75.6	0.0	28.2	45	122	96	2	-55	-1
Pilot Parachute	22.00	3	66.0	17.0%	11.2	77.2	81.4	7.0	-9.6	20	49	53	-5	2	4
Main Parachute	175.00	3	525.0	17.0%	89.3	614.3	75.5	2.7	-11.0	149	460	519	-12	27	15
PYROTECHNICS			245.1	15.6%	38.3	283.4	94.6	8.1	10.2	156	233	226	-11	-46	16
Landing Attenuation			70.0	25.0%	17.5	87.5									
Heatshield Jettison	10.00	4	40.0	25.0%	10.0	50.0	163.0	0.0	0.0	68	45	45	0	2	0
Uprighting Airbag Gas Generator	10.00	3	30.0	25.0%	7.5	37.5	71.2	7.7	-9.6	10	33	35	-3	1	2
Ingress/Egress Hatch Jettison	22.00	1	22.0	25.0%	5.5	27.5	112.3	62.1	25.7	29	9	24	-7	-4	12
Forward Aeroshell Thrusters	6.00	4	24.0	10.0%	2.4	26.4	73.8	0.0	0.0	6	22	22	0	-2	0
Parachutes			129.1	10.0%	12.9	142.0									
Drogue Mortar	21.62	2	43.2	10.0%	4.3	47.6	75.6	0.0	28.2	16	45	35	1	-20	0
Pilot Chute Mortar	12.35	3	37.1	10.0%	3.7	40.8	81.4	7.0	-9.6	10	26	28	-3	1	2
Drogue/Main Release	4.00	12	48.0	10.0%	4.8	52.8	75.1	0.0	29.7	16	52	36	1	-24	0
Reefing Line Cutters	0.04	20	0.8	15.0%	0.1	0.9	75.1	0.0	29.7	0	1	1	0	0	0
MECHANISMS			1,488.2	18.9%	281.8	1,770.0	80.8	8.9	5.3	755	2,057	2,194	-42	-156	105
Low Impact Docking System			765.0	17.7%	135.5	900.5									
LIDS Mechanical Components	600.00	1	600.0	12.0%	72.0	672.0	38.3	0.0	0.0	87	1,297	1,290	14	-98	-1
LIDS Electronics Box	11.67	6	70.0	43.0%	30.1	100.1	48.8	0.0	0.0	10	152	151	2	-13	0
LIDS Hatch	80.00	1	80.0	38.0%	30.4	110.4	58.5	0.0	0.0	5	129	127	2	-13	0
Hatch Mounting/Guide Hardware	15.00	1	15.0	20.0%	3.0	18.0	58.5	0.0	0.0	0	21	20	0	-2	0
Ingress/Egress Hatch	230.00	1	230.0	10.0%	23.0	253.0	112.3	62.1	25.7	271	88	229	-61	-33	109
Heatshield Separation	4.00	8	32.0	25.0%	8.0	40.0	163.0	0.0	0.0	55	36	36	0	2	0
LAS/CM Separation	2.00	4	8.0	25.0%	2.0	10.0	85.0	0.0	0.0	0	5	5	0	-1	0
CM Tension Ties & Compression Pads	8.00	8	64.0	25.0%	16.0	80.0	164.8	0.0	0.0	118	79	78	-1	4	0
Crew Seat Attenuation			288.0	25.0%	72.0	360.0									
Frame Attenuation	148.00	1	148.0	25.0%	37.0	185.0	121.3	0.0	10.8	123	84	85	0	4	-1
Seat Mounting Frame	140.00	1	140.0	25.0%	35.0	175.0	143.3	0.0	5.2	64	33	42	0	6	0
Vents	4.00	3	12.0	25.0%	3.0	15.0	91.0	0.0	0.0	0	5	5	0	-1	0
Umbilicals			1.6	25.0%	0.4	2.0									
CM Connectors to SM	1.00	1	1.0	25.0%	0.3	1.3	132.7	1.5	-78.7	1	1	0	0	0	0
CM Connectors to LAS	0.30	2	0.6	25.0%	0.2	0.8	85.0	0.0	0.0	0	0	0	0	0	0
Forward Bay Aeroshell Jettison			32.0	25.0%	8.0	40.0									
Retention Hardware/Guides	3.00	8	24.0	25.0%	6.0	30.0	73.8	0.0	0.0	7	25	25	0	-3	0
Separation Springs	2.00	4	8.0	25.0%	2.0	10.0	73.8	0.0	0.0	2	8	8	0	-1	0
LIDS Jettison System	55.60	1	55.6	25.0%	13.9	69.5	55.2	0.0	0.0	10	92	91	1	-8	0
TOTAL DRY MASS			12,020.9	19.1%	2,301.0	14,321.9	128.8	1.6	-8.2	10,919	10,668	9,912	-74	-365	176
LUNAR MISSION															

CEV CREW MODULE - CRC-3 FINAL CONFIGURATION - 4 CREW LUNAR SORTIE - LAUNCH CONFIGURATION - MASS PROPERTIES REPORT

DESCRIPTION	Unit Mass (lbm)	Qty	CBE Mass (lbm)	Growth %	Growth Mass (lbm)	Predicted Mass (lbm)	Center of Gravity X (in)	Center of Gravity Y (in)	Center of Gravity Z (in)	Moments of Inertia Ixx (slug-ft^2)	Moments of Inertia Iyy (slug-ft^2)	Moments of Inertia Izz (slug-ft^2)	Products of Inertia Ixy (slug-ft^2)	Products of Inertia Ixz (slug-ft^2)	Products of Inertia Iyz (slug-ft^2)
CREW			818.0	0.0%	0.0	818.0	126.1	3.3	6.5	233	186	81	-5	-3	5
Crewmember - CDR	204.50	1	204.5	0.0%	0.0	204.5	125.9	-13.7	32.3	87	78	18	3	-7	-26
Crewmember - PLT	204.50	1	204.5	0.0%	0.0	204.5	125.9	20.3	32.3	94	78	25	-5	-7	33
Crewmember - MS#1	204.50	1	204.5	0.0%	0.0	204.5	126.3	-12.7	-19.3	23	15	16	2	5	7
Crewmember - MS#2	204.50	1	204.5	0.0%	0.0	204.5	126.3	19.3	-19.3	29	15	23	-5	5	-10
FLIGHT CREW EQUIPMENT			691.2	10.0%	69.1	760.3	134.3	-18.7	-7.4	292	195	393	-98	37	-11
Personal Hygiene			11.9	10.0%	1.2	13.1									
Community Hygiene Kit	8.00	1	8.0	10.0%	0.8	8.8	156.9	-39.5	-2.5	3	1	4	-2	0	0
Emesis Bags	0.13	30	3.9	10.0%	0.4	4.3	156.9	-39.5	-2.5	2	1	2	-1	0	0
Sleeping Restraints	3.50	4	14.0	10.0%	1.4	15.4	160.4	2.9	-7.8	0	3	3	0	0	0
Housekeeping			46.9	10.0%	4.7	51.6									
Vacuum Cleaner	15.00	1	15.0	10.0%	1.5	16.5	159.9	-10.4	-19.4	1	3	3	-1	-1	0
Wet Wipes	0.40	18	7.2	10.0%	0.7	7.9	156.7	-61.3	-5.8	7	1	8	-3	0	0
Dry Wipes	0.20	29	5.7	10.0%	0.6	6.3	156.7	-61.3	-5.8	5	1	6	-2	0	0
Sanitary Wipe Kit	1.00	1	1.0	10.0%	0.1	1.1	154.5	-49.7	-3.7	1	0	1	0	0	0
Towels	0.30	60	18.0	10.0%	1.8	19.8	160.1	-19.7	-5.8	2	4	5	-3	0	0
Crew Provisions / Clothing			112.0	10.0%	11.2	123.2									
Personal Stowage	24.00	4	96.0	10.0%	9.6	105.6	89.9	0.0	-30.7	26	53	51	1	22	1
Tablet PC	4.00	4	16.0	10.0%	1.6	17.6	89.9	0.0	-30.7	2	9	6	0	4	0
IFM Standard Tool Kit	45.70	1	45.7	10.0%	4.6	50.3	158.9	-16.2	-27.3	8	13	12	-5	-6	4
Restraints & Mobility Aids			9.5	10.0%	0.9	10.5									
Bungees	0.25	18	4.5	10.0%	0.5	5.0	157.5	-46.5	-26.9	3	1	3	-1	-1	1
Multiuse Bracket (Bogen Arm)	2.50	2	5.0	10.0%	0.5	5.5	157.5	-46.5	-26.9	3	1	4	-1	-1	1
Food & Food Preparation			294.6	10.0%	29.5	324.1									
Food with packaging - Primary	4.55	55	250.4	10.0%	25.0	275.4	159.1	-31.1	10.3	105	68	134	-52	29	-33
Food with packaging - Contingency	4.55	5	22.8	10.0%	2.3	25.0	157.8	-46.5	-18.9	13	5	16	-7	-2	3
Utensils	0.37	4	1.5	10.0%	0.1	1.6	137.6	-66.1	-17.1	2	0	2	0	0	0
Food Warmer	20.00	1	20.0	10.0%	2.0	22.0	137.6	-66.1	-17.1	22	1	22	-2	0	3
Waste			51.4	10.0%	5.1	56.6									
Food Trash Volume Compartment	0.04	60	2.2	10.0%	0.2	2.4	163.6	34.8	-12.1	1	1	1	1	0	0
Dry Trash Volume Compartment	0.03	60	1.7	10.0%	0.2	1.8	163.6	34.8	-12.1	0	0	1	0	0	0
WCS Supplies	41.52	1	41.5	10.0%	4.2	45.7	163.6	34.8	-12.1	11	11	22	11	-2	-2
Contingency Urine Collection	0.10	60	6.0	10.0%	0.6	6.6	132.0	66.5	-20.0	6	0	6	0	0	-1
Medical Equipment			28.0	10.0%	2.8	30.8									
Medical Kit	10.00	1	10.0	10.0%	1.0	11.0	155.1	-44.5	-10.3	5	1	6	-3	0	0
Contaminant Cleanup Kit	10.00	1	10.0	10.0%	1.0	11.0	155.1	-44.5	-10.3	5	1	6	-3	0	0
Environment Health Monitoring	8.03	1	8.0	10.0%	0.8	8.8	156.4	-44.7	-3.5	4	1	5	-2	0	0
Exercise	22.00	1	22.0	10.0%	2.2	24.2	158.1	-20.4	-19.5	3	5	6	-3	-2	1
Digital Video Camcorder			10.7	10.0%	1.1	11.8									
Digital Video Camcorder	2.00	1	2.0	10.0%	0.2	2.2	156.0	-60.5	-21.4	2	0	2	-1	0	0
Rechargeable Batteries	1.00	2	2.0	10.0%	0.2	2.2	156.0	-60.5	-21.4	2	0	2	-1	0	0
Battery Charger & Power Supply	5.00	1	5.0	10.0%	0.5	5.5	156.0	-60.5	-21.4	5	1	5	-2	0	1
Power Cables	0.50	1	0.5	10.0%	0.0	0.6	156.0	-60.5	-21.4	0	0	1	0	0	0
Video Interface Cables	0.50	1	0.5	10.0%	0.0	0.6	156.0	-60.5	-21.4	0	0	1	0	0	0
Digital Video Storage Media	0.10	7	0.7	10.0%	0.1	0.8	156.0	-60.5	-21.4	1	0	1	0	0	0
Digital Still Camera			12.8	10.0%	1.3	14.1									
Digital Still Camera	3.81	1	3.8	10.0%	0.4	4.2	156.0	-60.5	-21.4	4	1	4	-1	0	1
Rechargeable Battery	0.50	1	0.5	10.0%	0.0	0.6	156.0	-60.5	-21.4	0	0	1	0	0	0
28V Battery Charger and Power Supply	4.60	1	4.6	10.0%	0.5	5.1	156.0	-60.5	-21.4	4	1	5	-2	0	1
28V Input Power Cables	0.50	1	0.5	10.0%	0.0	0.6	156.0	-60.5	-21.4	0	0	1	0	0	0
Camera Power Cables	0.50	1	0.5	10.0%	0.0	0.6	156.0	-60.5	-21.4	0	0	1	0	0	0
Memory Storage Device	0.07	30	2.1	10.0%	0.2	2.3	156.0	-60.5	-21.4	2	0	2	-1	0	0
Camera Flash	0.80	1	0.8	10.0%	0.1	0.9	156.0	-60.5	-21.4	1	0	1	0	0	0
Photo / TV Accessories			14.3	10.0%	1.4	15.7									
Camcorder Accessory Light	0.50	1	0.5	10.0%	0.0	0.6	156.0	-60.5	-21.4	0	0	1	0	0	0

CEV CREW MODULE - CRC-3 FINAL CONFIGURATION - 4 CREW LUNAR SORTIE - LAUNCH CONFIGURATION - MASS PROPERTIES REPORT

DESCRIPTION	Unit Mass (lbm)	Qty	CBE Mass (lbm)	Growth %	Growth Mass (lbm)	Predicted Mass (lbm)	Center of Gravity X (in)	Center of Gravity Y (in)	Center of Gravity Z (in)	Moments of Inertia Ixx (slug-ft^2)	Moments of Inertia Iyy (slug-ft^2)	Moments of Inertia Izz (slug-ft^2)	Products of Inertia Ixy (slug-ft^2)	Products of Inertia Ixz (slug-ft^2)	Products of Inertia Iyz (slug-ft^2)
Mounting Brackets	2.90	2	5.8	10.0%	0.6	6.4	156.0	-60.5	-21.4	5	1	6	-2	0	1
Binoculars, 8 X 20	0.40	1	0.4	10.0%	0.0	0.4	156.0	-60.5	-21.4	0	0	0	0	0	0
Lens Cleaning Kit	0.05	1	0.1	10.0%	0.0	0.1	156.0	-60.5	-21.4	0	0	0	0	0	0
Common Video Interface Unit	2.50	1	2.5	10.0%	0.3	2.8	156.0	-60.5	-21.4	2	0	3	-1	0	1
CVIU power cables	0.50	2	1.0	10.0%	0.1	1.1	156.0	-60.5	-21.4	1	0	1	0	0	0
Video Monitor	4.00	1	4.0	10.0%	0.4	4.4	156.0	-60.5	-21.4	4	1	4	-1	0	1
Lenses			17.4	10.0%	1.7	19.1									
Wide Angle Lens	1.00	1	1.0	10.0%	0.1	1.1	156.0	-60.5	-21.4	1	0	1	0	0	0
Lens Kit	16.36	1	16.4	10.0%	1.6	18.0	156.0	-60.5	-21.4	15	3	17	-6	-1	3
SUITS & CREW SURVIVAL			472.7	10.0%	47.3	520.0	127.8	4.9	10.6	185	134	69	-2	2	15
EVA			361.2	10.0%	36.1	397.3									
Pressure Suit	80.00	4	320.0	10.0%	32.0	352.0	126.1	3.3	6.5	100	80	35	-2	-1	2
Umbilicals (Seated/Suited)	10.30	4	41.2	10.0%	4.1	45.3	135.6	1.7	15.9	24	7	18	0	1	0
Survival Gear			111.5	10.0%	11.2	122.7									
Life Raft	18.30	1	18.3	10.0%	1.8	20.1	132.8	49.3	53.9	26	16	10	0	0	13
Personal Flotation	3.98	4	15.9	10.0%	1.6	17.5	126.1	3.3	6.5	4	3	1	0	0	0
Emergency Breathing Masks	3.50	4	14.0	10.0%	1.4	15.4	146.6	0.0	55.4	13	14	1	0	3	0
Crew Survival Kit	15.82	4	63.3	10.0%	6.3	69.6	126.1	3.3	6.5	17	13	5	0	-1	0
ATCS FLUIDS			135.0	0.0%	0.0	135.0	150.4	5.8	-69.3	156	130	50	1	-36	-12
Propylene Glycol Solution (60%)	36.00	1	36.0	0.0%	0.0	36.0	145.3	-3.1	-50.3	30	17	18	-3	-4	0
Water	63.00	1	63.0	0.0%	0.0	63.0	152.6	32.8	-76.2	80	73	21	9	-20	-30
Refrigerant	36.00	1	36.0	0.0%	0.0	36.0	151.7	-32.4	-76.2	46	40	12	-5	-11	18
ECLSS FLUIDS			631.8	0.0%	0.0	631.8	156.4	11.8	-4.4	58	121	141	41	9	7
CM Oxygen	0.50	1	0.5	0.0%	0.0	0.5	155.0	-59.3	-52.5	1	0	0	0	0	0
Atmosphere Mass at Launch	50.50	1	50.5	0.0%	0.0	50.5	130.0	0.0	-0.1	27	20	19	0	0	0
Water Boxes	15.70	37	580.8	0.0%	0.0	580.8	158.7	12.9	-4.7	31	101	121	41	9	7
TOTAL INERT MASS			14,769.7	16.4%	2,417.4	17,187.0	130.6	1.1	-7.3	11,843	11,434	10,647	-137	-356	180
PROPELLANT			434.0	0.0%	0.0	434.0	152.8	0.0	-6.4	639	290	439	-2	10	0
Usable RCS Propellant			288.4	0.0%	0.0	288.4									
Oxygen	55.25	4	221.0	0.0%	0.0	221.0	154.3	0.0	0.0	334	53	334	-1	8	0
Methane	33.70	2	67.4	0.0%	0.0	67.4	154.3	0.0	80.2	119	119	15	0	30	-1
Retrorocket Propellant			145.6	0.0%	0.0	145.6									
SRM Propellant - Vertical Rocket	15.51	4	62.0	0.0%	0.0	62.0	151.1	0.0	-21.7	83	12	81	0	-4	0
SRM Propellant - Horizontal Rocket	20.90	4	83.6	0.0%	0.0	83.6	148.5	0.0	-82.0	104	106	9	0	-24	1
TOTAL WET MASS			15,203.7	15.9%	2,417.4	17,621.1	131.1	1.1	-7.3	12,482	11,724	11,086	-139	-346	180

Mass Properties are calculated at the module's wet mass center of gravity
Products of Inertia are calculated using a "positive integral" formulation

Table 13.0-2 Service Module Detailed Mass Properties

CEV SERVICE MODULE - CRC-3 FINAL CONFIGURATION - 4 CREW LUNAR SORTIE - LAUNCH CONFIGURATION - MASS PROPERTIES REPORT

DESCRIPTION	Unit Mass (lbm)	Qty	CBE Mass (lbm)	Growth %	Growth Mass (lbm)	Predicted Mass (lbm)	Center of Gravity X (in)	Center of Gravity Y (in)	Center of Gravity Z (in)	Moments of Inertia Ixx (slug-ft^2)	Moments of Inertia Iyy (slug-ft^2)	Moments of Inertia Izz (slug-ft^2)	Products of Inertia Ixy (slug-ft^2)	Products of Inertia Ixz (slug-ft^2)	Products of Inertia Iyz (slug-ft^2)
AVIONICS			99.0	11.8%	11.7	110.7	209.9	-19.2	53.2	196	109	123	12	-14	3
Command & Data Handling			45.0	10.0%	4.5	49.5									
DAU (Data Acquisition Unit)	15.00	3	45.0	10.0%	4.5	49.5	208.5	-84.3	33.5	88	13	80	13	-5	-28
Comm & Tracking			54.0	13.3%	7.2	61.2									
Comm Equipment			54.0	13.3%	7.2	61.2									
S/Ka-band Dual Feed HGA	10.00	1	10.0	8.0%	0.8	10.8	274.8	48.8	48.8	11	12	12	6	6	5
S/Ka-band Antenna Electronics	20.00	1	20.0	8.0%	1.6	21.6	202.3	14.8	94.4	40	42	3	-1	-9	6
S-band Low Gain Antenna + Mount	2.00	3	6.0	20.0%	1.2	7.2	167.7	5.6	-5.6	16	13	13	0	1	1
S-band Antenna Electronics	6.00	3	18.0	20.0%	3.6	21.6	202.2	53.9	79.0	41	30	15	-5	-7	19
ACTIVE THERMAL CONTROL			666.0	19.3%	128.8	794.8	217.2	-3.3	8.8	1,281	768	704	9	-17	-25
GSE Heat Exhanger			17.5	8.4%	1.5	19.0									
GSE Heat Exhanger	13.50	1	13.5	5.0%	0.7	14.2	213.0	30.9	89.9	26	24	3	-1	-3	8
Quick Fluid Disconnect on GSE HX	2.00	2	4.0	20.0%	0.8	4.8	213.0	30.9	89.9	9	8	1	0	-1	3
Radiators			540.8	19.6%	105.8	646.6									
Radiator Isolation Valves (Latching Solenoid)	2.00	16	32.0	20.0%	6.4	38.4	208.4	0.0	0.0	0	2	2	0	0	0
Relief Valves	2.00	8	16.0	5.0%	0.8	16.8	208.4	0.0	0.0	0	1	1	0	0	0
Fairing Radiator	71.85	1	71.9	20.0%	14.4	86.2	179.7	0.0	0.0	188	129	129	1	2	0
Body Radiator	231.67	1	231.7	20.0%	46.3	278.0	208.4	0.0	0.0	608	325	325	1	2	0
Aft Cone Radiator	189.28	1	189.3	20.0%	37.9	227.1	247.3	0.0	0.0	323	196	195	-1	-3	0
Heat Acquisition			53.7	20.0%	10.7	64.4									
SPDU Coldplate	17.90	1	17.9	20.0%	3.6	21.5	209.2	-35.6	89.3	41	36	7	2	-5	-15
TCU Coldplate	17.90	1	17.9	20.0%	3.6	21.5	206.2	-15.1	95.3	41	41	2	1	-7	-7
DAU Coldplate	17.90	1	17.9	20.0%	3.6	21.5	209.3	-89.3	35.5	43	6	38	6	-2	-14
Fluid Loop			54.0	20.0%	10.8	64.8									
Plumbing	54.00	1	54.0	20.0%	10.8	64.8	217.3	-3.3	8.9	1	1	1	0	0	0
ENVIRONMENTAL CONTROL & LIFE SUPPORT			236.5	19.5%	46.1	282.5	210.4	2.2	-29.6	357	368	25	-1	23	5
Gas Management & Pressure Control			236.5	19.5%	46.1	282.5									
Oxygen Tank	63.00	2	126.0	20.0%	25.2	151.2	210.5	0.7	-83.7	249	253	17	0	33	0
Nitrogen Sweep Lines	1.46	1	1.5	15.0%	0.2	1.7	188.5	-10.7	-10.6	0	0	0	0	0	0
Nitrogen Tank	63.00	1	63.0	20.0%	12.6	75.6	210.5	5.4	78.4	96	100	6	-1	-15	6
Insulation and Valves	46.00	1	46.0	17.5%	8.1	54.1	210.5	2.3	-29.7	12	14	2	0	4	-1
PROPULSION			2,482.7	18.0%	446.1	2,928.8	227.5	0.1	0.0	2,384	1,493	1,975	0	-7	1
Engines and Related Hardware			610.0	20.9%	127.4	737.4									
Main Engine	300.00	1	300.0	30.0%	90.0	390.0	282.4	0.0	0.0	45	397	396	-4	-12	0
Main Engine Gimbal Actuators	17.00	2	34.0	20.0%	6.8	40.8	250.2	6.3	0.0	1	9	9	2	-1	0
900 lbf Engines	15.00	4	60.0	15.0%	9.0	69.0	245.1	0.0	0.0	84	89	10	0	-1	0
25 lbf RCS Thruster Assembly	54.00	4	216.0	10.0%	21.6	237.6	206.3	0.0	0.0	570	301	301	1	2	0
Propellant Distribution System			1,060.0	18.7%	198.4	1,258.4									
Main Engine Isolation Valves	8.00	2	16.0	10.0%	1.6	17.6	250.2	6.3	0.0	0	3	3	1	0	0
RCS Cluster Isolation Valves	4.00	16	64.0	10.0%	6.4	70.4	206.3	0.0	0.0	169	88	88	0	1	0
Propellant Tank Isolation Valves	6.00	4	24.0	10.0%	2.4	26.4	219.6	0.0	0.0	16	8	8	0	0	0
900 lbf Engine Isolation Valves	4.00	8	32.0	10.0%	3.2	35.2	245.1	0.0	0.0	43	45	5	0	0	0
MMH Tank	231.00	2	462.0	20.0%	92.4	554.4	219.6	0.0	0.0	418	253	252	0	1	166
NTO Tank	231.00	2	462.0	20.0%	92.4	554.4	219.6	0.0	0.0	418	253	252	0	1	-166
Miscellaneous	320.70	1	320.7	10.0%	32.1	352.8	229.4	0.0	0.0	0	4	4	0	-1	0
Pressurization			492.0	17.9%	88.2	580.2									
Isolation Valves	8.00	9	72.0	10.0%	7.2	79.2	212.2	0.0	0.0	0	2	2	0	0	0
Helium Tank	195.00	2	390.0	20.0%	78.0	468.0	210.7	0.0	0.0	581	41	604	1	3	0
Regulators	5.00	4	20.0	10.0%	2.0	22.0	210.7	0.0	0.0	27	1	27	0	0	0
Relief Valve	5.00	2	10.0	10.0%	1.0	11.0	210.7	0.0	0.0	13	0	14	0	0	0
POWER & WIRING			1,749.4	17.5%	305.7	2,055.1	253.5	13.0	36.3	3,393	3,886	3,072	-133	-307	-66
Battery System			12.2	21.3%	2.6	14.8									

CEV SERVICE MODULE - CRC-3 FINAL CONFIGURATION - 4 CREW LUNAR SORTIE - LAUNCH CONFIGURATION - MASS PROPERTIES REPORT

DESCRIPTION	Unit Mass (lbm)	Qty	CBE Mass (lbm)	Growth %	Growth Mass (lbm)	Predicted Mass (lbm)	Center of Gravity X (in)	Center of Gravity Y (in)	Center of Gravity Z (in)	Moments of Inertia Ixx (slug-ft^2)	Moments of Inertia Iyy (slug-ft^2)	Moments of Inertia Izz (slug-ft^2)	Products of Inertia Ixy (slug-ft^2)	Products of Inertia Ixz (slug-ft^2)	Products of Inertia Iyz (slug-ft^2)
LithiumIon Rechargeable Battery	4.10	2	8.2	17.0%	1.4	9.6	198.8	40.5	87.2	18	16	4	-2	-4	7
Off-Line Charge Regulator	2.00	2	4.0	30.0%	1.2	5.2	198.8	40.5	87.2	10	9	2	-1	-2	4
Solar Arrays			868.0	16.4%	142.7	1,010.7									
Wing	310.80	2	621.6	13.0%	81.1	702.7	311.1	0.0	0.0	1,090	1,799	1,798	-11	-31	-326
SADA Power Harness	8.80	2	17.6	25.0%	4.4	22.0	238.2	42.4	19.6	15	6	12	3	1	1
Stowed Panel Stack Support Truss	48.40	2	96.8	25.0%	24.2	121.0	289.4	0.0	0.0	103	182	182	-1	-4	-3
Stowed Panel Stack Insulation Blanket	66.00	2	132.0	25.0%	33.0	165.0	309.8	0.0	0.0	223	396	396	-2	-7	-70
Power Management & Distribution			486.0	15.5%	75.4	561.4									
Power Distribution Unit (PDU)	45.00	2	90.0	12.0%	10.8	100.8	210.2	-54.3	78.0	191	130	72	15	-20	-91
Secondary Power Distribution Unit (SPDU)	44.00	2	88.0	10.0%	8.8	96.8	209.2	-34.4	86.0	173	152	31	10	-23	-62
Array Regulator Unit	43.00	4	172.0	15.0%	25.8	197.8	202.9	83.9	38.7	363	82	315	-69	-30	125
Thruster Controller Unit	42.00	2	84.0	20.0%	16.8	100.8	205.7	-14.5	91.0	176	178	12	6	-32	-29
Pyro Controller	12.00	2	24.0	20.0%	4.8	28.8	198.3	29.2	90.9	54	52	9	-4	-13	16
SM-to-CM Umbilical	7.00	4	28.0	30.0%	8.4	36.4	166.5	-26.7	-99.7	88	106	31	12	45	22
Wiring			383.2	22.2%	85.0	468.2									
Primary Power Wiring Harness	202.70	1	202.7	30.0%	60.8	263.5	202.3	40.5	87.2	500	433	112	-45	-97	192
Secondary Power Wiring Harness	80.52	1	80.5	30.0%	24.2	104.7	195.3	40.5	87.2	198	180	52	-24	-52	76
Instrumentation & Avionics Wiring	100.00	1	100.0	0.0%	0.0	100.0	202.3	40.5	87.2	190	164	43	-17	-37	73
STRUCTURE			1,819.3	25.0%	454.8	2,274.1	219.1	0.3	1.2	3,025	1,995	1,989	3	10	2
Outer Shell	318.70	1	318.7	25.0%	79.7	398.4	201.7	0.0	0.0	848	489	488	1	4	0
Ring Frames/Longerons	319.00	1	319.0	25.0%	79.8	398.8	241.6	0.0	0.0	444	324	323	-1	-4	0
CM I/F (8 hardpoints & torque box)	443.00	1	443.0	25.0%	110.8	553.8	185.9	0.0	0.0	991	663	662	3	10	0
Prop Tank Support Cone	336.00	1	336.0	25.0%	84.0	420.0	246.3	0.0	0.0	559	343	342	-2	-5	0
OMS Thrust Cone	140.40	1	140.4	25.0%	35.1	175.5	253.7	0.0	0.0	48	65	65	-1	-3	0
Prop Tank Struts	97.20	1	97.2	25.0%	24.3	121.5	184.7	0.0	0.0	130	102	102	1	2	0
Secondary Structure	165.00	1	165.0	25.0%	41.3	206.3	233.8	3.7	12.8	5	11	6	1	5	1
PASSIVE THERMAL CONTROL			91.0	20.0%	18.2	109.2	201.7	0.0	0.0	232	134	134	0	1	0
MLI Insulation	91.00	1	91.0	20.0%	18.2	109.2	201.7	0.0	0.0	232	134	134	0	1	0
PYROTECHNICS			124.5	19.9%	24.8	149.3	198.8	-5.4	-20.3	301	230	167	10	38	18
CM/SM Separation	10.00	4	40.0	10.0%	4.0	44.0	169.7	0.0	0.0	77	65	65	0	1	0
SM/Adapter Separation	30.00	2	60.0	25.0%	15.0	75.0	229.0	0.0	0.0	151	76	76	0	0	0
Umbilicals			24.5	23.8%	5.8	30.3									
CM/SM Umbilical Cutters	11.25	2	22.5	25.0%	5.6	28.1	166.5	-26.7	-99.7	68	82	24	9	35	17
Umbilical Arm Release	2.00	1	2.0	10.0%	0.2	2.2	166.5	-26.7	-99.7	5	6	2	1	3	1
MECHANISMS			274.9	25.0%	68.7	343.6	246.7	2.3	-4.4	435	414	350	11	36	-54
High Gain Antenna Mechanisms			20.0	25.0%	5.0	25.0									
Launch Restraint Release	2.00	1	2.0	25.0%	0.5	2.5	229.9	64.5	64.5	4	2	2	0	0	2
Deployment Actuation	3.00	1	3.0	25.0%	0.8	3.8	229.9	64.5	64.5	6	3	3	0	0	3
Gimbal + Controller	15.00	1	15.0	25.0%	3.8	18.8	229.9	64.5	64.5	32	16	17	2	2	16
Solar Array Wing Deployment			38.0	25.0%	9.5	47.5									
Launch Restraint Release	4.00	2	8.0	25.0%	2.0	10.0	273.6	0.0	0.0	9	10	10	0	0	-4
Deployment Actuation	15.00	2	30.0	25.0%	7.5	37.5	273.6	0.0	0.0	32	37	37	0	-1	-16
Solar Array Wing			89.3	25.0%	22.3	111.7									
Array Stack Restraint/Release	14.10	2	28.2	25.0%	7.1	35.3	273.6	0.0	0.0	30	35	35	0	-1	-15
Array Deployment Synchronization Mechanism	11.77	2	23.5	25.0%	5.9	29.4	273.6	0.0	0.0	25	29	29	0	-1	-13
Swival Hinge Mechanism (Yoke to SADA adapter)	8.80	2	17.6	25.0%	4.4	22.0	273.6	0.0	0.0	19	22	22	0	-1	-9
Saddle Capture Mechanism	10.00	2	20.0	25.0%	5.0	25.0	273.6	0.0	0.0	22	25	25	0	-1	-11
Solar Array Drive Assembly			48.5	25.0%	12.1	60.7									
Single Axis Drive Actuator	19.87	2	39.7	25.0%	9.9	49.7	273.6	0.0	0.0	43	49	49	0	-1	-21
Drive Stepper Motor	2.20	2	4.4	25.0%	1.1	5.5	273.6	0.0	0.0	5	5	5	0	0	-2
Electronic Control Unit	2.20	2	4.4	25.0%	1.1	5.5	273.6	0.0	0.0	5	5	5	0	0	-2
SM Compression Pads	8.00	3	24.0	25.0%	6.0	30.0	169.7	0.0	0.0	52	44	44	0	1	0
SM/Adapter Separation	30.00	1	30.0	25.0%	7.5	37.5	229.0	0.0	0.0	76	38	38	0	0	0

CEV SERVICE MODULE - CRC-3 FINAL CONFIGURATION - 4 CREW LUNAR SORTIE - LAUNCH CONFIGURATION - MASS PROPERTIES REPORT

DESCRIPTION	Unit Mass (lbm)	Qty	CBE Mass (lbm)	Growth %	Growth Mass (lbm)	Predicted Mass (lbm)	Center of Gravity X (in)	Center of Gravity Y (in)	Center of Gravity Z (in)	Moments of Inertia Ixx ($slug\text{-}ft^2$)	Iyy ($slug\text{-}ft^2$)	Izz ($slug\text{-}ft^2$)	Products of Inertia Ixy ($slug\text{-}ft^2$)	Ixz ($slug\text{-}ft^2$)	Iyz ($slug\text{-}ft^2$)
Umbilicals			25.0	25.0%	6.3	31.3									
SM Connector Umbilicals to CM	20.00	1	20.0	25.0%	5.0	25.0	166.5	-26.7	-99.7	60	73	21	8	31	15
Pad Umbilicals	5.00	1	5.0	25.0%	1.3	6.3	166.5	-26.7	-99.7	15	18	5	2	8	4
TOTAL DRY MASS			7,543.3	19.9%	1,504.8	9,048.1	229.6	2.6	8.5	11,605	9,396	8,538	-88	-237	-115
LUNAR MISSION															
ATCS FLUIDS			12.0	0.0%	0.0	12.0	208.4	0.0	0.0	0	1	1	0	0	0
Propylene Glycol Solution	12.00	1	12.0	0.0%	0.0	12.0	208.4	0.0	0.0	0	1	1	0	0	0
ECLSS FLUIDS			248.6	0.0%	0.0	248.6	210.6	2.3	-28.9	376	384	22	-1	20	7
Oxygen	82.27	2	164.5	0.0%	0.0	164.5	210.6	0.7	-83.7	270	273	16	0	36	0
Nitrogen	84.07	1	84.1	0.0%	0.0	84.1	210.6	5.4	78.4	106	111	6	-1	-16	6
PRESSURANT			72.0	0.0%	0.0	72.0	210.8	0.0	0.0	88	5	92	0	0	0
Helium	36.00	2	72.0	0.0%	0.0	72.0	210.8	0.0	0.0	88	5	92	0	0	0
PROPELLANT			615.0	0.0%	0.0	615.0	219.6	0.0	0.0	425	242	242	0	1	-45
Unusable			615.0	0.0%	0.0	615.0									
Unusable Fuel (MMH)	116.00	2	232.0	0.0%	0.0	232.0	219.6	0.0	0.0	160	91	91	0	0	70
Unusable Oxidizer (NTO)	191.50	2	383.0	0.0%	0.0	383.0	219.6	0.0	0.0	265	151	150	0	1	-114
TOTAL INERT MASS			8,490.9	17.7%	1,504.8	9,995.7	228.4	2.4	7.0	12,494	10,028	8,893	-89	-216	-153
PROPELLANT			20,500.0	0.0%	0.0	20,500.0	219.6	0.0	0.0	14,174	8,075	8,054	10	29	-1,496
Usable			20,500.0	0.0%	0.0	20,500.0									
Usable Fuel (MMH)	3,868.00	2	7,736.0	0.0%	0.0	7,736.0	219.6	0.0	0.0	5,349	3,047	3,039	4	11	2,318
Usable Oxidizer (NTO)	6,382.00	2	12,764.0	0.0%	0.0	12,764.0	219.6	0.0	0.0	8,825	5,027	5,015	6	18	-3,814
TOTAL WET MASS			28,990.9	5.2%	1,504.8	30,495.7	222.5	0.8	2.3	26,668	18,102	16,947	-79	-186	-1,650

Mass Properties are calculated at the module's wet mass center of gravity
Products of Inertia are calculated using a "positive integral" formulation

Table 13.0-3 Launch Abort System Detailed Mass Properties

CEV LAUNCH ABORT SYSTEM - CRC-3 FINAL CONFIGURATION - 4 CREW LUNAR SORTIE - LAUNCH CONFIGURATION - MASS PROPERTIES REPORT

DESCRIPTION	Unit Mass (lbm)	Qty	CBE Mass (lbm)	Growth %	Growth Mass (lbm)	Predicted Mass (lbm)	Center of Gravity X (in)	Center of Gravity Y (in)	Center of Gravity Z (in)	Moments of Inertia Ixx (slug-ft^2)	Moments of Inertia Iyy (slug-ft^2)	Moments of Inertia Izz (slug-ft^2)	Products of Inertia Ixy (slug-ft^2)	Products of Inertia Ixz (slug-ft^2)	Products of Inertia Iyz (slug-ft^2)
ACTIVE CONTROL MOTOR			334.7	30.0%	100.4	435.1	-219.9	0.0	0.0	17	2,753	2,753	2	1	0
Active Control Motor Skin	151.50	1	151.5	30.0%	45.5	197.1	-218.1	0.0	0.0	13	1,225	1,225	1	0	0
Active Control Motor	183.10	1	183.1	30.0%	54.9	238.0	-221.4	0.0	0.0	4	1,528	1,528	1	1	0
ABORT MOTOR			2,780.0	13.9%	387.3	3,167.3	-69.3	0.0	0.0	426	1,973	1,973	2	1	0
Motor Case Assy	2,780.00	1	2,780.0	13.9%	387.3	3,167.3	-69.3	0.0	0.0	426	1,973	1,973	2	1	0
JETTISON MOTOR			547.8	21.0%	115.0	662.8	-173.5	0.0	0.0	35	2,252	2,252	3	1	0
Motor Case Assy Skin	217.00	1	217.0	21.0%	45.6	262.6	-174.3	0.0	0.0	17	907	907	1	0	0
Motor Case Assy	330.80	1	330.8	21.0%	69.5	400.3	-172.9	0.0	0.0	17	1,344	1,344	2	1	0
STRUCTURES & MECHANISMS			1,236.0	14.9%	184.4	1,420.4	-17.1	0.0	0.0	350	3,978	3,978	-1	-1	0
Nose Cone	106.00	1	106.0	25.0%	26.5	132.5	-251.6	0.0	0.0	5	1,177	1,177	1	0	0
CM/LAS Adapter	792.00	1	792.0	10.0%	79.2	871.2	49.7	0.0	0.0	321	2,071	2,071	-3	-1	0
Avionics Mount	116.00	1	116.0	20.0%	23.2	139.2	34.6	0.0	0.0	0	211	211	0	0	0
Interstage	222.00	1	222.0	25.0%	55.5	277.5	-141.1	0.0	0.0	25	519	519	1	0	0
AVIONICS			170.0	20.0%	34.0	204.0	34.6	0.0	0.0	1	309	309	-1	0	0
Power Distribution Unit	30.00	1	30.0	20.0%	6.0	36.0	34.6	0.0	0.0	0	55	55	0	0	0
Bus Interface Unit	30.00	1	30.0	20.0%	6.0	36.0	34.6	0.0	0.0	0	55	55	0	0	0
Pyro Control Unit	30.00	1	30.0	20.0%	6.0	36.0	34.6	0.0	0.0	0	55	55	0	0	0
Battery Pack	80.00	1	80.0	20.0%	16.0	96.0	34.6	0.0	0.0	0	146	146	0	0	0
PASSIVE THERMAL CONTROL			989.0	25.0%	247.3	1,236.3	119.1	1.6	0.8	1,673	8,608	8,631	63	29	11
Boost Protective Cover	989.00	1	989.0	25.0%	247.3	1,236.3	119.1	1.6	0.8	1,673	8,608	8,631	63	29	11
TOTAL DRY MASS			6,057.5	17.6%	1,068.4	7,125.9	-42.1	0.3	0.1	2,501	19,873	19,895	68	31	11
PROPELLANT			6,271.0	10.4%	652.1	6,923.1	-56.4	0.0	0.0	407	5,300	5,300	2	1	0
Jettison Motor Propellent	162.00	1	162.0	10.0%	16.2	178.2	-188.3	0.0	0.0	7	750	750	1	0	0
Active Control Propellent	500.00	1	500.0	15.0%	75.0	575.0	-210.9	0.0	0.0	5	3,249	3,249	3	1	0
Abort Motor Propellent	5,609.00	1	5,609.0	10.0%	560.9	6,169.9	-38.2	0.0	0.0	395	1,302	1,302	-2	-1	0
TOTAL WET MASS			12,328.5	14.0%	1,720.5	14,049.0	-49.2	0.1	0.1	2,909	25,173	25,196	70	32	11

Mass Properties are calculated at the module's wet mass center of gravity
Products of Inertia are calculated using a "positive integral" formulation

Table 13.0-4 Spacecraft Adapter Detailed Mass Properties

CEV SPACECRAFT ADAPTER - CRC-3 FINAL CONFIGURATION - 4 CREW LUNAR SORTIE - LAUNCH CONFIGURATION - MASS PROPERTIES REPORT															
							Center of Gravity			Moments of Inertia			Products of Inertia		
DESCRIPTION	Unit Mass (lbm)	Qty	CBE Mass (lbm)	Growth %	Growth Mass (lbm)	Predicted Mass (lbm)	X (in)	Y (in)	Z (in)	Ixx (slug-ft^2)	Iyy (slug-ft^2)	Izz (slug-ft^2)	Ixy (slug-ft^2)	Ixz (slug-ft^2)	Iyz (slug-ft^2)
POWER & WIRING			20.0	25.0%	5.0	25.0	290.4	0.0	100.0	52	52	1	0	5	0
Wiring			20.0	25.0%	5.0	25.0									
Wiring Harness	20.00	1	20.0	25.0%	5.0	25.0	290.4	0.0	100.0	52	52	1	0	5	0
STRUCTURE			740.9	25.0%	185.2	926.2	290.7	0.0	0.0	2,110	1,273	1,272	0	-5	0
Skin Panels (Composite)	136.93	1	136.9	25.0%	34.2	171.2									
Hat Stringers (Composite)	221.02	1	221.0	25.0%	55.3	276.3									
Intermediate Rings	97.00	1	97.0	25.0%	24.3	121.3									
Fwd Attach Ring	69.00	1	69.0	25.0%	17.3	86.3									
Separation Ring (SM Interface)	121.00	1	121.0	25.0%	30.3	151.3									
Aft Attach Ring (CLV Interface)	96.00	1	96.0	25.0%	24.0	120.0									
PYROTECHNICS			68.0	25.0%	17.0	85.0	229.0	0.0	0.0	171	134	134	0	2	0
SM/Adapter Separation	34.00	2	68.0	25.0%	17.0	85.0	229.0	0.0	0.0	171	134	134	0	2	0
MECHANISMS			90.0	25.0%	22.5	112.5	229.0	0.0	0.0	227	177	177	0	3	0
SM/Adapter Separation	90.00	1	90.0	25.0%	22.5	112.5	229.0	0.0	0.0	227	177	177	0	3	0
TOTAL WET MASS			918.9	25.0%	229.7	1,148.7	280.1	0.0	2.2	2,560	1,636	1,583	0	6	0

Mass Properties are calculated at the module's wet mass center of gravity
Products of Inertia are calculated using a "positive integral" formulation